FTD-MT- 64-526

AD622400

TT65-64167

TRANSLATION

THE EXTERNAL LOADS AND STRENGTH OF FLYING APPARATUSES

By:

A. I. Gudkov, P. S. Leshakov, and L. G. Ryakov

FOREIGN TECHNOLOGY DIVISION

AIR FORCE SYSTEMS COMMAND

WRIGHT-PATTERSON AIR FORCE BASE

OHIO

This document is a machine translation of Russian text which has been processed by the AN/GSQ-16(XW-2) Machine Translator, owned and operated by the United States Air Force. The machine output has been post-edited to correct for major ambiguities of meaning, words missing from the machine's dictionary, and words out of the context of meaning. The sentence word order has been partially rearranged for readability. The content of this translation does not indicate editorial accuracy, nor does it indicate USAF approval or disapproval of the material translated.

EDITED MACHINE TRANSLATION

THE EXTERNAL LOADS AND STRENGTH OF FLYING APPARATUSES

BY: A. I. Gudkov, P. S. Leshakov, and L. G. [illegible]

English Pages: 619

PREPARED BY:

TRANSLATION DIVISION
FOREIGN TECHNOLOGY DIVISION
WP-AFB, OHIO.

Date 20 July 19 65

A. I. Gudkov, P. S. Leshakov,
L. G. Ryakov

VNESHNIYE NAGRUZKI I PROCHNOST' LETATEL'NYKH APPARTOV

Gosudarstvennoye

Nauchno-Tekhicheskoye Izdatel'stvo

Oborongiz

Moskva 1963

Pages 1-480

BLANK PAGE

TABLE OF CONTENTS

U. S. BOARD ON GEOGRAPHIC NAMES TRANSLITERATION SYSTEM

Block	Italic	Transliteration	Block	Italic	Transliteration
А а	*А а*	A, a	Р р	*Р р*	R, r
Б б	*Б б*	B, b	С с	*С с*	S, s
В в	*В в*	V, v	Т т	*Т т*	T, t
Г г	*Г г*	G, g	У у	*У у*	U, u
Д д	*Д д*	D, d	Ф ф	*Ф ф*	F, f
Е е	*Е е*	Ye, ye; E, e*	Х х	*Х х*	Kh, kh
Ж ж	*Ж ж*	Zh, zh	Ц ц	*Ц ц*	Ts, ts
З з	*З з*	Z, z	Ч ч	*Ч ч*	Ch, ch
И и	*И и*	I, i	Ш ш	*Ш ш*	Sh, sh
Й й	*Й й*	Y, y	Щ щ	*Щ щ*	Shch, shch
К к	*К к*	K, k	Ъ ъ	*Ъ ъ*	"
Л л	*Л л*	L, l	Ы ы	*Ы ы*	Y, y
М м	*М м*	M, m	Ь ь	*Ь ь*	'
Н н	*Н н*	N, n	Э э	*Э э*	E, e
О о	*О о*	O, o	Ю ю	*Ю ю*	Yu, yu
П п	*П п*	P, p	Я я	*Я я*	Ya, ya

* ye initially, after vowels, and after ъ, ь; e elsewhere. When written as ё in Russian, transliterate as yё or ё. The use of diacritical marks is preferred, but such marks may be omitted when expediency dictates.

FOLLOWING ARE THE CORRESPONDING RUSSIAN AND ENGLISH

DESIGNATIONS OF THE TRIGONOMETRIC FUNCTIONS

Russian	English
sin	sin
cos	cos
tg	tan
ctg	cot
sec	sec
cosec	csc
sh	sinh
ch	cosh
th	tanh
cth	coth
sch	sech
csch	csch
arc sin	$\sin^{-1}$
arc cos	$\cos^{-1}$
arc tg	$\tan^{-1}$
arc ctg	$\cot^{-1}$
arc sec	$\sec^{-1}$
arc cosec	$\csc^{-1}$
arc sh	$\sinh^{-1}$
arc ch	$\cosh^{-1}$
arc th	$\tanh^{-1}$
arc cth	$\coth^{-1}$
arc sch	sech^{-1}
arc csch	csch^{-1}
rot	curl
lg	log

This book is dedicated to external loads having effect on a flight vehicle (aircraft and helicopter), and the durability of its construction. Basic attention in the book is allotted to actual problems of strength of contemporary flight vehicles: dynamic load, periods of service and strength of construction, strength during high speeds of flight, taking into account aerodynamic heating and others. Along with an account of theoretical questions in the book there are described experimental methods of investigating strength of construction.

The book is designed for engineers connected with designing, tests, and exploitation of flight vehicles. At the same time, it can be used as a training aid for aviation students of higher educational institutions.

PREFACE

Strength of construction is one of the basic factors guaranteeing flight safety of any flight vehicle. To investigations in the region of strength, considerable attention has been allotted from the very beginning of the development of aviation.

Consideration of strength of flight vehicles is impossible without knowledge of external loads appearing in flight and during motion on land and their influence on construction. Therefore, during first investigations of strength of aviation construction there arose the necessity of studying external loads in different conditions of flight.

In parallel with the study of external loads acting on an aircraft, methods of design for strength and laboratory tests have been improved.

Until the thirties basic attention was allotted to the study of static strength of aviation construction. Other questions, although they had value, were not determining. Subsequently, with increase in speeds of flight and, consequently, with the complication of interaction of structure with the air medium, the study of different aeroelastic phenomena — flutter, divergence, and reversal of control surfaces — became of great value.

Investigation of loads on structure, taking into account its elastic deformations and stability in flow of air, compose now an independent region of the science of strength — aeroelasticity.

In connection with a considerable increase in periods of service of aviation structures, of especially important value are questions of fatigue strength.

The range of questions on strength of flight vehicles is manifold. At present, it is possible to distinguish three basic directions in the science of strength of flight vehicles — aeroelasticity, static strength, and fatigue strength. To these questions, basically, is dedicated the contents of this book.

Solution of problems of strength of supersonic flight vehicles has been considerably complicated by the influence of aerodynamic heating. Therefore, in Chapter VIII is considered the influence of aerodynamic heating on the strength of flight vehicles.

In this book are not considered questions of structural mechanics of aircraft, since they are presented in sufficient detail in literature.

The authors do not claim a completed account of the considered questions. The majority of them, in themselves, present extensive regions of independent scientific investigation. Therefore, during the study of concrete problems of strength of flight vehicles one should use special literature. However, the authors consider that this book will be useful to specialists occupied in investigations of strength, in their practical work. In particular, engineer-operators material will help conduct exploitation of flight vehicles more correctly.

Concrete data on external loads, deformations, and stresses in construction are borrowed from native or foreign literature.

Main divisions of the book were written by P. S. Leshakov (Chapters I, II, IV, VII, X) and A. I. Gudkov (Chapters III, V, VI, IX, X). Chapter VIII about the influence of aerodynamic heating was written by L. G. Raykov.

The authors express their gratefulness to Corresponding Member of Academy of Sciences of USSR A. I. Makarevskiy, Doctors of Technical Sciences L. I. Balabukh and A. A. Umanskiy, Candidates of Technical Sciences A. I. Martynov, G. N. Rudykh, T. A. Frantsuz, and V. L. Raykher, V. I. Savel'yev, for reading the manuscript and giving valuable counsel to the authors.

MT-526.
External Loads and Strength of
Flying Apparatuses, State
Scientific and Technical
Publishing House, Oborongiz,
Moscow, 1963.
Pages: Cover-480

CHAPTER I

DESIGN CONDITIONS DETERMINING STRENGTH REQUIREMENT OF AIRCRAFT

List of Designations Appearing in Cyrillic

аэр = aero = aerodynamic

в = el = elevator

в = vert = vertical

г.о = h.e = horizontal empennage

г.п = h.f = horizontal flight

доп = per = permissible

несж = incompressible

огр = lim = limitation

пр = ind = indicated

сж = com = compressibility

ср = av = average

хв = emp = empennage

ш = hi = hinge

э = op = operational

эф = ef = effective

In the process of exploitation, an aircraft is subjected to influence of various kinds of loads.

When designing an aircraft, for its strength analysis it is necessary to know limiting external loads having effect on its construction. On the basis of laboratory, flying, and theoretical research, and generalizations of designing experience and exploitation, there are developed requirements on selection of basic initial data for strength analysis and methods of determining external loads. These requirements are presented in norms of strength of aircraft, which regulate magnitude and character of load distribution for separate parts of flight vehicle in different conditions of flight.

During load calculation there are chosen a number of aircraft attitudes which correspond to operating conditions determining the heaviest conditions of load of basic supporting members. These positions in norms are called "cases of design and tests." Each case has its own formulation and letter or numerical designation.

Norms of strength have continuously improved with development of aviation.

Basic parameters for determining external loads are maximum overload, terminal velocity (terminal velocity pressure) of flight and weight of aircraft.

Under overload is understood ratio of external (surface) forces acting on a flight vehicle to its weight. External forces are expressed in the form of aerodynamic and inertial forces, and also in the form of reaction of land.

During curvilinear flight, overload n is equal to ratio of lift of aircraft Y to its weight G:

$$n=\frac{Y}{G}.$$

Magnitude of maximum permissible speed of flight $V_{max\ max}$ and maximum operational G-force n^{op}_{max} is determined based on assignment and flying-technical data of aircraft.

Calculation conditions are established in reference to conditional (calculated) weight of flight vehicle, taking into account possible (while in operation) variants of distribution of separate loads.

1.1. Selection of Design Conditions in Norms of Strength at Different Stages of the Development of Aviation

In the first years of the development of aviation (before 1910) basically studied was the problem of flight. Numerous accidents in 1909-1910 because of aircraft breakdown in the air forced engineers to turn the most serious attention to the guarantee of sufficient strength of created structures. For solution of this question it was necessary to determine external loads acting on an aircraft in flight and during landing.

First attempts to establish requirements with respect to external loads and methods of strength analysis of an aircraft were in 1910-1912. In August 1910 a commission of representatives of aeronautical leagues of England, France, and Belgium indicated the necessity of state supervision of aircraft construction. Soon in France was developed the project "Evidence of fitness for flight," where it was indicated that an aircraft should satisfy defined conditions and also should be subjected to flight and laboratory (static) tests.

For determination of basic requirements for strength of aircraft, in 1911-1912 was started a study of basic cases of load of aircraft in flight — influence of a gust of bumpy air and load during maneuver. In this period, Russian designer D. P. Grigorovich established that the most severe case of load is the pull-out of an aircraft from diving, when overload can attain magnitude of 5-8. He also introduced for the first time in Russia static tests of parts of an aircraft.

By 1912, in a number of countries, researchers (in Russia V. M. Ol'khovskiy, in France A. Se, in Germany G. Reysener, and others) came to the conclusion that optimum value of breaking overload for an aircraft should be considered $n^p = 12$.

In 1913 German military department developed, for checking quality of aircraft "Special conditions" which contain requirements for strength. In these requirements magnitude of maximum overload was connected with speed of flight (in particular, during speed $V > 120$ km/hr calculation of overload n^p was taken as equal to 6). In 1914 in Germany, investigations were started of overloads in flight on an "Albatross" aircraft. For this purpose was prepared an instrument recording overload; measured overloads did not exceed $n = 2$.

In the same period in Russia questions of external loads and methods of appraising strength of aircraft were studied by N. Ye. Zhukovskiy, N. P. Grigorovich, N. A. Rynin and others.

By the beginning of the war of 1914-1918 there already were carried out the first works on definition of external loads and were fixed the most dangerous cases of load. In a number of countries there was recognized necessary state supervision of aircraft construction and were introduced tests of aircraft on land during static load.

In the First World War the role of the aircraft in military operations was sharply increased, and there appeared the necessity of introducing official requirements for its strength. In 1916 in Germany there were accepted official "Technical requirements on manufacture and delivery of military airplanes," which became the prototype of norms of strength of aircraft in a number of countries.

In Russia in 1916 at the Aerodynamic Laboratory of Moscow Technical School, on the initiative of N. Ye. Zhukovskiy there was created an Aviation Design and Testing Bureau, in the function of which entered, in particular, the study of external loads and development of methods of analysis and check of strength of the structure of aircraft. In the same year was created a commission for development of norms of strength. At the first session of this commission, 14-16 November 1916, in which participated N. Ye. Zhukovskiy, V. P. Vetchinkin, A. N. Tupolev, A. A. Arkhangel'skiy, basic requirements were accepted for strength of aircraft and thereby was assumed the beginning of the creation of domestic norms of strength.

In December 1918 was created Central Aero-Hydrodynamic Institute (Central Aero-Hydrodynamic Institute). From the moment of organization the Central Aero-Hydrodynamic Institute has studied questions of strength of aircraft and is a leading organization in the development of the science of aircraft strength.

In 1918 was conducted a number of test flights for investigation of overloads during maneuvers and in "turbulence." For measurement of overloads, V. P. Vetchinkin* at first applied the usual spring scales with weight of 4.5 pound, but then designed accelerometer with mark of maximum and minimum value of overload (Fig. 1.1). On the basis of analysis of the results of measurements he came to the conclusion that magnitude of overload on aircraft of that period can be changed from -2 to +4. He suggested preliminary norms, which should be maintained when designing aircraft. Subsequently, under his leadership proceeded development of first domestic norms of aircraft strength.

---

*V. N. Sokol'skiy, Development of methods of aircraft strength analysis before the First World War. Transactions of the Institute of Natural History and Technology, Academy of Sciences of the USSR, Vol. 21, 1959.

In 1920-1922 were developed norms of strength in England and the United States. By these norms maximum destroying overload was taken to be equal to 4.0-5.5 for bombers, 8.0 for trainer aircraft and 7.5-8.5 for fighter airplanes.

In the Soviet Union the first norms of strength were developed before 1924 ("Temporary union norms 1924"). In these norms maximum design overload was taken as equal to 8.5.

By 1923-1925 the upper limit of standardized breaking overloads approached 12, which corresponds to operational G-force of 8.

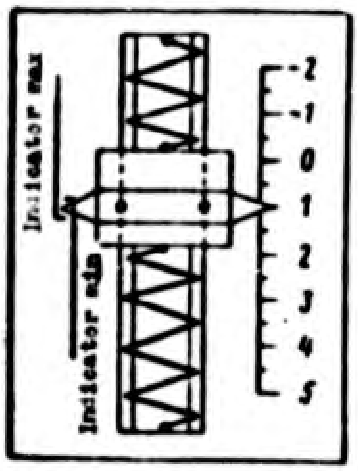

Fig. 1.1. Recorder of overloads of V. P. Vetchinkin.

For increase of strength reserve in norms of some countries, destroying overload was brought to 15 (Italian norms of strength 1924). However, in norms of strength of a majority of countries this magnitude composed 10-13 and virtually was not changed up to now. Possibility of achievement in flight of maximum overloads close to 8 was proved in 1924 by pilot I. C. Doolittle on aircraft "Fokker PW-7," when there was attained an overload of 7.8 during pullout at a speed of 260 km/hr.

Along with norms of strength were developed also methods of strength analysis of aviation structure. A great contribution in the development of theory of analysis was introduced by Soviet scientists. After introduction of the first norms (1924) there began regular and systematic work on improvement of domestic norms of strength. Considerable work on the development of norms was conducted by A. A. Goryainov and G. I. Kuz'min under the leadership of V. P. Vetchinkin and V. I.

Aleksandrov.*

In domestic norms of strength in 1925, aircraft were divided into two classes — civil and military. Each class in turn is divided into four groups by weight of aircraft. In the class of military aircraft considered also was assignment of aircraft. The following values of design overload were accepted during pullout:

Class of aircraft	Group			
	1	2	3	4
Civil	5.5	5.5 to 5.0	5.0 to 4.0	4.0
Military	12.0	8.0	6.0	4.0

For all aircraft overloads during landing were established depending upon landing speed:

Landing speed in km/hr	Less 80	80–120	More 120
Overload during landing	6	6-8	According to special coordination

For further, more precise definition of external loads in norms of strength, of great value was the work of V. S. Pyshnov.**

In 1927, during issue of new norms of strength, were definitized classifications of aircraft and a series of design cases. Subsequently,

*A. A. Goryainov and G. I. Kuz'min, Norms of strength of aircraft and static tests, Transactions of Central Aero-Hydrodynamic Institute, Issue 25, 1926.

**V. S. Pyshnov, Experiments on overloads of aircraft in flight, "War and technology," 1926, No. 257. Investigation of strength of aircraft, Transactions of Air Academy RKKA, Issue 6, 1932.

norms of strength were definitized and supplemented every 2-3 years. In particular, in the norms of 1934 was introduced a position about selection of design overload depending upon speed of flight. The foundation of this position was developed by S. N. Shishkin.* He later conducted flight tests of loads during takeoff and landing and a series of research in further development of norms of strength.

In 1935-1940 were conducted extensive investigations of loads on aircraft during maneuvers, during flight in bumpy air, during takeoffs and landings. At the same time work was started on measurement of overloads in conditions of mass exploitation of aircraft. Conducted investigations allowed the definitizing of strength norms and the separation of them into engineering discipline, based on strict fundamental positions and well-founded methods of extrapolation during determination of loads on promising aircraft. In the same period, in norms of strength were definitized safety factors, methods of analyzing distribution of aerodynamic load, and a series of new design cases.

Considerable work on the foundation of design cases and development of norms of strength was conducted by A. I. Makarevskiy. He investigated the influence of degree of longitudinal stability of an aircraft and basic structural and aerodynamic parameters on maximum overload of an aircraft; calculated loads on empennage were substantiated, and there were carried out a series of test flights.

Substantiated selection of rated loads for high-speed aircraft of the period of the Patriotic War (Yak-1, La-5, MiG-3, Ty-2, Pe-2, Il-2) ensured, during high tactical flying data, their reliable work in complex conditions of combat actions without breakdown from insufficient design strength of construction.

---

*S. N. Shishkin, Concerning the question of new classification of aircraft in norms of strength, "Technology of Air fleet," 1933, No. 8.

In period of Patriotic War work on development of norms of strength did not cease.

Subsequently, norms of strength were augmented by new requirements, taking into account peculiarities of load during transonic and supersonic speeds of flight and new conditions of exploitation of aircraft. Introduction of contemporary methods of test flights and wide theoretical and laboratory investigations permit, now, developing norms of strength taking into account prospects of development of different types of flight vehicles.

1.2. Speeds of Flight Taken for Aircraft Strength Analysis

Aerodynamic forces acting on a flight vehicle, basically, are determined by its speed with respect to air. Speed of flight vehicle with respect to air is called true or air speed. During the analysis of external loads is used the idea of equivalent (V_i) speed, which is connected with true speed (V_H) by relationship

$$V_i = V_H\sqrt{\frac{\rho_H}{\rho_0}} = V_H\sqrt{\Delta_H}, \qquad (1.1)$$

where ρ_H is air density on altitude H;

ρ_0 is air density for earth;

$\Delta_H = \frac{\rho_H}{\rho_0}$ is relative density on altitude H.

Measurement of speed in flight is conducted with the help of a pilot-static head extending out to the zone of air flow undisturbed by the aircraft. The indicator or recorder of speed records the so-called indicated airspeed V_{ind}, which is connected with equivalent airspeed by relationship

$$V_i = V_{\text{пр}} + \delta V_{\text{сж}} + \delta V_{\text{а.пр}} \qquad (1.2)$$

where δV_{com} is correction for compressibility of air;

δV_{aero} is correction considering distortion of static pressure at the place of installation of pickup on aircraft.

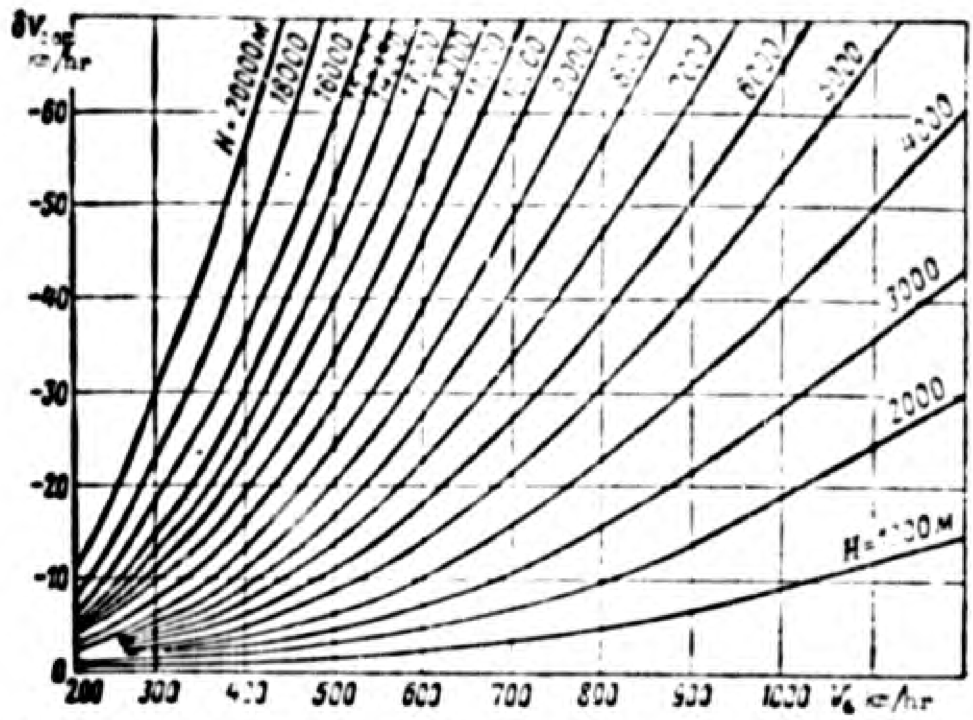

Fig. 1.2. Graph for determinating correction for compressibility.

Magnitude of correction for compressibility depends on altitude and speed of flight. On Fig. 1.2 is given graph for determination of δV_{com}. At transonic speeds of flight is considered additionally wave correction.

For convenience of pilot, maximum permissible operational speeds of flight usually are established by indicated airspeed. In analyzing aerodynamic loads only equivalent speed is taken. The difference between indicated and equivalent speeds because of correction for compressibility δV_{com} goes into safety factor, since correction for compressibility δV_{com} is less than zero (Fig. 1.3).

For appraisal of aerodynamic loads is used idea of dynamic (high-speed) pressure q, connected with speed by the following dependence:

$$q = \rho_H \frac{V_H^2}{2} = \rho_0 \frac{V_i^2}{2}.$$

Formula for analyzing magnitude of impact pressure by speed or Mach number it is possible to record so:

$$q = \frac{V_i^2}{207} \ \text{kg/m}^2, \qquad (1.3)$$

where V_i in km/hr,

or

$$q = 9.5 p_H M^2 \ \text{kg/m}^2; \qquad (1.4)$$

$$M = \frac{V_H}{a_H} \quad \text{and} \quad a_H = \sqrt{\frac{k p_H}{\rho_H}};$$

p_H - atmospheric pressure in mmHg;

a_H - speed of sound at altitude H;

$k = \frac{c_p}{c_v}$ - adiabatic coefficient (for air k = 1.4).

Using expression (1.3) and (1.4), we will define equivalent speed and Mach number by impact pressure:

$$V_i = 14.4\sqrt{q} \ \text{km/hr} \quad \text{and} \quad V_i = 44.4 M \sqrt{p_H} \ \text{km/hr}. \qquad (1.5)$$

$$M = 0.32\sqrt{q \cdot p_H}. \qquad (1.6)$$

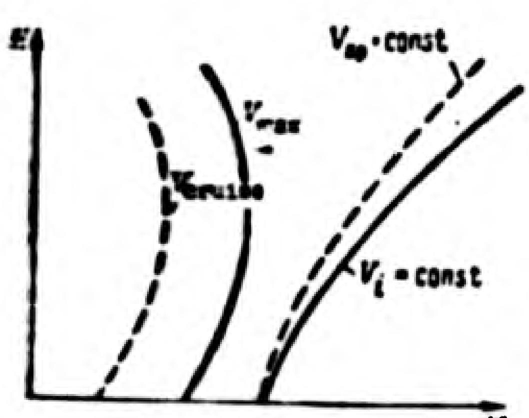

Fig. 1.3. Approximate character of limitation of flight speed of a piston-engined aircraft.

In Table 1.1 are given values of speeds and Mach numbers at different altitudes, calculated by formulas (1.5) and ( ).

Table 1.1

q kg/m²	V_i km/hr	Mach number		
		$H = 0$	$H = 10000$ m	$H = 30000$ m
500	326	0,262	0,514	2,43
1000	456	0,370	0,727	3,45
2500	720	0,587	1,15	5,45
5000	1020	0,830	1,63	7,70
7500	1250	1,018	1,98	9,42
10000	1440	1,172	2,30	10,[illegible]0
15000	1765	1,410	2,82	13,35
20000	2040	1,660	3,26	15,9
30000	2495	2,015	3,99	18,9
40000	2880	2,344	4,60	21,8
50000	3205	2,623	5,14	24,3

Aircraft when descending can develop a considerably higher speed than in horizontal flight during maximum thrust of motor. Increase of speed leads to growth of local and total loads acting on the flight vehicle. Therefore, guarantee of structural strength during essentially higher speeds of flight than maximum speed leads to unnecessary increase of structural weight. For every flight vehicle there are chosen such terminal velocities of flight that, on the one hand, tasks set before a given apparatus are fulfilled and, on the other hand, this does not lead to essential increase of weight of construction.

Selection of maximum permissible speed of flight $V_{max\ max}$, which is determining in aircraft strength analysis, depends on type and assignment of aircraft. For aircraft with piston motors, as a rule, is established a limitation only in equivalent (indicated) speed of flight (Fig. 1.3). For these aircraft maximum permissible speed is higher than maximum speed of horizontal flight (on all altitudes). For jet aircraft with subsonic speeds basic conditions of flight usually correspond to altitudes of more than 7-12 km. Therefore, on lower altitudes it is expedient to limit maximum speed of flight (Fig. 1.4). The altitude higher than which there are no limitations of maximum speed of flight is called altitude of limitation and is designated H_{lim}. At great heights, speed of flight, as a rule, is limited by a definite Mach number from conditions of preservation of stability and controllability of the flight vehicle. If limitation of speed at altitude by maximum permissible impact pressure coincides with limitation of speed by Mach number, i.e., if

$$V_{max\,max\,q} = V_{max\,max\,M},$$

then such an altitude is designated H_q.

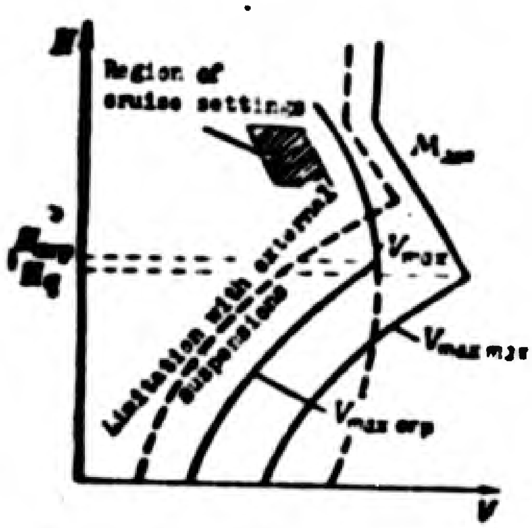

Fig. 1.4. Approximate character of limitation of speed of flight of aircraft with jet engine during subsonic speeds of flight.

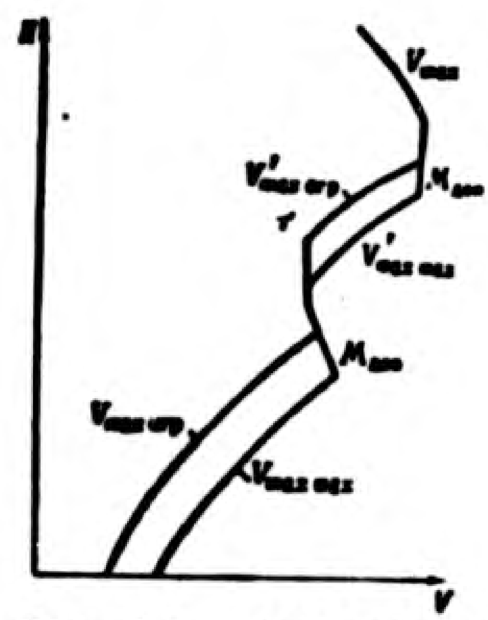

Fig. 1.5. Approximate character of limitation of speed of flight of supersonic aircraft. $V^T_{max\,max}$ and $V^T_{max\,lim}$ are limitations of speed from conditions of permissible heating.

For aircraft with supersonic speeds of flight there appear also other causes of limitation of speed. Thus, at speeds corresponding to M > 2 there is observed considerable heating of construction. In connection with this there is established additional limitation of speed from condition of permissible heating of construction. Approximate graph, characterizing limitation of speed of flight of supersonic aircraft, is shown in Fig. 1.5.

In the basis of the selection of terminal velocity of flight of aircraft are placed the results of study of maneuvers executed by them. Maneuvering aircraft must execute steep descent and sometimes nose dive. Therefore, during selection of magnitude $V_{max\ max}$ preliminarily is investigated diving of such aircraft with pull-out at different altitudes. In certain cases for deceleration of descent, on aircraft are established air brakes, which permits taking into calculation smaller maximum permissible speed of flight.

For passenger aircraft, basic cases for selection of terminal velocities are:

- climb on most advantageous conditions;
- conditions of descent at the end of flight;
- descent of aircraft in case of emergency decompression of passenger cabin.

For every condition there are determined terminal velocities of flight taking into account possible errors of pilot, horizontal gusts in bumpy air, and errors of speed indicator. It is assumed that terminal velocity $V_{max\ max}$ is permissible only for brief conditions of flight. For prolonged conditions of flight there is introduced additional limitation of speed, usually designated V_{lim}. Thus, by requirements of IKAO* $V_{lim} = V_{max\ max} - 113$ km/hr. During flight in conditions of strong atmospheric turbulence, for nonmaneuvered aircraft there can be introduced additional limitations of speed of flight.

---

*IKAO – International Organization of Civil Aviation.

For mass exploitation, as a rule, are established terminal velocities lower than those accepted during strength analysis. In this case, magnitude of reserves in speed are determined based on peculiarities of the aircraft. Besides limitations of speed from conditions of local and general strength, sometimes are introduced limitations of speed of flight, excluding appearance of structural flutter, divergence, and reverse controls.

Established also are a number of special limitations of speed during flight with open hatches for different assignments, lowered landing gear, deflected flaps, and so forth.

For instance, for well-founded selection of limitations of speed of flight with lowered landing gear and flaps calculations are conducted of highest possible speed during takeoff, taking into account possible errors of pilot. In this case, for lowering of limiting permissible speed it is expedient to establish powerful retracting mechanisms of landing gear (or flaps), since this reduced time of retracting of landing gear and, consequently, the considerable build-up of speed does not occur in the process of retracting. However, excessively fast retracting (lowering) of landing gear may cause unfavorable change of moments of aerodynamic forces on conditons of takeoff and landing. Therefore, in every concrete case optimum time of retracting and lowering of landing gear (or flaps) is found. For instance, in requirements of IKAO it is recommended that calculated speed with lowered flaps not be more than 60% higher than minimum speed of flight with retracted flaps or 40% higher than minimum speed with flaps in landing position.

On aircraft with external suspensions (suspension tanks, cargo containers, and so forth) there can be introduced additional limitations both in impact pressure (equivalent speed) and in Mach number. In certain cases, based on conditions of exploitation, there is no necessity for high speeds of flight on aircraft with external suspensions. Then terminal velocities of flight are somewhat lowered as compared to conditions of flight without suspensions. In case of necessity, the pilot can drop external suspensions, and the aircraft will have the same limitation of speed as without suspensions.

In selection of limitations of speed on supersonic aircraft, basic parameters are permissible temperatures of aerodynamic heating of structure. In this case, limiting Mach number is established depending upon material of construction, conditions of heat transfer, and time of stay in limiting conditions. There is considered also possible change of particular (rigidity) characteristics of construction of aircraft during heating.

During selection of limitations of speed of flight for a flight vehicle there are considered the operational peculiarities of its automation. For this purpose, there is conducted simulation on a stand of different conditions of flight with the imitation of possible influences of unfavorable factors or malfunctions of separate elements of automatic control system.

All fixed limitations of speed are checked in flight during test of aircraft. There is estimated local strength of construction, behavior of aircraft (stability, controllability, and others), and reality of achievement or exceeding of terminal velocities in exploitation. On the basis of tests values of terminal velocities of flight are definitized, and corresponding limitations of speed for mass exploitation of aircraft are established.

1.3. Forces Effective on Aircraft in Flight

In horizontal linear flight with constant speed, on an aircraft act the following forces (Fig. 1.6): weight of aircraft G, wing lift Y, load on horizontal empennage $P_{h.e}$, thrust of power installation of aircraft T and drag X.

Condition of equilibrium of forces and moments can be recorded in the form

$$Y-P_{г.о}-G=0; \quad T-X=0. \quad P_{г.о}L_{г.о}-Ya=0.$$

where $L_{h.e}$ is arm of aerodynamic force of horizontal empennage with respect to center of gravity of aircraft;

a — distance from center of gravity to point of application of lift of aircraft without empennage.

For aircraft in which magnitude $P_{h.e}$ in horizontal flight composes small part of lift Y (less than 5%), for simplification it is possible to assume

$$Y=G, \quad X=T.$$

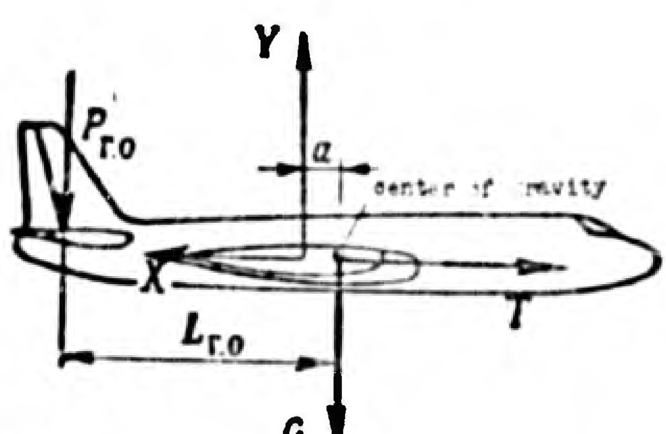

Fig. 1.6. Forces acting on an aircraft in horizontal flight.

Lift and drag are expressed through aerodynamic coefficients

$$\left.\begin{aligned} Y&=c_y\frac{\rho V^2}{2}S; \\ X&=c_x\frac{\rho V^2}{2}S. \end{aligned}\right\} \qquad (1.7)$$

where S is wing area;

c_x is drag coefficient;

c_y is coefficient of lift.

Besides shown forces, in curvilinear flight appear inertial forces: centrifugal force of mass of aircraft, acting in the direction of radius of curvature of trajectory from center of curvature,

$$F_c = m\frac{V^2}{R}$$

and tangential inertial force of mass of aircraft, effective along a tangent to trajectory,

$$F_t = m\frac{dV}{dt}.$$

In these expressions

m — mass of aircraft;

R — radius of curvature of trajectory;

g — acceleration due to gravity.

Diagram of forces acting on an aircraft in curvilinear flight is shown on Fig. 1.7.

For majority of forms of maneuvers, magnitude of tangential acceleration is comparatively small. For simplification of further analysis, we will assume dV/dt = 0. Then basic relationship for forces normal to trajectory will be

$$Y - G\cos\theta - F_c = 0,$$

or

$$Y = G\left(\cos\theta + \frac{V^2}{Rg}\right). \qquad (1.8)$$

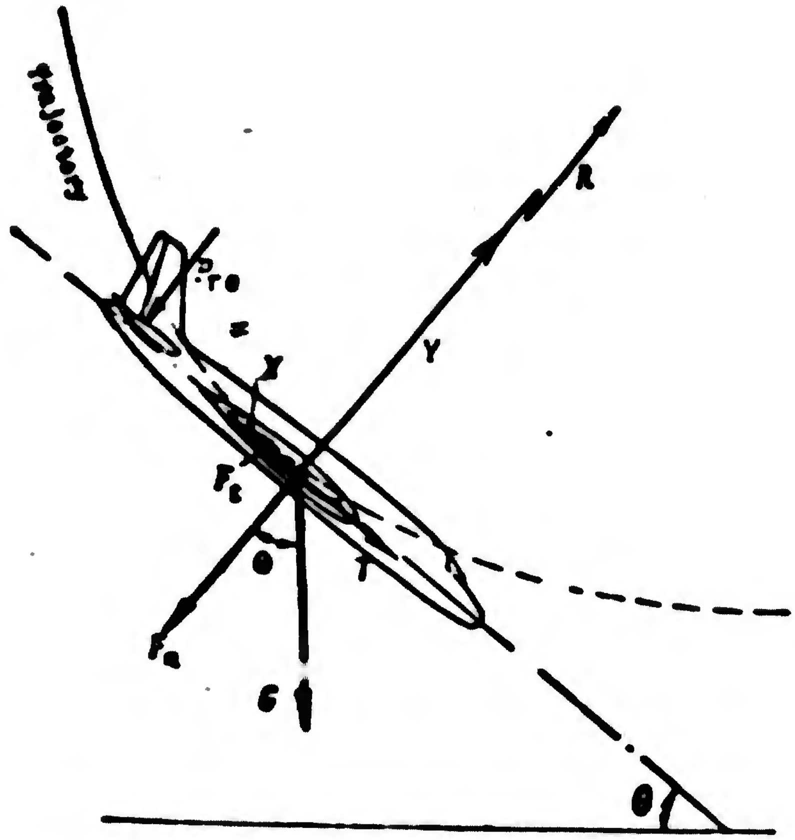

Fig. 1.7. Forces acting on an aircraft in curvilinear flight.

For comparison of loads during different conditions of flight of an aircraft is used the idea of overload – ratio of lift of aircraft to its weight, i.e., $n = Y/G$. For curvilinear flight, from formula (1.8) we will obtain

$$n = \cos\theta + \frac{V^2}{Rg}. \tag{1.9}$$

From expression (1.9) it is clear that magnitude of increase of overload in curvilinear flight is directly proportional to square of speed of flight and is inversely proportional to radius of curvature of trajectory. On a turn, magnitude of overload is determined by angle of bank γ; $n = 1/\cos\gamma$.

Overload can be less than unity and even negative when wing lift is directed in the opposite direction. Sign of overload determines direction of lift in curvilinear flight.

Below are given magnitudes of overloads during execution in aircraft of certain figures of aerobatics:

Chandelle....................4-5
Spiral.......................3-4
Barrel Role..................4-5
Multiple Barrel Roll.......5-7
Nesterov Loop..............3-6
Half-loop....................4-5
Spin.........................2-3
Turn.........................3-5

1.4. Maximum Overloads of Aircraft

Magnitude of overload of aircraft during constant gross weight is determined by lift.

During achievement of highest possible lift Y_{max} without loss of speed, maximum overload is

$$n_{max}=\frac{Y_{max}}{G}=\frac{c_{y\,max}\rho\frac{V^2}{2}S}{G}=\frac{c_{y\,max}q}{G/S}. \qquad (1.10)$$

where $c_{y\,max}$ is maximum value of lift coefficient. If we designate by $c_{y\,h.f}$ the value of lift coefficient corresponding to horizontal flight at given impact pressure q, then in horizontal flight weight of aircraft is

$$G=c_{y\,h.f}\,qS.$$

Then formula (1.10) it is possible to record in the form

$$n_{max}=c_{y\,max}/c_{y\,h.f}.$$

At low and medium altitudes, from condition of highest possible wing lift on aircraft theoretically can be obtained very high overloads (more than 15-20). However, the body of a person is able to endure only limited overloads. During action of overload exceeding 4-5, in the pilot appear sickly sensations. During further increase of overload pilot can lose ability to control aircraft normally.

On Fig. 1.8 ar given limiting overloads endurable by a person, depending upon direction of inertial forces. Magnitude of limiting endurable overload very strongly depends on time of its action. For instance, during overload of 6, effective for 15-20 sec, pilot "loses" sight and senses a number of sickly phenomena. During brief action (less than 2 sec) of overload of the order of 8-10, sickly phenomena are less perceptible.

During appraisal of maximum permissible overloads, one should consider that ability to control aircraft normally is lost during overloads considerably smaller than those shown on Fig. 1.8.

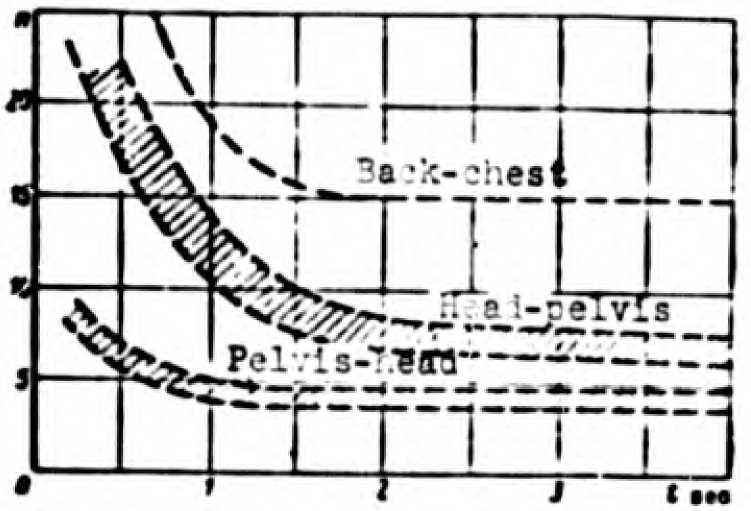

Fig. 1.8. Overload permissible for a person.

For increase of tolerance by pilot of overloads in maneuvering aircraft sometimes are used special G-suits.

It has long been tried to define maximum overload as that limiting endurable by pilot's body. However, absence of direct connection between physiologic influence of overload on body of pilot and magnitude of overload has forced a search for other ways of determining maximum overloads.

The highest, practically possible overload is determined by a number of factors:

— assignment and parameters (geometric and aerodynamic) of the aircraft;

— qualification and physical state of pilot;

— external conditions during fulfillment of maneuver, etc.

In real conditions of flight, at large angles of attack, there appears strong shaking of aircraft from local separations of flow, which hinders the attainment of angles of attack corresponding to $c_{y\,max}$. Value of coefficient of lift, at which shaking starts, is designated $c_{y\,per}$, and corresponding value of angle of attach is α_{per}.

With increase in angle of attack over α_{per}, besides shaking, there can appear instability in overload, loss of transverse controllability, and so forth. Therefore, in operation it is not recommended to exceed α_{per}.

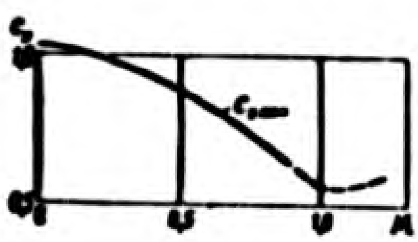

Fig. 1.9. Dependence of $c_{y\,per}$ on Mach number.

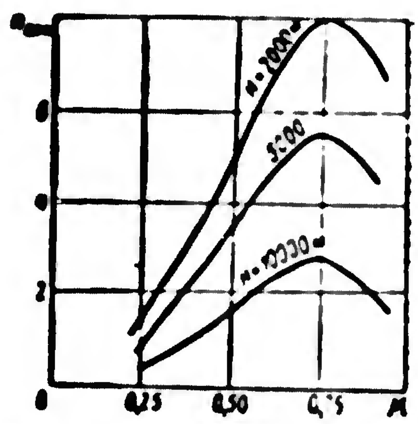

Fig. 1.10. Dependence of n_{per} on Mach number.

With increase in Mach number magnitude of $c_{y\,per}$ decreases (Fig. 1.9) because of influence of compressibility of air on distribution of pressure along profile.

Value of overload corresponding to $c_{y\,per}$ is called maximum permissible from conditions of aerodynamics and is defined as

$$n_{per} = \frac{c_{y\,per}\, a p_H M^2}{2G/S}. \qquad (1.11)$$

The higher the altitude of flight, the less will be the air density and speed of sound, and consequently, the less will be n_{per} at the same Mach number (Fig. 1.10).

At supersonic speeds of flight wing lift, in spite of decrease in c_y, is increased because of growth of impact pressure. Therefore, for supersonic aircraft at great heights there can be obtained overload of more than 8-10. However, realization of such overloads is hampered because of insufficient effectiveness of horizontal empennage and considerable fall of speed during maneuver due to sharp growth of c_x with increase of angle of attack.

1.5. Influence of Characteristics of Controllability and Stability of Aircraft on Maximum Possible Overload

Highest possible overload, determined from conditions of carrying ability of wing ($c_{y\,max}$), not always can be obtained during given parameters of stability and controllability of an aircraft. In connection with this, it is of interest to reveal dependence of probable maximum overload of aircraft on characteristic of its stability and controllability.

During elevator deflection (stabilizer) by angle δ_{el} is created moment M_δ, forcing aircraft to revolve with angular velocity ω_z about transverse axis:

$$M_\delta = c^{\delta}_{y\,г.о.}\delta_{в} S_{г.о.} kqL_{г.о.} \qquad (1.12)$$

Moment M_δ is balanced:

a) moment of damping M_ω, appearing from rotation of aircraft about transverse axis with angular velocity ω_z is:

$$M_\omega = k_\omega \frac{a_z}{\sqrt{k}} \frac{L_{г.о.}}{V} c_{y\,г.о.} kqS_{г.о.} L_{г.о.}\omega_z; \qquad (1.13)$$

b) static moment of aerodynamic forces is

$$M_s = m_z^{c_y} \Delta c_y q S b_A; \tag{1.14}$$

c) moment of inertial forces is $J_z \cdot d\omega_z/dt$.

Here are accepted following designations:

$c^{\delta}_{y\,h.e}$, $c^{\alpha}_{y\,h.e}$ – derivatives c_y with respect to δ and α for horizontal empennage;

$k = \frac{q_{emp}}{q}$ – coefficient of deceleration of flow for empennage ($k \approx 0.8$);

b_A – average aerodynamic chord of wing;

k_{ω} – coefficient, considering damping from other parts of aircraft, with the exception of horizontal empennage ($k_{\omega} \approx 1.3$);

$S_{h.e}$ – area of horizontal empennage;

$m_z^{c_y}$ – derivative of coefficient of moment of aircraft with respect to coefficient of lift;

J_z – moment of inertia of aircraft with respect to axis z;

Δc_y – increase of coefficient c_y during maneuver.

For curvilinear flight we have the following condition of equilibrium of moments and forces (along axis y):

$$M_t - M_d + M_s - J_z \frac{d\omega_z}{dt} = 0; \tag{1.15}$$

$$c_y qS = G\cos\theta + \Delta c_y qS. \tag{1.16}$$

In this case magnitude of overload is

$$n = \frac{c_y qS}{G} = \cos\theta + \Delta c_y q \frac{S}{G}. \tag{1.17}$$

Will replace

$$\Delta c_y q \frac{S}{G} = \Delta n. \tag{1.18}$$

Then

$$n = \cos\theta + \Delta n,$$

where θ is angle of inclination of tangent to trajectory with respect to horizon (Fig. 1.11).

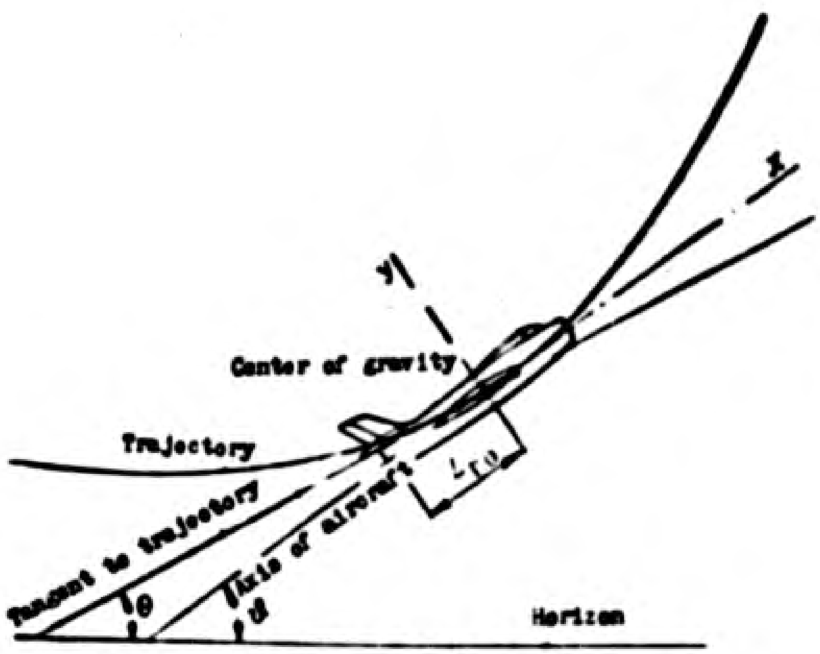

Fig. 1.11. Geometric parameters of trajectory of aircraft during maneuver.

Derivative of increment of overload

$$\frac{d\Delta n}{dt} = c_y^{\alpha} q \frac{S}{G} \frac{d\alpha}{dt}. \qquad (1.19)$$

Angle of attack α is defined as difference of angles ϑ and θ:

$$\alpha = \vartheta - \theta,$$

where ϑ is angle of inclination of longitudinal axis of aircraft to horizon. Then

$$\frac{d\alpha}{dt} = \frac{d\vartheta}{dt} - \frac{d\theta}{dt} = \omega_z - \frac{d\theta}{dt}. \qquad (1.20)$$

Let us define second member (1.20) through V and Δn.

It is known that

$$\frac{d\theta}{dt} = \frac{\Delta n g}{V},$$

where R is radius of curvature of trajectory:

$$R = \frac{V^2}{\Delta n g}.$$

Consequently,

$$\frac{d\theta}{dt}=\frac{V}{R}.$$

Using this expression, from (1.20) we will define

$$\frac{d\theta}{dt}=\omega_z-\frac{\Delta n g}{V}. \tag{1.21}$$

Substituting this expression into equation (1.19), we obtain

$$\frac{d\Delta n}{dt}+c_y^{\alpha}q\frac{S}{G}\frac{g}{V}\Delta n-c_y^{\alpha}q\frac{S}{G}\omega_z=0. \tag{1.22}$$

Having developed equation (1.15) in differential form, taking into account (1.18), we will obtain

$$J_z\frac{d\omega_z}{dt}-c^{\delta}_{y\,r.o}\delta_{в}S_{r.o}kqL_{r.o}+$$
$$+k_{\omega}\frac{\omega_z L_{r.o}}{\sqrt{k}V}c^{\alpha}_{y\,r.o}kqS_{r.o}L_{r.o}-m_z^{c_y}\Delta nGb_A=0. \tag{1.23}$$

For simplification, it is possible to take

$$\frac{dm_z}{dc_y}=f(c_y)=\text{const and } V=\text{const}.$$

We will introduce auxiliary designations:

$$A=c^{\delta}_{y\,r.o}\delta_{в}\frac{1}{J_z}kqS_{r.o}L_{r.o};\qquad E=c_y^{\alpha}q\frac{S}{G};$$

$$B=-\frac{1}{J_z}m_z^{c_y}Gb_A;\qquad F=c_y^{\alpha}q\frac{S}{G}\frac{g}{V}.$$

$$D=\frac{1}{J_z}k_{\omega}\sqrt{k}\,c^{\alpha}_{y\,r.o}\frac{L^2_{r.o}}{V}qS_{r.o}.$$

Substituting these designations into equations (1.22) and (1.23), we will obtain

$$\left.\begin{aligned}&\frac{d\omega_z}{dt}-A+D\omega_z+B\Delta n=0;\\&\frac{d\Delta n}{dt}+F\Delta n-E\omega_z=0.\end{aligned}\right\} \tag{1.24}$$

Reducing system (1.24) to one second order differential equation relative to Δn, we find

$$\frac{d^2\Delta n}{dt^2}+(F+D)\frac{d\Delta n}{dt}+(FD+BE)\,\Delta n=AE. \qquad (1.25)$$

At V = const equation (1.25) has constant coefficients B, D, E, and F. Coefficient A is changed in time and depends on type of maneuver (conditions of deflection of control surface). In this case, solution of equation (1.25) has the form

$$\Delta n=\frac{AE}{p^2}-\frac{1}{p^2}e^{-\frac{F+D}{2}t}\int_0^t\left[e^{\frac{F+D}{2}\tau}A\right]'E\cos p\,(t-\tau)\,d\tau \qquad (1.26)$$

where

$$p^2=FD+BE-\left(\frac{F+D}{2}\right)^2.$$

Second component characterizes throwing of dynamic system during action on it of external perturbation. At low and medium altitudes, where can be obtained large overloads from conditions of carrying ability of wing, this throwing is relatively small. Therefore, value Δn_{max} one can determine so:

$$\Delta n_{max}=\frac{AE}{FD+BE-\left(\frac{F+D}{2}\right)^2}. \qquad (1.27)$$

For stable aircraft

$$\left(\frac{F+D}{2}\right)^2\ll FD+BE.$$

Therefore, it is possible to take approximate dependence

$$\Delta n_{max}\approx\frac{AE}{FD+BE}. \qquad (1.28)$$

Substituting in this equation aerodynamic parameters of an aircraft, we will obtain

$$\Delta n_{max} = \frac{c^{\delta}_{y\,г.о}\,\delta_{в} q}{16\mu_{в}\sqrt{\Delta}\, c^{\alpha}_{y\,г.о} L_{г.о} - m_z^{c_y} \frac{S}{S_{г.о}} \frac{G}{S} \frac{b_A}{L_{г.о}}}. \qquad (1.29)$$

From expression (1.29) it is clear that magnitude of maximum overload depends on product of angle of displacement of control surface (stabilizer) by impact pressure. Product $\delta_{el}q$ characterizes divergence of control surfaces in a maneuver at a given speed, depending directly on actions of pilot. Degree of sharpness of maneuver the pilot senses and corrects, basically, by amount of movement of control stick and force applied to it and also by overload appearing during maneuver. For longitudinal control without booster, product $\delta_{el}q$ it is possible to express through pressure on control stick in the following way:

$$\delta_{в} q \approx \frac{P}{S_{в} b_{в\,ср}} \cdot \frac{1}{m^{\delta}_{ш}}. \qquad (1.30)$$

where m^{δ}_{hi} is derivative of coefficient of hinge moment of elevator with respect to angle of displacement of control surface;

S_{el} and $b_{el\ av}$ is area and average chord, respectively, of elevator.

In case of application of booster, force on the stick is simulated by loading mechanism approximately directly proportional to magnitude $\delta_{el}q$. As results of experiment show, force on handle can be described by the following relationship:

$$P_{max} = P_0 + \bar{P} n_{max}. \qquad (1.31)$$

where P_0 is maximum force applied by pilot in beginning of maneuver (P_0 = 80-100 kg);

$\bar{P} = \frac{dP}{dn}$ is gradient of decrease of force on handle with respect to overload ($\bar{P}$ = 8-10 kg).

Product $\delta_{el}q$ it is possible to replace by the following expression:

$$\delta_{в} q = \frac{P_0 - \bar{P} n_{max}}{S_{в} b_{в\,ср} m^{\delta}_{ш}}. \qquad (1.32)$$

Substituting expression (1.32) into formula (1.29), we will obtain expression for highest possible overload:

$$\Delta n_{max} = \frac{(\bar{P}_0 - \bar{P}) k c_y^{\alpha} m_z^{\delta}}{S_0 b_{cp}\left[\rho g k_{\circ} \sqrt{\lambda}\, c^{\alpha}_{y\,h.e} L_{h.e} - m_z^{c_y} \frac{S}{S_{h.e}} \frac{G}{S} \frac{b_A}{L_{h.e}}\right] + \bar{P} k c_y^{\alpha} m_z^{\delta}}. \qquad (1.33)$$

On Fig. 1.12 is given approximate graph of maximum overload. At low speeds magnitude of maximum overload is determined from conditions of maximum wing lift or taking into account $c_{y\ per}$, and at high speeds — by parameters of stability and controllability of aircraft.

Formula (1.33) gives the possibility of conducting analysis of the influence of different parameters on magnitude n_{max}. For the first time such analysis was done by A. I. Makarevskiy.

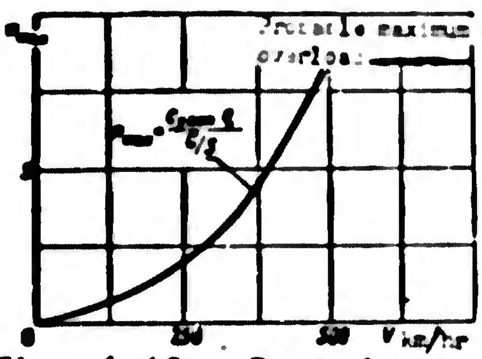

Fig. 1.12. Dependence of maximum overload on speed of flight for maneuvering aircraft.

For stable aircraft, maximum overload increases with increase in degree of compensation of elevator relative to stagger of empennage $L_{h.e}/b_A$, wing aspect ratio λ and horizontal empennage $\lambda_{h.e}$. The biggest influence on Δn_{max} is rendered by reserve of longitudinal static stability.

Magnitude n_{max} sharply increases with approach to neutral stability.

1.6. Forces Effective on Aircraft During Flight in Bumpy Air

In atmosphere, as a result of difference of temperatures and pressures, motion of air masses occurs. This motion causes turbulent atmospheric state, when there occurs intense mixing of streams of flow, accompanied by variable field of air velocities and vortexes.

On aircraft, rendering essential influence, are vortexes whose scale will be commensurate with dimensions of aircraft.

During load analysis it is accepted to distinguish shift of air by gradient of speed. If speed of air increases to maximum value during long period of time of flight (more than 2 sec, i.e., during a stretch of more than 300-500 m), then such shifts of air masses are called flows. Shift of air with large gradient of build-up of speed is called a gust.

Subsequently, we will be interested in gusts, since they cause considerable overloads of aircraft.

Gusts and flows are created in atmosphere by different causes; the main ones are:

a) nonuniform heating of surface of earth, creating so-called "therms" (Fig. 1.13);

b) influence of relief of site (Fig. 1.14);

c) circulation of air in clouds (Fig. 1.15);

d) jet streams.

Vertical gusts, caused by nonuniform heating of site, are considerably strengthened in second half of day. They have comparatively small speed (W = 2-8 m/sec) and spread to altitudes 2000-3000 m. Gusts, caused by influence of relief of site (see Fig. 1.14), are observed in mountain regions and their speed can be somewhat higher. They spread to altitude 1500-2000 m from the level of summits of mountains.

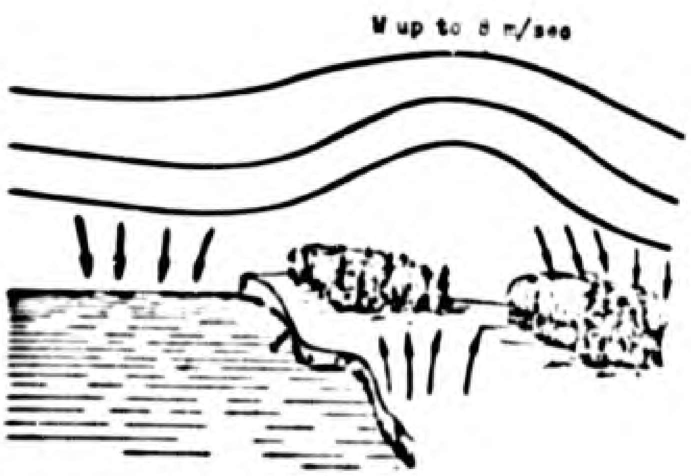

Fig. 1.13. Diagram of formation of thermal flows.

In thick cumulus overcast speeds of gusts increase. Gusts attain the highest speed in a thunderstorm front (up to 20-50 m/sec). Therefore, entrance into zone of thunderstorm activity for aircraft is dangerous.

Gusts caused by jet streams are observed in zone of tropopause, i.e., at altitudes 10-13 km, even during clear weather. In this case, turbulence in tropopause zone is encountered in isolated sections extending from 30 to 100 km and thickness near 1 km.

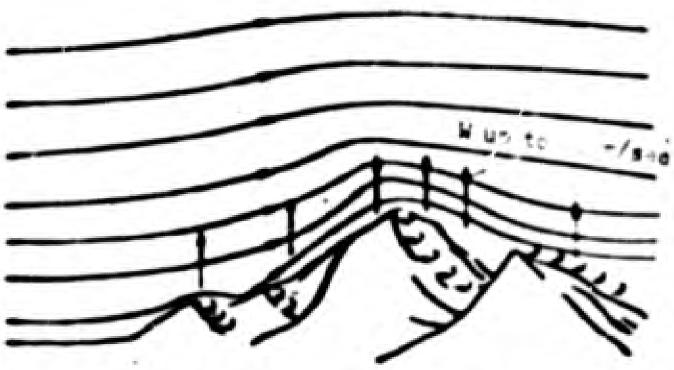

Fig. 1.14. Influence of relief of surface of earth on vertical air flows.

Let us consider simplified diagram of influence on aircraft of a vertical gust during following assumptions:

1) gust is normal to flight trajectory, is uniform in amplitude and its speed instantly increases from 0 to W (Fig. 1.16);

2) aircraft is absolutely rigid;

3) perturbed motion is symmetrical relative to longitudinal plane of aircraft;

4) motion of pitch is absent;

5) speed of aircraft is constant.

During influence of gust with speed W direction is changed of incident flow on aircraft by angle $\Delta\alpha = W/V_1$ (Fig. 1.17), which leads to increase of lift:

$$\Delta Y = c_y^{\alpha} \Delta\alpha S q = c_y^{\alpha} \rho \frac{V_1 W}{2} S. \quad (1.34)$$

Considering that vertical gusts act downward and upward, overload of aircraft one can determine in the following way:

$$n = \frac{Y \pm \Delta Y}{G} = 1 \pm \frac{1}{2} c_y^{\alpha} \rho \frac{V_1 W}{G/S}. \quad (1.35)$$

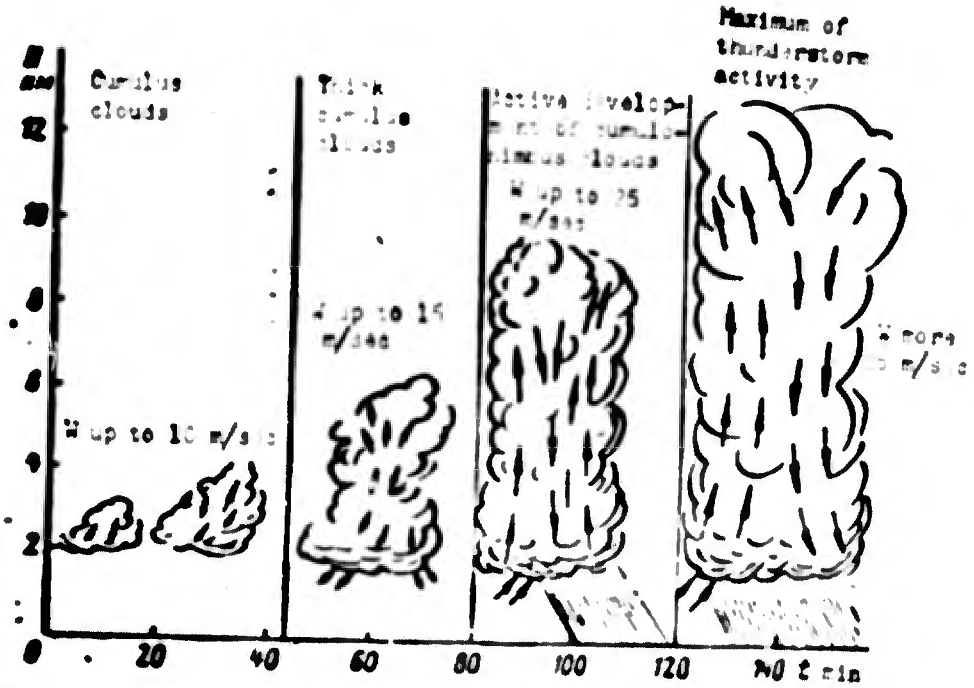

Fig. 1.15. Stages of development air turbulence in cumulus and cumulo-nimbus clouds.

At given value of speed of gust W, value of overload depends on speed of flight, wing loading G/S and value c_y^α.

For passenger aircraft, maximum overloads during flight in turbulent atmosphere are approximately 2.5-3.5. Lowering speed of flight, the pilot can decrease overload during strong gusts of bumpy air. However, during lowering of speed there is increased danger connected with flight at large angles of attack, i.e., approach to unstable conditions or stall of aircraft into a spin. Therefore, possible range of change of speed during flight in turbulent atmosphere at great heights is very limited. The safest conditions usually correspond to cruising speeds of flight.

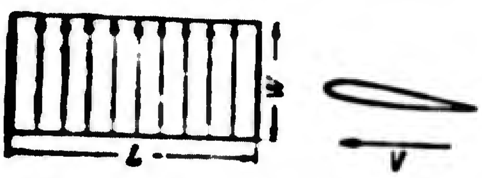

Fig. 1.16. Distribution of speeds during sharply outlined gust of air.

During the analysis of overloads possible during approach to large angles of attack, one should consider that linear dependence $c_y = f(\alpha)$ continues up to larger angles of attack than this follows from static testings in wind tunnel (see page 37).

We will consider action of a horizontal gust. During instantaneous encountered horizontal gust of air with speed W, lift will be changed by magnitude ΔY.

Fig. 1.17. Diagram of influence of vertical gust on aircraft.

Total lift

$$Y = Y_0 + \Delta Y = c_y S \frac{\rho}{2} (V_1 + W)^2 \tag{1.36}$$

will cause overload

$$n = \frac{Y}{Y_0} = \left(1 + \frac{W}{V_1}\right)^2 \approx 1 + \frac{2W}{V_1}. \tag{1.37}$$

Even during strong atmospheric turbulence, W/V_1 ratio does not exceed 0.15; consequently, n will not be more than 1.3-1.5.

During action of gust at angle φ to direction of flight (Fig. 1.18), increase of overload will be

$$\Delta n_\varphi = \frac{2W\cos\varphi}{V_1} + 0.5\, c_y^\alpha \rho \frac{V_1 W \sin\varphi}{G/S}. \tag{1.38}$$

Value of angle φ_0, corresponding to $\Delta n_{\varphi\ max}$ at given value of W, can be found from relationship

$$\frac{d\Delta n_\varphi}{d\varphi} = -\frac{2W\sin\varphi}{V_1} + 0.5\, c_y^\alpha \rho_0 \frac{V_1 W}{G/S} \cos\varphi = 0, \tag{1.39}$$

whence

$$\operatorname{tg}\varphi_0 = \frac{c_y^\alpha \rho}{2\,G/S}.$$

In cruising conditions for aircraft of type Il-14 $\varphi_0 = 65$-$70°$. For Il-18 $\varphi_0 = 70$-$75°$. Relative growth of Δn_φ during optimum φ_0, as compared to growth of overload during action of vertical gust of identical speed Δn_{vert}, one can determine from relationship (1.38):

$$\frac{\Delta n_\varphi}{\Delta n_0} = \operatorname{ctg}\varphi\cos\varphi + \sin\varphi = \frac{1}{\sin\varphi}. \tag{1.40}$$

For shown types of aircraft this growth, as compared to Δn_{vert}, composes 5-10%.

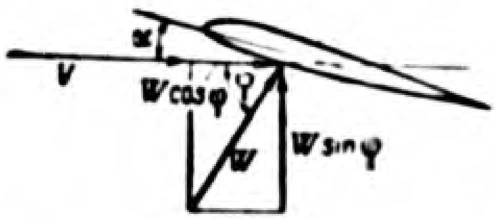

Fig. 1.18. Diagram of vectors of velocities during action of gust at angle φ.

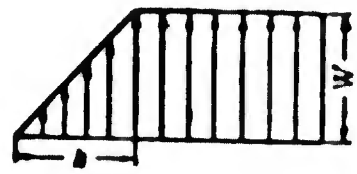

Fig. 1.19. Diagram of gust of air.

In real atmosphere, speed of gust grows at certain extent h (Fig. 1.19). During entrance into gust, with gradual build-up of speed of gust, aircraft is carried along by gust the greater the less the specific load on the wing. Therefore, in dependence (1.35) is introduced coefficient K, which considers this phenomenon, and expression for overload will be

$$n = 1 + 0.5 K c_y^{\alpha} \rho_0 \frac{W V_i}{G/S}. \tag{1.41}$$

Magnitude K is less than unity and can be determined from relationship

$$K = \frac{1 - e^{-\nu}}{\nu}, \tag{1.42}$$

where

$$\nu = \frac{\rho c_y^{\alpha} h}{2G/S}.$$

Intensity of influence of gust of air on aircraft is estimated by effective speed of conditional gust having assigned a gradient of build-up and provoking an overload of the same magnitude as would cause a real gust.

Magnitude of effective speed W_{ef} is determined with respect to overload measured in flight from dependence

$$W_{ef} = \frac{2(n-1)\,G/S}{K c_y^\alpha \rho_0 V_i}. \tag{1.43}$$

Recurrence of W_{ef} is determined on the basis of mass measurements of overloads in different conditions of exploitation.

During flight in bumpy atmosphere at supersonic speeds, overloads increase because of growth of speed and are somewhat lowered because of decrease in c_y^α. Expression (1.41), taking into account (1.5), it is possible to present in the form

$$n = 1 + 6.2 K \rho_0 \frac{W\sqrt{\rho_H}}{G/S} c_y^\alpha M \tag{1.44}$$

As can be seen, change of overload in Mach number (M) depends on magnitude $c_y^\alpha M$. For supersonic speeds, it is possible to consider approximately

$$c_y^\alpha = \frac{4}{\sqrt{M^2-1}}. \tag{1.45}$$

Consequently,

$$c_y^\alpha M = \frac{4M}{\sqrt{M^2-1}} = \frac{4}{\sqrt{1-\frac{1}{M^2}}}. \tag{1.46}$$

Dependence of $c_y^\alpha M = f(M)$ is given in Fig. 1.20. At $M > 1.5$ overload in turbulent atmosphere is lowered. For subsonic nonmaneuvered aircraft magnitude of product $c_y^\alpha M$ attains 4.5-4.8; for supersonic aircraft $c_y^\alpha M$ will be 4.2-5.0.

For aircraft with swept-back wing change of c_y^α with respect to M it is possible to express in first approximation by following relationships (for subsonic region of Mach numbers):

$$c_y^\alpha \approx c_{y\,\mathrm{incm}}^\alpha \frac{1}{\sqrt{1-M^2\cos^2\chi}}. \tag{1.47}$$

where χ is angle of sweepback;

$$c^{\alpha}_{y} = \frac{1.8a\lambda}{\lambda + 2(1+\tau)};$$

τ is coefficient characterizing positive sweepback; for form of ellipse and trapezoid $\tau = 1$.

For supersonic region of Mach numbers.

$$c^{\alpha}_{y} = \frac{4\cos\chi}{\sqrt{M^2\cos^2\chi - 1}}. \qquad (1.48)$$

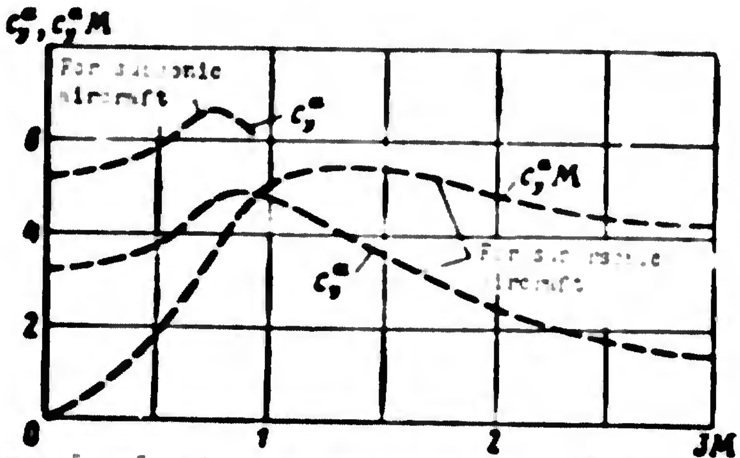

Fig. 1.20. Dependence of c^{α}_{y} and $c^{\alpha}_{y}M$ on Mach number.

Then

$$c^{\alpha}_{y}M = \frac{4\cos\chi}{\sqrt{\cos^2\chi - \frac{1}{M^2}}} \qquad (1.49)$$

Consequently, for swept-back wing at the same Mach number, overload during gusts at small supersonic speeds will be somewhat higher than for straight wing.

1.7. Influence of Angular Velocity on Magnitude of Maximum Overload

Fast change of angle of attack leads to certain peculiarities of change of aerodynamic properties. For incompressible flow one can determine approximate dependences of magnitude of coefficient of maximum lift from angular velocity of change in angle of attack.

On Fig. 1.21 is given dependence of c_y with respect to α for motionless wing during change of direction of flow.*

On Fig. 1.22 is shown dependence of c_y with respect to α, when at first angle of attack is increased, and then decreases. Speed of change of angle of attack $d\alpha/dt$ is expressed as dimensionless value by means of multiplying it by chord of wing b and dividing by flow rate of air V.

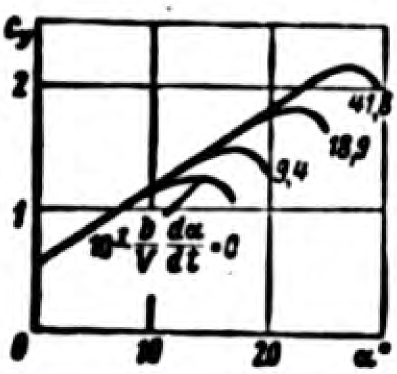

Fig. 1.21. Influence of speed of change of angle of attack on $c_{y\,max}$ ($\lambda = 5$, Re = $= 3.6 \cdot 10^5$, profile Gö 398, wing is motionless, direction of flow changes).

Increase in $\Delta c_{y\,max}$ higher than steady-state value, depending upon $\frac{b}{V}\frac{d\alpha}{dt}$, is depicted on Fig. 1.23. Approximately, it is possible to express $\Delta c_{y\,max}$ by linear dependence

$$\Delta c_{y\,max} = 21.7 \frac{b}{V}\frac{d\alpha}{dt}. \quad (1.50)$$

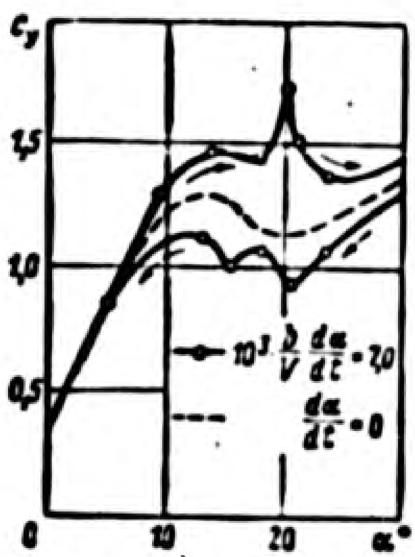

Fig. 1.22. Influence of speed of change of angle of attack on coefficient of maximum lift (profile of Klark UN, $\lambda_{ef} = \infty$, Re = $1.2 \cdot 10^5$); direction of flow is constant, angle of attack of profile changes.

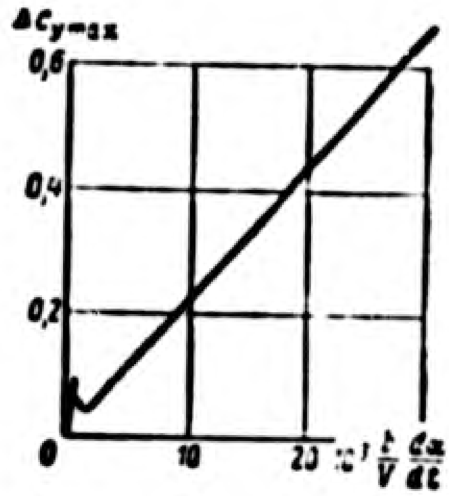

Fig. 1.23. Dependence of $\Delta c_{y\,max}$ on speed of change of angle of attack.

*Ya. Ts. Fyn, Introduction to the theory of aeroelasticity, Fizmatgiz, 1959.

This dependence is disturbed for small values of parameter of angular velocity ($\frac{b}{V}\frac{d\alpha}{dt} < 2\cdot 10^{3}$).

During linear increase of speed of gust from 0 to W at distance h we have

$$\frac{d\alpha}{dt} = \frac{W}{V}\frac{V}{h} = \frac{W}{h}. \tag{1.51}$$

Then during gusts of bumpy air

$$\frac{b}{V}\frac{d\alpha}{dt} = \frac{W}{h}\frac{b}{V}. \tag{1.52}$$

For contemporary subsonic aircraft magnitude $\frac{W}{h}\frac{b}{V}$ composes 0.002-0.015. Thus increase of maximum wing lift can be from 5 to 30%. This one should consider during calculation of limiting possible overloads. During fulfillment of maneuvers by light aircraft $d\alpha/dt$ can be 0.1-0.5 rdn/sec and, accordingly, $\frac{b}{V}\frac{d\alpha}{dt} = 0.001-0.010$. In this case during sharp maneuvers, also considerable will be increase in $c_{y\,max}$.

1.8. Instruments for Statistical Measurements of Overloads

For study of real magnitudes of overloads encountered during exploitation of aircraft there are conducted measurements of overloads by special (statistical) instruments. Main unit of these instruments is the accelerometer. Most widely used are such statistical instruments as meter of overloads, recorder of overloads with prolonged recording (1 hour and more), recorder of overloads with automation for switching-on, recorder of overloads and speed of type V-n, recorder of overloads, speed, altitude, and duration of flight of type V-n-H-t, sometimes with automatic switching-on.

There are also applied other types of statistical instruments with registration, for instance, of control surfaces deflection, pressure, course, temperature, and others. For control of overloads in flight, on pilot's instrument panel is established visual indicator of overloads. Indicator has two fixing pointers, which permit fixing the value of maximum and minimum overloads attained in flight.

When carrying out statistical measurement meter of overloads is the most convenient. In this instrument the range of measured overloads is divided into 5-10 degrees. During shift of seismic mass of instrument, under the action of overload, there occurs actuation of mechanical or electrical meters adjusted to a definite degree of overload. Application of meters permits determining only the quantity of encountered overloads of a certain magnitude. However, it is impossible to obtain data about weight of aircraft, speed, and altitude of flight, at which overload is registered.

For contemporary aircraft, during the time of flight, weight is considerably changed (30-50%). Due to this, load on certain units during the same overload is changed 1.5-2 times. Consequently, for judgement about load capacity of aircraft construction, data recorded by the meter is insufficient. Therefore, meters are used basically during investigations on passenger aircraft of type Li-2 and Il-14 and on light maneuvering aircraft.

Application of recorders of overloads with prolonged recording also is limited in view of complexity of exploitation, large consumption of tape, and difficulty of deciphering recordings. In such instruments is frequently applied an automation for switching-on, which permits considerable simplification of their exploitation and deciphering of recordings. The automation turns on a tape winder during action of overload

Fig. 1.24. Recording of instrument V-n.

larger than 1 + Δn and less than 1 - Δn, where Δn is the actuating threshold of the instrument. For maneuvering aircraft Δn = 0.7-1.0; for nonmaneuvering Δn = 0.2-0.3. During application of the automation for one charging of the instrument it is sufficient for measurements during 100-200 hours of flight.

In period of development of piston aircraft recorders of type V-n (in English literature designated V-g) found wide propagation. These instruments have nodes for registration of overload and speed. Recording is produced in the form of diagram V-n (Fig. 1.24). Such recording gives directly a diagram of overloads of aircraft at different speeds of flight.

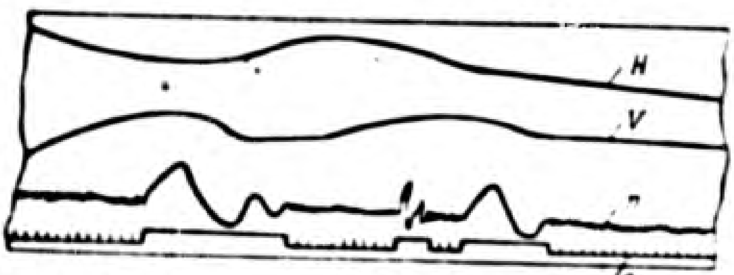

Fig. 1.25. Recording of instrument V-n-H-t.

For jet aircraft, having a great range of flight altitudes, it is expedient to apply statistical records of type V-n-H-t, recording speed, overload, altitude, and duration of flight. These instruments usually have an electric preselector gear of tape speed. In calm horizontal flight recorder works as barospeed recorder, recording speed and altitude of flight at low speed of tape 2-5 mm/min. During action of overload larger than actuating threshold 1 ± Δn, instrument has increased speed of drawing of tape 5-10 mm/sec. Such instruments permit obtaining sufficiently full statistical data about aircraft, atmospheric turbulence, etc. On Fig. 1.25 is given a sample of recording of instrument. Statistical instruments of such type can be used also for control of fulfillment of assignment by pilot and for analysis of causes of flight accidents.

Statistical measurements are used for more precise definition of initial data during strength analysis of an aircraft, for solution of question about its period of service, and for investigations of characteristics of atmospheric turbulence.

As an example on Fig. 1.26 are given characteristics of recurrence of gusts W_{ef}, obtained in conditions of mass exploitation of aircraft.

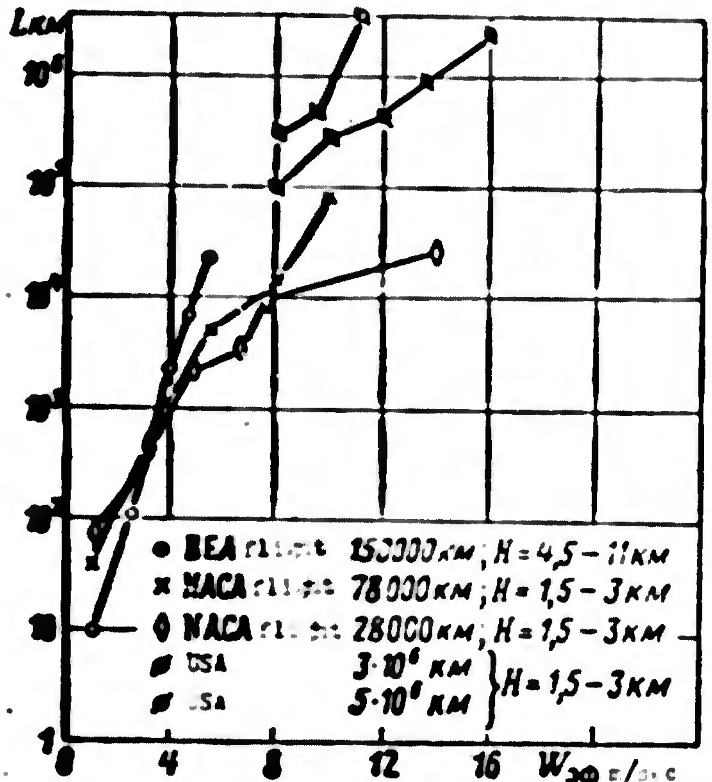

Fig. 1.26. Recurrence of W_{ef} on different altitudes (L – path which aircraft must fly in order to encounter, on the average, one gust of assigned intensity).

1.9. Initial Conditions for Aircraft Strength Analysis

For determination of loads acting on units of an aircraft, it is necessary to know quantity of overload in the center of gravity, speed of flight, weight of aircraft, and also possible variants of their combinations.

These factors are basic.

Additional factors can be: angular velocity of rotation, angles of displacement of control surfaces, force on control wheel (stick), and others.

In flight there is possible a rather wide range of combination of shown factors. During strength analysis there is considered a defined region of their combination, the most characteristic for a given type of aircraft. Graphic presentation about considered combinations of overloads and speeds is given in V-n diagram, where along the axis of abscissas are possible speeds of flight, and along the axis of ordinates — corresponding overloads.

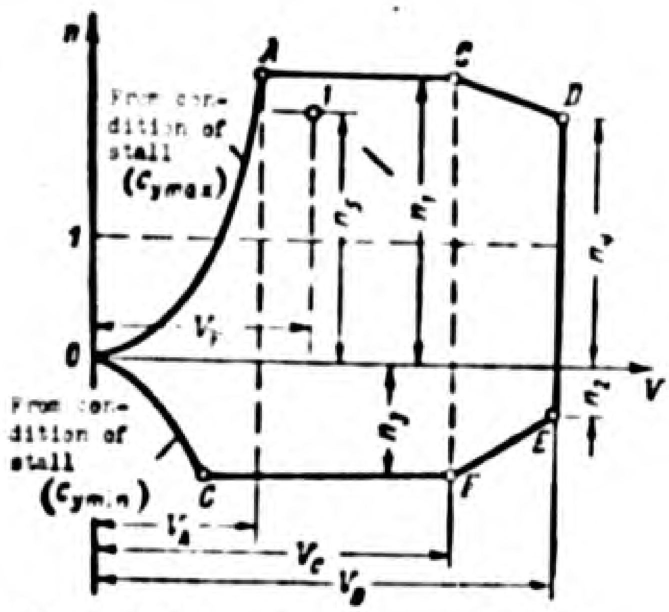

Fig. 1.27. Diagram V–n for maneuvering cases of flight.

On Figs. 1.27 and 1.28 are given V-n diagrams, accepted in requirements of IKAO on strength for aircraft in case of maneuver and flight in bumpy air.

Points of diagram A, C, and D on Fig. 1.27 correspond to calculated cases of load during positive angles of attack. Points E, F, and G correspond to calculated cases during negative angles of attack.

Points B', C', D', G', E' of the diagram (see Fig. 1.28) correspond to calculated cases of load during gusts of bumpy air of different speed and direction.

In calculated cases are considered characteristic speeds of flight:

V_D — calculated diving speed (gliding);

V_C — calculated cruising speed;

V_A — calculated speed of maneuver (case A);

V_P — calculated speed during open flaps;

V_B — calculated speed during maximum intensity of gust;

n_1 and n_4 — minimum positive overload during maneuver;

n_2 and n_3 — negative overload during maneuver;

n_5 — maximum overload during flight with open flaps.

In norms of strength all aircraft are usually divided into three classes: class A — maneuvering, class B — limited-maneuvering, class C — nonmaneuvering.

Maneuvering aircraft include those which can accomplish all figures of aerobatics and dive. Limited-maneuvering aircraft allow fulfillment of figures of pilotage. Nonmaneuvering aircraft include all types of passenger and transport aircraft. For every class, taking into account assignment of aircraft, gross weight, and speed of flight, there are assigned maximum and minimum operational overloads (n^{op}_{max}, n^{op}_{min}). Below are described approximate values of maximum operational overloads of certain types of aircraft.

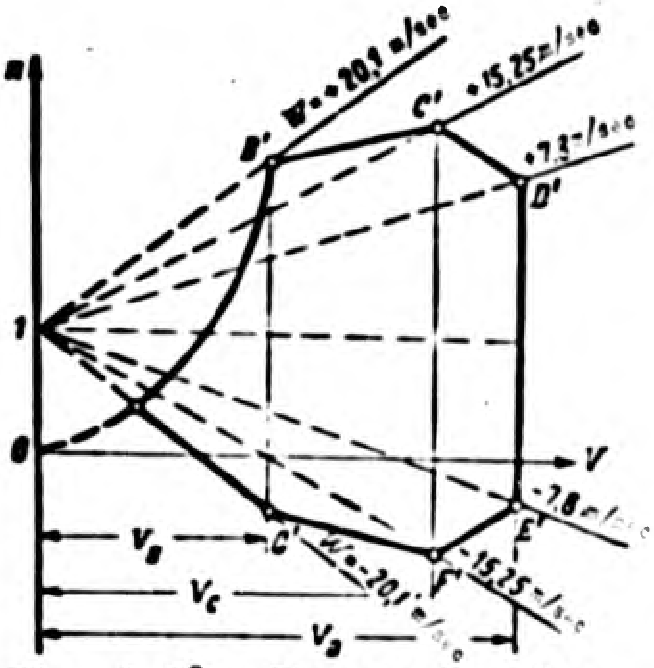

Fig. 1.29. Diagram V–n for overloads during flight in bumpy air.

Light maneuvering aircraft......... 7–9
Light high-speed passenger aircraft 4–5
Medium passenger aircraft..........3.0–4.0
Heavy passenger aircraft...........2.0–3.5

Selection of weight of aircraft is determined by basic form of loads. Weight of aircraft with defined variant of load, selected for strength analysis, is called <u>calculation weight</u>.

If an aircraft is presented with identical requirements for maneuvering during all gross weights and variable loads in wing are absent, then calculation weight will be maximum weight of aircraft. For high-altitude aircraft, for which the necessity of fulfilling maneuvers appears only after a climb, calculation weight can be correspondingly lowered, taking into account fuel consumption.

Since aircraft has in wing considerable variable loads (fuel, suspension), it is necessary to consider a whole range of gross weights of aircraft when determining the most unfavorable combination at which load on units of the aircraft will be maximum. Sometimes there can be several variants of gross weight, which are taken for calculation.

For determination of loads during takeoff and landing there are selected calculated takeoff and calculated landing weight, respectively. For a majority of jet aircraft calculated landing weight is considerably lower than takeoff.

1.10. Selection of Coefficient of Safety

On the basis of analysis of load peculiarities of an aircraft in model conditions of flight are determined maximum operational loads. For transition to calculated (breaking) loads P^p in norms of strength there is set a safety factor

$$f = \frac{P^p}{P^э_{max}}.$$

In norms of strength it is assumed that safety factor pertains to external and inertial loads, but not to stresses in construction, caused by these loads.

Basic assignment of safety factor is to ensure selection of such a rated load so that in operation there are no permanent deformations in supporting members of the structure. During selection of safety factor there are considered probability of obtaining assigned maximum overload, character of action of load (dynamic characteristic), wear of parts, possibility of inspection in operation, technology of production, and so forth. Furthermore, there is considered the necessity of guaranteeing safety of crew and passengers in emergency cases (for instance, there are selected raised safety factors for the fuselage for landing cases, for cargo bracing units, which in case of breakdown during crash landing, can inflict damage on crew or passengers, etc).

Selection of safety factor from conditions of probability of encountering large loads is illustrated on graph in Fig. 1.29, where is shown probable dependence of magnitude of load on time of flight.

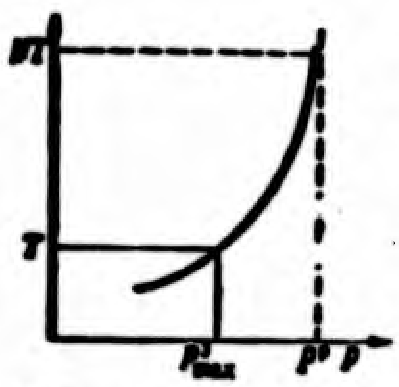

Fig. 1.29. Approximate dependence of probable maximum load on duration of flight.

If it is assumed to have a group of N aircraft with average flight time of T hours, then there should be selected such a magnitude of maximum operational load that it is not exceeded during time T. Quantity of rated load should be not less than load corresponding to total flight time of aircraft of the entire group. Usually magnitude of safety factor for aircraft is selected as f = 1.5-2.0.

For pilotless flight vehicles of single-time action, it is possible somewhat to decrease safety factor, taking, for instance, its value to equal 1.2-1.3. Such decrease in safety factor is justified by small number of recurrence of loads and the absence of a person.

1.11. Requirements for Rigidity of Construction

Elastic deformations of the structure render a strong influence on aerodynamic and inertial loads, and also on characteristics of stability and controllability of contemporary flight vehicles. Some cases of this influence will be considered below (redistribution of aerodynamic load along wing span, divergence, and reverse). Elastic deformations determine reaction of structure to dynamic loads (during landings, gusts of bumpy air, and so forth) and to vibrations of its parts. Therefore, there are a number of requirements for permissible elastic deformations of structure.

In particular, to guarantee corresponding aerodynamic shapes magnitudes of local deformations of plating are limited. Requirements for effectiveness of aircraft control set up a number of conditions relating to general deformations of wing (permissible sags and torsion angles), and deformations of control lines. Requirements for rigidity of control lines lead to assignment of permissible angles of deflection of control surfaces because of elastic deformations of control lines during operational load. It is necessary to consider also requirement for elimination of resonances of control cables in working range of engine revolutions. In a number of cases recommendations are introduced on dynamic arrangement of a flight vehicle (optimum combination of distribution of concentrated masses and elastic characteristics of construction, at which are observed the least forces on the structure in case of influence on it of dynamic load).

C H A P T E R II

EXTERNAL LOADS EFFECTIVE ON UNITS OF AIRCRAFT

<u>List of Designations Appearing in Cyrillic</u>

ам = s.a = shock absorber
аэр = aero = aerodynamic

в = air = air
в = h = holding
в = el = elevator
в.о = v.e = vertical empennage
возм = pos = possible
вр = rot = rotation

г.о = h.e = horizontal empennage
гр = lo = load

д = div = divergence
дв = mot = motor
доп = per = permissible

ж = liq = liquid
жестк = rigid = rigid

з = rear = rear

изб = exc = excess
изг = bend = bending
ин = in = inertial

к = end = end
кр = cr = critical
к = cr = critical
кр = wi = wing

л = le = left

м = man = maneuvering

List of Designations Appearing in Cyrillic Continued

н = rud = rudder
н.в = b.a = bumpy air

п = fr = front
пл = plu = plunger
пл = gl = gliding
пн = pn = pneumatic tire
пос = land = landing
пост = for = forward
пр = ri = right
пр = giv = given

р = rev = reversal
ред = red = reduced

ср = av = average
ст = sta = stabilizer
ст = str = strut

тр = fri = friction

упр = elas = elastic
ур = bal = balancing
уст = st = steady

ф = fus = fuselage

ц.т = c.g = center of gravity

ш = l.g = landing gear

э = ail = aileron
э = op = operational
экв = equi = equivalent

2.1. Basic Calculation Cases for a Wing

The wing is the basic carrier element of such flight vehicles as aircraft, gliders, and winged rockets. Loads on the wing serve as initial data during determination of loads of other units of an aircraft. In connection with this in norms of strength at first are considered rated loads of wing.

Character of distribution of aerodynamic load on the wing depends on angle of attack. Limiting values of angle of attack of a wing correspond to coefficients $c_{y\ max}$ and $c_{y\ min}$. During fulfillment by

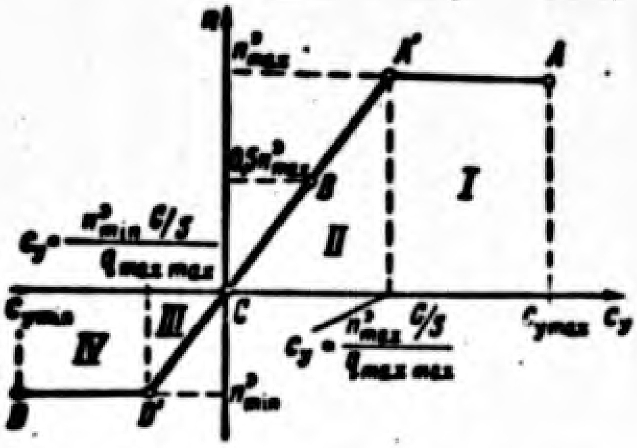

Fig. 2.1. Basic calculation cases of a wing.

aircraft of maneuvers in air overload can be changed from n^{op}_{min} to n^{op}_{max}, and impact pressure — from q_{min} to $q_{max\,max}$, where $q_{min} = \frac{G/S}{c_{y\,max}}$. Since in conditions of flight corresponding to q_{min} loads are relatively small, it is expedient to consider range of impact pressures from value q, determined by magnitude $c_{y\,max}$ or $c_{y\,min}$ during achievement, correspondingly, of overload n^{op}_{max} or n^{op}_{min}, up to $q_{max\,max}$.

On Fig. 2.1 are shown characteristic regions of combinations of c_y, n and q, possible in flight:

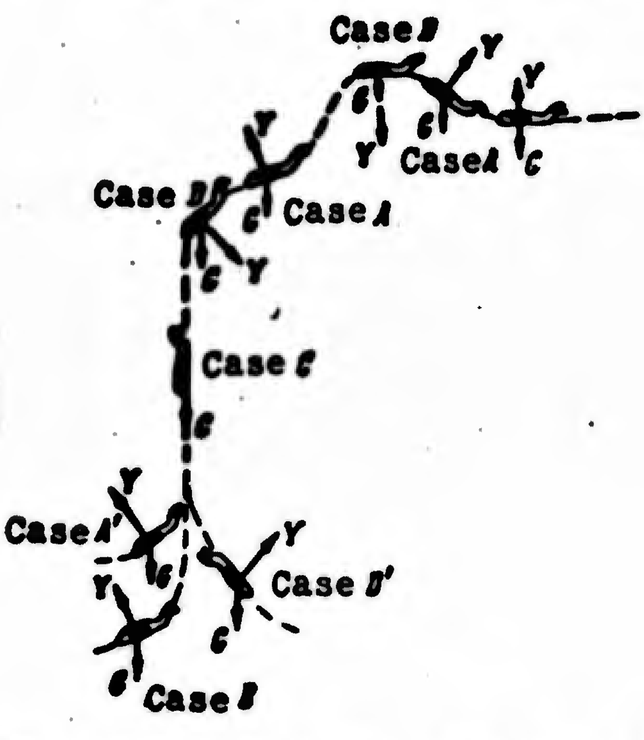

Fig. 2.2. Positions of aircraft on trajectories, corresponding to calculation cases.

Region I:

$$n = n^{\circ}_{max} = \text{const}; \quad \frac{n^{\circ}_{max} G/S}{c_{y\,max}} < q < q_{max\,max};$$

Region II:

$$q = q_{max\,max} = \text{const}; \quad n^{\circ}_{max} > n > 0.$$

Region III:

$$q = q_{max\,max} = \text{const}. \quad 0 > n > n^{\circ}_{min}.$$

Region IV:

$$n = n^{\circ}_{min} = \text{const}. \quad \frac{n^{\circ}_{min} G/S}{c_{y\,min}} < q < q_{max\,max}.$$

Model calculation cases for a wing lie on the boundary of these regions.

<u>Case A</u> — approach to large angles of attack, corresponding to $c_{y\,max}$, during achievement of overload n^{op}_{max} (climb).

Case A' — achievement of overload n^{op}_{max} at maximum permissible speed of flight $V_{max\ max}$ (pullout of dive or glide, ascending flow of bumpy air).

Case B — achievement of average overload ($0.5\ n^{op}_{max}$) at maximum permissible speed of flight with deflection of ailerons (aerobatics and maneuver with bank).

Case C — deflection of ailerons on terminal velocity of flight during $c_y = 0$ (diving).

Cases D and D' — correspond to entrance into dive, elements of figures of aerobatics with negative G, action of descending flow of bumpy air. Corresponding positions of aircraft on trajectory of flight in all these cases are depicted on Fig. 2.2.

2.2. Distribution of load on Wing

Magnitude of aerodynamic load on wing is determined by difference of pressures between upper and lower surfaces of wing. Distribution of pressures and, consequently, also distribution of load along the chord is determined by angle of attack, form of profile, and speed of flight. Distribution of pressures in case A (large angle of attack) usually corresponds to subsonic conditions of flight. Speed corresponding to this case is

$$V_A = \sqrt{\frac{2n^{2}_{max}G}{\rho c_{y\,max} S}}.$$

In Fig. 2.3 is given diagram of distribution of pressure along the chord at large angle of attack in subsonic conditions. In this case, center of pressure is 15-20% of chord from nose of profile.

At small angles of attack (case A') in subsonic conditions of flight, center of pressure is somewhat displaced backward. Due to growth of impact pressure local loads are increased on covering of wing. At critical mach number (M_{cr}) on wing there appear local speeds

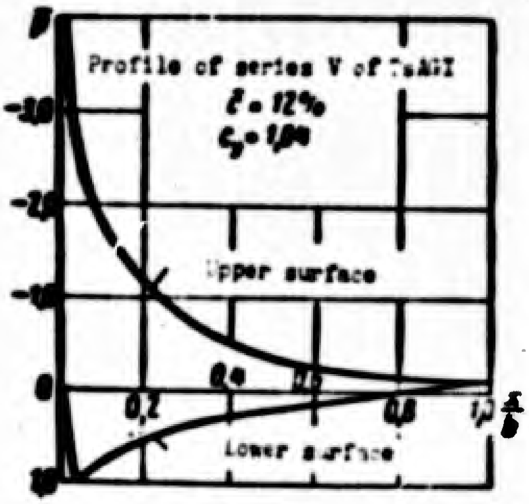

Fig. 2.3. Distribution of pressure along chord of wing at large angle of attack. $\overline{p} = \frac{p_{exc}}{q}$ – pressure coefficient, p_{exc} – excess pressure at point, x/b – distance from nose of profile in fraction of chord b.

equal to speed of sound. During further increase of speed will be formed a zone of local supersonic speeds. At the place of transition of speed into subsonic will be formed a shock wave, where pressure sharply increases.

On Fig. 2.4 is shown change of distribution of pressure on upper and lower surfaces of wing, depending upon Mach number at constant angle of attack. At M = = 0.6 on upper surface, at point A, located near nose, local speed attains speed of sound and pressure becomes critical (p_{cr}). Beyond this point pressure continues to drop, and speed to grow. With this is created small supersonic section up to point B, in which speed sharply decreases, and pressure increases, i.e., will be formed a shock covering supersonic section. During further increase of Mach number supersonic zone grows and at M > 0.8 appears also on lower surface. At M = 0.85 on both sides of profile there exist supersonic zones

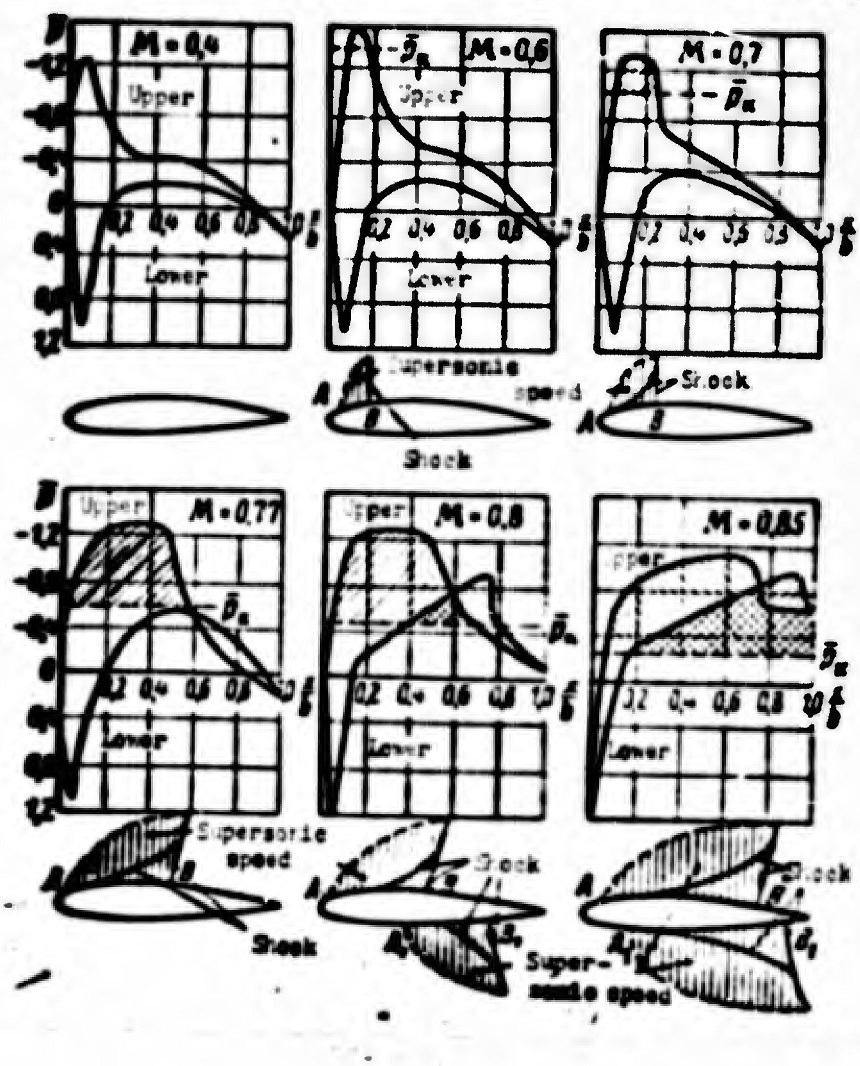

Fig. 2.4. Distribution of pressure on lower and upper surfaces of wing at different Mach numbers.

covering almost all the surface of the wing. At supersonic speeds of flight, center of pressure is on 45-50% of the chord of the wing.

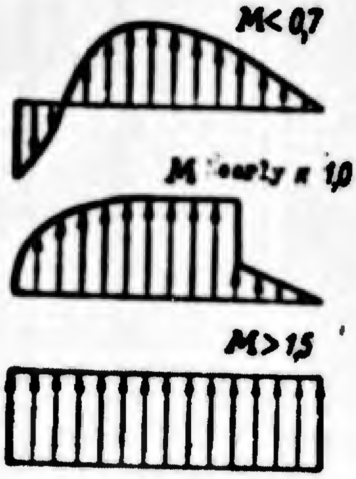

Fig. 2.5. Distribution of load along the chord at small angle of attack.

In case A' magnitude of c_y composes 0.3-0.5. Distribution of aerodynamic load in this case is shown schematically on Fig. 2.5. In cases B and C because of deflection of aileron there appear additional loads on end sections of the wing (Fig. 2.6). Due to this there is considerable increase in bending moment and torque of wing in sections where aileron is located.

General magnitude of aerodynamic load P_{aero} is determined by magnitude of lift $Y = nG$ and drag $X = c_x qS$. Aerodynamic force acting on wing can be found by the formula

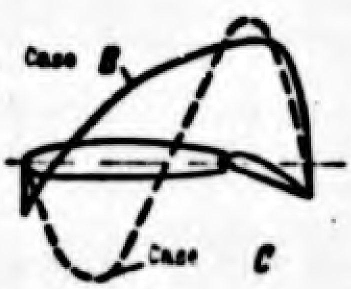

Fig. 2.6. Change of distribution of loads during deflection of aileron.

$$P_{aero}=\frac{Y}{\cos\theta}=\frac{nG}{\cos\theta}. \qquad (2.1)$$

Angle θ is determined from dependence

$$\mathrm{tg}\,\theta=\frac{c_{x\,wi}}{c_{y\,wi}},$$

where $c_{x\ wi}$ and $c_{y\ wi}$ – are drag coefficient and wing lift, respectively, which are chosen with respect to polar of wing for angle of attack corresponding to calculation.

For subsonic speeds of flight $\cos\theta \approx 1$.

On Fig. 2.7 are given approximate polars with points corresponding to calculated cases of wing.

Inertial load of wing P_{in} one can determine analogously to aerodynamic force:

$$P_{in}=\frac{nG_{wi}}{\cos\theta}. \qquad (2.2)$$

where G_{wi} is weight of wing.

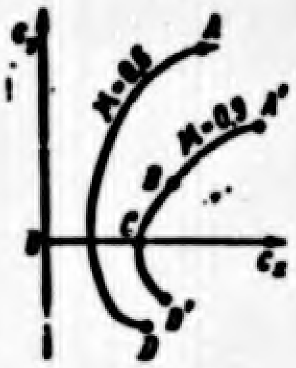

Fig. 2.7. Polars of wing at M = 0.6 and M = = 0.9.

Analogously, we find forces from concentrated load (motor, landing gear, and so forth):

$$P_{lo} = \frac{nG_{lo}}{\cos\theta}. \qquad (2.3)$$

where G_{lo} is weight of load.

On Fig. 2.8 is given diagram of aerodynamic and inertial loads on wing.

Distribution of aerodynamic load along wing span can be assumed to be according to the law of distribution of lift. There is allowed a certain error because of different laws of distribution c_y and c_x along span. Therefore, an approximately linear aerodynamic load is equal to linear load from lift:

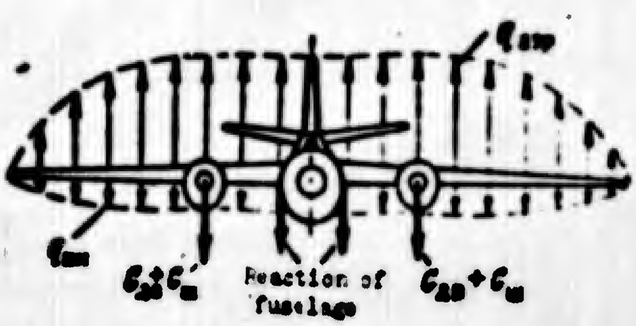

Fig. 2.8. Diagram of loads on wing (G_{mot} – weight of motor, $G_{l.g}$ – weight of landing gear). q_{aero} q_{in} – linear aerodynamic and inertial loads.

$$q_{aero} = q_y = c_y b \frac{\rho V^2}{2}, \qquad (2.4)$$

where c_y and b are coefficient of lift and chord of section (variables along span).

From equation of lift.

$$nG = c_{y\,wi} S \frac{\rho V^2}{2} \qquad (2.5)$$

we will define impact pressure:

$$\frac{\rho V^2}{2} = \frac{nG}{c_{y\,wi} S}. \qquad (2.6)$$

Substituting expression (2.6) into equality (2.4) and replacing $S = b_{av} l$, we will obtain

$$q_y = \frac{nG}{l}\,\frac{c_y b}{c_{y\,wi} b_{av}}. \qquad (2.7)$$

Magnitude $\frac{nG}{l}$ constitutes average linear load, which is definitized by variable relative circulation

$$\overline{\Gamma}=\frac{c_y b}{c_{y\,cp} b_{cp}}.$$

Then it is possible to record

$$q_y=\frac{nG}{l}\overline{\Gamma} \tag{2.8}$$

Approximate form of graph of relative circulation $\overline{\Gamma} = f\left(\frac{z}{l/2}\right)$ is shown in Fig. 2.9. Methods of determining relative circulation of aerodynamic load of different wings are presented in reference literature on aerodynamics.

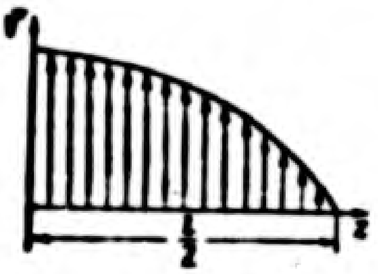

Fig. 2.9. Graph of relative circulation of wing.

On the section of the wing where are located fuselage and gondolas of motor, there occurs a certain fall of lift. Due to this, on remaining part of wing lift must correspondingly be increased. This redistribution is weakly expressed in large angles of attack (case A) and becomes essential during small angles of attack (case A', Fig. 2.10). Due to this, in case A' bending moment in root section will be somewhat more than in case A (10-15%). Influence of compressibility also leads to a certain increase of relative circulation on wing tip (Fig. 2.11).

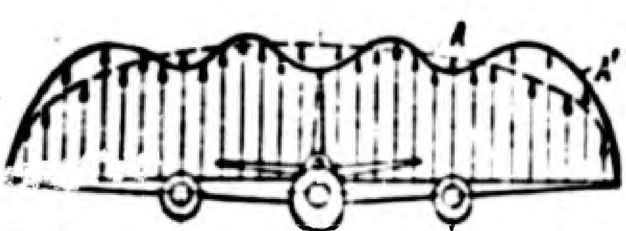

Fig. 2.10. Relative circulation of aerodynamic load during small and large angles of attack of wing.

On sweptback wing, in distinction from straight, there occurs redistribution of load (even if we do not consider deformation) which leads, in subsonic conditions, to increase of relative circulation, and consequently also load on wing tips (Fig. 2.12). During identical angle of attack, presence of sweepback leads to decrease of full wing lift by approximately 10-15%.

For lowering loads on structure of wing when arranging aircraft (especially heavy), it is useful to place the biggest quantity of weight on the wing, since inertial forces counterbalance aerodynamic forces directly on the wing. In aircraft having a large quantity of fuel in the wing, the order of fuel consumption must be such that it will ensure during flight maximum unloading of wing. For this, fuel located in end parts of the wing is used at the last, and in the beginning there is expended fuel from the fuselage and center section of the wing. Since with decrease in weight, overload of aircraft, possible during flight in turbulent atmosphere, increases, it is necessary that permissible overload, depending on strength of wing, somewhat increase with decrease of weight of aircraft.

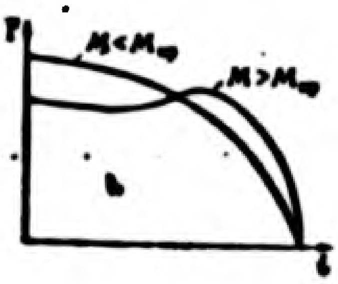

Fig. 2.11. Influence of compressibility of air on relative circulation of wing.

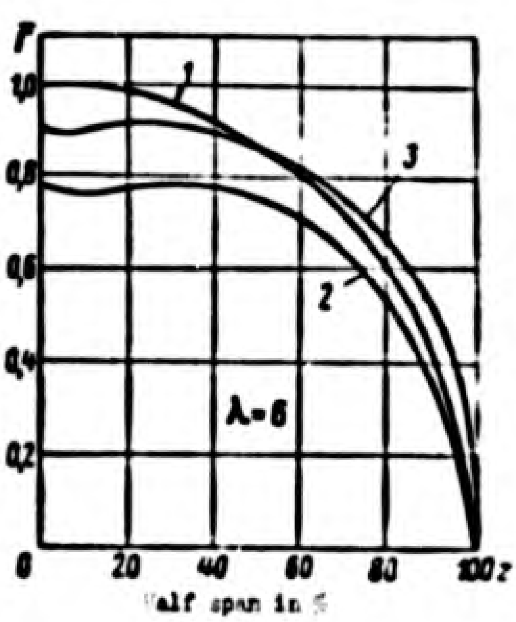

Fig. 2.12. Influence of sweepback on distribution of circulation along span. 1) for straight wing; 2) for sweptback wing during an angle of attack equal to angle of attack of straight wing; 3) for sweptback wing during lift equal to lift of a straight wing.

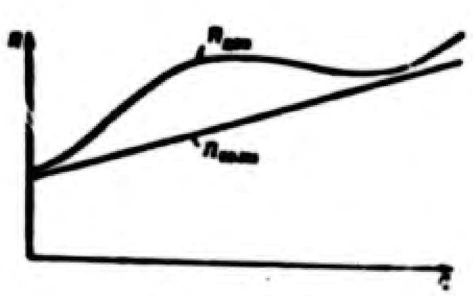

Fig. 2.13. Change of possible and permissible overload according to fuel depletion.

In Fig. 2.13 is represented approximate change of possible (n_{pos}) and permissible ($n_{per}^{\cdot}$) overloads of heavy aircraft. Analysis of strength of wing one should conduct along all the route of a flight during diverse variants of load.

2.3. Influence of Deformations of Wing on Distribution of Load

In connection with application of highly durable materials, by decrease of relative thickness of profile and by increase of sweepback of wing relative rigidity of wings of contemporary aircraft has been lowered. Sags of ends of wings for contemporary aircraft during maximum operational overlaod attain 5-10% swing. Considerable deformations of parts of aircraft in turn cause change in distribution of aerodynamic loads. At low speeds of flight influence of elastic deformations is small. With growth of speed of flight this influence increases, which leads to essential change of bending moment and torques of wing from aerodynamic forces, decrease of effectiveness of ailerons, change of characteristics of stability and controllability as compared to characteristics of rigid aircraft, and so forth.

Torsion of a straight wing changes angles of attack by magnitude $\Delta\alpha = \theta$, where θ is torsion angle of wing. At large angles of attack, because of location of center of pressure ahead of axis of rigidity there occurs an increase in angles of attack of end sections of wing. Torsion angle is changed from zero in root to maximum value on end. Due to this, load on wing tips is somewhat increased. With increase of speed of flight there occurs increase of torsion angle, and at a certain speed aerodynamic forces become larger than forces of elasticity of construction, which causes destruction of wing. This phenomenon is called divergence. In the early stages of the development of aviation, monoplane structures were frequently subjected to the phenomenon of divergence. For contemporary aircraft, critical speeds at which divergence starts are usually higher than speeds of flutter and other forms of aeroelastic instability.

We will analyze basic relationships during divergence. If in the process of established flight there accidentally is changed the angle of attack of the wing, then because of aerodynamic moment there will be additionally increased torsion angle of wing. However, this prevents moment of elastic forces. Inasmuch as aerodynamic moment is proportional to square of speed of flight, and elastic forces do not depend on speed of flight, then there can exist a critical speed at which elastic forces serve only to hold wing in position of equilibrium. At a speed higher than critical, accidental deformation will lead to unlimited increase of torsion angle. This speed is called critical <u>speed of divergence</u> V_{div}.

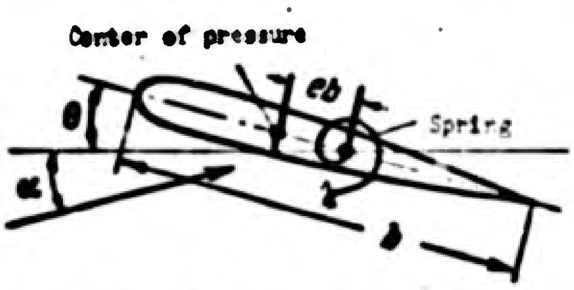

Fig. 2.14. Diagram of section of elastic wing.

We will consider a section of unit length from wing of infinite span of constant cross section. Elastic forces of structure of wing are replaced by a spring (Fig. 2.14). Let us assume that in initial moment direction of flow is parallel to chord of wing during zero lift. If angle of attack of all the wing is changed to angle α, then section of wing will turn because of twisting strain by angle θ. We will find position of equilibrium of a wing in flow with speed V.

Aerodynamic moment of wing of unit swing is

$$M_{aer} = M_0 + Yeb, \tag{2.9}$$

where $M_0 = c_{m0}qb^2$ is moment of profile during zero angle of attack:

c_{m0} is coefficient of moment during zero angle of attack;

Yeb is moment of lift $Y = qbc_y^\alpha(\theta + \alpha)$;

e is distance of center of pressure from axis of rigidity, referred to chord of wing.

Aerodynamic moment is equal to elastic turning point:

$$M_{аэр} = M_{упр} = k_\theta \theta, \tag{2.10}$$

where K_θ is conditional torsional rigidity of wing (spring force of spring).

During small increase of torsion angle $\Delta\theta$ change of aerodynamic moment is

$$\Delta M_{аэр} = qeb^2 c_y^\alpha \Delta\theta. \tag{2.11}$$

Correspondingly, change of elastic turning point is

$$\Delta M_{упр} = k_\theta \Delta\theta. \tag{2.12}$$

If during torsion, increase of elastic turning point ΔM_{elas} is larger than aerodynamic ΔM_{aero}, then wing tries to return to initial state, i.e., condition of equilibrium will be

$$\Delta M_{упр} > \Delta M_{аэр}.$$

Then critical condition is determined by equality

$$\Delta M_{упр} = \Delta M_{аэр}. \tag{2.13}$$

After substituting here expression for increases of moments, we will obtain

$$qeb^2 c_y^\alpha \Delta\theta = k_\theta \Delta\theta. \tag{2.14}$$

From (2.14) we can determine impact pressure corresponding to critical condition:

$$q_д = \frac{k_\theta}{eb^2 c_y^\alpha} \tag{2.15}$$

or critical speed of divergence

$$V_д = \sqrt{\frac{2k_\theta}{\rho e b^2 c_y^\alpha}}. \tag{2.16}$$

For wing of rectangular form in plan, V_{div} one can determine from following relationship:

$$V_{d}=\frac{\pi}{l}\sqrt{\frac{GJ_{w}}{2\rho e c_{y}^{\alpha}}}. \qquad (2.17)$$

where GJ_{wi} is torsional rigidity of wing;

l is wing span.

Sweepback of wing renders considerable influence on magnitude of V_{div}. During straight sweepback of wing, critical speed of divergence sharply increases with increase in angle of sweepback χ. During reverse sweepback, speed of divergence is considerably lowered with increase in χ, which hampers use of wings of such a diagram. This occurs due to the fact that during bend of sweptback wing, its chord changes its position with respect to incident flow, and this leads to change of angles of attack of sections of wing during bend.

Let us assume that function $w(x,z)$ describes surface of sags of wing. Then slope of this surface in direction of axis x is equal to

$$\frac{\partial w}{\partial x}=\frac{\partial w}{\partial \zeta}\frac{\partial \zeta}{\partial x}+\frac{\partial w}{\partial \xi}\frac{\partial \xi}{\partial x}. \qquad (2.18)$$

where ζ and ξ are orthogonal coordinates in directions parallel and perpendicular to axis of wing (Fig. 2.15).

Change of angle of inclination with respect to flow will be

$$\Delta\alpha=-\frac{\partial w}{\partial x}.$$

Since

$$\frac{\partial w}{\partial \xi}=-\theta,\quad \frac{\partial \xi}{\partial x}=\cos\chi \text{ and } \frac{\partial \zeta}{\partial x}=\sin\chi, \qquad (2.19)$$

then, after substituting these expressions into formula (2.18), we will obtain

$$\Delta\alpha=\theta\cos\chi-\frac{\partial w}{\partial \zeta}\sin\chi, \qquad (2.20)$$

where $\frac{\partial w}{\partial \zeta}$ is slope of a curve of sags along wing span.

First member gives at χ = 35-45° not more than 10-15% of total change $\Delta\alpha$. Thus magnitude $\Delta\alpha$ is basically determined by flexural rigidity of wing. On the basis of this, it is possible to judge factors, influencing $\Delta\alpha$:

a) application of structures of highly durable materials leads to increase of deformations (in view of increase of ratio of operating stress σ to elastic modulus E for these materials). For instance, application of titanium leads to increase of sags and angles of torsion of structure 1.5-2.0 times as compared to structures of alloy D16;

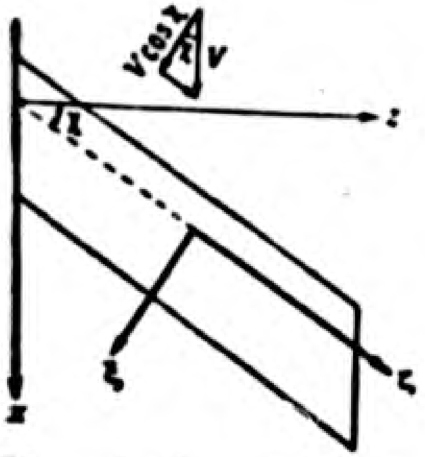

Fig. 2.15. Diagram of a sweptback wing.

b) increase of relative thickness of profile of wing $\bar{c}$ and narrowing of η promotes decrease of sags of wing and, consequently, change decreases in angles of attack of end sections of wing;

c) increase of aspect ratio and angle of sweepback of wing leads to increase of sags and, correspondingly, to increase in $\Delta\alpha$.

Sag of wing it is possible to express, with sufficient accuracy, by formula

$$w = w_e \left(\frac{z}{l}\right)^k. \tag{2.21}$$

where w_{end} is sag of end section.

Then

$$\frac{dw}{dz} = k\frac{w_e}{l}\left(\frac{z}{l}\right)^{k-1}\cos\chi. \tag{2.22}$$

where k is constant coefficient.

In particular, for end section at k = 2

$$\left(\frac{dw}{dz}\right)_e = \frac{2w_e}{l}\cos\chi. \tag{2.23}$$

Since at n^{op}_{max} sag composes 5-10% of wing span, then $\Delta\alpha$ in end sections it can attain 7-12° (at χ = 34-45°).

Distribution of aerodynamic load for rigid and elastic sweptback wing is shown on Fig. 2.16. Due to deformation on wings with reverse

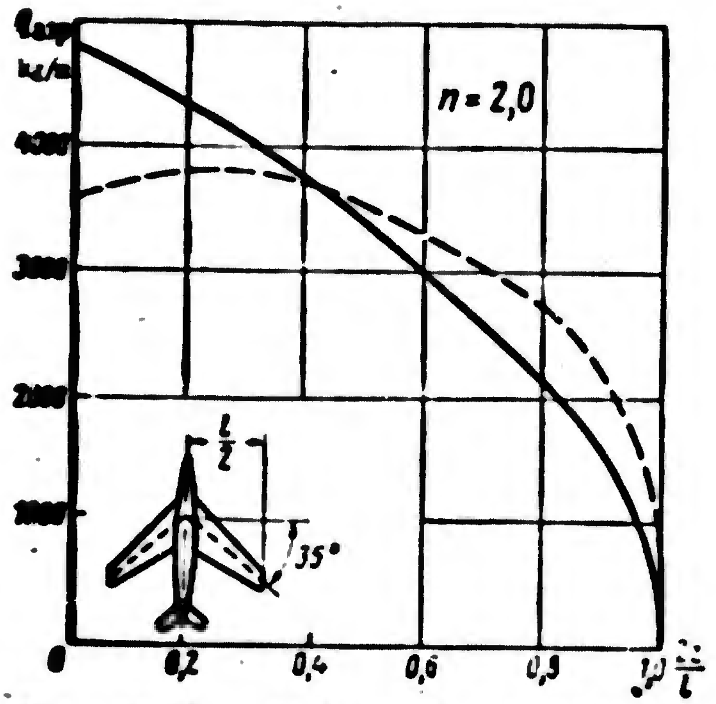

Fig. 2.16. Influence of deformations of sweptback wing on distribution of linear load along wing. ———elastic wing, - - - - -rigid wing.

sweepback, load on wing tips is considerably increased, and, conversely, during straight sweepback end sections of wing are unloaded. Correspondingly, in case of straight sweepback during elastic deformation bending moment of elastic wing is considerably lowered. This relative lowering of bending moment is increased by separation of flow from wing tips during large angles of attack, which leads to further decrease in M_{bend}. Therefore, change of bending moment with respect to overload has nonlinear character (Fig. 2.17).

2.4. Reversal of Ailerons

Elastic deformations of wing essentially affect effectiveness of ailerons. During deflection of aileron downward, lift on wing is increased and rolling moment of aircraft is created. However, this deflection of aileron creates also aerodynamic moment twisting wing in direction of decrease of lift, which lowers magnitude of rolling moment. Inasmuch as rigidity of wing does not depend on speed of flight, and aerodynamic force is changed proportionally to V^2, there exists critical speed at which aileron becomes absolutely ineffective. This speed is called critical speed of reversal of ailerons V_{rev}. The nearer the speed of flight to critical speed, the less effective is aileron control (Fig. 2.18). At a speed of flight higher than V_{rev} action of ailerons becomes reverse.

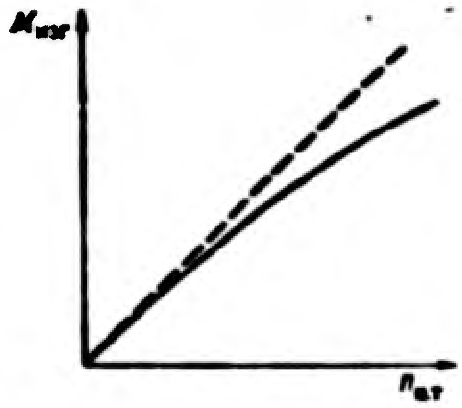

Fig. 2.17. Change of bending moment of swept-back wing with respect to overload. ——— elastic wing, - - - - - rigid wing.

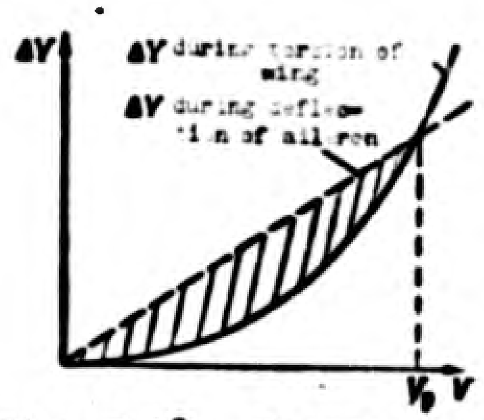

Fig. 2.18. Change in increase of lift during deflection of aileron with respect to speed of flight.

We will consider a wing of unit swing with chord b, supplied with an aileron with chord b_{ail}. Torsional rigidity of wing is replaced by a spring with rigidity k_θ (Fig. 2.19). Changes in coefficients of lift and moment during deflection of aileron by angle δ_{ail} it is possible to record in the form

$$\left.\begin{aligned}\Delta c_y &= c_y^\alpha\theta + c_y^\delta\delta_{ail}\\ \Delta c_m &= c_m^\delta\delta_{ail}\end{aligned}\right\} \tag{2.24}$$

where c_y^δ and c_m^δ are derivatives of coefficients of lift and moment of section of wing with respect to angle of displacement of ailerons.

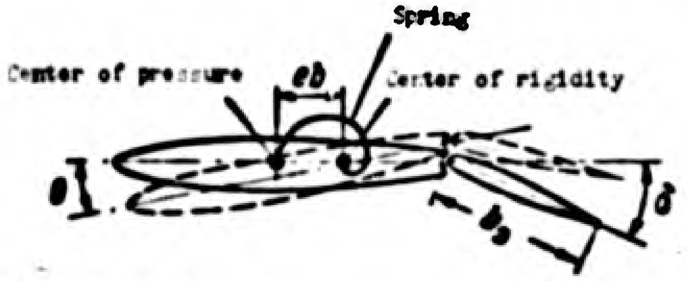

Fig. 2.19. Diagram of wing with aileron.

Change of torque relative to elastic axis during deflection of aileron by angle δ_{ail} will be

$$\Delta M = qb\left[eb\left(c_y^\delta\delta_a + c_y^\alpha\theta\right) + bc_m^\delta\delta_a\right], \tag{2.25}$$

where e is distance of center of pressure from center of rigidity in fractions of chord.

Torsion angle of wing is

$$\theta = \frac{\Delta M}{k_\theta} = \frac{qb^2}{k_\theta}\left[e\left(c_y^\delta\delta_a + c_y^\alpha\theta\right) + c_m^\delta\delta_a\right]. \tag{2.26}$$

From formula (2.26) we will define relationship between torsion angle of wing and aileron deflection angle:

$$\theta = \frac{e c_y^{\delta} + c_m^{\delta}}{\frac{k_\theta}{qb} - e c_y^{\alpha}} \delta_r \tag{2.27}$$

From equations (2.24) and (2.27) can be obtained ratio for Δc_y:

$$\Delta c_y = \frac{c_m^{\delta} + c_y^{\delta}\frac{k_\theta}{qbc_y^{\alpha}}}{\frac{k_\theta}{qbc_y^{\alpha}} - e} \delta_r . \tag{2.28}$$

Aileron will be ineffective at $\Delta c_y = 0$, i.e., condition of critical speed of reversal will be

$$c_m^{\delta} + \frac{c_y^{\delta} k_\theta}{qbc_y^{\alpha}} = 0 \tag{2.29}$$

Solving equation (2.29) with respect to speed, we will obtain expression for speed of reversal

$$V_p = \sqrt{\frac{-2c_y^{\delta} k_\theta}{c_y^{\alpha} \rho b c_m^{\delta}}} \tag{2.30}$$

From formula (2.30) if follows that magnitude V_{rev} does not depend on magnitude e. This is caused by the fact that aerodynamic moment twisting the wing, presents a pair of forces and does not depend on position of elastic axis.

Effectiveness of aileron on two-dimensional wing at $V < V_{rev}$ is determined by ratio

$$\frac{c_y}{c_y'} = 1 - \frac{V^2}{V_p^2}\left(\frac{V_d^2 - V_p^2}{V_d^2 - V^2}\right). \tag{2.31}$$

where c_y' is coefficient of lift of rigid wing.

In Fig. 2.20 are presented curves of aileron effectiveness depending upon relationship $R = q_{div}/q_{rev} = V_{div}^2/V_{rev}^2$.

During straight sweepback of wing, deformation of sag during deflection of aileron causes additional decrease of angle of attack of end sections, which leads to considerable lowering of effectiveness of aileron. During reverse sweepback of wing, effectiveness of aileron

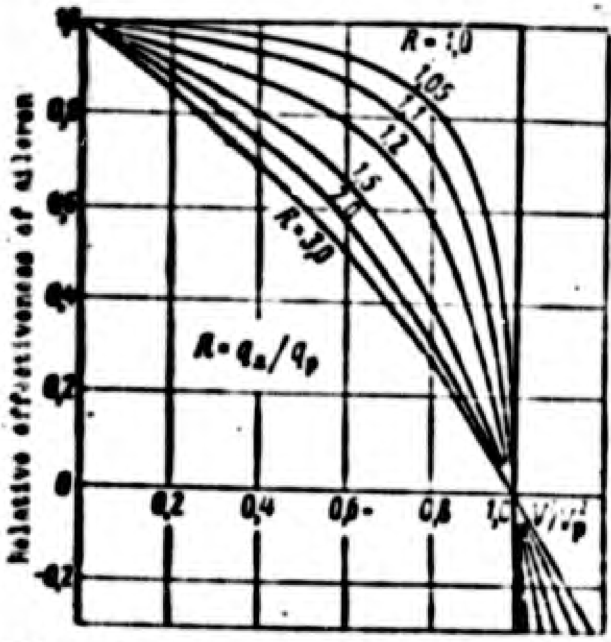

Fig. 2.20. Influence of critical speed of divergence on effectiveness of aileron.

is increased. Since at V_{rev} increase of lift during deflection of aileron is equal to zero, then there will not be additional bend of wing in this case. Therefore, sweepback of wing practically does not affect velocity of reversal.

As can be seen from formula (2.30), effectiveness of aileron and critical speed of reversal during constant rigidity of wing depend on relationship of derivative aerodynamic coefficients c_y^{α} c_y^{δ}, c_m^{δ}, which endure considerable change in Mach number. Since during transonic speed of flight magnitude c_m^{δ} increases and c_y^{δ} drops, then speed of reversal and effectiveness of ailerons in this zone of speeds drop because of influence of compressibility of air. During supersonic speeds of flight these coefficients are changed approximately by the same order. Therefore, indicated critical speed of reversal approximately remains constant or even somewhat increases.

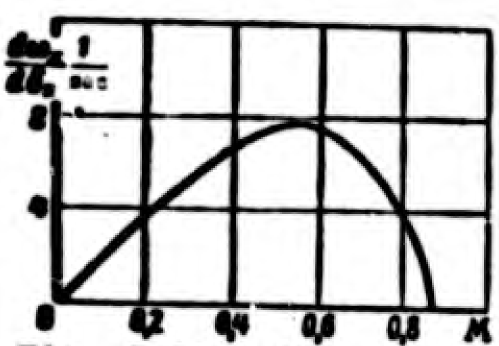

Fig. 2.21. Change in effectiveness of ailerons with respect to Mach number.

During test flights, effectiveness of ailerons is more conveniently estimated by magnitude $d\omega_x/d\delta_{ail}$ (ω_x is angular velocity of aircraft with respect to axis x), dependency of which on Mach number is shown on Fig. 2.21.

Deformations of aileron control lines cause increase of movement of stick (control wheel) for creation of one and the same rolling moment, which causes lowered effectiveness of ailerons with respect to movement of the stick.

2.5. Loads Effective on Horizontal Empennage

Loads acting on horizontal empennage it is possible to divide into three basic groups:

a) balancing loads;

b) maneuvering loads;

c) loads during flight in bumpy air.

In rectilinear flight, on the empennage act balancing aerodynamic load and its weight. Magnitude of load on horizontal empennage is basically defined as

$$P_{г.о}=\frac{M_z}{L_{г.о}}=\frac{m_z qSb_A}{L_{г.о}}, \tag{2.32}$$

where M_z is moment of aircraft relative to its center of gravity during given angle of attack, determined by wind-testing a model of an aircraft without horizontal empennage. During calculation, one should consider load during the most unfavorable centering;

$L_{h.e}$ is distance from center of gravity of aircraft at a given centering to center of pressure of aerodynamic load of horizontal empennage.

In a flying range of angles of attack $m_z = f(c_y)$ it is possible to consider linear function. Consequently, coefficient m_z it is possible to present in the form

$$m_z=m_{z0}+m_z^{c_y}c_y=m_{z0}+m_z^{c_y}\frac{nG/S}{q}. \tag{2.33}$$

where m_{z0} is value of coefficient of moment at $c_y = 0$. Then balancing load is

$$P_{ур}=-\left(m_{z0}+m_z^{c_y}\frac{nG/S}{q}\right)qS\frac{b_A}{L_{г.о}}=-m_{z0}qS\frac{b_A}{L_{г.о}}+m_z^{c_y}n\frac{Sb_A}{S_{г.о}L_{г.о}}\cdot\frac{G}{S}\cdot S_{г.о} \tag{2.34}$$

Thus balancing load on horizontal empennage consists of two components, of which one depends on magnitude of impact pressure, and the other — on magnitude of overload.

The biggest loads on empennage appear during maneuver. However, determination of maneuvering loads presents great difficulties, since along with characteristics of maneuverability of aircraft one should consider possible peculiarities of piloting. During determination of loads on horizontal empennage it is expedient to connect their magnitude with magnitude of maximum overload and maximum force applied by pilot to control stick.

Loads on horizontal empennage during elevator deflection are connected with magnitude of overload appearing with this deflection. However, this connection is not simple, and depends also on method of piloting (law of deflection of control surface with respect to time). During established regime of flight, to each magnitude of overload corresponds a definite position of control surface and value of balancing load. In the process of maneuver the pilot can deflect a control surface smoothly or sharply; with this there are obtained different magnitudes of angular acceleration $d\omega_z/dt$. Therefore, load on horizontal empennage at the same angle of elevator deflection depends on rate of its deflection. Magnitude of load on horizontal empennage and its distribution along chord is different in separate phases of maneuver.

With this one should distinguish three phases, which it is possible to show graphically during step-by-step deflection of control surface (Fig. 2.22).

a) the first corresponds to initial deflection of control surface, at which is obtained initial load P_{man} on horizontal empennage (point I);

b) the second corresponds to the moment when during rotation of aircraft there appears considerable damping load on horizontal empennage, in the direction reverse to load, caused by deflection of control surface (point II); this point corresponds to achievement of maximum overload:

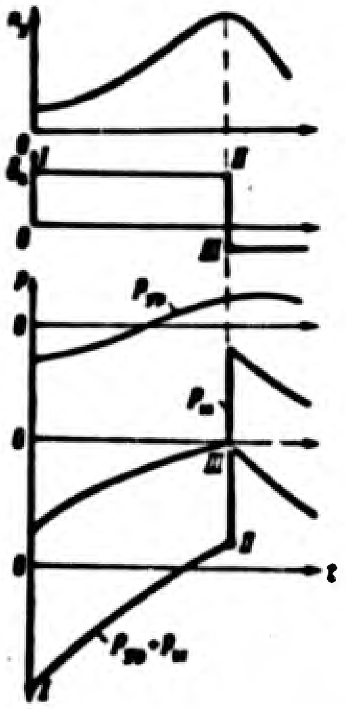

Fig. 2.22. Phases of elevator deflection.

c) the third corresponds to the position when during considerable damping load on empennage (considerable ω_z) the pilot, deflecting control surface for cessation of maneuver, creates additional load directed to the same side as damping (point III).

Total load on horizontal empennage is equal to sum of maneuvering and balancing loads:

$$P_{г.о} = P_{м} + P_{г}$$

Similar phases it is possible to observe also during any other law of elevator deflection in maneuver. Distribution of loads, corresponding to these phases, is shown on Fig. 2.23.

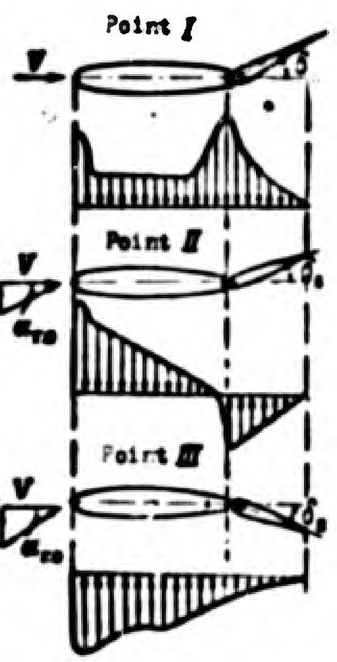

Fig. 2.23. Distribution of loads on horizontal empennage during different phases of elevator deflection (points I, II, III, correspond to Fig. 2.22).

All three phases present interest both in magnitude of loads on horizontal empennage and in their distribution along chord.

Determining loads on horizontal empennage during maneuver requires analysis of equation of aircraft motion. With this there is obtained complicated dependences of load on horizontal empennage on parameters of aircraft. For the first time loads on empennage were in detail investigated by A. I. Makarevskiy. The selection of basic calculation cases for the empennage was well-founded by him.

In the practice of designing and during standarization of loads it is expedient to use simplified formulas reflecting connection of load on horizontal empennage $P_{h.e}$ with conditional wing loading $n_{max}^{op} \frac{G}{S}$ and area of empennage $S_{h.e}$:

$$P_{г.о} = C \frac{n_{max}^{э} G}{S} S_{г.о}. \qquad (2.35)$$

Constant C one can determine for corresponding phase of deflection of control surface. Such dependence, as experience shows, with sufficient accuracy estimates loads on horizontal empennage.

In first phase of deflection of control surface, magnitude of maneuvering load P_{man} is determined by angular acceleration:

$$P_{м} = \frac{1}{L_{г.о}} J_z \frac{d\omega_z}{dt}. \qquad (2.36)$$

Thus determination of maneuvering overload is reduced to determination of angular acceleration $d\omega_z/dt$. The sharpest maneuvering will be instantaneous elevator deflection $\delta_{el} = f(t) = \text{const}$, which permits estimating boundary of possible magnitudes of maneuvering loads on horizontal empennage. For this case magnitude $d\omega_z/dt$ is determined from relationship (1.24):

$$\frac{d\omega_z}{dt} = A - D\omega_z - B\Delta n. \qquad (2.37)$$

In initial moment of maneuver, at $t = 0$ $\omega_z = 0$ and $\Delta n = 0$. Consequently,

$$\frac{d\omega_z}{dt} = A$$

Then

$$P_{м} = \frac{1}{L_{г.о}} J_z A = -c^{\delta}_{y\,г.о} \delta_{в} k q S_{г.о}. \qquad (2.38)$$

After determining product $c^{\delta}_{yh.e} \delta_{el} kq$ from equation (1.29), we will obtain

$$P_{м} = \left(\mu g k \sqrt{k}\, c^{\alpha}_{y\,г.о} \frac{S L_{г.о}}{G} - m_z^{c_y} \frac{S b_A}{S_{г.о} L_{г.о}}\right) \frac{G}{S} S_{г.о} \Delta n_{экс}. \qquad (2.39)$$

Magnitude in parentheses it is possible to consider constant. Then for P_{man} can be obtained approximate formula

$$P_{м} \approx C n_{max} \frac{G}{S} S_{г.о.} \qquad (2.40)$$

<u>In second phase</u>, taking into account damping load

$$P_{г.о} = c_{y\,г.о}^{\delta} \delta_{в} k q S_{г.о} - \frac{\omega_z L_{г.о}}{\sqrt{\Delta}\, V} c_y^{\alpha} k q S_{г.о} \qquad (2.41)$$

(second member characterizes magnitude of damping load). In this case load on horizontal empennage in magnitude is less than in the first case; however, it presents interest from the point of view of distribution of load along chord (Fig. 2.23)

<u>In third phase</u> maximum load is possible at great speed of flight, when pilot, protecting aircraft from excessive overload, deflects sharply controls from himself. This summarizes load caused by deflection of control surfaces and damping load. This case frequently is called second maneuvering load. It corresponds to large loads on horizontal empennage because of following circumstances:

a) deflection of stick from self for cessation of maneuver, as a rule, can be accomplished more sharply since during deflection of stick pilot does not fear obtaining excessive overload;

b) when pulling stick toward himself, the pilot must apply relatively large forces, but to deflect it from himself it is sufficient at first for the pilot only to weaken pressure on stick and for shift of control beyond neutral position it is necessary only to press on stick;

c) damping load somewhat increases total load on horizontal empennage. Therefore, in this case maneuvering load is 20-50% larger than in the first case. During determination of load by the formula (2.40), value of coefficient C increases 1.2-1.5 times.

During action of vertical gust of bumpy air on empennage

$$P_{\text{г.о}} = P_{\text{уп}} + P_{\text{б.в}}, \tag{2.42}$$

where $P_{b.a}$ is load on horizontal empennage from gust of bumpy air. Load $P_{b.a}$ one can determine, using relationship (1.34):

$$P_{\text{б.в}} = Kc^{\alpha}_{y\,\text{г.о}} \Delta 2q S_{\text{г.о}} = 0.5\, Kc^{\alpha}_{y\,\text{г.о}} \rho_0 W V_{\max} S_{\text{г.о}}. \tag{2.43}$$

During appraisal of coefficient K it is expedient to consider, for horizontal empennage, magnitude $J_z g/S_{h.e} L^2_{h.e}$, characterizing specific inertial load on horizontal empennage. If moment of inertia of aircraft is assumed approximately equal to

$$J_z \approx 0.026 \frac{G}{g} L^2, \text{ then } \frac{J_z g}{S_{\text{г.о}} L^2_{\text{г.о}}} \approx 0.3 \frac{G}{S},$$

and correspondingly, magnitude of coefficient K will be 0.5-0.6. Substituting in formula (2.43) numerical values of W, c^{α}_{y}, ρ_0 and K, we will obtain

$$P_{\text{б.в}} = C_{\text{б.в}} V_{\max} S_{\text{г.о}}, \tag{2.44}$$

where $C_{b.a}$ is constant coefficient.

For aircraft of large dimensions there is usually conducted analysis of loads on horizontal empennage taking into account entrance of aircraft in a gust of trapezoidal form (see Fig. 1.19). There is considered possible increase ("throwing") of angle of attack of empennage due to oscillations of aircraft in plane of pitch.

2.6. Loads Effective on Vertical Empennage

There are three forms of loads on vertical empennage:

a) maneuvering loads;

b) load in case of engine failure;

c) load during flight in bumpy air.

Maneuvering loads. Definition of maneuvering loads on vertical empennage also is connected with great difficulties and requires consideration of complicated dependences.

Experimental data show that loads on vertical empennage during fulfillment of usual maneuvers (turns, chandelles, spirals, and so forth) are very small. However, from operational experience it is known that sometimes in flight take place very large loads that in the period (before 1935-1937) sometimes led to destruction of vertical empennage. Analysis of possible loads on vertical empennage is hampered by the fact that the basic factors determining these loads (angle of slip, angle of control surface deflection), are not limited by limitations easily controlled by the pilot. Thus, for instance, even during fulfillment of sharp maneuvers, lateral overloads do not exceed 1.5, which does not cause any essential physiological sensations for the pilot. During the analysis of loads, in the case of a sufficient reserve of static stability for aircraft without boosters, it is possible to be oriented to force of pilot. For aircraft with boosters, rated load on vertical empennage is determined by permissible angle of sideslip. Character of change of loads on vertical empennage is shown in Fig. 2.24.

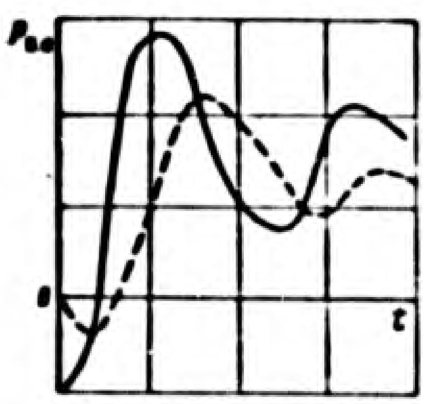

Fig. 2.24. Character of change of loads on vertical empennage during rudder deflection. ——sharp application of force to pedals (P_0 = const), - - - -smooth application of force to pedals $P = P_0\,(1-e^{-2t})$.

Phases of maneuver in horizontal plane and corresponding load on vertical empennage are shown in Fig. 2.25. Maximum loads take place in conditions of large angles of sideslip (βmax). During sharp rudder deflection at the time of achievement of the biggest β for return of aircraft to conditions $\beta = 0$ there appears the biggest load on the vertical empennage. Direction of this load is opposite to maneuvering load in the beginning of the maneuver.

Analogously to second maneuvering load on horizontal empennage, magnitudes of maximum loads on vertical empennage, to a very great measure, depend on stability of aircraft. For unstable aircraft $P_{max\ v.e}$ is limited only by maximum value of coefficient of lateral force $c_{z\ max}$. Sharpness of application of force on pedal shows both on magnitude and on character of load (see Fig. 2.24). From condition of achievement $c_{z\ max}$ it is expedient to consider load directly proportional to impact pressure. Therefore, load on vertical empennage it is possible to determine by the formula

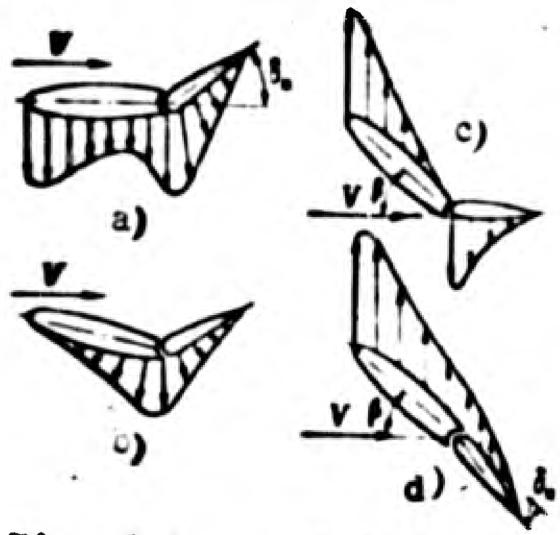

Fig. 2.25. Loads on vertical empennage in different phases of maneuver. a) beginning of maneuver, sharp rudder deflection, b) flight with small angle of sideslip ; c) flight with large angle of sideslip ; d) termination of maneuver, deflection of control surface for return to conditons of zero sideslip .

$$P_{\text{в.о}} = C q_{\text{макс}} S_{\text{в.о}} \qquad (2.45)$$

where C is constant coefficient.

<u>Load on vertical empennage in case of failure of engines located on wing</u>. During engine failure action of moment M_y from asymmetric thrust causes sideslip of aircraft. In the beginning aircraft obtains large angles of sideslip due to throwing, but then arrives at a steady angle of sideslip .

$$\beta_{\text{уст}} = \frac{M_y}{-m_y^{\beta} q S l}. \qquad (2.46)$$

where m_y^{β} is derivative of coefficient of moment with respect to angle of sideslip β.

Maximum angle of slip it is possible to express through β_{st}:

$$\beta_{\text{макс}} = \beta_{\text{уст}} k_{\text{д.с}}. \qquad (2.47)$$

where $k_{v.e}$ is coefficient characterizing throwing during sharp application of moment M_y.

Load on vertical empennage one can determine by the formula

$$P_{v.e} = -c^{\beta}_{zv.e} kqS_{v.e}\beta_{max} = \frac{c^{\beta}_{zv.e}}{m^{\beta}_{y}} k \frac{S_{v.e}}{S} \frac{M_y}{l} k_{v.e} \qquad (2.48)$$

where $c^{\beta}_{zv.e}$ is derivative of coefficient of lateral force with respect to angle of sideslip ;

k is coefficient of deceleration of flow for empennage.

For simplification of calculation, load on vertical empennage frequently is determined by approximate formula

$$P_{v.e} = \frac{M_y}{l_{v.e}} k_{v.e}. \qquad (2.49)$$

in which will be disregarded forces appearing on wing and fuselage. Formula (2.49) gives decreased value for $P_{v.e}$ as compared to value in formula (2.48), since aerodynamic forces acting on fuselage and wing cause moment, as a rule, directed to the side reverse to moment of forces acting on empennage. Coefficient of throwing for a specific aircraft depends on altitude and speed of flight. Magnitude of thrust of motor also depends on altitude and speed of flight. Therefore, one should determine maximum value of $P_{v.e}$ for the most unfavorable combination of M_y and $k_{v.e}$.

In formula (2.48) it is assumed that rudder is pressed and pilot does not manage to react to behavior of aircraft. In actual conditions pilot tries to prevent achievement by the aircraft of large angles of sideslip . During deflection of rudder by angle δ_{rud}, load on vertical empennage is

$$P^{\delta}_{v.e} = -c^{\beta}_{zv.e} kqS_{v.e}\beta - c^{\delta}_{zv.e} kqS_{v.e}\delta_{rud} \qquad (2.50)$$

where $c^{\delta}_{zv.e}$ is derivative of coefficient of lateral force with respect to rudder angle.

One may assume that pilot tries to deflect controls in such a manner that load on vertical empennage, caused by this deflection, parriès moment appearing due to engine failure. Then

$$-c^{\beta}_{z\,в.о}\,kqS\beta_{в}=-\frac{M_y}{L_{в.о}}. \qquad (2.51)$$

Let us assume that because of late reaction of pilot, deflection of controls happened at the time of achievement of β_{max}. In this case magnitude of load on empennage will be

$$P_{в.о}=\frac{c^{\beta}_{z\,в.о}}{m^{\beta}_{y}}k\frac{S_{в.о}}{S}\frac{M_y}{l}k_{в.о}+\frac{M_y}{L_{в.о}} \qquad (2.52)$$

or, using approximate relationship (2.49), we will obtain

$$P_{в.о}=\frac{M_y}{L_{в.о}}(1+k_{в.о}). \qquad (2.53)$$

<u>Loads during flight in bumpy air.</u> In this case expressions for load on vertical empennage are analogous to (2.44):

$$P_{в.о}=C_{в.о}V_{max}S_{в.о} \qquad (2.54)$$

where

$$C_{в.о}>C_{г.о} \text{ since } J_y>J_z.$$

Besides above-indicated cases of load, one should consider combined cases of load. Since it is doubtful to obtain simultaneously maximums of operational loads in both calculation cases, then in examining joint action of two forms of independent loads there is chosen a certain part from the maximum value of each form of load.

In practice it is necessary to consider the following cases of load:

a) load on vertical empennage from bumpy air during flight with stopped motor on one side of wing;

b) simultaneous load on horizontal and vertical empennage.

The latter case is the calculated for fuselage and vertical empennage, if on it is located horizontal empennage.

2.7. Asymmetric Loads of Tail Assembly

Asymmetiic distribution of load between halves of horizontal empennage is, to a certain degree, inherent to all conditions of flight. Degree of disymmetry is increased during maneuvers with side slip or rotation of aircraft. In many cases forces appearing in the structure of the empennage during asymmetric load, can be calculated.

During location of horizontal empennage on middle or upper part of fin, in the case of asymmetric loads there appear large additional bending moments on vertical empennage. This circumstance forces us attentively to analyze possible disymmetry of loads.

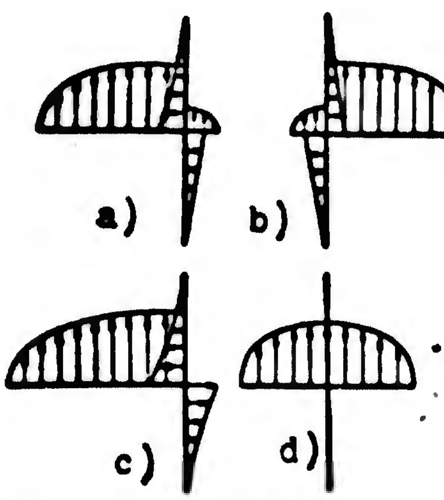

Fig. 2.26. Influence, on asymmetric loads, of the location of the horizontal empennage on the fin. a and b) low location of stabilizer; c) middle location of stabilizer; d) stabilizer is located in upper part of fin.

Basic factors determining degree of disymmetry of distribution of load on horizontal empennage are:

1. Influence of load of vertical empennage during sideslip and rudder deflection.

2. Influence of wings and fuselage on direction of flow near empennage during sideslip.

3. Rotation of aircraft during maneuver.

4. Influence of slipstream (or jet stream of motors).

5. Gusts of bumpy air.

Three first factors are determining factors during selection of rated loads.

Location of horizontal empennage with respect to height of fin, to a considerable degree, determines magnitude of asymmetric load (Fig.

2.26).

On two-fin empennage sideslip causes change of bending moments of stabilizer because of asymmetric loads on vertical empennage (Fig. 2.27). With this occurs an increase of load along ends of stabilizer.

On swept-back empennage degree of disymmetry of loads is increased because of the fact that during sideslip is changed effective angle of sweepback of each half of stabilizer (Fig. 2.28).

The change in character of flow around empennage during sideslip is also influenced by downwash near empennage from fuselage and wing. This leads additionally to considerable disymmetry of loads on horizontal empennage. Sign of moment of asymmetric load of horizontal empennage is inverse to sign of moment of asymmetric load of wing.

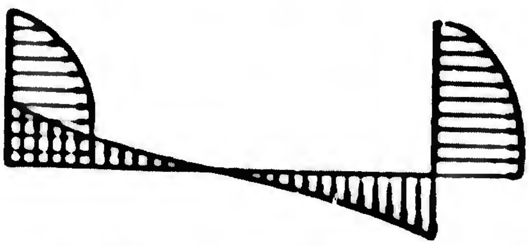

Fig. 2.27. Asymmetric loads on horizontal empennage with two-fin vertical empennage.

During rotation of aircraft with respect to axis x, angles of attack of sections of horizontal empennage are distributed asymmetrically:

$$\Delta\alpha_{г.о}=\frac{\omega_x z}{V},$$

which leads to asymmetric loads on it. In this case also degree of disymmetry of loads is increased from influence of wing. However, this influence is insignificant since rotation of aircraft around axis x is accompanied by deflection of ailerons, which to a considerable degree decreases magnitude of downwash caused by rotation of aircraft.

Asymmetric loads from different factors are algebraically summarized, which determines full disymmetry of loads on horizontal empennage. During sideslip at high speeds load on one half of horizontal

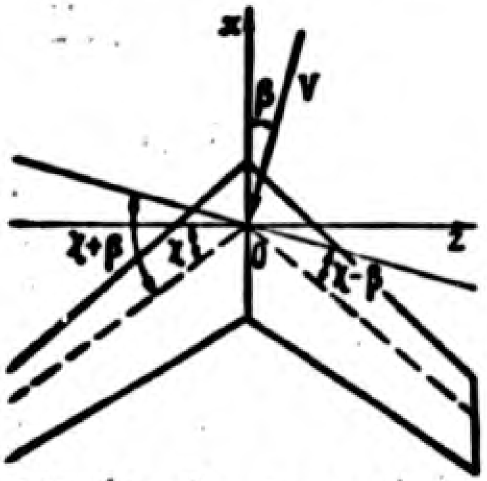

Fig. 2.28. Diagram of swept-back empennage during sideslip.

empennage can appear larger than corresponding maximum load during symmetric distribution.

Influence of compressibility of air at high speeds of flight considerably complicates analysis of asymmetric loads. In particular, at transonic speeds influence of Mach number somewhat increases disymmetry of loads.

2.8. Influence of Deformations of Structure of Aircraft on Effectiveness of Empennage

For analysis of influence of deformation of fuselage and empennage on effectiveness of longitudinal control we will consider an aircraft rigidly fixed in section of fuselage with respect to center of gravity; wing and nose part of fuselage we will consider absolutely rigid. In this case, moment from horizontal empennage it is possible to record in the form

$$M_z = -L_{г.о}P_{г.о} + M_{г.о} \tag{2.55}$$

Let us express component of moment through aerodynamic coefficients:

$$\left.\begin{aligned} M_z &= c_m qSb_A;\\ P_{г.о} &= \Delta c_{y\,г.о} kqS_{г.о};\\ M_{г.о} &= c_{m\,г.о} kqS_{г.о} b_{г.о} \end{aligned}\right\} \tag{2.56}$$

where b_A and $b_{h.e}$ are middle aerodynamic chords of wing and horizontal empennage respectively;

k is coefficient of retardation of flow for empennage.

Measure of effectiveness of horizontal empennage is the relative change of coefficient of pitching moment with respect to elevator angle, which it is possible to characterize by derivative of coefficient of moment with respect to elevator angle c_m^δ. For real aircraft, because of elastic deformation of structure c_m^δ is less than for absolutely rigid aircraft. Ratio $c_m^\delta / c_{m\ \mathrm{rigid}}^\delta$ characterizes elastic effectiveness of elevator.

From equation (2.55), taking into account formula (2.56), we have

$$c_m^\delta = -k\frac{S_{r.o}}{S}\left(-\frac{L_{r.o}}{b_A}c^\delta_{y\,r.o\,\Sigma}+\frac{b_{r.o}}{b_A}c^\delta_{m\,r.o}\right). \tag{2.57}$$

where $c^\delta_{m\ h.e}$ is derivative of coefficient of moment of horizontal empennage with respect to angle δ_{el};

$c^\delta_{y\ h.e\ \Sigma}$ is derivative with respect to angle δ_{el} of full coefficient of lift of horizontal empennage, taking into account its turn by angle θ.

For analysis of this relationship we will consider diagram of aircraft shown in Fig. 2.29. Angle of turn of horizontal empennage is changed along span. For simplicity in calculation we take section of horizontal empennage, located at distance 2/3 of a half span from fuselage.

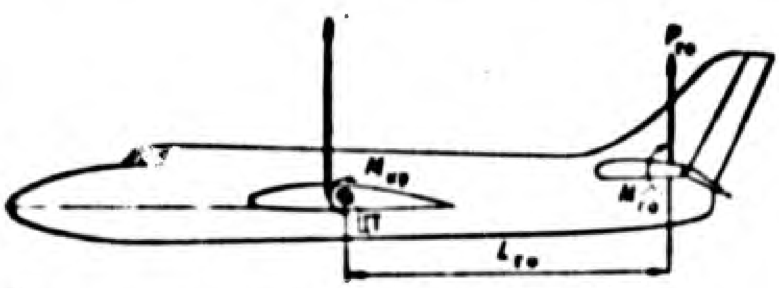

Fig.2.29. Diagram of aerodynamic forces acting on aircraft.

Elastic properties of the fuselage and empennage one can determine through influence coefficients E_1 and E_2. Let us assume that rigidity is characterized by magnitude E_1 equal to lift of empennage of both halves, which it is necessary to apply in center of pressure of empennage in order to turn calculation section by 1 rdn. Correspondingly, coefficient E_2 is equal to moment which it is necessary to apply in calculation section in order to turn it by the same angle. Then change of angle of attack of stabilizer will be

$$\theta = \frac{P_{r.o}}{E_1} + \frac{M_{r.o}}{E_2}. \tag{2.58}$$

During further analysis we will consider small changes in angles of elevator deflection δ_{el} and turn of stabilizer θ.

Let us compose equation of forces and moments:

$$\left.\begin{aligned} P_{г.о} &= kqS_{г.о}(c^{\alpha}_{y\,г.о}\theta + c^{\delta}_{y\,г.о}\delta_{в}); \\ M_{г.о} &= c^{\delta}_{m}\delta_{в}kqS_{г.о}b_{г.о}. \end{aligned}\right\} \tag{2.59}$$

Using relationships (2.58) and (2.59), we will obtain

$$\frac{d\theta}{d\delta_{в}} = \frac{A}{B}, \tag{2.60}$$

where

$$A = kqS_{г.о}\left(\frac{c^{\delta}_{y\,г.о}}{E_1} + \frac{c^{\delta}_{m}\,b_{г.о}}{E_2}\right);$$

$$B = 1 - \frac{1}{E_1}qkS_{г.о}c^{\alpha}_{y\,г.о}.$$

Increase of lift coefficient one can determine from formulas (2.56) and (2.59):

$$\Delta c_{y\,г.о} = \frac{P_{г.о}}{kqS_{г.о}} = c^{\alpha}_{y\,г.о}\theta + c^{\delta}_{y\,г.о}\delta_{в} \tag{2.61}$$

Let us take derivative $\Delta c_{y\ h.e}$ with respect to δ_{el} :

$$c^{\delta}_{y\,г.о\,э} = c^{\alpha}_{y\,г.о}\frac{A}{B} + c^{\delta}_{y\,г.о}. \tag{2.62}$$

After substituting expression (2.62) into formula (2.57), we will obtain

$$c^{\delta}_{m} = k\frac{S_{г.о}}{S}\left[-\frac{L_{г.о}}{b_A}\left(c^{\alpha}_{y\,г.о}\frac{A}{B} + c^{\delta}_{y\,г.о}\right) + \frac{b_{г.о}}{b_A}c^{\delta}_{m\,г.о}\right]. \tag{2.63}$$

If aircraft is absolutely rigid, then $E_1 = E_2 = \infty$. Then $A = 0$ and $B = 1$. In this case

$$c^{\delta}_{m\,жестк} = \frac{kS_{г.о}}{S}\left(-\frac{L_{г.о}}{b_A}c^{\delta}_{y\,г.о} + \frac{b_{г.о}}{b_A}c^{\delta}_{m\,г.о}\right). \tag{2.64}$$

Effectiveness of elevator of elastic aircraft it is possible to express in the following way:

$$\frac{c^{\delta}_{m}}{c^{\delta}_{m\,жестк}} = 1 - c^{\alpha}_{y\,г.о}\frac{A}{B}\frac{L_{г.о}}{b_A}\left(-\frac{L_{г.о}}{b_A}c^{\delta}_{y\,г.о} + \frac{b_{г.о}}{b_A}c^{\delta}_{m\,г.о}\right)^{-1}. \tag{2.65}$$

Second member in the denominator is considerably less than first and during qualitative appraisal it is possible to lower it.

Finally

$$\frac{\delta_{в}}{\delta_{в\,жестк}} = 1 + \frac{A}{B}\frac{\xi_{г.о}}{\zeta_{г.о}}. \tag{2.66}$$

Critical speed of divergence of horizontal empennage will be the speed at which small deflection of δ_{el} causes large torsion angles of empennage. From equation (2.66) it is clear that this takes place at $B = 0$.

Impact pressure, corresponding to critical speed of divergence of horizontal empennage, is

$$q_{д\,г.о} = \frac{E_1}{kS_{г.о}\zeta_{г.о}}. \tag{2.67}$$

Critical speed of reverse of horizontal empennage is defined as the speed at which effectiveness of control surface becomes equal to zero, i.e., deflection of control surface does not lead to change of moment. This condition can be obtained from equation (2.66):

$$1 + \frac{A}{B}\frac{\xi_{г.о}}{\zeta_{г.о}} = 0 \tag{2.68}$$

Substituting values of A and B, we will obtain expression for impact pressure, corresponding to critical speed of elevator reversal;

$$q_{р.о} = \frac{E_1}{kS_{г.о}a_{г.о}}\frac{\xi_{г.о}}{\zeta_{г.о}\delta_{в}}. \tag{2.69}$$

As can be seen, speed of elevator reversal does not depend on coefficient E_1 because at speed of reversal lift force of empennage, caused by deflection of control surface, is equal to zero.

From expressions (2.67) and (2.69) there can be obtained relationship for appraisal of elevator effectiveness:

$$\frac{\delta_{в}}{\delta_{в\,жестк}} = \frac{1 - q/q_{р.о}}{1 - q/q_{д\,г.о}}. \tag{2.70}$$

2.9. Loads on Landing Gear, Appearing During Landing

On contemporary aircraft the predominant type is the retractable in flight landing gear with nose strut. With such a diagram two main struts are located somewhat behind center of gravity and receive, when standing, 85-90% of the weight of the aircraft. The front strut is carried in the nose part of the aircraft.

On aircraft with piston motors widely have been applied landing gears with tail wheel (or skid). In this case center of gravity of the aircraft is located behind main struts. Applied also is a bicycle diagram of landing gear, where the main part of load is apportioned to two struts located under fuselage. With such a diagram, for protection of wing tips from damage during landing, on wing tips are established wing-tip struts.

On aircraft with large gross weight, frequently on each strut there is established several wheels. On heavy aircraft widely used are four-wheeled carts. Sometimes applied are struts (wheels) of landing gear, dropped after takeoff. In this case landing is carried out on special landing gear.

When parked only its weight acts on the aircraft. On each support strut acts reaction of land, the magnitude of which depends on relative location of center of gravity during a given load of aircraft. Load on one strut is called strut load P_{str}.

Wheels for an aircraft will be selected based on strut load and magnitudes of takeoff and landing speeds. There should be ensured corresponding pressure of wheels on surface of airport, taking into account strength of covering of runway. For a number of types of aircraft there is required a guarantee of operation on unpaved airfields. For certain types of aircraft, instead of wheels are applied skis.

Landing gear should absorb kinetic energy of aircraft on landing. Magnitude of this energy depends on vertical and horizontal components of speed during landing. Energy caused by vertical component is absorbed by shock absorbers and partially elastic deformations of structure of aircraft. Normal forces of reaction of wheels have to be relatively small in magnitude. Kinetic energy from horizontal component is basically absorbed by brakes of wheels and partially by aerodynamic drag of aircraft.

For maneuvering of aircraft on land nose (tail, wing-tip) strut is made to be controllable. This should ensure sufficient stability of motion of aircraft on land.

Vertical Velocity During Landing

The process of landing is divided into the following stages (Fig. 2.30): gliding, levelling out, holding off (H_h), incipient stalling (just before touch-down), landing, and landing run.

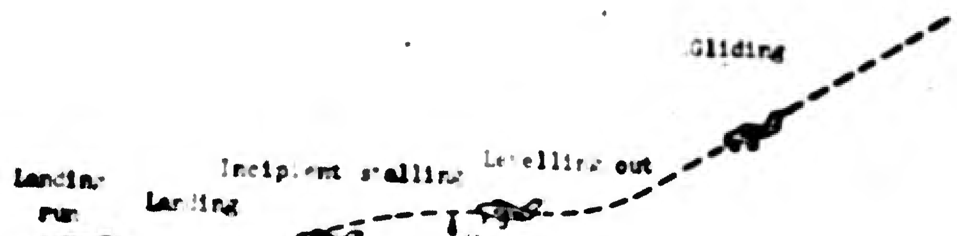

Fig. 2.30. Trajectory of landing.

When gliding, speed of aircraft must somewhat exceed minimum, since a certain speed margin is necessary for safety of flight and fulfillment of levelling out of aircraft.

Gliding is executed in conditions $c_{y\,gl} = 0.6\text{-}0.7\, c_{y\,max}$. Gliding angle is equal to $\theta = \text{arc tan}\,\frac{1}{K}$ (K – characteristics of aircraft in glide).

During approach to land the pilot, by moving stick to himself, levels the aircraft, i.e., increases angle of attack, and the aircraft shifts from gliding to horizontal flight (to section of holding).

For decrease in length of landing run and decrease in loads on landing gear during impact against land, in the holding section speed decreases to minimum possible. Observing equality of lift and weight, pilot gradually increases angle of attack of wing. Thrust of motor is minimum. Increase of lift is limited by maximum value c_y. After achievement of $c_{y\ max}$, further increase in angle of attack no longer can compensate loss of speed. Due to action of force corresponding to difference between weight and lift $G - Y$, there is created acceleration directed downward and aircraft "dips" (stalls) and touches land with its wheels. Horizontal speed of aircraft at the time of termination of incipient stall is called landing speed. In an aircraft with nose wheel and bicycle landing gear landing directly from glide is possible.

For normal landing, levelling out should be finished at low altitude. Usually it is recommended that altitude at the end of holding be near 1 m. In operation errors are possible in determining altitude of levelling out, and at the end of holding (beginning of incipient stall) altitude can attain 2-3 m.

Magnitude of load during landing is basically determined by vertical velocity V_y at touch-down. For determination of magnitude of V_y during incipient stall it is possible to use approximate formula of V. S. Pyshnov:*

---

*V. S. Pyshnov, Aerodynamics of aircraft, Oborongiz, 1943.

$$V_y = 9.5\sqrt[3]{\frac{c_x}{c_y}\frac{H^2}{V_{min}}}. \qquad (2.71)$$

where c_x/c_y is a magnitude reverse to performance characteristics of an aircraft during landing;

V_{min} is minimum speed of aircraft with lowered flaps and landing gear.

Assuming

$$\frac{c_x}{c_y} = 0.2 \text{ and } V_{min} = 50 \text{ m/sec},$$

we will obtain

$$V_y = 1.5H^{2/3}.$$

Approximate dependence of V_y on altitude of holding is shown in Fig. 2.31.

Altitude of holding and, consequently , also magnitude of V_y depend on qualifications of the pilot, meteorological conditions, and other causes. On Fig. 2.32 are given statistical data of recurrence of V_y during different landing conditions.*

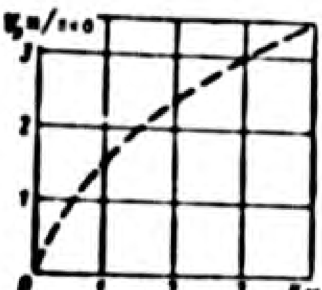

Fig. 2.31. Dependence of V_y on altitude of holding.

Levelling aircraft before landing, pilot orients it with respect to horizon. Because of local slopes of airport there appears additional component V_{land} tan α, where α is angle of encountered slope.

Consequently,

$$V_{y\alpha} = V_y + V_{land}\,\mathrm{tg}\,\alpha. \qquad (2.72)$$

On airports with artificial covering there usually are allowed the following magnitudes of longitudinal slopes in radians, depending

---

*H. Conway, Landing. Gear Design, London, 1958.

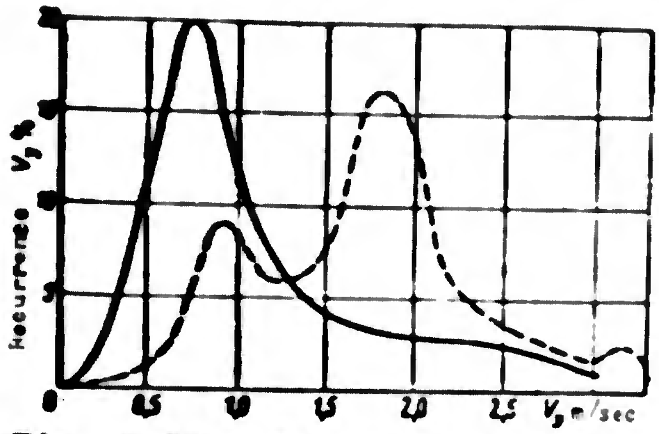

Fig. 2.32. Recurrence of V_y during landing in simple and adverse weather conditions. ——landing in simple weather conditions, - - - -landing in adverse weather conditions.

upon type of aircraft:*

Section of strip	Heavy high-speed aircraft	Other aircraft
Middle section	0.015	0.025
Extreme sections:		
Encountered slope	0.015	0.020
Incidental slope	0.005	0.010
Zone of safety:		
Encounter slope	0.025	0.030
Incidental slope	0.006	0.010

In Fig. 2.33 is given a diagram where are indicated permissible slopes for a runway with artificial covering and for ground surface of an

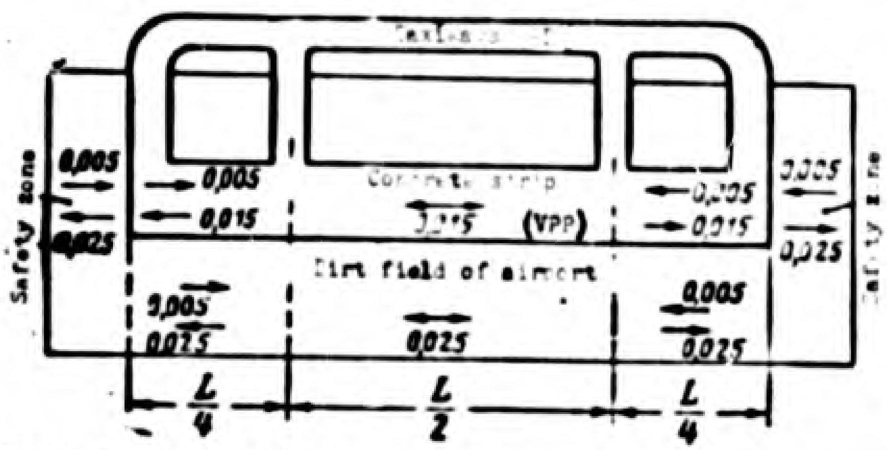

Fig. 2.33. Diagram of runway and taxiways of an airport, with indication of permissible slopes.

airport. Radius of curvature of surface of airport should be not less than 6000 m for the runway and not less than 4000 m in the zone of safety.

Magnitude of limiting local encountered slopes because of local unevenness of runway can be approximately 0.01 higher as compared to given magnitudes. Consequently, increase of magnitude V_y because of local slope can compose 1.2-2.0 m/sec.

---

*Search for and Designing of Airports, under editiorial office of V. F. Babkov, Avtotransizdat, 1959.

Energy which must be absorbed during landing is developed also due to lowering of center of gravity of aircraft during squeezing of shock absorber and pneumatic tire to height

$$H_{c.g} = \varphi h_{s.a} + \delta_{pn} \tag{2.73}$$

where $h_{s.a}$ is magnitude of pressing of shock absorber;

φ is proportionality factor, depending on construction and geometric relationships of landing gear;

δ_{pn} is magnitude of pressing of pneumatic tire.

Maximum value of $H_{c.g}$ will correspond to limiting values of $h_{s.a}$ and δ_{pn}.

The effect of lowering the center of gravity it is possible to estimate from consideration of shock absorption during landing. It is necessary that shock absorption of the landing gear absorb all energy developed during impact of the aircraft against land. This work is determined from dependence

$$A = 0.5\,mV_{y\,giv}^2 + kGH_{c.g}, \tag{2.74}$$

where k is coefficient considering work abosrbed by aerodynamic drag and elasticity of construction.

On the other hand, work during landing it is possible to express through given vertical velocity $V_{y\,giv}$ which would be obtained during fall of an aircraft in a vacuum:

$$V_{y\,giv} = \sqrt{2gH_{equi}}. \tag{2.75}$$

where H_{equi} is altitude, during fall from which in a vacuum there is developed kinetic energy equal to work absorbed by shock absorption during landing in real conditions.

Consequently, it is possible to write

$$A = 0.5H_{equi}G. \tag{2.76}$$

Using expressions (2.74) and (2.75), one can determine

$$V_{y\,giv} = \sqrt{V_{y\,e}^2 + 2gH_{c.g}}. \qquad (2.77)$$

Substituting into formula (2.77) value V_y and $H_{c.g}$, we will obtain

$$V_{y\,giv} = \sqrt{(V_y + V_{land}\,\mathrm{tg}\,\alpha)^2 + 2kg(\eta h_{am} + \delta_{t})}. \qquad (2.78)$$

Magnitude of $V_{y\ giv}$ usually is from 2 to 4 m/sec.

In examining structural strength of landing gear and of the entire aircraft it is necessary to know force in elements of construction, obtained during absorption of maximum work

$$A_{max} = A^{op} f_{l.g} \qquad (2.79)$$

where $f_{1.g}$ is safety factor, established by norms of strength;

A^{op} is operational work:

$$A^{op} = \frac{mV_{y\,giv}^2}{2}.$$

During absorption of this work by shock absorption of the landing gear, there should not be permanent deformations in the structure of the aircraft.

Peculiarities of Loads on Landing and the Operation of Shock Absorption

An aircraft with a nose wheel usually lands on the two main struts, and then during landing run after 5-10 sec the front strut is lowered. Similarly lands an aircraft having a landing gear with a tail wheel. Both types of landing gear allow landing on three points. Landing of an aircraft with a bicycle landing gear can occur both on both struts and on one. Load effective during first impact on strut of landing gear may be represented by vertical P_y, frontal P_x, and lateral P_z components.

Vertical component of load it is possible to express in the form of dependence $P_{max} \sin \omega t \left(0 \leq t \leq \frac{\pi}{\omega}\right)$ with imposition of higher-frequency components caused by elastic oscillations of structure (Fig. 2.34a). For contemporary aircraft $\omega = 3\text{-}12 \frac{1}{sec}$.

At first moment of impact during landing, peripheral velocity of wheel is equal to zero, and forward velocity of wheel is equal to landing speed of aircraft. Consequently, in this period will be slip of wheel with respect to surface of airport. In this case magnitude of frontal load basically depends on magnitude of vertical load on wheel and coefficient of sliding friction between wheel and covering of airport. Frictional force is balanced by inertial forces during spin-up of wheel. After wheel spins up to peripheral velocity equal to speed of aircraft, frontal load becomes practically zero (if brakes are not used).

Frontal load has usually two components of vibrations with frequencies 1-3 and 8-12 vibrations per second (see Fig. 2.34b). Lateral load appears during landing with drift, and basic frequency of its change coincides with frequency of change of vertical load. With this

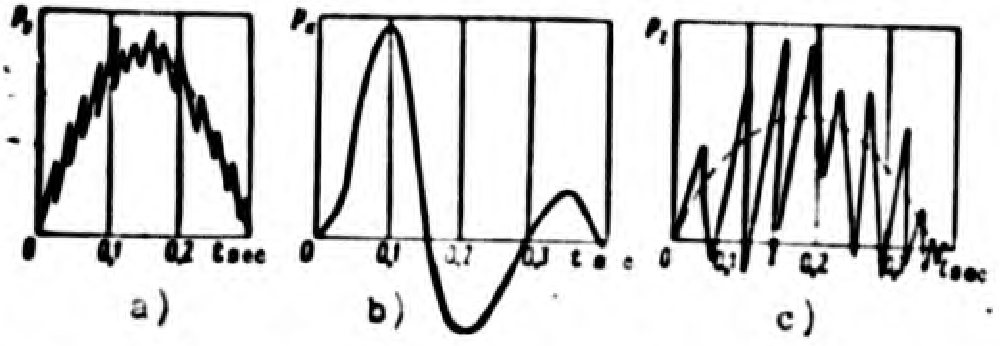

Fig. 2.34. Character of change of components of load on strut of landing gear during landing (first impact). a, b, c — vertical, frontal, and lateral components, respectively.

take place also impositions from elastic vibrations of parts of landing gear in a lateral direction (see Fig. 2.34c).

Characteristic of work of a pneumatic tire gives a diagram of dependence of load on wheel P on pressing tire δ for different values of initial pressure p_0 (Fig. 2.35). Maximum pressing of pneumatic tire δ_{max} corresponds to load P_{max}, at which begins contact of internal surfaces of pneumatic tire. Further increase of load leads to damage of pneumatic tire and wheel. For operation there is taken a maximum permissible pressing of pneumatic tire $\delta_{max\ per}$ equal to $0.95\delta_{max}$. Within limits of maximum permissible pressing, work absorbed by pneumatic tire one can determine by approximate formula

$$A_{max\ per} \approx 0.9\frac{P_{max\ per}\,\delta_{max\ per}}{2}. \tag{2.80}$$

Ratio of load on wheel during maximum permissible pressing of pneumatic tire to strut load $n_{lo} = \frac{P_{max\ per}}{P_{str}}$ is called coefficient of load capacity of wheel.

The main part of work on landing is taken by the shock absorber of the landing gear. At present are applied mainly oleo-pneumatic shock absorbers. In Fig. 2.36 is given a diagram of such a shock absorber. Shock absorber is charged with liquid and air with initial pressure p_0. During work of shock absorber air will be compressed and expanded on a politropic curve

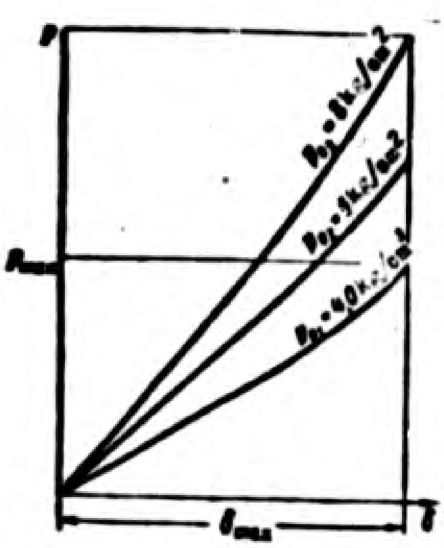

Fig. 2.35. Diagram of work of a pneumatic tire.

$$pv^n = p_0 v_0^n. \tag{2.81}$$

where v_0 and v are, correspondingly, initial and current volume of air in shock absorber;

p_0 and p are, correspondingly, initial and current value of air pressure in shock absorber;

$n \approx 1.2$ is, polytropic exponent.

In Fig. 2.37 a politropic curve is depicted by curve AmB.

On forward movement, pressure of liquid under plunger will be larger than air pressure. Due to difference of pressures, liquid will start to be pushed through calibrated holes of plunger and piston. During reverse movement, air pressure is higher than pressure of liquid under plunger, as a consequence of which air will drive liquid back. Resisting force of liquid is directed against pressure of air on piston. Pressure of liquid in space behind piston also is larger than air pressure in the cylinder; due to this check valve is closed, and liquid begins to overflow through decreased calibrated hole. Therefore, will be increased force of flow friction of shock strut, which will increase absorption of kinetic energy of aircraft.

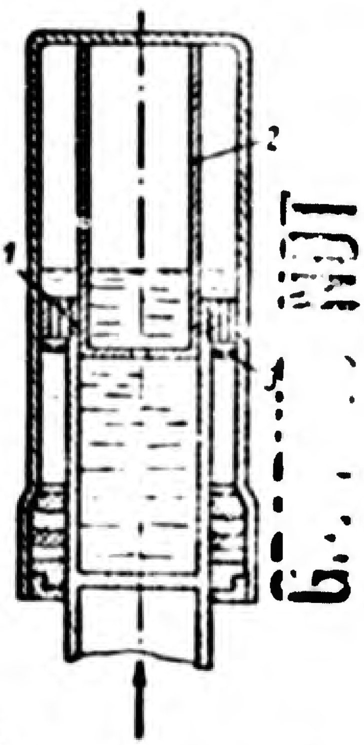

Fig. 2.36. Diagram of shock absorber of landing gear. 1) piston; 2) plunger; 3) check value.

In Fig. 2.37 is shown change of flow frictions: during forward movement — along curve AnB (above politropic curve), and during reverse movement — along curve BdA (below it). Area of figure AnBCOA constitutes work absorbed by air and liquid during pressing of shock absorber in forward movement. Area AnBdA depicts work of liquid changing into heat.

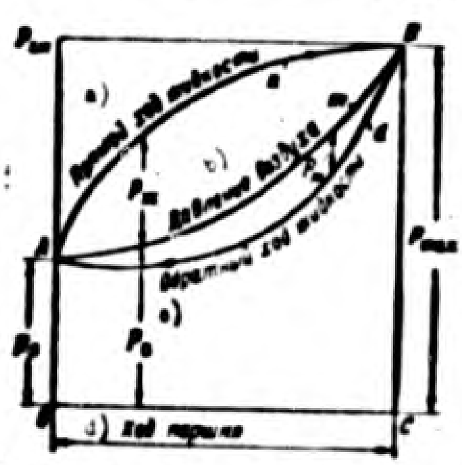

Fig. 2.37. Diagram of work of landing gear shock absorber.
KEY: a) forward movement of liquid; b) air pressure; c) reverse movement of liquid d) stroke of piston.

Additionally, in shock absorber act considerable frictional forces of cuffs and bushings. In shock absorber of telescopic landing gear frictional forces increase from frontal forces during first impact. Therefore, during first impact is increased force at which work of shock absorber starts.

During determination of kinetic energy which must be absorbed by front strut (wing-tip stand), reduced mass is considered. For front strut reduced mass is determined from analysis of eccentric impact, i.e., taking into account forward motion and rotation of the aircraft. During impact on front strut by force P_{fr} (Fig. 2.38), full acceleration of reduced mass will be

$$j = j_{пост} + j_{вр} \qquad (2.82)$$

where $j_{for} = \frac{P_{fr}}{G/g}$ is forward acceleration of aircraft;

$j_{rot} = \frac{P_{fr} b^2}{J_z}$ is circumferential acceleration, which is obtained from angular acceleration of aircraft due to action of unbalanced moment $P_{fr} b$;

$J_z = \frac{G}{g} i_z^2$ is moment of inertia of aircraft relative to its transverse axis;

i_z is radius of gyration of aircraft.

After substituting in expression (2.82) values J_{for} and J_{rot}, we will obtain

$$j = \frac{P_н}{G/g} + \frac{P_н b^2}{G/g\, i_z^2} = \frac{P_н}{G/g}\left[1 + \left(\frac{b}{i_z}\right)^2\right]. \qquad (2.83)$$

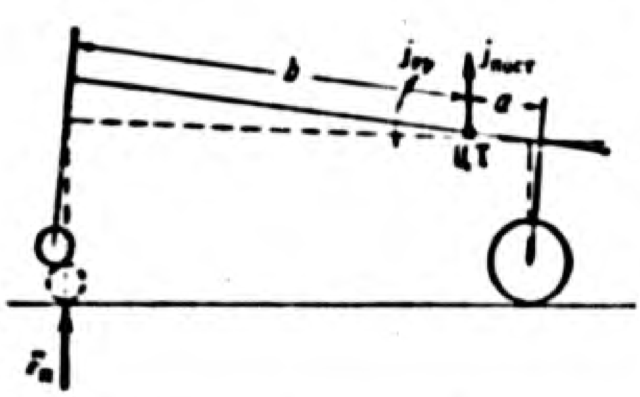

Fig. 2.38. Diagram of appearance of forces on front strut during impact on landing.

Since

$$P_н = m_{прив} j,$$

then

$$m_{прив} = \frac{G/g}{1 + \left(\frac{b}{i_z}\right)^2}. \qquad (2.84)$$

Analogously is determined mass for main struts. For three-wheeled diagram of landing gear, dimension a (see Fig. 2.38) is small as compared to i_z and, therefore, during calculations of loads for reliability one should assume magnitude m_{red} equal to all mass of aircraft m.

2.10. Basic Calculation Cases for Landing Gear

During landing and takeoff the landing gear works in complex conditions of combined load. For strength analysis of landing gear are chosen a series of calculation cases, basic ones of which are:

- three-point landing;
- two-point landing;
- landing with front impact;
- landing with drift;
- deceleration;
- taxiing
- landing run.

Cases of Load of Landing Gear During Landing

During a three-point landing there is assumed calculation value V_y and corresponding overload in center of gravity. Since relations of land are directed analogously to strut loads, then they are determined for main and front struts as a product of strut load (P_{str} or $P_{fr\ str}$) by overload in center of gravity of aircraft:

$$P^{э}_{max} = n_{E} P_{ст} \tag{2.85}$$

Resultant forces of reaction passes through center of gravity (Fig. 2.39). Magnitude of maximum overload is determined by load, corresponding to absorption of assigned work.

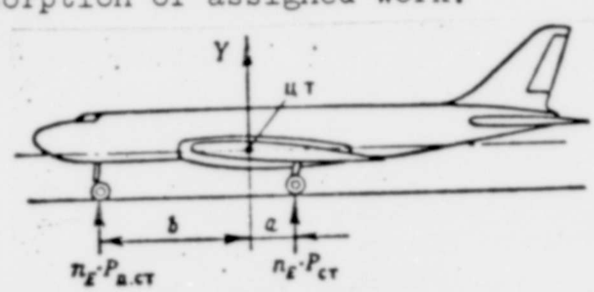

Fig. 2.39. Diagram of forces acting on aircraft during three-point landing.

During two-point landing all load is balanced by reactions of two main struts and lift of wing. Direction of all forces is close to vertical. Overload in center of gravity is assumed approximately the same as during three-point landing.

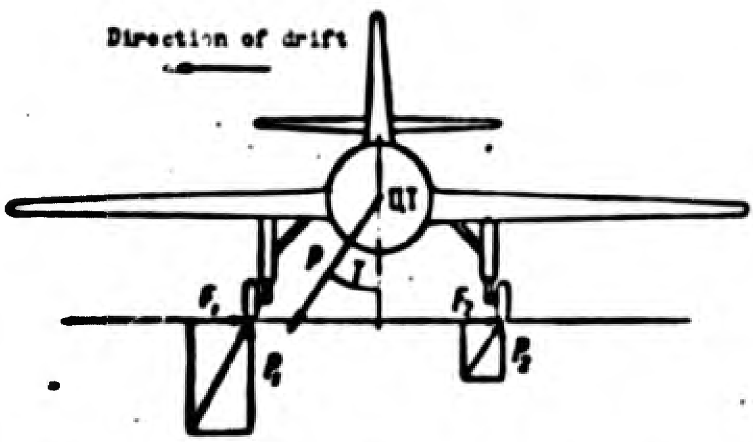

Fig. 2.40. Diagram of forces effective during landing with drift.

During landing with drift aircraft is somewhat turned against wind and is banked. At the time of contact of wheels with land, simultaneously with the vertical impact appears a lateral impact on the wheels. In this case, resultant forces of reaction will be directed at an angle to vertical (Fig. 2.40). Ratio of total lateral component of load to gross weight will be transverse acceleration $n_F = F/G$. Vertical and transverse acceleration on strut in the direction in which there is drift will be larger than in another direction. Irregularity of load is greater the larger the drift angle. Since combination of limiting V_y with maximum drift is doubtful, then magnitude of vertical load one should assume less than in case of symmetric landing.

During landing with front impact there always appear considerable frontal forces from spin-up of wheels and drag with respect to surface of airport. Attempts to lower magnitude of frontal load by means of preliminary spin-up of wheels as yet have not given positive results. Magnitude of frontal load depends on state of airport: on concrete it is less than on dry ground. With decrease in firmness of ground frontal load increases. During snow and ice cover of runway, frontal load is less than on concrete.

Load on Landing Gear, Appearing During Deceleration and Taxiing

On almost all contemporary aircraft there are brakes. Highest possible frictional forct T of wheel against surface of airport depends on limiting possible brake moment M_T for a given type of wheels. It is equal to ratio of operational moment M_T^{op} to radius of wheel R with pneumatic tire pressed by corresponding vertical load:

$$T = \frac{M_T^{op}}{R}.$$

On the other hand, frictional force of wheel completely braked against surface of airport composes

$$T = \mu P_y,$$

where μ is coefficient of friction.

For the most effective deceleration it is necessary that wheel does not slip with respect to surface of airport. This is attained by application of automata of deceleration, which lower pressure in brakes, as soon as slipping begins (decrease in angular velocity of rotation of wheels). During removal of slipping there occurs automatic feeding of pressure in brakes. Work of automaton leads to cyclical action of forces of friction with frequency 0.5-2.0 vibrations per second (Fig. 7.29). This considerably increases load nature of elements of landing gear by repeated loads.

We will consider the influence of speed and radii of turns on loads of landing gear (Fig. 2.41).

During curvilinear motion, on the aircraft acts centrifugal force

$$F = \frac{GV^2}{gr}, \tag{2.36}$$

where r is radius of turn.

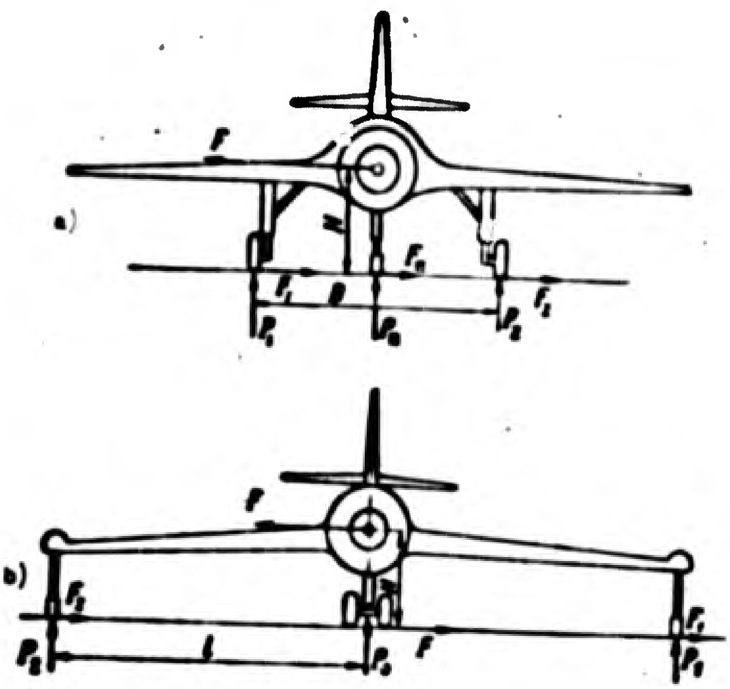

Fig. 2.41. Diagram of forces having effect on taxiing. a) tricycle landing gear; b) bicycle landing gear.

This force is balanced by frictional force of wheels:

$$F = F_1 + F_2 + F_n$$

Moment from centrifugal force is balanced by a pair of vertical forces P_1 and P_2 on struts:

$$FH = B(P_1 - P_2). \qquad (2.87)$$

We will assume wing lift equal to zero, since during speeds of taxiing it composes a small part of weight of aircraft. Then highest possible components of forces on landing gear will be obtained from following relationships:

$$\left.\begin{aligned} P_y &= \frac{1}{2}\left(1 + \frac{H}{B}\mu\right)G; \\ P_x &= \frac{\mu}{2}\left(1 + \frac{H}{B}\mu\right)G; \\ P_z &= \frac{\;}{2}\left(1 + \frac{H}{B}\mu\right)G \end{aligned}\right\} \qquad (2.88)$$

Frontal force P_x appears during deceleration for cessation of turn.

As can be seen from these relationships, limiting possible magnitude of load does not depend on speed and radius of turn. If landing gear is calculated on this load, then centrifugal force cannot be larger than one of two values:

1) value determined by frictional force (if $F > \mu G$, then slip of aircraft occurs and further increase of curvature of turn will be

impossible). Relationship between speed and radius of turn, taking into account formula (2.86), will be recorded in the form

$$V < \sqrt{\mu g r}; \tag{2.89}$$

2) value determined by moment of inversion:

$$FH > G\frac{B}{2},$$

whence

$$V < \sqrt{\frac{B}{2H} g r}. \tag{2.90}$$

For bicycle landing gear radius r and speed of turn V depend on permissible load on wing-tip strut.

Lateral force is connected with load on wing-tip strut by relationship

$$P_{\text{кр.ам}} = \frac{2H}{l} F.$$

Considering formula (2.86), we will obtain

$$V < \sqrt{\frac{lG}{2gH} P_{\text{кр.ам}} r}. \tag{2.91}$$

or, taking into account maximum frictional force μG,

$$V < \sqrt{\mu g r}. \tag{2.92}$$

Limiting vertical load in this case is determined from condition of motion of aircraft on unevenness of airport:

$$P_y = n_y \Delta G, \tag{2.93}$$

where n_y is overload caused by motion of aircraft on unevenness of airport;

ΔG is component of weight on one strut.

Limiting lateral load does not exceed frictional force ($P_z \leq \leq \mu \Delta G n_y$), since during large load will start slip of aircraft.

Loads Appearing During Motion of Aircraft on Uneven Surface of Airport

During landing run there can appear considerable loads and shock absorption, calculated from condition of absorption of work during first impact, can appear insufficient. In distinction from impact at touch-down, overloads on landing run are repeated with great frequency during a comparatively prolonged time (30-60 sec). Magnitude of overload (load on strut) depends on form and dimensions of unevenness of airport, speed, elastic characteristics of shock absorption and structure of landing gear.

For oleo-pneumatic shock absorption, during dynamic pressing of piston

$$P = P_{air+fri} + P_{man} \tag{2.94}$$

where P_{man} is force caused by flow friction during passage of liquid through hole;

$P_{air+fri}$ is force caused by drag of air and frictional force of piston.

Force P_{man}, pushing liquid through hole of plunger, is determined by excess pressure of liquid p_{liq}:

$$P_{man} = p_{liq} F, \tag{2.95}$$

where F is area of piston.

Excess pressure of liquid is determined by its impact pressure:

$$p_{liq} = \frac{\gamma v_{liq}^2}{2g}, \tag{2.96}$$

where γ is specific gravity of liquid;

v_{liq} is exhaust velocity of liquid: $v_{liq} = v_{plu} \frac{F}{\mu_{liq} f}$;

v_{plu} is speed of plunger;

f is area of passage hole for channel of liquid;

μ_{liq} is discharge coefficient, depending on form of hole, its depth, viscosity of liquid, and other factors.

Consequently,

$$P_{fr} = \frac{\gamma}{2g}\frac{F^3}{\mu^2_{liq} f^2} v^2_{sh}. \qquad (2.97)$$

Thus the main part of force on strut, caused by flow friction, is directly proportional to square of speed of piston of shock absorber. In this case force $P_{air+fri}$ it is possible not to consider, since it does not depend on speed of piston.

Selected curve of change of forces along the stroke of the piston corresponds to defined speed of the latter at different moments of pressing of strut. During motion on unevenness of airport, speed of shift of axis of wheel depends on form of unevenness, speed, and vibrations of aircraft.

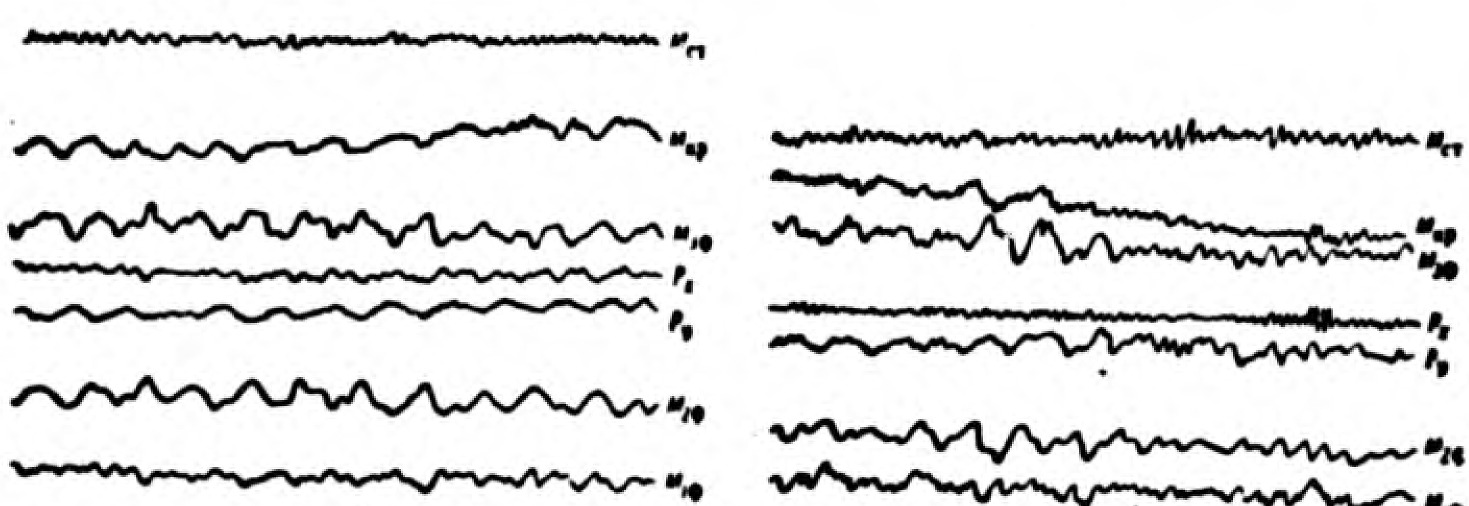

a) b)

Fig. 2.42. Character of loads during takeoff run a) and landing run b) of an aircraft. M_{sta}, M_{wi} and M_{fus} – bending moments of stabilizer, wing, and fuselage, respectively; 1, 2, 3 – numbers of sections, P_x and P_y are loadson main strut of landing gear.

On takeoff run motion of aircraft is calmer than on landing run, since there are no vibrations caused by first impact at touch-down and intense deceleration (Fig. 2.42). However, during takeoff run, weight of aircraft is maximum and for jet aircraft considerably exceeds landing. For instance, for heavy aircraft maximum takeoff weight can exceed landing weight 2 times. Due to this, loads on elements of structure of landing gear during takeoff run can be calculated loads.

Maximum loads during takeoff run appear during relatively low speed in the beginning of run. According to increase of speed, dynamic part of load considerably increases; however, maximum load nevertheless becomes less, since total load on landing gear decreases due to growth of wing lift. After breakaway of aircraft, wheels must be braked since rotation of wheels because of their instability may cause considerable vibrations and sign-alternating loads in elements of landing gear.

During landing run of aircraft it can happen that rate of climb of wheel on unevenness of airport will be larger than terminal velocity of motion of piston. In this case there will occur an unabsorbed impact, whose force will depend on elastic properties of structure and deformation of pneumatic tire.

Maximum loads on landing run appear at speed of aircraft (0.6-0.8) V_{land}. Since deformations of structure of aircraft are relatively small, then magnitude of load is basically determined by work of pneumatic tire. During large dimensions of wheels (D = 1000 mm), overload does not exceed 2.0 when crossing obstacles with unevenness 0.1-0.2 m high. During small dimensions of wheels, overloads can attain considerable magnitudes (up to 3-4).

For lowering loads during fast motion of piston of shock absorber there is established a safety valve for channel of liquid, adjusted to a defined magnitude of pressure, or there is ensured on part of the stroke an increased channel of liquid so that in this section works only air.

If height of unevenness is larger than possible pressing of pneumatic tire to rim δ_{max}, then at great speed, due to disturbance of operating conditions of shock absorber, overload acting on the aircraft during crossing of obstacles will be determined by form of obstacle and speed of aircraft.

We will consider for example motion of aircraft along a sinusoidal wave of unevenness with length L and height H. Motion of center of gravity during non-operating shock absorption will be determined by equation

$$h_{c.g} = (H - \delta_{max}) \sin \frac{\pi V}{L} t.$$

In this case overload will be

$$n = \frac{\ddot{h}_{c.g}}{g}$$

or

$$n = (H - \delta_{max}) \frac{V^2}{L^2} \frac{\pi^2}{g}, \qquad (2.98)$$

where V is forward velocity of aircraft.

For instance, at V = 30 m/sec, L = 2 m, $H - \delta_{max}$ = 3 cm, overload in center of gravity will be 6.8.

Forces Acting on Landing Gear in Flight

Loads experienced by landing gear because of drag or forces of inertia during fulfillment by aircraft of figures, are comparatively small. However, they can be calculated loads for retracting mechanism of landing gear, for locks holding landing gear in retracted position and for shields of landing gear. Mechanism of retracting works during lowering and retracting of landing gear, when speed of flight of aircraft does not exceed speed permissible for landing gear $V_{per\ l.g}$.

Gusts of bumpy air are possible. On landing gear act aerodynamic and inertial forces. Aerodynamic forces are determined for speed $V_{per\ 1.g}$ and, correspondingly, overloads from gusts of bumpy air at this speed are found. Inertial forces are determined by magnitude of overload of aircraft.

During calculation of aerodynamic forces acting on shields, one should consider possible deformations of shields, which can lead to considerable change of aerodynamic forces and disturbance of their calculated distribution during retracting of landing gear. Locks of landing gear are calculated on limiting overloads which are possible on a given aircraft.

On skis, in view of great their lifting surface, act considerable aerodynamic forces, which are calculated for shock absorbers, safety ropes, and separate nodes of bracing.

2.11. Loads Effective on Motor

Loads acting on mounting lugs of motor are determined by forces of inertia and reactions from thrust and torque of motor. Magnitude of these forces depends on type of motor, maneuverability of aircraft, and place of installation of motor on aircraft. During their determination are considered in different flight cases symmetric maneuvers with maximum and minimum overloads, slip, and spin. Inertial and aerodynamic forces are considered effective simultaneously with loads caused by work of motor at maximum and zero thrust. For motor with propellers one should additionally consider case of negative thrust, and also consider reactive moment of propeller. In landing cases action is considered of vertical and lateral loads.

Frames of piston and turbo-prop motors are subjected to action of vibrations caused by unbalanced forces of revolving parts of motor and propeller. Therefore, in their bracing nodes are placed shock absorbers preventing transmission of structural vibrations of aircraft. On turboprop motors level of vibration is small and their structural bracing usually is rigid. Calculation overloads for bracing of motor because of vibrations are somewhat larger than for remaining parts of structure of aircraft.

In the case of console bracing of motor on wing during dynamic loads (gust of bumpy air, landing) there are observed large vibrations of the motor. Overload in the center of gravity of the motor can increase 1.5-3 times as compared to overloads in the center of gravity of the aircraft.

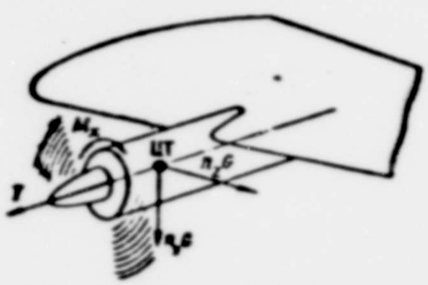

Fig. 2.43. Diagram of forces acting on turboprop motor.

As an example on Fig. 2.43 is given a diagram of basic forces acting on turboprop motor located on wing.

Mass force is determined by product of weight of propulsion system G_{mot} by corresponding overload n_y:

$$P_y = G_{mot} \cdot n_y \qquad (2.99)$$

Rocket moment one can determine from relationship

$$M_k = 716.2 \frac{N}{n}. \qquad (2.100)$$

where N is power of motor;

n is turns of propeller in minutes

In curvilinear flight overloads from acceleration increase overload in center of gravity of motor as compared to overload in center of gravity of aircraft:

$$n_{mot} = n_y + \frac{\varepsilon x}{g}. \qquad (2.101)$$

where ε is angular acceleration of aircraft;

x is distance between centers of gravity of motor and aircraft along longitudinal axis of aircraft.

In curvilinear flight there appears also gyroscopic moment of revolving masses of motor (turbines, compressor) and propeller. Value of gyroscopic moment is

$$M_g = J_x \omega_x \omega_1 \tag{2.102}$$

where J_x is moment of inertia of revolving parts of motor;

ω_x is angular velocity of rotation of parts of motor:

ω_1 is angular velocity of rotation of aircraft.

Plane of action of gyroscopic moment is perpendicular to plane of rotation of aircraft.

Magnitude of transverse accelerations of motor is relatively small and does not exceed unity. In most cases construction of bracing of motor in lateral direction is more durable than this is required by actual loads.

On cowlings of motors act aerodynamic and inertial loads. Inertial load composes a small part of total load. Aerodynamic loads increase because of influence of compressibility of air at high speeds of flight. Distribution of aerodynamic loads on gondolas of motor is determined by testing models in a wind tunnel. For bracing of cowlings it is necessary to take raised safety factors, since, besides aerodynamic forces, they are subjected to action of variables of loads from vibrations of motor.

2.12. Loads Acting on Fuselage

Basic forms of loads acting on fuselage, are reactions from forces applied to other parts of aircraft (wing, empennage, landing gear, power installation, and so forth). Simultaneously, fuselage is loaded by inertial forces of masses of cargo and units located inside aircraft and the mass of its own structure. Furthermore, on surface of fuselage act aerodynamic forces of rarefaction and pressure, at certain points attaining 0.7-1.0 kg/cm^2.

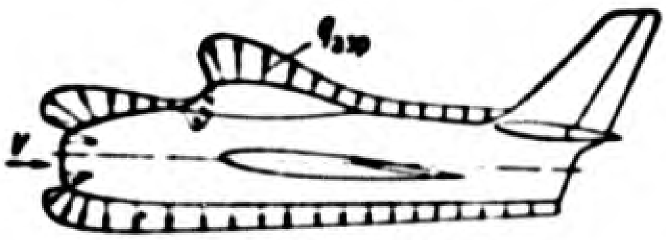

Fig. 2.44. Distribution of aerodynamic loads on surface of fuselage.

On Fig. 2.44 is presented approximate distribution of local aerodynamic loads acting on fuselage in flight. In central part of fuselage there occurs considerable redistribution of aerodynamic load, caused by influence of wing. In pressurized cabins of fuselages appear large forces from internal excess pressure (0.4-0.6 kg/cm^2).

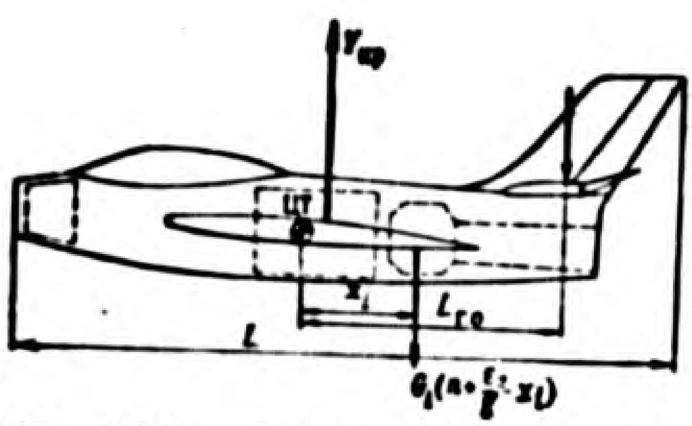

Fig. 2.45. Forces acting on fuselage in flight.

On Fig. 2.45 is shown a diagram of action of forces on fuselage in curvilinear flight — aerodynamic forces of wing and empennage, inertial forces appearing from action of overload along trajectory $n\Delta G_{1o}$ and angular acceleration $\frac{\varepsilon x}{g}\Delta G_{1o}$

Normal component from reaction of wing is

$$Y_{кр} = n(G - G_{кр}) - P_{г.о}. \tag{2.103}$$

Load on empennage is

$$P_{г.о} = P_{ур} + \Delta P. \tag{2.104}$$

where ΔP is maneuvering load.

Force ΔP leads to angular acceleration of aircraft

$$\varepsilon_z = \frac{\Delta P L_{г.о}}{J_z}, \tag{2.105}$$

where $J_z = \frac{G}{g} i_z^2$ is mass moment of inertia of aircraft around axis z;

i_z is radius of gyration of aircraft with respect to axis z ($i_z \approx 0.16L$);

L is length of aircraft.

From acceleration ε_z at any point of aircraft there appears additional overload

$$n_i = \frac{\varepsilon_z}{g} x_i$$

Full overload can be determined by algebraic sum of all components:

$$n_i = n \pm \frac{\varepsilon_z}{g} x_i \tag{2.106}$$

During first impacts on landing, aircraft experiences action of forces from landing gear; at the time of first contact, lift is approximately equal to weight of aircraft.

On cargo and fuselage acts overload at any point, equal to $n_1 = 1 + \frac{P_y}{G}$.

From moments $P_y a$ and $P_x b$ is obtained angular acceleration $\varepsilon_z = (P_y a + P_x b)J_z$, creating at point 1 additional overload

$$n_1 = \frac{\varepsilon_z}{g} r_1$$

perpendicular to radius r_1 (Fig. 2.46).

Full overload at point 1 is determined by geometric sum of both components of overload.

Loads during landing carry a dynamic character and cause considerable vibrations of fuselage, as a consequence of which appear

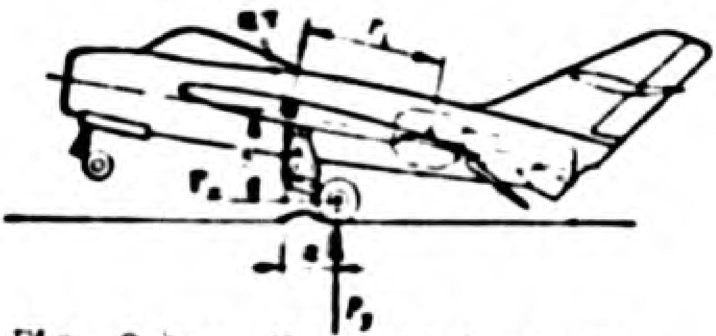

Fig. 2.46. Vertical loads on fuselage during landing.

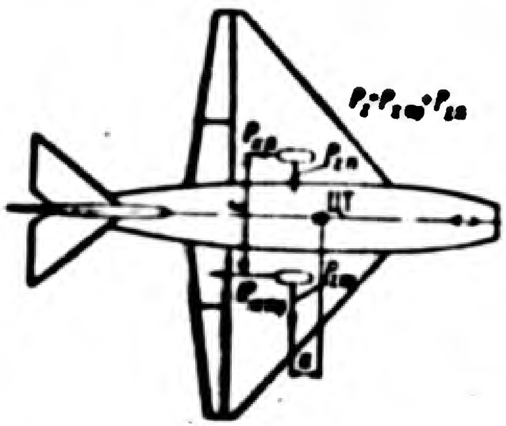

Fig. 2.47. Lateral loads on fuselage during landing.

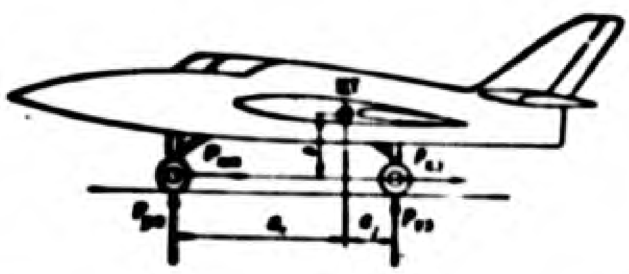

Fig. 2.48. Forces acting on fuselage of aircraft with bicycle landing gear during landing.

additional inertial forces. During landing run, as speed decreases, wing lift decreases, and magnitude of variables of loads from landing gear increase. These sign-alternating loads are caused by unevenness of surface of airport and nonuniform deceleration. During run also appear additional loads from front strut and corresponding moments M_z and M_y.

Besides symmetric loads, during landing lateral loads act (Fig. 2.47). Overload from lateral forces is

$$n_z = \frac{\Sigma P_z}{G}.$$

During three-wheeled diagram of landing gear, because of inequality of forces P_x on right and left struts and force P_z there appears moment

$$M_y = \Sigma P_z a + \frac{c}{2}(P_{x\,rl} - P_{x\,le}), \qquad (2.107)$$

where $P_{x\,rl}$ and $P_{x\,le}$ are frontal loads on right and left struts;

c are base of landing gear.

This moment corresponds to acceleration

$$\varepsilon_y = \frac{\Sigma P_z a + \frac{c}{2}(P_{x\,rl} - P_{x\,le})}{I_y}. \qquad (2.108)$$

In the considered case, inertial forces are determined by a method analogous to that shown during symmetric load.

For aircraft with bicycle landing gear (Fig. 2.48) moments acting on fuselage are determined from relationships

$$\left.\begin{aligned} M_y &= P_{z\,fr} a_1 - P_{z\,rear} a_2; \\ M_x &= P_{y\,fr} a_1 - P_{y\,rear} a_2 - (P_{z\,fr} + P_{z\,rear}) b. \end{aligned}\right\} \tag{2.109}$$

where $P_{z\,fr}$ and $P_{z\,rear}$ are lateral loads on front and rear struts, respectively;

$P_{y\,fr}$ and $P_{y\,rear}$ are vertical loads on front and rear struts, respectively.

Loads effective in flight in a lateral direction are basically determined by load of vertical empennage. During rudder deflection (fin) on vertical empennage acts force

$$P_{v.e} = P_{np} + \Delta P_{v.e}. \tag{2.110}$$

causing slip of aircraft. Moment from forces acting on empennage $M_{v.e} = P_{v.e} L_{v.e}$ is balanced by moment from forces acting on fuselage, wing, and gondola of motor, and also by inertial forces of aircraft. Additional overload at i-th point of aircraft from angular acceleration

$$\varepsilon_y = \frac{\Delta P_{v.e} L}{J_y} \tag{2.111}$$

is equal to $n_i = \frac{\varepsilon_y}{g} r_i$ and is perpendicular to radius r_i. In reference to masses found in fuselage, one can determine overload by the formula

$$n_i = n_0 + \frac{\varepsilon_y}{g} r_i$$

During asymmetric stop of motors located on wing, on fuselage additionally can act considerable loads. Sometimes these loads can be calculated.

Calculation Conditions for Fuselage of Passenger Aircraft

For guarantee of normal living conditions to passengers and crew cabins of high-altitude aircraft are hermetic and in them is created excess pressure p_{exc} = 0.4-0.6 kg/cm^2 (as compared to atmospheric pressure at altitude of flight). Character of change of pressure in cabin with respect to altitude of flight is shown in Fig. 2.49.

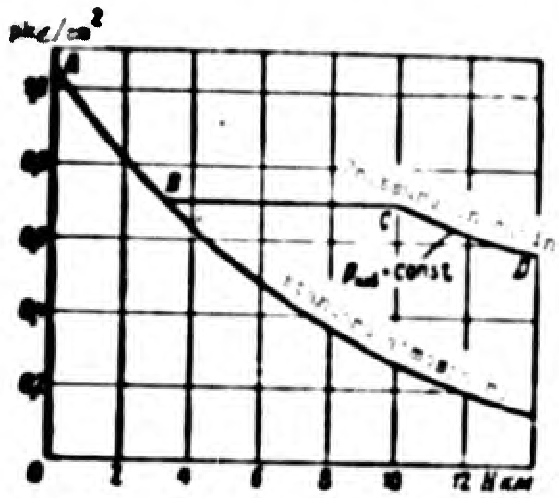

Fig. 2.49. Graph of change of excess pressure in pressurized cabin.

In section AB pressure in cabin is equal to atmospheric; in section BC in cabin is maintained constant pressure; in section CD is maintained constant pressure drop (p_{exc} as compared to atmospheric).

In flight, the structure of the pressurized cabin is constantly subjected to action of internal pressure. Considering possible errors in the operation of equipment for adjustment of excess pressure in the cabin, during calculation of strength p_{exc} is assumed 10-20% higher than nominal for a given aircraft. During design of pressurized cabin there should be considered possible joint action of flight loads (maneuver, flight in turbulence) and excess pressure.

In contemporary passenger aircraft the hermetically sealed section of the fuselage occupies large part of its length, and volume of pressurized cabin can attain 200-300 m^3. During supercharging of cabin, energy of compressed air in hermetic part of fuselage attains 1-3 million kgm. Appearance of a small crack in the sheathing of the fuselage, because of the great energy of the compressed air, can lead to explosive destruction of the fuselage. In connection with this, especially thoroughly conducted is the analysis of load and strength of a hermetic fuselage. Along with consideration of basic calculation cases, one should allot considerable attention to analysis of strength from the action of local loads (from influence of partitions, auxiliary nodes, and so forth), in order to prevent appearance in structure of fuselage of local cracks.

For strength of a hermetic fuselage are presented following basic requirements:

a) in zones of cuts and other places of concentration of stresses it is necessary to create a structure ensuring several ways of transmission of loads with general safety factor not less than 3.0;

b) for the remaining structure of the aircraft fuselage, during calculation of strength in case of action of pressure of supercharging, it is expedient to take safety factor 2, since operational excess pressure is created in every flight;

c) for flight loads, safety factor can be less since probability of obtaining maximum operational loads of this type is small;

d) for "glasswork" one should take a raised safety factor equal to 4-6 since the glass-like material has unstable characteristics of strength.

The fuselage of a passenger aircraft has raised requirements for strength also in landing cases of load, in order to ensure safety of passengers during exceptionally hard (emergency) landings, when structure of landing gear can completely exhaust its carrying ability. With this goal, during strength analysis of fuselage structure is taken a raised safety factor (10-20% larger than for design of landing gear).

Additionally are considered following cases of crash landing:

- landing with front gear up;
- belly landing;
- landing with a ground loop of the aircraft;
- landing on water of a landplane.

Magnitude of calculated overload is selected from 3 to 8 depending upon type of emergency case. Possibility of crash landing also presents raised requirements for bracing of seats, safety belts, and cargo. It is known that a person can sustain on safety belts a brief (emergency) overload in "spine-breast" direction up to 50-60. However, for such overloads it is practically impossible to ensure strength of bracing of seats and cargo. Usually for passenger aircraft, loads on safety belts are determined based on a calculated overload of the order of 8-12. Bracing of cargo, breakdown of which presents danger for passengers, should also be designed for these overloads.

CHAPTER III

BASIC INFORMATION FROM THEORY OF OSCILLATIONS. NATURAL OSCILLATIONS OF PARTS OF FLYING APPARATUSES

List of Designations Appearing in Cyrillic

вр = rot = rotation
в.ш. = d.h = drag hinge

изг = flex = flexural

кр = cr = critical
кр = wi = wing
кр = tor = torsional

ст = st = static

т = th = thrust
тон = tone

ц = cen = centrifugal

ш = h = hinge

For solution of many problems connected with study of dynamic loads and their action on structure assumptions from the theory of oscillations are used. Therefore, below described is basic information from the theory of oscillations.

During calculations of dynamic strength of aviation structures, during the analysis of flutter and action of dynamic loads on structure, it is necessary to know frequency and form of oscillations. In this chapter information is given on natural oscillations of parts of flight vehicles.

During the analysis of dynamic characteristics of elastic structures we distinguish natural, forced, parametric, and self-exciting oscillations (natural oscillation). In this chapter are considered natural and forced oscillations of the simplest systems and structures.

3.1. Oscillations of Linear Systems with One Degree of Freedom

During small oscillations, occurring within limits of linear dependence of deformation of system on acting force, fundamental equations of its motion are expressed by linear differential equations. Such oscillatory systems are called linear.

Natural Oscillation in Linear System with One Degree of Freedom

Let us assume that on a spring is suspended a body of mass m (Fig. 3.1). Mass of spring, as compared to mass of body, it is possible to disregard. Body has freedom of motion only in vertical direction and it is possible to consider it as a material point.

On such a system, removed from a state of equilibrium and left to itself, act restoring force of spring ky, directly proportional to rigidity k and deflection y(t) of system from position of equilibrium, and force of inertia $m\ddot{y}$.

From condition of equilibrium of these forces is obtained equation of motion of an oscillatory system with one degree of freedom in the absence of damping:

$$m\ddot{y}+ky=0. \tag{3.1}$$

Designating

$$p^2=\frac{k}{m}. \tag{3.2}$$

we will obtain equation of motion in the following form:

$$\ddot{y}+p^2y=0. \qquad (3.3)$$

Solution of this differential equation depends on initial

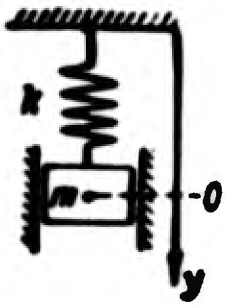

Fig. 3.1. Oscillatory system with one degree of freedom without damping.

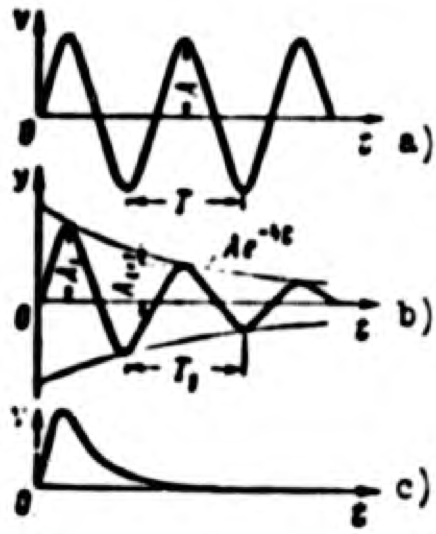

Fig. 3.2. Free oscillations in a system with different damping. a) h = 0; b) h < p; c) h > p.

conditions. Thus, if at time t = = 0, $y = y_0$ and $\dot{y} = \dot{y}_0$, then solution of equation will be

$$y=\frac{\dot{y}_0}{p}\sin pt+y_0\cos pt$$

or in other form

$$y=A\sin(pt+\alpha). \qquad (3.4)$$

where $A = \sqrt{\left(\frac{\dot{y}_0}{p}\right)^2 + y_0^2}$ is amplitude of displacement;

$\alpha = \text{arc tan}\,\frac{py_0}{\dot{y}_0}$ is initial phase.

Motion expressed by formula (3.4) is sinusoidal or harmonic. It is completely repeated after certain interval of time $T = 2\pi/p$, called period of oscillation (Fig. 3.2a).

Magnitude p is called angular frequency (name follows from vector interpretation of oscillatory motion).

From equation (3.3) it is clear that angular frequency is only parameter characterizing oscillatory system. It depends only on properties of the actual system and is called natural angular frequency of system.

Magnitude, reverse to period,

$$f=\frac{1}{T}=\frac{p}{2\pi} \qquad (3.5)$$

is called frequency of oscillations.

Period and frequency of oscillations, taking into account (3.2), it is possible to record in the form

$$T=2\pi\sqrt{\frac{m}{k}}, \qquad (3.6)$$

$$f=\frac{1}{2\pi}\sqrt{\frac{k}{m}}. \qquad (3.7)$$

They are determined only by parameters (mass and rigidity) of the oscillatory system itself and are called period and frequency of natural oscillations of system.

Harmonic oscillatory motion, expressed by formula (3.4), can be also characterized by speed and acceleration of this motion:

$$\dot{y}=pA\cos(pt+\alpha),$$

$$\ddot{y}=-p^2A\sin(pt+\alpha).$$

Oscillations of speed and acceleration have the same frequency p as oscillations of displacement, but are shifted in phase, correspondingly, by $\pi/2$ and π. Amplitude of speed is equal to $v = pA$, and amplitude of acceleration $j = p^2A$. If one were to replace p by the formula (3.5), then amplitude of acceleration is

$$j=4\pi^2f^2A.$$

This magnitude frequently is called vibration acceleration and can be expressed in fractions of g — acceleration due to gravity:

$$j \approx \frac{f^2 A}{250} g. \qquad (3.8)$$

where f is in oscillations per second, and A is in mm.

This magnitude, divided by g and equal to

$$n = \frac{f^2 A}{250}, \qquad (3.9)$$

is dimensionless and is called vibration overload.

Values of vibration acceleration and vibration overloads, calculated by the formulas (3.8) and (3.9), are 0.6% less than their exact values, but they are convenient for calculation and are frequently applied in practice.

In real oscillatory systems there always appear resisting forces to motion (frictional forces), and natural oscillations caused by initial external perturbation gradually attenuate.

Resisting forces can be external and internal. The most important are:

1) drag, proportional to speed (viscous drag);

2) drag, proportional to square of speed;

3) constant resisting force (dry friction);

4) internal drag (hysteresis).

During oscillations of parts of flight vehicles in the flow of air, resisting forces are composed of external forces (drag of medium) and internal forces (elastic hysteresis). For certain elements of structure (for instance, controls of the vehicle) force of dry friction can also appear essential.

For low speeds of flight (during small Re) resisting forces of air medium are proportional to first degree of speed. With increase of speed (Re) resisting forces become proportional to second degree of speed. During solution of problems of oscillations of aircraft and helicopters, resisting force of air medium it is possible to consider proportional to first degree of speed of oscillations.

Forces of internal friction, as yet, have been insufficiently studied. Considering that forces of internal friction (hysteresis losses) are comparatively small and compose only a certain share of total resisting forces acting on structure in flow of air during its small oscillations, it is possible to assume forces of internal drag in materials proportional to speed.

In the case of an oscillatory system with one degree of freedom during the action of resisting forces proportional to first degree of speed, equation (3.1) will take the form

$$m\ddot{y}+c\dot{y}+ky=0, \qquad (3.10)$$

where $c\dot{y}$ is resisting force;

c is coefficient of resisting force.

After dividing all members of this equation by m and designating

$$2h=\frac{c}{m}, \qquad (3.11)$$

we will obtain equation of damped oscillations:

$$\ddot{y}+2h\dot{y}+p^2y=0, \qquad (3.12)$$

where h is attenuation factor.

Process of motion, represented by equation (3.12), is determined by magnitudes p and h from formulas (3.2) and (3.11), which are connected with parameters of system and do not depend on perturbing forces. If $p > h$, i.e., if attenuation is not too great, equation (3.12) has a general solution of the form

$$y = Ae^{-ht}\sin(p_1 t + \alpha), \tag{3.13}$$

where amplitude A and phase α are determined by initial conditions, but angular frequency of damped oscillations

$$p_1 = \sqrt{p^2 - h^2}. \tag{3.14}$$

If attenuation is not great, then it little affects natural frequency and it frequently is disregarded.

A graph of motion described by formula (3.13) is presented on Fig. 3.2b. As can be seen, during damped oscillations motion is not completely repeated. But time between consecutive passages (in one direction) of a fluctuating system of position of equilibrium remains constant. This period is called period of damped oscillations. Period T_1 of damped oscillations little differs from period T of undamped natural oscillations of the system, if attenuation factor is small. During damped oscillations, just as during harmonic magnitude of extreme deflection of system from position of equilibrium is called amplitude of oscillations.

Amplitudes of damped oscillations decrease according to the law Ae^{-ht}. Relation of amplitudes of two neighboring deflections in one direction composes magnitude

$$\frac{A_i}{A_{i+1}} = \frac{Ae^{-ht}}{Ae^{-h(t+T_1)}} = e^{hT_1}. \tag{3.15}$$

Equality (3.15) is valid during any i. Natural logarithm of two consecutive amplitudes

$$\delta = \ln e^{hT_1} = hT_1 \tag{3.16}$$

is called logarithmic damping decrement, or damping decrement.

Considering expression (3.5), it is possible to present damping decrement in the form

$$\delta = 2\pi\frac{h}{p_1}. \qquad (3.17)$$

Attenuation factor h* has dimension of 1/sec. Damping decrement is dimensionless value and characterizes damping rate. Magnitude $1/\delta$ is equal to number of oscillations, after which amplitude decreases e times.

From expression (3.14) it is clear that, depending upon magnitude of attenuation factor, angular frequency p_1 can take real values (at $h < p$), zero value (at $h = p$) and imaginary values (at $h > p$). In the first case motion carries a periodic** (oscillatory) character; in the last one – nonperiodic; oscillations are absent, and slow motion toward position of equilibrium occurs (Fig. 3.2c). The case of zero angular frequency is the boundary between these two cases of motion of the system. Damping, corresponding to this case, is called critical:

$$\left.\begin{aligned} h_{\text{кр}} &= p = \sqrt{\frac{k}{m}}; \\ c_{\text{кр}} &= 2mh_{\text{кр}} = 2mp. \end{aligned}\right\} \qquad (3.18)$$

Forced Oscillations of a Linear System with One Degree of Freedom

Oscillation under the effect of external forces are called forced, and external forces – disturbing.

---

*There is also applied reciprocal

$$\tau_0 = \frac{1}{h} = \frac{2m}{c},$$

which has dimension of sec and is called time constant.

**It is necessary to consider conventionality of term "periodic," since during damped oscillations motion is not completely repeated, and, strictly speaking, it is not periodic.

During action of disturbing force always simultaneously appear free and forced oscillations. Free oscillations usually attenuate rapidly and in most cases forced oscillations present the basic interest. It is necessary, however, to consider conventionality of term "free" oscillations since they are caused by the same forces as forced oscillations.

Let us assume that on linear system (Fig. 3.3a) acts disturbing force P(t), which is an assigned function of time. Equation of motion of such a system has the form

$$\ddot{y} + 2h\dot{y} + p^2 y = \frac{1}{m}P(t). \tag{3.19}$$

It differs from equation of free oscillations (3.12) by the presence of a right side. General solution of equation (3.19) is composed of solution of uniform differential equation (3.12), determining natural oscillations of system, and particular solution of equation (3.19) with right side, determining forced oscillations. Solution has the form

$$y = y_1 + \frac{e^{-ht}}{mp_1}\int_0^t P(\tau)e^{h\tau}\sin p_1(t-\tau)\,d\tau, \tag{3.20}$$

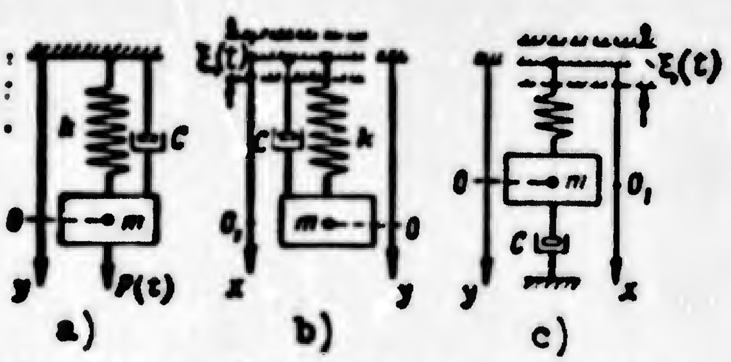

Fig. 3.3. Excitation of oscillation in linear systems with one degree of freedom. a) force is applied to mass; b and c) assigned motion of point of bracing (b-damping is proportional to relative velocity of mass; c-damping is proportional to absolute velocity of mass).

where first member signifies free oscillations determined by initial conditions, and has expression (3.13), and second member determines oscillations caused by disturbing force.

We will consider action of different disturbing forces on an oscillatory system.

Action of harmonic disturbing force. Beats. Resonance. Let us assume that disturbing force is changed according to the law

$$P(t)=P_0\sin\omega t. \tag{3.21}$$

where P_0 is amplitude of force;

ω is angular frequency of disturbing force.

In the absence of damping, equation of forced oscillations will be

$$\ddot{y}+p^2y=\frac{P_0}{m}\sin\omega t. \tag{3.22}$$

General integral of equation (3.22) we will find from formula (3.20), considering h = 0:

$$y=y_1+\frac{P_0}{mp}\int_0^t\sin\omega\tau\sin p(t-\tau)\,d\tau. \tag{3.23}$$

Calculating integral in expression (3.23) and designating

$$\frac{P_0}{mp^2}=\frac{P_0}{k}=y_{st} \tag{3.24}$$

for case $\omega \neq p$, we will obtain

$$y=y_1+\frac{y_{st}}{1-\frac{\omega^2}{p^2}}\left(\sin\omega t-\frac{\omega}{p}\sin pt\right). \tag{3.25}$$

where y_{st} is deflection which system will obtain during "static" application of force P_0.

If disturbing force acts on a system at rest (during zero initial conditions), then $y_1 = 0$.

We will consider in greater detail second member of expression (3.25), describing motion of system under action of disturbing force.

Disturbing force causes oscillations with frequencies p and ω, i.e., with frequency of natural oscillations and with frequency of disturbing force. Resultant oscillation will not be harmonic.

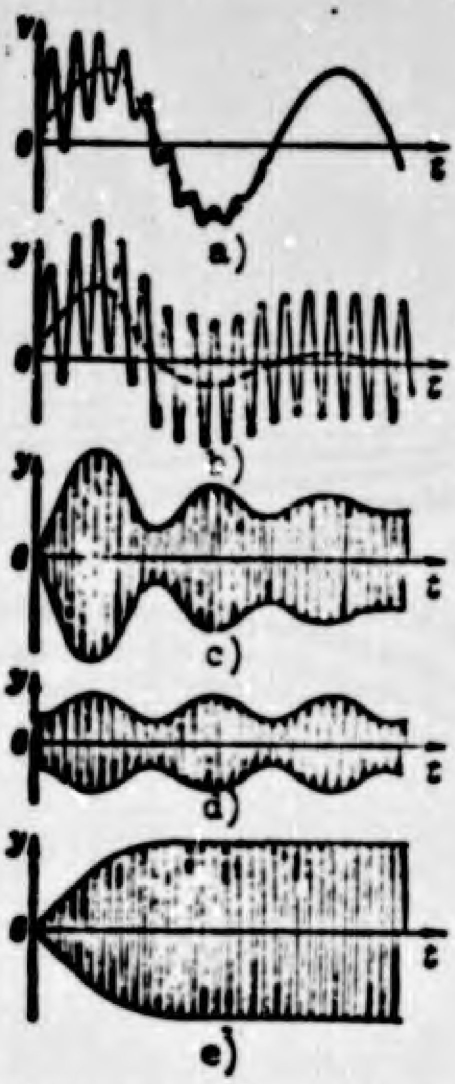

Fig. 3.4. Process of establishment of forced oscillations under the action of a disturbing force. a) $\omega \ll p$, b) $\omega \gg p$, c) $\omega \sim p$, d) $\omega_1 \sim \omega_2$, e) $\omega = p$.

Character of oscillations under action of a harmonic disturbing force, in many respects, depends on relationship of frequencies of forced and natural oscillations.

We will assume that $\omega \ll p$. Considering that in real systems natural oscillations attenuate rapidly, total oscillations under the action of disturbing force will have form shown on Fig. 3.4a. During $\omega \gg p$ oscillations will have form shown on Fig. 3.4b.

If $\omega \sim p$, then, assuming that $\omega/p = 1$ before sin pt, and considering only second member in expression (3.25), we will obtain

$$y = \frac{2y_{ст}}{1-\frac{\omega^2}{p^2}} \sin\frac{\omega-p}{2}t \cdot \cos\frac{\omega+p}{2}t. \qquad (3.26)$$

Motion described by expression (3.26), it is possible to consider as harmonic oscillations with frequency $\frac{\omega + p}{2}$ (period $T = \frac{4\pi}{\omega + p}$) and variable amplitude

$$A = \frac{2y_{ст}}{1-\frac{\omega^2}{p^2}} \sin\frac{\omega-p}{2}t,$$

period of change of which is equal to

$$T_1 = \frac{4\pi}{\omega-p}.$$

Graph of motion, corresponding to formula (3.26), is represented on Fig. 3.4c. From this graph it is clear that near resonance oscillations constitute beats. Basic oscillations with frequency $\omega - p$ have variable amplitude. Period of beat T_1 is determined by difference of frequencies of disturbing force and natural oscillations.

Because of damping of natural oscillations, beats also in time attenuate and pass into steady forced oscillations.

The same result will be obtained if on oscillatory system simultaneously act two disturbing forces with close frequencies ($\omega_1 \approx \omega_2$). But in this case, beats will have an undamped character (Fig. 3.4d).

Very important is case $\omega = p$. This is so-called case of resonance. During resonance amplitude of forced oscillations

$$A = \frac{y_{st}}{1 - \frac{\omega^2}{p^2}} \tag{3.27}$$

in the absence of damping will be infinitely large.

Designating by q the ratio of forced oscillations to natural frequency of system

$$\frac{\omega}{p} = q, \tag{3.28}$$

formula (3.27) it is possible to present in the form

$$A = \frac{y_{st}}{1 - q^2}. \tag{3.29}$$

During very small frequencies of disturbing force ($q \ll 1$) amplitude of forced oscillations is almost equal to static deflection of system; at $q \to 1$ amplitudes of oscillation begin to increase and at $q = 1$ become infinitely large. At $q > 1$ oscillations decrease and at $q \to \infty$ amplitude of oscillations approaches zero; system, as it were, cannot react to changes of external force (see Fig. 3.5).

Expression for amplitudes during resonance can be obtained if in the common solution (3.23), expression (3.21) for force P(t) is replaced by the following:

$$P(t)=P_0 \sin pt.$$

Then during zero initial conditions, expression for oscillations during resonance will have the form

$$y=-\frac{1}{2}\frac{P_0}{mp}t\cos pt.$$

Thus amplitude of oscillations during resonance

$$A=\frac{1}{2}\frac{P_0}{mp}t$$

linearly depends on time. Consequently, during resonance there will be no steady-state oscillations (in the absence of damping), and oscillations will increase proportionally to time as this is shown on Fig. 3.4e in the left part of graph. Damping strongly affects oscillations, namely in the region of resonance, limiting "resonance" amplitudes. However, in systems with little damping, build-up of amplitudes during resonance, in initial moment occurs approximately as shown on Fig. 3.4e. This deduction is important in that relation that is possible fast transition through resonance. Under this condition of amplitude of oscillations will not be too large.

Let us consider now the influence of damping on forced oscillations.

Equation of forced oscillations of a system with damping, under action of forced (3.21), has the form

$$\ddot{y}+2h\dot{y}+p^2y=\frac{P_0}{m}\sin\omega t. \tag{3.30}$$

Forced oscillations can be determined from general solution (3.20) by substitution of value $P_0 \sin \omega t$ instead of $P(t)$. It is simpler, however, to find particular solution of equation (3.30) in the form

$$y = a \sin \omega t + b \cos \omega t. \tag{3.31}$$

This solution has the final form

$$y = \frac{P_0 (p^2 - \omega^2)}{m[(p^2 - \omega^2)^2 + 4h^2\omega^2]} \sin \omega t - \frac{2P_0 h\omega}{m[(p^2 - \omega^2)^2 + 4h^2\omega^2]} \cos \omega t. \tag{3.32}$$

Considering formulas (3.24) and (3.28) and designating

$$2\frac{h}{p} = 2\frac{h}{h_{кр}} = \gamma, \tag{3.33}$$

it is possible to record expression (3.32) in the form

$$y = A \sin(\omega t - \alpha), \tag{3.34}$$

where A is amplitude of forced oscillations:

$$A = \frac{y_{ст}}{\sqrt{(1 - q^2)^2 + q^2\gamma^2}}; \tag{3.35}$$

α is phase angle between oscillations (shifts) system and oscillations of disturbing force:

$$\alpha = \operatorname{arctg} \frac{q\gamma}{1 - q^2}; \tag{3.36}$$

γ is damping factor, which constitutes relation of real damping in system to critical.

Damping factor, taking into account formulas (3.14), (3.17) and (3.33), is connected with logarithmic damping decrement by dependence

$$\delta = \frac{\pi\gamma}{\sqrt{1 - \left(\frac{\gamma}{2}\right)^2}}, \tag{3.37}$$

whence

$$\gamma = \frac{\delta}{\pi\sqrt{1 + \left(\frac{\delta}{2\pi}\right)^2}}. \tag{3.38}$$

During small damping $\gamma \approx \frac{\delta}{\pi}$.

Ratio of amplitude of forced oscillations (3.35) to deflection y_{st} of system during static application of force is called coefficient of dynamics λ (amplification factor):

$$\lambda = \frac{A}{y_{st}} = \frac{1}{\sqrt{(1-q^2)^2 + q^2\gamma^2}}. \qquad (3.39)$$

It shows degree of dyanmic "receptivity" ("responsiveness") of system to oscillations of disturbing force. Coefficient of dynamics depends only on relation of frequencies q and damping (damping factor γ).

Dependence of dynamics coefficient λ on q for different γ is shown on Fig. 3.5. Region of frequencies, where $\lambda > 1$, is called

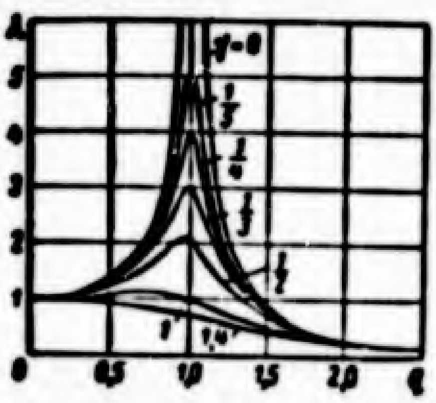

Fig. 3.5. Resonance curves.

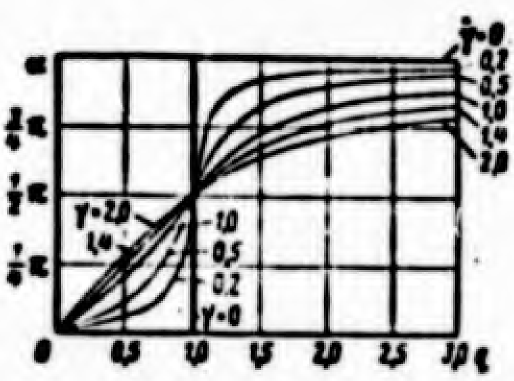

Fig. 3.6. Phase responses.

region of resonance. As can be seen from resonance curves, damping most strongly affects magnitude of amplitudes in region of resonance where maximum λ is attained during resonance frequency somewhat smaller than natural without damping. However, this distinction is small. Considering q = 1, by formula (3.39) we find

$$\lambda \approx \frac{1}{\gamma}. \qquad (3.40)$$

Outside resonance region (at $0.7 < q < 1.3$) influence of damping on amplitude is insignificant and it cannot be considered.

Dependence of α [formula (3.36)] on frequency (or relation of frequencies q) is phase response. During different damping factors phase responses are represented on Fig. 3.6. Phase shift α is changed from zero at low frequencies of disturbing force to π at frequencies $\omega \gg p$. During resonance ($\omega = p$) oscillations lag in phase from oscillations of disturbing force by $\pi/2$. In region of resonance, phase shift changes the faster the nearer to resonance and the less the damping. In the absence of damping, phase shift changes by a jump from 0 to π during $\omega = p$.

<u>Action of arbitrary periodic force on an oscillatory system.</u> If disturbing force $P(t)$ is any periodic function of period T, then it is possible to expand it into Fourier series:*

$$P(t) = \frac{a_0}{2} + \sum_{k=1}^{\infty} (a_k \cos k\omega t + b_k \sin k\omega t),$$

where $k = 1, 2, 3, \ldots$ is the order of harmonics of the expansion in Fourier series;

$a_0, a_1, a_2, \ldots, b_1, b_2, \ldots$ are Fourier coefficients.

Expansion of periodic functions in cosines and sines is the most wide-spread, but not the only method of expanding functions in a series. There is a large quantity of functions, with respect to which original function can be expanded in series. However, expansion in trigonometric functions (into harmonic components) in

---

*Periodic function can be expanded into Fourier series if it satisfies Dirichlet conditions. Functions describing real physical processes practically always satisfy to these conditions.

this case is the most convenient, since it depicts real processes occurring during oscillations.

Fourier series for function P(t) can be recorded in the following form:

$$P(t) = P_0 + \sum_{k=1}^{\infty} P_k \sin(k\omega t + \varphi_k), \qquad (3.41)$$

where

$$P_0 = \frac{a_0}{2}; \quad P_k = \sqrt{a_k^2 + b_k^2}; \quad \varphi_k = \operatorname{arc\,tg} \frac{a_k}{b_k}.$$

Separate components of disturbing force of the form $P_k \sin(k_\omega t + \varphi_k)$ are called harmonic components or harmonics. Harmonic $P_1 \sin(\omega t + \varphi_1)$ with main (or basic) frequency is called basic component or 1st harmonic. All subsequent harmonics with k-multiple frequency are called k-th component or k-th harmonic. Constant component P_0 coincides with mean value of function P(t).

Result of action of any periodic force, in accordance with the superposition principle valid for a linear system, will be obtained by simple summation of action of each of its harmonic components:

$$y(t) = y_{st} + \sum_{k=1}^{\infty} A_k \sin(k\omega t + \varphi_k - \alpha_k), \qquad (3.42)$$

where amplitude A_k and phase shift α_k of harmonic components of oscillations are determined by formulas (3.35) and (3.36). In this case, forced oscillations will have components with frequencies ω, 2ω, 3ω etc. each number of harmonics of expansion of forces in Fourier series. Furthermore, if natural frequency of system coincides with one of the components of the disturbing force, then resonance will appear.

Constant component y_{st} in formula (3.42) corresponds to deflection of system under action of mean value P_0 of disturbing force.

If force P(t) consists of several forces, variable by sinusoidal law, but with frequencies which, in general, are not multiples of frequency of change of total force,

$$P(t) = P_1\cos(\omega_1 t + \varphi_1) + P_2\cos(\omega_2 t + \varphi_2) + \ldots + P_n\cos(\omega_n t + \varphi_n),$$

then result of action of such force, in accordance with supersposition principle, will be obtained by summation of oscillations appearing from each component force. Total forced oscillations will have components with frequencies $\omega_1, \omega_2, \ldots, \omega_n$, in general not multiples of basic frequency ω_1.

Considered case of action of a disturbing force with a complex spectrum* has an important practical value. On flight vehicles oscillations of structure appear as a result of action of many disturbing forces occurring from different sources and having different frequencies, usually not multiples of each other. In these conditions, the determination of actual frequencies and amplitudes of components of oscillations, with respect to recording them, is the basic method of finding source of oscillations and manifestation of disturbances created by them. Formal application, for this purpose, of expansion of the recording of oscillations into Fourier series, i.e., into components with frequencies which are multiples of a certain, frequently arbitrarily taken, frequency, in many cases hampers manifestation of the source of oscillations and, consequently, cannot always be applied.

---

*Spectrum is totality of amplitudes or initial phase angles of harmonic components of oscillation (amplitude spectrum of oscillation or phase spectrum of oscillation).

Spectrum is called lined if harmonic components presented to it possess frequencies with discrete values; solid or continuous spectrum possesses continuous sequence of frequencies.

Action of force of variable frequency. Passage through resonance. This case corresponds, for instance, to acceleration of motors during starting of an aircraft or spin-up of rotor of a helicopter, when in the process of increasing rpm appearing oscillations pass through resonance.

Below described are certain results of investigations of the action of force of variable frequency on an oscillatory system. Let us assume that frequency of disturbing force increases evenly, force remains constant in amplitude and damping is small. From Fig. 3.7, on which are shown characteristics of oscillations during different speeds of acceleration $\frac{\varepsilon}{p^2}$ (ε – angular acceleration), it follows that the more speed of acceleration, the less the maximum of amplitudes and the later it sets in (after passage of natural frequency). During deceleration also maxima of amplitudes are less the faster transition is completed through resonance and the later it sets in (at frequencies smaller than natural).

Action of forces of small duration. Considerable practical interest is presented by the study of action of single disturbing forces on an oscillatory system with one degree of freedom. These forces usually grow relatively fast, attaining certain maximum value, and then somewhat more slowly (Fig. 3.8c).

Law of change of force in time can be various, but it is possible to present it by two functions:

$$\left.\begin{array}{lll} 0 < t < T_1, & P(t) = P_1(t) & \dot{P}_1(t) > 0; \\ T_1 < t < T_2, & P(t) = P_2(t) & \dot{P}_2(t) < 0; \\ t > T_2, & P(t) = 0 & \end{array}\right\} \qquad (3.43)$$

Definition of motion of an oscillatory system under the action of force, assigned in form (3.43), is reduced to finding solution of

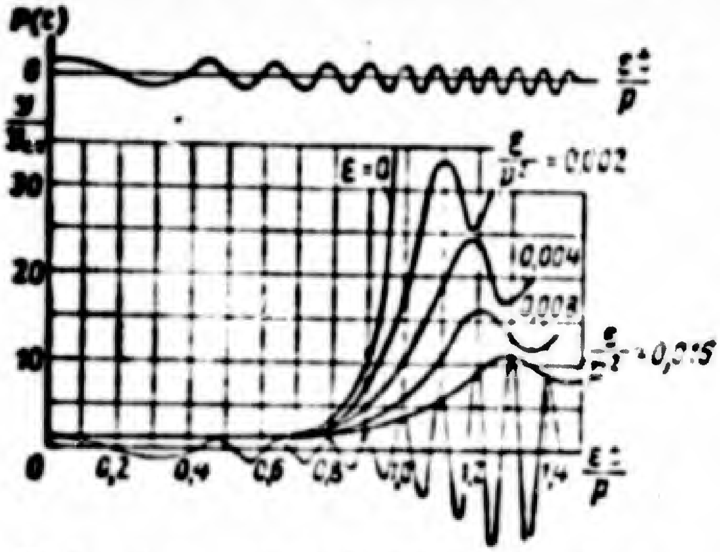

Fig. 3.7. Oscillations during passage through resonance.

equation of motion (3.19). Integrating by parts (3.20) and assuming that $y_1 = 0$ and forces of damping are small, general solution (3.20) of equation (3.19) it is possible to reduce to the form

$$y = y_{\text{ст}} - \frac{1}{mp^2}\int_0^t P(\tau)\cos p(t-\tau)\,d\tau. \quad (3.44)$$

Second member in formula (3.44) constitutes "dyanmic" correction, which one should add to static deflection in order to obtain dyanmic.

For slowly variable forces, when period of free oscillations of system is small as compared to time T_1, disturbing force acts "statically" and dynamic correction it is possible to disregard. In another case for fast variable forces, when duration of action of force T_2 is small as compared to period of natural oscillations, oscillations of system are determined by magnitude of pulse of disturbing force for the full time of its action. These two extreme cases were considered on the assumption that damping in the system is small.

In many cases it is necessary to estimate action of single disturbing forces with duration commensurable with period of natural oscillations of sys[illegible], during any magnitude of damping in system (for instance, duri[illegible] measurements of overloads on aircraft with help of seismic instruments (recorders of overloads) or during determination of effect of action on the structure of forces appearing during takeoffs, landings, and during flight in turbulent atmosphere).

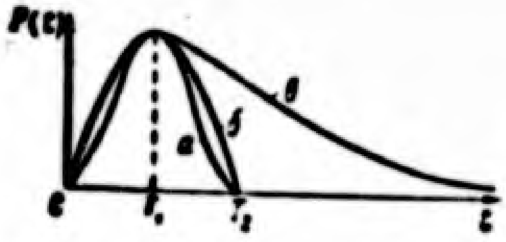

Fig. 3.8. Graphs of forces of small duration. a) $P(t) = P_0 \frac{1}{2}(1 - \cos wt)$, b) $P(t) = P_0 \sin wt$, c) according to formula (3.47).

As an example we will consider forces variable according to the following three laws (Fig. 3.8):

$$\left.\begin{aligned} &\text{a)}\ 0<t<\frac{2\pi}{\omega}, && P(t)=P_0\frac{1}{2}(1-\cos\omega t);\\ &t>\frac{2\pi}{\omega}, && P(t)=0. \end{aligned}\right| \quad (3.45)$$

$$\left.\begin{aligned} &\text{b)}\ 0\leqslant t<\frac{\pi}{\omega}, && P(t)=P_0\sin\omega t;\\ &t>\frac{\pi}{\omega}, && P(t)=0. \end{aligned}\right| \quad (3.46)$$

$$\left.\begin{aligned} &\text{c)}\ 0<t<\frac{\pi}{\omega} && P(t)=P_0\sin\omega t;\\ &t>\frac{\pi}{2\omega} && P(t)=P_0\frac{2\omega}{\pi}te^{1-\frac{2\omega}{\pi}t}. \end{aligned}\right\} \quad (3.47)$$

Graphs of dependence of dynamics coefficient on magnitude of q ratio during different values of attenuation factor are shown in Fig. 3.9. By these graphs it is possible to estimate dynamics coefficient depending upon magnitude q and attenuation factor h for single loads, which can be approximated by dependences of the form (3.45)-(3.47). From graphs it is clear that during attenuation factor h = (0.6-0.7)p, dynamics coefficient insignificantly differs from unity (not more than by 5-10%) during change of disturbing force with frequency from 0 to p.

Character of shift of oscillatory system (in reference to seismic instruments) under action of disturbing forces (overloads), variable by laws (3.45)-(3.47), is shown on Fig. 3.10.

<u>Assigned motion of point of bracing</u>. Let us assume that $\xi(t)$ is shift of point of bracing of elastic connection (see Figs. 3.3b, and c). We will examine forced oscillations which are the result

of motion of this point. On mass act force of inertia $m\ddot{y}$ and elastic reaction proportional to lengthening of elastic connection $k(y - \xi)$. From condition of equilibrium of these forces we will obtain

$$m\ddot{y} + ky = k\xi$$

or after division by m

$$\ddot{y} + p^2 y = p^2 \xi. \qquad (3.48)$$

This is equation of oscillations of system during assigned motion of point of bracing in the absence of damping in an absolute system of coordinates y with beginning at point 0 remaining in space motionless.

In relative system of coordinates x with beginning at point 0_1 rigidly joined with place of bracing, equation of motion of system will be

$$\ddot{x} + p^2 x = -\ddot{\xi} \qquad (3.49)$$

This equation is obtained from equation (3.48) by substitution of $y = x + \xi$.

During damping proportional tc relative speed of mass (see Fig. 3.3b), equations of motion have the form

a) in absolute system of coordinates

$$\ddot{y} + 2h\dot{y} + p^2 y = 2h\dot{\xi} + p^2 \xi; \qquad (3.50)$$

b) in relative system of coordinates

$$\ddot{x} + 2h\dot{x} + p^2 x = -\ddot{\xi}. \qquad (3.51)$$

During damping proportional to absolute velocity of mass (see

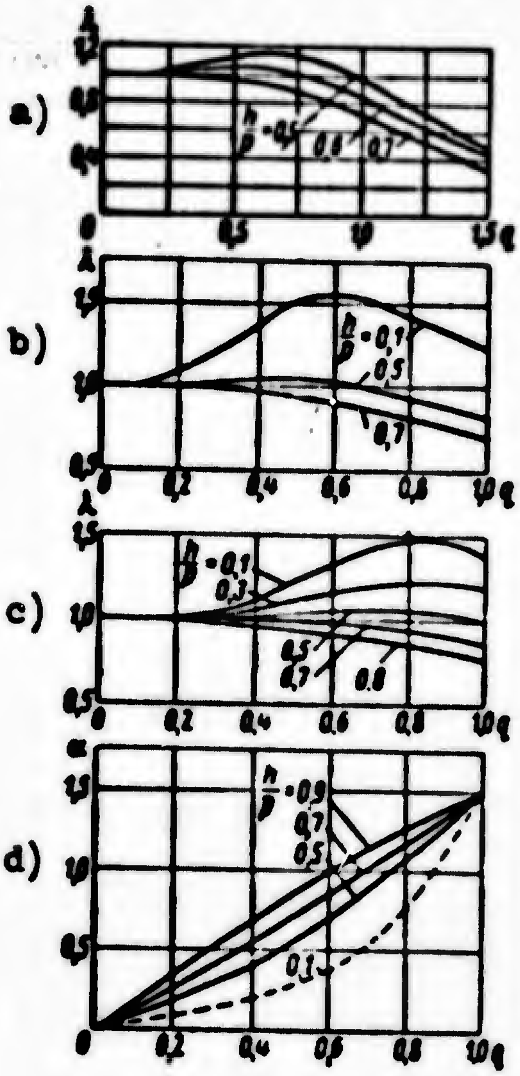

Fig. 3.9. Graphs of dynamics coefficient for forces of small duration. a) $P(t) = P_0 \sin \omega t$ — repeated force, b) $P(t) = P_0 \sin \omega t$ — single force, c) $P(t) = \frac{P_0}{2}(1 - \cos \omega t)$ — single force, d) phase response for force $P(t) = P_0 \cdot \frac{1}{2}(1 - \cos \omega t)$.

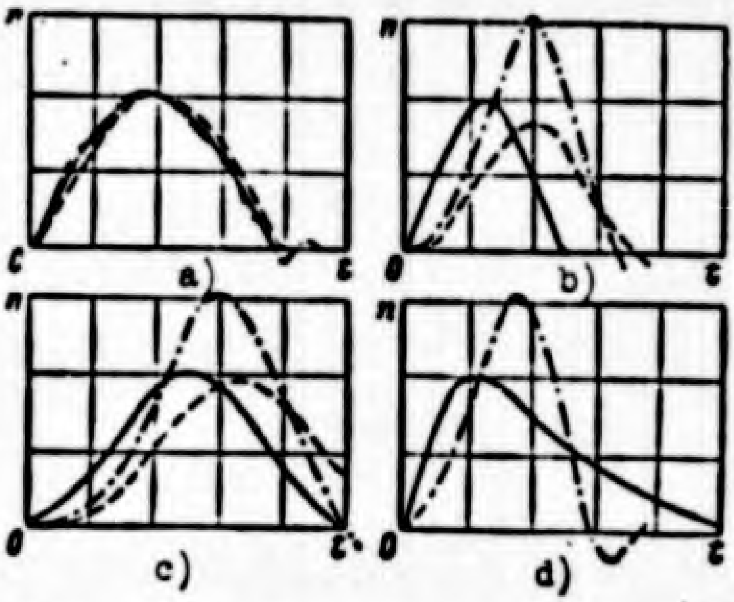

Fig. 3.10. Indications of instrument during action of overloads, determined by: a) formula (3.45) at $q = 0.1$; b) formula (3.45) at $q = 0.7$; c) formula (3.46) at $q = 0.7$; d) formula (3.47) at $q = 0.7$ —— actual overload, — • — indications of instrument at $h = 0.1\ p$, ------ indications of instrument at $h = 0.7\ p$.

Fig. 3.3c), equations of motion have the form

a) in absolute system of coordinates

$$\ddot{y} + 2h\dot{y} + p^2 y = p^2 \xi; \tag{3.52}$$

b) in relative system of coordinates

$$\ddot{x} + 2h\dot{x} + p^2 x = -\ddot{\xi} - 2h\dot{\xi}. \tag{3.53}$$

Solution of equations (3.48)-(3.53) is conducted analogously to the above-indicated.

As an example we will consider the case when a point of bracing oscillates by harmonic law

$$\xi(t) = \xi_0 \sin \omega t. \tag{3.54}$$

Then, substituting expression (3.54), for instance, into equation (3.51), we will obtain equation of motion in the following form:

$$\ddot{x} + 2h\dot{x} + p^2 x = \frac{P_0}{m} \sin \omega t, \tag{3.55}$$

where

$$P_0 = m\omega^2 \xi_0.$$

Equation (3.55) in form completely coincides with equation (3.30). Using obtained solutions, we have

$$x = x_0 \sin(\omega t - \varepsilon), \tag{3.56}$$

where

$$x_0 = \frac{\varphi^2}{\sqrt{(1-\varphi^2)^2 + \varphi^2\gamma^2}} \xi_0,$$

$$\varepsilon = \operatorname{arctg} \frac{\varphi\gamma}{1-\varphi^2}.$$

Study of oscillations under the action of any other forces applied to a point of bracing may be conducted analogously to that as was shown for a case of application of these forces to mass of system.

3.2. Oscillations of Elastic Nonlinear Systems with One Degree of Freedom

In the considered schematic systems force of elasticity linearly depends on deformation. For real structures such dependence takes place during small deformations. During considerable deformations linear dependence of force of elasticity on deformation is disturbed and system becomes nonlinear. Nonlinear dependence of force of elasticity on deformation is possible, for instance, in control cables of flight vehicles in the presence of gaps (Fig. 3.11a) or in landing gear of aircraft, when shock absorption of strut begins to work only after a defined pressing of pneumatic tires (Fig. 3.11c). Other cases of nonlinearity are possible (Fig. 3.11b, d, e, and f).

Equation of motion of systems with nonlinear elastic characteristic P(y) in the absence of damping, it is possible to present in the form

$$m\ddot{y}+P(y)=0. \tag{3.57}$$

Solution of this equation has the form

$$t=\int_a^y \frac{dy}{-\sqrt{\frac{2}{m}\int_y^a P(y)\,dy}}. \tag{3.58}$$

where $a = y_{max}$ (for beginning of count moment is selected at $\dot{y} = 0$).

For systems with symmetric elastic characteristic, period of natural oscillations one can determine by the formula

$$\frac{T}{4}=\sqrt{\frac{m}{2}}\int_0^a \frac{dy}{\int_y^a P(y)\,dy}.$$

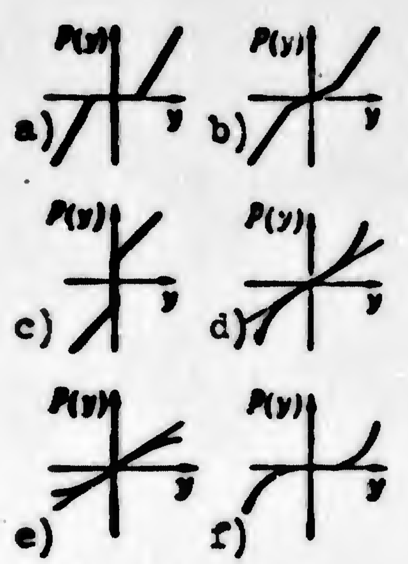

Fig. 3.11. Examples of nonlinear elastic characteristics.

Integrals entering into this formula, in most cases are not reduced to tabular and are calculated by methods of approximation. It is important to note that in nonlinear systems period of natural oscillations depends on amplitude; in "soft" systems it decreases with increase of amplitude of oscillations, and in "rigid" it increases.

Oscillations of nonlinear systems will not be strictly harmonic and are called pseudo-harmonic.

Forced oscillations in nonlinear systems with one degree of freedom during action of harmonic disturbing force are described by equation of the form

$$m\ddot{y} + P(y) = P_0 \sin \omega t. \qquad (3.59)$$

This equation does not have exact solution in closed form; therefore, it is solved by methods of approximation.

On Fig. 3.12 for qualitative analysis are given typical resonance curves for nonlinear systems. Center lines on these curves constitute change of natural frequency with increase in amplitude of oscillations.

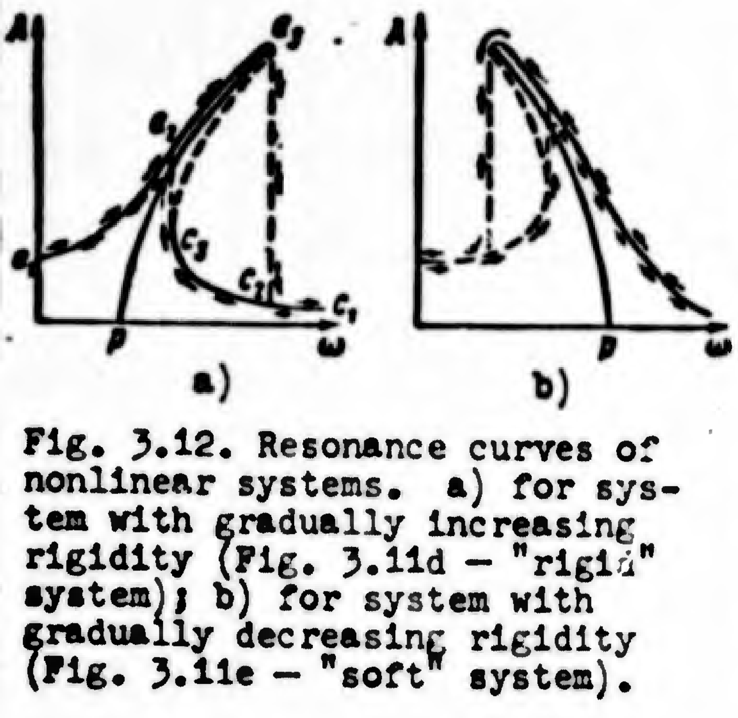

Fig. 3.12. Resonance curves of nonlinear systems. a) for system with gradually increasing rigidity (Fig. 3.11d — "rigid" system); b) for system with gradually decreasing rigidity (Fig. 3.11e — "soft" system).

In nonlinear systems, in principle, resonance is impossible in such a form as this is shown on Fig. 3.5. Amplitude of oscillations in system with nonlinear elastic characteristic always remains limited even in the absence of forces of damping. Forces of damping, always present in real oscillatory systems, lower resonance peak.

Oscillation in nonlinear systems during change of frequency of disturbing force occur in the following way (Fig. 3.12a). With increase of frequency amplitude increases along branch a from a_1 to a_3. During further increase of frequency, amplitude suddenly decreases from a_3 to c_2 and then is changed along branch c. With decrease of frequency of oscillations is observed reverse picture: in the beginning amplitude is changed along branch c from c_1 to c_3 then suddenly increases from value c_3 to a_2 and subsequently is changed along branch a.

During action of two disturbing forces on a nonlinear system it is impossible to use principle of independence of action of forces. However, in this case the principle of mutual exception is valid, which consists of the following.

If on a system act two disturbing forces, whose frequencies are ω_1 and ω_2 and separately calculated amplitudes $A_1 > A_2$, then total action of forces is determined only by amplitude A_1, i.e., "weak" component in this case is "suppressed" by "stronger."

These general peculiarities of forced oscillations of nonlinear systems are confirmed by experimental investigations.

3.3. Principles of Vibration Insulation

For decrease in harmful action of vibrations (for instance, created by work of motor) on the structure of a flight vehicle or for protection of instruments and equipment from vibrations, vibration insulation is applied. Structural fulfillment of vibration insulation can be varied. Vibration insulating devices can have different characteristics, but their assignment is one — to decrease forces transmitted from source of oscillations, or to decrease amplitude of oscillations transmitted to damped object.

Investigation of oscillations of a body during vibration insulation in general, taking into account all degrees of freedom of the body, is complex. However, in many cases, it is possible to consider oscillation of damped object as oscillation of a system with one degree of freedom. Analysis, with this, is considerably simplified, and basic regularities of oscillations are revealed sufficiently enough.

In aviation, for vibration insulation, in most cases, are applied shock absorbers with linear characteristics. Investigation of oscillations of objects with such vibration insulation is reduced to the consideration of forced oscillations of linear systems. Quality of vibration insulation is estimated by dynamics coefficient. If dynamics coefficient $\lambda < 1$, then vibration insulation is effective.*

In this case, forces transmitted from source of oscillations to structure

$$N = kA = \lambda P_0 \tag{3.60}$$

(where k is coefficient of elasticity of shock absorber; $\mathring{A}$ is amplitude of oscillations of damped object) will be less than maximum value of disturbing force. Analogously to this, amplitude of oscillations of damped object

$$y_0 = \lambda \xi_0 \tag{3.61}$$

will be less than amplitude of oscillations of point of bracing ξ_0.

If $\lambda > 1$, then transmitted forces or amplitudes, in accordance with formulas (3.60) and (3.61), are increased and damping even worsens work of equipment.

Using (3.39) and considering $\gamma = 0$, we find that vibration insulation becomes effective from moment when $q > \sqrt{2}$ or $\omega > \sqrt{2}p$ (Fig. 3.13).

---

*Usually vibration insulation is considered qualitative if transmitted forces or amplitudes decrease not less than 50%, i.e., dynamics coefficient must be $\lambda \leq 0.5$.

Thus, natural frequency of damped object is one of the important parameters characterizing quality of vibration insulation. In many cases, frequency of oscillations one can easily determine by experimental means, according to the following identical formulas:

$$f=\frac{1}{2\pi}\sqrt{\frac{g}{y_{st}}};\quad f=\frac{5}{\sqrt{y_{st}}}\,;\quad f=\frac{300}{\sqrt{y_{st}}}\qquad (3.62)$$

or by the graph on Fig. 3.14.

Formulas (3.62) are obtained from dependence (3.7), taking into account the fact that within limits of elastic deformation of shock absorbers $G = mg = ky_{st}$, and, consequently,

$$\frac{k}{m}=\frac{g}{y_{st}},$$

where G is weight of damped object;

y_{st} is static sag of shock absorbers in cm under action of weight of object.

Natural frequency of oscillations is determined in the following way. Object is removed from damping. Then it is placed again in damping and sag of shock absorbers y_{st} under action of gravity is determined. Using obtained value of sag y_{st}, by formulas (3.62) is determined natural frequency of oscillations.

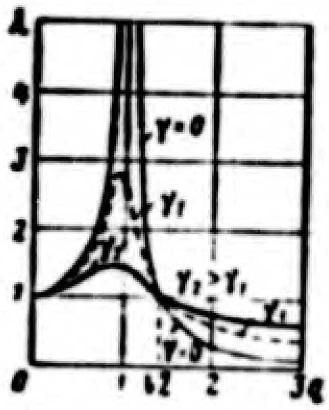

Fig. 3.13. Resonance charateristics of a damped object with different damping.

Increase in ratio of frequencies $q = \omega/p$ is the basic method of achieving good vibration-insulation.

It is necessary to note that different lead wires can render essential influence on oscillations of damped object, in particular, can change natural frequency of object if its gravity is

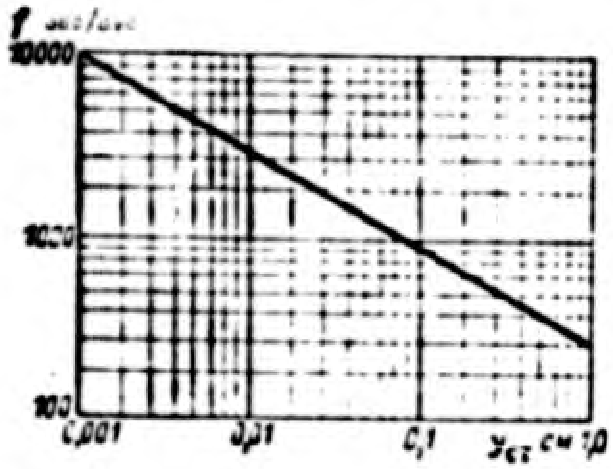

Fig. 3.14. Dependence of natural frequency of a damped object on static sag of shock absorber.

small. However, this influence is impossible to determine by means of calculation. In view of this, laboratory tests of damped instrument equipment and appraisal of its damping must be conducted in the presence of the entire lead wire in the same form in which it is executed in real operational conditions.

We will consider the influence of damping on vibration insulation. In the case of linear characteristics of shock absorbers, equations of motion of a damped object in the presence of resisting forces proportional to speed, are analogous to the above considered (3.30), (3.55).

On Fig. 3.13 are shown resonance curves for damped objects with one degree of freedom at different values of damping factors. As can be seen, all curves pass through point $q = \sqrt{2}$. In other words, damping in all cases becomes effective only if natural frequency of object in damping is at least 1.41 times less than frequency of disturbing force.

From the same curves on Fig. 3.13 it is clear that damping is useful only in zone of resonance, inasmuch as amplitudes of oscillations are considerably lowered. In remaining cases, i.e., for relation of frequencies $q > \sqrt{2}$, it worsens vibration insulation. With this, the more the damping, the worse the vibration insulation. However damping, if it not too large, is useful, inasmuch as it leads to comparatively fast cessation of natural oscillations of damped object after accidental shocks in operation. It is all the more so necessary if one considers that on a damped object act disturbances whose frequency on flight vehicles sometimes changes in wide limits.

It is necessary to note that on aircraft and helicopters oscillations with frequencies from 2 to 25 oscillations per second are basic. If the natural frequency of objects of special equipment on shock absorbers are in a given range of frequencies, then resonance of instruments is possible. In this case damping does not improve, and condition of work of objects of special equipment worsens.

Depending upon concrete conditions (place of installation of instrument on flight vehicle and frequencies of predominant oscillations in this place), it is possible to improve vibration-insulating properties of damping by individual selection of shock absorbers. However, the fundamental solution of question of vibration insulation is the application of shock absorbers with nonlinear power characteristics of the type shown on Fig. 3.11, inasmuch as in such oscillatory systems a state resonance is impossible.

3.4. Oscillations of a System with Several Degrees of Freedom

We will consider certain questions of oscillations of linear systems with several degrees of freedom. The most general method of composing equations of motion of oscillatory systems with any limited quantity of degrees of freedom is based on application of Lagrange equations of the second type, which in the absence of damping have the form

$$\frac{d}{dt}\left(\frac{\partial T}{\partial \dot{q}_i}\right)-\frac{\partial T}{\partial q_i}+\frac{\partial \Pi}{\partial q_i}=Q_i\ (i=1,\ 2\ \ldots). \qquad (3.63)$$

where T and Π are kinetic and potential energy of system;

Q_i is generalized disturbing force;

q_i is generalized coordinate.

During composition of equations of motion there is obtained a system of n equations based on number of degrees of freedom. With increase in number of degrees of freedom, complexity of calculation increases. At n > 4, without application of electronic computing mathematical machines it is practically impossible to conduct calculation.

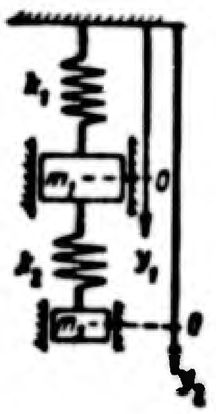

Fig. 3.15. System with two degrees of freedom.

Equations of free oscillations of a system with two degrees of freedom, depicted on Fig. 3.15, have the form

$$\left.\begin{aligned} m_1\ddot{y}_1 + k_1y_1 - k_2(y_2 - y_1) = 0; \\ m_2\ddot{y}_2 + k_2(y_2 - y_1) = 0. \end{aligned}\right\} \qquad (3.64)$$

Solution of these equations it is possible to look for in the form

$$\left.\begin{aligned} y_1 = A\sin(pt + \alpha); \\ y_2 = B\sin(pt + \alpha). \end{aligned}\right\} \qquad (3.65)$$

Substituting (3.65) in equations (3.64), we will obtain a uniform system of equations with respect to amplitudes A and B:

$$\left.\begin{aligned} (k_1 + k_2 - m_1p^2)A - k_2B = 0; \\ -k_2A + (k_2 - m_2p^2)B = 0. \end{aligned}\right\} \qquad (3.66)$$

Nontrivial solution of system of equations (3.66) is possible in the case when determinant, composed from coefficients of this system, is equal to zero:

$$\begin{vmatrix} k_1 + k_2 - m_1p^2 & -k_2 \\ -k_2 & k_2 - m_2p^2 \end{vmatrix} = 0. \qquad (3.67)$$

While analyzing determinant, we find frequency (determinant) equation for investigated oscillatory system

$$p^4-\left(\frac{k_1+k_2}{m_1}+\frac{k_2}{m_2}\right)p^2+\frac{k_1k_2}{m_1m_2}=0, \qquad (3.68)$$

while solving which we will determine two real roots p_1 and p_2.

Consequently, an oscillatory system with two degrees of freedom has two natural frequencies. Therefore, solution of equations (3.64) one should record in the form

$$\left.\begin{aligned} y_1&=A_1\sin(p_1t+\alpha_1)+A_2\sin(p_2t+\alpha_2);\\ y_2&=B_1\sin(p_1t+\alpha_1)+B_2\sin(p_2t+\alpha_2).\end{aligned}\right\} \qquad (3.69)$$

Amplitudes A_1, A_2, B_1, B_2 and phase angles α_1 and α_2 are determined by initial conditions, but natural frequencies p_1 and p_2, just as in systems with one degree of freedom, do not depend on initial conditions and are completely determined by parameters of the actual system, as one may see from equation (3.68).

During defined selection of initial conditions there can be obtained $A_2 = B_2 = 0$. Then oscillation will occur with one frequency p_1. Oscillation of such form is called <u>first normal oscillation</u>. Ratio of amplitudes, in accordance with system (3.66),

$$\frac{B_1}{A_1}=\frac{k_1+k_2-m_1p_1^2}{k_2}, \text{ or } \frac{B_1}{A_1}=\frac{k_2}{k_2-m_2p_1^2}, \qquad (3.70)$$

is fully defined, independent from initial conditions, and is determined only by parameters of the actual system. Ratio (3.70) determines first normal form of oscillations.

Analogously to this, it is possible to select such initial conditions at which $A_1 = B_1 = 0$, and oscillation will have only second frequency p_2. This oscillation is called <u>second normal oscillation</u>. Ratio of amplitudes for this case is analogous to equalities (3.70) and determines second normal form of oscillations.

Normal forms of oscillations possess important property of orthogonality, occurring in the fact that sum of products of each of the masses by amplitudes of their normal oscillations is equal to zero:

$$m_1 A_1 A_2 + m_2 B_1 B_2 = 0. \qquad (3.71)$$

If one of the amplitude ratios is known, for instance B_1/A_1, determining one form of oscillations, then by expression (3.71) can be found the other ratio, corresponding to the other form of oscillations.

The property of orthogonality is an expression of equality of kinetic energy of total (with respect to two forms) motion to sum of kinetic energy of both (with respect to each form separately) motions. Analogously to this, it is possible to show that linear systems with n degrees of freedom have n natural frequencies and normal forms of oscillations, corresponding to them (in number of degrees of freedom), where any two normal forms of oscillations are orthogonal.

Calculation of frequencies and forms of normal oscillations is complex and for n > 3 is conducted by methods of successive approximations.

We will consider now forced oscillations of a linear system with two degrees of freedom with assigned power disturbance in the absence of forces of damping (Fig. 3.16a). Recording equation of motion of each mass, we will obtain system of equations

$$\left.\begin{aligned} m_1\ddot{y}_1 + k_1 y_1 - k_2(y_2 - y_1) &= P_1(t); \\ m_2\ddot{y}_2 + k_2(y_2 - y_1) &= P_2(t). \end{aligned}\right\} \qquad (3.72)$$

Let us consider, at first, action on system of harmonic forces

$$P_1(t) = P_1 \sin\omega t; \quad P_2(t) = P_2 \sin\omega t. \qquad (3.73)$$

Taking particular solution in the form

$$y_1 = A\sin\omega t; \qquad y_2 = B\sin\omega t \tag{3.74}$$

and substituting it into equations of motion (3.72), after simple

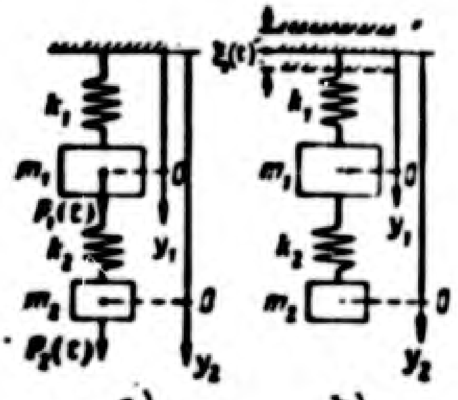

Fig. 3.16. Excitation of oscillations in a system with two degrees of freedom. a) assigned power disturbance; b) assigned motion of point of bracing.

Fig. 3.17. Resonance curves for a system with two degrees of freedom.

calculations we will obtain the following expression for amplitudes of oscillations:

$$\left.\begin{aligned} A &= \frac{P_1(k_2 - m_2\omega^2) + P_2k_2}{(k_1 + k_2 - m_1\omega^2)(k_2 - m_2\omega^2) - k_2^2}; \\ B &= \frac{P_2(k_1 + k_2 - m_1\omega^2) + P_1k_2}{(k_1 + k_2 - m_1\omega^2)(k_2 - m_2\omega^2) - k_2^2}. \end{aligned}\right\} \tag{3.75}$$

Denominator of expressions (3.75) during values $\omega = p_1$ or $\omega = p_2$ coincides with determinant (3.67) and turns into zero. Consequently, during coincidence of frequency of action of disturbing forces with one of the frequencies of natural oscillations of the system appears resonance. Of such resonances, in a system with two degrees of freedom, two are possible — at $\omega = p_1$ and at $\omega = p_2$ (with respect to number of natural frequencies of oscillations, see Fig. 3.17).

Values of amplitudes at $\omega = 0$ determine static deflection of masses:

$$A_{ст} = \frac{P_1 + P_2}{k_1}; \qquad B_{ст} = A_{ст} + \frac{P_2}{k_2}. \tag{3.76}$$

Ratio of amplitudes of oscillations to corresponding static deflections determines coefficients of dynamics for each of the masses:

$$\lambda_1 = \frac{A}{A_{ст}}; \qquad \lambda_2 = \frac{B}{B_{ст}}.$$

Zone of resonance ($\lambda > 1$) for systems with two degrees of freedom is expanded (Fig. 3.18).

It is necessary to note that in a case when disturbing force acts only on one mass ($P_1 \neq 0$, $P_2 = 0$), coefficient of dynamics for first mass turns into zero at defined frequency. From formulas (3.75) it is clear that this is obtained when (at $P_2 = 0$)

$$k_2 - m_2\omega^2 = 0. \tag{3.77}$$

Amplitudes become equal: $A = 0$ and $B = \frac{P_1}{k_2}$. Thus, in a given particular case, when is executed condition (3.77), mass, to which is applied disturbing force, does not oscillate. This phenomenon is used in practical conditions for extinguishing oscillations with the help of dynamic dampers (extinguishers) of oscillations. However, such a damper is effective if oscillations are accomplished with one defined frequency ω = const and damper is strictly adjusted for "absorption" of oscillations with this frequency, i.e., its mass and elasticity of spring are determined in accordance with condition (3.77).

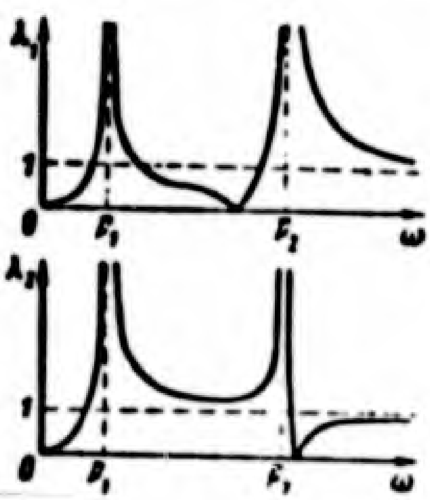

Fig. 3.18. Change of coefficients of dynamics λ_1 and λ_2 depending upon frequency during assigned motion of point of bracing.

During non-observance of this condition, damper can be ineffective.

We will consider a system during the action of oscillations at point of bracing (see Fig. 3.16b). Equations of motion of masses of such a system during the action of harmonic disturbance have the form

$$\left.\begin{aligned} m_1\ddot{y}_1 + k_1y_1 - k_2(y_2 - y_1) &= k_1\xi_0 \sin\omega t; \\ m_2\ddot{y}_2 + k_2(y_2 - y_1) &= 0, \end{aligned}\right\} \qquad (3.78)$$

where $\xi_0 \sin \omega t$ is assigned motion of point of bracing.

Particular solution of equations (3.78), corresponding to steady forced oscillations, we will look for in the form (3.74). After substituting this solution into equations (3.78), we will obtain for amplitudes the following expressions:

$$A = \frac{k_1(k_2 - m_2\omega^2)}{(k_1 + k_2 - m_1\omega^2)(k_2 - m_2\omega^2) - k_2^2}\xi_0;$$

$$B = \frac{k_1k_2}{(k_1 + k_2 - m_1\omega^2)(k_2 - m_2\omega^2) - k_2^2}\xi_0.$$

At $\omega \to \infty$ amplitudes A and B approach zero. During static disturbance ($\omega = 0$) $A = B = \xi_0$.

Ratios of amplitudes of oscillations to amplitude of disturbing oscillatory motion constitute coefficients of dynamics (see Fig. 3.18):

$$\lambda_1 = \frac{k_1(k_2 - m_2\omega^2)}{(k_1 + k_2 - m_1\omega^2)(k_2 - m_2\omega^2) - k_2^2};$$

$$\lambda_2 = \frac{k_1k_2}{(k_1 + k_2 - m_1\omega^2)(k_2 - m_2\omega^2) - k_2^2}.$$

3.5. Oscillations of Systems with Continuously Distributed Mass

Real structures of flight vehicles only in certain cases can be schematized as an oscillatory system with a finite number of degrees of freedom. More exact results are given by calculation of continuity of distribution of mass in an oscillatory system the number of degrees of freedom of which turns out to be infinite. Such a system possesses an infinite number of natural frequencies of oscillations and normal forms corresponding to them.

Oscillations in systems with continuous distribution of mass are described by equations in partial derivatives. Solution of such equations for complex oscillatory systems presents great mathematical difficulties and can be brought to an end only for the simplest systems.

Let us consider, for example, bend oscillations of a beam of constant cross section. From theory of strength of materials we know relationship

$$(EJy'')'' = P(t), \qquad (3.79)$$

where P(t) is intensity of distributed load;

y = y(z, t) is sag of beam (depends on coordinate z and time t);

E is elastic modulus;

J is moment of inertia.

Magnitude P(t) in our case is algebraically composed of external load and forces of inertia:

$$P(t) = g(z, t) - m\ddot{y}, \qquad (3.80)$$

where m is mass of unit of length of beam. After substituting expression (3.80) into equation (3.79), we will obtain

$$(EJy'')'' + m\ddot{y} = g(z, t). \qquad (3.81)$$

General solution of equation of forced oscillations (3.81) is composed of solution of corresponding equation without right side

$$\frac{\partial^2}{\partial z^2}\left(EJ\frac{\partial^2 y}{\partial z^2}\right)+m\frac{\partial^2 y}{\partial t^2}=0, \tag{3.82}$$

determining natural oscillation of system, and particular solution of equation (3.81) with right side. Having assumed that function y(z, t) can be presented in the form

$$y(z,t)=f(z)r(t), \tag{3.83}$$

after certain transformations we will obtain

$$-\frac{1}{mf(z)}\cdot\frac{d^2}{dz^2}\left(EJ\frac{d^2f(z)}{dz^2}\right)=\frac{\ddot{r}(t)}{r(t)}. \tag{3.84}$$

In equality (3.84) the left part depends on coordinate z, and the right on time t. For identical fulfillment of equality (3.84) it is necessary that each of its parts equal a constant which we will designate by $-p^2$. Then we will obtain two equations

$$\ddot{r}(t)+p^2r(t)=0; \tag{3.85}$$

$$\frac{1}{mf(z)}\frac{d^2}{dz^2}\left(EJ\frac{d^2f(z)}{dz^2}\right)=p^2. \tag{3.86}$$

Solution of equation (3.85) has the form

$$r(t)=A\sin(pt+\alpha), \tag{3.87}$$

where A is constant, determined by initial conditions. Solution (3.87) indicates oscillatory character of motion. Magnitude p has physical meaning of frequency of oscillations.

Equation (3.86) determines form of oscillations. For particular case of a beam of constant cross section (EJ = const) its solution has the form

$$f(z)=C_1\sin kz+C_2\cos kz+C_3\operatorname{sh}kz+C_4\operatorname{ch}kz. \tag{3.88}$$

where

$$k = \sqrt[4]{\frac{mp^2}{EJ}};$$

C_1, C_2, C_3, C_4 are constants depending on boundary conditions.

Solutions (3.87) and (3.88) of equation (3.84) are particular solutions. General solution is obtained by means of imposition of particular solutions of the form (3.83):

$$y(z, t) = \sum_{i=1}^{\infty} f_i(z) r_i(t). \qquad (3.89)$$

Forced Oscillations of Structures

We will assume that frequency and form of natural oscillations for structure of a flight vehicle are known. For solution of equation of forced oscillations of system (3.81) it is possible to apply method of expansion of external load and unknown function for sag, in eigenfunctions $f_i(z)$:

$$q(z, t) = f_1(z) Q_1(t) + f_2(z) Q_2(t) + \ldots; \qquad (3.90)$$

$$y(z, t) = f_1(z) R_1(t) + f_2(z) R_2(t) + \ldots, \qquad (3.91)$$

where $Q_i(t)$ and $R_i(t)$ are functions of time for external force and sag. Considering that each component of series (3.90) causes oscillation described by a corresponding component of series (3.91), equation (3.84), after certain transformations, it is possible to record so:

$$-\frac{1}{m f_i(z)} \frac{d^2}{dz^2}\left(EJ \frac{d^2 f_i(z)}{dz^2}\right) = \frac{1}{R_i(t)}\left(R_i(t) - \frac{Q_i(t)}{m}\right). \qquad (3.92)$$

Proceeding with equality (3.92) just as with equality (3.84), and considering that left parts of these equalities are identical, we will obtain two equations

$$\frac{1}{mf_i}\frac{d^2}{dz^2}\left(EJ\,\frac{d^2f_i}{dz^2}\right)=p_i^2; \qquad (3.93)$$

$$\frac{1}{R_i}\left(\ddot{R}_i-\frac{Q_i}{m}\right)=-p_i^2. \qquad (3.94)$$

The first of them indicates the fact that forms of forced and natural oscillations of a system, in a case of arbitrary distributed load $g(z, t)$, coincide; the second is a differential equation of function $R_i(t)$ for forced oscillations:

$$\ddot{R}_i+p_i^2R_i=\frac{Q_i}{m}. \qquad (3.95)$$

Equation (3.95) has a solution of the form (3.20):

$$R_i(t)=\frac{1}{mp_i}\int_0^t Q_i(\tau)\sin p_i(t-\tau)\,d\tau. \qquad (3.96)$$

Magnitude $Q_i(t)$ one can determine from series (3.90), using orthogonality of eigenfunctions:

$$Q_i(t)=\frac{\int_0^l g(z,t)f_i(z)\,dz}{\int_0^l f_i^2(z)\,dz}, \qquad (3.97)$$

where l is length of structure.

Full solution of equation (3.92) for a case of forced oscillations is obtained from particular solutions, analogous to (3.83):

$$y(z,t)=\sum_{i=1}^{\infty}f_i(z)R_i(t). \qquad (3.98)$$

Equality (3.98) indicates that forced oscillations of the considered system occur also with corresponding natural frequencies p_i of this system.

3.6. Natural Oscillations of the Wing

We will consider certain flexural and torsional oscillations of a wing in a vacuum in the absence of forces of damping. Such oscillations are possible if centers of gravity of sections of wing coincide with centers of rigidity. For sweptback wings, oscillations of bend and torsion always will be together. Let us consider in the beginning a wing for which the line of centers of rigidity of sections is a straight line coinciding with the line of centers of weight and perpendicular to the line of sealing in a nondisplaceable fuselage (Fig. 3.19).

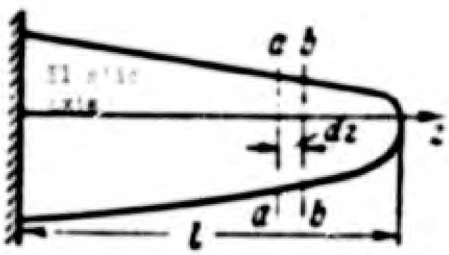

Fig. 3.19. Console diagram of a wing.

Flexural oscillations of the wing are characterized by deflections of its elastic line y = y(z, t), depending on coordinate z and time t. Differential equation of elastic line of a wing loaded by distributed forces of inertia coincides with equation (3.82) of natural oscillations of a beam. Method of solution of equation (3.82) will completely apply even in this case. Deflection of wing is presented in the form (3.83); after dividing variables, there are obtained from equation (3.84) two equations coinciding in form with equations (3.85) and (3.86):

$$\ddot{T}(t)+p^2T(t)=0; \qquad (3.99)$$

$$(EJf'')''-p^2mf=0. \qquad (3.100)$$

Boundary conditions for these equations will be

$$\left.\begin{array}{l} z=0;\ f=0;\ f'=0; \\ z=l;\ f''=0;\ (EJf'')'=0. \end{array}\right\} \qquad (3.101)$$

(deflection and angle of rotation for root, bending moment, and shear force on wing tip are equal to zero).

Equation (3.99) determines function of time $r(t)$. Its solution has the form (3.87), indicating harmonic character of motion. Equation (3.100) determines function of form $f(z)$. This equation has a solution only during defined values of p^2 corresponding to natural frequencies of oscillations of wing.

During calculation of natural oscillations, functions of form $f(z)$ are given approximate value. For this value $f(z)$ is determined angular frequency p. Then values $f(z)$ and p are definitized by method of successive approximations. Usually for this two or three approximations are sufficient.

As was shown above, systems with distributed mass have an infinitely large quantity of natural frequencies of oscillations p_i. Each value of natural frequency corresponds to a form of natural oscillations $f_i(z)$. General solution of equations (3.99) and (3.100) is obtained by imposition of particular solutions of form (3.83):

$$y(z, t) = \sum_{i=1}^{\infty} f_i(z) r_i(t). \qquad (3.102)$$

Components $f_1(z)r_1(t)$, $f_2(z)r_2(t)$, $f_3(z)r_3(t)$,... are called, respectively, first, second, third, and so forth, tones of natural flexural oscillations of the wing.

Any two tones of natural flexural oscillations of the wing are orthogonal. Property of orthogonality of natural oscillations is used during determination of i-th tone of natural oscillations during known i-1th tone of oscillations.

Torsional oscillations of the wing are determined analogously to flexural. Equation of torsional oscillations is obtained from condition of equilibrium of any section of wing, for instance, between sections a-a and b-b on Fig. 3.19. For this, change of elastic torque acting on section of wing $\frac{\partial}{\partial z}(GJ_{wi}\frac{\partial \vartheta}{\partial z})$ dz is adopted to moment of inertial forces acting on this section $J_m \ddot{\vartheta} dz$. As a result there is obtained equation of torsional oscillations of wing:

$$\frac{\partial}{\partial z}\left(GJ_{wi}\frac{\partial \vartheta}{\partial z}\right) - J_m\frac{\partial^2 \vartheta}{\partial t^2} = 0, \tag{3.103}$$

where GJ_{wi} is torsional rigidity of wing;

J_m is linear polar moment of inertia of mass of wing with respect to axis of rigidity;

$\vartheta = \vartheta(z, t)$ is torsion angle of section of wing during oscillations.

Boundary conditions for equation (3.103) will be

$$\left.\begin{array}{ll} z=0, & \vartheta=0; \\ z=l, & GJ_{wi}\vartheta'=0. \end{array}\right\} \tag{3.104}$$

Particular solution of equation (3.103), just as in case of flexural oscillations, is determined in the form

$$\vartheta(z, t) = \varphi(z) r(t). \tag{3.105}$$

Substituting (3.105) into equation (3.103), for φ and r we will obtain

$$\ddot{r} + p^2 r = 0; \tag{3.106}$$

$$(GJ_{wi}\varphi')' + p^2 J_m \varphi = 0. \tag{3.107}$$

Threshold conditions (3.104) will take the form

$$\left.\begin{array}{ll} z=0, & \varphi=0; \\ z=l, & \varphi'=0. \end{array}\right\} \tag{3.108}$$

During calculations there is assigned a law of change of torsion angles of section of the wing along the span and, in accordance with this, is determined natural frequency p. Furthermore, precise definitions of φ and p are conducted by method of successive approximations.

Equations (3.106) and (3.107) during boundary conditions (3.108), just as in the case of flexural oscillations, are satisfied only during defined values of parameter p. To each value of natural frequency p_i corresponds its own form of oscillations φ_i. General solution of equations (3.106) and (3.107) will be found by superposition of particular solutions of the form (3.105):

$$\theta(z, t) = \sum_{i=1}^{\infty} \varphi_i(z) r_i(t). \qquad (3.109)$$

Components $\varphi_1(z)r_1(t)$, $\varphi_2(z)r_2(t)$, $\varphi_3(z)r_3(t)$,... are called, respectively, first, second, third, and so forth, tones of natural torsional oscillations of the wing. During calculation of highest tones, property of orthogonality of natural oscillations is used.

Everything said pertains to certain flexural and torsional oscillations of the wing, calculated by "console diagram," i.e., in assumption of rigid sealing of wing in nondisplaceable fuselage. Such a calculation diagram gives good approximations for aircraft with straight wings of comparatively small dimensions.

In reality "purely flexural" and "purely torsional" oscillations of wing do not occur, since for real structures centers of gravity and rigidity of sections do not coincide and oscillations will be joint, i.e., wing will simultaneously accomplish both flexural and torsional oscillations. Initial bending strain of wing involves twisting strain and vice versa. However, during oscillations with frequency p_{flex} predominate flexural oscillations and, conversely, during frequency p_{tor} torsional oscillations. Therefore, in many cases it is permissible to calculate separately flexural and torsional natural oscillations of a wing.

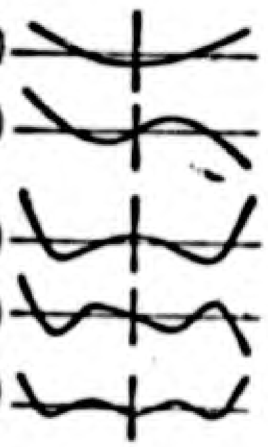

Fig. 320. Forms of natural flexural oscillations of a straight wing of a transport aircraft. a, c, e — symmetric bend, respectively, of I, II, and III tones; b, d — antisymmetric bends, respectively of I and II tones.

For sweptback wings, even in an ideal case, when centers of rigidity coincide with centers of gravity in every section, bending strain and torsion cannot occur separately. Therefore, the concept of "purely flexural" and "purely torsional" oscillations for such wings loses meaning. Joint flexural-torsional oscillations of a wing are considered on page 261.

Free-floating wing it is possible to schematize as a beam of variable section with load in the middle from weight of fuselage. It accomplishes oscillations around position of equilibrium. Wing is deformed in such a way that inertial forces of the mass of part of wing moving in one direction are mutually balanced by forces of inertia of remaining part of wing moving in opposite direction. For free-floating wing forms of oscillations are of two types — symmetric and antisymmetric. During symmetric oscillations, both wing tips simultaneously deflect to one side (upward or downward). During antisymmetric oscillations, wing tips at each given moment of time move to different sides. Symmetric forms it is possible to calculate on console diagram. Antisymmetric forms cannot be calculated on such a diagram. In this case, it is necessary to consider free-floating wing.

On Fig. 3.20 are represented forms of natural flexural oscillations of a straight wing of a real aircraft for several first tones. The lowest frequency of wing corresponds to symmetric form with least number of junction points (2 junction points, curve a). Then there are, in the order of growth of frequencies, antisymmetric form with three points (curve b), symmetric with four points (curve c), etc. At the junction points, at any moment of time displacement $y = 0$.

Amplitudes of fuselage during symmetric oscillations of wing are insignificant and are less the larger the mass of the fuselage at the same weight of wing. Antisymmetric oscillations of a wing practically do not depend on mass of fuselage, since it is located at a junction point of oscillations.

3.7. Natural Oscillations of an Aircraft (Helicopter)

Analogously to those considered for the wing can be calculated natural oscillations of all the main parts of a flight vehicle-fuselage, stabilizer, fin, etc. If, however, we consider aircraft (helicopter) as a single oscillatory system, then we will obtain not the natural frequency of separate assemblies, but their frequency of oscillations in the system of the entire aircraft or helicopter. Thus, for contemporary aircraft with sweptback wing and heavy aircraft with large masses on the wing it is impossible to calculate natural oscillations of separate parts of structure. For instance, for aircraft with sweptback wing the fuselage obtains large deformations during oscillations, which it is impossible to disregard. Therefore, in such cases during calculations of natural oscillations it becomes necessary to consider an aircraft on the whole.

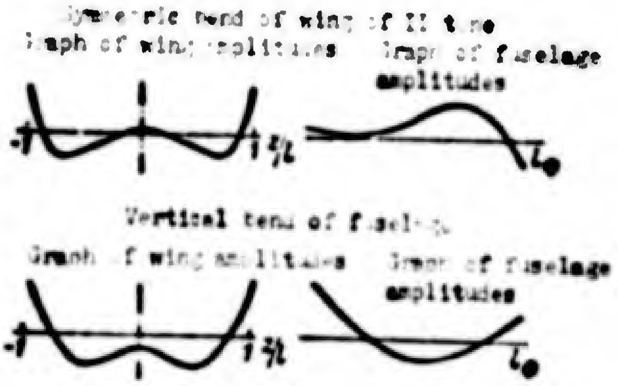

Fig. 3.21. Forms of oscillations of transport aircraft.

On Figs. 3.21 and 3.22 are presented certain forms of oscillations of a whole aircraft and a helicopter. From comparison, for instance, of forms of oscillations of symmetric bend of a wing and vertical bend of aircraft fuselage (see Fig. 3.21), it is clear that in both cases wing and fuselage obtain considerable deformations. Therefore, it is only conditionally possible to carry these or other oscillations to any part of the structure of the aircraft.

An aircraft (or other flight vehicle) constitutes a complex elastic system, all parts of which accomplish joint oscillations. Thus, symmetric flexural oscillations of a wing cause flexural oscillations of the fuselage and horizontal empennage; antisymmetric ones cause torsion of fuselage and flexural oscillations of empennage. Torsion of wing causes bend of fuselage, etc. Each form of oscillations of an elastic aircraft corresponds to a defined frequency. If one were to dispose these frequencies in order of growth, then it is possible to speak of I, II, III, etc., tones of oscillations of parts of an aircraft and forms corresponding to these tones. Thus it is possible only conditionally to carry these or other tones of natural oscillations of a whole aircraft to separate units of the aircraft. This conventionality gives only an idea concerning which elastic and mass characteristics and which unit any frequency or form of natural oscillations of a whole aircraft basically depends on. However, for convenience of analysis there are distinguished frequencies and forms of natural oscillations of wing, fuselage, empennage, control surfaces, etc.

Correctness of calculation of natural oscillations of an aircraft (or other flight vehicle) is checked by frequency (resonance) tests of full-scale aircraft (see p 543).

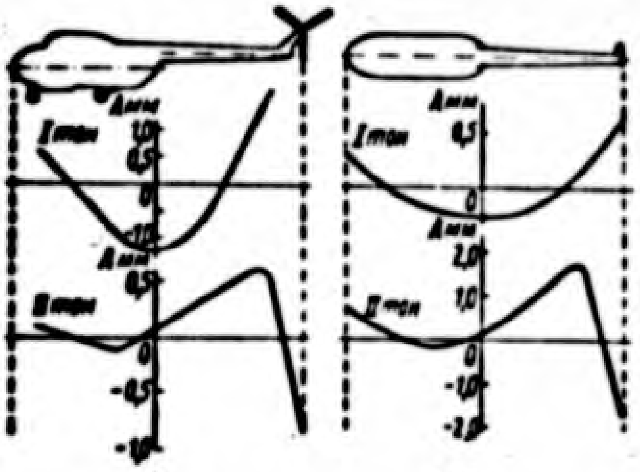

a) b)

Fig. 3.22. Forms of oscillations of a single-propeller helicopter. a) vertical bend of fuselage and tail beam; b) horizontal bend of fuselage and tail beam.

In Table 3.1 is given order of magnitudes of frequencies of natural oscillations for maneuvering and nonmaneuvering aircraft. From this table it is clear that for nonmaneuvering aircraft natural frequencies of lowest tones have small values; for maneuvering aircraft they are larger. A peculiarity of natural oscillations of contemporary aircraft is a thickening of spectrum of frequencies and a lowering of magnitudes of lowest tones. During frequency tests there are determined up to 40-50 tones of natural oscillations. Higher tones of oscillations usually do not have practical value.

Along with approximate values of frequencies of oscillations shown in Table 3.1 are determined also frequencies of natural oscillations of control surfaces, ailerons, trim tabs, flaps, etc. Lately there have been determined also horizontal oscillations of control surfaces, stabilizer, and wing. It is necessary to note that, depending upon friction and gaps in wiring of control, frequency of oscillations of control surfaces can change with change in amplitude of oscillations.

3.8. Resonance of Control Lines

In the practice of aircraft building there are usually not conducted full calculation of forced oscillations of control lines, but there are determined natural frequencies of thrusts of control lines

Table 3.1. Frequencies of Natural Oscillations of Structures of Aircraft in Oscillations Per Minute (Aircraft Without Fuel, Fuselage is Loaded)

Form of oscillations	Aircraft	
	Maneuvering	Nonmaneuvering
Wing		
Symmetric bend of I tone	400-500	100-150
Symmetric bend of II tone	1200-1400	300-330
Symmetric bend of III tone	2500-3000	550-570
Antisymmetric bend of I tone . . .	550-650	200-300
Antisymmetric bend of II tone . .	1600-1800	500-530
Antisymmetric bend of III tone . .	—	580-600
Symmetric torsion of I tone . . .	1800-2500	150-300
Symmetric torsion of II tone . . .	—	300-400
Symmetric torsion of III tone . .	—	1000-1100
Antisymmetric torsion of I tone .	—	120-150
Antisymmetric torsion of II tone .	—	200-250
Antisymmetric torsion of III tone	—	1000-1200
Fuselage		
Vertical bend of I tone	900-1300	200-250
Vertical bend of II tone	—	500-550
Horizontal bend of I tone	600-700	100-150
Horizontal bend of II tone	—	400-500
Torsion of fuselage	600-700	200-300
Stablizer		
Symmetric bend of I tone . . .	600-800	300-400
Symmetric bend of II tone	2500-3500	1000-1200
Antisymmetric bend of I tone . . .	700-900	900-1100
Symmetric torsion	900-1100	1200-1400
Antisymmetric torsion	1000-1500	1200-1500
Vertical Fin		
Bend of I tone	700-800	300-400
Bend of II tone	1900-2100	1200-1300
Torsion	2800-3100	900-1100

in order to not allow resonance from coincidence of their natural frequencies with frequencies of disturbing forces. It is recommended to select thrusts in such a way that frequency of fundamental tone of their natural oscillations differ from revolutions of engine and propeller no less than by 200-300 oscillations per minute. This reserve is selected taking into account the fact that calculation formulas for determination of natural frequencies of thrusts of control are derived without taking into account influence of longitudinal forces.

Definition of frequencies of natural oscillations of thrusts of control is based on the use of formula (3.88). Inasmuch as natural frequencies of oscillations are determined, a frequency equation is basic in this case. Method of composing frequency equation consists of determining for each case, depending upon support conditions of thrusts, the boundary conditions, while analyzing the recording of which leads to homogeneous equations relative to constants C_1, C_2, C_3, C_4 of equation (3.88). So that these coefficients do not turn simultaneously into zero, zero determinant of coefficients of system of ordinary equations relative to constants C_1, C_2, C_3, C_4 must be equal. Equating determinant to zero, we arrive at frequency equation

$$X = C_1A_x + C_2B_x + C_3C_x + C_4D_x, \qquad (3.110)$$

where

$$A_x = \frac{1}{2}(\operatorname{ch} kx + \cos kx);$$

$$B_x = \frac{1}{2}(\operatorname{sh} kx + \sin kx);$$

$$C_x = \frac{1}{2}(\operatorname{ch} kx - \cos kx);$$

$$D_x = \frac{1}{2}(\operatorname{sh} kx - \sin kx).$$

Functions A_x, B_x, C_x, D_x possess property of circular replacement. Therefore, derivatives from X (3.110) have the form

$$\left.\begin{aligned}\frac{1}{k}X' &= C_1D_x + C_2A_x + C_3B_x + C_4C_x;\\ \frac{1}{k^2}X'' &= C_1C_x + C_2D_x + C_3A_x + C_4B_x;\\ \frac{1}{k^3}X''' &= C_1B_x + C_2C_x + C_3D_x + C_4A_x.\end{aligned}\right\} \qquad (3.111)$$

At x = 0 $A_0 = 1$, $B_0 = C_0 = D_0 = 0$. Magnitude k has the same value as in formula (3.88).

For example we will consider determination of natural frequencies for a thrust with hinged supported ends (Fig. 3.23). In this case, on ends of thrust deflection and bending moment are equal to zero. This gives the following boundary conditions:

$$\left.\begin{aligned}x=0,\quad X=0,\quad X''=0;\\ x=l,\quad X=0,\quad X''=0.\end{aligned}\right\} \qquad (3.112)$$

Using expressions (3.110) and (3.111) during boundary conditions (3.112), we will obtain

$$C_1 = C_3 = 0;$$
$$C_2B_l + C_4D_l = 0;$$
$$C_2D_l + C_4B_l = 0.$$

Equating determinant of this system to zero, we find

$$B_l^2 - D_l^2 = 0.$$

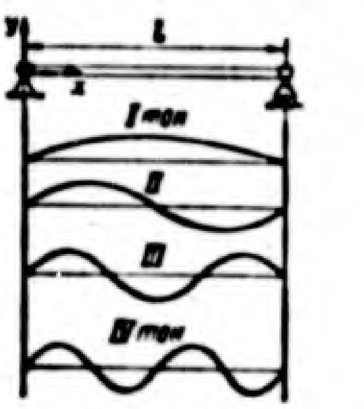

Fig. 3.23. Forms of oscillations of a homogeneous beam with hinged supported ends.

Substituting here values B_l and D_l from (3.110), after simple transformations we will obtain frequency equation

$$\operatorname{sh} kl \cdot \sin kl = 0.$$

Since $\operatorname{sh} kl \neq 0$, frequency equation takes the form

$$\sin kl = 0.$$

Roots satisfy to equality

$$kl = n\pi \quad (n = 1, 2 \ldots),$$
$$k = \frac{n\pi}{l}. \tag{3.113}$$

Substituting expression (3.113) into formula (3.88) for k, we determine

$$p_n = \frac{n^2\pi^2}{l^2}\sqrt{\frac{EJ}{m}} \quad (n = 1, 2, 3 \ldots)$$

or taking into account (3.5)

$$f_n = 94.2\frac{n^2}{l^2}\sqrt{\frac{EJ}{m}} \text{ osc/min}$$

Analogously there are determined natural frequencies of thrusts for other conditions on supports. Calculation of multispan thrusts with one or several supports in the middle part and thrusts with elastic supports is somewhat more complicated than in the given example. Calculation formulas are practical for all possible conditions on supports of thrusts of aircraft (helicopter) control, and necessary data on values of magnitudes E, J, m for pipes applied in aircraft construction are presented in reference books.

Of practical value usually is the first tone of oscillations of thrusts. Therefore, in most cases, there are limited by calculation frequencies of fundamental tone, which, to a considerable measure, simplifies the problem of resonance calculation of control lines.

3.9. Natural Frequencies of Power Installations

If one were to consider a motor with its assemblies as an absolutely rigid body, attached with the help of an elastic weightless frame to an aircraft (helicopter), where mounting lugs of frame are absolutely nondisplaceable, then such an oscillatory system in general possesses six degrees of freedom (forward displacements in the direction of three axes x, y, z and angular displacements φ, ψ, ϑ about the same axes) and, consequently, has six frequencies and forms of natural oscillations.

In a case of six degrees of freedom, equation of frequencies will be of the sixth order and full calculation of natural oscillations presents considerable difficulties. However, in many cases such an oscillatory system possesses one or two planes of symmetry. During one plane of symmetry a system of six differential equations is broken up into two systems of three equations, correspondingly, for symmetric (in plane of symmetry) and antisymmetric (perpendicular to plane of symmetry) forms of oscillations of motor. In this case, determination of natural oscillations is considerably simplified.

In many cases it is necessary to ensure only safety of propulsion systems with respect to appearance of resonance. Consequently, in such cases the basic problem is determination of frequencies of natural oscillations and there is no need for determination of forms of oscillations. However, knowledge of forms of natural oscillations is necessary when carrying out laboratory strength tests of frames of motors and during appraisal of influence on power installations of dynamic loads appearing during flight in bumpy atmosphere, during landing, etc.

Frequency of natural oscillations can be easily determined if one were to assume that oscillations of power installation are separate. Separate oscillations take place if center of gravity of power installation is combined with center of rigidity of elastic system of bracing of motor (frame and damping). If center of gravity and center of rigidity are not combined, but are on axis of symmetry, then will occur two-connected oscillations. If center of gravity is not combined with center of rigidity but they both lie in plane of symmetry, then oscillation will be three-connected.

Usually natural oscillations of propulsion systems are three-connected. However, thanks to selection of shock absorbers and construction of frame, it is possible to achieve the location of center of gravity of power installation and center of rigidity of system of bracing on the axis of symmetry or in the plane of symmetry, and sometimes combinations of centers of weight and rigidity and, consequently, separation of oscillations. The latter is very useful, since during separate oscillations it is possible by simple means to change any natural frequency of oscillations for removal of resonance without changing, besides, magnitude of other natural frequencies. In the absence of such separation, oscillations will always be joint, and change of one frequency of natural oscillations involves more or less considerable change of other frequencies.

For approximate determination of frequencies it is possible to use formulas of separate oscillations:

$$\left.\begin{aligned} f_x &= 9.55\sqrt{\frac{k_x}{M}}; & f_\varphi &= 9.55\sqrt{\frac{R_x}{J_x}}; \\ f_y &= 9.55\sqrt{\frac{k_y}{M}}; & f_\psi &= 9.55\sqrt{\frac{R_y}{J_y}}; \\ f_z &= 9.55\sqrt{\frac{k_z}{M}}; & f_\theta &= 9.55\sqrt{\frac{R_z}{J_z}}. \end{aligned}\right\}$$

where k_x k_y, k_z are rigidities of bracing of motor (frame and damping) in direction of axes x, y, z;

R_x, R_y, R_z are rigidities of bracing for torsion about the same axes x, y, z;

f is frequency in oscillations per minute.

Frequencies and forms of natural oscillations of power installation one can determine experimentally, directly on the aircraft (helicopter).

3.10. Natural Oscillations of Propeller Blades

Schematically it is possible to consider a propeller blade as a revolving beam of variable section. Change of twist along radius of blade and noncoincidence of centers of weight and centers of rigidity of sections of blade during calculation of natural oscillations is usually disregarded. This makes it possible to consider separate oscillations of bend and torsion of blade.

For nonrotating blades it is possible to use the same equations (3.99) and (3.100) which were applied during determination of natural oscillations of wing. Let us consider flexural oscillations of blade in plane of least rigidity (in direction of thrust of blade). We will consider that angle of incidence of blade in equilibrium state is close to zero (usually in section on relative radius $\bar{r} = 0.7$). Equation of natural flexural oscillations of blade in field of centrifugal forces has the form

$$\frac{\partial^2}{\partial r^2}\left(EJ_1 \frac{\partial^2 y}{\partial r^2}\right) - \omega^2 \frac{\partial}{\partial r}\left(N \frac{\partial y}{\partial r}\right) + m \frac{\partial^2 y}{\partial t^2} = 0, \tag{3.114}$$

where

$y(r, t)$ is deflection along radius of blade;

EJ_1 is least flexural rigidity of blade (in direction of thrust of blade);

r is radius of section of blade;

$m(r) = \rho_m F(r)$ is linear mass of blade, in the common case variable in radius of blade;

ρ_m is mass density;

$F(r)$ is area of cross section of blade, variable in radius;

$\omega^2 N = \omega^2 \int_r^R m r\,dr = \omega^2 \int_r^R \rho_m F r\,dr$ is centrifugal force of element of blade in section from r to R;

r is radius of propeller.

Equation (3.114) differs from equation (3.82) for a beam by the presence of a second member considering influence of centrifugal force.

If one were to assume $\omega = 0$, then equation (3.114), constituting equation of motion of a revolving blade, will take the form (for nonrotating blade), coinciding with equation (3.82).

Knowing condition of bracing of root of blade, it is possible to compose boundary conditions, and the problem about natural oscillations of blade will be completely determined. For aircraft propellers with rigid sealing of root, boundary conditions have the form (3.101):

$$\left.\begin{array}{l} r=0, \quad y=0, \quad y'=0; \\ r=R, \quad EJ_{y}y''=0, \quad (EJ_{y}y'')'=0. \end{array}\right\} \qquad (3.115)$$

For carrier or steering helicopter with horizontal hinge, boundary conditions have the form

$$\left.\begin{array}{l} r=0, \quad y=0, \quad EJ_{y}y''=0; \\ r=R, \quad EJ_{y}y''=0, \quad (EJ_{y}y'')'=0. \end{array}\right\} \qquad (3.116)$$

Equation (3.82), jointly with boundary conditions (3.115) or (3.116), determines natural oscillation for nonrotating blade, but equation (3.114) with those same boundary conditions determines natural oscillation of blade in field of centrifugal forces.

Centrifugal forces render essential influence on natural oscillations of blade. Centrifugal force tries to return blade to its middle position and by this increases rigidity of system, which thus is composed of two magnitudes — flexural rigidity k_{flex} and rigidity

k_{cen} created by centrifugal force during rotation of propeller. If one were to consider a blade as a system with one degree of freedom, having mass m, and suspended on two springs with rigidity k_{flex} and k_{cen}, then natural frequency of such a system is

$$p^2 = \frac{k_{flex} + k_{cen}}{m} = \bar{p}^2 + p_{cen}^2. \qquad (3.117)$$

Natural frequency of a revolving blade also can be represented in the form (3.117). Here $\bar{p}$ is natural frequency of nonrotating blade, possessing rigidity EJ_1 and mass m, in general, variable in radius. This frequency can be found from equation (3.82). Furthermore, it can be experimentally determined directly on propeller mounted on aircraft (helicopter).

Magnitude p_{cen} constitutes correction for influence of centrifugal forces and is equal to natural frequency of chain not having flexural rigidity in field of centrifugal forces. If dimensions of propeller hub are negligible as compared to length of blade, then

$$p_{cen} = \omega, \qquad (3.118)$$

i.e., natural frequency of such a chain is equal to angular velocity of its rotation. Formula (3.118) is valid for any law of distribution of masses. This formula is completely valid if configuration of system is not disturbed in the absence of one of rigidity. Real blade during rotation is deformed as compared to its configuration in the absence of rotation, and therefore formula (3.118) gives only approximate value of frequency. This approximation is considered by coefficient a:

$$p^2 = \bar{p}^2 + a\omega^2. \qquad (3.119)$$

Expression (3.119) is obtained by means of simple reasonings for a blade represented in the form of a system with one degree of freedom. The same result would be obtained if one were to solve equation (3.114) during corresponding boundary conditions. For this, as usually, y(r, t) is presented in the form

$$y(r,t)=\sum_{i=1}^{\infty} f_i(r)\sin p_i(t). \tag{3.120}$$

then it is substituted into equation (3.114) and, solving the equation, frequency of natural oscillations is found by the formula

$$p_i^2=\frac{\int_0^R EJ_1(f_i'')^2\,dr}{\int_0^R mf_i^2\,dr}+\omega^2\frac{\int_0^R N(f_i')^2\,dr}{\int_0^R mf_i^2\,dr}. \tag{3.121}$$

Thus expression for frequency of any tone of natural oscillations of an elastic blade (in the plane of least rigidity) in a field of centrifugal forces it is possible to record in the form, analogous to expression (3.119):

$$p_i^2=\bar{p}_i^2+a_i\omega^2. \tag{3.122}$$

For rigidly attached blades i = 1.2, ..., for blades with hinged bracing i = 0, 1, 2, ...

In equalities (3.121) and (3.122) first members determine natural frequency of nonrotating blade:

$$\bar{p}_i^2=\frac{\int_0^R EJ_1(f_i'')^2\,dr}{\int_0^R mf_i^2\,dr}. \tag{3.123}$$

and second members influence natural frequencies of centrifugal forces; coefficients a_i in formula (3.122) have value

$$a_i = \frac{\int_0^R N(r) f_i'^2 dr}{\int_0^R m f_i^2 dr}. \tag{3.124}$$

Calculations of hinged and rigidly attached blades differ little from each other. Essential peculiarity of the problem about oscillations of a hinged blade is the presence of zero tone, connected with the possibility of turn of blade as a solid body around hinge. Zero tone of natural oscillations ($i = 0$) corresponds to pendular oscillations of blade. Pendular frequency of a nonrotating blade is equal to zero ($p_0 = 0$), and for a revolving blade, due to action of centrifugal forces, is $p_0 = \omega$. All other tones of natural oscillations of a blade ($i = 1, 2, 3, \ldots$) are connected with its elastic deformations.

Oscillations of propeller blades in plane of the biggest rigidity (in plane of rotation) in the absence of rotation are described by the same equation (3.82) for natural oscillations of a beam during corresponding threshold conditions. Equation of natural oscillations of revolving blades in plane of least rigidity has the form

$$(EJ_2 x'')'' - \omega^2 (Nx')' - \omega^2 m x + m\ddot{x} = 0. \tag{3.125}$$

where EJ_2 is the biggest flexural rigidity of blade (in plane of rotation);

$x(r, t)$ is oscillation of blade in plane of greatest rigidity in distinction from its oscillations in plane of least rigidity $y(r, t)$;

$w^2 N$ is centrifugal force of element of blade;

$\omega^2 mx$ is expression considering action of component of centrifugal force, appearing due to noncoincidence of direction of its action (on radius from axis of rotation of propeller with elastic axis of blade during its oscillations about drag hinge.

In this case also applicable are boundary conditions (3.115) and (3.116), but in the presence of damper of the drag hinge in conditions of (3.116) one should take at $r = 0$ $y = 0$, $EJ_2 y'' = M_{d.h}$.

Natural frequencies of oscillations of a blade in plane of rotation are determined just as natural frequency of oscillations of a blade in plane of least rigidity. However, due to presence of third member in equation (3.125), relationship between natural frequencies of flexural oscillations of a blade in planes of rotation and thrust p_{rot} and p_{th} will be the following:

$$p_{rot}^2 = p_{th}^2 - \omega^2.$$

Due to this, formula (3.122) for the case of oscillations of a blade in plane of rotation will have the form

$$p_i^2 = \bar{p}_i^2 + (a_i - 1)\omega^2. \qquad (3.126)$$

Natural frequencies of flexural oscillations of a nonrotating blade $\bar{p}_1$ and coefficients a_1 in this case are determined by the same formulas (3.123) and (3.124), but form of oscillations $f_1(r)$ and rigidity have to correspond to oscillations of a blade in plane of the biggest rigidity; $p_0 = \bar{p}_0 \neq 0$ at $\omega = 0$ (caused by presence of elastic element in construction of drag hinge).

Coefficients a_1 in formulas (3.122) and (3.126) depend on angle of installation of blade. Calculations show that if angle of installation of blade φ is equal to zero approximately in section $\bar{r} = 0.70$-0.75, then twist of blades shows little on results of calculation. In this case it is possible to disregard it and to consider separate oscillations of blade in plane of least and in plane of the biggest rigidity. If $\varphi \neq 0$, then oscillations in both planes it is necessary to consider as connected, and calculations are strongly complicated.

Torsional oscillations of blade can be calculated similarly. They have comparatively high frequencies. For natural frequencies

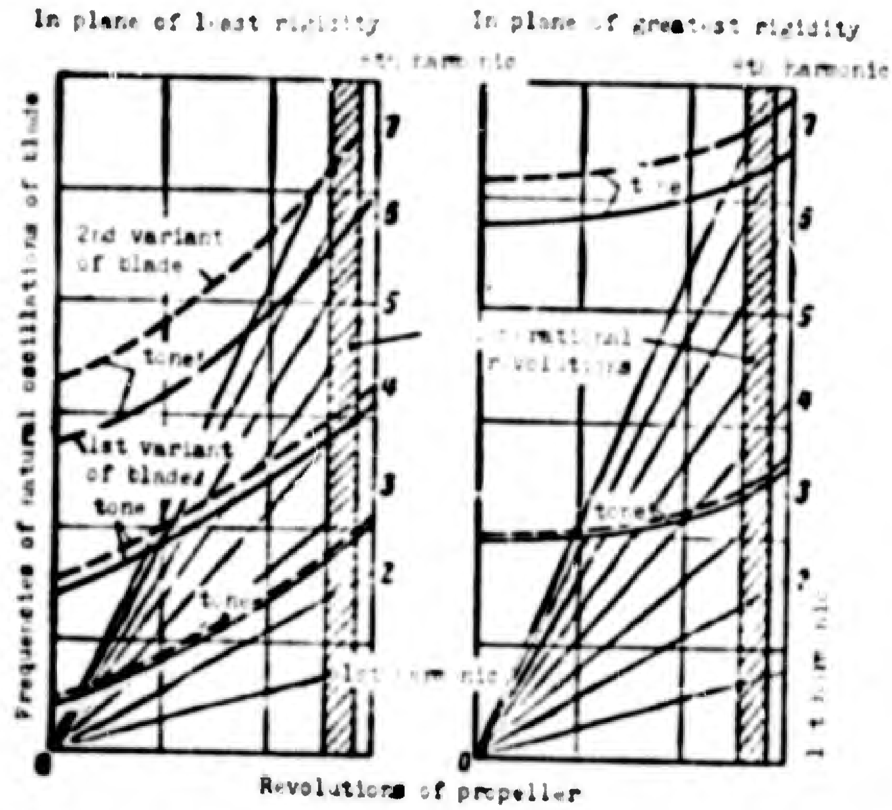

Fig. 3.24. Typical graph of change in natural frequencies of flexural oscillations of blade of helicopter rotor. 1st variant – blade with bad frequency responses, 2nd variant – blade with improved frequency responses.

of torsional oscillations of blades the same dependence is valid (3.122) as for bend oscillations in plane of least rigidity. Only during calculation of natural frequencies, instead of form of flexural oscillations $f(r)$ is taken form of torsional oscillations $\varphi(r)$ (3.105).

If purpose of calculation is the determination of natural frequencies of oscillations, then frequencies can be calculated for a nonrotating blade with correction for influence of centrifugal forces by formulas (3.122) and (3.126). In these formulas coefficients a_1

can be calculated or taken approximately from results of calculation of other blades.

Influence of centrifugal forces on natural frequencies it is possible to see from Fig. 3.24, where parabolas constitute change of natural frequencies with change in revolutions of propeller, and straight lines are harmonics of exciting forces.

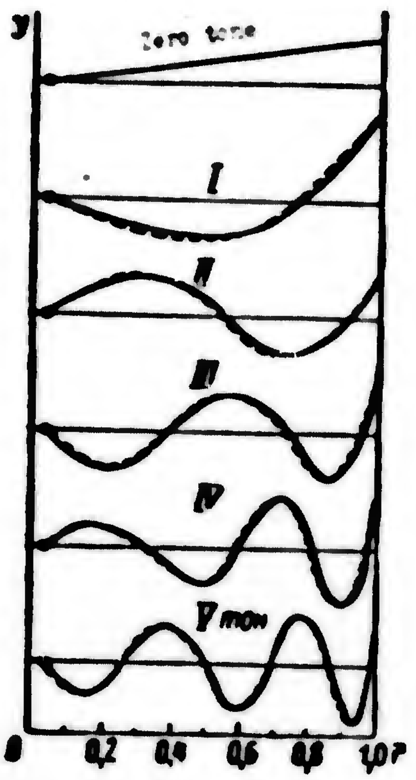

Fig. 3.25. Forms of oscillations (in plane of least rigidity) of blade of rotor of helicopter without rotation and in field of centrifugal forces. ——— revolutions are equal to zero, ---- operational revolutions $\bar{r} = \frac{r}{R}$ relative radius of section of blade.

Fig. 3.26. Dependence of frequencies of natural oscillations of blade of steering propeller of helicopter on angle of installation. 1st variant – blade with bad frequency responses, 2nd variant – blade with improved frequency responses.

Centrifugal forces render also an influence on forms of oscillations, especially for lowest tones. If for helicopter rotor distance from axis of rotation to hinge is $l_h = 0$, then zero form of oscillations is a straight line. If $l_h \neq 0$ (usually $l_h/R = 0.03$-0.10), then form differs from straight line; there is created a certain break in form of oscillations for hinge (Fig. 3.25).

Analogous breaks in form of oscillations are possible in places of drop in rigidity of blade in radius. Changes of form of oscillations of blade in a field of centrifugal forces especially strongly show on diagrams of bending moment and, consequently, on distribution of stresses on radius of blade, inasmuch as in their expression enter derivatives from function of deflections of blade y(r, t) and x(r, t). Influence of centrifugal forces is stronger the lower the tone of oscillations and the less flexural rigidity of the blade. Due to this centrifugal forces show less on forms of oscillations in plane of rotation than in direction of thrust, since flexural rigidity of blade in plane of rotation is usually considerably larger than in direction of thrust. Forms of oscillations of blades in plane of rotation (in plane of the biggest rigidity) differ little from forms of oscillations of a nonrotating blade. Forms of oscillations of blades in plane of least rigidity during relatively small flexural rigidity, as this occurs for carrying rotors of helicopters, depend little on their elastic properties and almost completely are determined by centrifugal and inertial forces. Due to this, influence is strengthened of concentrated loads and drops in rigidity on forms of oscillations in a field of centrifugal forces. This in turn leads to considerable increase of stresses on blades at places of distribution of concentrated loads and sharp change in rigidity.

At small angles of incidence of blade virtually separate oscillations are accomplished in planes of least and biggest rigidity. During turn of blade oscillations in both planes become connected, where due to change in rigidity of blade with its turn, frequencies of oscillations of blade change.

On Fig. 3.26 are represented frequency characteristics of blade of steering propeller of a helicopter. Shaded sections of diagram constitute limits of change in frequency of exciting forces in the range of working rpm of the propeller. With increase in angle of installation (pitch of propeller) frequency of lowest tone of joint flexural oscillations of blade (with degrees of freedom: bend in direction of thrust - bend in plane of rotation) essentially drops. Second tone of joint oscillations, conversely, increases. This is connected with the fact that with increase in angle of installation of blade in one plane, rigidity decreases (in plane of rotation), in the other it increases (in direction of thrust).

Besides the shown factors, oscillations of blades can be affected by torsional rigidity of propeller shaft. Usually this influence is small. Calculation of torsion of shaft is complicated by the fact that torsional rigidity of shaft is not always known beforehand. Therefore, during experimental determination of natural frequencies of propeller blades, one should establish on aircraft (helicopter) or simulate these conditions in a laboratory.

Natural oscillations (frequency and form) can render an essential influence on loads appearing in blades due to proximity of resonance with frequencies of disturbing forces. Therefore, a study of characteristics of natural oscillations of blades and their rational selection can essentially improve operational condition of a propeller on an aircraft (helicopter).

CHAPTER IV

STATISTICAL METHODS OF INVESTIGATING THE ACTION OF DYNAMIC LOADS ON A STRUCTURE

List of Designations Appearing in Cyrillic

вх = in = input

вых = out = output

гр = ld = load

ж = r = rigid

изг = bend = bending

кол/сек = osc/sec

крейс = cru = cruising

л = lef = left

м/рад = m/rad

м/сек = m/sec

н = rou = roughness

пр = rt = right

рад/м = rad/m

сек = sec

ф = f = fuselage

Ц.Т цт = CG (cg) = Center of Gravity (center of gravity)

ш = ldg = landing gear

Dynamic loads of structures are of two types:

a) rarely acting loads of considerable magnitude, provoking large stresses in the structure: time of action of such loads is commensurable with the period of lowest tone of natural elastic oscillations of the structure or less than it;

b) frequently repeating loads, the magnitude of which is small.

The first type of dynamic loads includes, for instance, aircraft loads appearing in gusts of air in a turbulent atmosphere and during sharp maneuvers, and loads appearing during takeoffs and landings.

Dynamic loads of the second type cause different forms of forced oscillations of aircraft structures (vibrations).

Dynamic loads acting on an aircraft depend on a large quantity of factors, the combination of which has a random character. For instance, loads during landing of an aircraft depend on the actions of the pilot, on weather conditions, on the lift-drag ratios of the aircraft, the character of the airport surface, the quality of shock absorption of landing gear, and several other factors. In a turbulent atmosphere the exact form of a gust is always indefinite to some extent. The influence of gusts on an aircraft has a random character. A random character is also carried by the majority of forms of oscillations of a structure in flight and during motion on the ground.

If, however, we consider the totality of a large number of random loads, it will appear that average results reveal stability in their own way.

The study of the regularities of random processes is the subject of mathematical statistics.

The basic concepts and methods of mathematical statistics which are used during the analysis of dynamic processes are set forth below.

4.1. The Concept of Probability.

Probability Distribution Functions

Let us consider a simple experiment of tossing a coin. Let us assume that the favorable event A will be tails. In the first N experiments event A happened ν times. Number ν, indicating how many times given event A happened, is called the frequency. Frequency of A is called the ratio of ν/N. It is obvious that

$$0 < \frac{\nu}{N} < 1. \tag{4.1}$$

Experiments indicate that upon increasing the number of experiments the frequency ν/N of defined event A tends to a certain more or less constant value. An illustration of this circumstance could be Fig. 4.1, where the dependence of frequency ν/N of the occurrence of "tails" on the number of tosses of the coin is depicted.

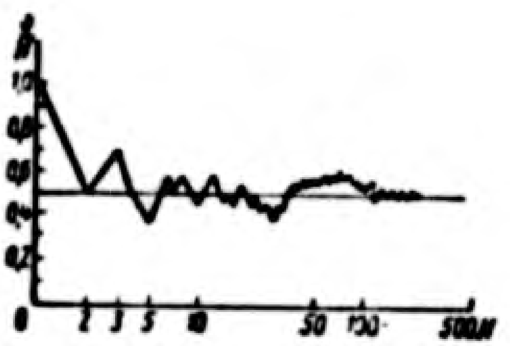

Fig. 4.1. Graph of the change of frequency with increase of the number of experiments.

The stability of frequency for a large volume of tests, repeated under identical conditions, has been known for a long time. There are foundations to assume that for any occurrence A, connected with a random experiment, one can determine such number P at which the frequency of appearance of event A with large repetition of the experiment will be approximately equal to P. This number P is called the probability of event A. In accordance with relationship (4.1) it is clear that

$$0 < P < 1.$$

If event A is impossible, then P = 0. If, however, A is a reliable event, then $P = 1$.

As an example of a random variable we shall consider force S, measured in an element of an aircraft design. Let us assume that in the first measurement we obtain the value of force S_1, in the second S_2, etc., and in the n-th measurement S_n.

On the graph along the axis of abscissas we shall plot magnitude S, and along the axis of ordinates we shall plot the probability of the fact that the force does not exceed the value of $S = x$. This probability can approximately be determined with the help of frequency summation of all values of forces less than or equal to x. Let us designate it $P(S \leq x)$. The curve obtained in such a way, $F(x) = P(S \leq x)$ (Fig. 4.2), is called the curve of integral probability distribution.

It is obvious that integral distribution function F(x) is a non-decreasing function of x and for it the following relationships are valid:

$$0 \leq F(x) \leq 1, \quad F(-\infty) = 0 \text{ and } F(+\infty) = 1.$$

The derivative at point

$$\frac{dF(x)}{dx} = w(x), \tag{4.2}$$

if it exists, is called the probability density or the probability distribution function of the random variable. Any probability density w(x) is non-negative function and the integral from it within the limits of $(-\infty, +\infty)$ is equal to one, i.e.,

$$\int_{-\infty}^{\infty} w(x)\,dx = 1. \tag{4.3}$$

Distributions occur in two types — discrete and continuous.

Random variable x is called a magnitude of the discrete type if it can take a finite or infinite denumerable set of values, i.e., such a set, the elements of which can be numbered in any order and written out in sequence $x_1, x_2, \ldots, x_n$. Discrete quantities are for instance the number of landings of an aircraft, the number of shots, etc.

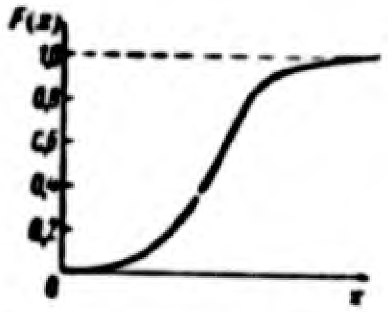

Fig. 4.2. Curve of integral probability distribution.

Distribution of discrete random variable x will be completely determined if one indicates for any value of $\nu(\nu = 1, 2, \ldots, N)$ the probability P_ν that x takes the value of x_ν. Since the probability that events $x_1, x_2, \ldots, x_n$ will take place is equal to one,

$$\sum_{\nu=1}^{n} P_\nu = 1.$$

The integral distribution function F(x) is then given by the relationship

$$F(x) = P(x_\nu < x) = \sum_{x_\nu < x} P_\nu, \qquad (4.4)$$

where summation is extended to all values of index ν, for which $x_\nu \leq x$. Thus, F(x) is a step function equal to a constant in any interval without point x_ν and having a jump of P_ν at every point x_ν. Distribution of the discrete type can be graphically represented by a step curve (Fig. 4.3).

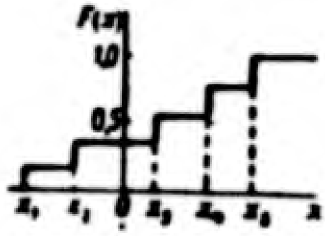

Fig. 4.3. Graph of step curve.

In the measurement of loads we investigate, as a rule, the continuous random variable, i.e., the variables which can take any value in one or several assigned intervals. For continuous magnitude X the distribution function F(x) is continuous (see Fig. 4.2); probability density $w(x) = F'(x)$ exists for all values of x.

In this case

$$F(x) = P(X < x) = \int_{-\infty}^{x} w(u)\,du. \qquad (4.5)$$

Probability is equal to zero at any x_ν, if X takes a particular value of x_ν:

$$P(X = x_\nu) = 0.$$

If magnitude X takes a value belonging to a finite interval (x_1, x_2), then in accordance with (4.5), the probability is

$$P(x_1 < X < x_2) = F(x_2) - F(x_1) = \int_{x_1}^{x_2} w(u)\,du. \qquad (4.6)$$

Obviously,

$$\int_{-\infty}^{\infty} w(u)\,du = 1.$$

Distribution of a continuous random variable can be represented by a graph of distribution function F(x) (see Fig. 4.2) or a graph of probability density of the given distribution w(x) (Fig. 4.4).

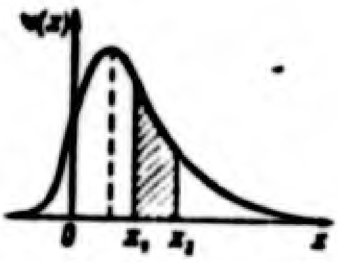

Fig. 4.4. Curve of probability density.

4.2. Characteristics of Distribution. Mean Values and Moments

In the investigation of a random variable it is important to know its value, around which is grouped the main mass of probabilities. From the graphic point of view it follows to represent the probability distribution in the form of corresponding masses on an axis. The sum of all masses is equal to one. Analogous to the center of weight of the masses, in mechanics the concept of mathematical expectation M(X) is introduced. Let us assume that the experiment is concerned with events $x_1, x_2, \ldots, x_n$, and let us assume that $P_1, P_2, \ldots, P_n$ are the probabilities of these events. The mathematical expectation or mean value of the magnitude is the sum of

$$M(X)=\sum_{\nu=1}^{N} P_\nu x_\nu \qquad (4.7)$$

which is the weighed mean of magnitude x, where by the scales are probabilities P_ν in points of concentration of mass. If with continuous random variable X the frequency of its values in an interval from x to x + Δx is approximately equal to $w(x)\Delta x$ and the value of magnitude X in this interval is approximately equal to x, the mean value is equal to $M(X) \approx \sum_{\Delta x_i} x_i w_i(x)\Delta x_i$, where summation is extended through all intervals of Δx. In the limit when $\Delta x \to 0$ we will obtain the exact formula for the mathematical expectation:

$$M(X)=\int_{-\infty}^{\infty} xw(x)\,dx. \qquad (4.8)$$

Integrals

$$\alpha_\nu=\int_{-\infty}^{\infty} x^\nu w(x)\,dx \qquad (\nu=1, 2, 3, \ldots) \qquad (4.9)$$

are called the first, second, third, etc, moments of distribution function is conformity with values of ν = 1, 2, 3, ... The first moment corresponds to the mean and is designated m.

Integrals

$$\mu_\nu=\int_{-\infty}^{\infty} (x-m)^\nu w(x)\,dx. \qquad (4.10)$$

are called central moments. By factoring $(x - m)^\nu$, we will find the relationships between moments and central moments:

$$\left.\begin{array}{l}\mu_0=1;\\ \mu_1=0;\\ \mu_2=\alpha_2-m^2;\\ \mu_3=\alpha_3-3m\alpha_2+2m^3;\\ \mu_4=\alpha_4-4m\alpha_3+6m^2\alpha_2-3m^4;\\ \ldots\ldots\ldots\ldots\end{array}\right| \qquad (4.11)$$

Mean magnitude m is in its own way a measure of the "position" of variable X; its concept is equivalent to the center of gravity of masses which are distributed along an axis in proportion to probability.

Second central moment μ_2 gives an idea on how far the values of the variable are distributed with respect to the mean value. This concept is analogous to the central moment of inertia with the indicated distribution of mass.

Second moment

$$\mu_2 = \int_{-\infty}^{\infty} (x-m)^2 w(x)\,dx. \tag{4.12}$$

is called the <u>dispersion</u> of the random variable.

As a characteristic of scattering, it has been accepted to consider a magnitude of the same dimension as the actual random variable which is called the <u>standard or mean quadratic deviation</u>, is designed by σ, and is taken to be equal to the nonnegative root of μ_2:

$$\sigma = \sqrt{\mu_2} = \sqrt{\alpha_2 - m^2}. \tag{4.13}$$

4.3. <u>Normal Distribution</u>

The most frequently encountered distribution is normal distribution, the integral function of which has the form

$$F(x) = \frac{1}{\sqrt{2\pi}} \int_{-\infty}^{x} e^{-\frac{v^2}{2}}\,dv. \tag{4.14}$$

Corresponding normal probability density is

$$w(x) = F'(x) = \frac{1}{\sqrt{2\pi}} e^{-\frac{x^2}{2}}. \tag{4.15}$$

Graphs of normal distribution functions are shown in Fig. 4.5. The mean value of this distribution is equal to zero and the mean quadratic value of random variable X, corresponding to it, is equal to one.

Random variable X is considered to be normally distributed with parameters m and σ if its integral distribution function $F(\frac{X-m}{\sigma})$ is determined by the formula

$$F\left(\frac{x-m}{\sigma}\right) = \frac{1}{\sqrt{2\pi}} \int_{-\infty}^{\frac{x-m}{\sigma}} e^{-\frac{v^2}{2}}\,dv. \tag{4.16}$$

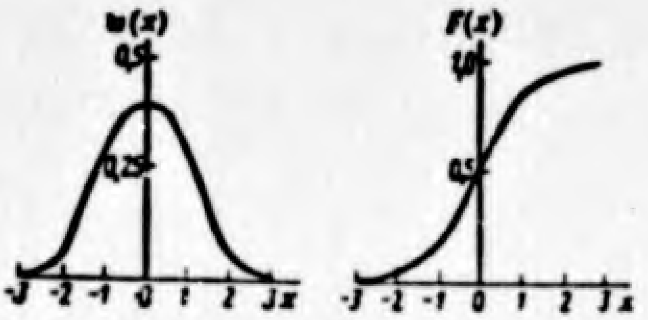

Fig. 4.5. Graphs of functions $w(x)$ and $F(x)$ for normal distribution.

where σ and m are constants ($\sigma > 0$). Then the probability density is

$$w(x) = \frac{1}{\sigma\sqrt{2\pi}} e^{-\frac{(x-m)^2}{2\sigma^2}}. \qquad (4.17)$$

It is easy to check that m is the mean value and σ is the standard deviation:

$$\left.\begin{aligned} &\int_{-\infty}^{\infty} x \frac{1}{\sigma\sqrt{2\pi}} e^{-\frac{(x-m)^2}{2\sigma^2}} dx = \frac{1}{\sqrt{2\pi}} \int_{-\infty}^{\infty} (m + \sigma x) e^{-\frac{x^2}{2}} dx = m; \\ &\int_{-\infty}^{\infty} (x-m)^2 \frac{1}{\sigma\sqrt{2\pi}} e^{-\frac{(x-m)^2}{2\sigma^2}} dx = \frac{\sigma^2}{\sqrt{2\pi}} \int_{-\infty}^{\infty} x e^{-\frac{x^2}{2}} dx = \sigma^2. \end{aligned}\right\} \qquad (4.18)$$

Magnitude m shows the displacement of curve $w(x)$ along the axis of abscissas without change of its form, while a change of magnitude σ causes a change of the scale along both coordinate axes.

Figure 4.6 gives the normal distribution curves for different values of σ. The smaller σ is, the closer the values of X are concentrated near point $x = m$.

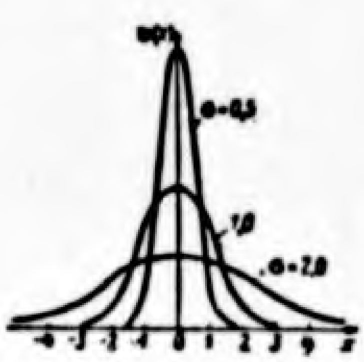

Fig. 4.6. Curves of normal distribution with different values of σ.

Analysis of the conditions of appearance of normal distribution shows that it is observed in all cases when the random variable characterizes the total effect of a large number of independent causes. Therefore, normal distribution is frequently encountered in practice.

In certain phenomena there predominates the influence of one independent magnitude and distribution has an asymmetric character. Such distribution can frequently be approximated by the logarithmically normal law of distribution (Fig. 4.7), when $v = \ln(x - m)$. In this case the distribution density is

$$w(x) = \frac{1}{\sigma (x-a)\sqrt{2\pi}} e^{-\frac{[\ln (x-a)-m]^2}{2\sigma^2}}, \qquad (4.19)$$

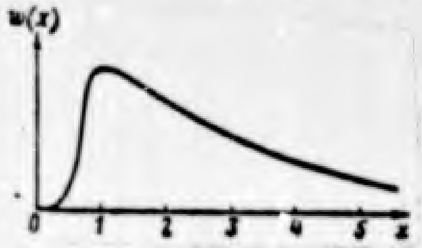

Fig. 4.7. Curve of logarithmically normal distribution.

where a is the lower bound of possible values of x.

During the analysis of experimental data for the determination of m and σ it is expedient to apply the graphic method. On the graph it is very easy to note the deviations of experimental points from theoretical the dependence if this dependence has a linear character. For obtaining a graph of normal distribution in the form of a straight line along the axis of ordinates we take probability scale in % corresponding to the linear scale of argument u (Fig. 4.8). Ordinates P are calculated by the formulas

$$\left.\begin{aligned} P &= \Phi(u) + 0{,}5 \quad u > 0; \\ P &= 0{,}5 - \Phi(u) \quad u < 0, \end{aligned}\right. \qquad (4.20)$$

where

$$\Phi(u) = \frac{1}{\sqrt{2\pi}} \int_0^u e^{-\frac{v^2}{2}} dv.$$

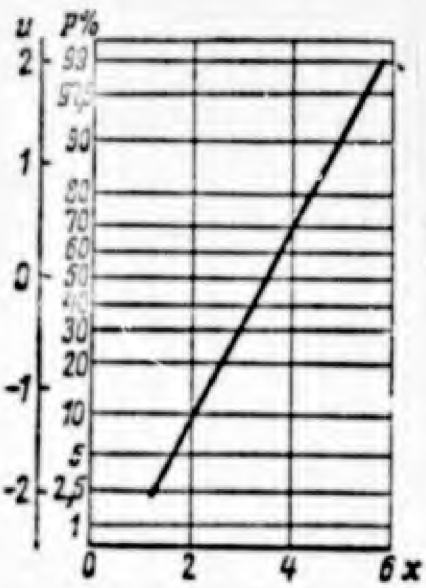

Fig. 4.8. Curve of normal distribution in probability scale.

Along the axis of abscissas we take the linear scale of the random variable. Paper with the probability scale drawn on it is commonly called probability paper. On such paper we plot the points of the experimental data in the form of accumulated frequencies:

$$F(x_i) = \frac{\nu_i}{N+1},$$

where ν_1 is the sum of frequencies of observations of values from 1 to x_1;

N is the total number of observations.

Then through the points we draw a straight line corresponding to normal distribution.

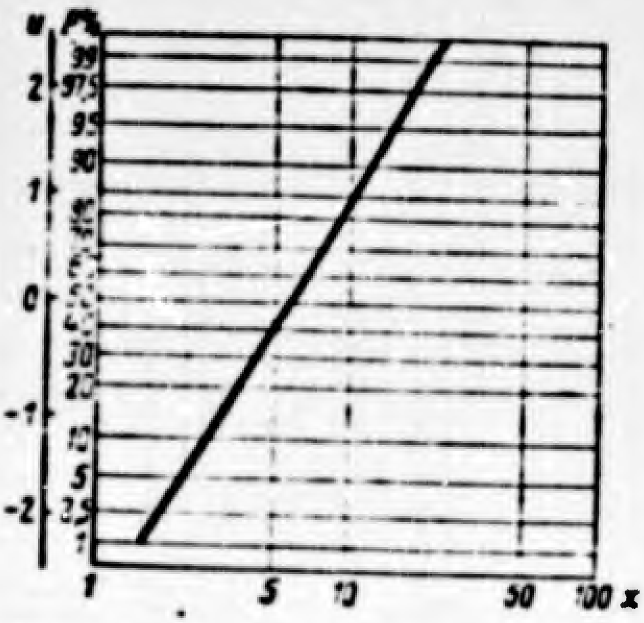

Fig. 4.9. Curve of logarithmically normal distribution in logarithmic probability scale.

Magnitude of mean m is determined by the value of x corresponding to the problem P = 50%. Standard deviation σ of distribution can be estimated by the distance $L_{P_1P_2}$ between points corresponding to probability of $P_1 = 10\%$ and $P_2 = 90\%$, from the relationship $\sigma = L_{P_1P_2}/2.56$.

The graphic method of estimating the mean value and mean quadratic deviation of a number of observations with simultaneous check of the normality of their distribution requires smaller expenditures of time than with the use of the usual calculation methods.

In asymmetric distribution a functional scale can be applied along the axis of abscissas. For instance, with the scale along the axis of abscissas log x, the logarithmically normal distribution will have the form of a straight line (Fig. 4.9).

4.4. Correlation. Correlation Coefficient

During the analysis of various kinds of loads it is frequently necessary to clarify their dependence on certain parameters. For random variables the concept of correlation is introduced. By correlation we mean such a connection of random variables when to each value of one variable there corresponds a probable value of another variable, with respect to which the observed values can be distributed according to some law of probability distribution. The nearer the observed values are to the probable value, the more defined is the dependence between the variables or, in other words, the stronger the correlation between them.

If both variables absolutely do not depend on one another, the correlation between them is absent. Correlation can be both linear and nonlinear, and exist between two, three, and larger numbers of variables.

For determination of the equation of correlation dependence the method of least squares is applied.

Let us consider the determination of the correlation dependence for two variables x and y.

Assuming the connection to be linear, we determine it in the form of a dependence between Δy and Δx:

$$\left.\begin{aligned}\Delta x &= x - m_x\\ \Delta y &= y - m_y\end{aligned}\right\} \tag{4.21}$$

where m_x and m_y are mean values of variables x and y.
It is necessary to select coefficient a in equation $\Delta y = a\Delta x$ in such a way so that the sum of $\sum_{i=1}^{n}(\Delta y_i - \Delta y)^2$ (where y_i are the observed values of Δy) is minimum.
The condition of minimum with be

$$\frac{\partial}{\partial a}\left[\sum_{i=1}^{n}(\Delta y_i - a\Delta x_i)^2\right] = 0, \tag{4.22}$$

whence

$$-2\sum_{i=1}^{n}\Delta y_i\Delta x_i + 2a\sum_{i=1}^{n}\Delta x_i^2 = 0,$$

and consequently,

$$a = \frac{\sum_{i=1}^{n}\Delta y_i\Delta x_i}{\sum_{i=1}^{n}\Delta x_i^2}. \tag{4.23}$$

The proximity of the experimental points to the obtained dependence is characterized by the correlation coefficient

$$\rho = \sqrt{1 - \left(\frac{\bar{\sigma}_y}{\sigma_y}\right)^2}. \qquad (4.24)$$

where $\bar{\sigma}_y$ is the standard deviation of observed values of Δy_i from the values of $\Delta y = a\Delta x$:

$$\bar{\sigma}_y = \sqrt{\frac{\sum_{i=1}^{n} (\Delta y - \Delta y_i)^2}{n}}; \qquad (4.25)$$

σ_y is the standard deviation from the mean value of y:

$$\sigma_y = \sqrt{\frac{\sum_{i=1}^{n} \Delta y_i^2}{n}}.$$

The maximum value of ρ is equal to unity when $\bar{\sigma} = 0$. This corresponds to the situation when all the observed points lie on the straight line $\Delta y = a\Delta x$. The minimum value of ρ is equal to zero, which corresponds to $\bar{\sigma}_y = \sigma_y$. When $\rho = 0$ the linear correlation is absent. However, there can exist some form of nonlinear correlation.

Usually for calculation of the correlation coefficient we use a somewhat different dependence.

Let us convert expression (4.25):

$$\begin{aligned} \bar{\sigma}_y^2 &= \frac{1}{n}\sum_{i=1}^{n} (\Delta y_i - \Delta y)^2 = \frac{1}{n}\sum_{i=1}^{n} (\Delta y_i - a\Delta x_i)^2 = \\ &= \frac{1}{n}\left(\sum_{i=1}^{n} \Delta y_i^2 - 2a\sum_{i=1}^{n} \Delta y_i \Delta x_i + a^2\sum_{i=1}^{n} \Delta x_i^2\right). \end{aligned} \qquad (4.26)$$

Further, substituting expression (4.23) instead of a, we obtain

$$\bar{\sigma}_y^2 = \sigma_y^2 - \frac{\left(\sum_{i=1}^{n} \Delta x_i \Delta y_i\right)^2}{n\sum_{i=1}^{n} \Delta x_i^2}. \qquad (4.27)$$

Placing expression (4.27) in formula (4.24), we find

$$\rho = \frac{\sum_{i=1}^{n} \Delta x_i \Delta y_i}{\sqrt{\sum_{i=1}^{n} \Delta x_i^2 \sum_{i=1}^{n} \Delta y_i^2}} = \frac{\sum_{i=1}^{n} \Delta x_i \Delta y_i}{n \sigma_x \sigma_y}. \tag{4.28}$$

Considering the denominator in expression (4.28) as a normalizing factor, as measure of correlation it is possible to take the magnitude $\sum_{i=1}^{n} \Delta x_i \Delta y_i$.

Analogous to this, by applying the method of least squares, we can find the form of the correlation for three and more variables.

4.5. Random Processes

In the practice of investigating the peculiarities of aircraft loading we frequently encounter random variables which vary in time or with respect to some other parameter, i.e., they are functions of this parameter. Gusts of air in a turbulent atmosphere, loads during motion on the ground, and so forth, are examples of such functions. In this case in every moment of time t the magnitude x(t) is not determined from conditions of the problem, but takes random values which are distributed according to the laws of probability.

A function whose value at every given magnitude of the independent variable is a random variable is called a random function. Thus a random function can be considered as an infinite totality of random variables depending on one or several continuously changing independent variables.

As a result of experiment a random function can take specific forms which are commonly called the realizations of the random function or the possible value of the random function, as for example the recording of pulsations air turbulence (Fig. 4.10).

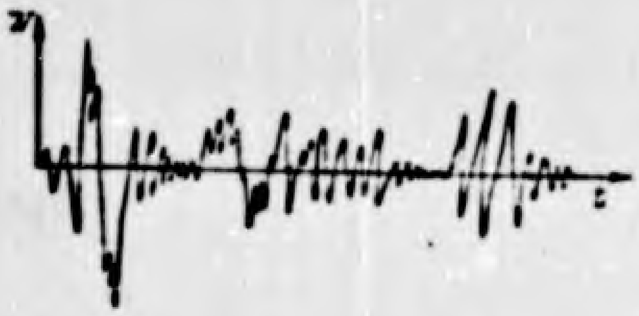

Fig. 4.10. Recording of pulsations of air turbulence.

It is possible to show that a large number of recordings of observations have been made in analogous conditions which form an ensemble or events. Let us number these recordings by $x_1(t)$, $x_2(t)$, ..., $x_n(t)$. It is possible to form the following statistical averages of the first, second order, etc:

$$\left.\begin{aligned}\widetilde{x(t)} &= \frac{1}{N}[x_1(t) + x_2(t) + \ldots + x_N(t)];\\ \widetilde{x^2(t)} &= \frac{1}{N}[x_1^2(t) + x_2^2(t) + \ldots + x_N^2(t)];\\ &\ldots\ldots\ldots\ldots\ldots\ldots\end{aligned}\right\} \qquad (4.29)$$

Let us assume that $\widetilde{x(t)}$, $\widetilde{x^2(t)}$, ... tend to defined limits when $N \to \infty$; then these limiting values $\widetilde{x(t)}$, $\widetilde{x^2(t)}$, ... constitute the averages with respect to the ensemble of a random process. Analogous to this it is possible to form the averages, which indicate the inner bond of the random process in time:

$$\left.\begin{aligned}\widetilde{x(t)x(t+\tau)} &= \lim_{N\to\infty}\frac{1}{N}\sum_{i=1}^{N}x_i(t)\,x_i(t+\tau);\\ &\ldots\ldots\ldots\ldots\ldots\ldots\\ \widetilde{x(t)x(t+\tau_1)\ldots x(t+\tau_n)} &= \lim_{N\to\infty}\frac{1}{N}\sum_{i=1}^{N}x_i(t)\,x_i(t+\\ &+\tau_1)\ldots x_i(t+\tau_n).\end{aligned}\right\} \qquad (4.30)$$

These averages are called the ensemble averages of correlation functions of the random process $x(t)$

A full statistical description of a random process requires averages of all orders.

Another type of average is the concept of the time average. For the first and second order these averages in the interval of time 2T have the form

$$\left.\begin{aligned}\overline{x(t)}^T &= \frac{1}{2T}\int_{t_0-T}^{t_0+T} x(t)\,dt;\\ \overline{x^2(t)}^T &= \frac{1}{2T}\int_{t_0-T}^{t_0+T} x^2(t)\,dt.\end{aligned}\right| \tag{4.31}$$

The limiting values of $\overline{x(t)}^T$ and $\overline{x^2(t)}^T$, when $T \to \infty$, we shall designate by $\overline{x(t)}$ and $\overline{x^2(t)}$. If the time averages at sufficiently large T do not depend on t_0 and T, then x(t) is a stationary function. For a stationary random process the probability distribution function does not depend on displacement of reading along the axis of time.

In the case of a stationary random process the time averages will be equal to the ensemble averages and, therefore, there is no necessity for the stationary process to distinguish the time average and the ensemble average.

The stationary character of a random process can be ascertained in the following way. Let us assume that we make a series of recordings (oscillograms) of a random process. If as a result of treatment of the oscillograms the obtained averages of $\overline{x(t)}$, $\overline{x^2(t)}$, and $\overline{x(t)x(t+\tau)}$ turn out to be the same for any moment of time t and any fixed value of τ, the process is stationary. If, however, the averages depend on moment of time t, for which they are determined, the process is non-stationary.

Random functions, which are functions of time, usually are called random or stochastic processes.

4.6. Correlation Function

For a stationary random process x(t) the correlation function $R(\tau)$ can be determined from the relationship

$$R(\tau) = \overline{x(t)\,x(t+\tau)} = \lim_{T\to\infty}\frac{1}{2T}\int_{-T}^{T} x(t)\,x(t+\tau)\,dt. \tag{4.32}$$

The physical meaning of the concept of correlation function consists of the following. The correlation function determines a certain averaged connection between values of the random function which are distant from each other at a defined interval τ, i.e., characterizes the mutual connection of $x(t)$ and $x(t + \tau)$.

If τ is sufficiently small, the interconnection between values of $x(t)$ and $x(t + \tau)$ is great and the relation of $R(\tau)/R(0)$ is close to unity, i.e., at small values of τ the probability that the value of function $x(t = \tau)$ hardly differs from the value of $x(t)$ is close to unity. With the increase of τ the component, which is determined by the initial values of x, attenuates, the connection between magnitudes $x(t)$ and $x(t + \tau)$ weakens, they become mutually independent, and function $R(\tau)$ tends to zero. Thus, at sufficiently large τ the probability that magnitude $x(t + \tau)$ will hardly differ from magnitude $x(t)$ is practically equal to zero:

Let us consider certain properties of the correlation function.

1. The correlation function $R(\tau)$ of a random function with mean value $m = 0$ for sufficiently large τ tends to zero:

$$\lim_{\tau\to\infty} |R(\tau)| = 0. \tag{4.33}$$

When $m \neq 0$ $\lim\limits_{\tau\to 0} |R(\tau)| = m^2$.

Figure 4.11 gives the approximate form of the correlation function.

2. The initial value of $R(0)$ of the correlation function $R(\tau)$ is equal to the mean value of the square of the random function and, therefore, is essentially positive:

$$R(0) = \overline{x^2}. \tag{4.34}$$

3. Correlation function $R(\tau)$ is an even function of τ:

$$R(\tau)=R(-\tau) \qquad (4.35)$$

Actually,

$$R(\tau)=\overline{x(t+\tau)x(t)}=\overline{x(t)x(t-\tau)}=R(-\tau).$$

4. The values of correlation function $R(\tau)$ at any value of τ never exceed its initial magnitude $R(0)$, i.e.,

$$R(0)>R(\tau). \qquad (4.36)$$

For proof of this relationship we shall consider the inequality

$$[x(t)\pm x(t+\tau)]^2>0$$

or

$$x^2(t)+x^2(t-\tau)>\pm 2x(t)x(t+\tau).$$

Taking the time average from both parts of this inequality and considering relationship (4.34), we obtain relationship (4.36).

Fig. 4.11. Approximate form of correlation function.

If function $x(t)$ contains a random function with a periodic component superimposed on it, the correlation function will also contain a periodic component with the same period and will have the form depicted in Fig. 4.12. However, the correlation function does not contain information about phases of the process. For an example we shall find the correlation function for the case of

$$x(t)=a\sin(\omega t+\varphi).$$

understanding the term "correlation function" as simply the result of application of the operation expressed by integral (4.32) to the function $x(t)$:

$$R(\tau)=\lim_{T\to\infty}\frac{1}{2T}\int_{-T}^{T}a^2\sin(\omega t+\varphi)\sin(\omega t+\omega\tau+\varphi)\,dt=$$

$$=\lim_{T\to\infty}\frac{1}{2T}\frac{a^2}{2}\int_{-T}^{T}[\cos\omega\tau-\cos(2\omega t+\omega\tau+2\varphi)]\,dt=$$

$$=\lim_{T\to\infty}\frac{a^2}{2}\left\{\cos\omega\tau-\frac{1}{2T}\frac{\sin(2\omega T+\omega\tau+2\varphi)+\sin(2\omega T-\omega\tau-2\varphi)}{2\omega}\right\}=$$

$$=\frac{a^2}{2}\cos\omega\tau.$$

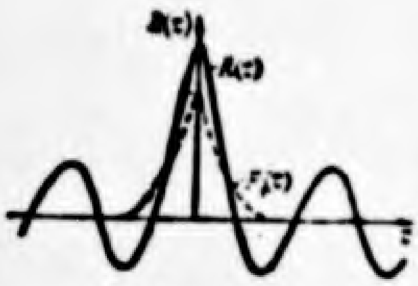

Fig. 4.12. Form of correlation function of a process having a periodic component. $R_1(\tau)$-correlation function corresponding to the random component of function $x(t)$.

Sometimes (usually in those cases when $\bar{x}\neq 0$) it turns out to be convenient to introduce into consideration the standardized correlation function

$$\rho(\tau)=\frac{\overline{[x(t)-\bar{x}][x(t+\tau)-\bar{x}]}}{\overline{x^2}-\bar{x}^2}. \qquad (4.37)$$

It is obvious that $\rho(0)=1$.

4.7. Spectral Density

As it is known, absolutely integratable functions $f(t)$, i.e., functions satisfying the condition

$$\int_{-\infty}^{\infty}f(t)\,dt<\infty,$$

can be represented in the form of a Fourier integral

$$f(t)=\int_{-\infty}^{\infty}F(i\omega)e^{i\omega t}\,d\omega, \qquad (4.38)$$

where

$$F(i\omega)=\frac{1}{2\pi}\int_{-\infty}^{\infty}f(t)e^{-i\omega t}\,dt.$$

Function $F(i\omega)$ is called the Fourier transform or the complex spectrum of function $f(t)$.

We shall consider a stationary random process $x(t)$ for which the mean value m is equal to zero. We shall "truncate" function x(t) in such a way that it is equal to zero outside the interval (-T, T). The truncated function will be designated as $x_T(\tau)$, i.e.,

$$\left.\begin{array}{l} x_T(t) = x(t) \text{ when } -T \le t \le T; \\ x_T(t) = 0 \quad \text{at all remaining values of t.} \end{array}\right\} \tag{4.39}$$

We shall define the concept of spectral density $S(\omega)$ as the Fourier transform from correlation function $R(\tau)$:

$$S(\omega) = \int_{-\infty}^{\infty} R(\tau) e^{-i\omega\tau} d\tau = 2\int_{-\infty}^{\infty} R(\tau)\cos\omega\tau\, d\tau. \tag{4.40}$$

Consequently,

$$R(\tau) = \frac{1}{2\pi}\int_{-\infty}^{\infty} S(\omega) e^{i\omega\tau} d\omega = \frac{1}{2\pi}\int_{-\infty}^{\infty} S(\omega)\cos\tau\omega\, d\omega. \tag{4.41}$$

For proof of this transformation we use the concept of current spectrum $X_T(i\omega)$ which is the Fourier transform for function $x_T(t)$:

$$X_T(i\omega) = \int_{-\infty}^{\infty} x_T(t) e^{-i\omega t} dt = \int_{-T}^{T} x_T(t) e^{-i\omega t} dt. \tag{4.42}$$

Then

$$S_T(\omega) = \int_{-\infty}^{\infty} R_T(\tau) e^{-i\omega\tau} d\tau = \frac{1}{2T}\int_{-\infty}^{\infty} e^{-i\omega\tau} d\tau \int_{-\infty}^{\infty} x_T(t) \times x_T(t+\tau)\, dt = \frac{1}{2T}\int_{-\infty}^{\infty} x_T(t) e^{i\omega t} dt \int_{-\infty}^{\infty} x_T(t+\tau) e^{-i\omega(t+\tau)} d\tau, \tag{4.43}$$

where

$$R_T(\tau) = \frac{1}{2\pi}\int_{-T}^{T} x_T(t)\, x_T(t+\tau)\, dt.$$

Conducting transformation in expression (4.43) and considering that $X_T^*(i\omega)$ signifies a complex number conjugate with $X(i\omega)$, i.e.,

$$X_T^*(i\omega) = X_T(-i\omega) = \int_{-\infty}^{\infty} x_T(t) e^{i\omega t} dt. \tag{4.44}$$

we obtain

$$S_T(\omega) = \int_{-\infty}^{\infty} R_T(\tau) e^{-i\omega\tau} d\tau = \frac{1}{2T} X(i\omega) X^*(i\omega). \tag{4.45}$$

Considering that the function $R_T(\tau)$ is even,

$$\int_{-\infty}^{\infty} R_T(\tau) e^{-i\omega\tau} d\tau = 2 \int_0^{\infty} R_T(\tau) e^{-i\omega\tau} d\tau = 2 \int_0^{\infty} R_T(\tau) \cos \omega\tau \, d\tau. \tag{4.46}$$

Consequently

$$S_T(\omega) = 2 \int_0^{T} R_T(\omega) e^{-i\omega\tau} d\tau = \frac{1}{2T} |X_T(i\omega)|^2. \tag{4.47}$$

As the spectral density it is possible to consider

$$S(\omega) = \lim_{T \to \infty} \frac{1}{2T} |X_T(i\omega)|^2. \tag{4.48}$$

Let us stop on certain properties of spectral density.

If $R(\tau)$ is monotonically diminishing function of τ, $S(\omega)$ is also a monotonically diminishing function of ω. The narrower function $R(\tau)$ is, the flatter and wider function $S(\omega)$ is. If $R(\tau)$ tends to zero during a very short interval of time Δ, then $S(\omega)$ keeps approximately a constant value up to a frequency of the order of $2\pi/\Delta$. Such a spectrum $S(\omega)$ is frequently called a white spectrum. A limiting case, when $S(\omega)$ = const, corresponds to the absence of any correlation between subsequent values of $x(t)$.

If $S(\omega)$ has a maximum at a certain frequency w_c and possesses symmetry with respect to this point, the correlation function will have the character of damped oscillations with frequency ω_c.

If $x(t)$, in addition a random component, contains a periodic component with frequency ω_0, the spectral density S_ω has discontinuity at the point $\omega = \omega_0$. Correspondingly, if $\overline{x(t)} \neq 0$, the function $S(\omega)$ will have a discontinuity in the origin of coordinates, i.e., when $\omega = 0$.

There exists the relationship

$$\overline{x^2} = \frac{1}{2\pi}\int_{-\infty}^{\infty} S(\omega)\,d\omega. \tag{4.49}$$

This relationship can be obtained in the following way.

We have

$$\int_{-\infty}^{\infty} |X_T(i\omega)|^2\,d\omega = \int_{-\infty}^{\infty} X_T(-i\omega)X_T(i\omega)\,d\omega = \int_{-\infty}^{\infty} X_T(-i\omega)\,d\omega \int_{-\infty}^{\infty} x_T(t)e^{-i\omega t}\,dt \tag{4.50}$$

or, changing the order of integration,

$$\int_{-\infty}^{\infty} |X_T(i\omega)|^2\,d\omega = \int_{-\infty}^{\infty} x_T(t)\,dt \int_{-\infty}^{\infty} X_T(-i\omega)e^{-i\omega t}\,d\omega = 2\pi\int_{-\infty}^{\infty} x_T^2(t)\,dt. \tag{4.51}$$

Thus,

$$\int_{-\infty}^{\infty} x_T^2(t)\,dt = \int_{-T}^{T} x_T^2(t)\,dt = \frac{1}{2\pi}\int_{-\infty}^{\infty} |X(i\omega)|^2\,dt. \tag{4.52}$$

Dividing (4.52) by 2T, with sufficiently large values of T it is possible to write

$$\overline{x^2} = \frac{1}{2T}\int_{-T}^{T} x_T^2(t)\,dt = \frac{1}{2\pi}\int_{-\infty}^{\infty} \frac{1}{2T}|X(i\omega)|^2\,d\omega = \frac{1}{2\pi}\int_{-\infty}^{\infty} S(\omega)\,d\omega. \tag{4.53}$$

Since in certain cases magnitude $\overline{x^2}$ gives an estimate of energy or power, then sometimes $S(\omega)$ is called spectral power. Element $S(\omega)\,d\omega$ gives component $\overline{x^2}$ from components of frequencies lying in a range from ω to $\omega + d\omega$.

4.8. Analysis of the Action of Dynamic Loads on a Linear System

During the dynamic action of an external load a considerable influence on the character and magnitude of forces in elements of a structure is rendered by the elastic oscillations of the structure.

An approximate solution of the problem concerning the action of dynamic loads on a structure can be obtained by two methods:

a) divide the entire aircraft structure into n sections having assigned mass m_i, moment of inertia J_i, and elastic constraints of defined rigidity connected between themselves. In this case the problem is reduced to integration of a system 2n of second order differential equations, since for each of the sections it is possible to compose two equations, one of which will describe forward motion of the i-th section, and the other, its rotation:

b) taking into consideration a limited number of natural vibration modes of the aircraft, reduce the solution to the problem of a system with a finite number of degrees of freedom. With the known modes of $f_i(z)$ the forced oscillations of the structure can be represented by a system of equations of the form (3.95):

$$\ddot{R}_i(t) + p_i^2 R_i(t) = \frac{Q_i}{m}. \tag{4.54}$$

It is usually sufficient to consider the first four modes of elastic oscillations.

Thus in both cases this problem is reduced to the solution of a system of second order equations with constant coefficients, i.e., to the investigation of a linear system.

Mechanical Conductivity of a System

Let us consider the solution of a second order differential equation (3.30) in complex form. Let us designate $F_0 = P_0/m$ and present the periodic force in the form of $F = F_0 e^{i\omega t}$. Then the solution of the equation can be written in the form of

$$y = \frac{F_0 e^{i\omega t}}{Z(i\omega)}. \tag{4.55}$$

where

$$Z(i\omega) = (i\omega)^2 + 2h(i\omega) + p^2.$$

Modulus $Z(i\omega) = \sqrt{(p^2-\omega^2)^2 + 4h^2\omega^2}$, and phase angle

$$\alpha = \operatorname{arc\,tg} \frac{2h\omega}{p^2-\omega^2}.$$

Magnitude $Z(i\omega)$ is called the mechanical impedance of the system described by equation (3.30). Reciprocal $Hi(\omega) = \frac{1}{Z(i\omega)}$ is called the mechanical conductivity of the system. In our example

$$H(i\omega) = \frac{1}{\sqrt{(p^2-\omega^2)^2 + 4h^2\omega^2}}.$$

The solution (4.55) of equation (3.30) can be written in the form of

$$y = H(i\omega) F_0 e^{i\omega t}.$$

Thus the reaction of a linear system to a perturbing force, which is variable according to harmonic law, is obtained by multiplication of the perturbing force by the magnitude of mechanical conductivity.

If systems, whose individual impedance is Z_1 and Z_2, are connected in series, the resultant impedance is

$$Z = Z_1 + Z_2.$$

If, however, the systems are connected in parallel, the resultant impedance will be determined from the relationship

$$\frac{1}{Z} = \frac{1}{Z_1} + \frac{1}{Z_2}$$

or the resultant mechanical conductivity is equal to

$$H = H_1 + H_2.$$

Since the differential equation is linear, the superposition principle is valid, i.e., if the right side of equation (3.30) has the form of $F_1 + F_2 = F_{10}e^{i\omega t} + f_{20}e^{i2\omega t}$, the solution can be written in form of

$$y(t)=\frac{F_{\omega}}{Z(i\omega)}+\frac{F_{2\omega}}{Z(i2\omega)}. \tag{4.56}$$

In more general form this principle can be represented if the right side of the equation is assigned a Fourier series:

$$F(t)=\sum_{n=-\infty}^{\infty} C_n e^{in\omega t}.$$

Then

$$y(t)=\sum_{n=-\infty}^{\infty} \frac{C_n}{Z(in\omega)} e^{in\omega t}. \tag{4.57}$$

where C_n are Fourier coefficients.

Further generalization of the principle consists in that F(t) is expressed with the help of a Fourier intergal:

$$F(t)=\frac{1}{\sqrt{2\pi}}\int_{-\infty}^{\infty} C(\omega) e^{i\omega t}\,d\omega, \tag{4.58}$$

where

$$C(\omega)=\frac{1}{\sqrt{2\pi}}\int_{-\infty}^{\infty} F(t) e^{-i\omega t}\,dt.$$

Then

$$y(t)=\frac{1}{\sqrt{2\pi}}\int_{-\infty}^{\infty} \frac{C(\omega)}{Z(i\omega)} e^{i\omega t}\,d\omega. \tag{4.59}$$

Transition Conductivity of a System and Impulse Response

Let us consider the reaction of a linear system to a certain form of perturbation. A simple example of a perturbation function is the unit step function 1(t) which is determined in the following way (Fig. 4.13):

$$\left.\begin{aligned} 1(t)&=0 \text{ for } t<0;\\ 1(t)&=\tfrac{1}{2} \text{ for } t=0;\\ 1(t)&=1 \text{ for } t>0. \end{aligned}\right| \tag{4.60}$$

Such a function can be obtained as the limit of a properly selected

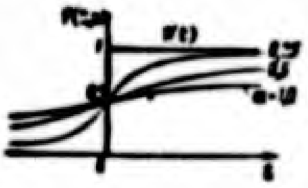

Fig. 4.13. Graph of unit step function 1(t).

continuous function (see Fig. 4.13):

$$f(t,a) = \frac{1}{2} + \frac{1}{\pi}\operatorname{arctg}\frac{t}{a} \qquad (4.61)$$

Actually if we limit ourselves to the consideration of the main values of a many-valued function (4.61) in the interval

$$-\frac{\pi}{2} < \operatorname{arctg}\frac{t}{a} < \frac{\pi}{2}.$$

then

$$\lim_{a\to 0} f(t,a) = \lim_{a\to 0}\left(\frac{1}{2} + \frac{1}{\pi}\operatorname{arctg}\frac{t}{a}\right) = 1(t).$$

If the step point shifts from point t = 0 to point t = τ (Fig. 4.14), the step function is recorded in the form of 1(t-τ).

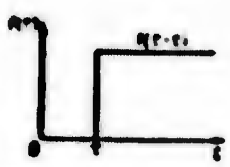

Fig. 4.14. Graph of unit step function 1(t-τ).

The reaction of a physical system to the unit step function is called the <u>transition conductivity of the system</u> A(t). Let us find the reaction of a linear system to the unit step function. Let us consider the equation

$$\ddot{y} + p^2 y = 1(t) \qquad (4.62)$$

under the initial conditions t = 0, $y = \dot{y} = 0$.

The general solution of this equation has the form of

$$y = \frac{1}{p^2} + C_1\sin pt + C_2\cos pt.$$

Using the initial conditions, we find that $C_1 = 0$ and $C_2 = -\frac{1}{p^2}$. Consequently the transition conductivity of the system (Fig. 4.15) is

$$A(t) = y = \frac{1}{p^2}(1 - \cos pt)\,1(t). \qquad (4.63)$$

The unit step function causes a sudden jump which is equal to two, i.e., dynamic coefficient $\lambda = 2$.

Of large value in the analysis of oscillatory systems is the reaction of a system to the δ-function, which may be considered as a derivative of the unit step function. With the exception of the point where $t = 0$, the derivative from $1(t)$ is equal to zero. For determination of the δ-function we shall consider the derivative from a corresponding continuous function (4.61):

$$\delta(t, a) = \frac{d\eta(t, a)}{dt} = \frac{a}{\pi(t^2 + a^2)}.$$

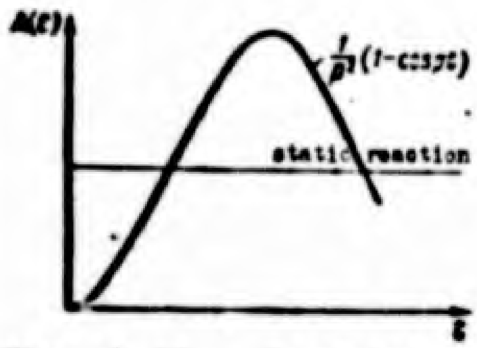

Fig. 4.15. Transition conductivity curve of a linear system with one degree of freedom.

The δ-function $\delta(t)$ may be considered as the limit of continuous function $\delta(t, a)$ when $a \to 0$:

$$\delta(t) = \lim_{a \to 0} \delta(t, a) = \lim_{a \to 0} \frac{d\eta(t, a)}{dt}.$$

Consequently, the δ-function is equal to zero when $t \neq 0$ and is equal to infinity when $t = 0$, since $\delta(0, a) = \frac{1}{\pi a}$. With the decrease of a the peak magnitude increases (Fig. 4.16), but the area limited by the curve $\delta(t, \delta)$ remains equal to unity independently of a:

$$\int_{-\infty}^{\infty} \delta(t, a)\,dt = 1.$$

For the δ-function the following equality is also valid:

$$\int_{-\infty}^{\infty} \delta(t)\,dt = 1.$$

If the δ-function is considered as being shifted along the axis of abscissas in point $t = \tau$, it is recorded in the form of $\delta(t-\tau)$. Frequently the δ-function is written in the following form:

$$\left.\begin{aligned}&\delta(t-\tau)=0 \text{ when } t\neq\tau;\\&\lim_{\varepsilon\to 0}\int_{-\varepsilon}^{\varepsilon}\delta(t-\tau)\,dt=1.\end{aligned}\right\} \tag{4.64}$$

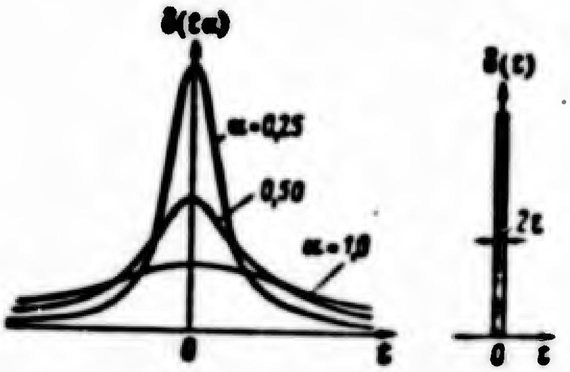

Fig. 4.16. Graph of δ-function.

Response to the δ-function is called the impulse response h(t). As an example we shall consider an equation of the form

$$\left.\begin{aligned}&\ddot{y}+p^2y=\delta(t);\\&y=\dot{y}=0 \text{ when } t<-\varepsilon\ (\varepsilon>0).\end{aligned}\right\} \tag{4.65}$$

Integrating equation (4.65) from $-\varepsilon$ to ε, where ε is a small number, we obtain

$$\int_{-\varepsilon}^{\varepsilon}\frac{d^2y}{dt^2}\,dt+p^2\int_{-\varepsilon}^{\varepsilon}y\,dt=1. \tag{4.66}$$

The first integral can be converted in the following way:

$$\int_{-\varepsilon}^{\varepsilon}\frac{d}{dt}\left(\frac{dy}{dt}\right)dt=\int_{-\varepsilon}^{\varepsilon}d\left(\frac{dy}{dt}\right)=\frac{dy}{dt}\Big|_{-\varepsilon}^{\varepsilon}=\left(\frac{dy}{dt}\right)_{t=\varepsilon},$$

since $\left(\frac{dy}{dt}\right)_{t=-\varepsilon}=0$.

The second integral of (4.66) tends to zero, since in the vicinity of $t=0$ y is a finite quantity, i.e., $|y|<M$ and the integral is limited by magnitude $2M\varepsilon$, which tends to zero in the limit when $\varepsilon\to 0$. Consequently, in the limit, relationship (4.66) will take on the form of

$$\left(\frac{dy}{dt}\right)_{t=0}=1.$$

Therefore, the initial equation (4.65) will be equivalent to the system of equations

$$\begin{aligned}&\ddot{y}+p^2y=0,\quad t>0;\\&y=0;\quad \dot{y}=1,\quad t=(0+).\end{aligned}$$

the solution of which has the form of

$$h(t) = \frac{1}{p}\sin pt \cdot 1(t).$$

Between the transition conductivity of the system and the impulse response there takes place the relationship

$$h(t) = \frac{dA}{dt}.$$

Duhamel Integral

Let us consider the reaction of a linear system to the action of a force F(t) which is arbitrarily variable in time. Function F(t) can be approximately represented in the form of the sum of step functions (Fig. 4.17a). As an independent variable we take the magnitude τ.

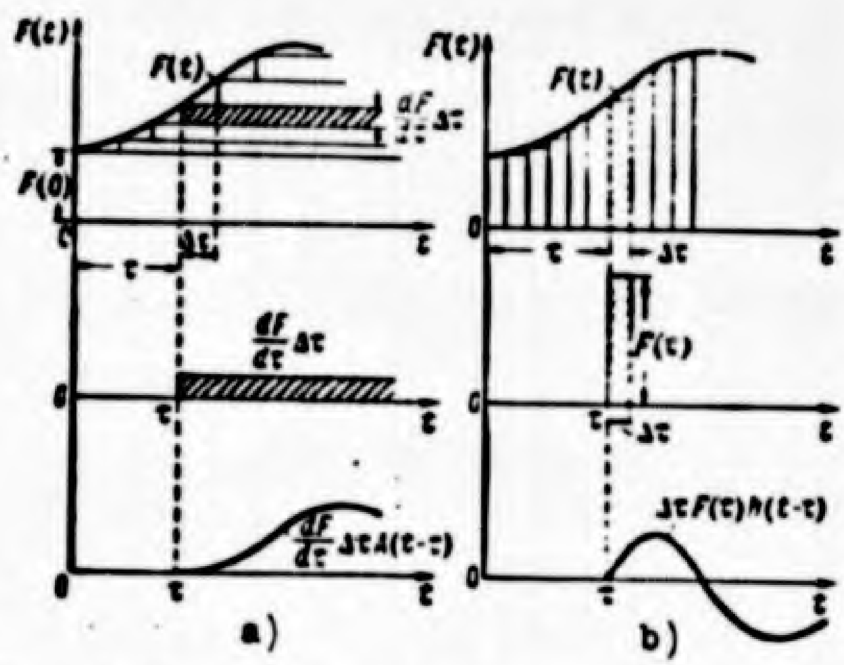

Fig. 4.17. Geometric representation of the Duhamel integral by the step function a) and δ-function b).

The reaction to the step function with ordinate $\Delta F(\tau)$, applied at the time $\tau + \Delta\tau$, is determined by the expression

$$\Delta y(t) = \Delta F(\tau) A[t - (\tau + \Delta\tau)].$$

The reaction to the entire totality of step functions from $\tau = 0$ to

$\tau = t$ is found on the basis of the superposition principle:

$$y(t) = F(0)A(t) + \sum_{\tau=0}^{\tau=t} \Delta F(\tau) A[t-(\tau+\Delta\tau)] =$$
$$= F(0)A(t) + \sum_{\tau=0}^{\tau=t} \frac{\Delta F(\tau)}{\Delta\tau} A[t-(\tau+\Delta\tau)]\Delta\tau.$$

Passing to a definite integral when $\Delta\tau \to 0$, we obtain

$$y(t) = F(0)A(t) + \int_0^t \frac{dF(\tau)}{d\tau} A(t-\tau)\,d\tau. \tag{4.67}$$

Partially integrating, we reduce expression (4.67) to the following form:

$$y(t) = -\int_0^t F(\tau) \frac{d}{d\tau} A(t-\tau)\,d\tau, \tag{4.68}$$

or

$$y(t) = \int_0^t F(\tau) h(t-\tau)\,d\tau, \tag{4.69}$$

where

$$h(t-\tau) = \frac{dA(t-\tau)}{dt}.$$

Integrals in formulas (4.68) and (4.69) are known under the name of Duhamel integrals.

Calculation of relationship (4.69) can be made by using the δ-function and impulse response $h(t-\tau)$. The sequence of calculation is graphically shown in Fig. 4.17b.

Reaction of a Linear System to Random Perturbation

We shall determine a relationship with help of which it is possible to conduct an analysis of the reaction of dynamic systems to random perturbations.

Relationship (4.69) for a stationary process (in this case the perturbation acts all the time) can be written in the form of

$$y(t) = \int_{-\infty}^{t} F(\tau) h(t - \tau) d\tau. \tag{4.70}$$

Expression (4.70) will not change if instead of t we put the upper limit of integration equal to $+\infty$, since magnitude $h(t-\tau)$ obviously is equal to zero for a non-negative argument. Therefore, for $t < \tau < +\infty$ the intergrand expression also equal to zero and consequently,

$$y(t) = \int_{-\infty}^{\infty} F(\tau) h(t - \tau) d\tau.$$

Introducing the variable $\sigma = (t-\tau)$, we obtain

$$y(t) = \int_{-\infty}^{\infty} F(t - \sigma) h(\sigma) d\sigma. \tag{4.71}$$

Using relationship (4.71), we can find the correlation function of the output magnitude

$$R(\tau) = \lim_{T \to \infty} \frac{1}{2T} \int_{-T}^{T} y(t + \tau) y(t) dt. \tag{4.72}$$

Putting expression (4.71) in formula (4.72) and introducing σ' into expression $y(t + \tau)$, we obtain

$$\begin{aligned} R(\tau) &= \lim_{T \to \infty} \frac{1}{2T} \int_{-T}^{T} \int_{-\infty}^{\infty} \int_{-\infty}^{\infty} F(t - \sigma) F(t + \tau - \sigma') h(\sigma) h(\sigma') d\sigma d\sigma' dt = \\ &= \int_{-\infty}^{\infty} \int_{-\infty}^{\infty} h(\sigma) h(\sigma') \left\{ \lim_{T \to \infty} \frac{1}{2T} \int_{-T}^{T} F(t - \sigma) F(t + \tau - \sigma') dt \right\} d\sigma d\sigma'. \end{aligned} \tag{4.73}$$

Since the position of interval 2T in the stationary function does not affect the result, by putting $t' = t - \sigma$, we can obtain

$$\lim_{T\to\infty}\frac{1}{2T}\int_{-T}^{T}F(t-\sigma)F(t+\tau-\sigma')\,dt=$$

$$=\lim_{T\to\infty}\frac{1}{2T}\int_{-T-\sigma}^{T-\sigma}F(t')F(t'+(\tau+\sigma-\sigma'))\,dt'=R_{in}(\tau+\sigma-\sigma'). \tag{4.74}$$

Putting formula (4.74) in expression (4.73), we obtain the relationship between values of input R_{in} and output R_{out} correlation functions:

$$R_{out}(\tau)=\int_{-\infty}^{\infty}\int_{-\infty}^{\infty}h(\sigma)h(\sigma')R_{in}(\tau+\sigma-\sigma')\,d\sigma\,d\sigma'. \tag{4.75}$$

A more important dependence is the relationship between spectral densities of input $S_{in}(\omega)$ and output signal $S_{out}(\omega)$. This relationship can be derived by using the dependence

$$S_{out}=\int_{-\infty}^{\infty}R_{out}(\tau)e^{-i\omega\tau}\,d\tau \tag{4.76}$$

Substituting (4.75) in (4.76), we find

$$\begin{aligned}S_{out}(\omega)&=\int_{-\infty}^{\infty}\int_{-\infty}^{\infty}\int_{-\infty}^{\infty}e^{-i\omega\tau}h(\sigma)h(\sigma')R_{in}(\tau+\sigma-\sigma')\,d\sigma\,d\sigma'\,d\tau=\\&=\int_{-\infty}^{\infty}\int_{-\infty}^{\infty}\int_{-\infty}^{\infty}e^{-i\omega(\tau+\sigma-\sigma')}e^{i\omega\sigma}h(\sigma)e^{-i\omega\sigma'}h(\sigma')R_{in}(\tau+\sigma-\\&-\sigma')\,d\sigma\,d\sigma'\,d\tau=\int_{-\infty}^{\infty}h(\sigma)e^{i\omega\sigma}d\sigma\int_{-\infty}^{\infty}h(\sigma')e^{-i\omega\sigma'}d\sigma'\int_{-\infty}^{\infty}R_{in}(\tau+\\&+\sigma-\sigma')e^{-i\omega(\tau+\sigma-\sigma')}d\tau\end{aligned} \tag{4.77}$$

The first two integrals of expression (4.77) are determined by the reaction of the linear system to the input value of unit amplitude which varies according to sine law and is effective for a prolonged interval of time. Therefore, the integrals are connected with mechanical conductivity $H(i\omega)$ by the following relationships:

$$\begin{aligned}\int_{-\infty}^{\infty}h(\sigma')e^{-i\omega\sigma'}d\sigma&=\int_{-\infty}^{\infty}h(\sigma')e^{-i\omega\sigma'}d\sigma=-\int_{\infty}^{t}h(t-\tau)e^{-i\omega(t-\tau)}d\tau=\\&=e^{-i\omega t}\int_{-\infty}^{t}e^{i\omega\tau}h(t-\tau)\,d\tau=H(i\omega)\end{aligned} \tag{4.78}$$

and

$$\int_{-\infty}^{\infty} h(s)e^{i\omega s}\,ds = e^{i\omega t}\int_{-\infty}^{t} e^{-i\omega t}h(t-\tau)\,d\tau = H(-i\omega) \qquad (4.79)$$

Putting expressions (4.78) and (4.79) in equation (4.77) and considering that

$$\int_{-\infty}^{\infty} R_{in}(\tau+s-s')e^{-i\omega(\tau+s-s')}\,d\tau = S_{in}(\omega),$$

we obtain

$$S_{out}(\omega) = H(i\omega)\cdot H(-i\omega)\,S_{in}(\omega)$$

or

$$S_{out}(\omega) = |H(i\omega)|^2 S_{in}(\omega). \qquad (4.80)$$

Expression (4.80) shows that spectral density $S_{out}(\omega)$ of the signal at the outlet of a linear dynamic system is equal to the square of mechanical conductivity $H(i\omega)$ multiplied by spectral dens. $S_{in}(\omega)$ of the signal at the input.

4.9. Reaction of an Aircraft to Gusts of Turbulent Air

Single Gust

For determination of loads appearing during gusts a number of simplifications are made, and the perturbed motion of an aircraft in this case is considered as the motion of a system having only one degree of freedom, i.e., vertical movement y. The equation of motion will have the form of

$$m\ddot{y} = -Y. \qquad (4.81)$$

where m is the mass of the aircraft;

y is the lift of the aircraft.

Assuming that the speed of the gust is a function of time W(t), the expression for lift Y can be written in the following manner:

$$Y = \frac{1}{2} c_y^{\alpha} \rho V^2 S\left(\frac{W}{V} + \frac{\dot{y}}{V}\right). \tag{4.82}$$

Introducing the parameter

$$\lambda = \frac{c_y^{\alpha} \rho V S}{2m},$$

equation (4.81) may be represented in the form of

$$\ddot{y} = -\lambda(W + \dot{y}) \tag{4.83}$$

under initial conditions $y = \dot{y} = 0$, when $t = 0$.

Let us consider the case of the action of a step gust:

$$\left.\begin{aligned} W(t) &= W_0, & t > 0; \\ W(t) &= 0, & t < 0. \end{aligned}\right| \tag{4.84}$$

In this case equation (4.83) has the form of

$$\ddot{y} + \lambda \dot{y} = -\lambda W_0. \tag{4.85}$$

Introducing the intergrating factor $e^{\lambda t}$, we obtain

$$\frac{d}{dt}(\dot{y} e^{\lambda t}) = -\lambda W_0 e^{\lambda t}. \tag{4.86}$$

Integrating equation (4.86) and using the initial conditions (4.84), we obtain

$$\dot{y}(t) = W_0(e^{-\lambda t} - 1). \tag{4.87}$$

Secondary integration gives

$$y = \frac{1}{\lambda} W_0 (1 - e^{-\lambda t}) - W_0 t. \tag{4.88}$$

This is the expression of transition conductivity of an aircraft under the influence of a gust on it. From it we obtain

$$\ddot{y} = -\lambda W_0 e^{-\lambda t}. \tag{4.89}$$

Putting the value of λ in formula (4.89), for increase G-force we obtain

$$\Delta n = -\frac{\ddot{y}}{g} = \frac{1}{2} c_y^\alpha \rho V \frac{W_0}{G/S} e^{-\lambda t}. \tag{4.90}$$

In this case [see formula (1.41)]

$$K = e^{-\lambda t}.$$

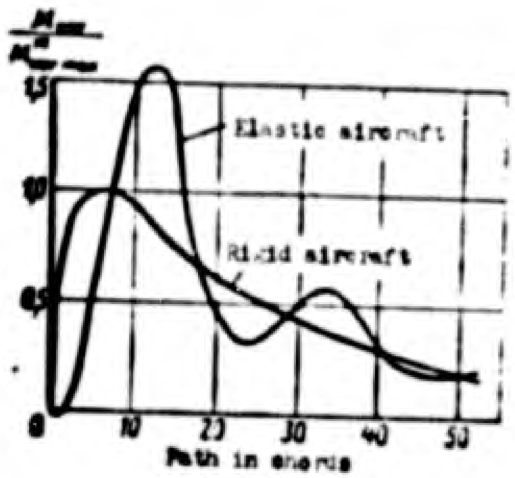

Fig. 4.18. Graph of bend-wind ($M^r_{bend.max}$ is the maximum magnitude of bending moment of the wing of a rigid aircraft).

Maximum G-force increment when $t = 0$ will be

$$\Delta n_{max} = \frac{1}{2} c_y^\alpha \rho V \frac{W_0}{G/S}. \tag{4.91}$$

Using the Duhamel integral we can obtain the expression for $y(t)$ with any law of change of $W(t)$:

$$y(t) = \int_0^t W(\tau) \left[e^{-\lambda(t-\tau)} - 1 \right] d\tau, \tag{4.92}$$

since in this case the impulse response is equal to

$$h(t) = e^{-\lambda t} - 1.$$

For further verification of the calculation it is necessary to consider the action of a gust on an aircraft taking into account the elasticity of the structure. As an example Fig. 4.18 gives curves of relative change of bending moment of a wing for rigid and elastic aircraft taking into account the transition processes of aerodynamic loading. As can be seen, the bending moment of the elastic wing considerably differs from the bending moment of the rigid wing.

Cyclical Gusts

In a turbulent atmosphere an aircraft is usually subjected to the influence of gusts which follow directly one after another (cyclical gusts). Therefore, it is necessary to consider the influence on an aircraft of cyclical gusts with a frequency equal to the natural frequency of oscillations of the aircraft wing. In this case the action of three or four consecutive gusts practically leads to resonance amplitude of oscillations (during damping). There is then a considerable increase of bending moments of the wing and loads from concentrated weights (engines, fuel tanks, and others) as compared to the static action of a single gust of the same magnitude.

Reaction of an aircraft to a gust depends on the length of the gust. We can find the length of a gust at which the reaction of the aircraft will be the least. This value of length is found in a defined relationship with wing chord.

Gusts of small length (as compared to chord) are "averaged" by the wing, and the aircraft practically does not react to them. Gusts of great length have a small gradient of build-up of W and correspondingly their influence on the aircraft is also small. Knowing the magnitude of length of a gust (wave length L) and speed of the aircraft, one can determine the frequency of influence of a gust on the aircraft

$$f=\frac{V}{L}.$$

It is obvious that frequency grows in direct proportion to the speed of flight.

If the speeds of flight of an aircraft are small, and the natural frequencies of the wing are relatively high (more than 10 oscillations per second), the phenomenon of resonance does not appear, since the frequency of action of gusts usually at small speeds of flight are relatively small (less than 10 oscillations per second).

In contemporary aircraft, due to the increase of speeds of flight, there is an increase in the frequency of action of gusts, and with a lowering of frequency of action of gusts, and with a lowering of frequencies of natural wing oscillations to 1-5 oscillations per second there appears a real possibility of resonance (Fig. 4.19).

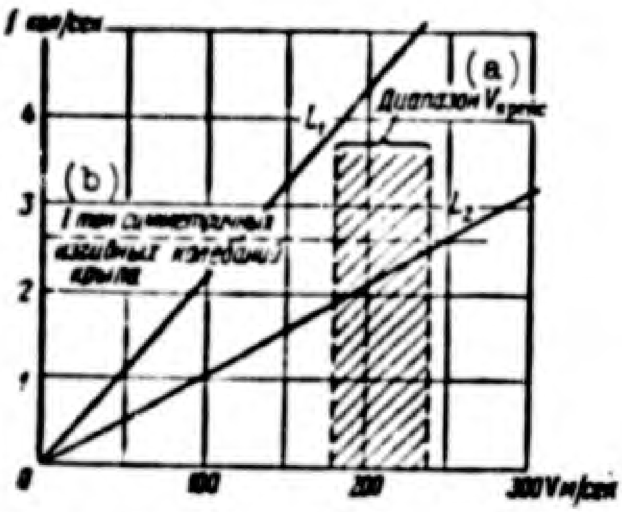

Fig. 4.19. Dependence of the frequency of influence of gust on the speed of flight. L_1 and L_2 – limiting values of length of gusts.
KEY: (a) Range V_{cru}; (b) 1st tone of symmetric bending oscillations of wing.

The magnitude of maximum amplitude of wing oscillations during cyclical gusts depends on magnitude W and on the damping of oscillations of the wing. The influence of gusts on an aircraft increases approximately in direct proportion to the speed of flight. However, the magnitude of damping of oscillations also increases. Due to this the maximum bending moments of the wing from the action of cyclical gusts cannot be on the maximum, but on a certain average speed of flight.

4.10. Spectral Characteristics of Turbulent Atmosphere

Processes occurring in a turbulent atmosphere are random. Therefore, it is expedient to apply statistical methods to the investigation of aircraft loads during gusts of turbulent air. The function of change of speed of gusts in space can be represented as a random function.

During the study of continuous turbulence it is assumed that the atmosphere in a defined zone of altitudes is isotropic, i.e., the components of speed of pulsations of air on three coordinate axes are identical in the statistical respect.

Correlation functions for isotropic turbulence of the atmosphere have the form of

$$\left.\begin{aligned} R_1(r) &= R_1(0)\,e^{-\frac{r}{L_1}}; \\ R_2(r) &= R_2(0)\,e^{-\frac{r}{L_2}}\left(1-\frac{r}{2L_2}\right). \end{aligned}\right| \tag{4.93}$$

correlation function $R_1(r)$ characterizes the statistical bond between components of speed of gusts which are found at distance r measured in the direction of the speed of flight, i.e., the statistical bond of horizontal components of gusts; $R_2(r)$ characterizes the statistical bond between components of speed of vertical gusts. Constants L_1 and L_2 carry the name of turbulence scales and are equal to the areas under the standardized curves of correlation:

$$L_1=\int_0^\infty \frac{R_1(r)}{R_1(0)}\,dr \text{ and } L_2=\int_0^\infty \frac{R_2(r)}{R_2(0)}\,dr. \tag{4.94}$$

These magnitudes characterize the duration of the correlation between gusts.

Subsequently we shall consider the statistical characteristics of only vertical gusts, since they are the determining ones for loads on an aircraft during flight in a turbulent atmosphere.

From relationships (4.93) there can be obtained an expression for spectral density of speed of vertical gusts:

$$S(\Omega)=S(0)\,\frac{1+3\Omega^2L_2^2}{(1+\Omega^2L_2^2)}. \tag{4.95}$$

where $\Omega=\frac{2\pi}{L}$ is the space frequency;

L is the length of a wave of gust.

The character of the curve of spectral density is approximately identical for different atmospheric compositions. Therefore, it is expedient to express the function of spectral density of gusts through the mean quadratic velocity of gusts σ_W and the function characterizing the change of $S(\Omega)$ in space frequency:

$$S(\Omega)=\sigma_W^2\frac{L_2}{\pi}\frac{1+3\Omega^2L_2^2}{(1+\Omega^2L_2^2)}. \qquad (4.96)$$

Figure 4.20 shows the form of curves of standardized spectral density for a different magnitude of L_2.
The form of curve $S(\Omega)$ in the region of frequencies 0.01 and above is very close to the dependence

$$S(\Omega)=\frac{C}{\Omega^{5/3}}. \qquad (4.97)$$

where C is a constant which depends on the intensity of turbulence of the atmosphere.

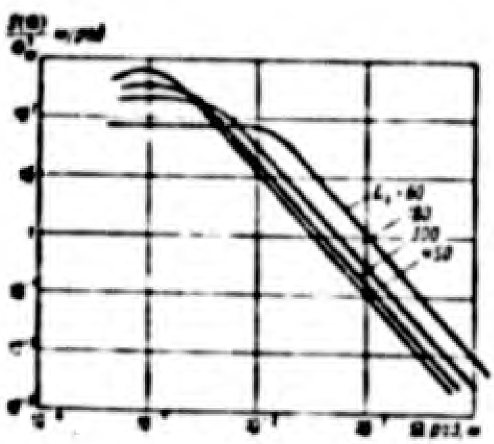

Fig. 4.20. Curves of the spectral density of air gusts.

Experimental measurements of spectral density give a dependence which is close to expression (4.97) (Fig. 4.21). Magnitude σ_W is connected with the meteorological parameters of the atmosphere.

During the analysis of the influence of atmospheric turbulence on an aircraft, as the argument of spectral density is expedient to use angular frequency, since it determines the frequency-response curves of the aircraft. It is obvious that $\omega = \Omega V$ and correspondingly,

$$S(\omega)=\frac{1}{V}S(\Omega).$$

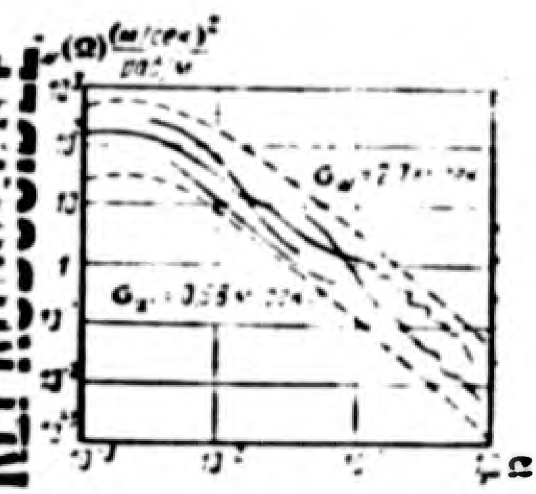

Fig. 4.21. Theoretical and experimental spectral curves of atmospheric turbulence.

Then

$$S(\omega)=\sigma_W^2\frac{L_1}{\pi V}\frac{1+3\left(\frac{\omega L_1}{V}\right)^2}{\left[1+\left(\frac{\omega L_1}{V}\right)^2\right]^2}. \tag{4.98}$$

4.11. Reaction of an Aircraft to the Random Influence of a Turbulent Atmosphere

Let us examine the action of vertical perturbations on a rigid wing of constant chord b, moving in a turbulent atmosphere with velocity V and having freedom of movement only vertically; amplitude of movement will be considered small as compared to chord. Under these conditions the change of the angle of attack of the wing will be

$$\alpha=\frac{W}{V}.$$

We shall assume that the pattern of turbulence does not change during the interval of time when the considered particle of air passes a distance along the profile. Then W may be expressed in the form of

$$W=W\left(t-\frac{x}{V}\right). \tag{4.99}$$

(Axes of coordinates are considered fixed to the wing, i.e., the turbulent formation as if moves past the wing with velocity V). In this case the equation of motion of the wing it can be written in the form of

$$m\ddot{y}+Y(\dot{y})=-Y(W). \tag{4.100}$$

where Y(W) is the lift appearing during the action of a gust with velocity W(t);

Y(y) is the lifting (damping) force caused by the motion of the wing.

Taking linear dependences for small perturbations, it is possible to analyze separately Y(W) and Y(y).

Spectral density of a vertical gust of turbulent atmosphere, determined by formula (4.98), may be written in the form

$$S_W(\omega) = \sigma_W^2 \frac{L_2}{\pi V} \frac{1+3\xi^2}{(1+\xi^2)^2}. \tag{4.101}$$

where $\xi = \frac{\omega L_2}{V}$;

σ_W is the mean value of the intensity of the gust squared. According to formula (4.82) the spectral density of lift is

$$S_y(\omega) = |H_y(i\omega)|^2 S_W(\omega). \tag{4.102}$$

where $H_y(\omega)$ is lift conductivity during a sinusoidal gust. Spectral density of wing accelerations is

$$S_n(\omega) = |H_y(i\omega)|^2 |H_n(i\omega)|^2 S_W(\omega). \tag{4.103}$$

where $H_n(i\omega)$ is acceleration conductivity during sinusoidal lift.

Consequently, the problem of determination of the reaction of a wing to the influence of a random function of gust is reduced to the investigation of $H_n(i\omega)$ and $H_y(i\omega)$.

If one considers that the vertical component of gust is determined with the help of the expression

$$W(x,t) = W_0 e^{i\omega\left(t - \frac{x}{V}\right)},$$

which shows that the sinusoidal gust moves with respect to the wing with velocity V, the lift for a wing of unit span during the influence of gusts on it with the velocity

$$Y = \pi\rho b V W_0 e^{i\omega t} \gamma(k). \tag{4.104}$$

where k is the given frequency: $k = \frac{\omega b}{2V}$,

$$|\varphi(k)|^2 \approx \frac{1}{1+2\pi k}.$$

Consequently, lift conductivity during a gust is

$$H_y(i\omega) = \pi\rho b V \varphi(k). \tag{4.105}$$

The wing conductivity during sinusoidal lift is

$$H_a(i\omega) = \frac{\ddot{y}}{Y} = \frac{1}{\pi\rho b S} \cdot \frac{k}{(1+k_c)k + 2G - 2iF}, \tag{4.106}$$

where $k_c = \frac{m}{\pi\rho S b}$;

G and iF are correspondingly the real and imaginary parts of the function C(k), considering the change of wing lift during its transient motion.

Figure 4.22 represents the change of F(k) and G(k).*

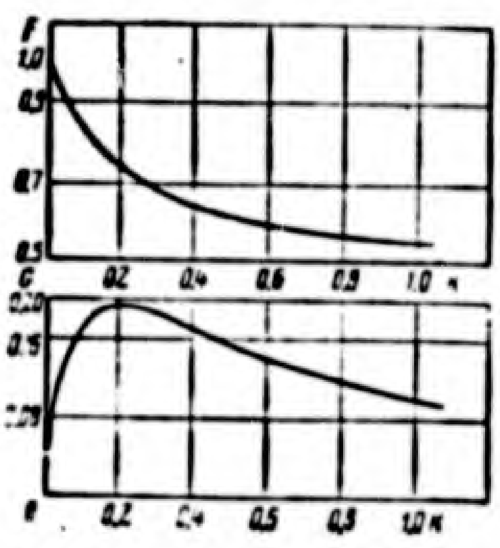

Fig. 4.22. Graphs of function F(k) and G(k).

From formula (4.106) one can determine

$$|H_a(k)|^2 = \left(\frac{1}{\pi\rho S b}\right)^2 \frac{k^2}{4(F^2+G^2) + 4Gk(1-k_c) + k^2(1+k_c)^2}. \tag{4.107}$$

According to formula (4.49) the mean value of the square of accelerations is

$$\overline{\ddot{y}^2} = \int_0^\infty |H_y(ik)|^2 |H_a(ik)|^2 S_w(\omega)\, d\omega. \tag{4.108}$$

The exact integration of this expression is hampered; however it is possible to execute approximate integration, considering that

$$|G| < 0.2, \quad |F| < 1 \text{ and } k_c \approx 30 \text{ to } 130.$$

A good approximation to relationship (4.107) will be the expression

---

*Ya. Ts. Fyn, Introduction to the theory of aeroelasticity, Fizmatgiz, 1959.

for the quasi-stationary case:

$$|H_n(ik)|^2 = \left(\frac{1}{\pi\rho S b}\right)^2 \frac{k^2}{4+k^2(1+k_c)^2}. \tag{4.109}$$

Designating

$$\gamma = \frac{b}{2L}, \quad \alpha = \frac{2}{\gamma(1+k_c)}$$

and putting expressions (4.101), (4.105), and (4.109) in formula (4.108), we obtain

$$\overline{y^2} = \sigma_w^2 \frac{V^2}{\pi b^2(1+k_c)^2}\int_0^\infty \frac{\xi^2}{\alpha^2+\xi^2}\,\frac{1}{1+2\pi\gamma\xi}\,\frac{1+3\xi^2}{(1+\xi^2)^2}\,d\xi.$$

Designating the integral in this expression by $J(\alpha, \gamma)$, we obtain

$$\overline{y^2} = \overline{\sigma_w^2} \frac{V^2}{\pi b^2(1+k_c)^2} J(\alpha, \gamma) \tag{4.110}$$

The character of change of $J(\alpha, \gamma)$ is shown in Fig. 4.23. When $\gamma \to 0$ or $\gamma \to \infty$ $J(\alpha, \gamma) \to 0$, and consequently $y^2 \to 0$. This means that if the scale of turbulence becomes negligible or infinitely large as compared to wing chord, the intensity of acceleration of the aircraft will tend to zero. This is possible to explain also from the consideration of the influence of gusts on the wing. If the scale of turbulence is small as compared to chord, the influence of gusts is averaged. On the other hand, if wing chord is small as compared to the scale of turbulence, the G-forces of the aircraft will be insignificant.

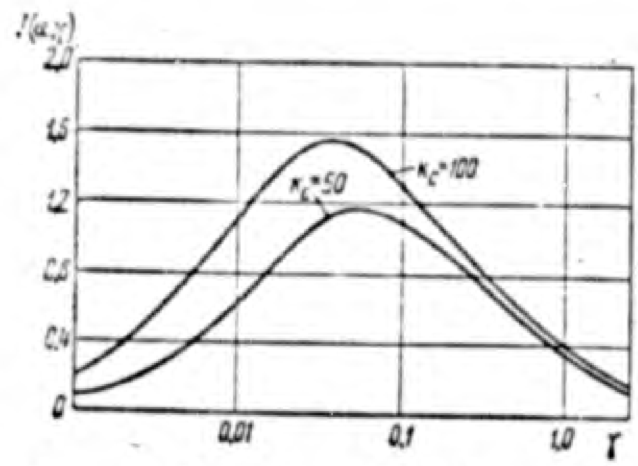

Fig. 4.23. Graph of function $J(\gamma, \alpha)$:

In order to compare formula (4.110) with the usual expression for G-force during gusts of turbulent air (4.91), we shall perform an additional transformation. Considering that usually $k_c > 50$, it is possible to put $(1 + k_c) \approx k_c$.

Then

$$\sqrt{\overline{\Delta n^2}} = \frac{\sqrt{\overline{\ddot{y}^2}}}{g} = \frac{2\pi V S\sqrt{\overline{w^2}}}{2mg}\sqrt{\frac{J(\alpha,\gamma)}{\pi}}$$

or, taking that $2\pi \approx c_y^{\alpha}$, we obtain

$$\sqrt{\overline{\Delta n^2}} = \frac{1}{2} c_y^{\alpha} \rho V \frac{\sqrt{\overline{w^2}}}{G/S}\sqrt{\frac{J(\alpha,\gamma)}{\pi}}. \tag{4.111}$$

Comparing the expressions obtained above for Δn with expression (1.41), it is possible to see that they are identical with an accuracy of factor $\sqrt{\frac{J(\alpha,\gamma)}{\pi}}$, which may be called an "easing of the gust." The presence of a maximum of $J(\alpha, \gamma)$, depending on parameter k_c, indicates the fact that the aircraft reacts to the scale turbulence which is commensurable with chord. This explains a rather interesting experimental result which consists in the fact that the distance of the gust gradient is more closely connected with wing chord than with meterological conditions. Thus, the earlier judgement is confirmed about the fact that on high-speed aircraft the coincidence of frequency of action of gust with the natural frequency of the wing of the aircraft became possible.

The influence of a gust on an elastic aircraft. During the analysis of the influence of a gust on the structure of an aircraft it is necessary to consider the influence of deformations on the magnitude of forces in a given section. In this case the mechanical conductivity of the aircraft is determined by taking into account the elastic deformations of the structure. For each section of the wing (fuselage) there will be its own function of mechanical conductivity of the structure $H(i\omega)$ with respect to the influence of gusts of turbulent air. A large influence on magnitude $H(i\omega)$ is rendered by rotation of the aircraft, which is considerably determined by the characteristics of stability of the aircraft.

Functions of mechanical conductivity are determined by means of calculation or experimentally on dynamically similar models. Knowing the function of mechanical conductivity with respect to force Q $H_Q(i\omega)$, one can determine spectral density $S_Q(\omega)$ for a given section of structure from the relationship

$$S_Q(\omega) = |H_Q(i\omega)|^2 S_w(\omega). \tag{4.112}$$

Hence one can determine the average of the square of forces:

$$\overline{Q^2} = \int_0^\infty |H_Q(i\omega)|^2 S_w(\omega)\,d\omega. \tag{4.113}$$

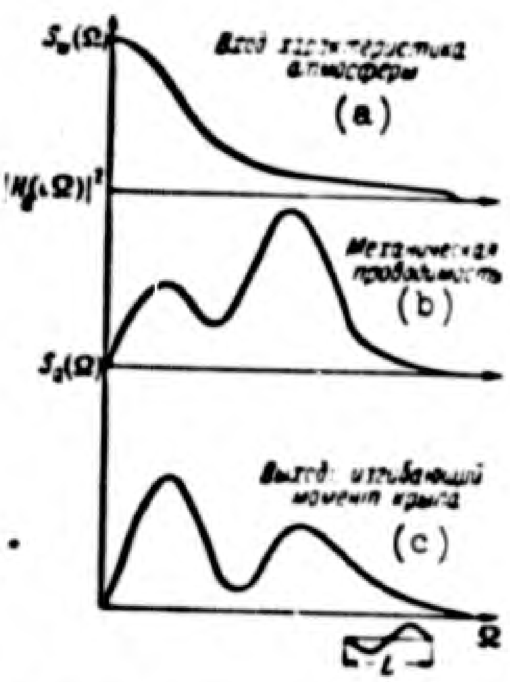

Fig. 4.24. Approximate form of the function of mechanical conductivity and spectral density of bending moment.
KEY: (a) input characteristic of atmosphere; (b) mechanical conductivity; (c) output: bending moment of wing.

Figure 4.24 gives approximate graphs of $/H_Q(i\omega)/^2$ and $S_2(\omega)$ for the root section of the wing of a transport aircraft, constructed for the space frequency $\Omega = \frac{2\pi}{L}$.

4.12. Influence of Dynamic Loads Appearing During Takeoff and Landing on the Structure of an Aircraft

Above we considered loads on landing gear during takeoff and landing, assuming that the aircraft structure was absolutely rigid.

In an elastic aircraft, part of the kinetic energy changes into strain energy of the aircraft structure. Fast change of loads during landing (during 0.1-0.5 sec.) excites the natural oscillations of the structure of lower tones. During the analysis of loads during landing, aerodynamic damping may be disregarded.

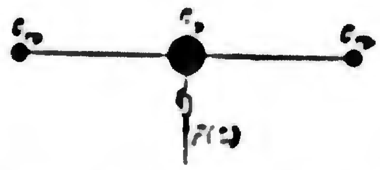

Fig. 4.25. Diagram of a model of an aircraft with loads on the wing.

Let us consider a simple diagram of an aircraft which consists of a fuselage, wing, and two loads on its ends (Fig. 4.25).

Along the axis of the aircraft during landing there is developed a force

$$F(t)=n_{max}Gf(t). \qquad (4.114)$$

where n_{max} is the maximum G-force during landing;

G, G_f, G_{ld} are correspondingly the weight of the aircraft, fuselage, and load:

$$G=G_{ф}+2G_{гр}.$$

It is easy to see that the model has two degrees of freedom and possesses the following forms of motion:

The form of motion of a solid

$$f_0(0)=1, \quad f_0(t)=1, \quad p_0=0;$$

The form of motion of an elastic body

$$f_1(0)=-\frac{2G}{G_{ф}}, \quad f_1(t)=1, \quad p_1=\sqrt{\frac{kG}{2G_{ф}G_{гр}}},$$

where k is the rigidity of the wing (the wing is considered to be weightless).

We shall determine the transverse force on the wing Q around the internal side of the end load.

We shall compose equations for the time function r(t):

$$\left.\begin{aligned}\ddot r_1 &= n_{max}\, g f(t);\\ \ddot r_2 + p^2 r_2 &= -n_{max}\, g f(t).\end{aligned}\right\} \qquad (4.115)$$

Transverse force Q may be expressed by acceleration:

$$Q(t) = -\frac{G_{rp}}{g}\left(\ddot r_1(t) + \ddot r_2(t)\right). \qquad (4.116)$$

Placing the expressions for $\ddot r_1$ and $\ddot r_2$ in formula (4.116), we determine

$$Q(t) = \frac{G_{rp}\, n_{max}}{g}\left[-f(t) + f(0)\cos\omega_2 t + \int_0^t \frac{df(\tau)}{d\tau}\cos\omega_2(t-\tau)\, d\tau\right]. \qquad (4.117)$$

If the force which is acting on a landing gear strut can be expressed by the dependence

$$\left.\begin{aligned} f(t) &= \sin\omega t, \qquad 0 < t < \frac{\pi}{\omega};\\ f(t) &= 0, \qquad t > \frac{\pi}{\omega}.\end{aligned}\right\} \qquad (4.118)$$

the transverse force is

$$Q(t) = G_{rp} n_{max}\left[-\sin\omega t + \frac{\omega}{p^2}\,\frac{\sin pt - \frac{\omega}{p}\sin\omega t}{1-\left(\frac{\omega}{p}\right)^2}\right],\quad 0 < t < \frac{\pi}{\omega}. \qquad (4.119)$$

Figure 4.26 shows the change of load for an elastic and rigid aircraft during landing. The load during oscillations of the structure in the first tone increases 1.6 times as compared to the load of the rigid structure. In the calculation of several modes of oscillations of an actual aircraft the increase of load can be considerably larger.

Oscillations of the structure during landing are caused not only by vertical forces, but also by the frontal and lateral forces of the landing gear. Oscillations of the fuselage in a lateral direction,

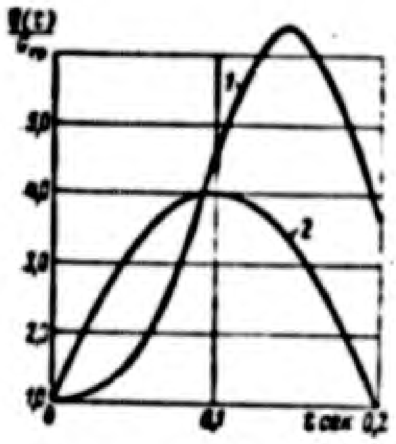

Fig. 4.26. Comparison of loads in the end section of the wing of an elastic (1) and absolutely rigid (2) aircraft during landing.

furthermore, are caused by the moment from the difference between frontal forces of the right and left struts.

Figure 4.27 shows the approximate change of bending moments M_1 and M_2 (with respect to the nose and tail sections) of a fuselage during landing. Oscillations of aircraft structure during landing lead to a considerable increase of loads on the fuselage, wing, engine frame, and other parts of an aircraft. Usually the biggest increase of inertial loads is observed at the end sections of the wing.

Figure 4.28 gives the distribution of relative G-forces along the fuselage length during landing.

During motion on the ground (takeoff run, landing run, and taxiing) an aircraft experiences the action of alternating loads caused by the local roughness of the airport and nonuniform braking of the wheels. With the increase of speed, while crossing the same roughness, the loads are increased in proportion to V^2; however, a constant load on a wheel due to the appearance of wing lift also decreases in proportion to V^2. Therefore, the biggest loads on landing gear are observed at a speed which is equal to 0.6-0.8 of the takeoff or landing speed.

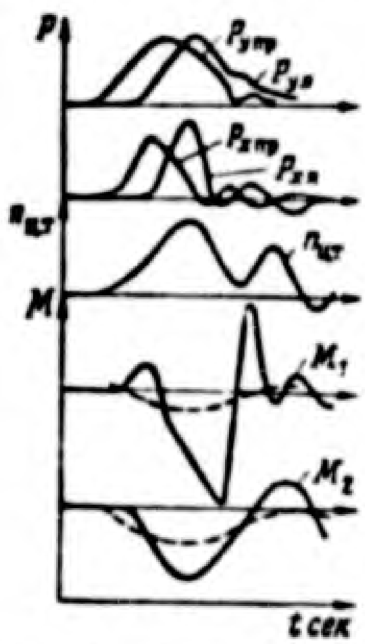

Fig. 4.27. Character of change of forces in a fuselage during landing. --- rigid aircraft, —— elastic aircraft.

With the increase of speed of the aircraft there is an increase in the frequency of action of pulses of roughness in proportion to speed. Spectrum of frequencies of oscillations of an aircraft structure during takeoff and landing contains basically the first 3 or 4 tones of natural oscillations.

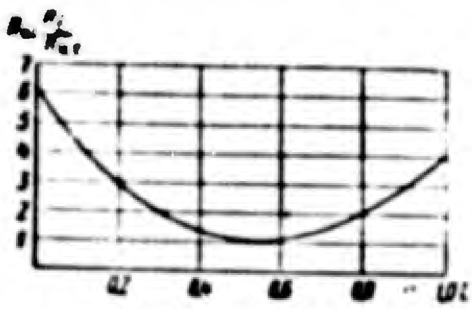

Fig. 4.28. Distribution of G-forces along the length of an aircraft.

For an analysis of loads during takeoff and landing it is possible to use methods of generalized harmonic analysis. Loads during the takeoff run, landing run, and taxiing may be considered as a random process.

Loads experienced by an aircraft during landing (the first shocks) can be approximated by the sum of an average typical curve of the load and the random perturbations. In this case it is possible to consider separately the reaction of the aircraft to an average load, and then to a random perturbation.

In order to apply the method of generalized harmonic analysis, the roughness of the airport must be represented in the form of a function of spectral density:

$$S_0(\Omega) = 2\int_0^\infty R(x)\cos\Omega x\,dx, \qquad (4.120)$$

where

$$R(x) = \lim_{x\to\infty}\frac{1}{2x}\int_{-x}^{x} y(\eta)\,y(\eta + \Delta x)\,d\eta; \qquad (4.21)$$

$\Omega = \frac{2\pi}{l}$ is the "space" frequency;

l is the length of a band of roughness;

$y(\eta)$ is the height of roughness.

For $\Omega > 0.01$ rad/m it is approximately possible to consider that the graph of the function of spectral density is expressed by the relationship

$$S(\Omega) = \frac{c}{\Omega^n}. \qquad (4.122)$$

where c and n are constants.

In certain cases it is possible to take n = 2.0. Magnitude C depends on the amplitudes of roughness. On the basis of materials of investigations in the United States for new runways $C \leq 2 \cdot 10^{-6}$ m; if $C > 6 \cdot 10^{-6}$ m, the runway requires repair, since in this case there is observed a strong flutter of the aircraft during takeoffs and landings.

Figure 4.29 gives graphs of $S_{rou}(\Omega)$ for one airport in the United States and the boundaries of permissible runway roughness.*

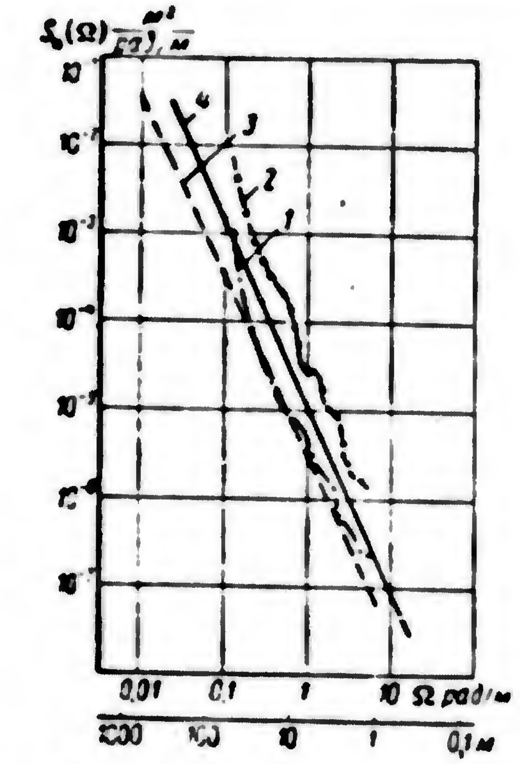

Fig. 4.29. Graphs of the spectral density of runway roughness. 1) runway; 2) taxiway; 3) permissible roughness of new runway; 4) permissible roughness after prolonged use.

In the determination of loads it is expedient to use the function of spectral density of roughness:

$$S_n(\Omega) = S_n\left(\frac{\omega}{V}\right) = \frac{1}{V} S_n(\omega). \qquad (4.123)$$

where $\omega = \Omega V$ (V = const is the velocity of the aircraft).

Then the spectral density, characterizing the loads (forces) in some section of the aircraft unit, can be determined from the relationship

$$S_Q(\omega) = \frac{1}{V} |H_{ldg}(i\omega)|^2 S_n(\omega). \qquad (4.124)$$

where $H_{ldg}(i\omega)$ is the function of

---

*John C. Haubolt. Runway Roughness Studies in the Aeronatical Field. J. Air Transp. Div. Proc. Amer. Soc. Civil Eng., V. 87, No. 1, 1961.

mechanical conductivity of the aircraft structure under the influence of external forces on the landing gear.

Since the characteristics of the landing gear are essentially nonlinear, there appear difficulties in the determination of the transfer function. In this case the methods of analysis of random processes in nonlinear systems are used.

CHAPTER V

AIRCRAFT VIBRATION

List of Designations Appearing in Cyrillic

в = p = propeller

д = e = engine
дб = db
доп = per = permissible

кГ/см = kg/cm²
кол/мин = vib/min
кол/сек = vib/sec

НП = DOF = Direction of Flight

об/мин = rpm

сек = sec

ф = f = fuselage

During tests of experimental aircraft we frequently encounter different oscillation modes of the structure. There arises a necessity to investigate the detected oscillations (for the most part the investigations are conducted experimentally). As a result of the investigations, measures are developed for removal of lowering the level of oscillations or providing reliable work of the structure and equipment of aircraft during increased oscillations (vibrations).

There are the following basic oscillation modes on contemporary aircraft:*

a) oscillations appearing during the operation of propulsion systems (motor vibration, including vibrations from the propellers;

b) aerodynamic oscillations connected with the peculiarities of air flow around the structure or its individual parts;

c) elastic oscillations during takeoffs and landings;

d) oscillations appearing during firing from airborne armament on military aircraft;

e) acoustic vibrations from the influence of noise of a jet engine on the elements of the structure.

5.1. Vibrations Appearing During the Operation of Power Plants (Propulsion Systems)

Perturbing forces appearing during the operation of a power plant are periodic forces, multiple turns of the revolving parts of the engine and propeller. Under the action of these forces the structure accomplishes forced oscillations.

Since the structure is not usually affected by one, but several perturbing forces, and all of them in this case are periodic, displacement of the structure y(z, t) under the action of these forces constitutes the result of imposition of displacements caused by each force (or each component of a complex force) separately:

$$y(z,t)=\sum_{i=1}^{n} F_i(z)\sin(\omega_i t+\beta_i), \qquad (5.1)$$

*Oscillations of the "flutter" type are considered in Chapter VI.

where $F_i(z)$ is the form of the forced oscillations in distinction from the form of natural oscillations $f_i(z)$;

ω_i is the predetermined angular frequency of the perturbing force;

β_i is the phase angle of the perturbing force;

n is the quantity of harmonic components of the perturbing force.

Forced oscillations of the structure are thus determined by the spectrum of perturbing forces. Of important value here is the relationship of frequencies of natural oscillations p_i and perturbing forces ω_i and the phenomenon of resonance connected with this. Forms of forced oscillations $F_i(z)$ upon necessity are determined experimentally.

The perturbing forces appearing during operation of the power plant can be divided into two groups:

1) forces appearing during engine operation and caused by the instability of moving masses of the engine;

2) forces appearing during propeller rotation and caused by propeller instability (static or dynamic), the difference in angles of blade setting, and also the aerodynamic effect during passage of propeller blades in front of the fuselage or wing.

Frequencies of engine (propeller) vibration always linearly depend on engine (propeller) rpm. The order of harmonics of variable forces and moments of engines, which may cause vibration of the structure, is the following:

a) for piston engines (PE): $\frac{1}{2}$, 1*, 2*, $\frac{a^*}{2}$, $\frac{a+1}{2}$ (a is the number of cylinders);

b) for turbojet engines (TJE): 1*, 2,...;

c) for turboprop engines (TPE): 1*, 2,....

The order of propeller harmonics for a k-bladed propeller is 1*, 2,..., k*, mk(m = 2, 3,...).

The order of harmonics during the study of engine (propeller) vibration is determined with respect to turns of the crankshaft or turbine of the engine (propeller turns).

Vibrations with frequencies corresponding to harmonics marked by an asterisk constitute the biggest danger in view of their considerable amplitudes.

Figure 5.1 shows the dependence of frequencies of engine vibration on engine revolutions for a real aircraft with piston engines. Dependences of frequencies of engine (propeller) vibration on engine rpm for aircraft with other propulsion systems are analogous to those shown in Fig. 5.1.

Figure 5.2 shows typical spectra of frequencies of engine (propeller) vibration and natural oscillations of aircraft with different propulsion systems. As can be seen, the most unfavorable with respect to ranges of frequencies of perturbing forces are piston power plants: the frequencies from the engine and propeller change almost continuously and form a region of comparatively low frequencies.

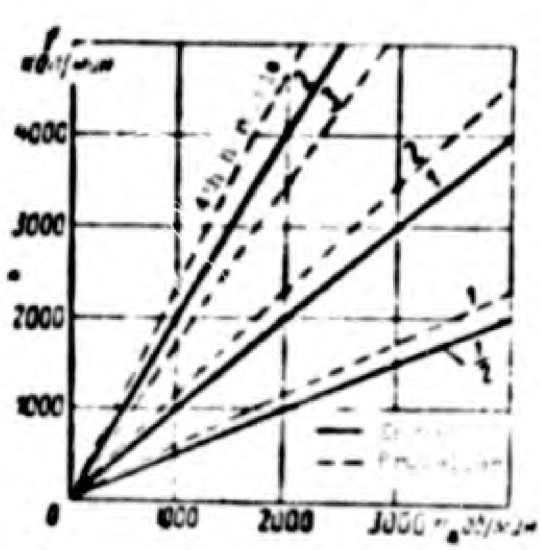

Fig. 5.1. Dependence of frequencies of engine (propeller) vibration of a passenger reciprocating aircraft on engine revolutions.

Table 5.1 gives data on engine vibration of several aircraft with piston engines of 1942-1946 vintage. Oscillations were measured on the engine, frame, and fuselage in three coordinate axes of each aircraft. The table gives maximum amplitudes on three axes. However, on all frames the oscillations along axis x practically were absent. Power plants of all the aircraft had vibration insulation.

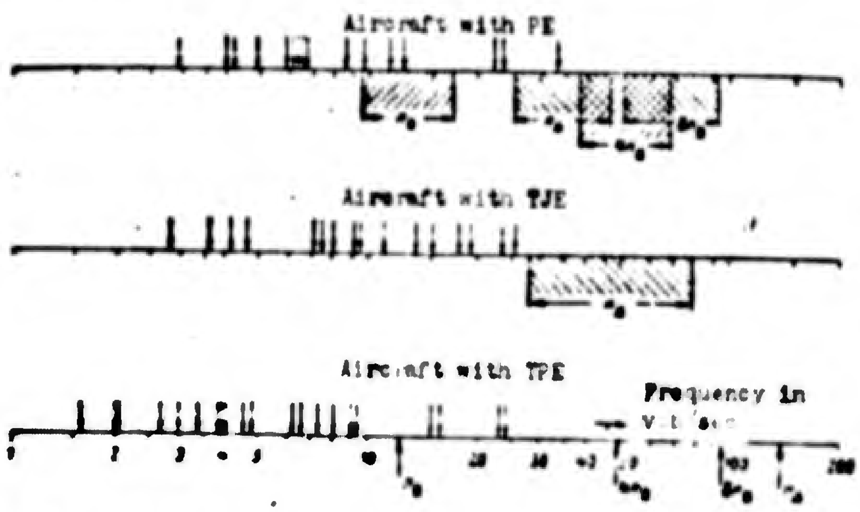

Fig. 5.2. Spectra of frequencies of natural and forced oscillations of three aircraft with different propulsion systems. n_p – propeller revolutions, n_e – engine revolutions, ↓ – frequencies of natural oscillations.

Table 5.1. Amplitudes (in mm) of Engine Vibration of Several Aircraft of 1942-1946 Vintage

Type of aircraft and engine	Place of measurement	Engine harmonics			
		1	2	6	7
Fighter with radial engine	Engine	0,12–0,20	0,11–0,13	–	0,003–0,009
	Frame	0,11–0,20	0,14–0,16	–	0,004–0,006
	Fuselage	0,05–0,08	0,05–0,07	–	0,003–0,004
Fighter with in-line engine	Engine	0,16–0,24	0,05–0,08	0,05	–
	Frame	0,08–0,17	0,05	None	–
	Fuselage	0,12	0,02	None	–
Ground-attack aircraft with in-line engine	Engine	0,18–0,20	0,11	0,010–0,025	–
	Frame	0,15	0,20	0,005–0,008	–
	Fuselage	0,05–0,08	0,03–0,05	None	–
Front-line bomber with two in-line engines	Engine	0,14–0,19	0,13–0,38	0,003–0,013	–
	Frame	0,12–0,13	0,08–0,12	0,003–0,007	–
	Fuselage	0,03–0,07	0,01–0,10	None	–
Front-line bomber with two radial engines	Engine	0,18–0,19	0,12–0,16	–	0,006–0,008
	Frame	0,07–0,13	0,10–0,12	–	0,005–0,007
	Fuselage	0,02	0,01–0,02	–	None

Note. Radial engines have 14 cylinders, in-line have 12.

Table 5.1 gives a presentation about the order of magnitudes of amplitudes of engine vibration on aircraft with piston engines. From the table it follows that engine vibration is basically experienced by the frame and certain other elements of the engine section. On the fuselage there appear vibrations with small amplitudes (basically not over 0.1 mm) and with a frequency corresponding to the 1st engine harmonic. High-frequency components on the structure generally either are not revealed during measurements, or they have extremely low amplitudes.

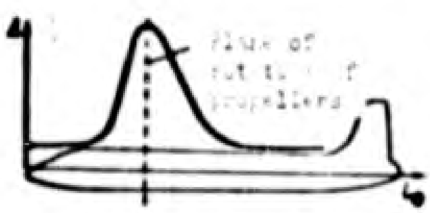

Fig. 5.3. Zone of increase propeller vibrations of sides of the fuselage of an aircraft with TPE.

Engine vibration can present serious danger usually for elements of the engine section and for control rods if they enter resonance. For decrease of engine vibration the engine is mounted on shock absorbers. By the selection of shock absorption of an engine the natural frequencies of the power plant are lowered to magnitudes smaller than the operational engine and propeller revolutions and consequently the possibility of its resonance is excluded. Due to internal friction in the shock absorbers there occurs energy dissipation of oscillations, and the amplitudes of oscillations to a considerable extent are lowered.

Selection of corresponding frequency-response curves of elements of the structure, in particular the selection of the response curves of the control rods, excludes their resonance with frequencies of engines vibration.

On aircraft with TJE engine vibration usually appears in a smaller degree than on aircraft with piston engines. This is explained both by the comparatively high frequencies of perturbing forces (see Fig. 5.2) and also by the absence of considerable unbalanced masses of these engines. It has been experimentally established that on a number of heavy aircraft with TJE in places located far from the engines, in particular on the wing tips, there is practically no engine vibration.

Amplitudes of engine vibration for such type of aircraft, at frequencies which are numerically equal to the number of engine revolutions, attain the following magnitudes: on the engine 0.04-0.13 mm, on the engine frame 0.02-0.12 mm, in the fuselage (on supporting members) 0.002-0.005 mm, on the wing 0.001-0.002 mm, and on the empennage 0.001-0.004 mm. Vibrations with higher frequencies are practically absent.

Turboprop engines have fixed rpm rates. Due to this, aircraft with TPE possess the peculiarity that the frequency of engine vibration have fixed, predetermined values. They are determined by the turbine revolutions of the engine and propeller and are practically constant during operation of the power plant on the ground and in the air.

For contemporary aircraft with TPE there sharply arose the question about vibrations caused by the aerodynamic influence of the propeller on the fuselage. The indicated vibrations have comparatively high frequency (see Fig. 5.2, aircraft with TPE) and can lead to comparatively fast fatigue damage of different elements of the fuselage and equipment of the aircraft. Fatigue damages of the skin and structural assembly of the fuselage during prolonged use of an aircraft present a definite danger of destruction due to vibrations, especially for passenger aircraft with pressurized fuselages.

The zone of increased vibrations of sides of the fuselage occupies a section 1.5-2.0 m in both directions from the plane of rotation of the propellers (Fig. 5.3), where the maxima of amplitudes of oscillations are somewhat displaced along the length of the fuselage with the change of the conditions of flight. Distribution of amplitudes, shown in Fig. 5.3, is characteristic for all aircraft with TPE.

Considerable vibrations with frequencies n_p and kn_p also occur on the empennage, inasmuch as in certain aircraft it is located in the stream from the propellers or near it.

Aircraft with TPE have the same order of magnitudes of amplitudes of oscillations with frequency of engine turbine revolutions as passenger turbojet aircraft.

Thus, of basic value for the structure is engine vibration with frequencies n_e, $2n_e$ – on aircraft with piston engines and n_e – on aircraft with TJE; n_p and kn_p – on aircraft with TPE. Amplitudes of oscillations with these frequencies are relatively small, but they act during the entire flight and can be a cause of fatigue breakdown of elements of the structure.

5.2. Aerodynamic Oscillations of Parts of Aircraft. Buffeting

Variable aerodynamic forces cause oscillations of parts of aircraft. These oscillations can conditionally be divided into two modes, i.e., aerodynamic and buffeting. The first are caused by variable aerodynamic forces appearing in the flow around the structure itself by an undisturbed flow; the second are caused by the variable aerodynamic forces appearing due to stall in the forward located parts.

Aerodynamic Oscillations

The forms of the appearance of aerodynamic oscillations, their character, and intensity essentially depend on the flight conditions and are connected with the aerodynamic peculiarities of the aircraft at different speeds and flight Mach numbers.

Certain properties and regularities of aerodynamic oscillations in a defined measure are studied by means of experimental investigations in flights on existing aircraft. There are oscillations appearing at subsonic, transonic, and supersonic speeds of flight (Fig. 5.4).

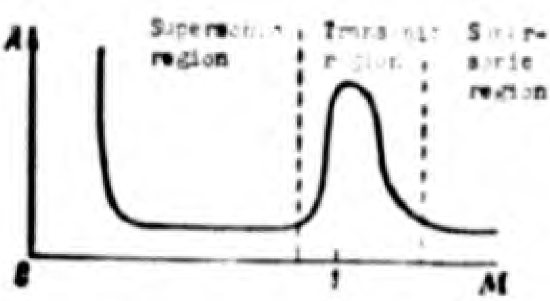

Fig. 5.4. Graph of the change of amplitudes of aerodynamic oscillations of aircraft according to flight Mach number.

Aerodynamic oscillations, appearing for various reasons at different speeds of flight, have one general property: the source of their appearance is the local disturbance of the streamlined flow of different parts of the structure. There appear pulsations of pressures and flow rates, which, influencing the aircraft structure, induce variable aerodynamic for es, and under their action the structure accomplishes elastic oscillations.

Variable aerodynamic forces can change in wide limits both in magnitude and also in frequency depending upon the causes of their appearance, conditions of flight, and other factors, the exact calculation of which is difficult to produce. Essentially these forces are random.

Thus, the problem of investigation of aerodynamic oscillations is reduced to the study of the reaction of an elastic oscillatory system to the perturbation function of a random process.

Random (stochastic) processes are studied with the help of corresponding statistical methods which allow, through recordings of aerodynamic oscillations, to make a conclusion with respect to the spectrum of oscillations and probability of achievement of defined magnitudes of amplitudes of oscillations. This information has an important value when estimating the fatigue strength of an aircraft structure, but it can be obtained only on the basis of experimental data of measurement of oscillations on a specific aircraft.

Having information with respect to the characteristics (pressures and speeds) of flow, with the help of estimators it is possible to rather sufficiently describe the process of aerodynamic oscillations under the condition of small oscillations of the structure and in the absence of such disturbance of the flow around the oscillating surface (stall) at which the dependence between lift and oscillations of speed in the flow becomes nonlinear. With non-observance of this condition, due to the introduced nonlinearity the calculation of oscillations presents a very complicated problem.

In the usual flight in the absence of stall in the indicated sense (when M is from M_1 to M_2), i.e., at a speed of flight from $1.2V_{min}$ to V_{max}, the oscillations of the structure with respect to amplitudes are small (Fig. 5.5). The largest oscillations appear during stalls when the determination of oscillations by means of calculation is very difficult. Therefore, at the basis of the study of aerodynamic oscillations we now find experimental methods.

Aerodynamic oscillations are aeroelastic, since they appear under the action of perturbing aerodynamic forces which appear due to the interaction of the incident flow and elastic structure.

An example of aeroelastic oscillations could be the oscillations of a cylinder which is suspended on an elastic spring and streamlined by a plane-parallel flow (Fig. 5.6a). At a certain defined flow rate there occurs its stall and behind the cylinder there form vortices which, converge from its ends with a defined frequency. Frequency of vortex stall depends on the geometric dimensions, configuration of the body, and approach stream velocity. In aeromechanics this frequency is determined by the relationship

$$f = \frac{V\,Sh}{d},$$

where Sh is the Strouhal number;

d is the diameter of the cylinder;

f is the number of oscillations per second.

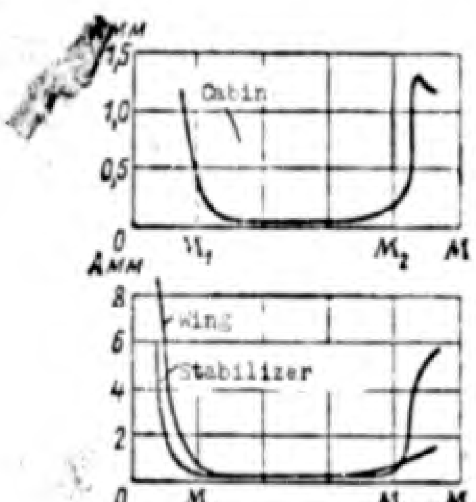

Fig. 5.5. Graphs of aerodynamic oscillations of a passenger aircraft.

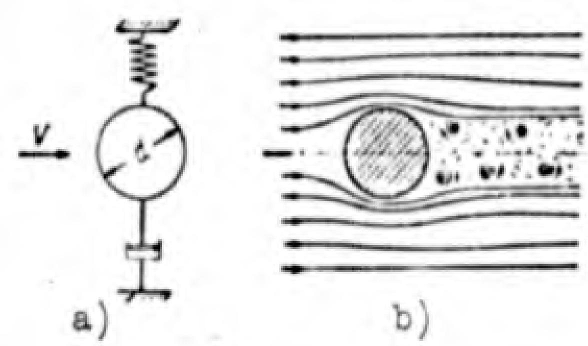

Fig. 5.6. Diagram of the appearance of oscillations of a cylinder in a flow of air. a) diagram of cylinder oscillations; b) diagram of vortices in the wake of a circular cylinder.

During vortex formation there appear periodic perturbing forces, directed across the flow, which bring the cylinder into oscillatory motion. Coefficient of lift, appearing during vortex stall with frequency $\omega = 2\pi f$, can be represented in the form

$$c_y = c_{y_0} e^{i\omega t}.$$

Consequently, the linear aerodynamic force can be written in the following manner:

$$P(t)=\frac{1}{2}\rho V^2 dc_m e^{i\omega t}.$$

The natural frequency of a cylinder in a flow of air (see Fig. 5.6a) approximately, without taking into account damping, can be determined by formula (3.2). The equation of forced oscillations of the cylinder in a flow of air will be

$$\ddot{y}+2h\dot{y}+p^2y=\frac{1}{2m}\rho V^2 dc_m e^{i\omega t}. \qquad (5.2)$$

Its form coincides with the equation of forced oscillations (3.30), if we designate

$$P_0=\frac{1}{2}\rho V^2 dc_m, \qquad e^{i\omega t}=\sin\omega t+i\cos\omega t.$$

Upon coincidence of the frequency of natural oscillations of the cylinder with the frequency of the perturbing force ω there appears resonance. Thus in this case, in examining the oscillations of the cylinder according to the "pattern of forced oscillations," one should expect that with an increase of flow rate V (and consequently, the frequency of change of perturbing force ω) the frequency and amplitude of oscillations of the cylinder will change approximate according to the same law as in a linear oscillatory system during the action of harmonic perturbation. However, observations of oscillations of different structures (bridges, metal pipes, steel cables, wires, etc.) at various wind velocities indicate that they oscillate with the same frequencies, equal to their natural ones. The behavior of such structures in a wind flow has a self-oscillatory character.

The experiments conducted with bodies of cylindrical form in wind tunnels indicated that, besides the so-called "Benard – Karman vortices," from an oscillating cylinder in its extreme positions, the powerful vortices stall, having a stalling frequency which is equal to the frequency of oscillations of the cylinder, and being the basic cause of oscillations of the cylinder. The biggest (with respect to amplitudes) oscillations of the cylinder occur across the flow. Longitudinal oscillations are insignificant.

The frequency of vortex stall in a wind stream from pipes and other bodies having a cylindrical form, and from cylinders in wind tunnels, is almost identical and corresponds approximately to the number Sh = 0.2. If the stalling frequency of "Benard – Karman vortices" when Sh ≈ 0.2 coincides with the natural frequency of the body, its oscillations (across the flow) sharply increase. Such conditions of flowing around is commonly called wind resonance. Wind resonance can present a large danger for structures.

If the stalling frequency of breakdown of vortices does not coincide with the natural frequency of the body, its oscillations are insignificant.

For excitation of sustained oscillations of a cylinder in a flow of air, a defined, "resonance" flow rate is necessary. If after the excitation of oscillations we change (decrease or increase) the flow rate, the oscillations will occur approximately with the same frequency in a rather large range of speed variation.

With a considerable difference between flow rate and "resonance" velocity the oscillations are cut off and subsequently there appear oscillations with another natural frequency of the body.

Consequently, in the region of natural frequencies with a change of the flow rate there is observed the phenomenon of pulling or "holding" of frequency. The frequency of oscillations of the body changes according to the flow rate not in a direct line, but along a certain step-like curve (Fig. 5.7). The arrows in Fig. 5.7 indicate the pattern of change of frequency of oscillations of the body with increase of flow rate.

At high speeds the flow in the wake is turned into turbulent flow with a continuous spectrum and random amplitude. The reaction of the cylinder to the action of such a flow no longer can be determined by the above-mentioned "pattern of forced oscillations," and should be studied by statistical methods. However, even in this case, in the wake of a circular cylinder there can predominate frequencies at which the spectral density has peaks, and consequently the frequencies "contain" the largest share of kinetic energy of the turbulent flow behind the cylinder. In such case it is possible to estimate the oscillations of the cylinder according to the pattern of forced oscillations.

The motion of airfoil profiles in a flow of air in many respects is analogous to that considered for a cylinder. Many experimental investigations were conducted on the behavior of airfoil profiles in a flow of air and the characteristics of the amplitude spectrum in wake behind these profiles. The basic purpose of these investigations was to illuminate the qualitative side of the phenomenon.

The data of different investigations in the qualitative evaluation of the phenomenon converge in the following. The frequency of predominant oscillations of flow in the wake behind an airfoil profile depends on the angle of attack of the profile and velocity (Mach number) of the flow. At the same flow rate in the subsonic region at average angles of attack which are common for horizontal flight of aircraft, the predominant frequency of vortices is almost

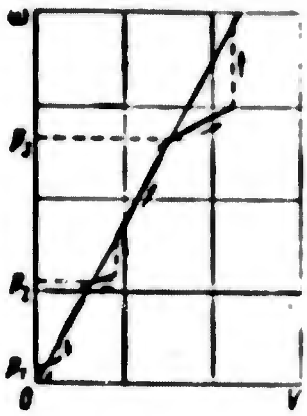

Fig. 5.7. Diagram of change of frequency of oscillations of a cylinder according to flow rate. (p_1, p_2, p_3 — natural frequencies of the cylinder).

proportionate to the angle of attack. In the region of large angles of attack (smaller, however, than the critical angle of attack of the profile) the predominant frequency of vortices drops. With an increase of the flow rate V with the preservation of constant angle of attack of the profile, the predominant frequency of vortices in the wake increases. At high flow rates in the wake behind the profile the predominant frequency is difficult to isolate.

During experiments on models it was established that with the increase of flow rate the frequency of vortices increases to a certain magnitude which is equal to the natural frequency of tone I of the model, and upon further increase of speed in a certain range it remains constant, analogous to that shown in Fig. 5.7 for a cylinder. In the "zone of resonance" the frequency of oscillations of the model and frequency of vortices in the wake behind the model in a certain range of variation of flow rates remain constant and equal. In other words, the model itself determines the frequency of vortices in the zone of its natural frequency of oscillations. Upon further increase of speed the determining factor again becomes the flow rate and the frequency almost linearly increases to a magnitude which is equal to the frequency of tone II of natural oscillations of the model. In the zone of second resonance the frequency of vortices in a certain range of variation of flow rate again remains constant. An analogous picture is repeated upon further increase of flow rate.

Thus, vortex formation is influenced not only by the aerodynamic properties of the model, but also its elastic ones: in the region of natural frequencies of the model the frequency of vortices is determined by oscillations of the model.

In the considered cases of oscillations of a circular cylinder and airfoil profile the incident flow of air was assumed to be uniform and consequently external perturbations are absent. Perturbing forces appeared due to the interaction of flow and elastic body. Therefore, oscillations of such type are called self-exciting (self-oscillations).

An aircraft in flight does not encounter a fully uniform flow of air, the turbulence characteristics of which (frequency and amplitude of oscillations of speed) are random variables. Slight turbulence of the incident flow of air practically does not affect the general aerodynamics of an aircraft, but can render a definite influence on the oscillations of its structure.

For a qualitative evaluation of aerodynamic oscillations it is important to know with that frequencies these oscillations occur.

Let us consider the wing of an aircraft during the action on it of a distributed aerodynamic load, which depends on coordinate z and time t:

$$g = g(z, t). \tag{5.3}$$

We shall not place any special conditions on the form of the function in this instance. The load can arbitrarily change along the wing span and its frequency spectrum is generally infinite (white noise).

We shall determine the frequencies and modes of forced oscillations of the wing under the action of an arbitrary perturbing load (5.3).

Inasmuch as in this case we are interested only in the qualitative side of the phenomenon, the wing may be schematized in the form of a beam on which there acts a load (5.3). We can analogously

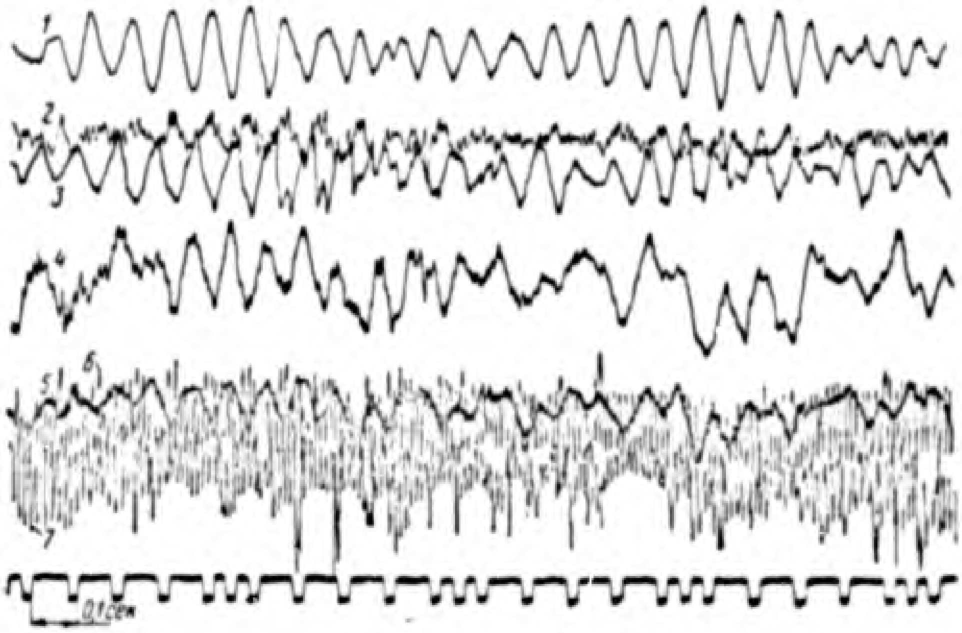

Fig. 5.8. Typical recording in flight of oscillations of an aircraft with TPE. 1) wing tip; 2) and 5) nose and afterbody (along axis y); 3) and 4) ends of stabilizer and fin, 6) and 7) side of fuselage in zone of propeller rotation.

schematize the fuselage or empennage of an aircraft. With such assumptions we shall formally apply the method of solution which includes expansion of the solution of the equation of forced oscillations of a distributed system with respect to the eigenfunctions of an oscillatory system. From solution (3.98) it follows that forced oscillations of the considered system occur with corresponding natural frequencies p_i of this system. The same result can be obtained by applying the method of spectral characteristics.

This general property of aerodynamic oscillations, obtained as a result of formal application of the method of expansion of the solution of the equation of forced oscillations with respect to the eigenfunctions of the system, is confirmed by experiment: frequencies of predominant (with respect to magnitude of amplitudes) aerodynamics oscillations always are close or coincide with frequencies of natural oscillations of a structure. Where upon the biggest amplitudes are possessed by oscillations which correspond to the lowest tones of natural oscillations of the structure, since the higher the frequency, the greater the damping, and consequently the smaller the peak of resonance.

Figure 5.8 gives a typical recording of oscillations of parts of an aircraft with TPE in horizontal flight. As can be seen from this recording (especially from recordings on channels 1 and 3), aerodynamic oscillations of the structure have low frequencies which correspond to its natural oscillations. It is necessary to note that the amplitudes of aerodynamic oscillations even at steady regimes of flight frequently are not constant, and the recording has the form of beats. The shown aerodynamic oscillations are characteristic for all types of aircraft with any propulsion systems. For aircraft with TPE high-frequency propeller vibrations are also substantial, especially for the sides of the fuselage in the plane of propeller rotation (see channels 6 and 7).

The shown peculiarity of aerodynamic oscillations is explained by the different dynamic receptivity of oscillatory systems to perturbations with various frequency. During aerodynamic oscillations the structure as if regulates itself, or more exactly, determines the frequency of oscillations. It is a unique filter which separates only those oscillations whose frequencies are in the zone of resonance with its natural frequencies.

Figure 5.9 shows the approximate distribution of amplitudes of oscillations with respect to frequencies of the wing, fuselage, stabilizer, and fin, obtained on actual aircraft. Vertical arrows show the values of natural frequencies for these parts of the structure. As can be seen, predominant oscillations are concentrated near the natural frequencies of the structure and with increase of frequency the amplitudes quickly decrease.

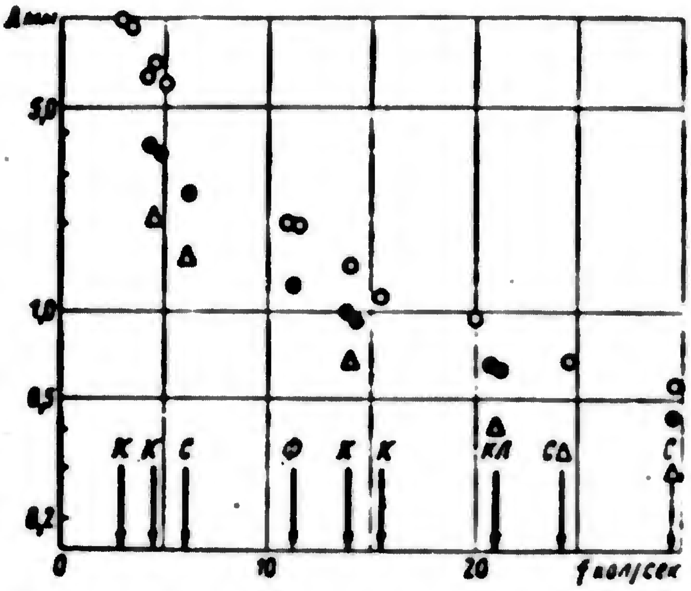

Fig. 5.9. Combined graph of aerodynamic oscillations of an aircraft. ○ — wing, ● — stabilizer, Δ — fin. ↓ — frequencies of natural oscillations: К — wing, Ф — fuselage, С — stabilizer, КЛ — fin.

The conclusion obtained with respect to the frequency spectrum of aerodynamic oscillations is very important in the practical aspect, since by the known frequencies and modes of natural oscillations it is always possible to indicate beforehand the predominant frequencies of aerodynamic oscillations and the approximate distribution of amplitudes through the structure. Absolute values of amplitudes can be obtained only from experiment during flying tests.

The general tendency of the change of the characteristics of aerodynamic oscillations with respect to speed (Mach number) in rectilinear flight consists of the following (see Fig. 5.4). At speeds of flight that are close to minimum (high c_y), the amplitudes of oscillations increase rapidly with deceleration. In the subsonic region (excluding speeds which are close to minimum) the oscillations are relatively small and comparatively slowly increase with the

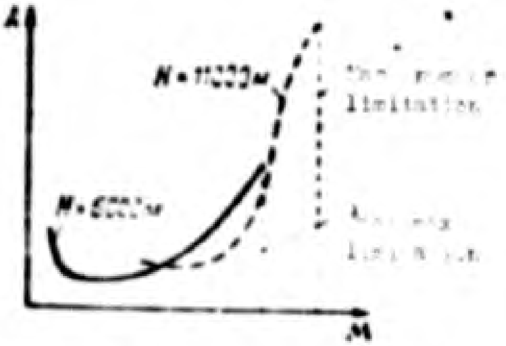

Fig. 5.10. Dependence of aerodynamic oscillations on Mach number for two altitudes of flight.

increase of the speed of flight. In the region of transonic speeds there begins a sharp growth of amplitudes of oscillations which attain maximum at Mach numbers corresponding to the moment of achievement of the speed of sound in the biggest quantity of points of the surface of the aircraft. Upon further increase of speed of flight the oscillations remain constant, and then decrease as the flow rate of air on the main parts of the structure become supersonic.

It is necessary, however, to consider that although the amplitudes of aerodynamic oscillations are limited, their maximums can be excessively large and can present a definite danger of partial destruction of the structure in flight. Therefore, in the investigation of these oscillations the appropriate measures of precaution (gradual increase of speed of flight during measurements, thorough analysis of the level of oscillations, etc.) are taken.

Speeds of flight, at which maxima of oscillations set in, and the maximum level of oscillations depend on many factors, in particular on the characteristics of profiles, angle of sweep of the wing and empennage, and others. Maximum amplitudes of oscillations on a given aircraft occur at the same Mach number, but their level increases with the growth of velocity head (with decrease of altitude of flight, see Fig. 5.15). The dependence of amplitudes of oscillations on Mach number for a subsonic aircraft is shown in Fig. 5.10.

Buffeting

Buffeting is the reaction of a structure to a strongly turbulized

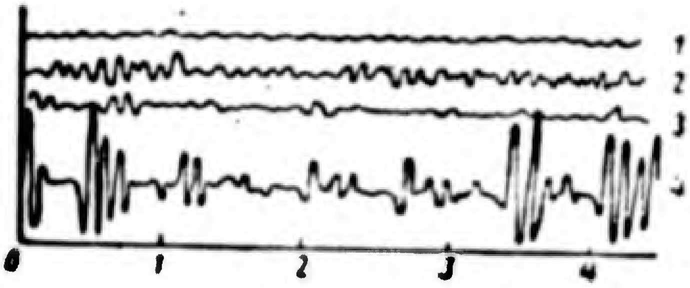

Time in seconds

Fig. 5.11. Recording of oscillations during buffeting of the empennage on a glider. 1 and 2) fuselage correspondingly on axes z and y, 3) wing; 4) elevator.

flow. Externally, buffeting is sensed as shocks on the empennage sometimes with almost regular periodicity (Fig. 5.11). If the frequency of these shocks is close to the natural frequency of the empennage or fuselage there appears resonance, which presents the biggest danger. Sometimes oscillations during buffeting carry an irregular character and have many components with different frequencies, whereby the magnitudes of total amplitudes of oscillations and the relationship of different components with respect to amplitudes strongly change in time (Figures 5.12 and 5.13).

Inasmuch as the basic causes of buffeting are stalls in the flow around parts of an aircraft, the struggle against it is conducted in the first place by improvement of the aerodynamics of the aircraft.

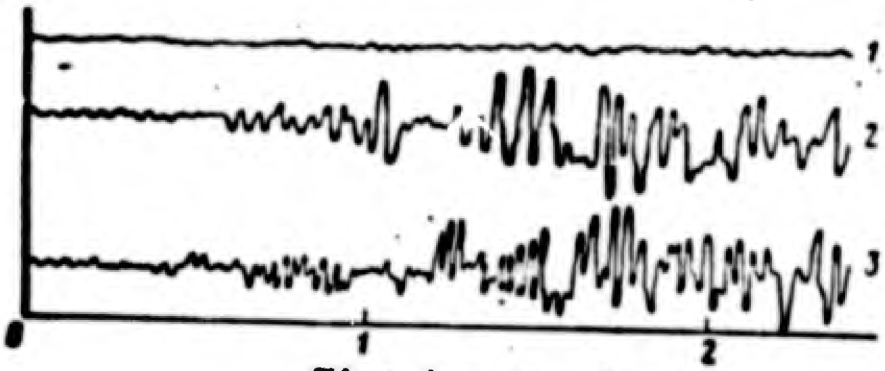

Time in seconds

Fig. 5.12. Recording of oscillations during buffeting of the empennage on an aircraft. 1) wing; 2) afterbody; 3) elevator.

There have been attempts of theoretical calculation of buffeting. However, the accuracy of such calculation is so small that it loses practical meaning. Therefore, the manifestation of the conditions of appearance of vibrations and the struggle against them are conducted with the help of an experiment, determining the places of the stalls and the characteristics of oscillations of the aircraft. Afterwards, in each specific case we find the structural solutions for the removal of stalls or we establish the necessary limitations of flight conditions.

We experimentally found certain recommendations which permit, in the majority of cases, the avoidance of considerable oscillations in operating conditions of flight. These recommendations basically concern measures for the improvement of aerodynamics of the aircraft.

Stall can occur from a wing (at large angles of attack), from different secondary structures on a wing and fuselage, in places of connection of wing and fuselage due to interference of flow, etc. Places of stall are determined by filming the flow field, for the obtainment of which, on the surface of the investigated part of the aircraft, tapes ("silk threads") are glued in the direction of flow in a given point (Fig. 5.14).

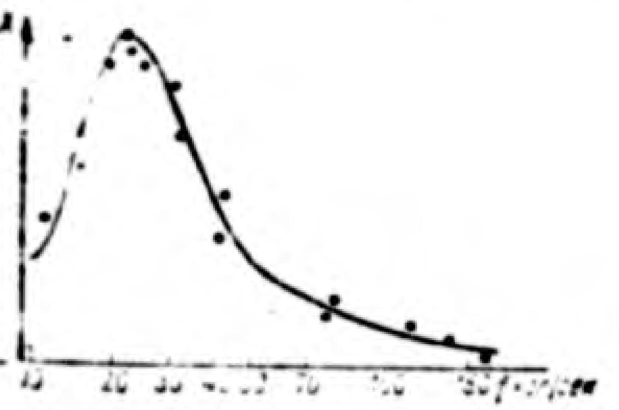

Fig. 5.13. Distribution of amplitudes with respect to frequency during buffeting of an aircraft (see recording in Fig. 5.12).

Preventing stalls along with the removal of buffeting signifies at the same time an improvement of the aerodynamic shapes of the design and a lowering of its parasite drag.

Improvement of the aerodynamics of an aircraft is the main method for the elimination of buffeting. In certain cases an increase of rigidity of the empennage had an effect.

Destructions to the structure, caused by buffeting, can occur not at once at the onset of oscillations, but upon the expiration of

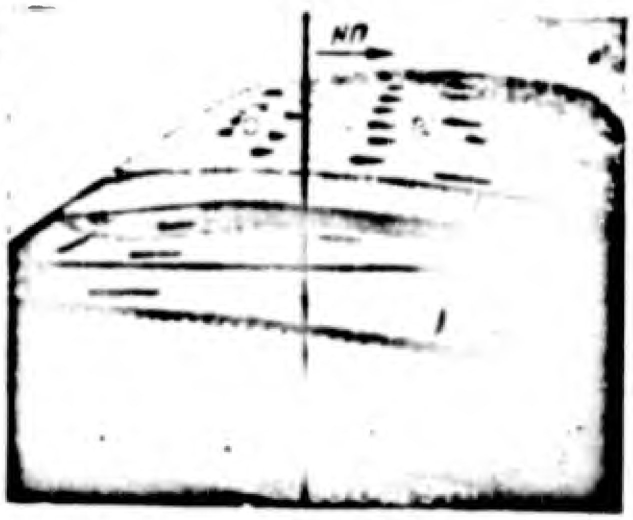

Fig. 4.14. Example of determination of flow field with the help of silk threads. a) zone of streamlined flow; b) stall zone.

a certain time due to the phenomenon of fatigue. In most cases this permits the investigation to be carried out directly in flight conditions, in which buffeting appears. However, one should note the danger of buffeting, especially in moments of appearance of intense oscillations. During aircraft tests there were cases when buffeting led to fast destruction of separate elements of the empennage. Intense oscillations of the buffeting type appeared at speeds of flight that are close to minimum (high c_y); on certain contemporary aircraft excessively large oscillations appeared at transonic speeds of flight.

The general cause of buffeting which occurrs in a stall with the forward located parts of an aircraft was shown above. However, the direct causes of buffeting and the forms of its appearance are usually different. The deficiencies of some aircraft are rarely repeated on others. The presence or absence of buffeting is checked on a completed aircraft during flying tests. On the basis of the results of the tests, specific measures for the removal of this phenomenon are determined.

This situation is illustrated by the following cases of buffeting.

On a jet aircraft there appeared buffeting of the empennage upon executing turns at small speeds of flight when the empennage went into the vortex flow from the wing. Amplitudes of oscillations of the empennage as compared to normal flight were increased by more than 20 times, whereupon the oscillations of the wing remained insignificant (see Fig. 5.12). The reaction of the stabilizer-elevator unit to perturbations created by flow from the wing was such that the oscillations had a clearly expressed predominant frequency (see Fig. 5.13). Large oscillations during buffeting were removed by increasing the torsional rigidity of the stabilizer and eliminating resonance phenomena.

On a heavy glider which had spoilers there appeared considerable oscillations of the tail section with open spoilers. Oscillations constituted separate shocks with almost regular periodicity along the empennage, which then were transformed into natural oscillations of parts of the glider (see Fig. 5.11). For removal of buffeting, spoilers were cut on the side of the fuselage, owing to which the empennage was removed from the spoiler stall zone.

On an aircraft with frontal shields on the landing grear there appeared intense oscillations with lowered landing gear. The cause of the oscillations was the stall at the indicated shields. Oscillations were removed by means of replacement of the frontal shields of the landing gear by lateral flaps.

On an aircraft with two turbojet engines located in the fuselage and having one air inlet in the nose of the fuselage, there appeared intense oscillations during engine throttling. The cause of the oscillations was the stall at the entrance to the air inlet due to a decrease of the flow rate of air during engine throttling. The oscillations were removed by the installation of flaps for bypass of air during engine throttling, connected with the gas sector.

From the given examples it follows that the direct causes of buffeting can be very diverse. Therefore, the main problem in the study of buffeting is the determination of its causes and the

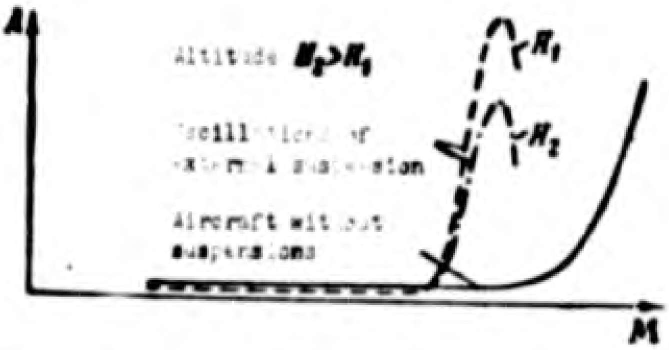

Fig. 5.15. Graphs of aerodynamic oscillations of an aircraft without external suspension and with suspension.

conditions of its appearance, depending upon which the methods of its removal are determined.

On contemporary aircraft different external suspensions are widely applied which frequently are made under completed aircraft, and, therefore, they are not always successful in the aerodynamic respect (in combination with the aircraft). In view of this there also appear intense oscillations, especially at transonic speeds of flight (Fig. 5.15). Aircraft with such suspensions obtain additional limitations for flying use due to excessive oscillations.

Contemporary transport aircraft with large cargo hatches that open in flight also sometimes obtain limitations on speed of flight due to increased oscillations which appear during flight with open hatches.

The basis for a judgement about the permissibility of any conditions of flight during the appearance of oscillations are the results of determination of the characteristics of oscillations of the aircraft structure during flying tests. Permissible conditions of flight, from the condition of flow around the wing, are established by the coefficient of lift $c_{y\ per}$ corresponding to the angle of attack at which stall has not yet occurred. The curve of $c_{y\ per}$ for different Mach numbers can be determined by the results of testing profiles or aircraft models in a wind tunnel. However, this curve can considerably differ from the curve for an actual aircraft. Therefore, the value of $c_{y\ per}$ should be ascertained during flying tests.

In the considered cases of buffeting, oscillations were experienced basically by the empennage upon colliding with a flow that is perturbed, in particular by a wing. The wing practically did not experience oscillations in this instance (see Fig. 5.12), or more exactly, it experienced only oscillations of insignificant amplitude. During flights at wing angles of attack close to critical, from the wing there begins an intense stall.

The stall creates large variable aerodynamic forces on the wing and causes intense oscillations (see Fig. 5.5 when $M < M_1$). An analogous phenomenon can occur at transonic speeds of flight due to the formation of a shock wave and separation of the boundary layer of the wing. These wing oscillations can be dangerous, especially at transonic speeds of flight.

5.3. Oscillations Appearing During Takeoffs and Landings

During takeoffs and landings there appear elastic oscillations of the aircraft structure. The problem of oscillations of the structure in this case may be formulated in the following manner: on an elastic oscillatory system with a distributed mass, the natural oscillation of which are determined by equation (3.82), there act n concentrated arbitrarily changing forced $P_i(t)$ (n is the number of landing gear struts). It is required to determine the forced oscillations of such a system.

In the given problem, forces are considered that are transmitted from the landing gear to the aircraft. No special conditions are placed on the force function $P_i(t)$: each of these forces can arbitrarily change in time, and all of them can affect the structure in any combination. The physical essense of this consists in that aircraft can have different shock absorption and consequently, the forces transmitted from the landing gear to the structure have different laws of change in time: landing can be made on one, two, or three points with different vertical and lateral speeds of the aircraft, i.e., the combination of forces $P_1(t)$ and their magnitudes have a random character.

An exact solution of this problem, even upon disregarding aerodynamic damping, is quite complicated. The solution of this problem was given above by the method of generalized harmonic analysis. Let us consider the qualitative side of oscillations appearing during takeoff and landing.

For this case the wing or fuselage will be considered as a beam and the unknown function for deflections and the perturbing force will be expanded in a series according to the eigenfunctions of a system, analogous to how this was done for $y(z, t)$ and $g(z, t)$ [equations (3.90) and (3.91)]. However, in this case one should consider that concentrated forces are applied in fixed points of the axis of abscissas. Equations (3.93) and (3.94) remain valid for the given case, only function $Q_1(t)$ of series (3.90), in distinction from its indicated value (3.97), has the form

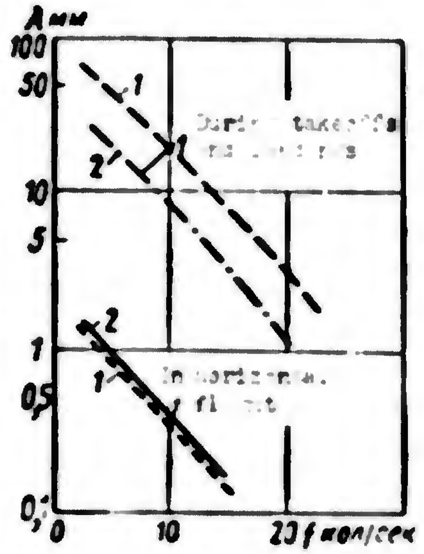

Fig. 5.16. Comparison of aerodynamic oscillations and oscillations appearing during takeoffs and landings. 1) stabilizer; 2) wing.

$$Q_1(t) = \frac{P_1(t) f_1(z_1) + P_2(t) f_1(z_2) + \dots}{\int\limits_0^l f_1(z)\, dz}. \tag{5.4}$$

where $P_1(t)$, $P_2(t)$,... are the forces from the 1st, 2nd,... shock struts of the landing gear;

z_1, z_2,... are the abscissas of the rigging points of the landing gear shock struts.

Hence the conclusion can be made that forced elastic oscillations of the structure during takeoffs and landings of an aircraft occur with natural frequencies and forms of oscillations. This oscillation mode differs from other forced oscillations by large amplitudes.

Elastic oscillations during takeoffs and landings for contemporary aircraft are relatively large and considerably exceed the amplitudes (practically with those same frequencies) of oscillations appearing in flight (Fig. 5.16). Here, for instance, the G-forces of the wing tips and fuselage increase 3 to 5 and more times as compared to the G-force in the center of gravity of the aircraft (see Fig. 4.28). Therefore, it is necessary in the determination of the service life of the structure to consider these oscillations, especially during use on unpaved airfields.

5.4. Acoustic Vibrations

On contemporary aircraft and rockets, in connection with the growth of power of propulsion systems and speeds of flight, there was an increase in the level of noises.

In engineering, noise is a complex sound process with a continuous spectrum of frequencies. The following concepts are used for evaluating noises: sound pressure, force of sound, and level of sound.

Sound pressure p is the difference between the instantaneous value of continuously variable pressure in a sound wave and constant atmospheric pressure existing at a given point of space in the absence of sound.

Force of sound J is the amount of energy, passing in unit of time through a single area, perpendicular to the direction of propagation of the sound.

The most wide-spread is the evaluation of the level of sound (noise) in decibels. The sound level L is the common logarithm of the ratio of the actural force of sound in a given point of space to the so-called threshold force of sound $J_0 = 10^{-16}$ w/cm^2:

$$L = 10 \lg \frac{J}{J_0}. \quad (5.5)$$

Figure 5.17 gives an approximate diagram of noise levels and corresponding magnitudes of sound pressure created by different noise sources, and also shows the approximate lower bounds of the noise level at which there are possible damage to a structure.

The spectrum of noise source can consist of discrete frequencies (propeller noise) or can be almost continuous with random frequencies (noise of jet engine).

The character of change of the noise level depends on the source. Thus, the biggest noise from the propeller is observed in the plane of its rotation (Fig. 5.18). In a wing stall the noise level varies with respect to chord and attains its maximum in the region of the beginning of the stall (Fig. 5.19).

Stresses in a structure are basically determined by the form of the function of mechanical conductivity. Therefore, certain elements have the biggest oscillations with natural frequencies. Figures 5.20 and 5.21 give the form of spectral stress-strain diagrams in the skin during the influence of continuous and discrete noise.

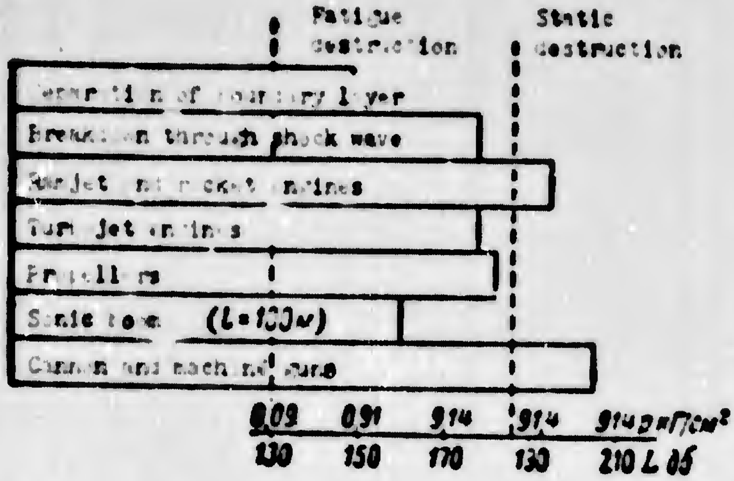

Fig. 5.17. Diagram of noise levels and sound pressure from different sources.

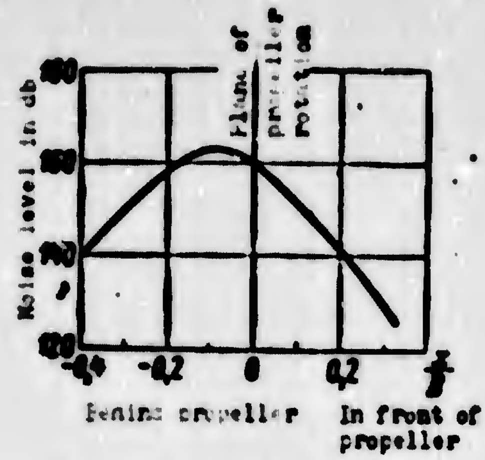

Fig. 5.18. Curve of noise level in the plane of propeller rotation. x/D – distance (along length of fuselage) in fractions of propeller diameter D.

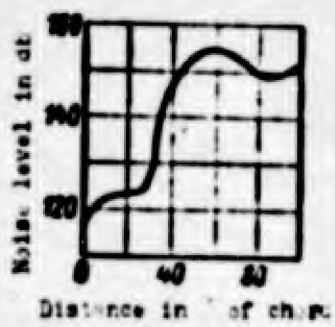

Fig. 5.19. Curve of noise level on a wing during stall.

Oscillations of the skin can essentially be increased due to the mechanical transmission of oscillations from one surface to another (ailerons, controls, and so forth).

During the analysis of vibration caused

Fig. 5.20. Graphs of the function of mechanical conductivity and stresses for a panel with continuous noise spectrum.

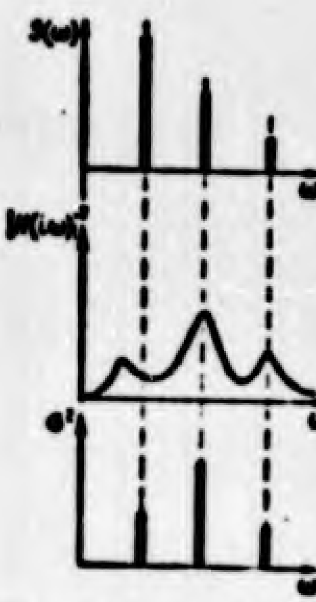

Fig. 5.21. Graphs of functions of mechanical conductivity and stresses with discrete noise spectrum.

by the noise of a jet engine it is necessary to consider the probability characteristics of distribution of amplitudes. This distribution is close to the Rayleigh distribution and can be described by the equation

$$P\left(\frac{\sigma}{\bar{\sigma}}\right)=\frac{\sigma}{\bar{\sigma}}e^{-\frac{1}{2}\left(\frac{\sigma}{\bar{\sigma}}\right)^{2}}. \quad (5.6)$$

where σ is the peak stress in the skin;

$\bar{\sigma}^2$ is the mean square of stress in the skin;

P is the probability of encounter of peak stresses of magnitude $\sigma/\bar{\sigma}$.

The mean square of stress in the skin is determined by the relationship

$$\bar{\sigma}^2=\frac{\pi}{4\gamma}\omega_0 S(\omega_0)\sigma_0^2. \quad (5.7)$$

where σ_0 is the stress in the skin caused by a constant unit pressure;

γ is the damping factor;

ω_0 is the natural frequency of oscillations of the structure;

$S(\omega_0)$ is the corresponding ordinate of the function of spectral density of noise.

The force of noise is approximately proportional to the fourth degree of relative flow rate. Therefore, the biggest acoustic vibrations are observed in the beginning of takeoff, when the relative flow rate of the jet stream is the biggest.

Acoustic vibrations of a structure can be decreased by means of optimum selection of places of engine location, application of silencers, selection of panel shape (from considerations that its natural frequency ω_0 be outside the range of the spectrum of maximum noise level), and also by increasing the skin thickness, and introduction of additional shock absorption of the skin (double skin with an absorbing layer, for instance a skin with honeycomb filler).

CHAPTER VI

FLUTTER

List of Designations Appearing in Cyrillic

б = b = balancer

д = div = divergence

ин = inert = inertia

кр = wing = wing or kp = crit = critical

несж = incom = incompressible

р = con = controls

сек = sec
стрел = swept = sweptback

ф = f = flutter or ф = fus = fuselage

ЦТ = c.g. = center of gravity

э = a = aileron

Flutter is a very dangerous form of self-exciting oscillations which are determined by the interaction of aerodynamic, elastic, and inertial forces, that are acting on a structure in an air current. The study of flutter reduces to the investigation of the problem of dynamic stability of the structure. Under certain conditions the structure becomes dynamically unstable: with a certain random deviation of it from the state of equilibrium there appear oscillations which are supported by the energy of flow and can increase until destruction of the structure.

The phenomenon of flutter on aircraft was noted for the first time in 1916. The first investigations of flutter date back to approximately the same time.

The basic causes of the appearance of flutter were the absence of weight balancing of ailerons (in certain cases, the controls) and low torsional rigidity of the wing. Before 1935 there appeared chiefly wing flutter. In the pre-war years (1935-1940) in connection with the rapid development of military aviation, which was outstripping the scientific investigations, there were many cases of flutter not only of wings, but also the empennage of aircraft. The main cause of flutter in these years was also the insufficient mass balancing of the control surfaces of aircraft.

In war period (1940-1945) and after the war the majority of cases of appearance of flutter occurred due to the influence of the tabs of the control surfaces and insufficient mass balancing of the controls, ailerons, and wing.

In connection with the growth of speed of contemporary aircraft and the lowering of relative rigidity of design there is an increase in the necessity of a more thorough study of the characteristics of flutter for guarantee of flight safety.

If for aircraft of past years the comparatively simple measures for guarantee of mass balancing of control surfaces and the selection of appropriate torsional rigidity of the lifting surfaces in most cases could ensure safety of an aircraft from flutter, then for contemporary aircraft the problem of flutter has become considerably more complicated and have not yet been completely studied. In connection with this, the analysis of aeroelasticity of a structure in the designing stage of every new aircraft became so important that recently the requirement of aircraft construction with the consideration of safety under conditions of flutter is becoming obligatory.

6.1. Causes of the Appearance of Flutter

The causes and the mechanism of the appearance of flutter will be considered in simple examples of aeroelastic oscillations of clear wing and a wing with an aileron (Figures 6.1 and 6.5).

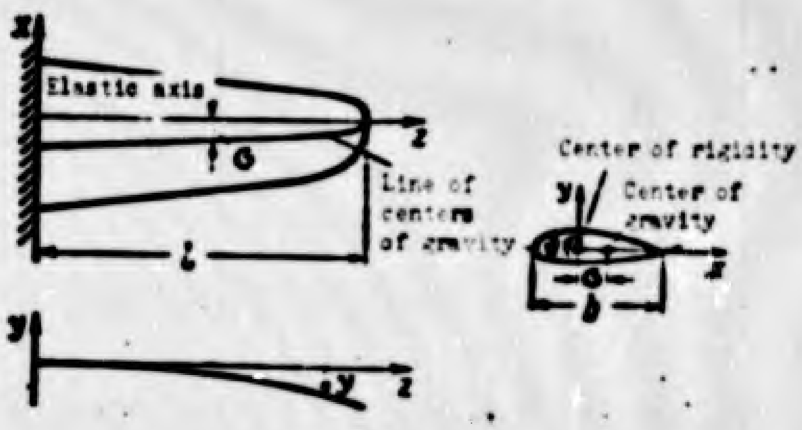

Fig. 6.1. Diagram of a wing for the calculation of flexure-torsion flutter ("cantilever diagram").

Above (see p. 152) we considered natural individual oscillations of wing flexure and torsion which were schematized in the form of a cantilever. Individual oscillations are possible only when the centers of gravity and centers of rigidity of sections of a cantilever wing coincide.

The centers of gravity of sections in real wings do not coincide with the centers of rigidity. Therefore, such wings accomplish joint (flexural and torsional) oscillations. The natural oscillations in this case are described by the system of equations

$$\left.\begin{aligned}&\frac{\partial^2}{\partial z^2}\left(EJ\frac{\partial^2 y}{\partial z^2}\right)+m\frac{\partial^2 y}{\partial t^2}-m\sigma\frac{\partial^2 \theta}{\partial t^2}=0;\\&\frac{\partial}{\partial z}\left(GJ_{\text{кр}}\frac{\partial \theta}{\partial z}\right)+m\sigma\frac{\partial^2 y}{\partial t^2}-J_m\frac{\partial^2 \theta}{\partial t^2}=0.\end{aligned}\right\} \qquad (6.1)$$

where σ is the distance between the center of gravity and the center of rigidity of a section of wing (see Fig. 6.1);

J_m is the linear moment of inertia with respect to the axis of rigidity.

The other designations are the same as in equations (3.82) and (3.103). When $\sigma = 0$ system (6.1) is broken up into two independent equations which coincide with equations (3.82) and (3.103).

Boundary conditions for system of equations (6.1) will be

$$\left.\begin{aligned}&z=0, \quad y=0, \quad \frac{\partial y}{\partial z}=0, \quad \theta=0;\\&z=l, \quad \frac{\partial^2 y}{\partial z^2}=0, \quad \frac{\partial}{\partial z}\left(EJ\frac{\partial^2 y}{\partial z^2}\right)=0; \quad \frac{\partial \theta}{\partial z}=0.\end{aligned}\right\} \qquad (6.2)$$

Integrating equation (6.1) under boundary conditions (6.2), we can find the frequencies and forms of joint oscillations of flexure and torsion of the cantilever. In the absence of damping the total amount of energy in such an oscillatory system remains constant: it is only transformed from flexural energy into torsional energy and black. In an air medium, and also due to hysteresis losses, these oscillations gradually subside.

Fig. 6.2. Diagram of the change of the damping decrement of oscillations of a structure for different forms of aeroelastic oscillations.

If the considered oscillatory system is placed in an air current, then during wing oscillations there are developed aerodynamic forces, one of which supports the oscillations and the others counteract the oscillations, so that the wing reacts to the total action of these forces. Experiments in wind tunnels show that with the growth of flow rate the oscillations in the beginning quickly subside, then damping decreases and there sets in a moment when there appear undamped harmonic oscillations with constant amplitude (damping is equal to zero, Fig. 6.2). The speed of flight at which the damping decrement of oscillations is equal to zero is called the critical flutter speed V_f. This state is neutrally stable. With an insignificant exceeding of V_f the damping decrement becomes "negative" and there appear increasing oscillations, i.e., flutter.

The oscillations during flutter are self-exciting. Its appearance does not require an external exciter of oscillations, and the energy of oscillations is derived from uniform steady-state (potential) flow during its interaction with the wing.

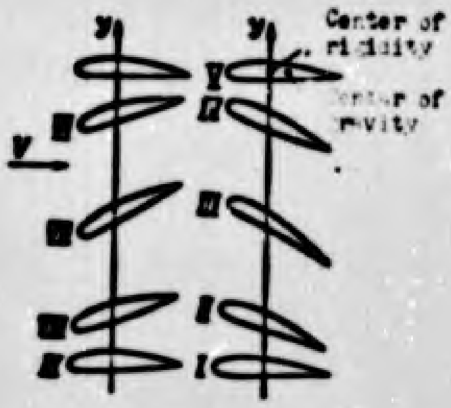

Fig. 6.3. Diagram of the appearance of flexure-torsion wing flutter. I-IX) consecutive positions of wing section during oscillations.

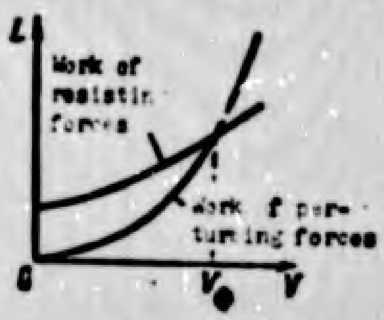

Fig. 6.4. Diagram of change of work L of excitation forces and resisting forces according to flow rate.

Let us consider in a simple example the mechanism of the appearance of flutter (Fig. 6.3). Let us assume that a wing is affected by an undisturbed air current, whereby it is situated at a small angle of attack (there is no wing stall). For some reason the wing was removed from the state of equilibrium, for instance due to bending. Then with an accelerated motion of the wing from position I upwards into positions II and III the motion of the center of gravity is retarded due to inertia as compared to the motion of the center of rigidity, and the wing is twisted in the direction of an increase of the angle of attack. There then appears additional lift in the direction of wing motion (upwards).

Under the action of aerodynamic forces and forces of elasticity the wing reaches a certain upper position V. In the opposite, also accelerated, motion of the wing downwards under the action of forces of elasticity the wing twists in the direction of a decrease of the angle of attack and there appears an additional aerodynamic force which acts in the direction of wing motion (positions VI-VIII).

During the motion of the wing, in addition to the internal hysteresis forces and resistance of air, there appears a damping force due to the influence of the rate of flexure oscillations, since during flexure oscillations there occurs a change in the angle of attack to magnitude $\Delta\alpha = y/V$. The additional lift, which appears in this instance, is a damping force, since it always acts against the motion of the wing. In addition to the indicated forces, on a wing that is fluctuating in an air current there also appear other perturbing and damping forces. At low speeds of flight the damping forces exceed the perturbing ones and the oscillations subside. With the increase of speed of flight there sets in such a moment when the work L of the perturbing forces exceeds the work of damping forces and flutter becomes possible, i.e., oscillations with increasing amplitude. The speed at which the work of the perturbing forces becomes equal to the work of the damping forces is the critical flutter speed (Fig. 6.4). In this case there are possible harmonic oscillations with constant amplitude.

Analogously to the considered flexure-torsion oscillations of the wing there occur oscillations with degrees of freedom: wing flexure (absolute torsional rigidity) and aileron deviation (Fig. 6.5). With probable deviation of a wing upwards from a certain

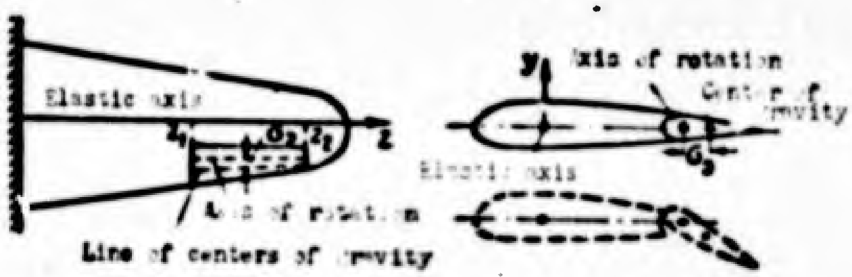

Fig. 6.5. Diagram of wing with aileron.

central position I (Fig. 6.6) the aileron with its mass unbalance (centers of gravity of aileron sections are behind its axis of rotation, $\sigma_a \neq 0$, see Fig. 6.5) lags behind the motion of the wing and deviates under the action of forces of inertia downwards with respect to the wing. Due to this there appears an additional lift which is directed towards the motion of the wing and increases its deflection (positions II-IV). During reverse motion of the wing downwards from the upper position of equilibrium V, the aileron deviates upwards and there is created an additional aerodynamic force, which also acts in the direction of wing motion (positions VI-VIII). Thus, during flexural oscillations of a wing with aileron there appear aerodynamic forces supporting the oscillations. There simultaneously appear damping forces which prevent the development of oscillations. At low speeds of flight the damping forces accomplish more work than the perturbing forces, and the wing oscillations are damped. At a certain critical speed of flight the work of the perturbing forces becomes equal to the work of the damping forces and wing oscillations of flexure-aileron form with constant amplitude become possible. At speeds of flight $V > V_f$ there are possible oscillations with increasing amplitudes. Analogous to the considered forms of flutter there appears flutter of other forms.

It is important to note that in both cases flutter appears during the interaction of two forms of wing deformations: in the first case, flexure and torsion of the wing and in the second, flexure of the wing and rotation of the aileron. If the wing accomplishes only flexural or only torsional oscillations, then such oscillations will always be damped (in the absence of wing stall). During stalls, flutter is possible with one degree of freedom, i.e., torsional stalling flutter of the wing or flutter of the control surfaces. In the absence of stalls and potential flows flutter is possible only in systems with several degrees of freedom. Such flutter is sometimes called "classical" to distinguish it for instance from stalling flutter.

The design of an aircraft or other flight vehicle has an infinite number of modes and frequencies of aeroelastic oscillations. It is possible to assume that in an air flow around a structure all modes of aeroelastic oscillations are excited. At small flow rates all of them are damped, but their damping decrements depend differently on speed. With the increase of flow rate from zero to a defined magnitude, in the beginning in one oscillation mode the damping decrement becomes equal to zero. Upon further increase of speed the damping decrements for another, third, etc. mode of aeroelastic oscillations consecutively become equal to zero (see Fig. 6.2). Thus the first critical state is attained, the second critical state of flutter, etc. If at low speeds all parts of the structure oscillate approximately with identical intensity, then upon achievement of a

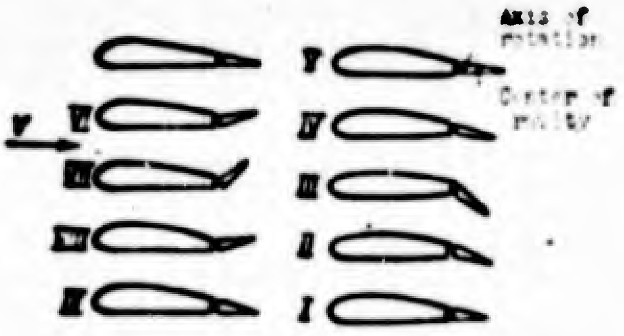

Fig. 6.6. Diagram of the appearance of flexure-aileron wing flutter. I-IX) consecutive positions of aileron during oscillations.

certain critical speed (with decrease of damping decrement to zero) the oscillations in corresponding mode become predominant. Considering this, during calculations of flutter it is possible to select a design with the least quantity of degrees of freedom, i.e., only with such degrees of freedom, which decisively affect oscillations of a corresponding aeroelastic mode. Successful schematization of the phenomenon considerably simplifies the analysis of flutter.

Usually the phenomenon of flutter of any form is determined by two, three, or more degrees of freedom of motion of the structure. With an increase of the number of degrees of freedom the analysis of flutter becomes very complicated; therefore, oscillation modes with number of degrees of freedom not more than three or four are usually considered. However, the excessive tendency to simplify the problem is not always justified. This especially pertains to the problem of analysis of flutter of the empennage with a great number of possible forms of flutter and comparatively large quantity of degrees of freedom, to which the individual forms of flutter are very sensitive. Application of high-speed mathematical machines expands the possibilities of theoretical analysis of flutter and permits the consideration of a large number of degrees of freedom.

6.2. Forms of Flutter. Influence of Structural Parameters on Critical Speed

There can be very many forms of flutter. Of practical value are the forms of flutter with the least critical speeds. It is impossible to indicate the calculation (with respect to least V_f) forms of flutter beforehand. Therefore analysis of flutter is conducted for several forms which are selected on the basis of accumulated experience. Selection of calculation forms of flutter to a considerable extent depends on the researcher. In view of this the study of cases of flutter, appearing on flight vehicles during operation, is an important condition for predicting the possible calculation forms of flutter for new designs. From the whole variety of possible forms of flutter at present we count 10-12 forms which are encountered in practice, present the biggest danger, and require obligatory checkout on new designs.

A large influence on flutter is rendered by certain design and operational parameters, whereby they affect the different forms of flutter differently.

Let us consider some of the most important forms of flutter and corresponding parameters, by modifying which it is possible to change the critical speed of flutter.

The Effect of Dynamic Balancing of Mass on Flutter

With noncoincidence of elastic axis and line of centers of gravity of sections ($\sigma \neq 0$, see Fig. 6.1) independently of the type of initial deformation – flexure or torsion – oscillations of flexure and torsion of the wing will be connected due to the presence of inertial connections, i.e., the inertial connection of flexure with torsion (during flexure there appears an inertial moment $m\sigma\ddot{y}$, which causes torsion) and the inertial connection of torsion with flexure (during torsion there appear forces of inertia $m\ddot{\theta}$ which cause flexure).

Besides the inertial connections, there exist aerodynamic connections. Since initial wing flexure leads to twisting (see Fig. 6.3), there occurs an increase of the aerodynamic forces that are acting in the direction of motion and creating a prerequisite for further increase of oscillations. Thus, due to aerodynamic and inertial connections there occurs a flow of energy to the system which is oscillating in the air flow.

For preventing flutter it is necessary to have such an influence on these connections that would ensure withdrawal of energy from the system during oscillations. However, it is difficult to influence the aerodynamic and elastic connections. It is considerably easier to change the inertial connections. For instance, in the wing this is attained by displacement of the centers of gravity of sections. Therefore, dynamic balancing (weight balancing) is an important means of preventing flutter.

During flexural-torsional oscillations wing flutter becomes impossible if $\sigma = 0$. In this case the wing accomplishes separate oscillations of flexure and torsion. For decrease of magnitude σ the wing is fitted with counterpoises (usually in the wingtips) for displacement of the centers of gravity of sections of the wing forward. In case of joint flexure-aileron oscillations of the wing the inertial interaction may be excluded if the mass of the aileron is distributed in such a way that during oscillations the forces of inertia do not cause oscillations of the aileron with respect to its axis of rotation ($\sigma_a = 0$, see Fig. 6.5). This is attained by installation of appropriate balancers in the nose of the aileron. Balancing of the controls is done.

The measure of mass unbalance of an aileron (control) is its moment of inertia M_{inert} with respect to the axis of rotation (see Fig. 6.5):

$$M_{inert} = -\int_{z_0}^{z_1} m_a \sigma_a \ddot{y} \, dz$$

or taking into account (3.102)

$$M_{inert} = -\ddot{r} \int_{z_0}^{z_1} m_a \sigma_a f \, dz = c\ddot{r}, \tag{6.3}$$

where

$$c = -\int_{z_0}^{z_1} m_a \sigma_a f \, dz.$$

If $M_{inert} = 0$, the inertial interaction at the given mode of oscillations is excluded.

If mass balancing is not produced with distributed, but with concentrated loads, the full inertial moment will be

$$M_{inert} = -\ddot{r} \int_{z_0}^{z_1} m_a \sigma_a f \, dz + \ddot{r} \sum_{i=1}^{n} m_{bi} \sigma_{bi} f(z_{bi}), \tag{6.4}$$

where m_{bi} is the mass of the i-th balancer;

m_a is the mass of the aileron;

σ_a is the distance between the axis of rotation and center of gravity of the aileron section (see Fig. 6.5);

z_{bi} and $f(z_{bi})$ are the coordinate and value of the function of oscillation mode in the section where the balancer is located.

Minimum necessary mass of the balancer for preventing flutter will be determined by the condition

$$m_b = \frac{\int_{z_0}^{z_1} m_a \sigma_a f(z) \, dz}{\sigma_b f(z_b)}.$$

What was said with respect to mass balancing of ailerons also pertains to other control surfaces.

It is important to note that the degree of balancing strongly depends on the function of mode $f(z)$. A system, which is completely balanced with respect to one oscillation mode, can be unbalanced with respect to another mode. For instance, if a balancer is located in the oscillation mode ($f(z_b) = 0$), it will be ineffective. For this reason the criterion of static balancing is not useful for evaluating the oscillatory properties of a system with respect to flutter. A design with unbalanced masses does not exclude all forms of flutter. Therefore, an analysis of the state of balance of masses is made in reference to definite (calculated) forms of flutter.

Torsion Flutter of a Wing

This form of 1. .. is the most dangerous. Flutter can develop very quickly and destruction of the structure occurs in 2 to 4 seconds (sometimes in 3 to 4 cycles of wing oscillations).

Selection of design parameters can ensure safety of the design from the appearance of flutter at known maximum speed of flight. The main parameters which may be changed for increasing V_f are the rigidity of the design, the ratio GJ_{wing}/J_m, position of the axis of centers of gravity along wingspan and distribution of masses along wing chord. These parameters affect V_f in the following way.

1. With a definite change of flexural, and torsional rigidity of a wing n times the critical speed of flutter V_f is changed $\sqrt{n}$ times. This position is valid not only for the case of flexure-torsion flutter, bur also for any form of flutter: an increase of all rigidities of the system increases V_f in the indicated ratio.

2. The biggest influence on critical speed of flexure-torsion flutter of a wing is rendered by the torsional rigidity of the wing. Flexural rigidity of the wing scarcely affects V_f. If torsional rigidity is increased all along the wingspan n times, V_f changes almost in exact proportion to $\sqrt{n}$.

3. The critical speed of flutter V_f has a minimum value upon coincidence of frequency of flexure and frequency of torsion. This phenomenon is called internal resonance. It is observed when the frequencies of different modes of oscillations are close to one another.

4. The character of change of the ratio GJ_{wing}/J_m along wingspan affects the mode of torsional oscillations $\varphi(z)$. Usually this ratio decreases toward the end of the wing, as a consequence of which there are relatively large amplitudes of its oscillations.

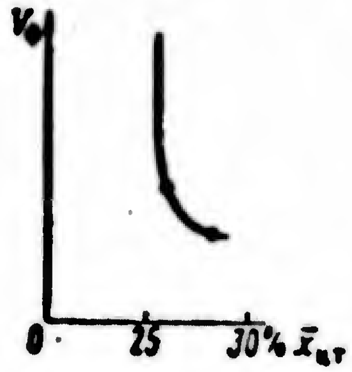

Fig. 6.7. Influence of the position of centers of gravity of wing sections on V_f.

It is necessary to see to it that the ratio GJ_{wing}/J_m is as large as possible (especially toward the end of the wing).

5. Of the three wing axes (foci, centers of rigidity, and centers of gravity) the position of the axis of centers of gravity (especially in the end sections) renders the biggest influence on V_f (Fig. 6.7). The critical speed of flutter may be essentially increased by forward displacement of the centers of gravity in the wing tips. For this we lighten the wing shanks, place counterpoises (balancers) in the nose, and so forth.

For wings of identical span and area the highest critical speed is possessed by the wing with maximum taper.

A large influence on the critical speed of flutter can be rendered by loads on the wing, e.g., power plants, external suspensions, etc. Depending upon weight of the load, its spacing along the wingspan and wing chord stagger, the critical speed of flutter V_f can both increase and decrease. In certain cases even the form of flutter is changed. A substantial influence on V_f is also rendered by the elasticity of suspension of weights, the landing gear, and attachment of the propulsion systems. A large destabilizing influence is rendered by empty fuel tanks on the wing tips and floats, especially for wings of small elongation. V_f also can essentially drop due to the influence of the weight of the fuel placed in the wing, which must be considered in the selection of the fuel consumption program.

Aileron Forms of Flutter

The main cause of the appearance of these forms of flutter is the mass unbalance of ailerons. In the majority of known cases aileron flutter was comparatively easy to eliminate on completed designs by the appropriate selection of weight balancing of ailerons.

Aileron flutter is of the torsion-aileron form with torsional wing strain and rotation of ailerons (this form is comparatively rarely encountered in practice) and flexure-aileron form with flexural wing strain and rotation of ailerons. Let us consider in greater detail this form of flutter.

Flexure-aileron flutter is symmetric and antisymmetric. In symmetric flexure-aileron flutter the wing is deformed by one of the symmetric forms of flexure oscillations (see Fig. 3.20), and the ailerons deviate simultaneously to one side due to the elasticity of the control wiring, which is characterized by frequency of symmetric oscillations of ailerons. In antisymmetric flexure-aileron flutter the wing is deformed by one of the antisymmetric forms of flexure oscillations, and the ailerons deviate in various directions. In this case the ailerons can deviate both without strain on the control wiring (control stick is free, wiring works as a mechanism, frequency of ailerons is equal to zero), and also due to elastic strain on wiring, which is determined by the frequency of antisymmetric oscillations of the ailerons (control stick is held). In connection with this, the analysis of flexure-aileron flutter is conducted both by taking into account, and also without taking into account the action of the elastic restoring force from the wiring strain.

Aileron flutter is a very dangerous phenomenon. However, it is less intense than flexure-torsion flutter of a wing. Thus, on subsonic aircraft 8-15 seconds passes before destruction of the wing during aileron flutter, and in many cases the crew succeeds in reducing the speed of flight and lands. The smaller intensity of aileron flutter is connected with the fact that the flow of energy in this case is ensured basically due to deflection of the aileron (the aileron "rocks" the wing), while during flexure-torsion flutter the flow of energy occurs due to torsion of the entire wing.

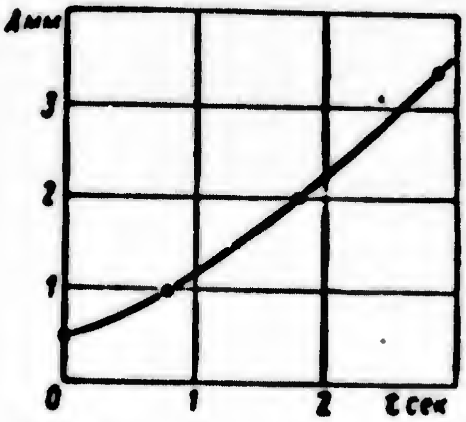

Fig. 6.8. Change of amplitudes of oscillations during antisymmetric flexure-aileron flutter of a glider.

Figure 6.8 gives the curve of build-up of amplitudes of oscillations during antisymmetric flexure-aileron flutter of a glider obtained by partial recording of oscillations at the time of appearance of flutter. Flutter continued for 5-6 sec. and during that time the mounting lugs of wing were destroyed and the glider was damaged. The cause of flutter was the mass unbalance of the ailerons.

At 100% dynamic balancing flexure-aileron flutter becomes impossible. However, for preventing flutter in the range of operational speeds of flight there can be sufficient partial balancing of the ailerons. The degree of necessary balancing is difficult to indicate without carrying out a calculation. Therefore, in practice they either calculate flutter and carry out balancing in accordance with the results, or conduct full dynamic weight balancing of the ailerons. In last case the aileron flutter calculation is not required.

Weight balancing of ailerons is a basic measure of preventing flexure-aileron flutter. Figure 6.9 shows a typical graph of the

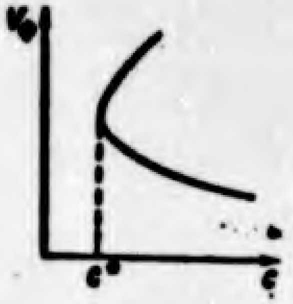

Fig. 6.9. Influence of weight balancing of ailerons on flexure-aileron flutter.

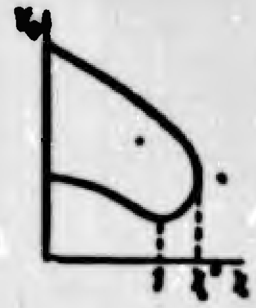

Fig. 6.10. Influence of the ratio of natural aileron, and wing frequencies on flexure-aileron flutter.

critical speed of flexure-aileron flutter depending upon coefficient c (6.3). There exists such a value of coefficient c* that if $|c| < |c^*|$ flutter is impossible. Selection of balancing in accordance with calculation attains the fulfillment of this condition.

Effective means of increasing the critical speed during aileron forms of flutter, especially on completed vehicles, are power dampers, which are devices with viscous resistance or with dry friction resistance, introduced between the aileron and wing and absorbing the energy of oscillations. There are also other types of dampers.

The critical speed of flexure-aileron flutter to a considerable degree depends on the ratio of frequencies of natural oscillations of the ailerons and the bending oscillations of the wing $\chi = f_a/f_{wing}$ (Fig. 6.10). When $\chi \approx 1$, V_f is minimum due to the internal resonance of the system. When $\chi > \chi^*$ ($\chi^* \approx 1.2$ to 1.5) flutter is impossible.

Control-Surface Forms of Flutter

In examining control-surface forms of flutter, in many cases one may assume that wing oscillations are small and may be disregarded. The fuselage is depicted as a nonuniform elastic cantilever, rigidly fixed in one of its sections (for instance in the center of gravity of the aircraft) and on the other end carrying the empennage. Oscillations of the vertical and horizontal empennage are considered to be independent. The stabilizer, fin, and rudder are frequently considered to be absolutely rigid.

Calculation under such assumptions does not always give sufficient accuracy of results. In particular, for aircraft with adjustable stabilizers the assumption of nondeformability of the stabilizer during oscillations is unacceptable. Disregard of fin deformations is also not always permissible. In those cases, when the indicated schematization is not fully satisfactory, it is necessary to consider the aircraft as a free-floating elastic system.

Control-surface forms of flutter are quite numerous. The most important forms are:

1) flexure-control-surface flutter of the horizontal empennage

with two degrees of freedom: bending of the fuselage and elevator deflection;

2) torsion-control-surface flutter of the horizontal empennage with two degrees of freedom: twisting of the fuselage and elevator torsion;

3) flutter of vertical empennage with three degrees of freedom: horizontal flexure and torsion of the fuselage and rudder deflection.

It is also necessary to calculate the deflection of trim tabs and servo-tabs. Servo-tab and trim tab forms of tail flutter are considerably more complicated than the enumerated control-surface forms. For aircraft with small relative thickness of vertical and horizontal empennage it is necessary to consider deformations of the fin and stabilizer during oscillations and compliance of the supports of the control hinges. In certain cases it is necessary to consider horizontal oscillations of the empennage.

The action of the controls on the empennage during oscillations in many respects is analogous to the action of the ailerons on the wing. Accordingly, the calculation of the control-surface forms of flutter in many respects is also like the calculation of wing forms, only into the equations of motion there are introduced corresponding fuselage deformations.

In most cases the cause of tail flutter was unbalance of the controls. Therefore, the calculation of the horizontal empennage is usually conducted only for control-surface flutter of the horizontal empennage, while the vertical empennage requires rudder balancing.

A sufficient condition for preventing control-surface flutter is the observance of full dynamic balancing of the controls. The necessary degree of balancing may be established by calculation.

The influence of weight balancing of the controls on V_f is analogous to that indicated for the ailerons (see Fig. 6.9). It is especially necessary to emphasize that a disturbance of balancing of the controls can essentially lower V_f.

Upon coincidence of frequencies of the stabilizer (or fin) and fuselage it is necessary to calculate flutter without control. In this case the controls are considered to be fixed with respect to the stabilizer (fin).

Control-surface flutter, in additional weight balancing, is essentially influenced by the magnitude of moment of inertia of the controls, aerodynamic compensation, and frequency of oscillations of the controls. With the increase of aerodynamic compensation the critical speed of flutter V_f increases. The greater the axial compensation, the less the necessary degree of weight balancing of the controls. V_f may also be increased by increasing the moment of inertia of the controls. The dependence of V_f on the ratio of frequency of the controls and frequency of the fuselage $\chi = f_{con}/f_{fus}$ is analogous to that indicated for the ailerons (see Fig. 6.10). Furthermore, magnitude V_f of torsion-control-surface flutter is essentially influenced by the torsional rigidity of the elevator. An increase of rigidity when $\chi > 1$, as this usually occurs on aircraft, always leads to an increase of V_f.

It is necessary to emphasize the necessity of the analysis of "stabilizer" forms of flutter of contemporary aircraft with adjustable stabilizers. The natural frequency of torsion of an adjustable stabilizer is considerably lower than a nonadjustable one. Correspondingly, magnitude V_f is also considerably lower in an aircraft with adjustable stabilizer. The calculated forms flutter of an adjustable stabilizer are cantilever (bending and twisting of stabilizer) and fuselage (with vertical bending of fuselage). V_f of an adjustable stabilizer can be increased by installing balancers on the stabilizer and by increasing the torsional regidity of the stabilizer.

Flutter with One Degree of Freedom

As was indicated above, the presence of two and more degrees of freedom in an oscillating system is an essential, but not necessary condition for the appearance of flutter. In transient aerodynamic processes at high subsonic and supersonic speeds of flight there is possible flutter in systems with one degree of freedom. The known examples of such flutter are explained by pitch oscillations of rigid wings and control surfaces. The majority of them present only theoretical interest. However, in practice there were observed cases of the appearance of intense oscillations of ailerons and controls at transonic speeds of flight. Recordings of such oscillations indicate the harmonic character of rotation of the ailerons or controls, which is common during flutter. This form of aeroelastic instability appears in connection with shock oscillations on the lower and upper surfaces of the wing (stabilizer) ahead of the axis of rotation of the ailerons (controls). The means of preventing this phenomenon are found experimentally, based namely on this physical explanation of instability of ailerons and controls. Quantitative calculations of instability of this form with the help of existing aerodynamic theories are difficult.

A sufficiently effective means of removal of the indicated natural oscillations of ailerons and controls is the introduction of a damper for absorption of the energy of oscillations. Inasmuch as a prediction of this phenomenon is now impossible due to the absence of developed calculation methods, and it is revealed only in a finished design, the introduction of friction into the system (which does not require serious alterations in design) is a sufficiently economic and reliable means.

In representing the motion of self-oscillation systems in the phase plane (in displacement – speed coordinates) the graph of motion, described by depicting point $(y, \dot{y})$, – the phase curve – when $t > 0$,

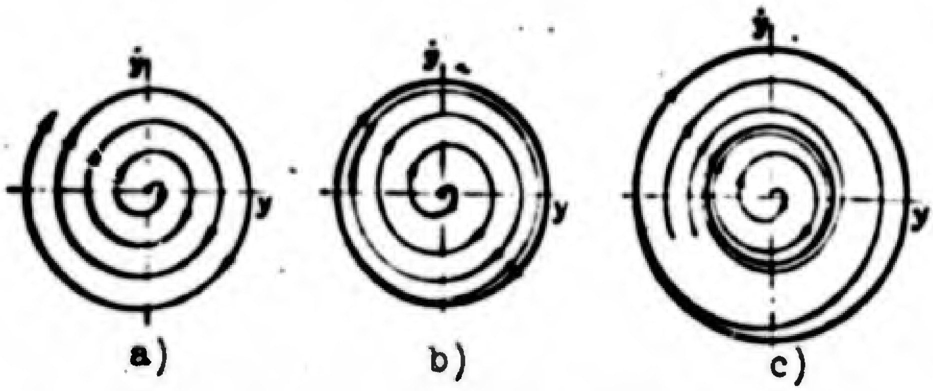

Fig. 6.11. Phase diagrams of oscillations. a) increasing oscillations; b) oscillations with a limit cycle; c) case of oscillations with several limit cycles.

emerges from the origin of coordinates in spiral form (Fig. 6.11a). This is explained by the fact that the origin of coordinates is the point of unstable equilibrium, and the oscillations themselves are divergent (increasing).

In certain nonlinear systems, with the growth of time (in the limit) the oscillations become periodic. Any periodic motion on the phase plane corresponds to a closed curve (Fig. 6.11b). In the considered case the spiral-like phase curve tends to a closed curve when $t \to \infty$. Poincare called this closed curve the limit cycle.

An oscillatory system under certain conditions can have not one, but several limit cycles (Fig. 6.11c). Inside the cycle the depicting point moves along a divergent spiral-like curve and nears the cycle, while outside the cycle the motion is along a twisted spiral-like curve and the depicting point also nears the cycle. The limit cycle constitutes steady-state oscillations with defined amplitude.

Aerodynamic forces at transtransonic speeds, which appear during oscillatory motion of control surfaces, are nonlinearly connected with speed. Therefore limit cycles of oscillations of ailerons and controls and corresponding changes of their stability are possible. The experimental data obtained during flying tests confirms the presence of such cycles. However, excessively large oscillations can lead to breaking of the structure, without reaching the limit cycle. In connection with this, it is impossible to make a definite preliminary conclusion concerning the presence of safe limit cycles in the considered type of natural oscillations of ailerons. Therefore, a thorough inspection of this phenomenon is required in wind tests and flying experiments.

Analogous natural oscillations in principle are also possible on the flaps and the wings themselves at transtransonic speeds of flight. These oscillations essentially depend on Mach flight number and are connected with the appearance of transient aerodynamic processes on streamlined surfaces. During stable supersonic flowing around such oscillations are absent.

Influence of Hydraulic Booster in the Control and Automatic Pilot Linkage on the Critical Speed of Control-Surface Flutter

The inclusion of a hydraulic booster changes the rigidity of control. The linkage rigidity then becomes dependent also on the characteristics of the booster. Due to this, the inclusion of a booster affects the magnitude of critical speed of control-surface flutter. In the case of unbalanced controls the inclusion of a booster in the control linkage can lead both to a lowering and to an increase of V_f.

The presence of a booster cannot be a cause of the appearance of flutter if the control system is stable in ground conditions. Consequently, with full balancing of the controls and observance of the indicated condition, inclusion of a booster should not lead to flutter.

Stability of a system with a hydraulic booster increases with the increase of rigidity of the structure, to which it is attached.

For a control system with an automatic pilot, the ratio of natural frequencies of the attitude gyroscope and fuselage deformations is of value. Due to the proximity of these frequencies natural oscillations are possible.

During natural oscillations with a booster or automatic pilot there usually is attained a certain limit cycle and further oscillations are not divergent (with respect to amplitudes). This phenomenon in its character differs from flutter. However, it presents a danger to the structure and is absolutely impermissible in operation.

It is especially necessary to emphasize the necessity of thorough study of the influence of a hydraulic booster and automatic pilot on the stability of a control system in ground conditions and in flight. Considering the difficulty of reliable determination of this influence by means of calculation, frequency tests are desirable to conduct with boosters and automatic pilot both off and on. In the last case the reaction of control to pulses of different duration and form should be investigated: the magnitude of these pulses should be such that control deviations under their action exceed the threshold of sensitivity of the automatic pilot.

Stalling Flutter

In distinction from classical flutter, which was considered above on the assumption of a smooth (without stall) flow around the structure, in stalling flutter, during at least part of the time of the full cycle of oscillation, the flow separates from the structure. This introduces peculiarities into the oscillatory process. Inasmuch as the wings and empennage of aircraft in the usual conditions of flight are far from the angles of attack, at which separation of flow begins, the problem of stalling flutter for them has a smaller value. More wide-spread is the separation from propeller blades of aircraft and helicopters in which stalling flutter was observed. Recently this question obtained value for jet engines in connection with observed breakages of blades of turbines and compressors at subcritical angles of attack.

The first experimental investigations of stalling flutter go back to 1935-1936. In connection with the appearing nonlinearities of the process a theoretical analysis of stalling flutter is hampered. However, investigations of this phenomenon on models indicate that in a steady flow with increase of wing angle of attack there is observed a considerable lowering of critical speed of flutter (more than 50%) at a certain critical value of the angle of attack. In view of this, stalling flutter presents a serious danger.

The peculiarities of stalling flutter may be seen in an example of testing propeller models. In the region of small angles of attack (angle of attack is taken in a section on relative radius $\bar{r} = 0.7$) in the absence of stall the critical speed of flutter with the increase of angle of attack from zero to a certain value at first drops, and then remains constant in a certain region of angles of attack.

This critical spe orresponds to classical flutter. Upon further increase of the angle of attack to a magnitude when stalling begins during oscillations, the critical speed sharply drops. This speed corresponds to stalling flutter.

The influence of design parameters on stalling flutter is frequently different than for classical flutter. Stalling flutter is chiefly torsional. Flexural oscillations during stalling flutter are relatively small, while in classical flutter the flexural and torsional oscillations cause deformation of the structure of one order. The position of the axis of centers of gravity of sections during stalling flutter practically does not have any value. The critical speed of stalling flutter can be defined as the speed at which the structure is twisted to angles of attack at which there occurs a separation of flow. It can be increased by increasing the torsional rigidity.

In this connection one should note the distinction between flutter, stalling flutter, buffeting, and aerodynamic oscillations, although all of them are "aerodynamic," i.e., there appear due to the in action of the air current and the structure. Flutter and aerodynamic oscillations are self-oscillation phenomena, inasmuch as they can appear in a steady air current in the absence of an external source of perturbing forces.

Flutter corresponds to dynamic instability of a structure in an air current, while during aerodynamic oscillations the structure is dynamically stable. Flutter oscillations are distinguished by their regularity, are almost harmonic, and have a defined frequency. Aerodynamic forces during flutter appear due to oscillations of the lifting surface and they support these oscillations.

The motion of a structure during aerodynamic oscillations does not have a fully regular character and can occur with many of its natural frequencies.

Buffeting is distinguished by its intensity and irregular character. The appearing aerodynamic forces during buffeting are determined basically by the turbulent characteristics of flow.

Oscillations of a wing (propeller blade) during a stall are boundaries between flutter and buffeting. On the one hand, oscillations in this case appear during the action of steady flow on the structure and are consequently a self-oscillation phenomenon. On the other hand, during a stall there appear stochastic aerodynamic processes and the elastic reaction of the structure to these processes will also be stochastic; the appearing aerodynamic forces depend very little on the oscillations of the structure, and therefore, the oscillations may be called buffeting. If the motion with such oscillations is distinguished by regularity (sinusoidality) with respect to one of the degrees of freedom, the phenomenon is sometimes called buffeting flutter.

Panel Flutter

In the above-considered forms of flutter, deformations of the structure along chord did not render a noticeable influence on flutter and they were disregarded. In panel flutter the main role is played by deformations of the skin (panel) which is rigidly supported along the edges.

Supersonic flutter of a panel for the first time was considered in connection with damages due to vibrations of the skin of the German V-2 rockets. In a subsonic flow, theoretically, certain self-exciting oscillations accompanied by skin buckling are also possible. The first theoretical research on panel flutter began in 1950.

The skin is enveloped by air from the external side; from the other side the air remains motionless. Due to this, on the skin panel, which is rigidly supported by elements of the internal assembly, at a defined impact pressure, depending on the dimensions and curvature of the panel and conditions on the supports, there can appear self-exciting oscillations.

Theoretical analysis and experiments indicate that loss of stability of the skin (buckling) and flutter and closely connected together.

By tightening the skin it is possible to prevent flutter, but it reappears when it becomes loose. Skin panels will be stable with respect to self-exciting oscillations when they possess sufficient rigidity and their mass is great as compared to the mass of the apparent air. From this point of view, a decrease in rigidity and an increase of skin buckling due to aerodynamic heating of the structure unfavorable shows up in the characteristics of panel flutter.

6.3. Basic Positions of the Theory of Flutter. Methods of Determination of Critical Speed

Basic Assumptions and Limitations of the Theory of Flutter

For practical purposes the most important problem is the guarantee of safety of a structure from the appearance of flutter. The oscillations themselves during flutter do not have any practical interest, since in view of the extreme danger it is important not to allow it to be used. Therefore, of all the characteristics of flutter the main one is the magnitude of critical speed. This gives a basis for the introduction of the following two assumptions which considerably simplify the mathematical apparatus for the investigation of such a complex physical phenomenon as flutter.

First, the problem of flutter constitutes a problem of dynamic stability of a structure in an air current and reduces to finding such (critical) a speed at which small perturbations withdraw the structure from dynamic equilibrium, or more exactly, the speed, upon exceeding which, small perturbations lead to increasing self-exciting oscillations. Consequently, during the analysis of flutter it is permissible to use the results of the theory of small oscillations.

Secondly, inasmuch as critical speed is determined during the study of flutter, and upon the achievement of critical speed there are possible harmonic oscillations of the structure, in the determination of the aerodynamic forces acting upon the oscillating structure we assume that it accomplishes harmonic oscillations. This also simplifies the problem.

We shall consider, for an example, flexural-torsional oscillations in an air current of a thin (two-dimensional) cantilever wing under the action of an initial small perturbation. Equations of joint flexural-torsional oscillations can be written in the form

$$\left.\begin{aligned}&\frac{\partial^2}{\partial z^2}\left(EI\frac{\partial^2 y}{\partial z^2}\right)+m\frac{\partial^2 y}{\partial t^2}-m\sigma\frac{\partial^2\theta}{\partial t^2}+Y=0;\\&\frac{\partial}{\partial z}\left(GJ_{ep}\frac{\partial\theta}{\partial z}\right)+m\sigma\frac{\partial^2 y}{\partial t^2}-J_m\frac{\partial^2\theta}{\partial t^2}+M=0.\end{aligned}\right| \tag{6.5}$$

where $Y = \frac{1}{2}c_y\rho V^2 b$ is the wing lift per unit of span;

$M = \frac{1}{2}c_m\rho V^2 b^2$ is the aerodynamic moment of the wing (per unit of span) with respect to the axis of rigidity.

The other designations are the same as in formulas (6.1) and in Fig. 6.1. The boundary conditions for equations (6.5) remain as before (6.2).

The basic difficulty in the composition of equations (6.5) consists in finding aerodynamic force Y and moment M, the exact determination of which for a wing that is fluctuating in an air current is a very difficult problem. Attempts at an exact determination of these forces led to very complicated solutions that were absolutely unfit for practical applications. Therefore the methods of flutter calculation are based on approximate aerodynamic theories which simplify the problem.

There are two such aerodynamic theories. One of them – the stationary theory – orignates from the assumption of the stationarity of derivatives c_y^α and c_m^α of an oscillating wing. The essence of this theory reduces to the following.

In the flow around a thin wing by a steady flow of ideal incompressible fluid, the lift per unit of span is

$$Y=\rho V\int_0^b \gamma(x)\,dx, \qquad (6.6)$$

where $\gamma(x)$ is the circulation (intensity of adjacent vortices) of a wing of unit span on an element of chord dx;

b is the wing chord.

In the flow around a wing profile by an unsteady flow of fluid, in addition to the adjacent vortices located along the wing (Fig. 6.12), there will appear vortex whiskers (free vortices) and formula (6.6) is unacceptable for the determination of lift. Since in the flow of an ideal fluid the total circulation around the contour, including the wing and vortex whiskers, should remain constant, and during oscillations the lift (and consequently the circulation) on the wing changes, the vortices should be removed from the wing and be carried away by the flow. The plane stationary theory of aerodynamic forces is based on disregarding the vortex sheet which converges from an oscillating wing due to the change of circulation in time. The aerodynamic properties of an oscillating wing with variable linear and angular velocities are replaced in each moment of time by the properties of the same wing with constant linear and angular velocities that are equal to the real instantaneous values of these speeds. The slope of the velocity vector of flow to the profile is also considered to be constant in each given moment of time and equal to the real instantaneous slope at this instant of time.

Fig. 6.12. Diagram of vortices in the air flow around a wing.

Thus, the unsteady flow near the wing is replaced by a steady one, circulation on the wing in every given moment of time will be constant, the adjacent (transverse) vortices in these moments will not depart from the wing, and formula (6.6) is applicable for computing the aerodynamic forces.

In accordance with the stationary theory it is relatively simple to determine the aerodynamic forces on a wing without an aileron, on a wing with an aileron, and on the empennage. Not stopping on the determination of these forces, which are presented in sufficient detail in various works and in special handbooks on the calculation of aircraft flutter, one should note that flutter calculations according to the theory of stationarity give good coincidence of results with given tests of models in wind tunnels basically in the subsonic region of speeds of flight. In the transonic and supersonic regions in certain cases this theory gives an overestimate of the critical speed of flutter.

The other aerodynamic theory — the non-stationary one — is based on disregarding the change of adjacent (longitudinal) vortices along the wingspan. In accordance this theory it is considered that every section of an oscillating wing is in conditions of plane-parallel flow and works independently of the other sections. The profile is considered to be moving in the flow with variable forward and angular velocities, circulation around the wing changes in time, and a vortex sheet runs from the wing. The aerodynamic forces, calculated under these conditions, are transferred to the elements of a real wing of finite span in conditions of nonplanar flow.

The non-stationary theory of aerodynamic forces in many cases is more exact, but it is also more complicated as compared to the stationary theory.

The question concerning the limits of applicability of the stationary and non-stationary theories of aerodynamic forces during the analysis of flutter is impossible to consider as fully answered. Evident simplifications, introduced by the stationary theory into engineering analysis of flutter, make it necessary to perform an experimental check of the limits of its applicability. The results of such a check indicate that it is fully applicable in the entire subsonic region of speeds of flight. At transonic speeds of flight, strictly speaking, both theories are inapplicable. In the region of supersonic speeds of flight (approximately for numbers M = 2.0 to 2.5) the non-stationary theory gives computed values of critical speed that are closer to the actual values. In view of this, the non-stationary theory for supersonic speeds is more reliable.

At high supersonic speeds of flight, corresponding to numbers $M > 2.0$ to 2.5, changes of airspeed in the flow near the wing become commensurable with the speed of sound, and the linearized aerodynamic theory is not fully useful for determination of aerodynamic forces. In these cases it is necessary to calculate the nonlinearity in the problem of aerodynamic forces on the wing, in consequence of which the analysis of flutter is considerably complicated. The influence of aerodynamic heating on the characteristics of flutter is considered in Chapter VIII.

The considered theories of flutter are linearized, i.e., the aerodynamic forces are determined according to the linearized aerodynamic theory, and the stability of the systems is investigated in the vicinity of critical speed during small perturbations. The limitations of the theory follow from this. Thus, within the limits of the linearized theory, oscillations cannot be calculated during flutter. With the help of this theory it is possible only to establish the presence of aeroelastic instability of the oscillatory system, but it is impossible to determine the characteristics of the oscillations. At the same time, for practical purposes, especially for flying tests, it is very important to know the magnitudes of maximum amplitudes upon achievement of limit cycles (in those cases when they exist) and intensity of build-up of oscillations during flutter. However, these characteristics can be obtained only if the nonlinear characteristics of the structure and the aerodynamic forces are known.

In the linearized theory of flutter it is assumed that perturbations are small. These perturbations should obviously have a defined minimum magnitude (amplitudes of oscillations should exceed the boundary layer thickness). With perturbations smaller this magnitude, flutter will not be excited. At the same time, during strong initial perturbations (during flights in a strongly turbulent atmosphere) flutter develops very intensely and at several smaller speeds of flight than during flight in a calm atmosphere.

The influence of large perturbations on critical speed and intensity of flutter within the limits of the linearized theory is impossible to reveal. This means that flutter is investigated for rectilinear flight in a calm atmosphere. Critical speed, determined for these conditions, extends to all other conditions of flight. This position does not fully exactly reflect the real processes. In particular, according to the linearized theory the angle of attack of the lifting surfaces in the position of equilibrium is taken to be equal to zero and it is considered that the real angle of attack does not render an influence on critical speed. However, the angles of attack, even considerably smaller than critical (in the static position of the structure), can lead to a lowering of critical speed of flutter at transonic speeds of flight, especially for structures with thin profiles. Upon approach to angles of attack that are close to critical (stalling), the critical speed of flutter can be lowered.

It is impossible to also consider the sufficiently effective linearized theory of flutter for supersonic speeds of flow.

In addition to those indicated, there exists a number of other limitations of application of the considered theories of flutter. In many cases, especially for small subsonic speeds of flow, they give practically acceptable results. In other cases, in particular those connected with the investigation of flutter at speeds of transonic and supersonic flow, the introduction is required of different more precise definitions which approximate the calculated picture of the phenomenon to the real picture. Therefore, along with theoretical analysis it is necessary to conduct experimental investigations.

Analysis of Flutter in an Incompressible Flow

If aerodynamic force V and moment M in equations (6.5) are determined, then considering that these forces continuously depend on ϑ, $\dot{\vartheta}$, $\dot{y}$, and the equations (6.5) themselves are linear equations with constant coefficients, the solution of the system of equations (6.5) can be written in the form

$$Y = Af(z)e^{\lambda t}, \quad \vartheta = B\varphi(z)e^{\lambda t}. \tag{6.7}$$

where f(z) and φ(z) are oscillation modes which must be determined from equations (6.1) under boundary conditions (6.2);

A and B are coefficients determined from initial conditions;

λ is a constant which continuously changes with the flow rate; λ is determined from the equation obtained from (6.5) and (6.2) and called the characteristic equation.

In general λ is a complex number:

$$\lambda = \delta + ip. \tag{6.8}$$

The following values of damping decrement δ and frequency p, which determine the important forms of motion of the oscillatory system are possible:

1. $p = 0$. This case corresponds to aperiodic motion. If the real part of (6.8) is negative ($\delta > 0$), the system, which is removed from the state of equilibrium, by aperiodic motion tries to return to

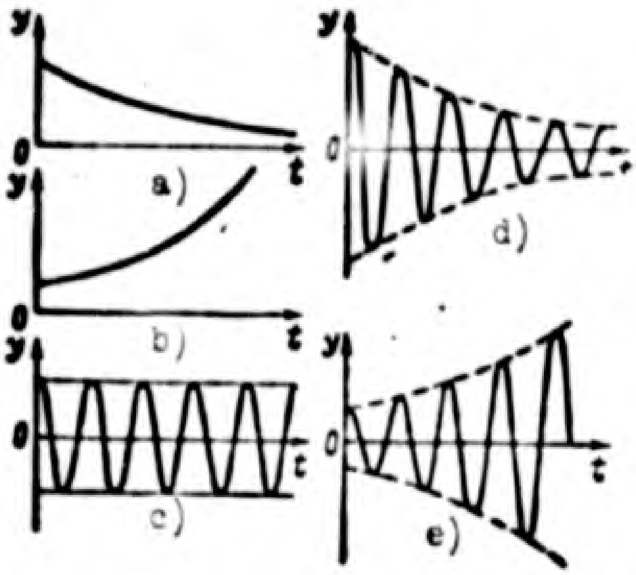

Fig. 6.13. Motion of a system at different values of damping decrement δ and frequency p. a) $\delta < 0$, $p = 0$; b) $\delta > 0$, $p = 0$; c) $\delta = 0$, $p \neq 0$; d) $\delta < 0$, $p \neq 0$; e) $\delta > 0$, $p \neq 0$.

the state of equilibrium (Fig. 6.13a) and consequently, the system is statically stable. If $\delta > 0$, the system, which is removed from the state of equilibrium, by aperiodic motion monotonically leaves the state of equilibrium (Fig. 6.13, b) until damage to the structure, and consequently the system is statically unstable. Such aperiodic motion – divergence – was considered above (see p.56). The case of $\delta = 0$ and $p = 0$ corresponds to the critical state of divergence and determines the condition upon fulfillment of which the system is neutrally and statically stable.

2. $p \neq 0$. Here two cases are possible: $\delta = 0$ or $\delta \neq 0$. In the first case λ is a purely imaginary magnitude and expression (6.7), with the help of Euler formulas

$$\left.\begin{aligned} e^{ipt} &= \cos pt + i \sin pt; \\ e^{-ipt} &= \cos pt - i \sin pt. \end{aligned}\right\} \qquad (6.9)$$

may be reduced to the form

$$\left.\begin{aligned} Y &= A_1 f(z) \cos(pt + \alpha); \\ \theta &= B_1 \varphi(z) \cos(pt + \beta). \end{aligned}\right\} \qquad (6.10)$$

Consequently, when $\delta = 0$ the oscillation will be harmonic and magnitude p is the angular frequency of oscillations.

In the second case, when $\delta \neq 0$, expression (6.7) with the help of the same Euler formulas (6.9) can be reduced to the form

$$\left.\begin{aligned} Y &= A_1 f(z) e^{\delta t} \cos(pt + \alpha); \\ \vartheta &= B_1 \varphi(z) e^{\delta t} \cos(pt + \beta). \end{aligned}\right\} \qquad (6.11)$$

If $\delta < 0$, the motion in accordance with formulas (6.11) will be damped (Fig. 6.13d). A system, removed from the state of equilibrium, by oscillatory motion tries to return to the position of equilibrium and consequently the system is dynamically stable. If $\delta > 0$, then in accordance with formulas (6.11) with the passage of time the oscillations will increase (Fig. 6.13b). A system, obtaining small perturbation, with the passage of time departs by oscillatory motion from the position of equilibrium and consequently such a system is dynamically unstable. Oscillatory (dynamic) stability of a system is called flutter.

The case of $\delta = 0$ when $p \neq 0$ is a boundary case and corresponds to the critical state of flutter when the system is neutrally and dynamically stable. In this case, in accordance with formulas (6.10), the system accomplishes harmonic oscillations (Fig. 6.13c).

Magnitude δ, which is the damping decrement of oscillations, can become equal to zero with the change of the flow rate several times (see Fig. 6.2), and consequently the same form of flutter can have several critical speeds. However, practical interest is presented by the lowest critical speed.

Analysis of the characteristics of flutter and divergence reduces to the analysis of roots λ (6.8) of the characteristic equation. With the use of the results of the non-stationary theory much calculating work is necessary and analysis of flutter becomes very complicated. Methods of calculating flutter and divergence, based on the hypothesis of stationarity, are simpler and more graphic.

For the case of flexural-torsional oscillations of a wing, calculated according to a cantilever diagram, the characteristic equation has the form

$$A\lambda^4+B\lambda^3+C\lambda^2+D\lambda+E=0. \qquad (6.12)$$

The coefficients of this equation depend on the rigidity and mass characteristics of the wing; the magnitude of these coefficients changes with the change of the speed of flight.

Equation (6.12) has four roots corresponding to its power. If among the roots of this equation there is at least one root with a positive real part, then such a system, as was shown above, is unstable: any small perturbation with the passage of time will withdraw the system as far as possible from the position of equilibrium. If all roots have a negative real part, then the system is stable, i.e., after a small initial perturbation it will gradually return to the position of equilibrium.

The real parts of the roots of equation (6.12) are functions of flow rate (see Fig. 6.2) and can change their sign upon change of the flow rate. In these conditions, with the change of the flow rate, the system can become unstable from stable. For stability of the system it is necessary that the real parts of all roots of the characteristic equation (6.12) be negative. A necessary and sufficient condition, upon the observance which this is fulfilled, consists in that the coefficients of the equation and the discriminant

$$R=BCD-B^2E-D^2A \qquad (6.13)$$

must be of one sign.

The critical speed of flow, at which a structure is neutrally stable, is determined by one of the equations

$$E = 0, \quad R = 0. \tag{6.14}$$

The first one determines the critical speed of divergence, since when E = 0 equation (6.12) has root $\lambda = 0$ and according to the above-stated there appears a critical state of divergence. For the considered case the critical speed of divergence is determined by the equality

$$V_d^2 = \frac{\int_0^l GJ_{\kappa p}\varphi'^2 dz}{\frac{1}{2}\rho\int_0^l c_m^\alpha b^2 \varphi^2 dz}. \tag{6.15}$$

The second equation of (6.14) determines the critical speed of flutter. It is obtained from equation (6.12) upon substitution of the value of $\lambda = ip (p \neq 0)$, which corresponds to the presence of harmonic oscillations in the system. Substitution of the values of coefficients A, B, C, D, E of equation (6.12) in the expression for the discriminant (6.13) leads to the flutter equation

$$LV^4 + MV^2 + N = 0, \tag{6.16}$$

the coefficients of which do not depend on speed. This equation gives two values for V_f. Practical interest is presented by the smaller value. Analogously, (according to the "cantilever diagram") the critical speeds of other forms of flutter can be determined.

Influence of Compressibility of Air on Flutter

Compressibility of air starts to appear from $M > 0.5$ to 0.6. At these Mach numbers the derivatives c_y^α and c_m^α are noticeably changed. Formally the calculation of flutter for a compressible flow can be conducted for any Mach numbers by the same formulas as for an incompressible flow. Only the aerodyanmic members in these formulas should be selected by taking compressibility into account.

The influence of compressibility in the region of subsonic and low supersonic speeds in general is small and may cause a change of the magnitude V_f on the order of 10%, but in certain cases this change reaches 20-30% (for straight wings). Therefore, in the region of such speeds of flow the calculation may be conducted for incompressible flow, and the influence of compressibility may be considered as a certain coefficient which depends on Mach number and is determined from experiments in wing tunnels. For high supersonic speeds the influence of compressibility is considerable. The forms of wing flutter in a supersonic flow can essentially differ from the forms of flutter in a subsonic flow.

Coefficients L, M, N of the flutter equation depend on the derivatives of the coefficients of aerodynamic forces and moments, the magnitude of which is influenced by the compressibility of air. Therefore, in the calculation of compressibility, equation (6.16) is transformed from an algebraic equation into a transcendental one:

$$L(V)V^4 + M(V)V^2 + N(V)V = 0 \qquad (6.17)$$

Three possible cases of the roots V^* of this equation are shown in Fig. 6.14. Curve 1 is tangent to line $V^* = V_{f\ incom}$ at a certain transonic Mach number. Curve 2 indicates the absence of flutter under the selected calculation conditions. Curves similar to curve 3 and intersecting line $V^* = V_{f\ incom}$ indicate the existence of a region of instability in a certain range of change of speeds (Mach numbers) of flow. This curve is characteristic for straight wings which usually have instability at transonic speeds.

The critical speed of flutter due to the influence of compressibility can decrease. The most dangerous speed in the sense of the possibility of appearance of flutter (with errors in the calculation assignment of wing rigidity as compared to its actual rigidity) is not maximum speed, but a certain average speed which corresponds to critical Mach number and depends on the aerodynamic properties of the wing.

The influence of certain design parameters on V_f in a compressible flow is intensified. In particular, if one does not consider the influence of compressibility, then with the climb to an altitute (with the decrease of density ρ) V_f is increased, but it always remains a finite quantity. In the calculation of compressibility there exists such a value of ρ at which the equation of flutter gives

Fig. 6.14. An analysis of the roots of the flutter equation (6.17).

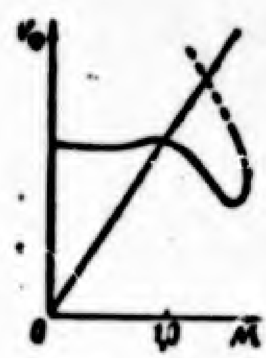

Fig. 6.15. The dependence of critical speed of flutter on Mach number in a compressible flow for the wing of a jet transport.

imaginary roots. In other words, at a defined altitude of flight flutter becomes impossible, even if there is a finite quantity of critical speed on the ground.

The indicated peculiarities of wing flutter in a compressible flow in equal measure also pertain to the empennage.

Figure 6.15 gives a graph of the dependence of V_f on Mach number for bending-twisting flutter of an unswept cantilever wing of a transport aircraft in a compressible flow.*

Influence of Sweepback of Wings on Flutter

Theoretical determination of the conditions of appearance of flutter for wings (or other streamlined surfaces) with large sweepback is hampered by the fact that such wings frequently are used for large subsonic and transonic speeds of flight, i.e., in the interval of speeds for which the aerodynamic theories are not fully strict. The use of approximate th[eor]ies of flutter calculation of sweptback wings leads to the necessity of a more thorough check of the results of such calculations on models or by other methods.

Aerodynamic loads on an oscillating swept-back wing are determined by two methods and flutter of swept-back wings is correspondingly calculated by two methods. One method considers sections of the wing that are normal to the elastic axis and uses the components of speed in these sections for the calculations (see Fig. 2.15); the other method considers sections in the direction of flow. The first method has obtained much development and is simpler, especially for wing designs whose wing ribs are normal to the axis of elasticity and consequently remain undeformed during flexural and torsional oscillations of the wing.

The majority of wings of swept-back aircraft work like a

---

*L. R. Bisplinhoff et al., Aeroelasticity, IL, 1958.

cantilever which is fixed in the root section and is normal to the elastic axis of the wing. Application of the first method is fully justified in this case. Application of the method of sections directed towards flow is more justified for wings with their ribs located towards the flow. However, application of this method is limited, although in certain cases it has definite advantages, in particular in the calculation of degrees of freedom of wing motion on the whole.

In the calculation of flutter of a swept-back wing according to the method of sections normally located to the elastic axis, the functions of deformations $y(z, t)$ and $\varphi(z, t)$ are taken in the direction of the structural wing span, and the structural and aerodynamic components, connected with the determination of air loads acting upon an oscillating swept-back wing, are selected by taking into account $\cos\chi$ (χ is the angle of sweep): instead of the magnitudes V, b, etc., the components $V\cos\chi$, $b\cos\chi$, etc. are taken.

According to the theory of two-dimensional flow the aerodynamic forces on a swept-back wing are created only by the transverse component of speed $V\cos\chi$. Therefore, the critical speed of flutter grows in proportion to $1/\cos\chi$:

$$V_{\phi\,\text{стрел}} = \frac{V_\phi}{\cos\chi}. \qquad (6.18)$$

Formula (6.18) for finite wings with large angle of sweep due to the change of the interaction of flexure and torsion strains is not fully exact. The actual change of V_f is proportionate to a certain magnitude which is the average between $1/\cos\chi$ and $1/\sqrt{\cos\chi}$.

The indicated principles of calculation of sweepback* in the

*Only wings with positive sweepback are considered.

determination of flexure-torsion flutter of wings give fully satisfactory results for an incompressible flow. Mach flight numbers almost do not render an influence on critical speed approximately up to values of $M = 0.8$. If it is necessary to consider the influence of compressibility for swept-back wings, one should take the effective Mach number which corresponds to the component of speed that is perpendicular to the structural wing span:

$$M_{\text{эфф}} = M\cos\chi. \tag{6.19}$$

Flutter of Wings of Low Aspect Ratio

Wings of low aspect ratio, applied on supersonic aircraft, have dimensions and rigidity in directions of chord and span of one order. These wings are of small thickness, are deformed like plates, and due to this the wing deformations in any direction cannot be disregarded. This hampers calculations considerably, inasmuch as it is necessary to apply the three-dimensional aerodynamic theory in the absence of bases for simplification of the problem. If for wings of high aspect ratio the change of aerodynamic forces was investigated along the span (along a line), on the assumption of the nondeformability of cross sections, then for wings of low aspect ratio (on the order of 2) it is necessary to determine the load distribution along the entire area.

In connection with the appearance of aircraft having wings of very low aspect ratio, in the last few years the methods of calculating the flutter of such wings have been made more exact. However, in view of the complexity of the calculation methods, a large place in the investigations of flutter of wings of low aspect ratio is occupied by experimental methods.

Calculations and mainly experiments on models in wind tunnels have established that due to the increase of rigidity the critical speed of wings of low aspect ratio is relatively high. It was also established that the "calculated" forms of flutter for such wings in certain cases were different than for wings of high aspect ratio. The influence of certain parameters on critical speed is also changed. In particular, the distribution of large loads (for instance, engines), on the nose of a wing which has small thickness, leads to oscillations with nose deformations. The calculated forms of flutter for wings of low aspect ratio have larger frequencies than for wings of high aspect ratio.

Methods of Determination of Critical Speed of Flutter

There exists a large quantity of methods for determining the critical speed of flutter. Not one of them has any evident advantages over the others.

The applicability of calculation method one or another depends on the type of design, the considered form of flutter, the complexity of the problem (number of degrees of freedom), and the degree of mechanization of the calculating processes. Selection of a method is sometimes determined by tradition.

Calculation is not the only method for determining the critical speed of flutter. At present the determination of V_f by means of tests on dynamically similar models (flutter models) in wind tunnels is considered as obligatory. Recently the electromechanical method of flutter simulation obtained development.

The indubitable advantage of the calculation method is the possibility, in the initial stage of designing, of conducting an analysis of the aeroelastic structure, investigating different versions of arrangement of the flight vehicle, studying the influence of individual design parameters on critical speed, and selecting the most optimum arrangement with guarantee of safety of the structure from the appearance of flutter. The deficiencies of this method include the inevitable schematization, the known arbitrariness in the selection of calculation forms of flutter, and a number of simplifications in the determination of aeroelastic forces.

Experimental method. A number of the indicated deficiencies is removed during tests of dynamically similar models in wind tunnels; first, because it is possible to manufacture the entire structure in a definite scale and its oscillations can be studied, not oscillations of its separate parts; secondly, the model is tested directly in the flow of air and consequently the errors are excluded, which were introduced in the determination of critical speed in calculations due to the imperfection of the theories of aerodynamic forces.

The experimental method, however, in addition to high costs and complexity, also has other deficiencies: the flutter model is made in accordance with the initial data and the results of preliminarily conducted flutter calculation, and consequently the tests of these models above all are a check of the results of the calculation. Due to this it is not not always possible to reveal the peculiarities of oscillations which were not "foreseen" in the calculation. For instance, if the tab form of flutter was not calculated and in view of the difficulties of simulation this component was not carried out on the model, the peculiarities of oscillations of the structure, which are connected with the presence of tabs, naturally will not be revealed during the tests. In many cases due to the difficulty of experimenting in supersonic wind tunnels, tests of flutter models are conducted at lower speeds (Mach numbers) than they should, and extrapolation of the results is made at high speeds of flow. In spite of the "limitations" this method is very valuable and at present is being widely applied.

The method of electromechanical simulation of flutter (see Chapter X) is economically more profitable (wind tunnels are not required) and can be more exact, inasmuch as it is possible to use full-scale designs. However this method has the same deficiencies as the calculation method, since the aerodynamic forces in both cases are assigned by calculation.

Other methods for determining the critical speed of flutter are also used. The advantage of application of method one or another depends on the problem of investigation on hand, on the required accuracy and reliability of the results, and also on the degree of urgency of the solution of the problem.

The magnitude of critical speed of flutter must be known for determining the safe range of operational speeds of flight. It is taken usually that critical speed should not exceed the highest possible speed of flight by more than 20-35%

$$V_f = (1.20 - 1.35) V_{max} \qquad (6.20)$$

The magnitude of exceeding depends on the accuracy of the method of determining V_f, the degree of influence of the design parameters on V_f, and on the reality of achievement of V_f in flight.

For estimating the safety of flight from the appearance of flutter it is not necessary to know the actual value of critical speed.

It is important to know that flutter is absent in the range of flying speeds and that there are definite reserves of speed. These data in many cases facilitate the problem, inasmuch as the necessity of determining the numerical value of critical speed V_f exceeding the real speeds of flight is dropped.

New Problems of the Theory of Flutter

The problem of aeroelastic analysis of designs of contemporary flight vehicles has been considerably complicated. There have appeared new problems of the theory of flutter, connected with new factors which affect critical speed. Such new problems in the first place include:

a) elastic oscillations of a structure with an automatic pilot and hydraulic booster: the connection of elastic oscillations through the automatic pilot with the controls; questions of stability of the control system (natural oscillations in ground conditions and in flight);

b) influence of aerodynamic heating: drop in rigidity upon lowering the elastic modulus; decrease in rigidity due to nonuniform heating;

c) wing flutter during flight at very high altitudes (the problem of aerodynamic forces on a wing that is oscillating in a strongly rarefied gas and at high Mach numbers).

When $M > 2.5$ a considerable influence is rendered on the characteristics of flutter by the nonlinearity of parameters. According to the nonlinear theory the critical speed at these Mach numbers is considerably less than according to the linear theory. This must be considered in calculations of flutter at flight Mach numbers of more than 2.5.

The results of the investigation of flutter indicate that the actual reserves of maximum speeds of flight up to the critical speed of flutter for contemporary aircraft are minimum and it is difficult to increase these reserves. From this it follows that questions of flutter for contemporary aircraft remain very urgent.

CHAPTER VII

FATIGUE STRENGTH OF FLIGHT VEHICLE STRUCTURES

List of Designations Appearing in Cyrillic

в = b = breaking point.
вибр = vib = vibration.
ВТ = VT

г = g = guarantee.

Д = D

з = safe = safety.

изб = ex = excess.
исп = test = tested.

к = c = concentrator.
к = str = structure.
кГ/мм^2 = kg/mm^2.
кол/сек = osc/sec.
кол/мин = osc/min.

м/сек = m/sec.
м = m = mechanical

нач = init = initial.

обр = sam = sample.

пер = var = variable.

разр = break = breaking.
расч = cal = calculated.
рт.ст = Hg

= sec

ср = av = average

ХГСА = KhGSA

цикл = cycles
цикл/мин = cycles/min.
цикл/сек = cycles/sec.

э = eq = equivalent
э = op = operational.
эф = ef = effective.

Up to the forties basic attention in the designing of aircraft was allotted to guarantee of static strength of a structure during the action on it of maximum, rarely encountered loads. Subsequently, along with guarantee of strength during a single load, considerable attention was allotted to questions of fatigue strength (resistance), i.e., the ability of a structure to sustain the action of relatively small loads, but repeated a large number of times in the operational period of an aircraft.

In the designing of passenger aircraft, questions of fatigue strength frequently are decisive for determining the dimensions and form of structural parts.

The catastrophes of a number of aircraft due to fatigue breakdown of structural elements (the American transport "Martin 2-02" in 1948, the British transport "DAV" in 1951, the passenger aircraft "Comet" in 1954) and the appearance of cracks in components of many aircraft after prolonged use served as an impetus to the rapid development of investigations of fatigue strength of aircraft structures.

Questions of fatigue strength of structures has acquired an especially important value in recent years, since considerably the periods of service of aircraft and the speeds of flight were increased; this led to an increase in both the absolute number of loading cycles of the structure, and also the number of loads per hour of flight; operating stresses in the structure were increased due to the application of more reliable methods of strength calculation; laboratory tests and methods of determining external loads were worked out.

Furthermore, improvement of naviagational and piloting equipment made it possible to fly aircraft in very unfavorable meteorological conditions, when the magnitude and recurrence of loads from gusts of wind are raised. Application of highly durable materials, more sensitive to the action of variable stresses, leads to a lowering of fatigue strength of aircraft structures.

The structure of aircraft with flight number $M > 2.0$ is considerably heated, in consequence of which the mechanical qualities of the materials are lowered, which also lowers the fatigue strength of the structure.

The problem of guarantee of aircraft strength during prolonged use includes work in three directions:

a) study of aircraft loading in conditions of actual use;

b) investigation of the work characteristics of structures during the action of repeated loads;

c) transition from the results of flying and laboratory investigations to the determination of a safe period of service of the structure.

The period of service of an aircraft is the period determined only from the conditions of strength during the action of repeated variable loads. This idea is conditional, since the actual period of service (operational period) of an aircraft depends on a number of other causes (obsolescence, corrosion, wear of equipment, and others).

7.1. Strength of Materials

The simplified mechanism of destruction of components under variable loads may be presented in the following form.

During the action of variable stresses there appear microcracks near the zones of local overstrains of materials. At a determined level of stresses the cracks gradually develop and an increase of the number and dimensions of such cracks gradually reduces a section of full value material. The ends of each crack in turn are places of the action of increased stresses, in which there form new cracks. Destruction during variable stresses occurs slowly, but in the last stage the rate of development of cracks progressively increases, and before the actual destruction the process proceeds almost as fast as during the static destruction of brittle materials.

A typical break due to fatigue has two zones: a smooth surface where the cracks spread slowly and their edges have been smoothed out due to the friction during repeated strains, and a rough surface, along which final destruction of the sample occurred (Fig. 7.1). A study of the character of a fatigue break permits us to judge the type and level of forces causing the destruction. The larger the relative area of the rough zone, the higher the level of variable stresses. The outline of the rough zone indicates the character of acting forces (flexture, torsion, tension, and so forth).

For an explanation of destruction under variable stresses different theories have been advanced. Wide propagation has been obtained by the theory of fatigue breakdown of N. N. Afanas'yev.* If the stresses are sufficiently great, then during the first cycles of change of these stresses in certain grains of metal there appear plastic deformations

*N. N. Afanas'yev, Statistical theory of fatigue strength of metals, Academy of Sciences USSR, 1955.

which cause distortion of the crystal lattice. This leads to hardening of the most stressed grains. As a result of hardening of grains and the increase of yield point connected with it the stresses appearing in grains with those same deformations are increased. In connection with the increase of stresses in individual "defective" places of grains there can appear the phenomenon of slip with a slight tear that will create a "loosening" in the grains along the sliding surface. The number of places of loosening (tears) is increased owing to the variable shifts to one and then to the other side. Grains weakened by the loosening can be deformed as a result of misalignment in places of loosening. Loosening can lead to the formation of cracks. Thus, destruction occurs during maximum stresses in individual grains, where in some cases the zone of appearance of cracks is located on the surface and in others, in the thickness of the material of the component.

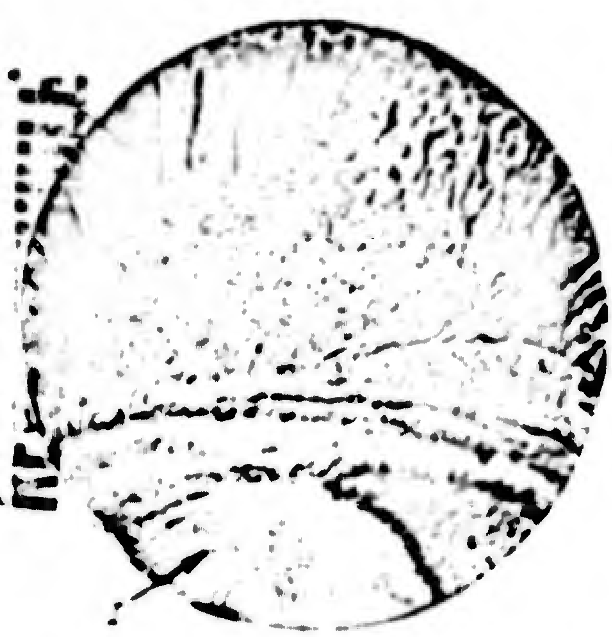

Fig. 7.1. Form of a break during fatigue testing of a sample. I) zone of fatigue break; II) zone of fast break.

The study of fatigue strength of structures and materials until now has almost completely been based on experiment.

Recently large propagation has been obtained by statistical theories of fatigue strength of materials.

At present, questions of fatigue strength were developed in an independent branch of science on the strength of a structure and they have formed their own terminology. Therefore, described below are the main definitions that have been adopted in investigations of the characteristics of strength of aircraft structures.

Most experimental investigations of fatigue strength are conducted during variable stresses which are periodic cyclical functions of time. The basic characteristics of variable stresses are the sign and magnitude of maximum and minimum stresses (σ_{max} and σ_{min}). The totality of all values of stresses during the time of one period corresponds to loading one cycle. As characteristics of the cycle we take the constant or average stress of the cycle

$$\sigma_{cp}=\frac{\sigma_{max}+\sigma_{min}}{2}$$

and variable stress (amplitude of the cycle)

$$\sigma_{ap}=\frac{\sigma_{max}-\sigma_{min}}{2}.$$

We can correspondingly consider average load P_{cp} and variable load P_{var}. If σ_{max} and σ_{min} are identical in magnitude, but are opposite in sign, the cycle will be symmetric ($\sigma_{av} = 0$), otherwise it will be asymmetric. The relation $r = \sigma_{min}/\sigma_{max}$ characterizes the asymmetry of the cycle and is called the coefficient of skewness of the cycle.

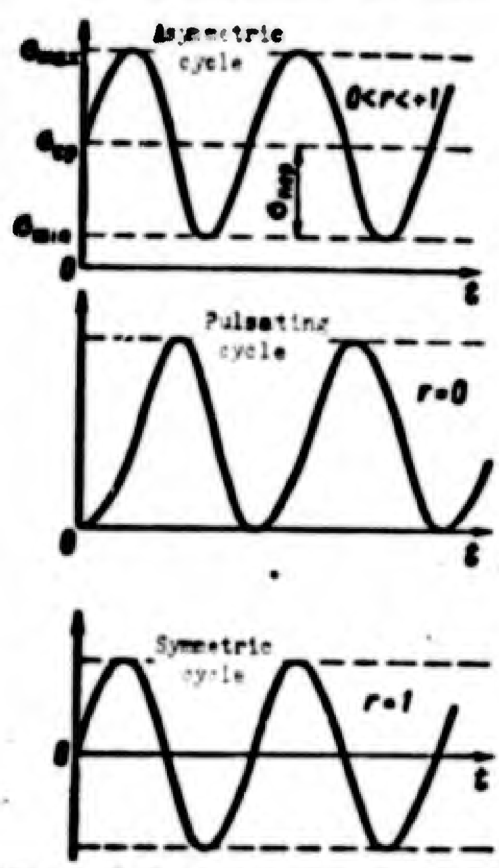

Fig. 7.2. Types of cycles of variable stresses.

Figure 7.2 shows different types of cycles of change of stresses. For the pulsating cycle the magnitude σ_{min} or σ_{max} is equal to zero ($r = 0$ or ∞).

Numerous tests of materials under variable loads allowed the establishment of two basic rules:

1) materials can be destroyed under variable (repeated) stresses σ_{max}, considerably less than the tensile strength σ_b if these stresses are repeated a sufficient number of times;

2) with the increase of amplitude of variable stresses (with constant value

of σ_{max}) the material sustains a smaller number of loading cycles before destruction.

Maximum stress of a cycle, at which the material is not destroyed upon the achievement of a predetermined large number of cycles (the base) of variable stresses, is called the endurance limit or fatigue strength. The endurance limit depends on the properties of the material, the type of cycle, and the conditions of carrying out the tests. In a uniaxial state of strain the endurance limit is designated by σ_r, where r indicates the type of cycle.

As the results of experimental investigations show, samples of the majority of ferrous metals, sustaining 10^7 cycles are not destroyed for a long time during further tests. Therefore, for ferrous metals the base is usually taken as 10^7 cycles.

For aluminum alloys and a number of high-alloy steels it is impossible to establish such a number cycles, after sustaining which the sample would not be destroyed during further tests. This is explained by the fact that with an increase of the number of cycles there is a corresponding continuous drop in the stress which can be sustained by the material. Therefore, for nonferrous metals in the determination of the endurance limit the base is taken from $2 \cdot 10^7$ to $10 \cdot 10^7$ cycles.

Characteristics of Strength of Materials

Endurance limit is usually determined at a frequency of change of stresses from 1500 to 6000 oscillations per minute. The dependences of maximum stresses on number of loading cycles until destruction — strength curves — can be constructed in coordinates N, σ (Fig. 7.3a) (N is the number of cycles up to destruction of a sample, σ is the stress during the tests), in semilogarithmic coordinates log N, σ

(Fig. 7.3b), when the logarithmic scale (log N) is plotted along the axis of abscissas, and in logarithmic coordinates log N, log σ. Application of logarithmic scales permits a compact depiction of the results of tests. Most frequently used are the semilogarithmic coordinates.

The strength curves for the majority of ferrous metals have a more or less expressed horizontal section when N is more than $2 \cdot 10^6$ (see Fig. 7.3), corresponding to the endurance limit. For certain forms of samples it was possible to establish an approximate relationship between the endurance limit and ultimate strength. For instance, the endurance limit for smooth steel samples during symmetric bending can be approximately estimated by the formula

$$\sigma_{-1} = 0{,}27\,\sigma_b + 1850 \text{ kg/cm}^2.$$

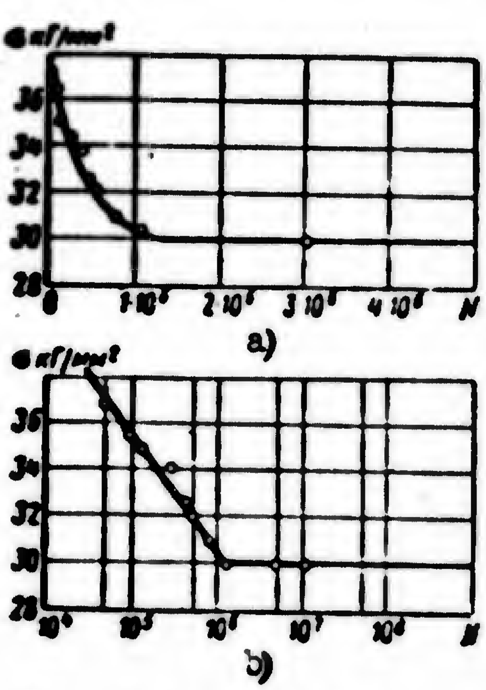

Fig. 7.3. Strength curves in different coordinates. a) linear coordinates; b) semilogarithmic coordinates.

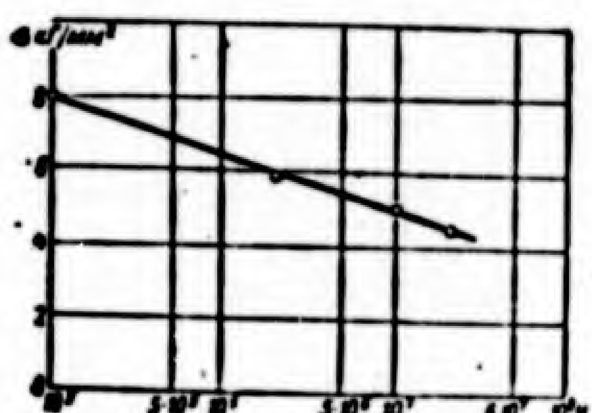

Fig. 7.4. Strength curve of an aluminum alloy.

The strength curves for aluminum alloys do not have a horizontal section (Fig. 7.4). However, it is possible to consider that approximately the conditional endurance limit for smooth samples made from nonferrous metals (on base $5 \cdot 10^7$) is connected by the following relationship to ultimate strength σ_b: $\sigma_{-1} \approx (0.25 \text{ to } 0.50)\sigma_b$. In particular, for alloy D16 $\sigma_{-1} \approx 0.25\ \sigma_b$.

In most cases, during tests the stress varies according to the asymmetric cycle. For estimating the endurance limit with different cycle forms strength diagrams are constructed in coordinates σ_{av}, σ_{max}, σ_{min} (Fig. 7.5). This diagram permits the determination of the limiting values of variable load at the assigned level of average load. Symmetric cycles are depicted by points lying on the axis of ordinates. The limiting symmetric cycle is represented by points A and B. Limiting asymmetric cycles, the biggest stress of which constitute the endurance limits σ_r, are depicted by points lying on limiting curves AC and BC. They are obtained experimentally for each material. Line OC gives the magnitude of average stress σ_{av} of the asymmetric cycle. The pulsating cycle is depicted by points D and E.

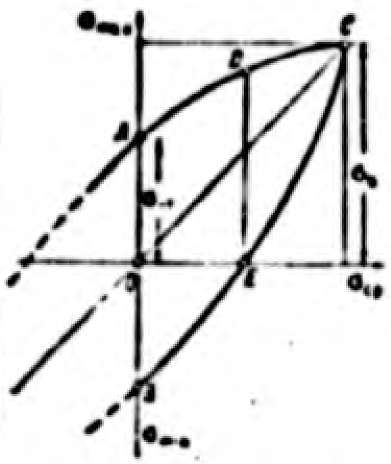

Fig. 7.5. Complete strength diagram.

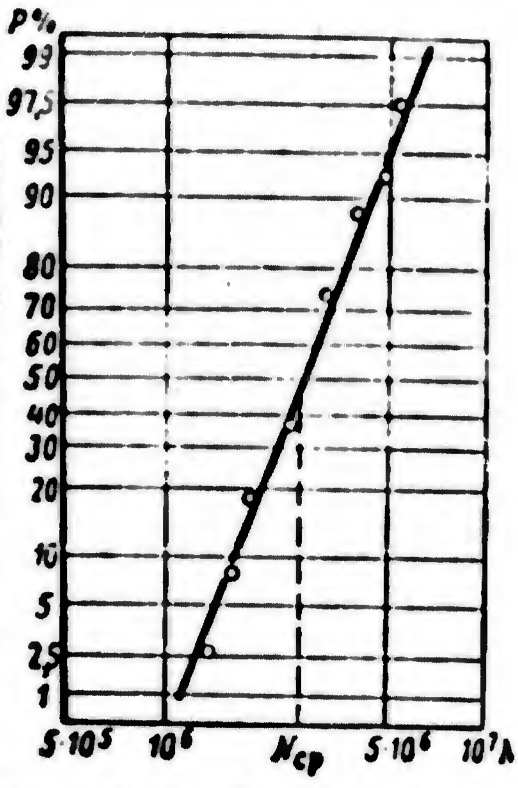

Fig. 7.6. Results of endurance tests of a group of samples.

The results of endurance tests of a large quantity of identical samples give large divergence in the number of cycles before destruction (up to 10 and more). Therefore, it is important to estimate with sufficient reliability the minimum number of cycles before destruction at the given level of stresses. For this purpose distribution curves of the number of cycles N are constructed which can logarithmically approximate the normal law of distribution (Fig. 7.6). On these curves in the logarithmic-probability coordinates one can determine the characteristics of distribution and estimate, with the assigned reliability, the probability of the lower bound of the number of cycles in which the sample can be destroyed.

7.2. Influence of Concentration of Stresses on the Characteristics of Strength

The strength characteristics of a material are largely influenced by the zones in which there appear internal forces which are more intensive than in the main mass of material. The phenomenon of sharp local disturbance of the field of internal forces in the material of a component is called the concentration of stresses, and the local peculiarities of the structure, which cause this phenomenon, are called the concentrators of stresses. Stresses which appear in the vicinity of a concentrator are called local stresses. Concentrators may be divided into two groups: geometric concentrators (holes, flanges, hollows, scratches, and others) and power concentrators (the character of contact forces).

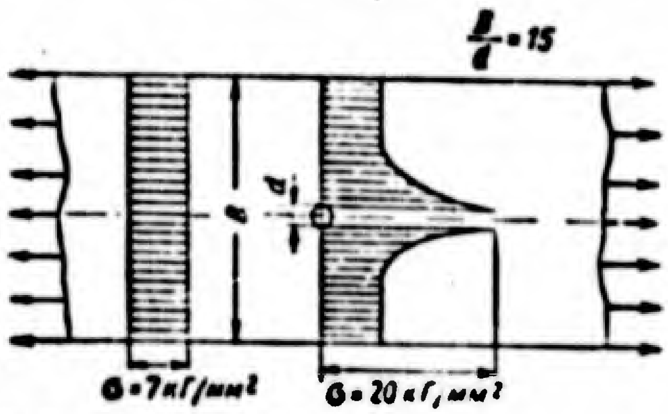

Fig. 7.7. Distribution of stresses in a plate which has a hole in it.

Local stresses basically depend on the geometry of the concentrator (radius of curvature, depth of scratch, etc.). Figure 7.7 shows the distribution of stresses during the extension of a plate with a small hole. Near the concentrator the stresses grow very intensely, and the maximum value of stress can exceed the average by a few times. With the increase of the load the stresses in the region of the concentrator reach their yield point earlier than in the other places. As a result of this, in the vicinity of the concentrator there will form a local zone of plastic deformation when the main mass of material is still deformed elastically and there occurs a certain leveling out of local stresses. The more plastic the material, the more considerable the redistribution. This explains the fact that the influence of concentrators shows up less on the endurance limit of plastic materials.

The influence of a concentrator is estimated by the effective coefficient of concentration k_r, which shows how many times the endurance limit of a sample without a concentrator σ_r is higher than the endurance limit of a sample with a concentrator σ_{rc}:

$$k_r = \frac{\sigma_r}{\sigma_{rc}}.$$

The magnitude of this coefficient depends on the material and the type of cycle. The coefficient of concentration for steel samples with a hole B/d = 5 (B is the width of a band, d is the diameter of the hole) and σ_b = 70 kg/mm^2 during extension and compression is given in Table 7.1. For a plate made from alloy D16 when B/d = 7 to 10, k_1 = 1.3 to 1.8.

Table 7.1.

Type of cycle	r	k_r
Positive pulsating	0	1.54
Symmetric	1	1.72
Negative pulsating	∞	2.07

The quality of treatment of components strongly shows up on the endurance limit (Fig. 6.8) due to the surface scratches remaining after treatment, which are concentrators. Highly durable steels are more sensitive to the quality of surface treatment. Since aircraft building uses highly durable steels (σ_b > 100 kg/mm^2), the obtainment of the necessary characteristics of strength requires an especially high quality of machining.

The endurance limit may be increased by additional treatment of the surface of a component. For instance, methods for hardening the surface layer include rolling, shot peening, and hydropolishing (treatment of surface by a stream of liquid under high pressure), and also chemical-heat treatment of the component: surface hardening by currents of high frequency, carburization, nitration, cyanidation, and others.

Corrosion of metal promotes the spread of fatigue cracks and lowering of the endurance limit. Thus, the endurance limit of steel samples during tests in sea water is lowered by 2.0-4.0 times and aluminum alloys by 3-5 times. Lowering of the characteristics of fatigue during tests in sea sprays is obtained approximately the same as and in sea water. Even air as a corrosional medium affects the endurance limit.* Investigations conducted on samples made from an aluminum alloy showed that a change of air pressure from 10^{-5} to 760 mm Hg lowers the number of cycles until destruction at the assigned level of stresses by approximately 10 times (Fig. 7.9).**

Application anticorrosional coatings can essentially increase the endurance characteristic of a metal in a corrosional medium as compared to an unprotected metal. Therefore, the protection of components of an aircraft from corrosion with different surface coatings and the preservation of these coatings has a large value for preventing premature fatigue breakdowns.

The strength of an actual structure depends not only on the level of stresses, but also on damage of the contact surfaces of connection (rivet seams, joints, and so forth) under variable loads. In a joint

---

*Questions of corrosional-mechanical strength of metals, Transactions of the Central Scientific Research Institute, Moscow Branch, No. 22, 1959.

**Internal Stresses and Fatigue Metals. Procedings of the Symposium on Internal Stresses and Fatigue Metals, Detroit and Warren, 1958.

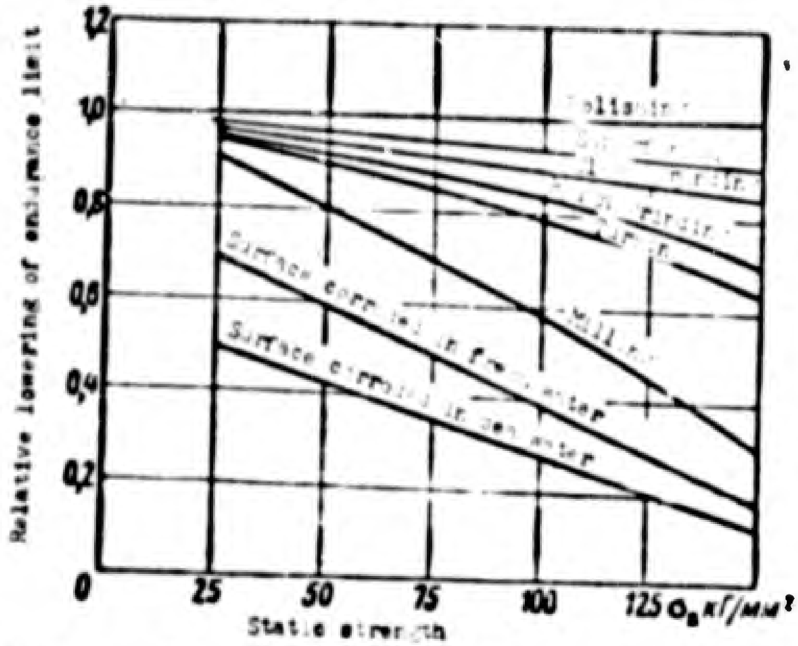

Fig. 7.8. Influence of quality of treatment on endurance limit of steel depending upon its static strength.

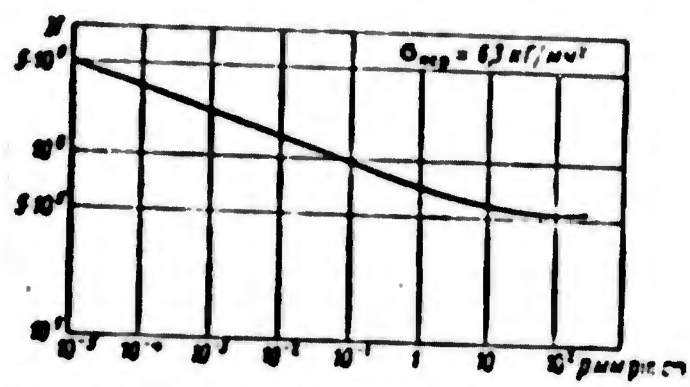

Fig. 7.9. Influence of an air medium on the endurance of an aluminum alloy.

under the action of contact pressure there occurs local cohesion of points of contact surfaces. During the influence of loads on a joint there appears a certain displacement of surfaces relative to one another, which leads to a break of local cohesions, i.e., there occurs damage to the surface of the material. Chemical cooro-sional phenomena increase the damage to the surfaces of connection.

During damage to the surface of a material the fatigue strength of connections is noticeably reduced, since the number of potential sources of concentration of stresses is increased and the spread of cracks is accelerated. Surface damage also strongly affects the stability of anticorrosive coatings. The influence of damage to a surface on the endurance characteristics of a structure depends on the type of connection. For lowering the possibility of surface damage, linings, lubrication, and so forth are used.

7.3. Influence of Loading Frequency on Endurance Characteristics

A structure that is in use is acted upon by variable loads with different frequencies. Some loads act several times in a flight (for instance, maneuvering loads), and others cause variable stresses with high frequency (for instance, acoustic vibrations occur with frequencies of more than 1000 oscillations per second). As a rule, with the increase of frequency of loads the level of maximum stresses drops in the structure. In estimating fatigue strength the level of stresses in a structure is expediently related to the breaking stress:

$$k=\frac{\sigma_{\text{макс}}}{\sigma_{\text{разр}}},$$

where σ_{max} is the maximum stress acting upon the sample (structure);

σ_{break} is the breaking stress for the structure.

Coefficient k is called the load factor of the structure (sample). An approximate dependence of the load factor of an aircraft structure on the frequency of its action is shown in Fig. 7.10.

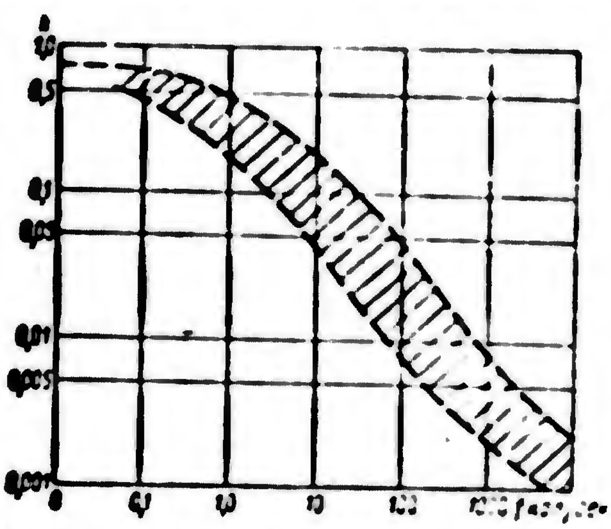

Fig. 7.10. Approximate dependence of load factor on the frequency of its action.

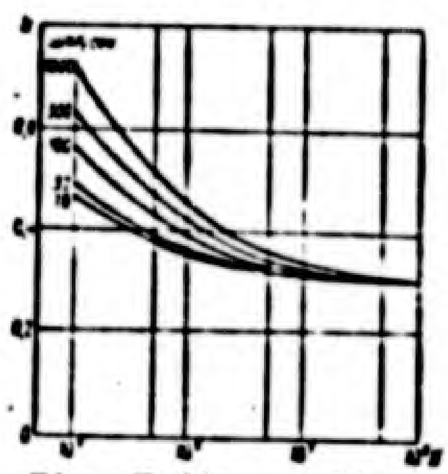

Fig. 7.11. Influence of frequency of loads on the endurance of an aluminum alloy in a vacuum.

The influence of loading frequency on endurance characteristics was noted long ago. However, only recently were there conducted extensive investigations which showed that at low loading frequencies the endurance characteristics are considerably lowered at a load factor of more than 0.3. This is evidently explained by the fact that at high loading speeds plastic deformations spread in a smaller zone and, therefore, there occurs slower development of fatigue cracks.

As an example, Fig. 7.11 gives the results of tests of samples at different loading frequencies. During tests of samples made from an alloy of the type D16 in a vacuum the endurance limit on a base of 10^8 cycles practically remains constant. The endurance characteristics on a base of 10^5 cycles are lowered by 37% with a decrease of loading frequency from 1000 to 10 cycles/sec. At the same comparatively high level of loads the number of cycles that the sample sustains is lowered with the decrease of loading frequency. For instance, when k = 0.5 this number of cycles decreases 10 times.

In a corrosional medium the influence of loading frequency on endurance characteristics is intensified (Fig. 7.12). With a lowering of loading frequency the endurance limit is also lowered. Thus, with a decrease of loading frequency from 1000 to 10 cycles/sec the endurance limits of samples are lowered by 40 to 50%.*

During tests in sea water the influence of loading frequency is intensified a few times as compared to tests in the air. For instance, for certain samples of steel a change of loading frequency from 1760 to 36 cycles/min lowers fatigue strength with respect to number of cycles until destruction by 10 times.** This is explained by the fact that during tests in aggressive media the time factor obtains a decisive value.

Upon further lowering of loading frequency to 8 cycles/min the fatigue strength continues to be lowered. For instance, for alloys D16 and 30KhGSA under a relative load of k = 0.4, the fatigue strength with respect to number of cycles until destruction is lowered in the following way (see Table 7.2).

With an increase of the relative load level the influence of

*W. J. Harris. Cyclic Stressing Frequency Effect on Fatigue Strength. Aircraft Engineering. 1959, 31, N 370.

**Questions of corrosional-mechanical strength of metals, Transactions of TSNIIMF, No. 22, 1959.

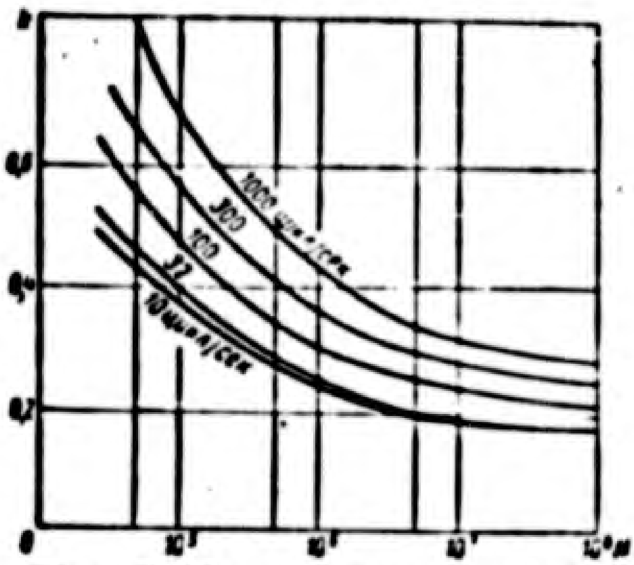

Fig. 7.12. Influence of loading frequency on fatigue strength of an aluminum alloy in an air medium.

Table 7.2.

Material	Frequency in cycles/min	N_f/N_{4500}
D16	8 130 4500	0.19 0.24 1.0
30KhGSA	8 130 4500	0.32 0.39 1.0

N_{4500} is the number of cycles which the sample sustains at a loading frequency of 4500 cycles/min;
N_f is the corresponding number of cycles at frequency f cycles/min.

frequency is somewhat lowered (Fig. 7.13).*

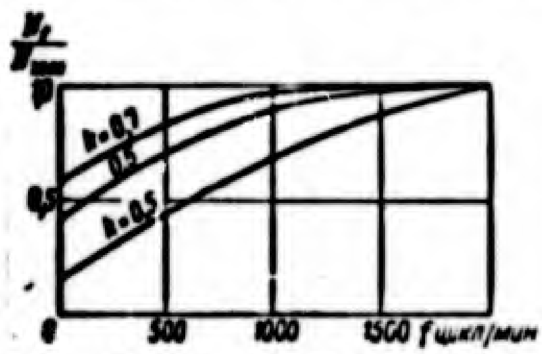

Fig. 7.13. Influence of loading frequency on fatigue strength of an aluminum alloy when k = = 0.5 to 0.7.

Since many forms of loads acting upon an aircraft have comparatively small loading frequencies, in investigations of fatigue of aircraft structures considerable attention has been allotted to the study of endurance characteristics at low loading frequencies (10-15 cycles/min and less). The characteristics of fatigue strength at low frequencies (less than 20 cycles/min) are sometimes called "strength under repeated loads" or "static strength of materials." All aircraft materials at present are subjected to checks on strength at low frequencies both in samples and also in the form of typical designs.

Figure 7.14 gives some typical strength curves of basic aircraft materials in a pulsating cycle with loading frequency of 15 cycles/min

*S. I. Ratner, Destruction during repeated loads. Oborongiz, 1959.

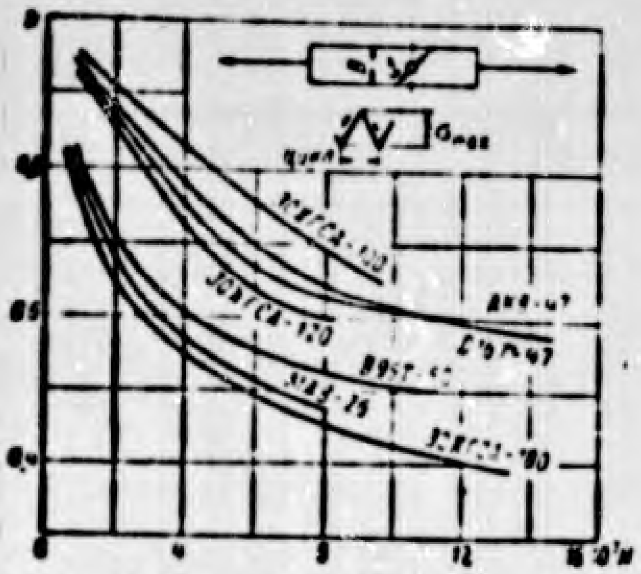

Fig. 7.14. Static strength of basic structural materials.

obtained for flat samples with a hole (B/d = 5). On these curves it is possible to see that highly durable materials (steel 30KhGSA with hardening to σ_b = 180 kg/mm^2 and aluminum alloy V95) have considerably lower endurance characteristics than materials of average strength (steel with hardening to σ_b = 120 kg/mm^2 and aluminum alloy D16). For instance, when k = 0.7 samples made from highly durable materials sustain only 1000-2000 cycles, whereas samples made from materials of average strength withstand 4000-6000 cycles. Furthermore, highly durable materials are more sensitive to concentration of stresses.

7.4. Strength of Structural Samples

Structural samples (joints, wing panels, and others) have lower endurance characteristics than typical samples with holes. This is explained by the large quantity of concentrators, which are rivet and bolt connections, and so forth. Tests of one type of wing panel showed that at an identical value of load factor k the wing panel sustains 5-7 times fewer cycles than samples with holes. As noted above, highly durable materials are more sensitive to the influence concentrators. Therefore, the fatigue strength of panels made from highly durable materials has lower characteristics as compared to panels made from materials of average strength.

The endurance limit of panel structures and complete aircraft assemblies with concentrators can be estimated by the effective coefficient of concentration

$$k_{ef} = \frac{\sigma_{sam}}{\sigma_{str}}.$$

where σ_{str} and σ_{sam} are the stresses which a structure and a sample sustain at the same number of loads.

According to certain researchers the effective coefficient of concentration for a wing structure is 4 to 6.* With an increase of average stress the value of k_{ef} is lowered somewhat, which can be explained by the influence of plasticity of the material at a higher level of stresses.

Aircraft structures widely employ bolt connections, particularly in the responsible joints of assemblies. Experimental investigations show that with an increase of preliminary tightening to a defined level the fatigue strength of bolts is somewhat increased.

7.5. Summation of Damages

Theory of Linear Summation of Damages

For estimating the period of service of a structure it is necessary to know, how the fatigue damages build up with respect to operational time.

If a structure experiences a variable load with constant frequency and amplitude, and at this level of variable stress the structure sustains N cycles, then in an operational period of T hours, during which there were n loading cycles, the relative damage will be $\xi = n/N$.

An aircraft (helicopter) during operation experiences, in an indefinite sequence and in a disorderly manner, alternating loads of different amplitude and frequency. It is necessary to establish how the fatigue damages introduced by the action of such loads build up.

*R. Carl and T. Wegeng, Investigations Concerning the Fatigue of Aircraft Structures, "Proceeding Amer. Society Testing Materials," v. 54, 1954.

At present, extensive use has been obtained by the hypothesis of linear summation of damages. It is considered that fatigue damages to a structure ξ_i from various load levels are independent from each other and are linearly summarized, i.e., total damage ξ_Σ can be determined from the relationship

$$\xi_\Sigma=\sum_{i=1}^{\nu}\frac{n_i}{N_i}. \tag{7.1}$$

where n_i is the number of load cycles of a given magnitude, having an effect on a structure in a defined period of operation;

N_i is the number of load cycles of the same magnitude, necessary for destruction of a structure;

ν is the number of separate levels (stages) of loads.

Upon strict fulfillment of the conditions of the hypothesis of linear summation

$$\sum_{i=1}^{\nu}\frac{n_i}{N_i}=1. \tag{7.2}$$

For checking the validity of this hypothesis we conducted numerous experimental investigations with many stages of change of load.

Figure 7.15 gives the generalized results of 222 tests, where the number of load levels was more than 2. The median of the diagram of distribution of test results is close to one (1.1), i.e., in 50% of the tests $\sum_{i=1}^{\nu}\frac{n_i}{N_i}>1.1$; for 97% of all tests the magnitude $\sum_{i=1}^{\nu}\frac{n_i}{N_i}>0.5$. This circumstance subsequently permits, when estimating the period of service of a structure, to take $\sum_{i=1}^{\nu}\frac{n_i}{N_i}=0.5$.

A large influence on magnitude $\sum_{i=1}^{\nu}\frac{n_i}{N_i}$ is rendered by overstrain in the initial stage of the tests and the number of load levels during the tests. In certain cases during tests with a large number of loading stages the magnitude $\sum_{i=1}^{\nu}\frac{n_i}{N_i}$ is lowered to 0.1-0.3.

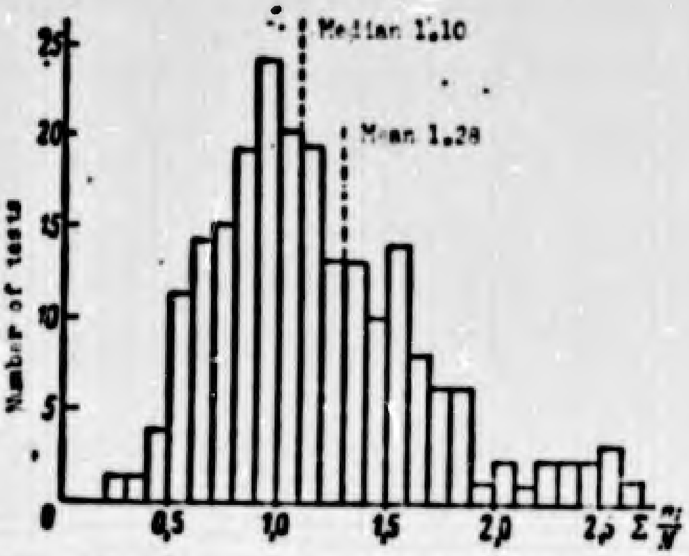

Fig. 7.15. Diagram of the results of fatigue tests with several loading stages (according to foreign data).

A more precise definition of the theory of summation of damages proceeds by way of calculation of the influence of variable stresses of different amplitude. As a result of this influence the strength curve is somewhat displaced downwards (Fig. 7.16, curve 2). This influence is estimated by the relation of the number of cycles to destruction on the displaced curve to the number of cycles on the initial curve

$$\omega_i = \frac{N_i'}{N_i}, \qquad (7.3)$$

which may be called the coefficient of the effect of a given aggregate of variable loads of different level on the strength of a structure.

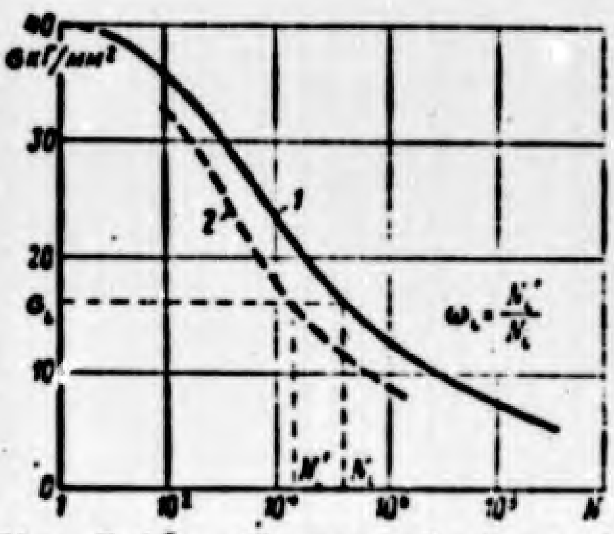
Fig. 7.16. Change of strength characteristics during tests with several levels of stresses. 1) curve, each point of which is determined at one level of repeated stresses; 2) strength curve determined by taking into account the action of stresses of several levels.

For estimating the effect coefficient ω we conducted investigations of smooth samples with a spectrum of loads close to the real spectrum on aircraft, where the probability of a load of given level was expressed by exponential function

$$P(x) = he^{-hx}, \qquad (7.4)$$

(h is the standard deviation of real distribution).* Results obtained in four to six stages of

*A. M. Freudenthal and A. Heller. On Stress Interaction in Fatigue and a Cumulative Damage rule, Aero/Space Science, 1959, 26, N 7.

loads and stresses more than (0.35 to 0.65) σ_b are shown in the graphs of Figs. 7.17 and 7.18.

During disorderly alternating of loads the actual strength of samples N_{test} is less than the strength determined according to the hypothesis of linear summation of damages N_{cal}. In particular, for smooth samples the effect coefficient ω can be less than 0.1. However, inasmuch as in actual structures there always are concentrators, this coefficient will be larger. In investigations by A. P. Ficher of samples made from a highly durable aluminum alloy with a concentrator (k_{-1} = 4) in 10 stages of variable load, changing approximately according to exponential law, the magnitude ω was equal to 0.65 to 0.82.*

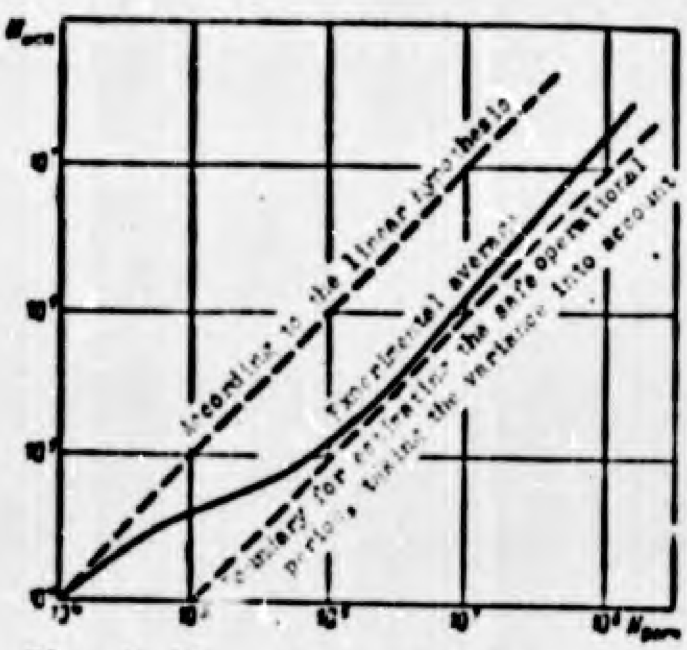

Fig. 7.17. Strength of samples made from aluminum alloy 2024 at a variable loading level.

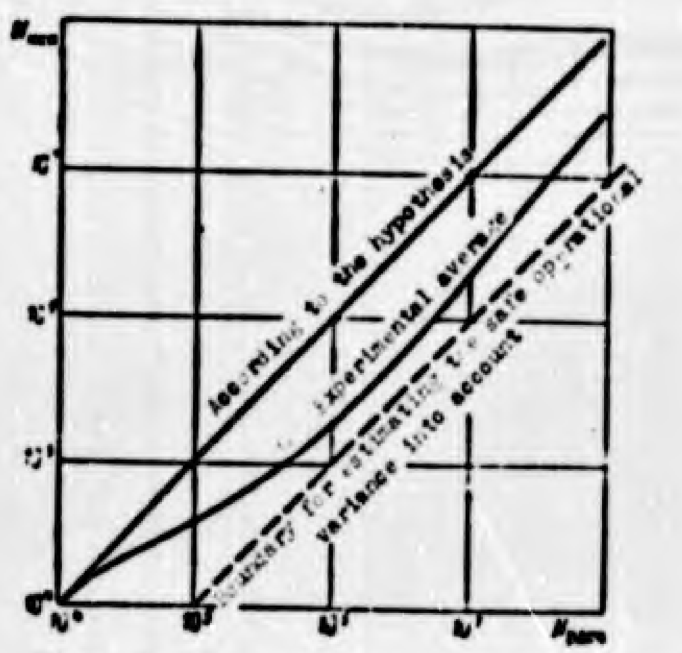

Fig. 7.18. Strength of samples of steel 4343 at a variable loading level.

Influence of Vibration Stresses

It is necessary to note that variable stresses, whose magnitudes are lower than the endurance limit, during multistage tests render a noticeable influence on the endurance characteristics, since small

*A. P. Ficher. Royal Aircraft Establishment Programme Fatigue Test on Natched Bars to a Gust Load Spectrum. Aeronat. Res. Council Current Rapers, N 498, 1960.

loads, after the appearance of initial cracks, affect their further development. Therefore, a disregard of the loads corresponding to stresses lower than the endurance limit while carrying out tests can give oversized endurance characteristics.

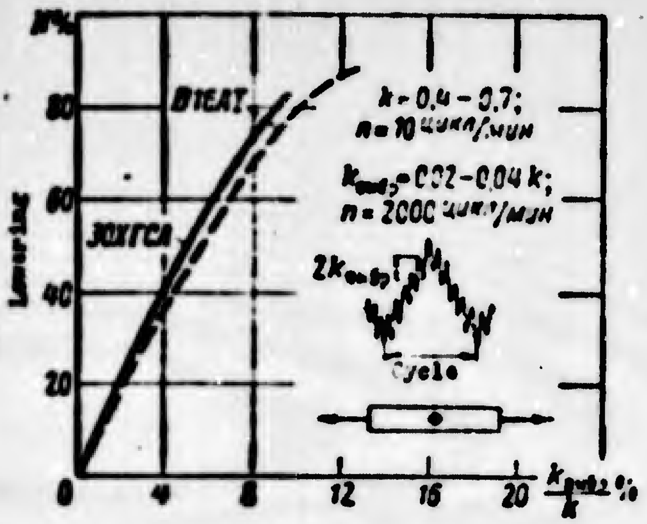

Fig. 7.19. Influence of vibrations on strength during repeated loads.

It is necessary to attentively refer to the selection of the lower level of loads considered during program tests. For instance, in certain cases it may be necessary to consider the stresses appearing during vibrations with comparatively small amplitudes (k_{vib} = 0.04 to 0.10). In this case the problem of summation of damages is complicated in connection with the considerable deviations from the hypothesis of linear summation of damages. Investigations of the influence of high-frequency build-ups showed that if a sample is given a basic load with a frequency of 10 cycles/min and is a vibrations build-up with a frequency of 2000 cycles/min, the high-frequency build-ups lead to a considerable lowering of strength (Fig. 7.19).* In this case a vibration stress with a magnitude near 1% of the basic magnitude lowers the period of service of the sample by approximately 10%. It is possible to assume that this lowering of fatigue strength is explained by the influence of the increase of the level of stresses on coefficient k_{vib} (see Fig. 7.20).

For estimating this influence we conducted tests of samples at an

*N. I. Marin, Influence of repeated loads on the strength of machinery designs, collection, "Strength and wear of mining equipment," Gosgortekhizdat, 1959.

increased amplitude of the level of variable load (k_{max} = 0.73 and k_{min} = 0.03). In low-frequency tests with increased amplitude a loaded sample made from alloy D16A-T sustained 4300 cycles and a sample made from alloy 30KhGSA withstood 3380 cycles. At the same time these samples in low-frequency tests with vibration build-ups at the same values of k_{max} and k_{min} (see Fig. 7.20) sustained respectively 1665 cycles and 850 cycles, i.e., 2.8 and 4.6 times less. This lowering of fatigue strength is also impossible to explain by the linear theory of damage summation.

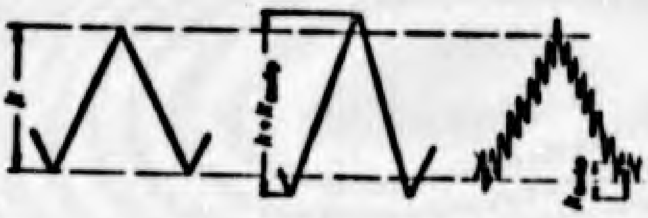

Fig. 7.20. Amplitudes during comparative fatigue tests of samples.

Thus, when compiling programs for fatigue, one should introduce the conditions of tests with the consideration of the vibration loads of the structure.

Influence of Preliminary Overstrain

During the operation of aircraft (helicopters) there can sometimes be single large loads, close to those maximum permissible. For a study of the influence of these loads on the strength of a structure in laboratory tests loads are used that considerably exceed the load level accepted for fatigue tests. Preliminary application of a static load of large magnitude renders an essential influence on the endurance characteristics of the elements of a structure. In a pulsating cycle a preliminary static load of the same sign causes an increase in strength of the structure. Figure 7.21 gives

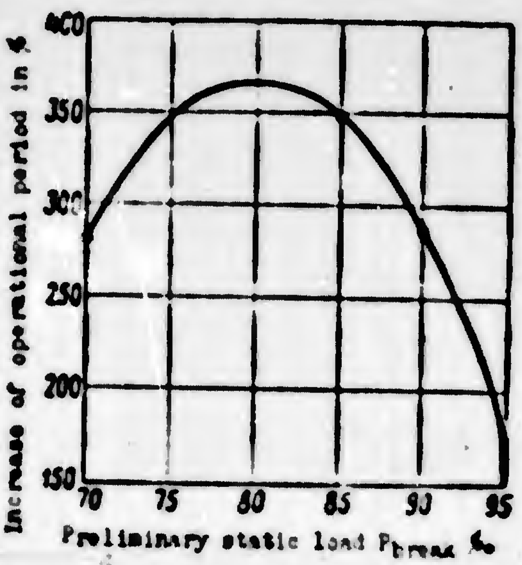

Fig. 7.21. Influence of preliminary load on the strength of a structure.

data on the influence of such a load on the strength of structural elements. A preliminary static load of reverse sign lowers the strength of the structure.

In connection with this it should be noted that the use of assemblies which have undergone static tests (i.e., assemblies having a large preliminary overload) is inexpedient, since their strength does not correspond to the strength of the structure in actual operation.

Influence of Average Level of Stresses

In the structure of an aircraft (helicopter), as a rule, there act variable stresses with different levels of average stress. As shown above, strength depends on the magnitude of average stress. Therefore, for typical samples and structural elements it is necessary to have a so-called complete strength graph which considers the level of average stress. The magnitude of average stress is characterized by coefficient $k_{av} = \sigma_{av}/\sigma_{break}$.

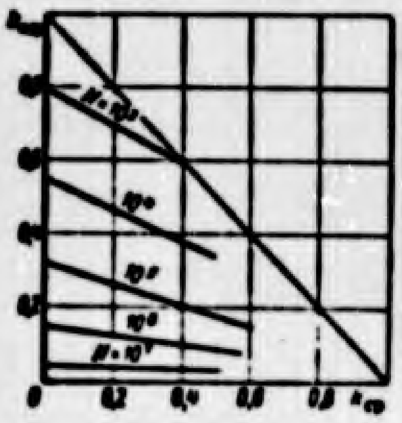

Fig. 7.22. Complete strength graph in coordinates $k_{var} = f(k_{av})$ when $N = \text{const}$.

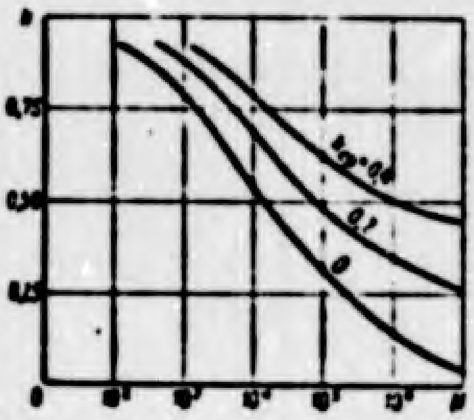

Fig. 7.23. Complete strength graph in coordinates $k = f(N)$ when $k_{av} = \text{const}$.

Figure 7.22 gives a graph of the dependence of number of cycles to destruction N on parameters k_{av} and $k_{var} = \sigma_{var}/\sigma_{break}$. A similar graph can also be constructed in usual coordinates: k is plotted along the axis of ordinates and N is plotted along the axis of abscissas (Fig. 7.23).

Complete strength graphs of typical constructions make it possible to estimate the strength of aircraft structures working on an aircraft (helicopter) under variable loading conditions with different levels of average stress.

The construction of a complete strength graph requires the carrying out of tests on a large number of samples. Since for the obtainment of each point of curve $K = f(N)$ when k_{av} = const, taking into account the variance of strength characteristics, it is necessary to test 6-10 samples, and for the construction of each curve it is necessary to take not less 5-8 points; then for obtaining a complete strength graph of a structural element it is necessary to bring 200-400 samples to destruction. This hampers the obtainment of complete strength graphs of various typical components of aircraft structures.

7.6. Loading Conditions of an Aircraft Structure During Operation

As regards the origin of loads having effect on an aircraft, they are very diverse. This may be seen from a simple enumeration of the main forms of loads, which include loads from gusts of wind, maneuvering loads, loads during takeoff and landing, loads from the influence of engine flow, loads of pressurized cabins from pressurization, combat loads (firing, launching of rockets, etc.), loads from aircraft control, systems, and others. Magnitudes and recurrence of loads affecting an aircraft depend on the assignment of the aircraft, its performance data, and the specific conditions of operation.

Special test flights are conducted for finding the magnitudes and recurrence of loads affecting an aircraft. The aircraft is outfitted with equipment for measurement of loads acting upon its main assemblies (see Chapter X). As a result of the measurements a dependence of loads on the conditions of maneuvering, landing, etc. is obtained. In particular, a relationship is determined between the overload in the center of gravity and the forces in the main components of the aircraft.

Furthermore, loading parameters are measured on a large quantity of aircraft in conditions of mass operation. These measurements make it possible to obtain averaged (statistical) data on the loading conditions. The most frequently measured are overloads in the center of gravity of the aircraft, since it is considered that they are the main characteristics of loading.

For contemporary heavy aircraft the forces in the structural elements not only are determined by the magnitude of overload, but also depend on the character of its change in time (see Chapter IV). Therefore, in statistical measurements, along with the magnitude of overload, the period of its action is also determined.

We shall briefly consider the main forms of loads below.

Loads From Wind Gusts

As shown above, overloads from gusts of wind are determined by the speed of the gust, the speed of flight, the aerodynamic and weight characteristics of the aircraft. The biggest interest is presented by the investigation of the recurrence of gusts of wind, since the remaining necessary characteristics are rather simply determined in the designing of the aircraft. Statistical measurements for investigations of wind gusts are conducted basically on nonmaneuverable aircraft.

Usually every passage of an aircraft through a gust with sharp build-up and fall of speed W corresponds to positive and negative G (Fig. 7.24). Therefore, the load cycle in gusts of wind may be taken as symmetric with the magnitude of static load k_{av} corresponding to horizontal flight (n = 1). The magnitude and recurrence of the variable of part of a load is determined by the characteristics of the atmosphere.

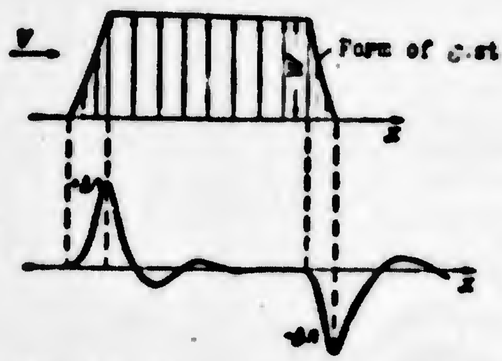

Fig. 7.24. Character of change of G-force during passage of an aircraft through a gust.

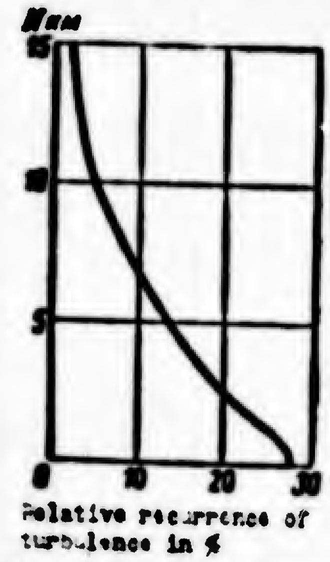

Fig. 7.25. Recurrence of turbulent zones.

Above (see Chapter II) we presented graphs of the recurrence of wind gusts, obtained as a result of investigations. According to this graph it is possible to estimate the magnitude and frequency of recurrence of gusts depending upon the route flown by the aircraft.

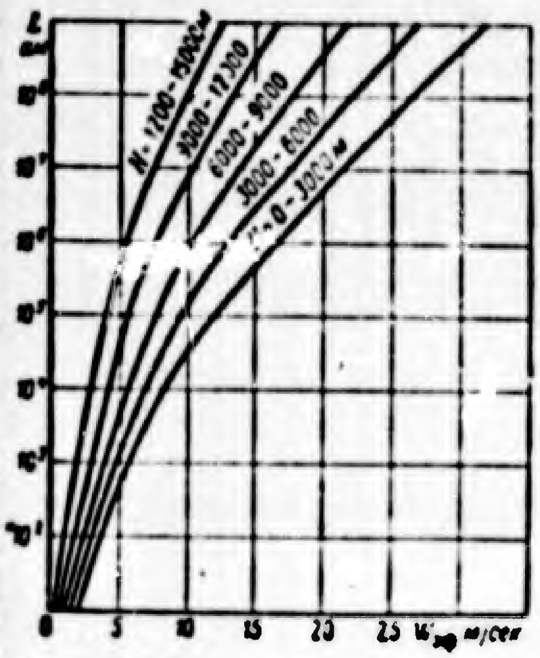

Fig. 7.26. Recurrence of gusts at different altitudes.

With an increase of the altitude of flight the quantity of encountered turbulent zones of air drops. If at altitudes up to 6000 m the relative time of flight in a turbulent atmosphere on the average is approximately 15% of the total duration of flight, then in the troposphere it is approximately 6%, and in the stratosphere approximately 4%.

Considering that the probability of encounter of the true speed of a gust of a given value remains constant with respect to altitude and the distribution of recurrence of zones of bumpy air with respect to altitudes is determined by Fig. 7.25, it is possible to estimate the approximate distribution of recurrence of gusts with respect to altitudes (Fig. 7.26).*

The number of gusts and their magnitude depend on the atmospheric composition and on the average they have a definite recurrence. Therefore, the number and magnitude of overloads of an aircraft from wind gusts are determined by length of the route flown by the aircraft. High-speed aircraft, flying a great distance in a unit of time, have large recurrence of gusts.

An aircraft flying at a small altitude, encounters considerably larger gusts during the passage of the same route than a high-altitude aircraft. The recurrence of gusts is quite intensely increased in flights at altitudes of 150-500 m. In this case the altitude should be counted off not from sea level, but from the surface of the earth.

Maneuvering Loads

All aircraft accomplish definite forms of maneuvers. However, only for maneuvering aircraft (fighters, ground-attack, primary training aircraft, and so forth) loads during maneuvers are decisive for the period of service of their design. A maneuvering overload is quite accurately determined by the magnitude of overload in the center of gravity of an aircraft. The magnitude and recurrence of maneuvering overloads depend on the type of the aircraft, its tactical performance data, and its characteristics of controllability and stability.

The characteristics of recurrence of manuvering overloads may be found by the use of simple statistical instruments (g-meters or V-n instruments).

*Mangurian, Brooks, Effects of Operational Factors on Structural Fatigue in Fighter Type Aircraft, SAE Preprint, 1954, X, N 387.

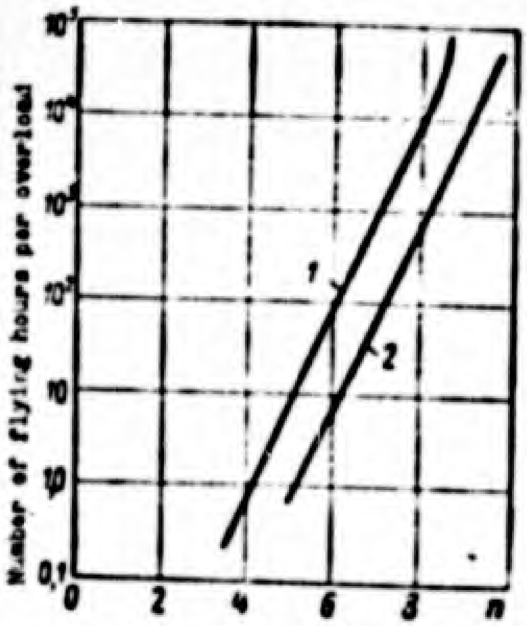

Fig. 7.27. Recurrence of maneuvering overloads.

Figure 7.27 gives a graph of the recurrence of maneuvering overloads of a fighter in conditions of combat and training flights, obtained on the basis of generalization of the results of measurements in the war period (1939-1945) on a number of aircraft (Me-109, "Typhoon," "Spitfire," and others) with the help of V-n instruments. As can be seen, in conditions of ordinary training flights the recurrence of maneuvering overloads of fighters turns out to be considerably larger (by 5-10 times) than in conditions of combat flights. In estimating the period of service of an aircraft one should be oriented on the recurrence in training flights, since the periods of service of fighters in combat conditions do not have a practical value.

In estimating the period of service of maneuvering aircraft it is possible, with sufficient reliability probabiltiy, to present the change of maneuvering overload in the form of a pulsating cycle, i.e., to consider that each maneuvering overload varies from zero to its maximum value. In certain cases the calculation of average level of maneuvering overloads permits us to somewhat definitize the characteristics of their recurrence, which in turn makes it possible to more exactly estimate the period of service of an airframe.

Loads During Takeoff and Landing

During motion on the ground an aircraft structure experiences the action of variable loads caused by the roughness of the airport surface and deceleration. Loads during motion along an airfield depend on the form surface roughness of the flying field (elevation, length, recurrence), the characteristics of shock absorption of the landing gear, the elasticity of the structure, the speed, the conditions of deceleration, the conditions of maneuvering of the aircraft, and so forth.

The decisive parameter for these loads are the characteristics of roughness of the airport surface. Permissible roughness magnitudes are determined by the corresponding requirements for relief of the airport surface, the fulfillment of which is controlled during the construction and use of the airport.

Corresponding measurements can obtain the spectral characteristics of roughness of airports. Methods of spectral analysis can determine the characteristics of recurrence of loads on the main parts of an aircraft (see Chapter IV).

Certain peculiarities are inherent in the determination of recurrence of loads during the first landing impacts, when a main role is played by the aerodynamic properties of the aircraft and the technique of landing. Recurrence of these loads is determined by statistical measurements of overloads or loads during landings in conditions of mass operation of aircraft. An approximate form of graph of recurrence of overloads during landing is shown in Fig. 7.28.

Recurrence of loads during takeoff and landing runs can be established by special investigations with the use of tensometric equipment. In Fig. 2.42 we see the character of loads on the main assemblies during the landing run of an aircraft. As a result of analysis of recordings of loads we can obtain complete graphs of their recurrence. For the obtainment of characteristics of recurrence of loads at a given airport is is sufficient to measure loads for 4-6 takeoffs and landings. More exact data can be obtained on the basis of the results of flights at several types of airports. If an aircraft must be used on unpaved airfields, the measurements of loads at each of the typical airports are conducted in a different season, i.e., in the summer, spring, autumn, and winter.

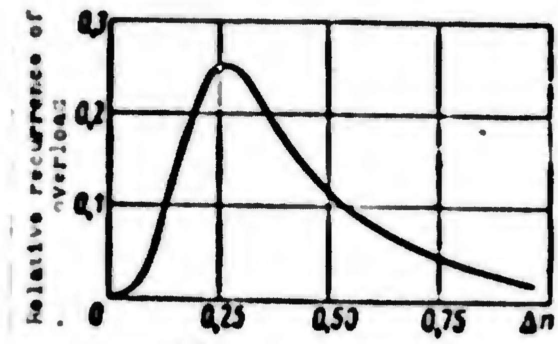

Fig. 7.28. Recurrence of overloads during the first landing shocks.

As investigations show, damage to a structure due to loads caused by the roughness of the airport, for certain assemblies can comprise most of the total damage appearing in the process of operation. The recurrence of loads during takeoffs and landings is considerably influenced by the conditions of wheel braking. The use of automatic brakes leads to cyclical loads with the frequency of work of the device (Fig. 7.29). The magnitude of load from braking is close to the maximum operational magnitude. Therefore, in the designing of components which perceive forces from braking moment, one should consider that they work at a high level of loads (approximately k = 0.4 to 0.6) and with a recurrence of 20-40 times per takeoff and landing.

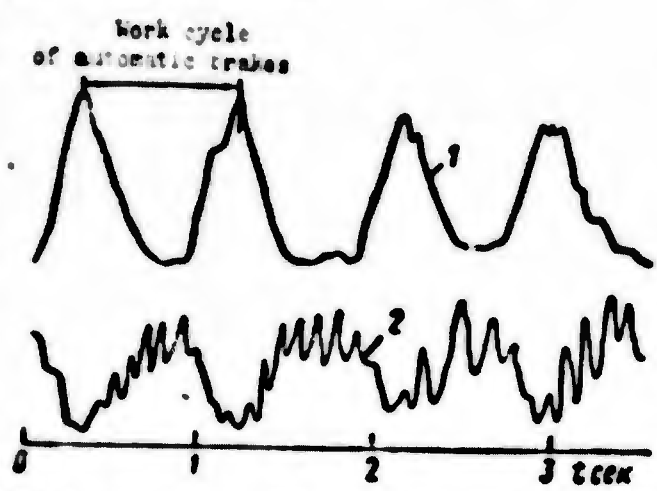

Fig. 7.29. Character of loads during braking in a landing run. 1) force in brake rod of bogie; 2) force in landing gear strut.

During calculation and designing the relationship of the design overload and the level of frequently repeated loads is considered. For instance, in the designing of landing gear the shock absorption should be made as soft as possible, since this permits a lowering of the design overload during landing and allows the structure to be made lighter. However, with the lowering of design overload there is an increase in the relative level of variable loads. For instance, a lowering of design overload during landing from 4.0 to 3.0 leads to an increase in the level of variable loads for landing gear from k = 0.30-0.35 to k = 0.6-0.7 and for the entire airframe structure from k = 0.25-0.30 to k = 0.35-0.40. This leads to an increase of damage with respect to number of cycles by 5 to 10 times.

Special Forms of Loads

In the selection of design conditions and in the designing of an aircraft one should conduct an additional analysis of safety factors when the loading cycle is determined by the work of the systems of the aircraft, for instance cabin pressurization, forces in hydraulic lifts, etc.

During every high-altitude flight the pressure drop in the pressurized cabin varies from 0 to p_{ex}^{op}. Thus, the load from excess pressure in every flight attains its operational value. In this case the load factor is

$$k = \frac{1}{f\eta f_{safe}}. \tag{7.5}$$

where f is the safety factor;

η is safety margin factor;

f_{safe} is pressure safety factor, considering the accuracy of work of the safety valves.

When η = 1.0 and when the usually adopted safety factors for excess pressure are f_{safe} = 1.5 to 1.65 and f_{safe} = 1.1 to 1.3, magnitude k comprises 0.5 to 0.6.

With such a load factor a structure can sustain the action of only several thousand pressurizations, which of course is insufficient for a passenger aircraft. Therefore, in the designing of pressurized cabins it is necessary to have a safety margin factor greater than one in structural elements which are designed for excess pressure.

Jacks for retracting landing gear, release of dive brakes, and release of flaps in every work cycle are subjected to the action of a limiting operational load. They are additionally acted upon by loads from pressure pulsations in the hydraulic system. Therefore, in such cases the safety factors should also be increased.

The action of loads during firing is a specific case. A dynamic load is applied with equal intervals. In addition to the stresses caused by an external dynamic load, there are also local stresses from structural oscillations and acoustic pressures. This causes a number of peculiarities in strength analysis and in the designing of aircraft parts which perceive loads during firing. In particular, one should select increased safety factors in the strength analysis of these aircraft parts.

The magnitudes and character of loads on the control linkage are determined by the peculiarities of the given type of aircraft or helicopter (the presence of hydraulic boosters, the degree of aerodynamic compensation of the controls, and so forth). In view of the special importance of control for the flight safety of an aircraft (or helicopter) special test flights are conducted for studying the loads acting upon the components of control.

In carrying out laboratory tests loads are taken with corresponding factors as compared to those measured in flight.

Magnitudes of Operational Stresses in a Structure

Breakages of aircraft assemblies, occurring due to structural oscillations, appear in the first place on the thin skin in the connections of wing ribs with stringers, etc. For oscillations (vibrations), as compared to other loads of an aircraft, a relatively low level of stresses (less than 1 to 2 kg/mm^2) and high frequency of action are characteristic. Table 7.3 gives the loading characteristics of a jet passenger aircraft for 1000 flying hours.

Table 7.3. Loading Characteristics of an Aircraft for 1000 Flying Hours

Form of load	Number of load cycles per 1000 flying hours	Loading frequency osc/sec	Load factor k
Gusts of bumpy air	$(1-15)\cdot 10^6$	0,3–5,0	0,05–0,70
Airport roughness	$(1-5)\cdot 10^5$	1–5	0,05–0,70
Oscillations of structural parts (buffeting, and so forth)	$(0,7-5)\cdot 10^7$	2–20	0,01–0,05
Motor vibrations	$(0,7-3)\cdot 10^8$	20–100	0,005–0,02
Acoustic vibrations	$(0,5-50)\cdot 10^9$	100–10 000	0,001–0,01
Maneuvers	$(1-5)\cdot 10^5$	5–20 times per flight	0,1–0,7
Pressure in cabin	$(2-10)\cdot 10^3$	1 per flight	0,2–0,4

As can be seen from Table 7.3, the number of cycles of oscillations per 1000 flying hours can reach up to 10^7 to 10^9. Considering that the stress concentration factor of actual riveted designs has magnitude 4 to 8, it is possible to estimate the permissible high-frequency variable stresses. For instance, if for alloy D16 the endurance limit of a smooth sample during a symmetric cycle is equal to 11.5 kg/mm^2, then for an actual design taking into account the coefficient of concentration, a stress of the order of 1.0-2.0 kg/mm^2 is permissible. The influence of a corrosional medium can additionally lower the permissible stress to 0.5-1.0 kg/mm^2. Increase of operating temperature also leads to a lowering of permissible stresses during vibrations.

Stresses in a structure due to common loads on an aircraft (maneuvering, gust of bumpy air, landing) are usually combined with variable stresses from oscillations (vibrations). As shown above, high-frequency stresses to a considerable extent lower the strength characteristics during repeated loads, which should be considered in the determination of period of service.

In most cases motor vibrations may be considered quite simply, since these vibrations carry a relatively stable character. Other oscillation modes (aerodynamic, during takeoff and so forth) are difficult to consider in view of their random character. In this case fatigue tests should be employed, taking into account the random sequence of stresses of different level or an evaluation should be made of the permissibility of oscillations according to the root-mean-square value of stresses.

7.7. Application of Generalized Harmonic Analysis in Estimating Load Recurrence of a Structure

In analyzing loads during flight in bumpy air, the influence of gusts may be considered as a stationary random process. In this case the concept of spectral density can also be used for estimating the service life of the structure.

As shown above, the spectral density of stresses $S_M(\omega)$ in a given section of an assembly can be determined through the mechanical conductivity $H_M(i\omega)$ of the structure and the spectral density of perturbations from gusts $S_W(\omega)$:

$$S_M(\omega)=|H(i\omega)|^2 S_W(\omega). \tag{7.6}$$

The number of loads exceeding the assigned level ξ is determined by the dependence

$$N(\xi)=N_0 e^{-\frac{\xi^2}{2\sigma_M^2}}=N_0 e^{-\frac{\xi^2}{2A^2\sigma_W^2}},$$

where

$$N_0=\frac{1}{2\pi}\left[\frac{\int_0^\infty \omega^2 S_M(\omega)\,d\omega}{\int_0^\infty S_M(\omega)\,d\omega}\right]^{\frac{1}{2}}=\frac{1}{2\pi}\left[\frac{\int_0^\infty \omega^2 |H_M(i\omega)|^2 S_{W_0}(\omega)\,d\omega}{\int_0^\infty |H(i\omega)|^2 S_{W_0}(\omega)\,d\omega}\right]^{\frac{1}{2}}; \tag{7.7}$$

$$S_{W_0}(\omega)=\frac{S_W(\omega)}{\sigma_W^2};\quad A^2=\int_0^\infty |H(i\omega)|^2 S_{W_0}(\omega)\,d\omega,\ \text{or}\ A=\frac{\sigma_M}{\sigma_W}.$$

Magnitude A is equal to the ratio of the mean square of stresses in the structure σ_m to the mean square of speed of the gust σ_w. In different atmospheric compositions $S_{wo}(\omega)$ remains practically constant.

During flight of an aircraft only the magnitude of the mean square of speed of gusts σ_w along the route is variable. In order to determine total recurrence $N(\xi)$ of a given level of stresses during flight on a typical route, it is divided into a number of sections in which the magnitude σ_{wi} remains approximately constant. Then magnitude $N\xi$ can be expressed in the form

$$N(\xi)=N_0\sum_{i=1}^{n}F(\sigma_{wi})e^{-\frac{\xi^2}{2A^2\sigma_{wi}^2}}, \tag{7.8}$$

where $F(\sigma_{wi})$ characterizes the time or distance covered in bumpy air when σ_{wi} = const.

Passing to continuous distribution of σ_w along the route of flight, we obtain

$$N(\xi)=N_0\int_0^{\infty}f(\sigma_w)e^{-\frac{\xi^2}{2A^2\sigma_w^2}}\,d\sigma_w, \tag{7.9}$$

where $f(\sigma_w)$ is the distribution density function of magnitude σ_w.

Analogous relationships can be used during the analysis of recurrence of loads appearing during motion of an aircraft on the ground and during vibrations.

7.8. Calculation-Experimental Method of Determination of the Service Life of a Structure

At present there do not exist conventional methods of determining the service life of an airframe. The solution of this problem is conducted in two ways.

In the first approach we originate from the necessity of creating a sufficiently reliable calculation method which allows us to estimate the safe service life of the structure and to carry out corresponding tests with repeated loads.

The supporters of the other approach deny the possibility of determining the service life of an airframe on the basis of any calculation methods or laboratory tests. The first plan advances the requirement of careful designing of units and structural parts of an aircraft for the purpose of reducing the concentration of stresses to minimum, attentive control in the process of production, and frequent inspections of structure when in use, allowing timely detection of initial fatigue cracks.

Practice requires the application of both methods jointly, since only with their joint use is it possible to sufficiently and reliably ensure a prolonged service life of an aircraft. Proceeding from this, in the process of designing a structure it is necessary to consider the peculiarities of work of each component and to ensure them with a longer life, with respect to fatigue breakdowns. In a number of cases it is expedient to construct a design which would sustain a considerable part of the operational load even after the destruction of one of its elements.

The influence of local damages on the overall strength of a structure can be removed either by duplicating the elements, or by considerably increasing their size. In order not to cause a considerable increase of weight, it is expedient to duplicate or to reinforce only those elements of a structure, the breakage of which leads to catastrophe. It is necessary to consider the possibility of timely detection of fatigue cracks.

At present a number of designers have proposed recommendations on the development of designs with increased life. In such designs they also try to see to it that the rate of propagation of cracks is sufficiently low and the danger of sudden catastrophic damage to structures in flight is excluded. For evaluating the effectiveness of the developed measures undertaken for increasing design life special tests are being conducted on repeated loads with the simulation of fatigue and operational damages.

Method of Calculating the Service Life of a Structure

For calculating service life the most wide-spread method is that of linear summation of damages. This method considers that destruction occurs at $\sum_{i=1}^{s}\frac{n_i}{N_i}=1$. Although this method is not sufficiently accurate, it makes it possible to perform a comparative evaluation of the service life of the structural elements of an aircraft. Probable deviations of the linear law of summation from actual conditions of structural damage can be considered by the introduction of safety factors and by carrying out special tests on structural assemblies which have been utilized a great deal.

By applying the method of linear summation of damages, it is possible to use the following means of estimating the service life of a structure.

On the basis of results of statistical measurements on aircraft there has been constructed a curve of load recurrence for a typical flight of an aircraft, in which the recurrence of stresses H_t has been determined in the most loaded main structural elements, referred to 1 flying hour (Fig. 7.30).

Using the strength curve of a structural element, typical for a given aircraft assembly (Fig. 7.31), one can determine the portion of damage to the structure caused by a given form of load in the defined flying period (for instance, in 1000 hours). The number of stresses with amplitude within limits of σ_i, $\sigma_i + \Delta\sigma$, effective during 1000 hours of flight, is equal to

$$n_i = -\frac{dH(\sigma_i)}{d\sigma}\Delta\sigma. \tag{7.10}$$

The amount of damage caused by the action of stresses (σ_i, $\sigma_i + \Delta\sigma$) in 1000 hours of flight, comprises

$$\frac{n_i}{N_i} = -\frac{dH(\sigma_i)}{d\sigma}\Delta\sigma\frac{1}{N(\sigma_i)}.$$

Upon strict fulfillment of the theory of linear summation, destruction will occur when $\sum_{i=1}^{\nu}\frac{n_i}{N_i} = 1.0.$ Correspondingly, in our case it will be

$$\sum_{i=1}^{\nu}\left(-\frac{TdH(\sigma)}{d\sigma}\right)\frac{1}{N(\sigma_i)}\Delta\sigma = 1.0, \tag{7.11}$$

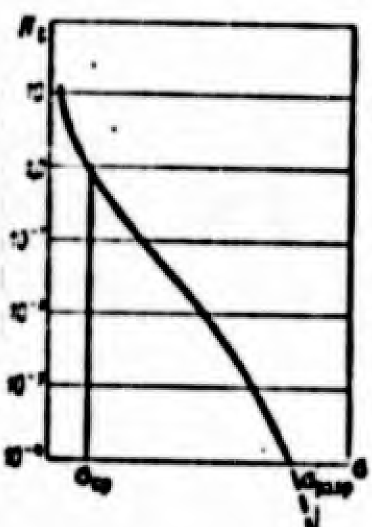

Fig. 7.30. Recurrence of stresses.

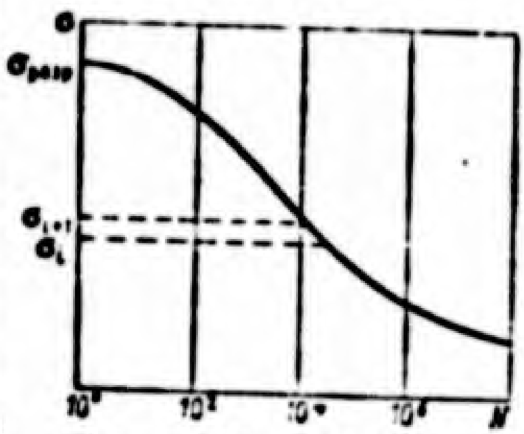

Fig. 7.31. Strength characteristics of a structural element.

where ν is the number of intervals into which the whole range of stresses is divided from σ_{av} to σ_{break} (σ_{av} corresponds to n = 1).

By passage to the limit we obtain

$$-T\int_{\sigma_{\text{ср}}}^{\sigma_{\text{разр}}}\frac{dH(\sigma)}{d\sigma}\frac{1}{N(\sigma)}d\sigma = 1.0, \tag{7.12}$$

The relationship for determining service life per thousand hours will be

$$T = \frac{1}{\int_{\sigma_{\text{ср}}}^{\sigma_{\text{разр}}}\xi d\sigma}. \tag{7.13}$$

Magnitude $\xi = -\frac{dH(\sigma)}{d\sigma}\frac{1}{N(\sigma)}$ characterizes the amount of damage to the structure by stresses of a given level and is called the function of damage intensity. This function usually has a clearly expressed maximum which characterizes the magnitude of stresses (loads), the action of which causes the greatest amount of damages.

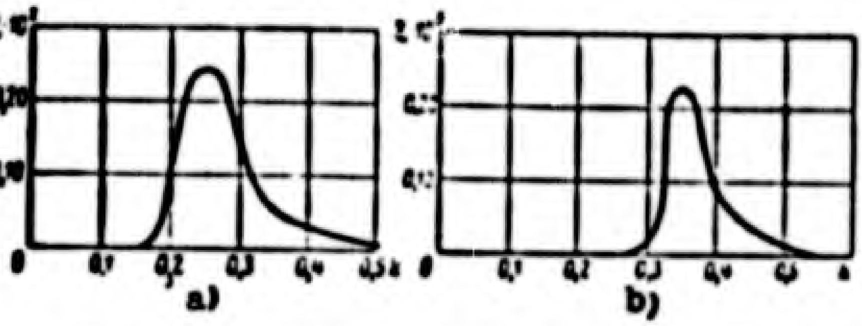

Fig. 7.32. Change of the function of damage intensity. a) maneuvering aircraft; b) non-maneuvering aircraft.

Figure 7.32 shows the approximate change of the function of damage intensity for different types of aircraft. The greatest amount of damage is usually introduced by relatively small loads when $k_{av} = 0.2$ to 0.4 and $k_{var} = 0.05$ to 0.10. Such loads are obtained for non-maneuvering aircraft during gusts of bumpy a. with a velocity of about 3 m/sec or during an overload of about 4.0 for maneuvering aircraft.

Example of Calculating Service Life

For calculating service life we will use the linear theory of damage summation. For simplification we shall take the following assumption:

1. The magnitudes of stresses in the main supporting members of a wing are directly proportional to the overload in the center of gravity of the aircraft. Consequently, recurrence of stresses is equal to the recurrence of corresponding overloads in the center of gravity of the aircraft. This assumption is valid for aircraft for which it is possible to disregard the influence of deformations on forces during the dynamic action of loads from gusts of bumpy air.

2. A wing is equally strong for a static load and its safety

factor is equal to 1.0.

3. The amount of damage introduced from overloads during takeoff and landing is predetermined and is equal to λ.

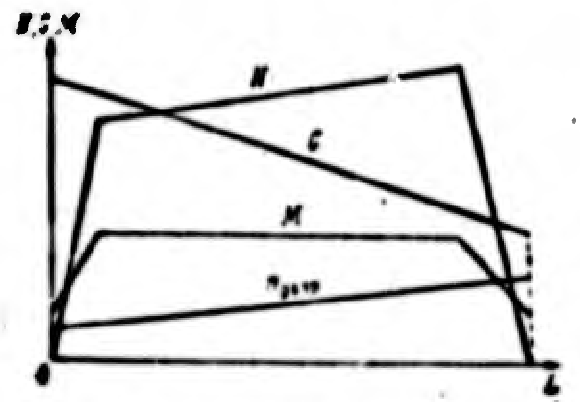

Fig. 7.33. Flight profile.

In accordance with the assignment and flying data of an aircraft we construct a typical flight profile (Fig. 7.33). The flight is divided into a number of intervals. In each interval the destructive overload, the altitude, and the speed of flight are approximately constant.

The magnitude of the destructive overload is determined from the following relationship:

$$n_{\text{разр}} = \frac{M_{\text{разр}}}{M_{n=1}},$$

where M_{break} is the destructive bending moment of the wing;

$M_{n = 1}$ is the bending moment of the wing when $n = 1$.

For each interval the calculation is conducted in the following sequence:

1. On the basis of integral recurrence of gusts of wind W_{ef} (Fig. 7.34a) we construct graphs of integral recurrence of overloads n (Fig. 7.34b), using the dependence

$$n = 1 + \frac{1}{2} K c_y^{\alpha} \rho_0 \frac{V_i W_{\text{эф}}}{G/S}. \qquad (7.14)$$

Then we construct a graph of differential recurrence dH/dk with respect to k, where $k = n/n_{break}$ (Fig. 7.35).

2. On the basis of available data we construct the strength curve of the considered structural element in the form of the dependence of k and $k_{av} = n_{av}/n_{break}$ on N of the type shown in Fig. 7.23. Since loads change near the middle position, corresponding to horizontal

flight when n = 1, then $k_{av} = 1/n_{break}$.

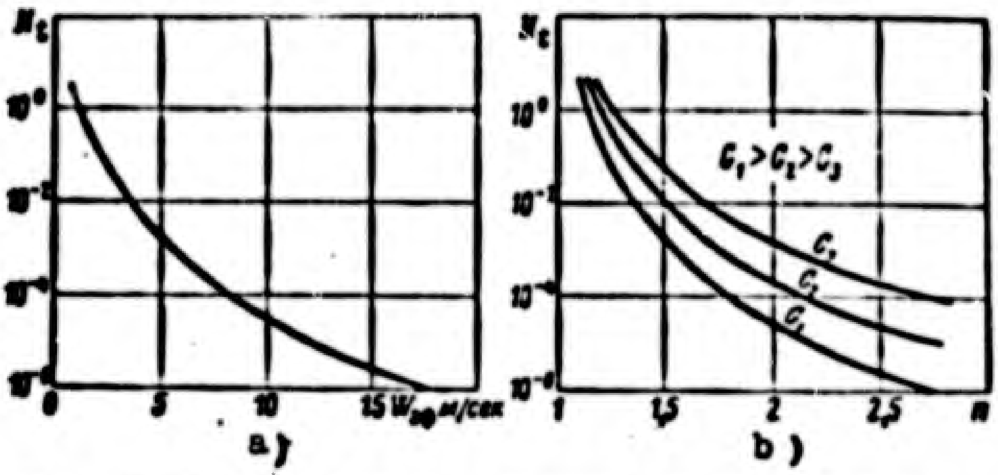

Fig. 7.34. Graphs of integral recurrence of gusts of wind (a) and overloads of an aircraft (b).

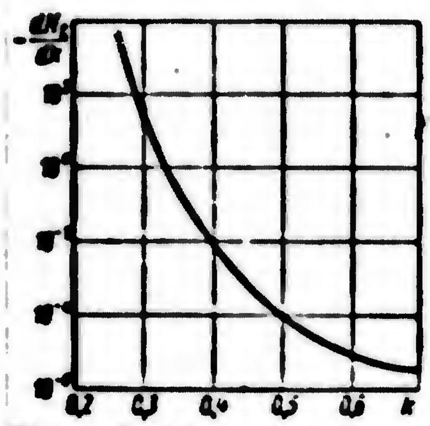

Fig. 7.35. Graph of differential recurrence of loads on a wing.

3. We construct the function of damage intensity $\xi = -\frac{1}{N}\frac{dH_t}{dk}$ depending upon k, whereby for every value of k the magnitude dH_t/dk is taken from the graph of differential recurrence, and the value of N is taken from the graph of static strength.

4. We calculate the damage in each section $\int_0^1 \xi dk$.

5. We determine the amount of damage from gusts of bumpy air in one typical flight. Magnitudes $\int_0^1 \xi dk$ for each interval of the route are multiplied by the time of flight, corresponding to the defined interval of the route, L_i/V_i, where L_i is the length of a segment of the route and V_i is the speed of flight in a considered interval of the flight route, i.e.,

$$l_i = \frac{L_i}{V_i}\int_0^1 \xi dk.$$

6. We calculate the amount of damage λ introduced by takeoff and landing of the aircraft, and we determine the total damage in one typical flight:

$$1=\sum_{i=1}^{\nu}\frac{t_i}{V_i}\int_0^1 t\,dk+\lambda \qquad (7.15)$$

where ν is the number of sections.

7. Knowing the damages obtained in one flight, we can determine the number of typical flights which the aircraft can accomplish in its entire service life and the computed value of service life in hours:

$$T=T_0\frac{1}{\sum\limits_{i=1}^{\nu}\frac{t_i}{V_i}\int_0^1 t\,dk+\lambda} \qquad (7.16)$$

where T_0 is the duration of a typical flight.

For contemporary aircraft, stresses in structural elements during the action of dynamic loads to a considerable extent are determined not only by the magnitude, but also by the character of change of the external load in time. In these cases it is expedient to apply methods of spectral analysis for finding the statistical dependences of stresses on external loads in the main supporting members of the structure.

For clarification of specific peculiarities of loading of a given aircraft we conduct measurements of forces in the main structural elements. The results of measurements are presented in the form of graphs of integral recurrence for each assembly. On the basis of these graphs it is possible to calculate the service life.

7.9. Strength of a Structure During Acoustic Vibrations

Damages caused by acoustic vibrations can be decisive for the strength of thin skins which are located in a noise zone of high level.

The theoretical basis for determining variable stresses which are created by acoustic pressures is the study of the dynamic receptivity of a structure which is under the action of a randomly variable load. It is considered that the distribution of amplitudes of acoustic pressure obeys the Rayleigh law and the summation of fatigue damages agrees with the linear hypothesis. The last condition can be written in integral form

$$\int_0^{\sigma_{max}} \frac{dn(\sigma)}{N(\sigma)} = 1, \qquad (7.17)$$

where $n(\sigma)$ is the number of loading cycles with stress σ;

$N(\sigma)$ is the allowed (destructive) number of cycles with the same value of σ.

In this case the dependence of N on σ is expediently considered not for the peak value of σ, but for $\bar{\sigma}$ [see formula (5.7)].

Function $N(\bar{\sigma})$ can be determined in the form

$$N(\bar{\sigma}) = \left[\int_0^{(\sigma/\bar{\sigma})_{max}} P(\sigma/\bar{\sigma})\, d(\sigma/\bar{\sigma}) / N(\sigma) \right]^{-1}. \qquad (7.18)$$

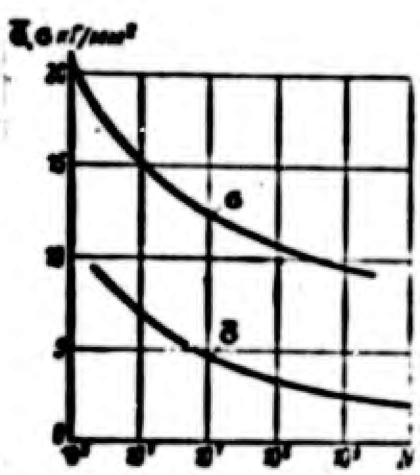

Fig. 7.36. Strength of an aluminum alloy during random alternation of stresses.

where $P(\sigma/\bar{\sigma})$ is the probability of skin loading when $\sigma/\bar{\sigma}$. Using this dependence, it is possible to construct the curve $N = f(\bar{\sigma})$ (Fig. 7.36). With the help of this curve and taking into account the results of fatigue tests one can determine the dependence of longevity of a sample on noise level.

Fatigue tests of structure during acoustic vibrations are performed with the help of powerful sirens or with the use of the exhaust of a turbo jet engine.

7.10. Tests of Components and Full-Scale Assemblies

Laboratory tests of typical components (fittings, joints, compound panels, fuselage sections with cutouts, and so forth) are conducted for clarification of the characteristics of their strength at different levels of loads. Usually under all conditions of loads no less than three identical samples are tested. The full investigation of variance of strength characteristics requires tests of a considerably large quantity of samples, since variance with respect to number of cycles which can be sustained by samples of a given type to destruction may be very great.

It is necessary to note that in the system of an entire aircraft the loading conditions of individual elements of the structure usually differ somewhat from the loading conditions of isolated elements. Therefore, sometimes certain elements, showing fully satisfactory strength during tests of them as isolated samples, turn out to be insufficiently durable during tests of them in the whole aircraft structure. Since tests on repeated loads of a whole aircraft and its assemblies are extraordinarily expensive and time consuming, usually only a very limited number of aircraft or individual assemblies are tested.

Tests of full-scale assemblies and aircraft on the whole permit the defection of weak places of the structure, the checking of the convergence of results of tests with the results of tests of individual elements, the study of the character and speed of propagation of cracks, and the obtainment of an estimate of the possible service life of an aircraft.

With respect to the complexity of fatigue tests of aircraft structures, it is possible to divide them into three categories: tests with single-stage loading; tests with combined loading according to a schematic program; tests with multistage loading according to a complex program which simulates operating conditions.

<u>Tests with single-stage loading</u> are the simplest, were used long ago, and are the most wide-spread. In these tests the assembly

(structure element) is given a variable load of constant amplitude. The measure of strength is the number of loading cycles the assembly to destruction.

The magnitude of repeated load is expediently selected in such a manner so that the accepted load level causes damage in the structure that is approximately equivalent to the damage caused by all repeated operational loads acting upon the structure. However, at the time there is no reliable method for determining the magnitude of such a load. Frequently the conditional characteristic magnitude of the load is taken, for instance, equal to 0.5 P_{cal}, or the magnitude of the load corresponding to the highest intensity of the damage function, or the most frequently encountered load magnitude.

Tests with loads of 0.7 P_{cal} and 0.5 P_{cal} are widely used. Such tests are used for estimating the strength of the main assemblies of an aircraft (wing, fuselage, empennage, controls, landing gear, etc.).

In a number of countries attempts have been made to find methods of transition from results of fatigue tests to an estimate of the service life of an aircraft. Thus, in the United States at the North American Company it was taken, for instance, that 3000 recycles with a load equal to 67% P_{cal} correspond to 2000 flying hours of a maneuvering aircraft. This is considered sufficient for fighters and trainers.

In Sweden the SAAB Company proposed tests with a load of 53.4% P_{cal} and necessary number of cycles equal to 25,000.

Recently, for estimating the service life of nonmaneuvering aircraft, a lower load level was used.

Tests on a single-stage program basically give the possibility of a comparative estimate of strength of new structural elements with respect to "reliable" elements, the strength of which is confirmed by prolonged use.

For estimating the service life of a structure the obtained number of cycles to destruction is sometimes recomputed for service life in hours of flight with the help of an equivalent coefficient k_{eq}. For the determination of this coefficient in an identical program tests are conducted on new structural elements and those in use. A comparison of the results of these tests permits us to find the value of k_{eq}. For instance, a new structure sustains N_0 number of cycles to destruction, and after T_1 flying hours the structure withstands a number of cycles N_1, and correspondingly after T_2 hours, N_2, etc. (Stages of flight should not be less than 500 hours for maneuvering aircraft and 3000-5000 hours for passenger aircraft). Then the equivalent coefficient k_{eq} is determined from the relationship

$$k_{eq}=\frac{T_1}{N_0-N_1}. \qquad (7.19)$$

The problem of determination of coefficient k_{eq} is complicated by the fact that different aircraft of one type in operation are subjected to the action of repeated loads of various intensity. Furthermore, there exists considerable variance in the strength characteristics of materials and structures.

An estimate of the equivalent coefficient can also be conducted on the basis of a study of the recurrence of the action of loads in operation. The linear theory of damage summation is then used. Knowing the value of k_{eq}, the service life of the structure (in hours) is determined from the relationship

$$T=k_{eq}N_0. \qquad (7.20)$$

The magnitude of coefficient k_{eq} depends on the type of aircraft, the design, and the material used. The value of k_{eq} should be determined specially for every aircraft. For certain types of wing structures of maneuvering aircraft during test with a load of 0.7 P_{cal}, k_{eq} has a magnitude of the order of 0.7-0.8, and during tests with a load of 0.5 P_{cal}, $k_{eq} \approx 0.20$ to 0.25. For nonmaneuvering aircraft a criterion is proposed for the determination of service life in the form*

$$T = 1.9 \frac{N}{V}, \tag{7.21}$$

where N is the number of cycles to destruction during a variable overload corresponding to a gust of 30.5 m/sec at the cruising speed of an aircraft;

V is the speed in km/hr.

A variable load is put on a static load when n = 1. In this case $k_{eq} = 1.9/V$. The higher the speed of flight, the lower the magnitude of coefficient k_{eq}.

Tests with combined loading according to a schematic program (programmed tests). In this case the structure is subjected to loads of several forms and levels. The magnitude of loads and the sequence of their action are determined by means of studying aircraft loads in actual operation. Loads experienced by an aircraft in operation are schematized and united in defined groups. On the basis of the obtained data loading program is compiled, which corresponds to a defined stage of flight.

In recent years this form of testing has become the chief means of estimating the service life of passenger aircraft. Tests of fuselages with pressurized cabins are the most wide-spread. In such tests the following loads are applied:

1. Excess pressure in cabin, the change of which corresponds to the flight profile.

*P. Wolker, Design Criterion for Fatigue of Wings, RAS, I, v. 57, N 505, I, 1953.

2. Loads on wing and empennage, which change in the cycle from standing loads to loads in horizontal flight.

3. Loads from gusts of wind.

4. Loads during takeoff and landing.

Usually the loading program for one cycle is composed for one typical flight, including takeoff, climb, cruise setting, descent, landing, and taxiing. Magnitudes of loads on assemblies of an aircraft and their number in one cycle are determined as a rule on the basis of measurements during flying tests.

Figure 7.37 gives a program of similar tests of a passenger aircraft.

Programmed tests permit the detection in an aircraft structure of weak places that were not detected in tests of individual elements. They permit the checking of the correctness of fatigue tests of elements, the determining of typical damages, the character of propagation of cracks, the formation of recommendations for inspections of an aircraft structure during operation, the development of recommendations for the repair of the aircraft structure, and an estimation of the service life of the airframe.

During the tests the fuselage is placed in a basin filled with water (Fig. 7.38). The change of pressure in the cabin is carried out by increasing the water pressure in it. This method of creating excess pressure excludes the danger of explosive damage to the fuselage upon the appearance of a crack in its skin, which is possible during air pressurization. In the creation of excess pressure by water it is easy to determine the onset of initial destruction, to observe the propagation of cracks, and in good time to repair the structure.

Calculation of service life is conducted with the dependence

$$T=\frac{1}{\eta}NT_{0} \qquad (7.22)$$

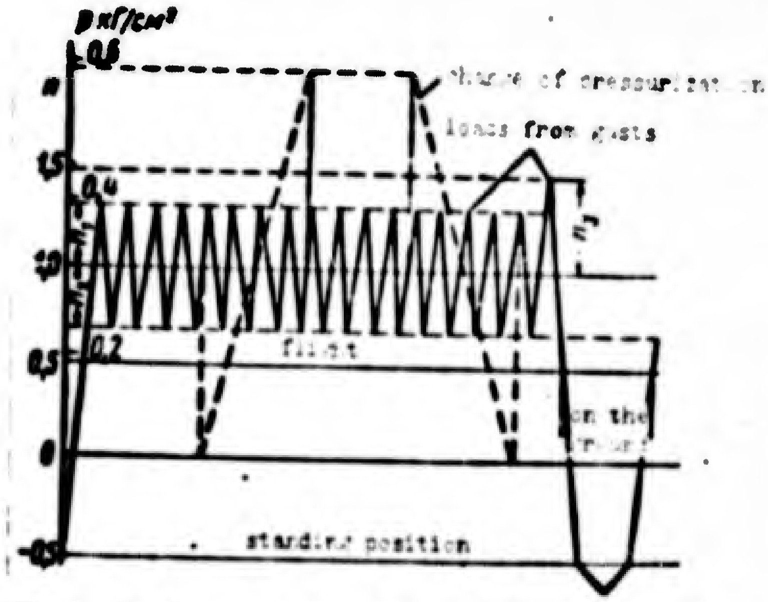

Fig. 7.37. Diagram of the loading program of the aircraft "Caravel" in one cycle, corresponding to a typical flight. n_1 – overload corresponding to an ascending gust of w_{ef} = 3 m/sec, n_2 – overload, corresponding to a descending gust of w_{ef} = 3 m/sec, n_3 – overload corresponding to an ascending gust of w_{ef} = 5 m/sec.

where T_0 is the duration of a typical flight;

η is the coefficient considering the variance in number of cycles.

<u>Tests with multistage loading</u>. Recently, tests have come into use with combined multistage loading. This method makes it possible to approximate the conditions of the tests as much as possible to the loading conditions in operation.

The program of loading for such tests is constructed on the basis of data on the recurrence of operational loads, i.e., the loading spectrum. The continuous loading spectrum will be converted into a gradual spectrum (Fig. 7.39); then the number of loads is determined for every stage of the load (stress) for the assigned number flying hours (100-500 hours). Grouping the loads with respect to frequency of application, we obtain the loading program (Fig. 7.40). Such a program is repeated to the destruction of the structure. The quantity of repetitions of the program (number of loading periods) is a measure of strength of the structure.*

Inasmuch as the program corresponds to a defined number of flying hours, the service life is equal to the product of the number of loading cycles N and the number of flying hours T_0 corresponding to one loading cycle:

$$T=\frac{1}{\eta}NT_0$$

*"Construction," 1954, I, v. 6, N 3, P. 97-104.

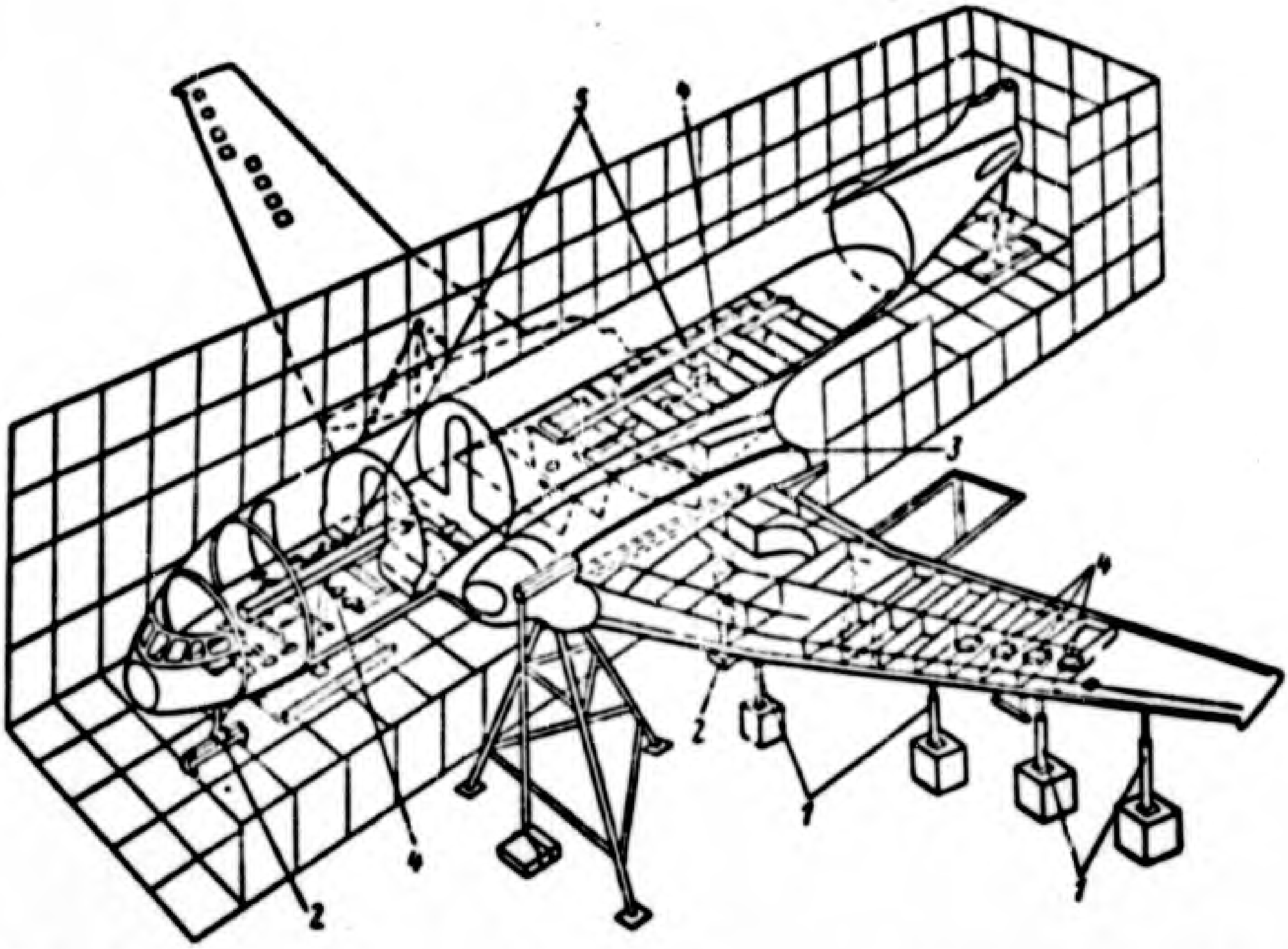

Fig. 7.38. Overall view of tests in a hydrobasin. 1) loading system of wing; 2) attachment of landing gear; 3) packing; 4) ballast; 5) lever system of fuselage loading.

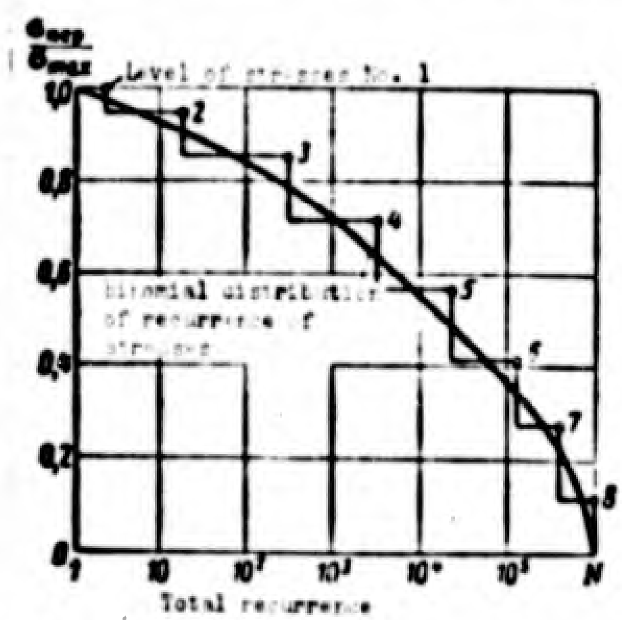

Fig. 7.39. Continuous and gradual spectrum of recurrence of stresses.

For the development of a program of tests with multistage loading it is possible to present the following considerations:

1. The number of stages in the program should be on the order of 6-8. A larger number strongly complicates the program, and a smaller number leads to too rough and too inaccurate reproduction of operational loads.

2. The number of loading periods to destruction should be on the order of 10. A smaller number leads to very inaccurate results, since

it is difficult to estimate the value of an incomplete period. A larger number of loading periods complicates the tests.

3. Tests should be started from the average stage of loading, then the loading stages should follow in order of growth up to maximum load, and further in decreasing order, etc.

4. It is necessary to also include in the program small loads (up to 10% of the biggest load).

5. Large and average loads should have low frequency.

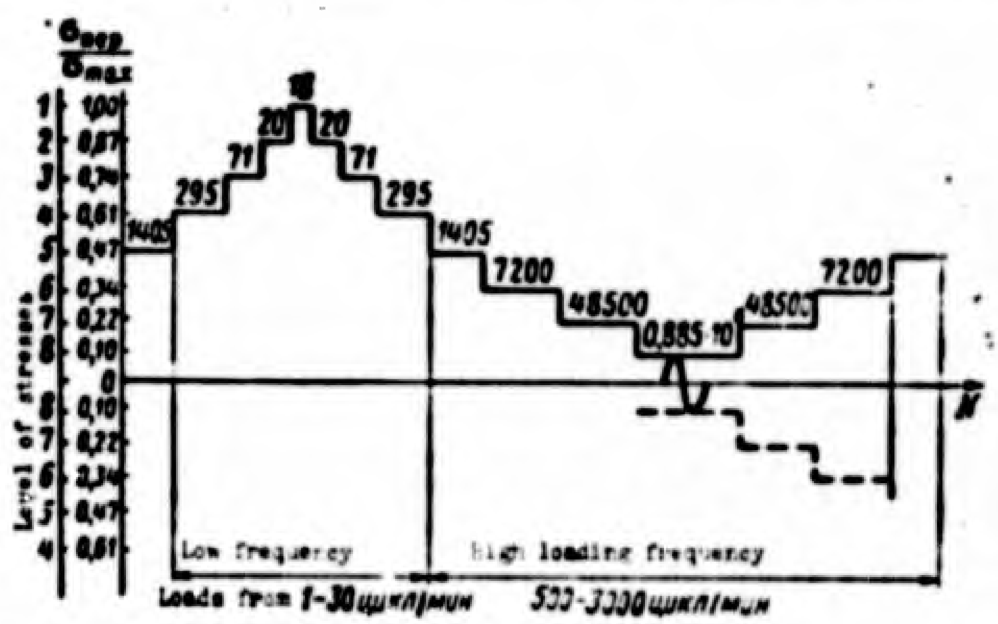

Fig. 7.40. Diagram of one loading cycle (1 cycle of the program contains 10^6 loads).

Programs are also used in which loads of different magnitude are alternated in random sequence as this occurs in the operation of an aircraft. Such tests even more approximate loading conditions to actual conditions during laboratory tests. They are conducted according to a program developed on the basis of available data on the magnitudes and recurrence of operational loads.

It is necessary to note that during tests with one constant load level it is impossible to detect a sufficient quantity of sections of a structure, which are dangerous with respect to fatigue strength. During tests with a different load factor (with constant amplitude) initial cracks appear in different places and the development of these cracks frequently does not correspond to that observed under operating conditions. Conversely, in tests according to a program with randomly alternating loads, places of the appearance of fatigue cracks are detected in a structure where the conditions of their development correspond to flying conditions. Therefore, in spite of their large complexity, tests with randomly alternating loads are expedient, since at the time there are no other methods of more reliably detecting sections of a structure that are dangerous with respect to fatigue strength.

Propagation of Fatigue Cracks

For the creation of a structure which is safe from fatigue breakdown and for the establishment of a safe service life the investigation of conditions of development of fatigue cracks has an important value. For increasing operational reliability it is very important in good time to opportunely detect cracks during inspections.

As a result of investigations of samples, it was discovered that the intensity of propagation of cracks is lowered with the decrease of the total level of stresses.

For preventing the propagation of fatigue cracks so-called limiters can be applied. Limiters of cracks can be stringers, wing ribs, frames, etc. In a thick skin and in elements with large cross sections (spar flanges) cracks spread comparatively slowly. In highly durable materials cracks spread faster (Fig. 7.41) and, therefore, for increasing reliability it is sometimes expedient to manufacture the skin from a less durable material.

Tests on repeated loads make it possible to find the dependence of rate of propagation of cracks on the type of structure. Depending upon the rate of propagation of cracks, the periodicity of inspections of a structure is established.

Table 7.4 gives certain data on the appearance of the first cracks noticed during visual inspection and in a structure during tests on repeated loads (0.5 P_{break}), which characterizes the rate of propagation of cracks.

Table 7.4

Assembly	N_{init}/N_{break}*
Wings:	
shell type	0.50—0.70
spar type	0.10—1.00**
Stabilizer:	
skin	0.01—0.10
joints	0.10—0.95
Fuselage skin	0.10—0.25
Aileron	0.30—0.85

* N_{init} is the number of cycles in which a crack is visually detected; N_{break} is the number of cycles in the destruction of a structure.

** When $\frac{N_{init}}{N_{break}} = 1.0$ place of appearance of crack was not examined.

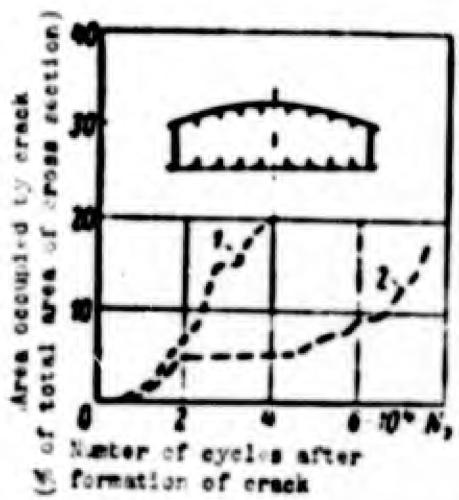

Fig. 7.41. Character of crack development in a wing structure. 1) aluminum alloy of type V95; 2) aluminum alloy of type D16.

7.11. Selection of a Reliability Factor in Determining Service Life

For every aircraft there exists such a limited service life, above which operation is not safe from conditions of fatigue strength and further structural repair is inexpedient.

A limited service life of a structure depends on the characteristics of the same structure, the character of damage summation during random alternating loads. Furthermore, the magnitude of the limited service life is essentially affected by the thoroughness inspections of the structure during operation, thorough consideration and quality of repair, the conditions of operation (flight conditions, quality of airports, weather conditions, corrosion, operational damages, and so forth). Therefore, the limited service life of a given specific aircraft in the beginning of its designing cannot be determined.

However, on the basis of the study of questions of strength of aircraft structures and the fulfillment of a necessary volume of laboratory tests, one can determine the minimum guarantee service life. The minimum guarantee period is the service life in hours, during which, with a definite reliability probability, it can be guaranteed that in operation with respect to fatigue conditions there will not occur any essential disturbance of strength. Subsequently, with the obtainment of information about the conditions of actual operation of aircraft and the results of tests on repeated loads, the service life is definitized. For determination of the minimum guarantee service life of an aircraft during design and construction comparative fatigue tests are made on structural elements (joints, panels, and so forth) and the best variant is selected. In process of this work the fatigue characteristics of the main structural elements are determined.

During test flights on the first models of an aircraft the loads (stresses) and oscillation of its parts are measured. Then tests are made on the aircraft structure on the whole or on its assemblies and estimates are made on the service life taking into account the results of all the work done.

With respect to a fixed minimum guarantee service life a certain safety factor is selected or, as it is otherwise called, the reliability factor. Total safety factor η is defined as the product on particular safety factors $\eta = \eta_1 \eta_2 \ldots$, on the selection of which only preliminary considerations can be given, since at present the data are still insufficient for the reliable establishment of their magnitudes.

In determination of a period one should introduce a correction η_1 for probable deviation of total damage, during tests on a simplified program, from total damage in real conditions of operation. As shown above, $\sum_{i=1}^{s} \frac{n_i}{N_i}$ can considerably differ from 1.0. In a single-stage test for the case of irregular loads one should take an increased value of the safety factor. In programmed tests with several stages of loads the coefficient η_1 can be lowered. If the structure is subjected to the action of only regular loads, which can be accurately reproduced in laboratory tests, then η_1 may be equal to 1.0.

For the selection of a safety factor the authenticity of loads used during fatigue tests has a large value. This factor is considered by coefficient η_2. If loads are taken by measurements during flying tests on a given aircraft and their magnitudes are increased by no less than 20% as compared to those actually measured, it is possible to take $\eta_2 = 1$. An increase of loads by 20% is produced for calculation of the error of measurements and the probable deviations of loads on different aircraft models.

If the calculation uses data on recurrence, obtained on the basis of statistical data, then η_2 is increased depending upon how close to the given aircraft are the parameters of the aircraft on which the statistical materials were obtained. It is necessary to consider that for aircraft of the same type the recurrence of loads can be different depending upon the specific conditions of operation.

In the selection of the safety factor the possibility of inspecting the places where initial destructions appear, and the rate of propagation of cracks have a large value. This factor is considered by coefficient η_3. If destruction begins in places that are hidden and inaccessible for inspection during operation, the coefficient η_3 is expediently taken as greater than 1.0. If initial cracks appear on the external skin, develop comparatively slowly, and can be easily noticed during postflight (preflight) inspection of an aircraft, the coefficient η_3 can be taken as equal to one. For pressurized fuselages during fast crack development the value of η_3 should be increased.

Of large value in the selection of the magnitude of the safety factor is a correct account of the analysis of the results of tests of identical samples and structures. This factor is considered by coefficient η_4.

According to different investigations (mainly foreign ones) the variance coefficient of fatigue characteristics, with respect to the number of cycles for full-scale structural samples with load factor 0.5-0.7, is:

Wing, empennage, and fuselage	1.5-2.5
Landing gear	2.5-3.5
Control linkage	3.0-4.0

These variance magnitudes are obtained in a comparatively small number of tested samples (from 2 to 5). (In tests of a large quantity of samples the variance coefficient can reach 9-11).

The distribution curve of results of fatigue tests of samples agrees well with the log-normal law of distribution. If there is a sufficient number of tests, one can then determine the parameters of distribution, the average number of cycles N_{av}, and the standard divation σ. Then, using the methods of mathematical statistics, a certain minimum number of loading cycles to destruction N_{min} can be found by proceeding from the condition that the actual value of the destructive number of cycles, with a probability for instance of 0.99

or 0.999, will be greater than N_{min}. In this case the safety factor η_4 may be taken as equal to one. However, the use of this method is difficult, since a small number of samples of full-scale structures (from 1 to 6) is tested. Magnitude η_4 is usually selected depending upon the number of tested samples.

Thus, with the number of tested samples less than 5-6 the magnitude of coefficient η_4 may be taken as equal to approximately three. In this case, in the calculation of the service life, the mean value of the number of cycles to destruction is taken. During the test of only one sample the magnitude η_4 should be more than 3.0.

In the process of operation an aircraft is under conditions which promote the development of corrosion of its components (sharp change of temperatures, increased humidity, and so forth). As was shown, corrosion considerably affects the strength of a structure, which should be considered by coefficient η_5. For aircraft flying under conditions of humid sea climate the coefficient η_5 should be increased. For aircraft, flying in a dry continental climate the magnitude η_5 can be lowered.

By means of calculation with the use of available experimental data the calculated service life of a structure T_{cal} is determined. Minimum guarantee service life $T_{min\ g}$ is determined by the formula

$$T_{min\ g} = \frac{T_{cal}}{\eta}, \tag{7.23}$$

where

$$\eta = \eta_1 \eta_2 \eta_3 \eta_4 \eta_5.$$

This method of determining service life of course is complicated, but on the given stage of development of investigations in this region its application should be considered expedient.

In order to obtain data for the solution of the problem of increasing the service life of an aircraft structure above the minimum guarantee period, from the very beginning of operation it is expedient to conduct the following measures:

1. Separate from the number of aircraft of a given type in operation the so-called leader group. Aircraft of this group should have maximum flying hours (usually more than the flying hours of aircraft of the main fleet) and should have been used as much as possible under the most difficult conditions. The number of leader aircraft depends on the total aircraft fleet and usually comprises a definite percent of it. The leader aircraft are outfitted with statistical equipment for registration of recurrence of loads. In certain cases, for the study of the conditions of work of an aircraft structure, tensometric and vibration-measuring equipment should be installed.

2. Assemble materials for timely detection of weak places in the structure, check the quality of repair and the correctness of use. It is expedient to install statistical instruments on groups of aircraft which are used under special conditions.

3. After a defined flying time (usually 0.7-1.0 $t_{min\ g}$) fatigue tests should be made on several aircraft models. These tests clarify the influence of flying time on fatigue characteristics and determine the degree of depletion of the service life.

On the basis of the results of these works sufficiently reliable data can be obtained for determining the service life of a structure taking into account the actual conditions of operation of the aircraft (external loads, maintenance, repair).

CHAPTER VIII

THE INFLUENCE OF AERODYNAMIC HEATING ON THE STRENGTH OF FLIGHT VEHICLES

List of Designations Appearing in Cyrillic

аэр = aer = aerodynamic

в = a = air
в = b = breaking point
в.ср = shear = shear strength

д = d = divergence
дв = en = engine
доп = per = permissible

изл = rad = radiation

к = con = convective
кГ/мм^2 = kg/mm^2
кг/мм^2 = kg/mm^2
кГ·м = kg·m
кГ/см^2 = kg/cm^2
ккал/кг·град = kcal/kg·deg
ккал/м^{2}час = kcal/m^2·hr
ккал/м·час·град = kcal/m·hr·deg
кон = con = convective
кон = str = structure
кр = crit = critical
кр = tor = torque

мин = min

нач = init = initial

об = equip = equipment
об = sk = skin

пр = giv = given

п.с. = b.l. = boundary layer

рад/см = rdn/cm

с = s = sun
стр = strin = stringer

ф = f = flutter

эк = eq = equivalent
экв = eq = equivalent
эф = ef = effective

At supersonic speeds of flight of vehicles the temperature of flow is increased near the surface of the structure. This leads to heating of the structure itself (aerodynamic heating). The mechanism of heating and propagation of heat in the structure consists of several processes. The external surface of a flight vehicle receives convection heat flow from the circumfluent air, the heat flow for radiation of the Sun, Earth, and atmosphere, and at cosmic speeds of flight, the heat flow of gas radiation. From the surface of a flight vehicle heat is radiated into the surrounding space and it spreads inside the structure by means of thermal conduction and convection. Between separate parts of the structure there occurs heat exchange. A general diagram of heat flow, acting upon a flight vehicle in flight, is shown in Fig. 8.1.

With the increase of temperature of the structure the mechanical properties of the materials are lowered. Besides this, during heating of the structure there occurs thermal expansion of separate elements, in consequence of which there appear thermal stresses. The sustained influence of high temperatures and external loads on the structure can lead to creep of materials. Calculation of the state of strain of structures in conditions of high temperatures is difficult. In

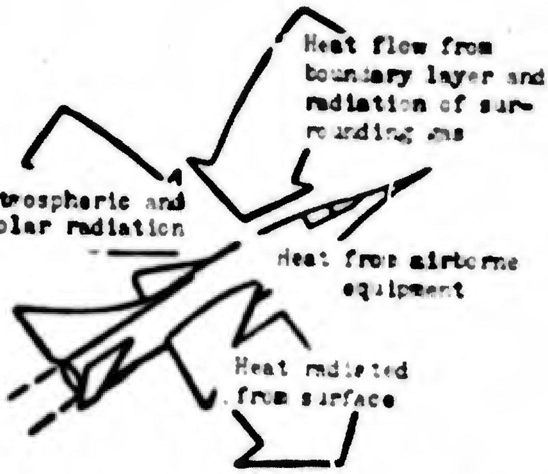

Fig. 8.1. Diagram of heat flow acting upon a flight vehicle in flight.

connection with this, experimental methods of investigating the performance of a structure in conditions of heating during laboratory and flying tests are widely applied.

Analysis of the strength of a structure, taking into account heating, consists in determining the field of temperatures, investigating the change of properties of the materials at these temperatures, and calculating the strength of structural elements during the action of an external load taking into account the first two factors.

Basic information is given below on the physical essence of aerodynamic heating, the laws of heat transfer, and the mechanical properties of materials at high temperatures, and a qualitative picture is given of the influence of heating on the aeroelastic characteristics of a structure and the service life of a flight vehicle during heating.

8.1. Temperature of Gas in Boundary Layer

Heating of the skin of a flight vehicle appears in flight upon acceleration of particles of air, located near its surface. The acceleration (in inverse motion — for deceleration) of air particles requires energy, part of which inevitably passes into heat, causing heating of the surface of the body.

In the case of complete transformation of kinetic energy of flow into thermal energy the temperature of decelerated flow is

$$T_0 = T_H\left(1 + \frac{k-1}{2} M^2\right). \qquad (8.1)$$

where k is the adiabatic index (for air k = 1.4);

T_H is the temperature of undisturbed air at altitude of flight H.

During the transformation of kinetic energy into thermal energy, part of it is dispersed and the temperature of the air at the adiabatic wall, i.e., the wall which does not absorb and does not radiate heat, will be

$$T_r = T_H\left(1 + r\frac{k-1}{2}M^2\right). \qquad (8.2)$$

where r is the temperature recovery factor.

Figure 8.2 shows the character of flow around a flight vehicle and the regions in which the temperature and flow rate sharply change.

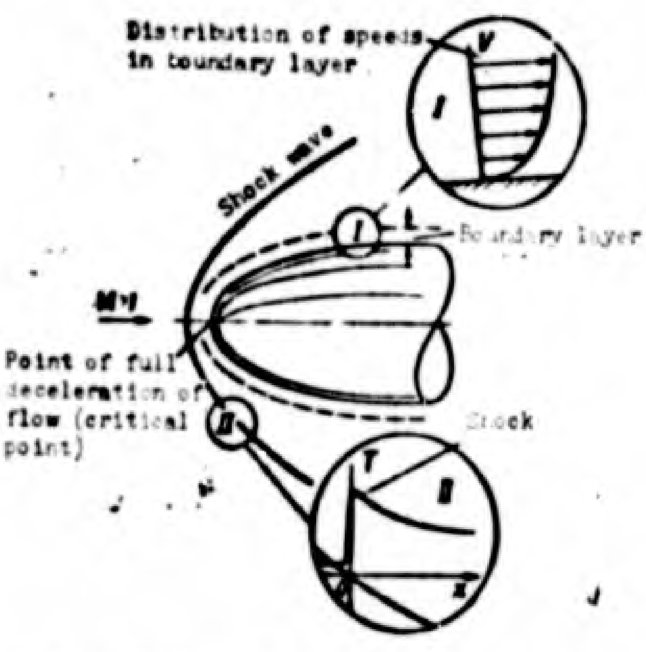

Fig. 8.2. Diagram of supersonic flow around a body and the character of change of temperature T in a shock.

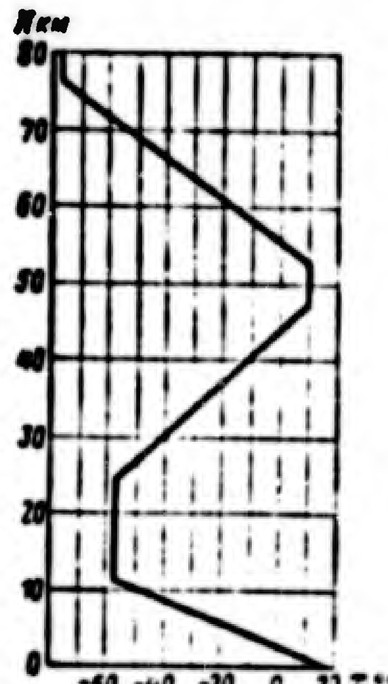

Fig. 8.3. Change of air temperature with altitude.

The points of full deceleration, deceleration of the flow of air in shock waves, and the deceleration of air particles in the boundary layer pertain to these regions. Increase of temperature in the first two cases is connected with the dynamic change of pressure (compression) during the flow of air without friction.

Deceleration and compression of air in shock waves are connected with large losses of mechanical energy, irreversibly transfered into thermal energy with subsequent heat dissipation.

Of large value in the determination of surface temperatures of a flight vehicle is the temperature of the surrounding atmosphere. The values of parameters of undisturbed atmosphere essentially depend on the season, the day, etc. Usually the parameters of undisturbed atmosphere at different altitudes are calculated according to standard atmosphere, in which the law of change of temperature with respect to altitude is determined on the basis of perennial measurements and statistical treatment. The change of temperature with the increase of altitude is shown in Fig. 8.3.

During the flight of a vehicle different conditions can be encountered with respect to T_H and ρ_H, which are different than standard. Therefore, during calculations of heating temperatures of a structure one should consider the highest air temperatures for every altitude of flight. The latter can be done on the basis of statistical data of distribution of air temperatures at different altitudes.

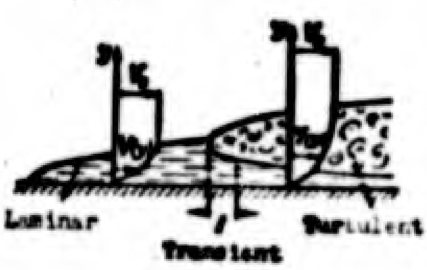

Fig. 8.4. Approximate structure of boundary layer.

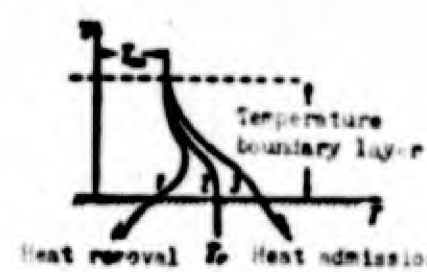

Fig. 8.5. Profile of air temperatures on the boundary layer. 1) wall temperature less than T_r ("cold" wall); 2) wall temperature equal to T_r (heat-insulated wall); 3) wall temperature greater than T_r (hot wall). T_∞ – temperature of undisturbed flow.

The increase of the temperature of flow behind a shock is determined by its intensity, which is connected with the form of the streamlined body and with the flow rate. The biggest increase of temperature of air is observed in a normal shock. In an oblique shock the relative increase of temperature drops with the decrease of cone angle of the front part of the streamlined body.

Furthermore, the structure of a flight vehicle experiences a heat flow which appears due to transformation of part of the mechanical energy of the air flow into thermal energy by the friction in the boundary layer. In the boundary layer, due to deceleration, airspeed decreases from the value in the external flow to zero on the surface (see Fig. 8.2). The thickness of the boundary layer varies practically from zero (for instance, near the nose section of the fuselage) to several centimeters (at the afterbody).

In connection with the different character of flow in the boundary layer (laminar or turbulent) the velocity profile of air particles throughout the thickness of the boundary layer will be different (Fig. 8.4).

Near a body which is moving in a compressible fluid, not only is there a speed boundary layer in which there is observed a change of speed, but also a temperature boundary layer in which the temperature also quickly changes from its value on the boundary of the body to the value in the external (undisturbed) flow (Fig. 8.5).

The heat liberated at the surface of the body is partially transmitted to the upper regions of the boundary layer, where the flow rates are not equal to zero and full deceleration does not occur.

8.2. Forms of Heat Exchange and Basic Laws of Heat Transfer

In the theory of heat transfer three basic forms of heat exchange are considered: thermal conduction, convective heat exchange, and heat exchange by radiation. Convective heat exchange is subdivided into free and forced convection.

The basic principles of the theory of heat transfer are briefly presented below.

Thermal conduction is the transmission of heat by means of direct contact of parts of a body during micromotion of elementary particles. Thermal conduction in pure form is observed basically in solids. In this case the heat flow, i.e., the quantity of heat passing through a unit of surface in a unit of time, is determined by Fourier law:

$$q=-\lambda\frac{\partial T}{\partial y}. \qquad (8.3)$$

where λ is the coefficient of thermal conduction;

$\frac{\partial T}{\partial y}$ is the gradient of temperatures.

The sign "–" shows that the heat flow is directed opposite the temperature increase.

The values of coefficient λ are determined experimentally and can be taken from reference books.

Convective heat exchange between a fluid (gas) and a solid is divided into free and forced convection. In this instance the heat flow is determined by Newton's law:

$$q_{к}=\alpha(T_1-T_2). \qquad (8.4)$$

where α is the coefficient of heat radiation;

T_1 and T_2 correspondingly are the temperature of the fluid and the body.

The determination of coefficients of heat radiation is conducted basically by experimental means with the use of the theory of similitude. Then the connection between parameters, which determines the heat exchange, may be expressed in the form of a criterial equation of dimensionless values.

The mechanism of flow of thermal processes in unventilated sections of a structure is basically determined by free convection. The dependence between criteria of similarity in this case can be represented by exponential function:

$$Nu = C(Gr \cdot Pr)^n. \tag{8.5}$$

where $Nu = \frac{\alpha l}{\lambda_a}$ is the Nusselt number;

$Gr = \beta \frac{g l^3}{\nu^2} \Delta T$ is the Grashof number;

$Pr = \frac{c_p g \mu}{\lambda_a}$ is the Prandtl number;

$\Delta T = T_1 - T_2$ is the difference of temperatures between the surface of the body and the medium;

l is the linear dimension;

β is the expansion coefficient;

c_p is the specific heat capacity of gas at constant pressure;

C and n are constant coefficients;

λ_a is the coefficient of thermal conduction of air;

ν is the kinematic coefficient of viscosity;

$\mu = \nu\rho$ is the dynamic coefficient of viscosity.

Coefficients C and n depend on the product of Gr times Pr (Table 8.1).

Table 8.1

$Gr \cdot Pr$	C	n
$1 \cdot 10^{-3} - 5 \cdot 10^{2}$	1.18	1/8
$5 \cdot 10^{2} - 2 \cdot 10^{7}$	0.54	1/4
$2 \cdot 10^{7} - 1 \cdot 10^{13}$	0.135	1/3

The dynamic coefficient of viscosity for air at different temperatures can be determined by Sutherland's formula:

$$\mu = \mu_0 \left(\frac{T}{T_0}\right)^{3/2} \frac{1 + \frac{110.4}{T_0}}{\frac{T}{T_0} + \frac{110.4}{T_0}}. \tag{8.6}$$

where the coefficient of viscosity μ0 is selected as the value corresponding to initial temperature. For instance, for a temperature of $0^{\circ}C$ the coefficient of viscosity of air is equal to $1.75 \cdot 10^{-6}$ $kg \cdot sec/m^2$.

The coefficient of heat radiation from wall to medium of the internal section of a structure can be determined from (8.5) by the formula

$$\alpha = \frac{\lambda_c}{l} C (Gr \cdot Pr)^n. \tag{8.7}$$

This formula with values of the constants shown in Table 8.1 is applicable for any liquid and gaseous mediums when $Pr \geq 0.7$ and for bodies of any form and any dimension.

Transmission of heat by convection is closely connected with thermal conduction. For small geometric spaces the process is basically determined by thermal conduction.

Usually the small spaces in which there occurs heat exchange by means of free convection are called slots (layers). In horizontal slots the process is determined by the mutual location of heated and cold surfaces and the distance between them.

If the heated surface is located above, the circulation of air particles does not occur. If, however, the heated surface is located below, there appear ascending and descending flows alternating between one another. Therefore, in a closed limited space the conditions of flow of the process of heat exchange are considerably more complicated than in large volumes. In the theory of heat transfer such a complicated process of heat exchange is commonly considered as the transmission of heat by means of thermal conduction. This introduces the concept of equivalent coefficient of thermal conduction λ_{eq}. In the use of the equivalent coefficient of thermal conduction there is no necessity for determining the heat-transfer coefficient, since the value of λ_{eq} is found directly from experiment. Usually in calculations they determine the values of λ_{eq} by the formula

$$\lambda_{eq} = \varepsilon_{con}\lambda_{f} \qquad (8.8)$$

where ε_{con} is the coefficient which considers the influence of convection. This coefficient is also a function of the dimensionless parameters Gr•Pr.

With the values of $(Gr \cdot Pr)_f < 1000$ $\varepsilon_{con} = 1$, i.e., heat transfer from a hot wall to a cold one in layers is caused only by the thermal conduction of the medium. With values of $10^3 < (Gr \cdot Pr)_f < 10^6$,

$$\varepsilon_{con} = 0.105 (Gr \cdot Pr)_f^{0.3} \qquad (8.9)$$

and when $10^6 < (Gr \cdot Pr)_f < 10^{10}$

$$\varepsilon_{con} = 0.40 (Gr \cdot Pr)_f^{0.2}. \qquad (8.10)$$

A large influence on the magnitude of coefficient α is rendered by the form of liquid (gas) and the motion of its particles.

In ventilated sections (engine sections, equipment sections, crew cabins, etc.) transmission of heat from more heated elements of the structure to less heated ones is carried out by forced convection.

For a well-developed turbulent flow ($Re > 10^4$) in the calculation of heat exchange in channels of different size the following criterial equation is used:

$$Nu_f = 0.021 Re_f^{0.8} Pr_f^{0.43} \left(\frac{Pr_f}{Pr_w}\right)^{0.25}. \tag{8.11}$$

Subscript f indicates that the physical parameters entering the expression of criteria are taken at the temperature of flow inside the channel, and w means that the criteria are calculated taking into account the physical parameters taken at wall temperature.

A characteristic dimension for cylindrical channels is the diameter d and for channels of other form the equivalent diameter d_{eq}.

In the calculation of heat transfer from internal surfaces of ventilated sections of small curvature it is possible to use the criterial equation for a flat plate:

$$Nu_f = C Re_f^n Pr_f^{0.43} \left(\frac{Pr_f}{Pr_w}\right)^{0.25}. \tag{8.12}$$

whereby when $Re < 4.85 \cdot 10^5$, $C = 0.76$ and $n = 0.5$; when $Re > 4.85 \cdot 10^5$, $C = 0.037$ and $n = 0.8$.

Besides convection and thermal conduction, heat exchange occurs by means of radiation. Heat flow of radiation is determined by Stefan – Boltzmann law:

$$q_{rad} = \varepsilon\sigma T^4, \tag{8.13}$$

where ε is the radiation factor or blackness;

σ is the Stefan – Boltzmann constant;

$$\sigma = 4.96 \cdot 10^{-8}\ ккал/м^2 \cdot час \cdot град^4.$$

Coefficient ε lies within the limits of $0 \leq \varepsilon \leq 1$, is determined experimentally, and can be taken from a reference book.

In the calculation of the temperature field of a structure it is necessary to consider heat exchange by radiation between its separate parts. For instance, in heat exchange by radiation between parallel surfaces it is possible to use the expression

$$q_{12} = \varepsilon_{np}\sigma(T_1^4 - T_2^4), \qquad (8.14)$$

where $\varepsilon_{giv} = \dfrac{1}{\dfrac{1}{\varepsilon_1} + \dfrac{1}{\varepsilon_2} - 1}$ is the given coefficient of blackness of the system;

ε_1, ε_2, T_1 and T_2 are correspondingly the coefficients of blackness and the temperature of the first and second surfaces.

This expression can also be used for the case of heat exchange between upper and lower wing surfaces.

The basic calculation formula of radiant heat exchange between two black bodies, arbitrarily located in space, has the form

$$q_{12} = 4.96 \cdot 10^{-8}(T_1^4 - T_2^4)H_{12}, \qquad (8.15)$$

where T_1 and T_2 correspondingly are the temperature of the first and second bodies.

The mutual surface of radiation of these bodies H_{12} is calculated by the formula

$$H_{12} = \int_{F_1} dF_1 \int_{F_2} \frac{\cos\varphi_1 \cos\varphi_2}{\pi r^2} dF_2, \qquad (8.16)$$

where F_1 and F_2 are the surfaces of bodies participating in heat exchange;

φ_1, φ_2 are the angles of incidence of radiation on centers of elementary sites dF_1 and dF_2;

r is the distance between these sites.

In calculations it is more convenient to use angular coefficients determined by the relationships

$$\varphi_{12} = \frac{H_{12}}{F_1};$$

$$\varphi_{21} = \frac{H_{12}}{F_2}.$$

Coefficients φ_{12} and φ_{21} show what part of the hemispheric radiant flux, emitted by one body, drops on the other body, which is located in radiant heat exchange with the first body.

Thus, heat flow by radiation from body to body is equal to

$$Q_{12} = \varphi_{12} F_1 \sigma (T_1^4 - T_2^4). \quad (8.17)$$

On the basis of the formula for heat exchange by radiation of ideal black bodies, the radiant heat exchange between two gray bodies, arbitrarily located in space, is described by the equation

$$Q_{12} = 4.96 \cdot 10^{-8} \varepsilon_{np} (T_1^4 - T_2^4) H_{12} \quad (8.18)$$

The given coefficient of blackness of the system from two gray bodies can be approximately calculated by the formula

$$\varepsilon_{np} = \varepsilon_1 \cdot \varepsilon_2 \quad (8.19)$$

In the calculation of radiant heat exchange between gray bodies it is necessary to determine the given degree of blackness of the system (the given radiation factor).

In the determination of temperature of a structure it is important to know what role is played by radiation heat exchange between the gas and the surface of the flight vehicle. Monatomic and diatomic gases are practically transparent for thermal beams in the usual state. However, at very high temperatures, when the gas starts to pass into the "fourth state," i.e., plasma, it is necessary to consider gas radiation. Temperatures, at which the density of radiation energy σT^4 becomes equal to the density of the energy of thermal motion of particles 3/2 kTn of an ideal gas in equilibrium state, can be found from the relationship

$$\sigma T^4 = \frac{3}{2} kTn, \qquad (8.20)$$

whence

$$T = \sqrt[3]{\frac{3kn}{2\sigma}}.$$

Here n is the number of particles per unit of volume;

k is the Boltzmann constant.

At gas pressure p = 0.01 mm Hg, when the density of particles is $n = 10^{15} \frac{1}{cm^3}$ (which corresponds to an altitude of ~80 km), this temperature is equal to 40,000°K.

At high altitudes, where flights are possible with supersonic speeds, the dry air does not contain impurities of polyatomic gases (H_2O, CO_2), having considerable radiative and absorptive ability at comparatively low temperatures. Therefore, even at cosmic speed the heat flow caused by radiation is many times less the total aerodynamic heating which takes place during the return of a spacecraft to the ground.

Nonetheless, the transmission of heat by radiation from gas to skin at a speed of flight, equal to the first cosmic speed and higher, is sufficiently high and it should be considered in calculations.

Being limited to the consideration of vehicles, flying with a speed less than first cosmic, we subsequently shall disregard gas radiation.

8.3. Heat Exchange in Supersonic Gas Flows

The quantity of heat given off in the flow around a body by a gaseous medium is considered by the theory of heat exchange in a boundary layer. Transmission of heat in a laminar boundary layer is carried out basically by thermal conduction, which is prompted by heat transfer with molecules between separate layers of gas. In a turbulent boundary layer the heat is transmitted basically by the pulsational motion of macroscopic gas particles and therefore the heat transfer in it can be a few times more intense than in the laminar layer. In a mixed boundary layer both forms of heat exchange are noted. In every case the solution of the system of equations of the boundary layer has its own peculiarities, for which heat exchange in different boundary layers is considered separately.

The basic laws of the theory of heat exchange in a boundary layer permit the construction of a system of equations describing the phenomenon on the whole. These equations may be solved in certain cases with the application of contemporary computer technology. Approximate calculations can be conducted according to Newton's generalized law of heat transfer:

$$q_{conv} = \alpha(T_1 - T_w). \tag{8.21}$$

where T_1 is the gas temperature;

T_w is the surface temperature.

The coefficient of heat radiation α, by means of convection between a liquid and a solid, is determined experimentally from the following relationship:

$$\alpha = \frac{q}{\Delta T}. \tag{8.22}$$

where q is the heat flow per unit of time through a unit of area;

ΔT is the difference of temperatures of gas and solid:

$$\Delta T = T_1 - T_w.$$

For gas flows moving at low speeds the difference of temperatures in relationship (8.21) is taken as the difference between gas temperature outside the boundary layer and temperature on the surface of the body (heat flow is directed from gas to body).

In examining gas flows moving at high supersonic speeds the picture of the phenomenon of heat exchange is complicated. Since gas temperature along the thickness of the boundary layer is variable, in equation (8.21) the gas temperature is conditionally taken as recovery temperature.

In the flow around a body by a gas the temperature inside the boundary layer will differ from recovery temperature T_r; however, this temperature is conveniently used in the composition of the difference of temperatures ΔT, i.e., it may be substituted so that in these conditions

$$q_{aer} = \alpha(T_r - T_w). \qquad (8.23)$$

The use of $T_r - T_w$ for expression of temperatures has some foundation, inasmuch as it obviously satisfies the requirement of $q_{aer} \to 0$, when $T_w \to T_r$. However, the difference $T_r - T_w$ in a gas flow moving at high speeds does not have such a physical value as does the difference $T_H - T_w$ in a gas flow moving at low speeds, since the coefficient of heat radiation depends on T_w and on Mach number. However, in any case expression (8.23) is convenient to use for further analysis.

Determination of the coefficient of heat radiation at supersonic speeds is a complicated problem and at present there are comparatively exact solutions only for laminar flow along a flat plate at a zero angle of attack.

Calculations of heat transfer in a boundary layer show that the dependence of the coefficient of heat radiation on numbers Re and Pr remains the same for a compressible gas as for an incompressible liquid, and is determined by a criterial equation of the form

$$\mathrm{Nu}_w = \frac{\alpha x}{\lambda_w} = 0.332\mathrm{Re}_w^{0.5}\mathrm{Pr}_w^{1/3} f\left(M, \frac{T_w}{T_r}\right). \tag{8.24}$$

where λ_w is the thermal conduction of air at skin temperature;

x is the distance from the leading edge or the nose.

The influence of compressibility appears through factor $f(M, \frac{T_w}{T_r})$. Its exact values can be determined on graphs given in an article,* where the values of α are given taking into account the dissociation of air molecules at high temperatures.

For a turbulent flow, i.e., for a flow when $\mathrm{Re} > \mathrm{Re}_{crit} = 5\cdot 10^5$, sufficiently accurate semi-empirical dependences are obtained. For a flat plate the coefficients of heat exchange may be determined by the formula

$$\mathrm{Nu}_w = \frac{\alpha x}{\lambda_w} = 0.029\mathrm{Re}_w^{0.8}\mathrm{Pr}_w^{0.4}\left(\frac{T_w}{T_r}\right)^{0.39}\left(1 + \frac{k-1}{2} r M^2\right)^{0.11}. \tag{8.25}$$

The most intensely heated are the leading edges of bodies. Heat flow in the front critical point can be calculated by the formulas:

for an axially symmetric body

$$q_w = 0.763\lambda_w (T_0 - T_w)\sqrt{\frac{\beta}{\nu_w}}\cdot \mathrm{Pr}^{0.4}\left(\frac{\rho_0 \mu_0}{\rho_w \mu_w}\right)^{0.4}. \tag{8.26}$$

---

* V. S. Avduyevskiy et al. Fundamentals of heat transfer in aviation and rocket technology, Oborongiz, 1960.

for a flat body

$$q_w = 0.57\lambda_w (T_e - T_w)\sqrt{\frac{\beta}{\nu_w}}\,\mathrm{Pr}^{0.4}\left(\frac{\rho_{b.l.}\mu_{b.l.}}{\rho_w\mu_w}\right)^{0.4}, \qquad (8.27)$$

where the subscript "b.l." means that the physical parameters of gas are taken under the conditions on the external boundary of the boundary layer.

Magnitude $\beta = (dV/dx)_{x=0}$ is found by proceeding from the experimental distribution of pressure in the vicinity of the critical point. For the rounded edge of a body, $\beta \approx 2a_{crit}/b$, where a_{crit} is the critical speed of sound and, b is the thickness of the edge.

Besides the coefficient of heat radiation, in the determination of heating of a surfaces of a flight vehicle according to equation (8.23) it is necessary to know the recovery temperature. The latter is calculated by expression (8.2). In it the local Mach number can be found from gas-dynamic calculation or wind tests. However, for the use of dependence (8.2) it is necessary to also know another quantity, i.e., the temperature recovery factor r. The recovery factor is a composite function of a number of parameters and depends on the form of the boundary layer, the form of surface, and Mach number. Experiments showed that at low supersonic speeds for a laminar boundary layer on a flat plate $r = \sqrt{\mathrm{Pr}}$. If we take the Pr number of air to be equal to 0.70, then $r = 0.83$. For a turbulent boundary layer the temperature recovery factor on a flat plate is approximately equal to

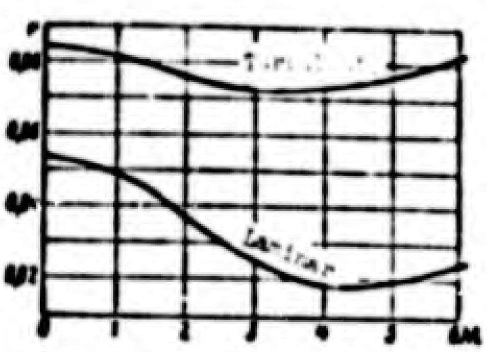

Fig. 8.6. Change of temperature recovery factor with respect to Mach number for turbulent and laminar boundary layers.

$$r = \sqrt[3]{\mathrm{Pr}}. \qquad (8.28)$$

Taking the same value of Pr = 0.70, we obtain r = 0.89.

Figure 8.6 gives the approximate change of recovery factor for a flat plate as functions of Mach number. Since there is usually observed flowing around (laminar and turbulent), in the use of the given formulas it is necessary to determine the moment of transition of the laminar boundary layer (Re_{crit}) to the turbulent one.

Transition of boundary layer from laminar to turbulent depends on many factors. In particular, an increase of Mach number decreases the influence of the degree turbulence of the incident flow on the position of the transition point. Surface roughness promotes transition of boundary layer from laminar to turbulent. However, the influence of roughness decreases with the increase of Mach number. Cooling of the boundary layer delays the onset of transition of the laminar layer to the turbulent.

In ordinary conditions on a flat plate the transition of a laminar boundary layer to a turbulent one is noted at approximately $Re = 0.5 \cdot 10^6$.

The process of heat transfer at flow rates, corresponding to Mach number more than 5, is complicated by the processes of dissociation and ionization of air due to high temperatures which arise in this instance. Processes of dissociation and ionization (and inverse processes of recombination) occur with terminal velocities. In these conditions the boundary layer experiences thermochemical reactions in which the heat transfer depends on the rate of the chemical reactions, the diffusion, and the catalytical properties of the wall.

The physical essence of the phenomenon in broad terms may be characterized in the following way. At a high air temperature behind a normal shock wave and in the boundary layer the atoms dissociate into ions. This expends a certain amount of energy, which lowers the temperature of flow. For instance, at a speed of flight $M = 20$ the stagnation temperature of gas without taking into account dissociation should be $17{,}500^{\circ}K$, and taking into account absorption of energy for dissociation it will be $6500^{\circ}K$.

Ions diffuse towards the wall, the temperature of which is less than the temperature of dissociation and can have catalytical properties.

In the recombination of ions near the wall the heat absorbed by the gas during ionization is released.

Specific heat flow to a body q_{aer} is defined as the sum of heat flow due to thermal conduction and diffusion, where the considered heat flow at the expense of diffusion is included when there occurs recombination of atoms on the wall. Conducted experimental research in the determination of temperatures at different Mach numbers at which dissociation is noted, confirmed the role of dissociation in the process of heat exchange. Calculation and experimental data show that a disregard of the phenomenon of dissociation of air molecules in the process of gas-dynamic heat exchange on the surface of a structure can lead to considerable errors.

In the composition of an equation of heat balance, the flows brought to the skin surface are taken with the sign "+," and those withdrawn have the sign "-."

A basic member of the equation of heat balance, characterizing the temperature of a structure in a wide range of speeds and altitudes of flight, is the convective heat flow which is determined in accordance with equation (8.23).

The coefficient of heat radiation α is determined depending upon the character of flow according to equations (8.24)-(8.27). At hypersonic speeds one should consider the influence of dissociation on heat transfer.

From the skin surface the thermal energy is radiated into the surrounding space. Heat of radiation into the surrounding space depends on the wall temperature and emissivity of the surface:

$$q_{rad} = \varepsilon\sigma(T_w^4 - T_H^4).$$

Up to Mach numbers M = 2.0 to 2.5 the magnitude of radiation heat is insignificant. According to the increase of speed and altitude of flight, its role in the heat balance of a structure is increased.

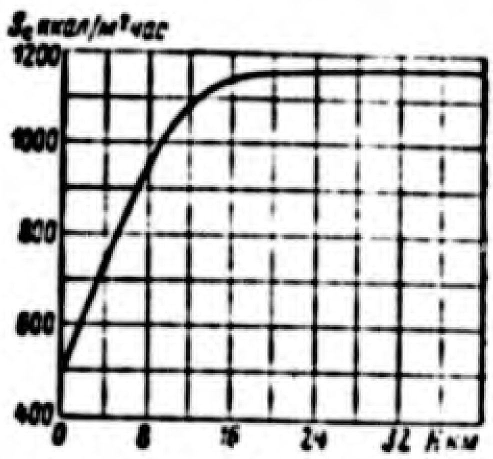

Fig. 8.7. Change of solar heat flow according to altitude H.

For instance, by calculations during flight at an altitude of 15 km and speed M = 2, the temperature of a flat plate will be less than the temperature of the adiabatic wall by 10°C; during flight at an altitude of 30 km and M = 5, the temperature of a flat plate at the expense of radiation will be lower (for instance, when ε = 0.8 at a point at a distance of 1 m from the leading edge the temperature will be 740°K, i.e., 460° less than T_r).

In many cases for steady-state conditions of heating q_{aer} and q_{rad} are decisive in the heat balance of a structure.

Besides the enumerated heat flow, a flight vehicle is influenced by thermal solar energy. The heat flow of the Sun q_s is determined by the expression

$$q_s = \beta_s S_s \cos\varphi. \qquad (8.29)$$

where β_s is the coefficient of absorption of solar energy by the surface of the craft;

S_s is the flow of solar energy;

φ is the angle between a solar ray, striking a given point of surface, and the normal to this surface.

The magnitude of solar heat flow is increased with the growth of the altitude of flight.

As can be seen from Fig. 8.7, the change of solar heat flow occurs up to an altitude of 22 km (in reference to mean latitudes). Above this altitude the solar heat flow is considered to be constant and equal to the solar constant $S_s = 1140$ kcal/m^2•hr.

The heat proceeding directly from the surface of an engine is transmitted to the structure and the skin, and is located near the equipment. It is considered that nearly two percent of the heat during fuel burning in turbojet engines goes through the engine walls into the surrounding space. For a preliminary estimate, the heat flow from an engine may be taken as equal to

$$q_{дв} = 0.001 \frac{c_e P H_u}{F_{об}} \text{ ккал/м}^2 \text{ час}, \qquad (8.30)$$

where c_e is the specific fuel consumption of an engine in kg/kg thrust per hour;

P is the engine thrust in kg;

H_u is the lowest calorific value of fuel in kcal/kg;

F_{sk} is the area of skin, surrounding the engine, in m^2.

Relatively weak sources of heat (electronic equipment, electrical equipment, radio equipment, heat exchangers, and so forth), rendering thermal influence basically only on themselves and on the equipment closely connected with them, are considered only in certain problems of heating.

Heat flow from electronic equipment q_{equip} is calculated from the condition that approximately 95% of the power drain of the equipment goes for thermal losses. Part of this heat goes for increasing the natural temperature of the equipment, and another part is given off into the surrounding space. A certain part of the heat proceeding to a structure is removed from the surface. The magnitude of this heat flow is determined by Fourier's law:

$$q_{\text{тепл}} = -\lambda\left(\frac{\partial T}{\partial y}\right)_w. \qquad (8.31)$$

The sum of all enumerated heat flows of a structure also composes the heat balance, which is written out in the following manner:

$$q_{\text{аппар}} + q_c + q_{\text{эл}} + q_{\text{об}} - q_{\text{изл}} - q_{\text{акк}} = 0. \qquad (8.32)$$

8.4. Analysis of Heat Flow

In the steady-state process of heat exchange the magnitude of heat accumulated by a structure is equal to zero:

$$q_{\text{акк}} = 0.$$

Equation (8.32) may be written out in expanded form:

$$\alpha(T_r - T_w) + \beta_c S_c \cos\varphi + q_{\text{об}} + q_{\text{эл}} - \varepsilon\sigma(T_w^4 - T_H^4) = 0. \qquad (8.33)$$

The solution of this equation gives the highest possible (steady-state) temperature of the structure of a flight vehicle under the given flight conditions.

During one-dimensional heating of a thin plate (skin) the solution of equation (8.33) for non-stationary conditions is expressed in the form

$$T = T_r - (T_r - T_{\text{нач}})e^{-\frac{\alpha}{c\gamma\delta}t}. \qquad (8.34)$$

where T_{init} is the initial skin temperature;

δ is the skin thickness;

c is the specific heat capacity of the skin material;

τ is the time of heating;

γ is the specific weight of the skin material.

Heating of the skin will set in when $T = T_r$. Steady-state heat exchange for thin-walled structures of a flight vehicle can occur after several minutes of flight under the same conditions.

Equation (8.33) may be solved graphically. The magnitudes of temperatures of the steady-state process of heat exchange, calculated by this equation, are shown in Fig. 8.8. These values are obtained without taking into account the heat flow of solar radiation and the internal airborne sources of heat.

The relative role of different heat flows in the common heat balance under certain conditions is different and it depends on the altitude and speed of flight. Calculations show that during flight at comparatively low speeds, $M = 1.5$ to 2.0, and altitudes, $H = 10$ to 15 km, the skin temperature is very close to recovery temperature T_r. With an increase of the speed of flight ($M > 2.5$ to 3.0) at altitudes less than 30 km, the skin temperature is strongly increased. The heat absorbed by the surface of the flight vehicle, as a result of atmospheric and solar radiation, then remains negligible as compared to the heat released in the boundary layer. In these conditions, besides the considered heat flows, thermal radiation from the surface of the structure begins to play a significant part, and skin temperature essentially differs from T_r. A disregard of the calculation of heat flow due to radiation from the surface of a flight vehicle when $M > 3$ leads to large errors.

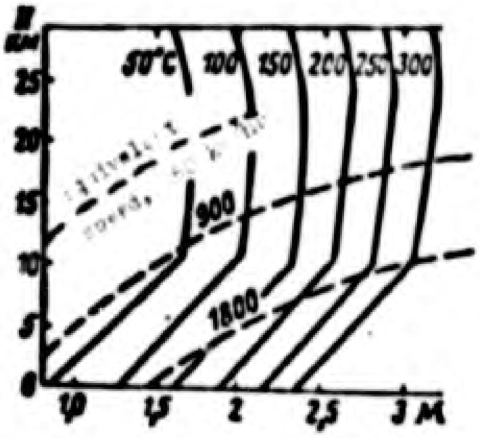

Fig. 8.8. Curves of equal steady-state skin temperatures as functions of Mach number and altitude of flight H.

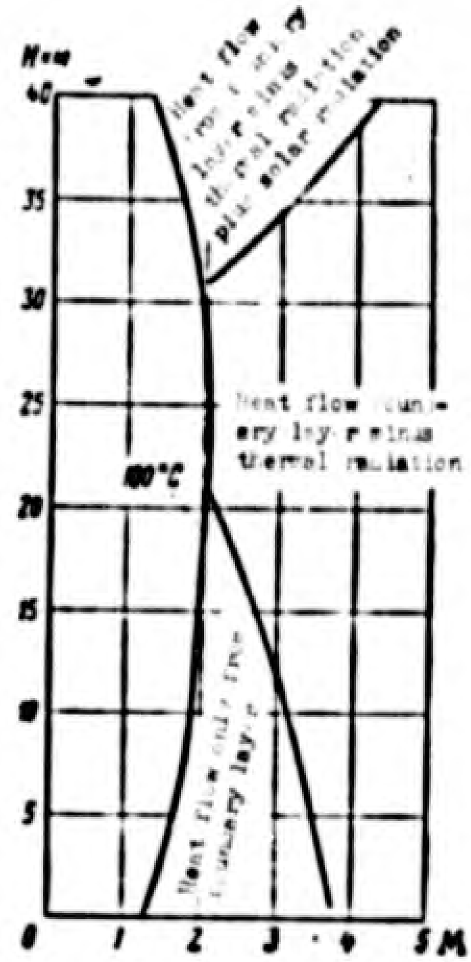

Fig. 8.9. Regions of conditions of flight and heat flow which are predominant in the common heat balance.

At altitudes H > 30 km the heat of solar radiation becomes commensurate with the remaining heat flow in view of the decrease of q_{aer}. Solar radiation cannot be considered for parts of a flight vehicle if the angle of inclination of a solar ray from the normal to the surface of the structure is $\varphi > 20^{\circ}$.

The relative significance of different heat flows in the common heat balance is shown in Fig. 8.9, where the regions of conditions of flight are given, which show the components of heat balance that determine the magnitude of steady-state temperature in these regions.

During heating of air behind a shock wave its intensity of radiation is increased. At transonic speeds behind a normal shock wave the intensity of radiation of air is so great that it is able to create flows of radiant energy, which strike the frontal area, of the same order as convective heat flow.

In the solution of the equation of non-stationary heat balance on the surface of a structure in the form

$$\alpha(T_r - T_w) + \beta_s S_s \cos\varphi - \varepsilon\sigma(T_w^4 - T_H^4) = -\lambda\left(\frac{\partial T}{\partial y}\right)_w \qquad (8.35)$$

it is necessary to consider the dependence of temperature in structural elements on the coordinate and time.

The temperature field of a solid is generally determined by a Fourier equation:

$$\frac{\partial T}{\partial \tau} = a\left(\frac{\partial^2 T}{\partial x^2} + \frac{\partial^2 T}{\partial y^2} + \frac{\partial^2 T}{\partial z^2}\right) \qquad (8.36)$$

In a one-dimensional temperature field the equation has the form

$$\frac{\partial T}{\partial \tau} = a\frac{\partial^2 T}{\partial y^2}, \qquad (8.37)$$

where a is the coefficient of thermal conductivity:

$$a = \frac{\lambda}{c\gamma}.$$

The first integral in the coordinate of this equation will be

$$c\gamma\int_0^\delta \frac{\partial T}{\partial \tau}dy = \lambda\left(\frac{\partial T}{\partial y}\right)_\delta - \lambda\left(\frac{\partial T}{\partial y}\right)_w, \qquad (8.38)$$

where δ is the thickness of a structural element.

In the absence of heat release from the internal surface (when y = δ) and at constant temperature along the thickness, we have

$$-\lambda\left(\frac{\partial T}{\partial y}\right)_w = c\gamma\delta\frac{dT_w}{d\tau}. \qquad (8.39)$$

Consequently, the equation of non-stationary heating of a thin skin will be

$$\alpha(T_r - T_w) + \beta_s S_s \cos\varphi - \varepsilon\sigma(T_w^4 - T_H^4) = c\gamma\delta\frac{dT_w}{d\tau}. \qquad (8.40)$$

The solution of equation (8.39) can be obtained by a numerical method. For instance, upon replacement of the derivative dT_{t_w}/dt with finite differences, we have

$$\Delta T_{wi} = \frac{\Delta\tau_i}{c\gamma\delta}\left\{\alpha_{i-1}(T_{ri} - T_{w,i-1}) - 4.9\cdot 10^{-8}\varepsilon(T^4_{w,i-1} - T^4_H) + A_s S_t \cos\varphi\right\}. \qquad (8.41)$$

where i is the number of the calculation interval.

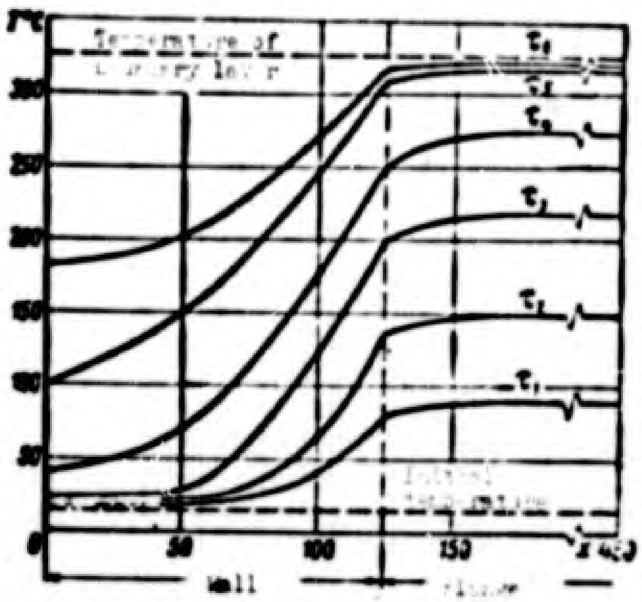

Fig. 8.10. Temperature field of the wall of a spar and skin for different durations of heating. x – distance from center of wall

In the presence of a gradient of temperatures on a structural element, there can be obtained a solution to equation (8.36) under corresponding boundary conditions.

Figure 8.10 gives the approximate change of temperature field of the system skin – wall in different intervals of time of heating τ_1, τ_2,... τ_6.* From these curves one may see when and where it is possible to expect the biggest gradients of temperatures.

Figure 8.11 shows the approximate distribution of temperatures for a section of a thin-walled wing at an angle of attack different from zero. Calculation is conducted on the assumption of the absence of heat transfer of sections inside the wing and internal thermal radiation. Due to the radiant heat exchange between structural

*F. Rohle and H. Oliver. Temperature Distribution and Thermal Stresses in a Model of a Supersonic Wing, IAS, V. 21, N I, 1954.

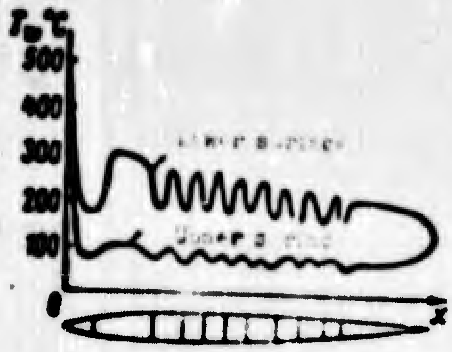

Fig. 8.11. Temperature field of the surface of a thin-walled wing.

elements the temperature gradients, especially for the walls, will be considerably lower.

8.5. Thermal Stresses

Calculation of temperature fields of the structure of a flight vehicle and data on the thermal-physical and mechanical properties of materials during heating permit the conducting of a strength analysis of the structure. The basic principles of the calculation of structural elements remain the same as under conditions of ordinary temperatures. However, at raised temperatures there appear many new phenomena which should be considered during calculations. In the first place they include the mechanical properties of the materials and the thermal stresses. Thermal stresses in structural elements appear both due to the temperature gradient, and also owing to the different in coefficients of linear expansion for various metals. Thermal stresses can lead

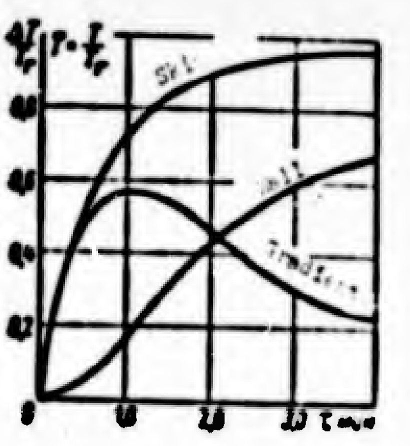

Fig. 8.12. Change of temperature drop and temperature gradient, with respect to time of heating.

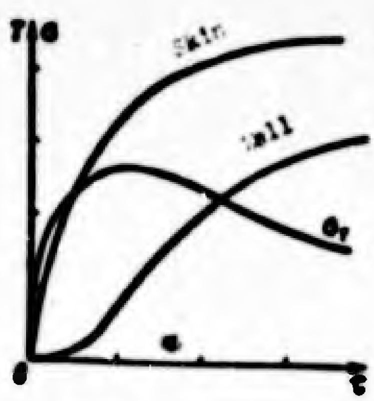

Fig. 8.13. Character of thermal stresses appearing in a wall during heating.

to loss of stability of individual structural elements and to a change in the rigidity of the structure. The structure can then be deformed due to the thermal stresses without an external load. In this case the structure has as if zero rigidity, which must be considered in the strength analysis of structures under conditions of raised temperatures, inasmuch as a change of rigidity in many respects determines the critical flutter speed, divergence, and so forth.

It is usually considered that up to the moment of onset of the yield point the magnitudes of thermal stresses and stresses from external load are added up algebraically. With the onset to destruction, i.e., upon exceeding the yield point, the thermal stresses quickly decrease.

In conditions of non-stationary heating in the structure of a flight vehicle there appear temperature drops both along the length of a structural element, and also along its thickness (in the case of massive structural parts).

Figure 8.12 gives an example of the change of relative temperature $\bar{T} = T/T_r$ of the skin and wall of a structural element and the relative gradient of temperatures $\Delta T/T_r$ in the structure with respect to time of acceleration of a flight vehicle. In the beginning of acceleration the difference of temperatures between the skin and the wall reaches its maximum. The temperature gradients lead to thermal stresses in structural elements.

Knowing the magnitude of the coefficient of linear expansion α, the change of length of a structural element during heating can be determined by the formula

$$\Delta l = \alpha l(T - T_{[illegible]}) \qquad (8.42)$$

If all structural elements can be freely expanded or compressed, the change of temperature does not cause stresses. However, expansion or compression of structural elements usually cannot occur freely. Due to this, in them there appear thermal stresses. Furthermore, external enclosure of a structural assembly prevents the change of length of its elements during heating, which leads to the appearance of thermal stresses.

Deformations Δl of a structural element are connected with stresses σ by a known relationship

$$\Delta l = \frac{\sigma l}{E}. \tag{8.43}$$

If the length of an element cannot be changed, then the elongation caused by the change of temperature (8.42) is removed by the action of equivalent thermal stresses σ_T. Consequently, it is possible to write

$$\alpha(T - T_{\text{нач}})l = -\frac{\sigma_T l}{E}, \tag{8.44}$$

whence

$$\sigma_T = -\alpha E(T - T_{\text{нач}}). \tag{8.45}$$

The sign "-" indicates that with an increase of temperature there appear compressive stresses.

Magnitudes E and α, entering equation (8.45), depend on the temperature of heating of the structure. The approximate change of thermal stresses is shown in Fig. 8.13. The maximum value of σ_T corresponds to the moment of appearance of maximum temperature gradient.

Calculation formulas of thermal stresses are generally very complicated. They may be simplified by allowing that if the

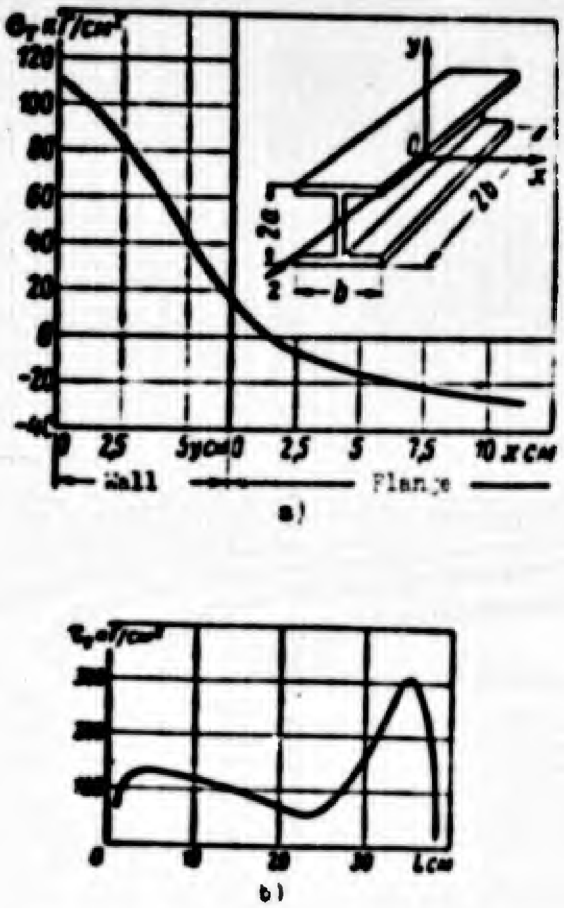

Fig. 8.14. Normal (a) and tangential (b) thermal stresses in the wall of a spar during non-stationary heating.

considered section is sufficiently far from the ends of the structural elements, the distribution of thermal stresses does not depend on the enclosure conditions, i.e., the hypothesis of flat sections is taken. Furthermore, it is considered that the temperature field is one-dimensional. The use of symmetry of cross sections of profiles permits simplifying the calculation of stresses.

However, in spite of these simplifications, the dependences for thermal stresses are quite complicated. Calculation formulas of thermal stresses for elements of different form are presented in corresponding reference literature and special handbooks.

In practice, thermal stresses, both in individual elements and also in complex structures, are determined experimentally. For this, electrical tensometers are applied.

As an example, Fig. 8.14a, gives a graph of normal thermal stresses on an average cross section of a welded beam, appearing during non-stationary heating, at the time of maximum gradient of temperatures. Tangential stresses, measured on the wall near one of the ends of the beam and near the connection of the wall to the band in the same moment of time, are shown in Fig. 8.14b. In this case the maximum tangential stress arises in the section close to the end of the beam.*

If in a certain zone the stress of a structural element exceeds the yield point, the distribution of thermal stresses is changed as compared to their distribution according to the law of elastic deformation. In this case the maximum thermal stresses are lowered.

At transient temperature the stress depends not only on the position of the point in a section of the structural element, but also on the duration of heating.

Stresses from an external load and thermal stresses may be summarized if each of them and their sums are in an elastic zone. When any of these stresses or their sums are in a plastic zone, the stresses may be summarized by proceeding from deformation curve. The equations are then composed in total deformations. For instance, in the case of uniform temperature during heating of the skin — stringer connection, made from different materials, the calculation equations have the form

$$\left.\begin{aligned} \varepsilon_{об} &= \frac{\dfrac{P}{F_{стр}E_{стр}} - (\alpha_{об}T_{об} - \alpha_{стр}T_{стр})}{1 + \dfrac{b\delta E_{об}}{F_{стр}E_{стр}}}; \\ \varepsilon_{стр} &= \varepsilon_{об} + (\alpha_{об}T_{об} - \alpha_{стр}T_{стр}). \end{aligned}\right\} \quad (8.46)$$

The subscripts "sk" and "strin" designate the magnitudes pertaining to the skin and stringer, respectively.

Dependences of stresses on relative time $\bar{\tau}$, obtained during heating of the skin — stringer connection, are shown in Fig. 8.15. Here $\bar{\tau}$ is equal to the ratio of time of heating to time of acceleration (from start to emergence into steady-state conditions). In

---

*G. Isakson. A simple Model Study of Transient Temperature and Thermal Stress Distribution due to Aerodynamic Heating, IAS, VIII, V. 24, N 8, 1957.

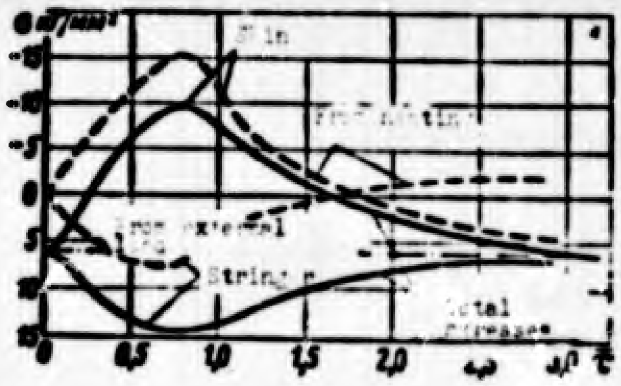

Fig. 8.15. Total stresses from an external load and temperature.

spite of the fact that stresses in no moment of time reach the yield point, they nevertheless differ from those which would be obtained from the addition of elastic stresses to the normal stresses from an external load. After the application of an external load in some time interval in the beginning of acceleration ($\bar{\tau}$ varies from 0 to 0.6) the stresses from the external load and heating are summarized. When $\bar{\tau} > 0.6$, due to the plastic deformation of the stringer the character of summation of stresses is changed and simple addition becomes impossible.

8.6. Influence of Heating on Characteristics of Materials

Strength During Brief Loading

During heating the basic mechanical characteristics of materials σ_b, E, and G are lowered. Figures 8.16-8.17 give approximate graphs of the change of these characteristics with the increase of temperature of material during brief loading.

Strength of a material under the action of tangential stresses in conditions of brief loading during heating changes approximately the same as under the action of normal stresses. Relationships, which exist between σ and τ at ordinary temperatures, also remain at high temperatures.

During heating also the strength of joints of structural elements (rivets, bolts, and welds) is lowered. The dependence between shear strength τ_{shear} and temperature hardly differs from a broken line consisting of two segments of straight lines. With a certain assumption this dependence (up to defined temperatures) for simplification of calculations may be approximated by a linear function. For instance, the dependence for permissible shearing stresses may be written in the form

$$\left.\begin{aligned} \tau &= \tau_{init}\left[1 - a\left(\frac{T}{T_{init}} - b\right)\right] \text{ at } \frac{T}{T_{init}} > b, \\ \tau &= \tau_{init} \text{ at } \frac{T}{T_{init}} < b, \end{aligned}\right| \tag{8.47}$$

where a and b are the corresponding experimental coefficients;

τ_{init} is the shear strength at $T_{init} = 20°C$.

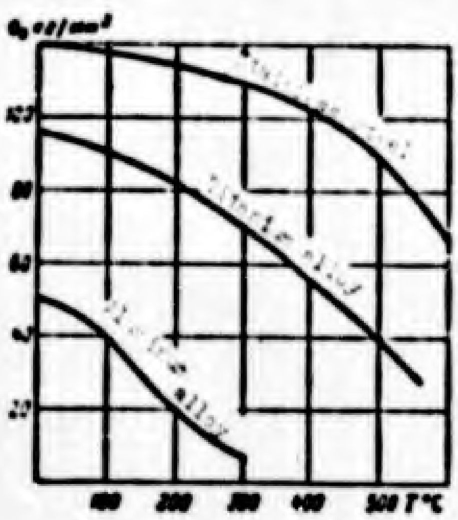

Fig. 8.16. Change of ultimate strength σ_b of certain alloys, depending upon temperature.

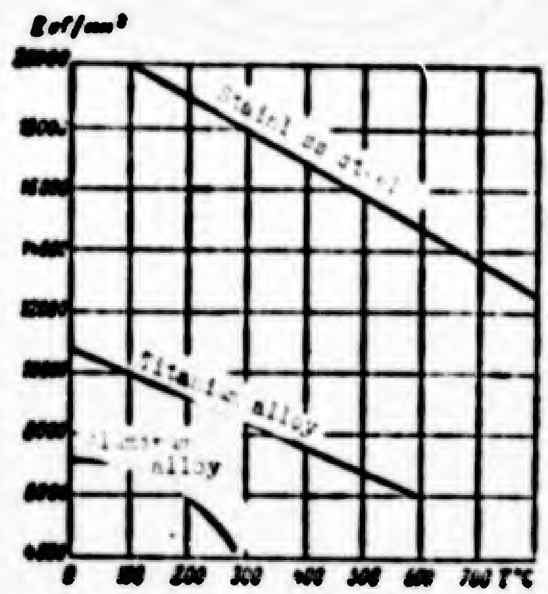

Fig. 8.17. Change of the first elastic modulus E of structural alloys, depending upon temperature.

When $\frac{T}{T_{init}} > b$ the breaking load of a riveted joint is

$$P = n\frac{\pi d^2}{4}\tau_{init}\left[1 - a\left(\frac{T}{T_{init}} - b\right)\right]. \tag{8.48}$$

where d is the diameter of the rivet;

n is the number of rivets.

Inasmuch as various materials have a different character of change of basic mechanical properties with the increase of temperature, for every type of structure the temperature zones of possible use of a certain material are determined. In conditions of steady-state heat exchange of a flight vehicle the zones of permissible temperatures for each material can be reduced to the conditions of flight with respect to Mach numbers and altitudes H.

Fatigue Strength of Materials at Raised Temperatures

At raised temperatures, simultaneously with the lowering of static characteristics, there is a considerable lowering of the fatigue strength of materials. The fatigue strength of materials during heating is influenced not only by loading cycles, but also by temperature cycles. In connection with this it is necessary to consider considerably larger variants of loading. In practice there are wide-spread investigations which are similar to the investigations of the characteristics of fatigue strength at normal temperature, i.e., tests are conducted at constant temperature and with variable stresses.

Furthermore, there is a form fatigue testing at raised temperatures, which is different from testing at room temperature. In these tests, along with the change of the load in a defined cycle, there also occurs cyclical heating.

In the investigation of fatigue strength in conditions of high temperatures, tests are used in which thermal stresses are created in the plastic region of deformation owing to cyclical heating and loading. Upon lowering the temperature to its initial value the stress changes sign due to the preceding plastic effect. The latter may cause plastic deformation in the opposite direction. Such a phenomenon strongly lowers the characteristics of fatigue strength of material.

In actual designs, during a change in temperatures there can appear large thermal stresses which in turn can lead to a lowering of the characteristics of fatigue strength. Such a form of loading of material is observed in practice, for instance during heating and cooling of the skin connected to a wing rib.

Besides the slow build-up of destruction from fatigue, the material can experience rather fast destruction from a considerable gradient of temperatures. For instance, if a body is subjected to the action of a sharp gradient of transient temperature, which causes large thermal stresses, there appears a state of thermal shock. Since certain materials are influenced by the rate of build-up of stresses, they can behave differently during thermal shock than during the usual thermals stresses or stresses caused by an external load.

In a thermal shock (fast heating) there appears a surface compressive stress and destruction of surface can occur from chipping or from shear stresses caused by compression. Furthermore, there can appear cracks not on the surface, but in the depth of the material. The magnitude of the biggest tensile stress depends on the time of heating and the thermal conduction of the material. If the material conducts heat poorly, then in a short time the thermal shock will spread only on the fibers nearest to the surface. In this case on surface there appear high compressive stresses. Tensile stresses in the remaining part will be low, since high compressive stresses in small number of fibers are balanced by extension of almost the entire body. If the material is a good conductor of heat, then at a determined moment the compressive surface tension on the surface will be lower than in a poor conductor; however, a large quantity of fibers will be subjected to compression, and therefore the tensile stress in the remaining part will be larger. Thus, under certain conditions a material having good thermal conduction with respect to resistance to thermal shock will be worse than material with poor thermal conduction.

In order to select best material it is necessary in detail to consider the conditions of its application and the assignment of the article.

Creep of Materials During Heating

The strength of materials at raised temperatures depends not only on the magnitude of the load and the temperature, but also on the duration of action of the load. Strength during prolonged loading will be lower than the strength during brief loading. The longer the time the material is under a load in conditions high temperatures, the more its strength is lowered.

Lowering of ultimate strength with the increase of time of action of a load in conditions of high temperatures is explained by the fact that a material under a constant load starts to be plastically deformed. The property of materials to be continuously plastically deformed due to the prolonged action of a load is called creep. The phenomenon of creep may be explained in the following way. As a result of the application of a load, in the material there occurs plastic deformation which is accompanied by hardening (cold hardening). However, at a high temperature there appears the

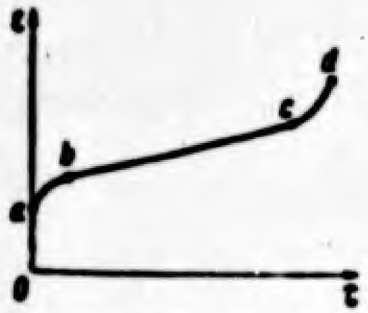

Fig. 8.18. Typical curve of creep of material.

process of recrystallization (removal of cold hardening), i.e., a softening process, and the material continues to be continuously deformed. The rate of deformation (creep) depends on the temperature and magnitude of the load.

The relationship between the processes of hardening and softening of material changes with the passage of the time of loading.

Figure 8.18 gives a typical curve of creep in the form of the dependence of increase of relative deformation ε on time τ. On section a-b of the creep curve the hardening process prevails. On section b-c the hardening process and the softening process are in equilibrium. On section c-d the softening process prevails.

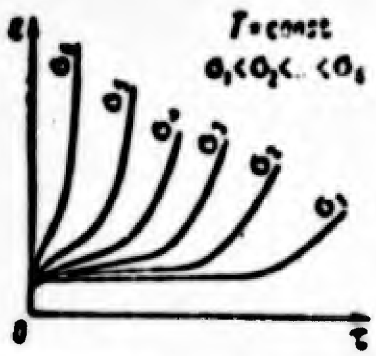

Fig. 8.19. Approximate change of the characteristics of creep with the increase of stresses.

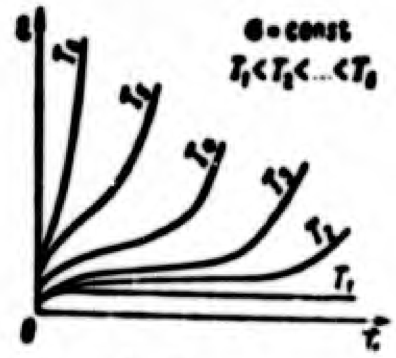

Fig. 8.20. Approximate change of the characteristics of creep with the increase of temperature.

The stage of the creep process with constant speed has been best studied (section b-c of the curve). It is necessary to emphasize that the rate of creep is strongly influenced by stress in the material of a structural element. The lower the stress, the less the slope of section b-c and the lower the creep rate, i.e., an increase of relative deformation per unit of time (Fig. 8.19).

Calculation of deformation from creep is especially important in the strength analysis of flight vehicles which have a low safety factor, in consequence of which the structural elements will be under the action of large stresses. In this case it is necessary to standardize the permissible permanent deformations caused by creep in one flight or in the whole service life of the flight vehicle.

For supersonic aircraft with the usual safety factor, the stresses effective in structural elements during horizontal flight are such that the creep rate is small.

Increase of temperatures leads to increase of creep (Fig. 8.20). Inasmuch as materials applied in flight vehicles are subject to creep at raised temperatures, during the prolonged action of a load the structure can obtain large deformations. So that these structural deformations do not exceed the allowed magnitudes, the effective stresses from the external load are decreased. The latter is attained by the fact that in calculations such an allowed stress is given, which in a defined time will cause only a defined given allowed deformation.

Influence of Heating on the Thermal-Physical Properties of Materials

With the increase of temperature there is a change not only in the mechanical characteristics of materials, but also in their physical and chemical properties: thermal conductivity, heat capacity, the coefficient of linear expansion, and also the properties connected with corrosion. The coefficient of thermal conduction of a material depends on the temperature. For an overwhelming majority of materials, linear dependences of the following form are valid:

$$\lambda = \lambda_{in}(1 + BT). \qquad (8.49)$$

where λ_{init} is the coefficient of thermal conduction at 0°C;

B is a constant determined experimentally.

In practical calculations the value of the coefficient of thermal conduction is usually taken for the average temperature of the considered range.

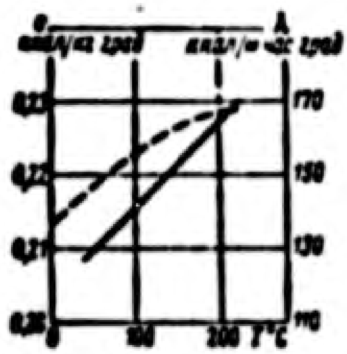

Fig. 8.21. Change of the thermal-physical properties of an aluminum alloy with respect to temperature. —— heat capacity, --- thermal conduction.

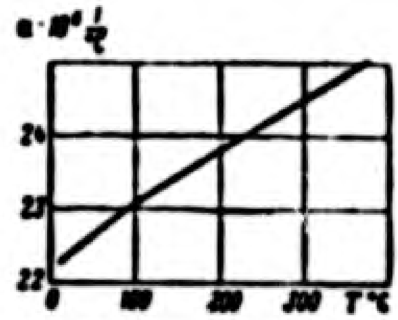

Fig. 8.22. Change of the coefficient of linear expansion of an aluminum alloy with respect to temperature.

The coefficient of thermal conduction of metals lies within the limits of values of λ = 10-360 kcal/m·hr·deg. For instance, for duralumin $\lambda \sim$ 140-160 kcal/m·hr·deg; titanium ~12-18; steel ~30-50; nickel alloy ~10-14. With the increase of temperature the coefficient of thermal conduction for the majority of metals decreases and for aluminum alloys it increases.

Together with the coefficient of thermal conduction, during heating there is a change in another characteristic, i.e., the specific heat capacity (Fig. 8.21). The mean value of heat capacities for aluminum alloys consists of 0.22 kcal/kg·deg, for titanium 0.15, and for steel 0.1.

In the investigation of the state of strain of structures, of large value is the coefficient of linear expansion. Its magnitude is also changed with the increase of temperature (Fig. 8.22).

Materials applied for the manufacture of aircraft structures are presented with requirements of high corrosional stability in various media and at different temperatures. There is chemical, gas, and electrochemical corrosion. Chemical corrosion is the process of destruction of a metal as a result of simple chemical interaction of it with the external medium. Under ordinary temperature conditions all structural materials as a rule well resist this form of destruction. Small chemical activity of materials is determined by the presence of a protective oxide film on their surface. However, at raised temperatures this film is usually destroyed.

Gas corrosion is the destruction of a material as a result of its interaction with gases at high temperatures. Gas corrosion in the first place is the result of the interaction of materials with air. The basic components of air — oxygen and nitrogen — while influencing a metal, saturate its surface layer and form different chemical compounds, i.e., oxides and nitrides, which are products of corrosion. Gas corrosion is accompanied not only by destruction of a metal or an alloy due to the formation of chemical compounds, but also by a change in the properties of the metal owing to its saturation by oxygen and nitrogen. With the increase of temperature, gas corrosion is increased.

In the manufacture of components from such materials as duralumin and titanium, on their surfaces there will form a so-called modified layer (an oxide-nitride film) which possesses increased strength and lowered plasticity, and hampers further corrosion. The diffusion rate of oxygen through a protective film at low temperatures is very small, owing to which the metal is reliably protected from further destruction. At raised temperatures (for duralumin $T > 200^{\circ}C$ and for titanium $T > 550^{\circ}C$) diffusion through the film is intensified and the metal starts to be destroyed faster. For the majority of metals, with the increase of temperature the rate of gas corrosion increases (approximately according to exponential law).

Selection of Materials for Work in Conditions of Raised Temperatures

In designing a flight vehicle, taking into account the influence of temperature and time of load action, there appears the necessity of extensive analysis of the properties of materials. All those changes, which were briefly considered above, force us to approach the evaluation and selection of materials in a new fashion.

At present there are several approaches to the solution of this problem.

Since a structure which can sustain an assigned load with the lowest gravity should be considered the most effective as a parameter for the comparison of the effectiveness different materials in the first place we take the ratio of permissible stress to specific weight of the material σ_{per}/γ or the so-called specific strength. The most convenient will be the material having the highest of value σ_{per}/γ. However, there exist many forms of permissible stresses, depending upon the type of load, the geometry of the structure, and the temperature (compression, shear, longitudinal bending, loss of stability, yield origin, etc.). A material which is the most suitable for one form of state of strain can be very unsuitable for other. Therefore,

STOP HERE STOP HERE

it is sometimes necessary to use the magnitude E/γ – specific rigidity – since the characteristics of rigidity have large value for the design of contemporary flight vehicles.

In analyzing the change of the mechanical characteristics of materials, it is possible to estimate the approximate temperature boundaries of their application. Thus, elementary calculations show that up to ~200-250°C the most suitable materials are aluminum alloys; up to 450-500°C – titanium alloys; up to 700-750°C – heat-resistant steel; and up to 900-1000°C – special heat-resistant alloys. However, in certain cases, caused by the specific peculiarities of the given form of design, these materials can be applied at temperatures higher than those shown.

8.7. Calculation of Heating During Designing

In the structure of a flight vehicle in conditions of flight at high hypersonic speeds there are possible numerous combinations of stresses from an external load and heating. Determination of the most severe combinations of these stresses, with respect to strength, requires the consideration of not only the limiting conditions as regards maximum loads, but also the conditions of heating. In other words, such an analysis requires data about the weight and speed of the vehicle, the altitude and the time of flight.

Obtainment of the necessary strength of structures in conditions of heating is connected with the increase of relative weight of the structure in view of the impairment of the mechanical properties of materials and the addition of thermal stresses to stresses from the load. In a number of cases it is expedient to conduct measures for lowering the heating of a structure and for decreasing the temperature gradients. For instance, thermal insulation is used in flights of short duration at high supersonic speeds. The total weight of the structure and thermal insulation can be less than the weight of only one structure which was made taking into account the lowering of mechanical properties of heated materials. In view of shown difficulties in a long flight at high supersonic speed, thermal insulation and cooling should be applied.

For preventing excessive thermal stresses it is necessary to provide the structural elements with the possibility of displacements appearing from thermal expansion. However, it is difficult to provide a structure with the required freedom of displacements while still preserving the rigidity of the structure. Facilitation, of the fulfillment of this task,can be promoted by the application of corrugation for thin spar walls. In conditions of aerodynamic heating the weight of the structures of high-speed flight vehicles is increased due to a lowering of the strength characteristics of the material, the appearance of thermal stresses during non-stationary heating, and also because of the application of thermal insulation, which is necessary for decreasing the temperature of the supporting members of the sturcture, and the installation of a cooling system.

For an estimate of the relative increase of weight of a structure we introduce a dimensionless parameter G, i.e., the ratio of the weight of a unit of area G_T of a panel perceiving operational loads during heating to the weight of a unit of area G_0 perceiving the same load without heating:

$$\bar{G} = \frac{G_T}{G_0}. \tag{8.50}$$

Magnitudes G_T and G_0 can be calculated in each specific case.

8.8. The Influence of Heating on the Aeroelastic Characteristics of a Structure

For the convenience of estimating the rigidity of a structure it is expedient to retain the usual equations of structural mechanics, which connect external loads with structural deformations. However, in this case the geometric constants of a section, multiplied by the corresponding elastic moduli (EJ, GJ_p), must be considered as effective rigidities which are variable in magnitude depending upon temperature and temperature gradients. As an example we shall consider the change of effective rigidities of a continuous double-wedge wing. For the calculation of temperatures and thermal stresses we shall take the flight profile which is represented in Fig. 8.23.

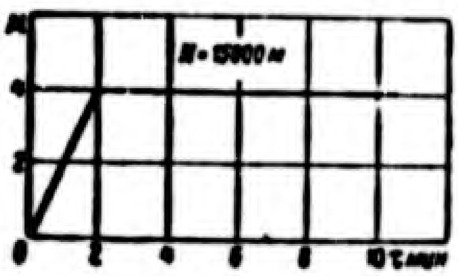

Fig. 8.23. Diagram of flight profile.

Effective torsional rigidity. Let us consider a double-wedge wing (Fig. 8.24) which perceives torque M_{tor} in conditions of aerodynamic heating under the conditions of flight as represented in Fig. 8.23.

Due to wing torsion from an aerodynamic load the vectors of thermal stresses will not lie in the plane xz. The angle of inclination of the vector at a point of cross section, which is at distance x from the axis of rigidity (mid-chord), is equal to $x\frac{d\theta}{dz}$. The resultant of forces applied to element dx in the direction of axis y is expressed by

$$c\sigma_T x \frac{d\theta}{dz} dx,$$

where c is the profile thickness. Resultant torque of thermal stresses will be written in the following way:

$$M_{\text{кр}\,T} = \frac{d\theta}{dz}\int_{-b/2}^{b/2} \sigma_T c x^2\, dx. \tag{8.51}$$

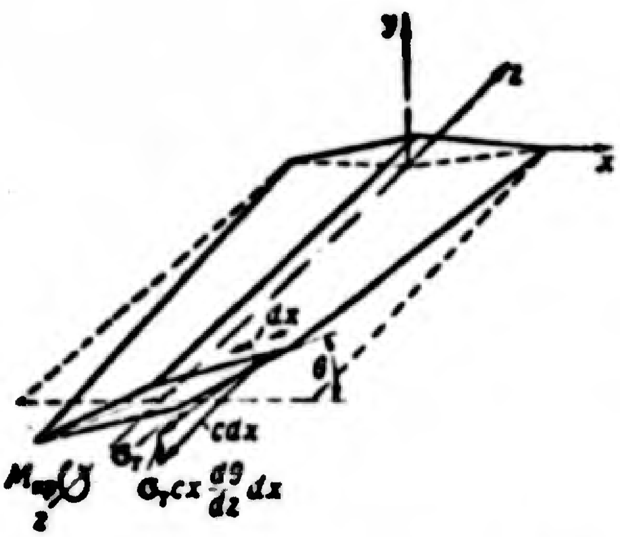

Fig. 8.24. Diagram of the action of torque and stresses in a double-wedge wing.

Consequently, total torque of tangential stresses will be

$$(GJ_p)_T \frac{d\theta}{dz} = M_{\text{кр}} - \frac{d\theta}{dz}\int_{-b/2}^{b/2} \sigma_T c x^2\, dx, \tag{8.52}$$

where $(GJ_p)_T$ is the torsional rigidity at temperature T.

In this case

$$(GJ_p)_T \approx \frac{1}{3}\int_{-b/2}^{b/2} G_T c^3\, dx. \tag{8.53}$$

This magnitude constitutes wing torsional rigidity according to Saint-Venant and is determined by taking into account the change of the mechanical properties of the material and the thermal stresses during heating.

Equation (8.52) is valid for an arbitrary section of the wing (not necessarily continuous) in the presence of normal stresses in general form

$$(GJ_p)_T \frac{d\theta}{dz} = M_{\text{кр}} - \frac{d\theta}{dz}\int_F \sigma_T \rho^2\, dF, \tag{8.54}$$

where ρ is the distance from the center of torsion.

Equation (8.54) can be rewritten in the form

$$\left[(GJ_p)_T + \int_F \sigma_T \rho^2\, dF\right]\frac{d\theta}{dz} = M_{\text{кр}} \tag{8.55}$$

The behavior of the wing of a flight vehicle can thus be describe by the ordinary dependence of the derivative of the angle of rotation of cross section on torque $\frac{d\theta}{dz} = \frac{M_{tor}}{GJ_p}$, if as the rigidity we consider the effective rigidity, equal to

$$(GJ_p)_{эф} = (GJ_p)_T + \int_F \sigma_T \rho^2 \, dF. \tag{8.56}$$

In this formula, in the right part the first member designates the usual rigidity which is calculated by taking into account the change of mechanical properties of material during heating; the second member constitutes the influence of thermals stresses on torsional strain.

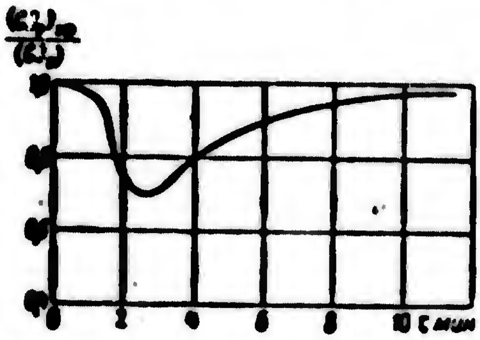

Fig. 8.25. Change of effective rigidity of a double-wedge wing during heating.

Figure 8.25 gives the change of the ratio of effective torsional rigidity to torsional rigidity at ordinary temperature with respect to the heating time for the considered example. As can be seen, the rigidity of a wing during aerodynamic heating in the process of accelerated flight can decrease as compared to the initial rigidity. This leads to an increase of wing deformation.

At large angles of wing torsion the external torque will be balanced not only by tangential stresses, but also by normal stresses σ_N. Under these conditions the generatrix of the wing, passing at distance x from mid-chord, is inclined to plane xz (see Fig. 8.24) at an angle of $x\frac{d\theta}{dz}$. If the initial length of the given generatrix was equal to z, then after deformation, the length of its projection on plane xz will be $z \cos\left(x\frac{d\theta}{dz}\right)$. Then normal torsional deformation ε_N will be defined as

$$\varepsilon_N = -\frac{1}{2}x^2\left(\frac{d\theta}{dz}\right)^2. \tag{8.57}$$

Proceeding from the hypothesis of plane sections and taking the distribution E along chord to be symmetric with respect to axis x, the expression for σ_N can be written out in the following manner:

$$\sigma_N = \sigma_T + \frac{1}{2}E\left(\frac{d\theta}{dz}\right)^2\left[x^2 - \frac{\int\limits_{-b/2}^{b/2} Ecx^2dx}{\int\limits_{-b/2}^{b/2} Ecdx}\right]. \tag{8.58}$$

Introducing the designation

$$\bar{\sigma}_0 = \frac{E}{2E_0}\left[x^2 - \frac{\int\limits_{-b/2}^{b/2} Ecx^2dx}{\int\limits_{-b/2}^{b/2} Ecdx}\right]. \tag{8.59}$$

we obtain

$$\sigma_N = E_0\bar{\sigma}_T + E_0\left(\frac{d\theta}{dz}\right)^2\bar{\sigma}_0,$$

where E_0 is the elastic modulus at 20°C; $\bar{\sigma}_T = \sigma_T/E_0$.

The relationship between the quantity of torque M_{tor} and the derivative of torsional angle $d\theta/dz$ is defined as

$$(GJ_p)_T\frac{d\theta}{dz} = M_{\text{кр}} - E_0\frac{d\theta}{dz}\int\limits_{-b/2}^{b/2}\bar{\sigma}_T cx^2dx - E_0\left(\frac{d\theta}{dz}\right)^3 \times \int\limits_{-b/2}^{b/2}\bar{\sigma}_0 cx^2\,dx, \tag{8.60}$$

whence

$$M_{\text{кр}} = \left[(GJ_p)_T + E_0\int\limits_{-b/2}^{b/2}\bar{\sigma}_T cx^2\,dx + E_0\left(\frac{d\theta}{dz}\right)^2\int\limits_{-b/2}^{b/2}\sigma_0 cx^2\,dx\right]\frac{d\theta}{dz}.$$

Figure 8.26 shows the change of the derivative of the angle of wing torsion from the magnitude of torque M_{tor} in the calculation of torsion according to Saint-Venant and taking into account large deformations. The results of both calculations will agree at small values of torque.

Effective flexural rigidity. Let us also consider flexure of a double-wedge wing (Fig. 8.27) which perceives bending moment M_x in conditions of aerodynamic heating under the conditions of flight as shown in Fig. 8.23. Under the action of an external aerodynamic load there will appear vertical deflections of chord, which will change along the length. Under these conditions the thermal stresses will create an additional moment with respect to axis x

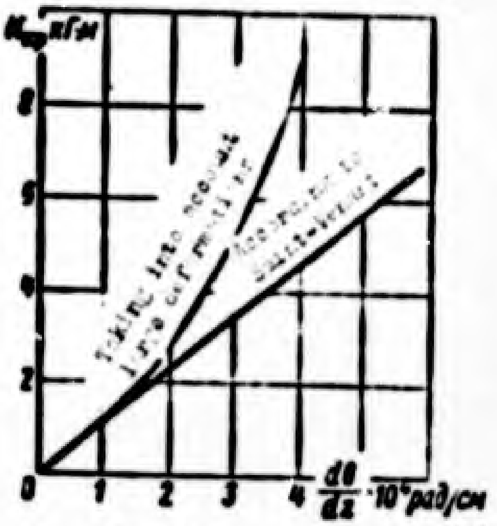

Fig. 8.26. Change of $\frac{d\theta}{dz}$ during torsion of a double-wedge wing.

$$M_T = \int_{-b/2}^{b/2} \sigma_T c v \, dx,$$

where v is the wing deflection along the center line. Equation equilibrium of moments with respect to an axis x will be

$$\int_{-b/2}^{b/2}\int_{-c/2}^{c/2} \sigma_z y \, dy \, dx + \int_{-b/2}^{b/2} \sigma_T c v \, dx = M_x. \qquad (8.61)$$

In conditions of flight with aerodynamic heating, the curvature in the chord plane, as a result of the influence of thermal stresses, is larger than under the usual conditions. Thermal stresses give a resultant (see Fig. 8.27)

$$\frac{\partial^2 v}{\partial z^2} \sigma_T c \, dx \, dz,$$

in the direction of positive values of y. Thus, the wing is subjected to the action of an additional lateral load, the intensity of which per unit of area composes

$$p_y = \frac{\partial^2 v}{\partial z^2} \sigma_T c.$$

The resultant of this load causes bending moment M_x in the plane of a section, the intensity of which per unit of span is equal to

$$m_z = -\frac{\partial^2 v}{\partial z^2} \int_{-b/2}^{b/2} \sigma_T c z dx. \qquad (8.62)$$

For normal stress along axis x we have

$$\sigma_z = \frac{12 m_z}{c^3} y.$$

We shall determine the connection between wing curvature with respect to spand and bending moment M_x with the help of the usual methods of strength of materials. Deformations in the direction of axes x and z, caused by flexure of the wing, are correspondingly equal to

$$\varepsilon_x = -\frac{\partial^2 v}{\partial x^2} y, \quad \varepsilon_z = -\frac{\partial^2 v}{\partial z^2} y \qquad (8.63)$$

or, expressing them through stresses, we obtain

$$\varepsilon_x = \frac{1}{E}(\sigma_x - \mu\sigma_z); \quad \varepsilon_z = \frac{1}{E}(\sigma_z - \mu\sigma_x). \qquad (8.64)$$

Thus we have

$$\sigma_x = -E \frac{\partial^2 v}{\partial x^2} y + \frac{12 \mu m_z}{c^3} y. \qquad (8.65)$$

Putting this relationship in equation (8.61), we obtain

$$M_x = -(EJ)_T \frac{\partial^2 v}{\partial x^2} + \int_{-b/2}^{b/2} \mu m_z dx + \int_{-b/2}^{b/2} \sigma_T c z dx. \qquad (8.66)$$

Magnitude $(EJ)_T = \int_{-b/2}^{b/2} \frac{Ec^3}{12} dx$ constitutes the flexural rigidity of the wing, which is decreased in view of the change of mechanical properties of the material under the influence of high temperatures.

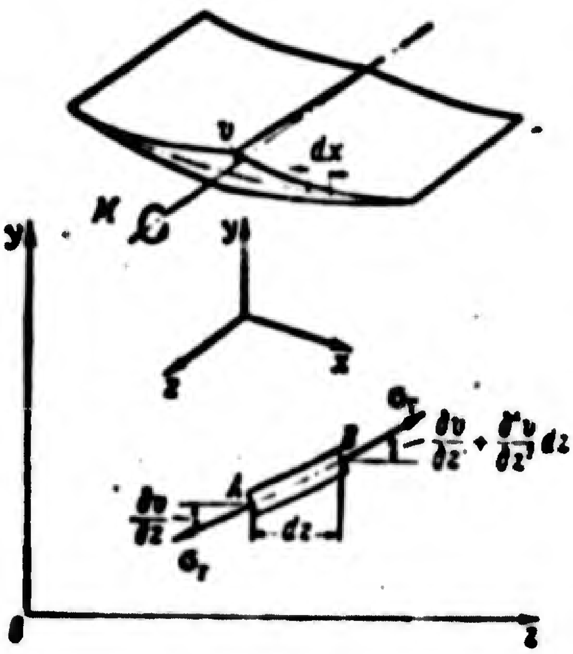

Fig. 8.27. Diagram of the action of stresses in a double-wedge wing during bending.

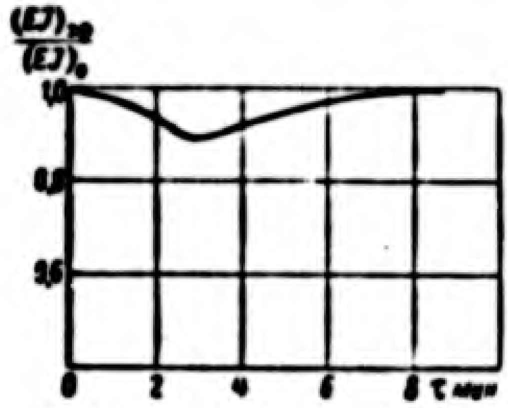

Fig. 8.28. Change of effective flexural rigidity of a double-wedge wing during heating.

The expression for bending moment may be written analogous to the expression of torque through effective rigidity:

$$M_z = -(EJ)_{ef}\frac{\partial^2 v}{\partial z^2}. \qquad (8.67)$$

where

$$(EJ)_{ef} = (EJ)_T - \frac{1}{\partial^2 v/\partial z^2}\int_{-b/2}^{b/2} p m_z\, dx - \frac{1}{\partial^2 v/\partial z^2}\int_{-b/2}^{b/2} \sigma_T c x\, dx.$$

The first member considers the decrease of rigidity at the expense of a lowering of the mechanical characteristics of the mateial at raised temperatures; the following members consider the influence of thermal stresses.

Figure 8.28 gives a curve of change in time of the ratio of effective flexural rigidity of a wing $(EJ)_{ef}$ to its rigidity at ordinary temperature $(EJ)_0$.

Change of structural rigidity of a flight vehicle during heating leads to a change of the frequencies of its oscillations, which renders a direct influence on the different oscillation modes of the structure in the flow of air. At present the general problem of analysis of the behavior of a structure, taking into account external loads, its elasticity, and aerodynamic heating, may be called a problem of aerothermoelasticity.

Change of rigidity characteristics of a wing during heating leads to a lowering of the critical speed of divergence V_d. An approximate dependence of V_d on the duration of heating for wings

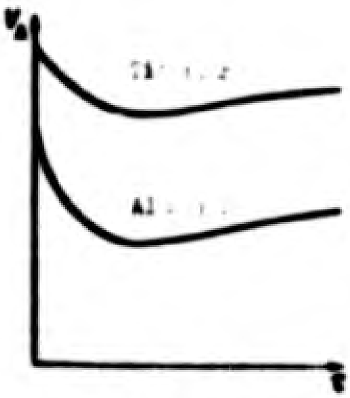

Fig. 8.29. Change of critical speed of divergence during heating.

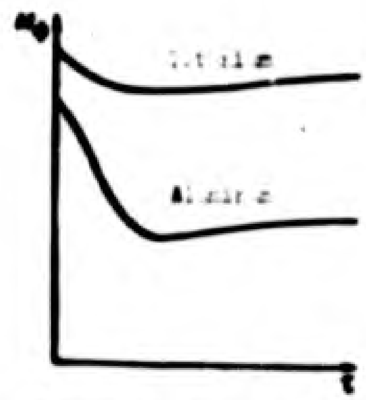

Fig. 8.30. Change of critical Mach number of flutter during heating.

made from titanium and aluminum alloys is shown in Fig. 8.29. In this case, aerodynamic heating is a stabilizing factor. Aerodynamic heating also renders considerable influence on the effectiveness of ailerons.

In the determination of critical speeds of divergence and reversal the influence of thermal stresses should be considered through effective rigidity.

During heating of a structure the critical speed of flutter V_f is lowered. At small temperature gradients the influence of aerodynamic heating on flutter is qualitatively illustrated by the curve of change of Mach number of flutter (M_f) with respect to time of acceleration (Fig. 8.30). During fast deceleration in the transition from conditions of flight at a high supersonic speed to conditions of flight at transonic or subsonic speed there can be sometimes created even more dangerous conditions for the appearance of flutter than during acceleration.

The influence of thermal stresses and large deformations at high temperature gradients is usually considered in flutter calculations by the introduction of effective torsional and flexural rigidity.

8.9. Service Life of a Flight Vehicle at Raised Temperatures

At raised temperatures the service life of a flight vehicle is lowered. It is determined by the characteristics of fatigue strength and creep of the structure. The service life, from conditions of fatigue strength, can be determined according to the method presented in Chapter VII by taking into account the fatigue strength of materials at high temperatures and the growth of intensity of corrosion during heating.

The service life of reusable flight vehicles, in connection with the appearance of creep, may be established by determining the moment of onset of critical deformation which is allowed for normal operation. This deformation is composed of instantaneous elastic deformation and plastic deformation under a load.

The origin and development of permanent deformations has a complicated character and depends on many factors. The change of heating and the external aerodynamic load causes a corresponding distribution of stresses in the structure. Moreover, in certain structural elements there can appear creep. Starting creep of any structural element leads in turn to load redistribution.

The probable service life of a reusable vehicle to destruction also depends on the selected criterion of destruction.

It is known that destruction criteria can be destructive stresses, losses of stability caused by creep, destruction from creep, and permanent deformations of the maximum permissible level, for instance 0.2, 1, or 2%.

Selection of an appropriate criterion is determined by the assignment of the structural element.

Of special value in the determination of service life the cyclic load recurrence of the structure (duration, magnitude of load, and temperature). It is necessary to consider that brief loads can render an essential influence on the creep of a structure. In particular, in spite of the fact that maneuvering loads are applied in a comparatively short period of time as compared to loads which are effective in rectilinear flight, the large stresses which then appear at high temperature can render considerable influence on the service life of the structure.

In actual structures creep can occur in complicated loading conditions. Experimental data on creep in various conditions give materials which allow us to make a number of simplifications. The rate of creep under a dynamic load insignificantly differs from the rate of creep under a constant load which corresponds to average stresses. Consequently, creep during gusts of wind will not strongly differ from creep which corresponds to conditions of constant loading.

Calculations of creep characteristics under a cyclical load may be conducted according to creep under a constant load, assuming that the average rate of creep is equal to the rate of creep which is caused by raised stress plus the rate of creep which is caused by normal stress, referred to the time of action of every stress. Proceeding from this, the total deformation ε_{Σ} in conditions of variable and cyclical loads at constant temperature can be determined from the following equation

$$\varepsilon_0 = \sum_{i=1}^{n} \varepsilon_i. \tag{8.68}$$

where ε_i is the relative deformation during stress σ_i and its time of action $k_i\tau_0$;

k_i is the coefficient which indicates the relative time of action of stress σ_i;

n is the number of levels of stresses;

τ_0 is the selected service life, for which deformations are analyzed.

In turn the total relative deformation ε_i can be considered as the sum of elastic deformation ε_{0i} and plastic deformation δ_i:

$$\varepsilon_i = \varepsilon_{0i} + \delta_i. \tag{8.69}$$

Putting expression (8.69) in equation (8.68), we obtain

$$\varepsilon_0 = \sum_{i=1}^{n} \varepsilon_{0i} + \sum_{i=1}^{n} \delta_i. \tag{8.70}$$

On the basis of laboratory and theoretical research the magnitude of permissible relative deformation ε_{per} is established. Then the permissible service period of a structure can be determined from the relationship

$$\tau = \frac{\varepsilon_{per}}{\varepsilon_0}\tau_0. \tag{8.71}$$

Since elastic deformations are small as compared to plastic ones during creep, it is expedient to consider only plastic deformations. Then, using the hypothesis of deformation summation during creep, relationship (8.71) can be presented in another form. Let us designate by τ_i the time in which deformation ε_{per} is attained during the action of stress σ_i. In the whole service life of a structure under a load with stress σ_i there will be obtained part of the permissible deformation, equal to $\frac{k_i \tau}{\tau_i} \varepsilon_{per}$. During the total action of all loads we have the relationship

$$\sum_{i=1}^{n} \frac{k_i \tau}{\tau_i} \varepsilon_{per} = \varepsilon_{per}$$

or

$$\tau = \frac{1}{\sum_{j=1}^{m} \sum_{i=1}^{n} \frac{k_{ij}}{\tau_{ij}}}, \tag{8.72}$$

From expression (8.72) we can determine the service life of the structure:

$$\tau \sum_{i=1}^{n} \frac{k_i}{\tau_i} = 1. \tag{8.73}$$

In general, in the operation of a flight vehicle there takes place both variable loads, and also variable temperatures. Then the relationship for determination of service life will be

$$\tau = \frac{1}{\sum_{i=1}^{n} \frac{k_i}{\tau_i}}. \tag{8.74}$$

where k_{ij} is the coefficient which indicates the relative time of action of stress σ_i at temperature T_j;

τ_{ij} is the time to destruction during stress σ_i and at temperature T_j;

m is the number of temperature stages.

CHAPTER IX

FEATURES OF HELICOPTER LOADING

List of Designations Appearing in Cyrillic

АП = AP = Automatic Pitch-Control Mechanism

р = bfc = blade-flapping control

ГШ = FH = Flapping Hinge

ВШ = DH = Drag Hinge

ЦТ = CG = Center of Gravity

л = b = blade

ц = cen = centrifugal

К = Cor = Coriolis

г.ш = f.h. = flapping hinge

ц.т = c.g. = center of gravity

в.ш = d.h. = drag hinge

в = rot = rotor

взм = flap = flapping

вр = rotat = rotation

н.в = m.r. = main rotor

в = h = hub

х.в = t.r. = tail rotor

о.ш = fe. h. = feathering hinge

ф = f = flutter

кр = crit = critical

изг = bend = bending

ст = st = static

НВ = MR = Main Rotor

крейс = cruis = cruising

р = r = rated

э = op = operational

ОШ = FEH = Feathering Hinge

The basic features of helicopters, as compared to other flight vehicles, are their increased structural vibrations.

Operational experience shows that dynamic loads and stresses, which arise due to vibration, are decisive for helicopters. The solution of the problem concerning structural strength of helicopters essentially reduces to a guarantee of dynamic strength and a correct determination of service life of their supporting elements under assigned dynamic loading.

Questions of dynamic strength and service life of helicopters are closely connected with questions of static strength of their structures. This is caused, first of all, by the fact that a structure is designed for general loads in the severest cases of loading that are encountered in operation, and consequently the dimensions and forms of the supporting members in the first place are determined namely by these external loads, which are essentially static. Secondly, limiting cases of static loading in flight frequently are accompained by the largest variable stresses in the structure, and its strength can essentially depend on the combination of static and variable stresses.

Cases of loading of helicopters in operation are considered in norms of strength, which originate from the same principles as aircraft. The norms anticipated conditions, in the fulfillment of which the operation of a helicopter will be safe with respect to structural strength.

Together with that, the strength norms of helicopters essentially differ from aircraft norms. In particular, considerable attention in strength norms of helicopters is allotted to questions of dynamic strength and service life of structures.

There are the following modes of helicopter vibrations:

a) vibrations caused by rotation of main and tail rotors;

b) motor vibration;

c) oscillations appearing from the aerodynamic forces which are acting upon the fuselage and nonrotary parts of a helicopter.

Of practical interest are the two first modes of vibrations. The third oscillation mode, due to the relatively low speeds of flight of comtemporary helicopters, is of the least interest.

These oscillation modes pertain to forced oscillations. They appear under the action of periodic external forces and are damped after the cessation of their action. Besides forced oscillations, helicopters can also experience self-exciting oscillations. Self-exciting oscillations include flutter of rotor blades and ground resonance.

The main and tail rotors of contemporary helicopters have a special device for cyclical change of blade pitch with respect to azimuth, i.e., an automatic pitch-control mechanism (AP). Blades are hinged to hubs. Such attachment allows both flapping of the blade around the flapping hinge (FH) and also blade oscillations near the drag hinge (DH). Angles of lag ξ and sweep β are limited by stops. Oscillations blades around the DH in the plane of rotation are damped with the help of dampers, the characteristics of which are selected in order to avoid ground resonance. Furthermore, such attachment permits the changing of collective rotor pitch φ_0 (rotor-blade pitch φ) by turning the blades around their longtudinal axis (feathering hinges FEH).

In flight the blades are acted upon by variable aerodynamic forces which cause oscillations. The blades experience inertial forces. Vibrations of the helicopter itself are a consequence of the action of perturbing forces and moments created on the rotor hubs basically (disregarding of friction in the hinges) by the aerodynamic and mass forces of individual blades. These forces are periodic with periods multiple to rotor revolutions.

In view of the presence of flapping and drag hinges in the rotor blade attachment, the moments of perturbing forces are not transmitted to the rotor hub and consequently, they themselves do not cause vibrations of the helicopter (with the exception of the moment which is transmitted to the hub by the DH damper). However, they affect the magnitude of forces which are transmitted to the hub, since under their action the blade-flapping angles, and consequently, also the variable forces on the blade are change.

The main oscillations for helicopters are those connected with the change of relative flow rates on rotary blades and the appearance of flywheel motions of blades. These oscillations are caused by the work of the rotor system of the helicopter in an oblique flow and are inevitable on helicopters.

Helicopters can also experience oscillations which are a consequence of inaccuracies in rotor adjustment. The intensity of these oscillations depends on the degree of misadjustment (unbalance) of

Fig. 9.1. Airflow conditions of rotor. a) axial airflow; b) transitional airflow (small values of μ); c) oblique airflow (large values of μ).

rotors and can vary in operating conditions.

Vibrations of helicopters depend on the airflow conditions of the rotor. Therefore, the conditions of flight are divided into three groups: axial airflow of rotor, oblique airflow, and transitional airflow. The approximate forms of airflow through the rotor disk under different conditions of its airflowing are schematically shown in Fig. 9.1.

9.1. Oscillations of Rotor Blades in Forward Flight

During the forward flight of helicopter the rotor has an oblique airflow that is determined by μ, which is called rotor performance:

$$\mu = \frac{V \cos \alpha}{\omega R},$$

where V - is the horizontal speed of flight;

α - is the rotor angle of attack;

R - is the rotor radius;

ω - is the angular velocity of rotor rotation.

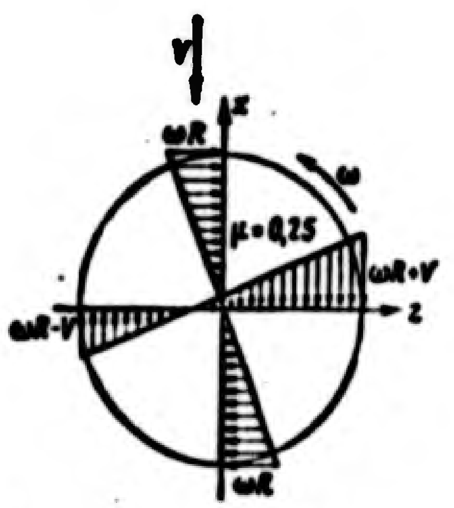

Fig. 9.2. Field of speeds of airflow on the blades of a moving rotor during flight at horizontal speed.

In an oblique airflow the rotor blades in each given moment of time will work in a field of various relative speeds of airflow (Fig. 9.2). The presence of hinges in the blade attachment provides them with flapping, at the expense of which the blade thrust is balanced. These two factors determine a number of essential peculiarities of oscillations of helicopter parts in conditions of oblique airflow of the rotor.

Flapping of Rotor Blades

Rotation of absolutely rigid rotor blades occurs around the surface of a cone, the angle at the summit of which is determined by the condition of equality to zero of the sum of moments of all forces which are acting on the blade. The blades then accomplish oscillations, i.e., flapping, with respect to their hinges. In steady flights, blade flapping is also steady and periodic, and cyclically repeated in every rotor revolution. They are continuous and periodic functions of blade aximuth ψ, and they consequently can be represented in the form of a trigonometric series with any degree of accuracy:

$$\beta = a_0 - \sum_{n=1}^{\infty} (a_n \cos n\psi + b_n \sin n\psi). \tag{9.1}$$

$$\xi = c_0 - \sum_{n=1}^{\infty} (c_n \cos n\psi + d_n \sin n\psi). \tag{9.2}$$

Coefficient a_0 in expression (9.1) is the cone angle of the rotor, which is part of the flapping angle, not depending on the azimuthal position of blades, and consequently it does not cause variable forces on the rotor by itself. In hovering conditions (undeflected AP) $\beta = a_0$.

Coefficient a_1 characterizes the angle of inclination behind the axis of the cone described by the blades, and b_1 is the angle of inclination of the axis of the rotor cone sideways, in the direction of the blade, proceeding forward. Motions of blades, determined by

equations $\beta = -a_1 \cos \psi$ and $\beta = -b_1 \sin \psi$, constitute simple cosinusoidal and sinusoidal motion.
Coefficients a_2, b_2 are amplitudes of second harmonics. Motions determined by equations $\beta = -a_2 \cos 2\psi$ and $\beta = -b_2 \sin 2\psi$, describe oscillations of blades with respect to the surface of the cone of blade rotation, which is formed during their motion according to the first harmonic law in expression (9.1).

Subsequent harmonics of blade flapping describe its oscillations with respect to the surface formed by the motion according to the law of the first two harmonics. Coefficients a_3, b_3; ...; a_n, b_n constitute the amplitudes of these oscillatory blade motions.

Coefficients c_0; c_1, d_1; c_2, d_2; ...; c_n, d_n of oscillatory blade motion with respect to the DH in expression (9.2) have a value which in general is analogous to that shown for coefficients of flapping in expression (9.1). Coefficient c_0 is the angle to which the blades are displaced with respect to the axis of the rotor hub during its rotation. The magnitude of this angle is determined by condition of equality to zero basically of moments resisting forces and moments of centrifugal forces of the blades, which try to turn them around the drag hinge. This angle does not change with the change of azimuthal position of the blades under given operating conditions of the rotor and consequently does not cause variable forces on the rotor by itself. In conditions of hovering during an axial airflow around the rotor $\xi \approx c_0$. Coefficients c_1, d_1; ...; c_n, d_n constitute the amplitudes of oscillatory blade motions in the plane of rotation with respect to their central position, determined by angle c_0.

Blade flapping to a great degree depends on the distribution of induced speeds around the rotor disk and on the work of the automatic pitch-control and the blade-flapping control (blade-flapping balance).

With undeflected AP plane and in the absence of blade-flapping control, the blade-setting angle with respect to the plane of the rotor hub (the plane passing through the axes of the FH) does not change with the change of their azimuthal position ($\varphi = \varphi_0 = \text{const}$).

With inclination of the AP plane the setting angle will cyclically change with respect to azimuth. Due to this there will also be a cyclic change in the aerodynamic forces on the blades and their flapping. For calculation of the effect of inclination of the AP ring, instead of φ we take $\varphi = \varphi_0 + \Delta\varphi_{AP}$. Angle $\Delta\varphi_{AP}$ is equal to

$$\Delta\varphi_{\text{АП}} = \delta \frac{\cos(\psi - \tau + \sigma)}{\sin\sigma}, \tag{9.3}$$

where δ is the angle of inclination of the AP;

τ is the angle that determines the plane is which the AP inclination occurs (computed from the plane of symmetry of the helicopter;

$\sigma = \text{const}$ is the designed advance angle.

The indicated formula is valid both for blades with stiffening and also those that are hinged.

Upon deflection of the AP plane to angle δ on azimuth ψ_1 the resultant of the aerodynamic forces of the rotor deviates to angle δi_a on azimuth $\psi_2 = \psi_1 + \Delta\psi$, where i_a is the AP transmission factor. Consequently, for a rotor with automatic pitch-control mechanism there exists an angle of advance (with respect to azimuth) of the deflection of the resultant of the aerodynamic forces as compared to the angle of deflection of the automatic pitch-control mechanism, in consequence of which the longitudinal and lateral control of helicopter turns out to be interconnected. For excluding this interconnection the rig points of the longitudinal and lateral control bars of the automatic pitch-control mechanism are moved along the longitudinal and transverse axes of the helicopter at angle σ, which is, therefore, called the designed advance angle. The latter can differ from advance angle $\Delta\psi$, which is equal to

$$\Delta\psi = \sigma_1 + c_0,$$

where σ_1 is the angle between the lines connecting the end of the blade guide with the center of the FH axis and with axis of rotor rotation;

c_0 is the constant part of the blade lag angle.

In this case the interconnection between longitudinal and lateral control of the helicopter is completely excluded.

The guides on the blades are levers on butt parts, which are connected by bars to the mobile AP ring, revolving together with the rotor shaft,and serve for control of the blade-setting angle. If the ends of guides, to which the bars are braced, do not lie on the FH axes, the rotor has a "blade-flapping control." In the absence of a blade-flapping control, the blade-setting angle φ practically does not depend on its flapping angle β. The presence of a blade-flapping control creates a dependence of φ on β: at positive β the magnitude φ decreases and at negative, it increases. Besides balancing the flapping, the blade-flapping control decreases the angle of advance $\Delta\psi$. The smaller the spacing of the FH from the axis of rotor rotation, the smaller the angle of advance. When $\mu \neq 0$ the blade-setting angle φ also depends on blade revolution with respect to the DH.

The general change of φ from blade flapping, in the presence of a blade-flapping control, will be

$$\Delta\varphi_\beta = \Delta\varphi_1 + \Delta\varphi_2 = -\beta(\mathrm{tg}\,\sigma_1 - \sin c_0) = -k_p\beta. \qquad (9.4)$$

where $\Delta\varphi_1 = -\beta \tan \sigma_1$ is the change of the blade-setting angle due to the influence of its oscillations in the flapping plane (with respect to the FH);

$\Delta\varphi_2 = \beta \sin c_0$ is the change of the blade-setting angle due to the influence of its oscillations in the plane rotation (with respect to the DH);

$k_{bfc} = \tan \sigma_1 - \sin c_0$ is the blade-flapping control factor.

Thus, for calculation of the effect of AP inclination and the action of the blade-flapping control, the expression for the blade-setting angle should be written in the form

$$\varphi = \varphi_0 + \Delta\varphi_{AP} + \Delta\varphi_\beta$$

or taking into account expressions (9.3) and (9.4)

$$\varphi = \varphi_0 + \delta\frac{\cos(\psi - \tau + \sigma)}{\sin\sigma} - k_p\beta. \qquad (9.5)$$

From this formula it is clear that angle φ, and consequently also the blade flapping, depend on angle τ, i.e., on the direction of inclination of the AP ring.

Flapping is also influenced by the elasticity of the blades, especially on rotors of large diameters and at high-frequency oscillations. The shank of an elastic blade oscillates in a different way as that of an absolutely rigid one (see Fig. 9.3). Oscillations of elastic and absolutely rigid blades in end sections differ even more.

In an absolutely rigid blade the oscillations of the first harmonic of angle β [formula (9.1)] usually composes up to 90% of the total value. Every subsequent harmonic with respect to magnitude of amplitude is 3-4 times less than the preceding one. In certain conditions of flight the second harmonic is essential.

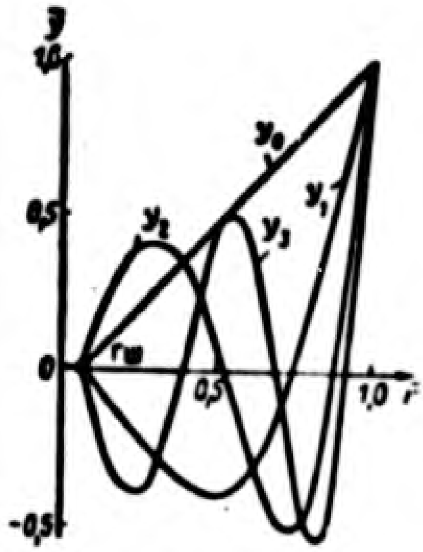

Fig. 9.3. Forms of oscillations for an absolutely rigid blade (y_0) and for the first three tones of a real elastic blade (y_1, y_2, y_3).

For an elastic blade, with respect to magnitude of flapping, the first harmonic is also a main one, but the amplitudes of the subsequent harmonics decrease considerably slower than in an absolutely rigid blade, especially in the region of higher harmonics, where, due to the possible resonance of blades, frequently observed at low speeds of flight ($\mu < 0.12$), the blade oscillations increase. Since flapping (with respect to magnitude of amplitudes) determines the first harmonic of angle β, and higher harmonics usually compose a slight portion of total flapping, the influence of elasticity of blades on their flapping is not a determining factor. However, with respect to the strength of blades, the most important (due to the possible resonance of blades) are flapping oscillations, namely with higher harmonics, occurring in the form of higher tones of natural oscillations of blades.

The use of the first harmonics in expressions (9.1) and (9.2) makes it possible to determine angles β and ξ with an accuracy of 1°, and the use of the second harmonics increases the accuracy to a tenth of a degree. The thus-obtained accuracy of determination of the trajectory of blade motion can be increased by the introduction of subsequent members of these series.

For steady conditions of flight, as shown by the results of measurements on helicopters in flight, in the expressions for angles β and ξ it is sufficient to preserve only the first two harmonics of their series expansion:

$$\beta = a_0 - a_1 \cos\psi - b_1 \sin\psi - a_2 \cos 2\psi - b_2 \sin 2\psi; \tag{9.6}$$
$$\xi = c_0 - c_1 \cos\psi - d_1 \sin\psi - c_2 \cos 2\psi - d_2 \sin 2\psi. \tag{9.7}$$

For transient and transitional flight conditions the high-frequency components of flapping and lag angles become essential. In these cases, in the expressions for β and ξ one should consider at least 8-10 harmonics.

Calculation of high-frequency components of blade flapping, in the determination of variable forces on the rotor, leads to considerable technical (calculating) difficulties. However, the application of high-speed computers makes it possible to considerably facilitate this problem. Owing to this it is possible to directly calculate the variable forces having an effect on the rotor.

Forces Acting Upon Rotor Blade

On the i-th blade of a rotor in flight the following aerodynamic and mass forces are effective (Fig. 9.4): thrust P_i, rotation resistance Q_i, gravity of blade G_b, centrifugal force of blade (in plane of rotation) $P_{cen\ i}$, Coriolis force (in plane of rotation, perpendicular to axis of blade) $P_{Cor\ i}$, tangential force of inertia from blade flapping around the FH (in flapping plane $P_{\beta i}$, inertial force from blade oscillations around the DH (in plane of rotation) $P_{\xi i}$.

These forces, with the exception of blade gravity G_b, are variable (in forward flight) and cause blade oscillations. Upon being transmitted to the rotor hub, they cause vibrations of the helicopter fuselage.

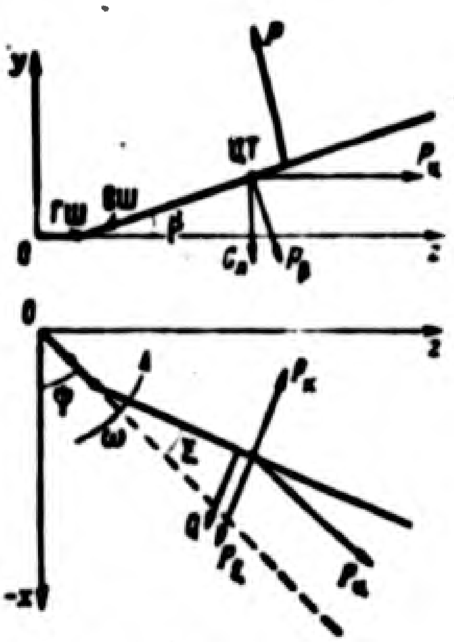

Fig. 9.4. Forces acting upon a rotor blade.

Let us consider the forces acting upon a blade. For simplicity we shall consider that the blade is absolutely rigid, flat, untwisted (setting angle $\varphi(r)$ = const on radius of blade) and have constant width (t = const). This assumption will not affect the qualitative side of the results which it is required to obtain, but considerably simplifies calcluations. The permissibility of different simplifications in quantitative calculations of variable forces should be studied for each specific rotor.

<u>Thrust</u> P_1. For a certain blade

$$P_1 = \frac{1}{2} \rho c_y^{\alpha} b \int_0^R (\varphi W_x^2 + W_x W_y)\, dr, \qquad (9.8)$$

where W_x and W_y are the longitudinal and axial components of resultant speed W of flow on an element of the blade during forward flight;

r is the radius of a section of the blade;

R is the radius of the blade.

Resultant speed W of flow is formed by the summation of induced speed, the speed of forward flight, the peripheral velocity of rotation, and the blade-flapping rate.

Component W_x lies in the plane of rotation and is perpendicular to

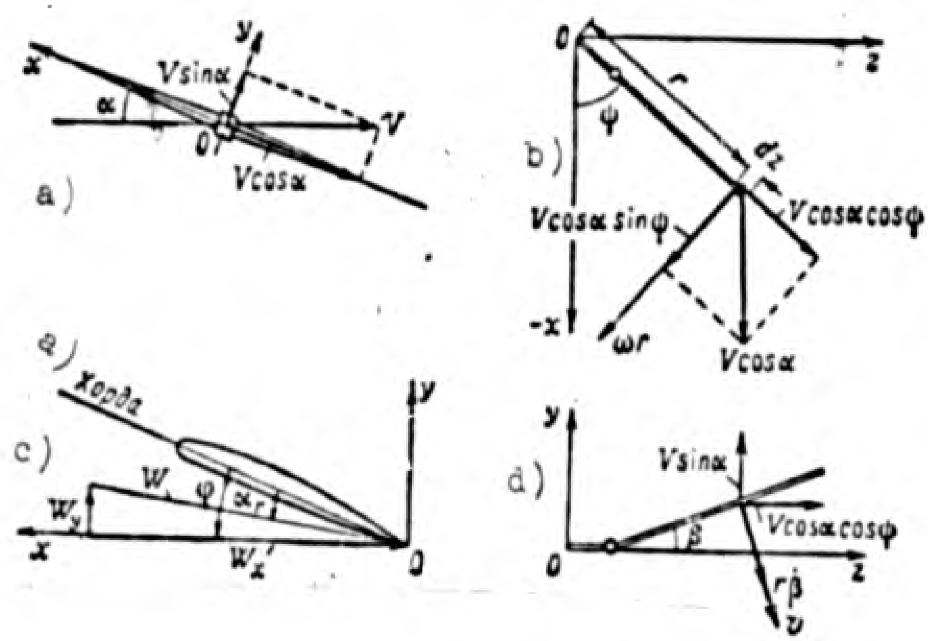

Fig. 9.5. Components of flow rate on blade. a) breakdown of flow rate V into components along rotor axes; b) flow rate on blade element in plane of rotation; c) component of resultant speed W on blade element during forward flight (α_r is the angl- of attack of blade element); d) flow rate on blade element in flapping plane.

the blade axis, while W_y is perpendicular to W_x and is directed parallel to axis y of the rotor (Fig. 9.5). These components are equal to

$$W_x = \omega r + V \cos\alpha \sin\psi; \tag{9.9}$$

$$W_y = V \sin\alpha \cos\beta - v - r\dot{\beta} - V \cos\alpha \cos\psi \sin\beta, \tag{9.10}$$

where v is the average induced speed along the rotor disk;

V is the horizontal speed of flight;

α is the rotor angle of attack (between vector of flow rate and hub plane, passing through axes of flapping hinges).

The statement concerning the constancy of induced speeds along the rotor disk is a defined assumption which significantly simplifies calculations, but lowers their accuracy. The true distribution of induced speeds differs from uniform distribution both with respect to the length of a blade, and also with respect to its azimuthal position. This distinction depends on the form of blades in the plan, their aerodynamic twist, the rotor angle of attack, the speed of flight, and other factors. For hinged blades with setting angle variable with respect to azimuth, the irregularity is distribution of induced speeds is greater than in rigidly fixed blades. In horizontal flight with sufficiently high speeds ($\mu \geq 0.15$) the absolute values of induced speeds are less and are distributed more uniformly than at low speeds of flight ($\mu = 0.03$-0.10), when induced speeds are large in magnitude and are distributed around the rotor disk very nonuniformly.

The majority of theoretical works on the determination of aerodynamic loads on blades originates from the simplifying assumption about the fact that a rotor has an infinite number of blades. For a real rotor with a finite number of blades the relative position of the vortex sheet and revolving blade is variable in time, in consequence of which the induced speed at some point of the rotor disk also (sometimes very strongly) changes due to the change of structure of the vortex sheet which passes through this point. Magnitudes of instantaneous induced speeds essentially differ from the time average value of induced speed. Experimental investigations of the rotor vortex system testify to the large influence of wingtip vortices descending from the ends of the blades on the instantaneous induced speeds.

Variable aerodynamic loads, acting upon a blade, depend on the instantaneous induced speeds. Therefore, the introduction of instantaneous induced speeds into the calculation will allow a fuller investigation of the peculiarities of the aerodynamic forces acting upon a rotor blade. However, theoretical research on the vortex system of a rotor with finite number of blades and the interconnection of this system, the instantaneous induced speeds, and aerodynamic loads on a blade still are not completed. Therefore, in engineering calculations we usually use different simple dependences for induced rotor speeds. One of such simplifications is the assumption about the fact that induced speeds are uniformly distributed around the rotor disk. As shown by the comparison of calculations with results of experiments, such an assumption is permissible in design calculations for comparatively high speeds of flight ($\mu \geq 0.20$). In carrying out more exact calculations or in calculations for low speeds of flight ($\mu < 0.20$) it is necessary to consider the variability of induced rotor speed. In these cases the values of induced speed are usually determined experimentally for specific rotors or dynamically similar models in wind tunnels.

Passing in formulas (9.9) and (9.10) to relative speeds, we obtain

$$\overline{W}_x = \frac{W_x}{\omega R} = \bar{r} + \mu \sin\psi; \tag{9.11}$$

$$\overline{W}_y = \frac{W_y}{\omega R} = \mu \operatorname{tg}\alpha \cos\beta - \bar{v} - \bar{r}\frac{d\beta}{d\psi} - \mu\cos\psi\sin\beta, \tag{9.12}$$

where $\bar{r} = \frac{r}{R}$ is the relative radius of a blade section.

Formula (9.8) may be written in the form

$$P_1 = C\omega^2\rho\left(\varphi\int_0^1 \overline{W}_x^2\,d\bar{r} + \int_0^1 \overline{W}_x\overline{W}_y\,d\bar{r}\right). \tag{9.13}$$

where

$$C = \frac{1}{2} c_y^a b R^3 = \text{const.}$$

In the future, it will be useful to calculate the integrals which enter expression (9.13). Putting in the first integral the value of W_x (9.11), after integration we obtain

$$\int_0^1 \overline{W}_x^2 d\overline{r} = \left(\frac{1}{3} + \frac{1}{2}\mu^2\right) + \mu \sin\psi - \frac{1}{2}\mu^2 \cos 2\psi. \tag{9.14}$$

Let us calculate the second integral.

Considering the dependences (9.11) and (9.12), we obtain

$$\int_0^1 \overline{W}_x \overline{W}_y d\overline{r} = \left(\frac{1}{2} + \mu \sin\psi\right)(\mu \operatorname{tg}\alpha \cos\beta - \overline{v} - \mu \cos\psi \sin\beta). \tag{9.15}$$

Blade-setting angle φ (9.5) does not remain constant with respect to azimuth upon deflection of the automatic pitch-control mechanism.

In horizontal flight, angle τ, which determines the direction of inclination of the automatic pitch-control mechanism, has an insignificant magnitude. For simplicity we shall take $\tau = 0$.

Then

$$\varphi = \varphi_0 + \delta k_\sigma \cos\psi - \delta \sin\psi - k_\beta \beta, \tag{9.16}$$

where

$$k_\sigma = \operatorname{ctg}\sigma = \text{const.}$$

Putting the values of integrals (9.14) and (9.15) and angle φ (9.16) into formula (9.13), we can determine the thrust of an individual blade P_i.

Resisting force Q_1. For an individual blade in the plane of rotation

$$Q_1 = \frac{1}{2}\rho b \int_0^R (c_{xp} W_x^2 - c_y' \varphi W_x W_y - c_y' W_y^2)\, dr, \tag{9.17}$$

where c_{xp} is the average coefficient of profile drag of blade, which is taken as constant (in reality it varies somewhat).

Passing to relative speeds, formula (9.17) can be written in the following form:

$$Q_1 = C\omega^2\rho \left[\frac{c_{xp}}{c_y'} \int_0^1 \bar{W}_x^2\, d\bar{r} - \varphi \int_0^1 \bar{W}_x \bar{W}_y\, d\bar{r} - \int_0^1 \bar{W}_y^2\, d\bar{r}\right], \tag{9.18}$$

where C = const has the same value as in formula (9.13).

The first two integrals in expression (9.18) are already determined. It remains to determine the third integral. Let us place, instead of W_y, its value by formula (9.12). Raising W_y to a square, integrating, and producing the appropriate conversions, we obtain

$$\int_0^1 \bar{W}_y^2\, d\bar{r} = \sum_{n=1}^{6} F_n(\psi), \tag{9.19}$$

where

$$F_1(\psi) = \frac{1}{2}\mu \operatorname{tg}\alpha + \bar{v}^3 + \frac{1}{2}\mu\cos\psi + \bar{v}\frac{d\beta}{d\psi}; \qquad F_2(\psi) = \frac{1}{3}\left(\frac{d\beta}{d\psi}\right)^2;$$

$$F_3(\psi) = -\mu \operatorname{tg}\alpha \left(2\bar{v} + \frac{d\beta}{d\psi}\right)\cos\beta; \qquad F_4(\psi) = \mu\cos\psi \left(2\bar{v} + \frac{d\beta}{d\psi}\right)\sin\beta;$$

$$F_5(\psi) = \frac{1}{2}\mu(\operatorname{tg}\alpha - \cos\psi)\cos\beta; \qquad F_6(\psi) = -\mu^2 + \operatorname{tg}\alpha\cos\psi\,\sin\beta.$$

Putting the values of integrals (9.14), (9.15), and (9.19) into formula (9.18) and taking into account expression (9.16), we can determine resisting force of rotation of an individual blade Q_1.

<u>Centrifugal force</u> $P_{cen\ i}$. During blade flapping there occurs a displacement of the blade's center of gravity (CG) in the plane of rotation. Due to this there appears an unbalanced centrifugal force on the blade. Since the centrifugal force is many times greater than the other forces (in usual flight it is approximately 100-150 times more than the weight of a blade), one should expect that a change in the magnitude of centrifugal forces of individual blades during their flapping can be an essential source of vibrations of both the blades themselves, and also of the entire helicopter.

Centrifugal force of a blade is

$$P_{ц i} = m_л \omega^2 [l_{г.ш} + (r_{ц.т} - l_{г.ш}) \cos\beta].$$

or during steady motion (ω = const)

$$P_{ц i} = k_1 \omega^2 + k_2 \omega^2 \cos\beta. \tag{9.20}$$

where $k_1 = m_b l_{f.h.}$ = const;

$k_1\omega^2$ is the constant part of centrifugal force, not depending on blade flapping;

$k_2 = m_b(r_{c.g.} - l_{f.h.}$ = const;

$l_{f.h.}$ is the distance from the axis of rotor rotation to the axis of the flapping hinge;

$r_{c.g.}$ is the distance (along radius) from the axis of rotor rotation to the center of gravity of the blade;

m_b is the mass of the blade.

<u>Coriolis force</u> $P_{Cor\ i}$. In flight, the moment which excites blade

oscillations with respect to the drag hinge is basically created by the Coriolis forces which appear due to blade flapping and act in the plant of rotation. These forces are transmitted to the rotor hub and are an essential source of helicopter vibrations, which is embodied in the actual principle of work of the rotor in an oblique flow.

In the calculation of force $P_{Cor\ 1}$ we shall disregard the additional angular blade velocity from oscillations with respect to the DH as compared to the basic velocity ω = const (this velocity does not exceed 2% of velocity ω).

The Coriolis force appearing on an individual blade is

$$P_{K_1} = 2\omega m_{л}\dot{\beta}\,[(r_{ц.т} - l_{в.ш})\cos\xi + l]\sin\beta\cos\xi, \tag{9.21}$$

where $l_{d.h.}$ is the distance from the axis of rotor rotation to the axis of the drag hinge;

$l = l_{d.h.} - l_{f.h.}$ is the distance (along length of blade) between the drag and flapping hinges.

With respect to the smallness of the angle of lag ξ, for simplification of calculations we shall take cos ξ = 1. Then, considering that

$$\dot{\beta} = \omega\frac{d\beta}{d\psi},$$

it is possible to write

$$P_{K_1} = 2k_2\omega^2\sin\beta\frac{d\beta}{d\psi}, \tag{9.22}$$

where k_2 = const has the same value as in formula (9.20).

<u>Inertial force of blade flapping</u> $P_{\beta 1}$. Tangential inertial force of blade flapping is

$$P_{\beta_1} = m_a\ddot{\beta}\,(r_{\text{ц.т}} - l_{\text{г.ш}}). \qquad (9.23)$$

Considering that

$$\ddot{\beta} = \omega^2 \frac{d^2\beta}{d\psi^2},$$

formula (9.23) can be reduced to the form

$$P_{\beta_1} = k_2\omega^2 \frac{d^2\beta}{d\psi^2}, \qquad (9.24)$$

where k_2 = const has the same value as in formula (9.20).

Force of inertia $P_{\xi 1}$. Due to blade oscillations in the plane of rotation there appears a force of inertia

$$P_{\xi_1} = m_a\ddot{\xi}\,(r_{\text{ц.т}} - l_{\text{в.ш}}). \qquad (9.25)$$

Producing the same actions as for force $P_{\beta 1}$, expression (9.25) may be reduced to the form

$$P_{\xi_1} = k_3\omega^2 \frac{d^2\xi}{d\psi^2},$$

where

$$k_3 = m_a\,(r_{\text{ц.т}} - l_{\text{в.ш}}) = \text{const}. \qquad (9.26)$$

These forces completely appear on rotors with triple-hinged blades, i.e., in the presence of feathering, flapping, and drag hinges. At present such hinging is possessed by blades of helicopter rotors. The attachment of tail rotor blades of contemporary helicopters have no hinges that are analogous to the drag hinges of main rotors. Due to this, the tail rotor blades have no forces P_ξ (more exactly, only part of this force is active, depending on the elastic oscillations of the blade in the plane of rotation). In other respects, the forces acting upon the tail rotor blades are analogous to the forces acting upon the main rotor blades.

As can be seen from expressions for forces, which are acting upon a blade, they contain the squares and products of components of speeds on blade elements, trigonometric functions of azimuth ψ, flapping angle β and angle of lag ξ, their products and derivatives. If we expand the fuctions of complex arguments of β and ξ in a series, then after involution and reduction of powers and products of trigonometric functions to functions of multiple angles, we obtain that in expressions for forces on blades there are possible variable components of the first, second, third, and higher harmonics with respect to rotor revolutions.

The expression for any of the indicated forces on an individual rotor blade may be written in general form:

$$P = P_0 - \omega^2 \sum_{n=1}^{\infty} (A_n \cos n\psi + B_n \sin n\psi). \tag{9.27}$$

where P_0 is the constant component of force on the blade;

A_n and B_n are the amplitudes of variable components of force on the blade;

n is the order of harmonics to rotor revolutions.

Depending upon the number of harmonics taken in the calculation for angles β and ξ, and the number of members of expansion of cosines and sines of these angles in a series, the quantity of harmonics n in expression (9.27) can change. We shall correspondingly change coefficients A_n and B_n.

Coefficients A_n and B_n are complex functions of many parameters, including the structural ones (spacing of blade hinges, designed angle of advance, blade-flapping control factor, mass characteristics of blade, and others). In the investigation of oscillatory properties of the blades of a new rotor, one should consider the influence of all these parameters.

For a specific rotor, the number of parameters which enter the expressions for forces is constant. In the investigation of oscillatory features blades, with respect to conditions of flight, they may be considered constant. In this case, the formulas for forces on blades are somewhat simplified.

Coefficients of aerodynamic forces for a rotor depend on the following basic parameters: speed of flight (or characteristics of rotor performance μ), magnitude of collective rotor pitch φ_0, angle of deflection of automatic pitch-control mechanism δ, and coefficients of blade flapping a_0, a_n, b_n, and c_0, c_n, d_n. Expressions for coefficients of aerodynamic forces have the form

$$\left.\begin{aligned} A_n &= f_{0n} + \mu(f_{1n} + f_{2n}\varphi_0 + f_{3n}\delta) + \mu^2(f_{4n} + f_{5n}\varphi_0 + f_{6n}\delta); \\ B_n &= \varphi_{0n} + \mu(\varphi_{1n} + \varphi_{2n}\varphi_0 + \varphi_{3n}\delta) + \mu^2(\varphi_{4n} + \varphi_{5n}\varphi_0 + \varphi_{6n}\delta), \end{aligned}\right\} \tag{9.28}$$

where f_{in} and φ_{in} are functions of coefficients of flapping, induced speeds, and rotor angle of attack.

Inertial forces on blades, arising due to their flapping around the flapping and drag hinges, depend basically on the coefficients of blade flapping, determined by equations (9.6) and (9.7). The form of coefficients A_n and B_n in this case is considerably simplified, since in formulas (9.28) there are no members which contain μ and μ^2, due to the fact that in expressions for inertial forces the speed of flight or parameter μ do not enter in evident form. Expressions for coefficients A_n and B_n of inertial forces are quite simply determined from the formulas given above.

Coefficients of variable components of forces on blades may be calculated with the known coefficients of flapping and induced speeds. Consequently, the change of forces on absolutely rigid blades can be studied, depending upon the variation of parameters of flight μ, φ_0, δ, and others. The accuracy of the calculation determination of variable forces on blades depends on the degree of authenticity of the information concerning flapping and induced speeds on the rotor.

The external aerodynamic forces on flexible blades differ somewhat from the forces on rigid blades due to their deformations. In particular, for flexible blades we must additionally consider the aerodynamic forces caused by the oblique flow around a bent blade and the change of the effect of deflection of the automatic pitch-control mechanism and the operation of the blade-flapping control for flexible blades due to their deformations. The inertial forces will also change somewhat, since flapping oscillations $y(r, t)$, and consequently also accelerations $\ddot{y}(r, t)$ of different points of the blade along its radius, will depend on its elastic deformations.

Oscillations of Rotor Blades in Flight

Under the action of external aerodynamic and inertial forces, rotor blades experience forces oscillations.

A revolving blade, which is flapping, is equivalent to an oscillatory system with many degrees of freedom. The resultant motion of a blade can be broken down into simple motions, i.e., oscillations of a blade near its hinges. For an absolutely rigid blade each of these simple motions is equivalent to the motion of a oscillatory system with one degree of freedom.

The motion of such simple oscillatory systems can be described by the equation

$$m\ddot{y}+2h\dot{y}+p^2y=P(t),$$

where the right side represents, in general form, the perturbing force on the blade, under the action of which the blade accomplishes forced oscillations.

The equation of forced oscillations of a flexible blade in the plane of least rigidity (in the flapping plane), taking into account equation (3.114) for natural oscillations of a revolving blade, may be written in the form

$$\frac{\partial^2}{\partial r^2}\left(EJ_1\frac{\partial^2 y}{\partial r^2}\right)-\omega^2\frac{\partial}{\partial r}\left(N\frac{\partial y}{\partial r}\right)+2h\frac{\partial y}{\partial t}+m\frac{\partial^2 y}{\partial t^2}=P_1(t), \tag{9.29}$$

where member $2h\frac{\partial y}{\partial t}$ considers the damping properties of the blade.

The equation of forced oscillations of a flexible blade in the plane of rotation, taking into account formula (3.125), has the form

$$\frac{\partial^2}{\partial r^2}\left(EJ_2\frac{\partial^2 x}{\partial r^2}\right)-\omega^2\frac{\partial}{\partial r}\left(N'\frac{\partial x}{\partial r}\right)+2h\frac{\partial x}{\partial t}-\omega^2mx+m\frac{\partial^2 x}{\partial t^2}=P_2(t). \tag{9.30}$$

Forced oscillations of revolving flexible blades depend both on the properties of the oscillatory system itself [its natural oscillations, determined by the left part of equations (9.29) and (9.30)], and also on the form of the function of perturbing force P(t). In view of the periodic change of flow rates on the blades during flight with forward velocity, the perturbing forces are also periodic and variable with every rotor revolution [see, for example, formula (9.27)]. The

Calculating the current by distribution function (2), we obtain

$$j_{0y}^{\alpha} = \left\langle e\int v_{\perp}\sin\theta f^{\alpha} d\vec{v}\right\rangle = -\frac{e c}{H_0}\left[\left\langle\int F_1^{\alpha} d\vec{v}\, \ldots\right\rangle - \left\langle\int F_1^{\alpha} d\vec{v}\,\frac{\hat{\Omega}}{\omega_H} E_x\right\rangle\right] + \frac{c}{H_0}\frac{\partial P^{\alpha}}{\partial x}, \tag{10}$$

where

$$P^{\alpha} = \int \frac{m v_{\perp}^2}{2} f_0\, d\vec{v},$$

and

$$j_{0z}^{\alpha} = \left\langle e\int v_{\perp}\cos\theta f^{\alpha} d\vec{v}\right\rangle = \frac{e c}{H_0}\left[\left\langle\int F_1^{\alpha} \ldots\right\rangle + \left\langle\int F_1^{\alpha} d\vec{v}\,\frac{\hat{\Omega}}{\omega_H} E_x\right\rangle\right]. \tag{11}$$

From (10) and (11) it follows that to determine currents with an accuracy of $\frac{1}{H_0^2}$ it is sufficient to determine F_1^{α} with an accuracy of $\frac{1}{H_0}$. With this accuracy F_1^{α} is determined by relationship (5). Substituting (5) in (10) and averaging (here it is necessary to allow for the fact that $\overline{k_y} = \overline{k_z} = \overline{k_y k_z} = 0$; the bar over the members signifies averaging for all possible values of components of vector $\vec{k}$), we obtain

$$j_{0y}^{\alpha} = -\frac{c}{H_0}\left\{\frac{\partial P^{\alpha}}{\partial x} + \frac{e^2}{2m^{\alpha}}\sum_{k_y k_z}\int d\vec{v}\, \frac{\partial F_0^{\alpha}/\partial v_z}{(k_z v_z - \omega_k')^2 + \gamma_k^2}\left[i(k_z v_z - \omega_k') \times (E_{xk}E_{xk}^{*} - E_{xk}^{*}E_{xk}) + \gamma_k (E_{xk}E_{xk}^{*} + E_{xk}^{*}E_{xk})\right]\right\}. \tag{12}$$

Inasmuch as oscillations are longitudinal, $E_{zk} = -\frac{1}{ik_z}\frac{\partial E_{xk}}{\partial x}$, therefore, finally for j_{0y}^{α} we obtain

$$j_{0y}^{\alpha} = -\frac{c}{H_0}\left[\frac{\partial P^{\alpha}}{\partial x} - \frac{1}{8\pi}\sum_{k_y k_z}\mathrm{Re}\left(\varepsilon_{xx}^{\alpha}(\omega, k) - 1\right)\frac{\partial}{\partial x}|E_{xk}|^2\right]. \tag{13}$$

helicopters are mounted on the tail beam. Under the action of the main and tail rotors the tail beam experiences vibrations. Due to the proximity of certain frequencies of oscillations of the beam, occurring from the main and tail rotors, it experience the phenomenon of oscillation beating. Beats, appearing due to oscillations of the tail beam, lead to a considerable increase of amplitudes of oscillations of tail rotor blades. Thus, in the study of oscillations of rotor blades one should turn attention both to the possible cases of resonance of blades, and also to cases beating due to oscillations of the rotor mounting bases.

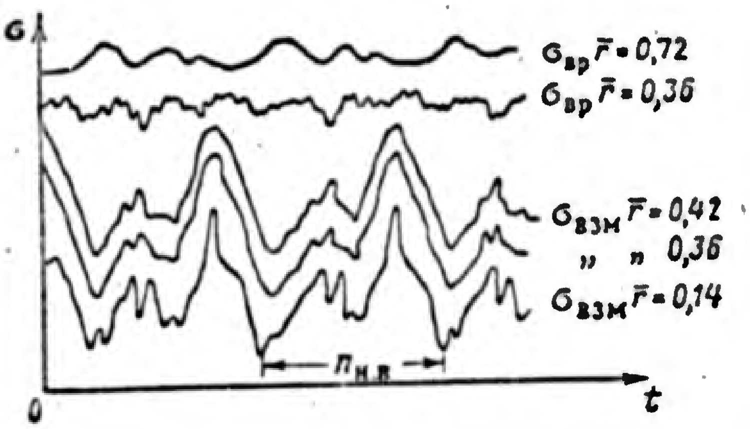

Fig. 9.6. Recording (oscillogram) variable stresses in a rotor blade spar in horizontal flight. σ_{flap} – in flapping plane, σ_{rotat} – in plane of rotation of blade, $\bar{r}$ – relative radius of blade section, $n_{m.r.}$ – period of oscillation, corresponding to one turn of main rotor.

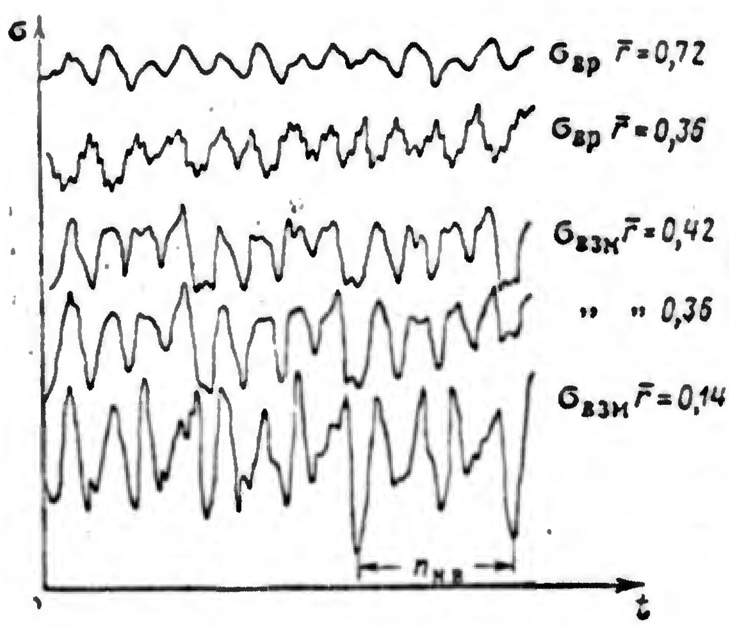

Fig. 9.7. Recording of variable stresses in a rotor blade spar in conditions of deceleration before landing.

Oscillations of helicopter rotor blades are combined and can essentially change with the change of the conditions of flight (Fig. 9.6 and 9.7). These oscillations, as noted, depend on many factors. By means of calculation it is difficult to find the conditions of flight at which there can appear dangerous oscillations of rotor blades. In view of this, special attention is allotted to the experimental study of oscillations and dynamic loading of rotor blades directly on helicopters during flying tests.

9.2. Helicopter Vibrations

In view of the fact that blades are hinged to rotor hubs, it has been considered, in disregarding the friction in the hinges, that only the forces acting upon the blades are transmitted to the hubs. From the forces of separate blades on rotor hubs there appear the following forces and moments (Fig. 9.8):

1) from blade thrust P_i – vertical force $P_{yi} = P_i \cos \beta$, rolling moment $M_{xi} = P_{yi} l_{f.h.} \sin \psi$, and pitching moment $M_{zi} = P_{yi} l_{f.h.} \cos \psi$ (Fig. 9.8a);

2) from the resisting force of blade rotation Q_i – longitudinal force $P_{xi} = -Q_i \sin \psi$, lateral force $P_{zi} = -Q_i \cos \psi$, torque $M_{yi} = Q_i l_{d.h.}$ (Fig. 9.8b);

3) from centrifugal force $P_{cen\ i}$ – longitudinal force $P_{cen\ xi} = P_{cen\ i} \cos \psi$ and lateral force $P_{cen\ zi} = P_{cen\ i} \sin n\psi$ (Fig. 9.8c);

4) from Coriolis force $P_{Cor\ i}$ – longitudinal force $P_{Cor\ xi} = P_{Cor\ i} \sin \psi$, lateral force $P_{Cor\ zi} = P_{Cor\ i} \cos \psi$, and moment $M_{Cor\ yi} = P_{Cor\ i} l_{d.h.}$ (Fig. 9.8d);

5) from inertial flapping force $P_{\beta i}$ – vertical force $P_{\beta yi} = -P_{\beta i} \cos \beta$, moments $M_{\beta xi} = P_{\beta yi} l_{f.h.} \sin \psi$, and $M_{\beta zi} = P_{\beta yi} l_{f.h.} \cos \psi$ (Fig. 9.8e);

6) from inertial forces $P_{\xi i}$ – component forces $P_{\xi xi} = -P_{\xi i} \cos \xi \sin \psi$, and $P_{\xi zi} = -P_{\xi i} \cos \xi \cos \psi$, and moment $M_{\xi yi} = -P_{\xi i} \cos \xi [l_{f.h.} + (l_{d.h.} - l_{f.h.}) \cos \psi]$ (Fig. 9.8, f).

This case pertains only to rotors that have drag and flapping hinges in the blade mounting.

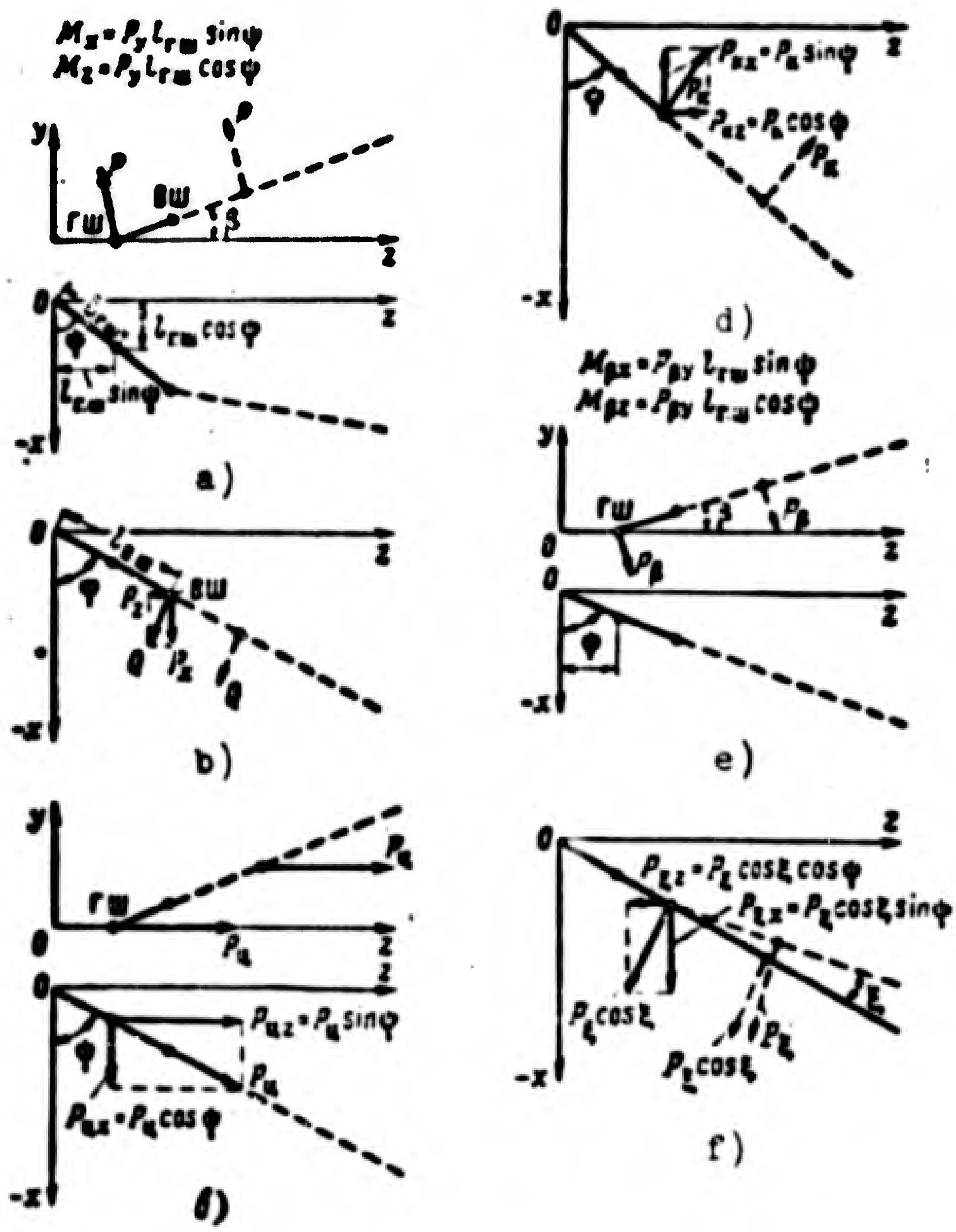

Fig. 9.8. The determination of forces and moments on a rotor hub.

It is obvious that if the variable parts of forces acting on the blades have frequencies which are multiple to rotor revolutions, then the variable forces and moments, created by them on the rotor hub, will also have frequencies that are multiple to rotor turns. In general, each of the enumerated forces and moments, formed on the hub by forces of a separate blade, may be represented by a trigonometric series with any degree of accuracy:

$$P_i = P_0 - \omega^2 \sum_{n=1}^{\infty} (A_n^0 \cos n\psi_i + B_n^0 \sin n\psi_i). \qquad (9.31)$$

where "h" means that the forces are applied to the hub.

The resultant force on the hub of a k-bladed rotor constitutes the sum of forces created on the hub by all blades:

$$P^0_{\Sigma}=\sum_{i=1}^{k}\left[P^0_{0i}-\omega^2\sum_{n=1}^{\infty}(A^0_{ni}\cos n\psi_i+B^0_{ni}\sin n\psi_i)\right]. \tag{9.32}$$

Considering the known property of trigonometric functions, including the fact that when $\psi_i = \psi_0 + (i - 1)\frac{2\pi}{k}$ and $n \neq mk$ $(m = 1, 2 \ldots)$

$$\sum_{i=1}^{k}\cos n\psi_i=0,\quad \sum_{i=1}^{k}\sin n\psi_i=0, \tag{9.33}$$

under the condition of full identity of blades, we obtain

$$P^0_{\Sigma}=P^0_{0\Sigma}-\omega^2\sum_{m=1}^{\infty}(A^0_{mk}\cos mk\psi+B^0_{mk}\sin mk\psi). \tag{9.34}$$

In other words, the total components of variable forces and moments, formed on the hub by the forces of all blades, have frequencies that are multiple to the number of rotor blades k. All component forces of other harmonics are mutually damped and are not transmitted to the helicopter fuselage.

Coefficients A_{mk} and B_{mk} of the total forces on the hub are analogous in form to coefficients A_n and B_n of the forces of separate blades in formulas (9.28). They are functions of the same parameters and constitute a linear combination of coefficients A_n and B_n. Consequently, they may be presented in the form

$$\left.\begin{aligned}A_{mk}&=f^0_{0mk}+\mu(f^0_{1mk}+f^0_{2mk}\varphi_0+f^0_{3mk}\delta)+\mu^2(f^0_{4mk}+f^0_{5mk}\varphi_0+f^0_{6mk}\delta);\\ B_{mk}&=\varphi^0_{0mk}+\mu(\varphi^0_{1mk}+\varphi^0_{2mk}\varphi_0+\varphi^0_{3mk}\delta)+\mu^2(\varphi^0_{4mk}+\varphi^0_{5mk}\varphi_0+\varphi^0_{6mk}\delta).\end{aligned}\right\} \tag{9.35}$$

where f_{imk} and φ_{imk} are functions of coefficients of flapping, induced speeds, and angle of attack.

"h" means that the indicated coefficients pertain to forces on the rotor hub.

Total forces on a hub may be calculated with respect to the known forces of separate blades and can be used for analysis of vibration phenomena which appear in a helicopter. In practice, however, such calculations are rarely conducted because of their complexity and low accuracy. Usually preference is given to experimental investigation of vibrations, conducted directly on a helicopter during flying tests.

The peculiarity of forced oscillations of helicopter parts consists in that the total vibrations of a helicopter fuselage have frequencies that are multiple to the number of rotor blades. Therefore, it is always possible beforehand to indicate the frequencies of predominant vibrations of parts of a helicopter. This is fully confirmed by the results of investigation of fuselage vibrations and variable stresses in its assemblies.

The change of amplitudes of oscillations of helicopter parts with conditions of flight and the stresses appearing in the supporting members of the structure basically correspond to the change of dynamic loads on the main and tail rotors.

Vibrations of helicopters, caused by rotor rotation, independently of conditions of flight, occur in two types:

– vibrations which appear due to periodic changes of forces acting on rotor blades in forward flight; these vibrations have frequencies that are multiple to the number of rotor blades;

– vibrations which appear due to poor balancing of blades and rotor adjustment; these vibrations have a frequency that is equal to the rotor revolutions.

Vibrations of the first type are inevitable on helicopters and they are of basic interest for study. The intensity of vibrations of the second type changes depending upon the quality of balancing of blades and rotor adjustment on the whole.

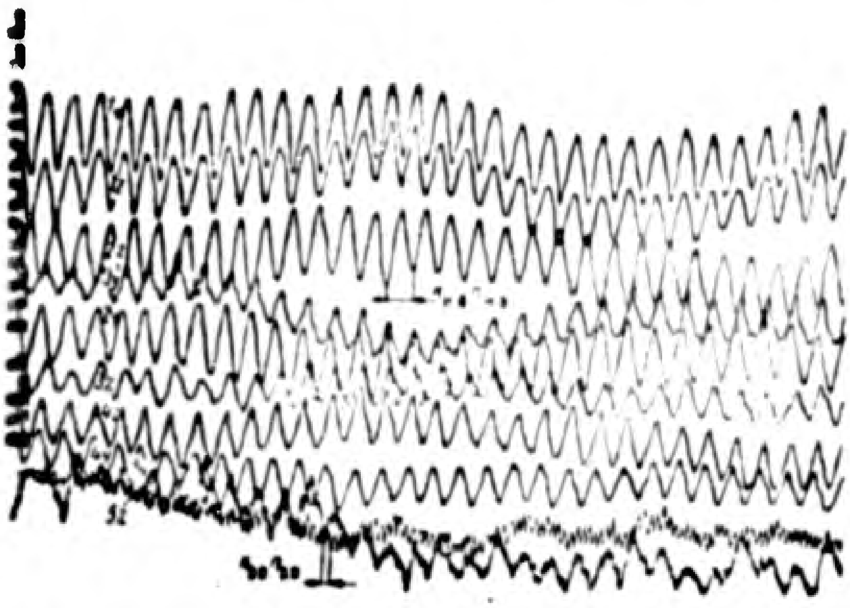

Fig. 9.9. Typical recording of vibrations of a single-rotor helicopter. 1) cockpit; 2) cargo cabin; 3) nose section of fuselage; 4) tail beam; 5) end beam, y and z – coordinates of helicopter, in the direction of which the vibrations were recorded, $k_{m.r.}n_{m.r.}$ – oscillation period, corresponding to $k_{m.r.}$ rotor turns ($k_{m.r.}$ is the number of rotor blades, $n_{m.r.}$ are the rotor turns), $k_{t.r.}n_{t.r.}$ is the oscillation period corresponding to $k_{t.r.}$ turns of the tail rotor ($k_{t.r.}$ is the number of tail rotor blades, $n_{t.r.}$ are the turns of the tail rotor).

From the oscillograms that are shown in Figures 9.9 and 9.10, it is clear that vibrations with frequency $k_{m.r.}n_{m.r.}$ are predominant for helicopters with k-bladed rotors. The variable stresses caused by them in the structural elements have the same frequency. These vibrations and stresses have frequencies that are multiple to the number of rotor blades.

On the tail and end beams, which the tail rotor is mounted on, besides the vibrations which were mentioned above, there also appear vibrations, a source of which is the tail rotor, with frequencies that are multiple to the number of its blades.

In certain conditions of flight, oscillations of the 2k-th harmonic of rotors also become essential. Oscillations of higher harmonics are practically nonexistant on helicopters.

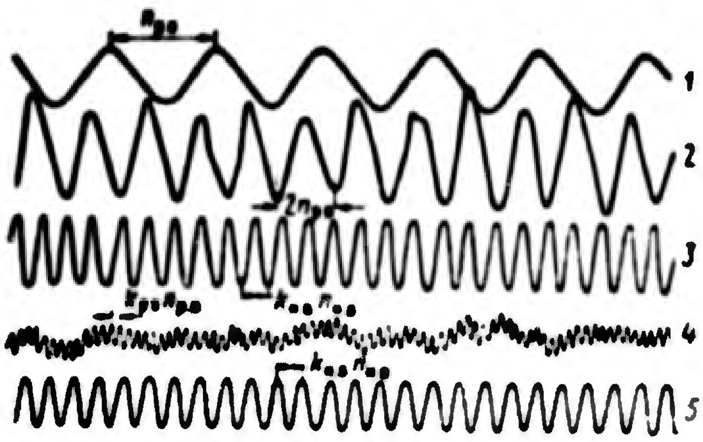

Fig. 9.10. Typical recording of vibrations and stresses in helicopter assemblies during horizontal flight. 1) flapping angle β of tail rotor blade; 2) bending moment of tail rotor blade in plane of rotation; 3) normal stresses in mounting rods of rotor reduction gear; 4) normal stresses in stringer of end beam; 5) vibrations in cockpit.

All other forms of vibrations, in particular motor vibration, have a smaller value than the vibrations caused by the main and tail rotors. The results of measurements of motor vibration on helicopters show that it essentially does not differ from that observed on aircraft with identical propulsion systems.

Thus, predominant (with respect to amplitudes and dynamic loads caused in assemblies) vibrations of helicopters have frequencies $n_{m.r.}$, $k_{m.r.}n_{m.r.}$, $k_{t.r.}n_{t.r.}$. The physical values of these frequencies vary in small limits and for contemporary helicopters they are correspondingly 2-3, 9-14, 40-55 oscillations per second.

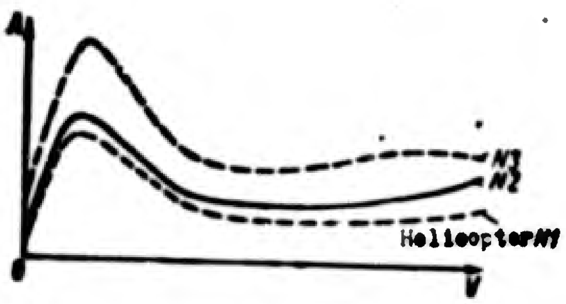

Fig. 9.11. Graph of amplitudes of oscillations in cabins of three different helicopters for frequencies equal to $k_{m.r.}n_{m.r.}$.

In distinction from aircraft, where predominant oscillations are usually observed in one (vertical for the most part) direction, on helicopters vertical and horizontal oscillations are equally as large. The character of change of amplitudes of basic oscillations with respect to conditions of flight for all helicopters is practically identical (Fig. 9.11). The lowest amplitudes of oscillations are observed in hovering, when the rotors work in conditions of axial airflow. In this case all rotor blades are enveloped by a flow of air with identical (with respect to azimuth) speeds, and vibrations with frequency $k_{m.r.}n_{m.r.}$ appear only due to the flapping of blades because of the small deflection of the automatic pitch-control mechanism while hovering. At low forward speeds of flight helicopter vibrations are sharply increased, and upon further increase of flight speed they at first decrease, and then again increase.

The causes of the increase of vibrations at low speeds of flight are still insufficiently studied. One of them is the sharp redistribution of high induced speeds along the rotor disk. The level of oscillations in these conditions also depends on the position of the rotor disk with respect to the vector of forward velocity. Thus, in conditions of deceleration before landing, upon lifting the nose of the helicopter, when the rotor has a large angle of attack, the rear part of rotor disk goes into the wake and helicopter vibrations reach their highest magnitude. In conditions of acceleration of a helicopter, in takeoff, and at low steady speeds of flight, when the rotor has a smaller or negative angle of attack, the vibrations decrease. The biggest vibrations on helicopters appear in a rather narrow range of low speeds (20-40 km/hr). In transitional flight regimes (during acceleration and deceleration) intense vibrations act for a short time, corresponding to the time of passage by the helicopter of the indicated speeds of flight. However, vibrations and dynamic loads on assemblies of the helicopter can be so considerable that it is impossible to disregard them.

The boundaries of the appearance of considerable vibrations at low speeds of flight on all helicopters have been inspected quite sufficiently. The dynamic loading of all basic structural elements of helicopters at these speeds of flight has been studied. However, ways for the full removal of this phenomenon on helicopters have not yet been found.

For the purpose of lowering the harmful effect of vibrations, for flying operation of helicopters limitations on flying time (service life) are sometimes introduced under conditions of the appearance of increased vibrations. Furthermore, in flight instructions of helicopters indications are usually given to the crew about piloting methods during acceleration and deceleration before landing, which have the purpose of limiting the time the helicopter remains in conditions of raised vibrations and lowering the level of these vibrations. Thus, lowering of vibrations may be attained upon the fulfillment of a shallow approach glide. In certain helicopters it is possible to avoid the appearance of large vibrations in the fulfillment of a steep glide with subsequent sharp deceleration to hovering of the helicopter and smooth landing. However, it is not always possible to execute such landings, especially with poor approaches and small dimensions of landing strips.

9.3. Oscillations of Helicopter Parts Appearing with Rotor Misadjustment

The basic causes, leading to disturbance of balancing of mass and aerodynamic forces on a rotor, are the inaccuracies in weight balancing of the rotor on the whole, in transverse balancing of blades (with respect to their longitudinal axis), and in the blade setting angles allowed during assembly, and also incorrect adjustment of trim tabs and blade dampers.

Due to the inaccuracy of weight balancing of the rotor on the whole, the center of gravity of the rotor does not coincide with the axis of rotation and there appears an unbalanced centrifugal force.

Weight unbalance of a rotor can appear in operation for various reasons, in particular due to the change of weight of blades from weather effects, fall of moisture on the blades, damage to the skin, and others.

With inaccurate transverse weight balancing of blades the centers of gravity of sections of an individual blade are not on its longitudinal axis. Due to this, under the action of centrifugal forces there appears a certain moment which turns the blade around the feathering hinge (Fig. 9.12):

$$M_{fe.h.} = P_{cen}\sigma_b \sin\beta,$$

where P_{cen} is the centrifugal force of the blade;

σ_b is the distance between the center of gravity of the blade and its longitudinal (flexible) axis;

β is the blade-flapping angle with respect to the flapping hinge.

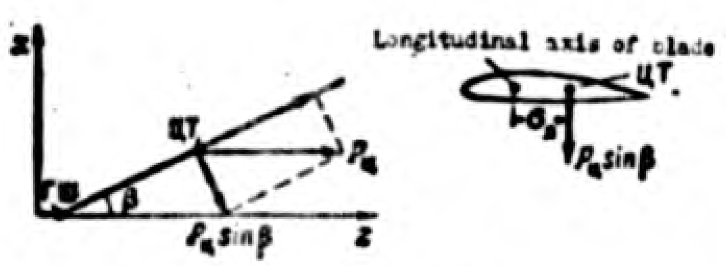

Fig. 9.12. Diagram of appearance of moment $M_{fe.h.}$ with inaccurate transverse weight balancing of a blade.

In this case (with reversible control) the bar of the automatic pitch-control mechanism receives a force which leads to a certain deflection of it. During rotor rotation the automatic pitch-control mechanism will also deviate. Due to oscillations of the ring of the automatic pitch-control mechanism the thrust vector of the rotor will describe a certain cone and balancing of aerodynamic forces will be disturbed.

Blade thrust, due to the difference in setting angles, will be unequal, and consequently the balancing of aerodynamic forces will be disturbed. The "co-taper" of blades will be disturbed, i.e., a blade with changed setting angle will "fall" from the cone of rotation which was formed by the motion of the other blades. Due to this, the balancing of mass forces is additionally disturbed.

Incorrect adjustment of trim tabs of blades, intended for compensation of moments appearing on the blades due to the disturbance of aerodynamic properties, leads to phenomena which are analogous to those which appear with incorrect transverse mass balancing of blades, and it also causes unbalance of aerodynamic and mass forces on the rotor.

In unbalance of mass forces on the rotor there appears an unbalanced centrifugal force of the rotor $P_{cen.\ rot}$ (in distinction from the centrifugal force of the blade P_{cen}), which causes oscillations of the entire helicopter:

$$P_{ц.в} = m_в \omega^2 e,$$

where m_{rot} is the mass of the rotor;

e is the eccentricity of the rotor's center of gravity.

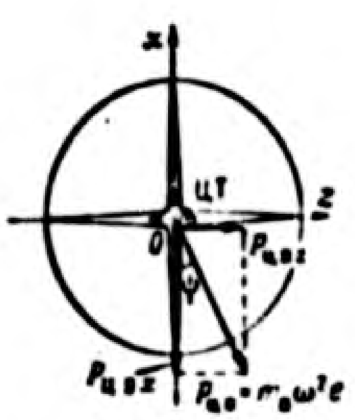

Fig. 9.13. Diagram of formation of components of unbalanced centrifugal force $P_{cen.\ rot}$ with unbalance of mass forces on a rotor.

The components of this force, along the rotor axes x, z, coinciding in directions with the connected axes of the helicopter, will be (Fig. 9.13):

$$P_{ц.в.x} = m_в \omega^2 e \cos\psi;$$
$$P_{ц.в.z} = m_в \omega^2 e \sin\psi.$$

Upon deflection of the automatic pitch-control mechanism to angle δ, for instance due to inaccuracies in transverse weight balancing of blades and incorrect adjustment of trim tabs of blades, there appears a revolving unbalanced force

$$P_y i_a \sin\delta \approx P_y i_a \delta,$$

where i_a is the transmission ratio of the automatic pitch-control mechanism.

This force will form variable components: longitudinal $P_{x\delta} = P_y i_a \delta \cos\psi$ and transverse $P_{z\delta} = P_y i_a \delta \sin\psi$.

With inaccuracies in blade setting angles there appears an additional blade thrust ΔP_y, which leads to the formation of variable moments on the rotor hub:

$$\Delta M_z = \Delta P_y l_{f.h.} \sin\psi,$$
$$\Delta M_x = \Delta P_y l_{f.h.} \cos\psi,$$

where $l_{f.h.}$ is the distance from the axis of rotation to the flapping hinge of the blade.

With unequal adjustment of the dampers of drag hinges of the rotor the variable part of total torque from all blades on the hub cannot be equal to zero. Due to this the dampers of the blades transmit a certain perturbing torque to the hub

$$M_{d.h.} = k\dot{\xi},$$

where k is a certain constant;

ξ is the lag angle of the blade.

In basic flight conditions with a sufficient degree of accuracy, angle ξ may be approximated by the first harmonic of expansion in Fourier series. Consequently, moment $M_{d.h.}$ also will vary basically according to the law of the first harmonic to rotor turns (more exact, according to the law of change of angle ξ).

Thus, due to the different inaccuracies in rotor adjustment there appear variable forces and moments, which always have a frequency that is equal to rotor turns. They cause oscillations of helicopter parts with the same frequency. The amplitudes of these oscillations, all other conditions being equal, are proportional to the magnitudes of variable forces and moments; in other words, they are proportional to the degree of rotor misadjustment.

If with normal rotor adjustment the oscillations of parts of a helicopter have a basic frequency which is multiple to the number of rotor blades, then with rotor unbalance there predominate oscillations with a frequency that is equal to rotor turns. This is confirmed by the results of measurements of oscillations on helicopters. Usually the amplitudes of these oscillations are small, but depending upon the degree of rotor unbalance they can attain a considerable magnitude.

Oscillations of a rotor through its mounting (reductor frame) are transmitted to the entire helicopter. The biggest amplitudes of oscillations of the reductor frame, with a frequency that is equal to rotor turns, are observed in the plane of its rotation. Amplitudes of the reductor frame in the direction of axes x and z of the helicopter, as shown by the results of measurements, are changed equally with the change of rotor turns. The lateral oscillations are then larger in amplitude than the longitudinal ones, and vertical oscillations are practically absent. Amplitudes of oscillations in other places of the helicopter are changed in conformity with the change of amplitudes of oscillations of the reductor frame.

Operational experience shows that even insignificant rotor unbalance leads to the appearance of large vibrations of a helicopter. The causes of such vibrations frequently are the DH dampers, especially the frictional dampers. Considerable vibrations, which can appear in operation due to rotor misadjustment, are undoubtedly impermissible. They are eliminated by improving the balancing of blades during manufacture, assembly, and mounting of the rotor on the helicopter, and also by checking the correctness of rotor adjustment in operation.

In practice there frequently occurs rotor misadjustment because of operational reasons (moisture on blades, nonuniform wear of covering, especially wooden coverings with varnish and paint coatings, a certain change in the adjustment of DH dampers, etc.). The permissible limits of such misadjustment are determined by the permissible level of vibrations on the helicopter. In the determination of parameters of dynamic loading of assemblies connected with the helicopter fuselage, it is necessary to consider the possibility of some rotor misadjustment. For this, flights are sometimes made with defined, predetermined, rotor misadjustment in order to determine the influence of the degree of misadjustment on the level of dynamic loading of the helicopter structure.

9.4. Flutter of Helicopter Rotor Blades

Flutter of blades of main and tail rotors can appear in flight and in ground conditions (in the absence of forward velocity) at a defined speed of airflow around blades, which is composed of the peripheral velocities of rotation of blades and the speed of flight (see Fig. 9.2). Therefore, the critical state of flutter of blades is usually estimated by rotor turns (critical flutter revolutions n_f) and by speed of flight (critical speed V_f).

Divergence of blades in existing helicopters does not have practical value, since the rotor turns, at which this phenomenon appears, is usually greater than the critical turns n_f or maximum operation turns of the rotor.

However, in certain cases the divergence of blades can present a real danger.

Flutter of blades presents a large danger for helicopters due to the possibility of fast destruction of the rotor in flight.

Cases of flutter of helicopter rotors were sometimes accompanied by "fall" of the blades from the cone of rotation. There is even a case of blades touching the helicopter cabin during flutter. On helicopters with coaxial propellers this can lead to "whipping" of blades of the upper and lower rotors.

On helicopters, cases of flutter were noted in basically two forms: stalling flutter of tail rotors at large blade-setting angles and flexural-torsional flutter of rotor blades (it is also called torsional-flapping flutter).

Stalling flutter was considered in Chapter VI. The basic measures for preventing it are limitations of blade-setting angles (rotorpitch) in operation, increase of torsional rigidity of blades, and forward displacement of centers of gravity of end sections of blades.

For convenience of analysis we distinguish flapping and bending forms of flutter of rotor blades, although both of these forms are flexural-torsional flutter, but have different tones of natural blade oscillations.

Flutter of rotor blades is called flapping or torsional-flapping, if during oscillations the motions of the blades as a solid about the flapping hinge are predominant (zero tone of natural oscillations); bending strain of a blade in the flapping plane is insignificant.

Flutter is called flexural or flexural-torsional, if during oscillations of blades bending strain of blades is predominant. In both cases it is assumed that blades during flutter accomplish collective flexural-torsional (torsional-flapping) oscillations.

In practice, basically flapping flutter of rotor blades was encountered.

Flutter of rotor blades can be in two forms: without shift of phases between oscillations of blades, and with phase shift. In the first case the problem can be reduced to the investigation of flutter of one isolated blade, secured in the shank, and the analysis of flutter is considerably simplified. In the second case the analysis of flutter is considerably complicated, since it is necessary to consider the rotor on the whole, and not a separate blade. But in this case it is also possible to reduce the problem to the investigation of one isolated blade under certain simplifying assumptions, which somewhat lower the accuracy of calculations however.

In the first case flutter is more intense; therefore it presents the biggest danger. Main loads in this form of flutter are experienced by the collective rotor pitch-control system. In the second case flutter is less intense, and main loads are experienced by the cyclical-control system.

Thus the simplest, and at the same time, the most important calculation cases in the investigation of flutter are the joint flexural-torsional oscillations of one isolated blade taking into account the different tones of flexural oscillations of the blade in the flapping plane, including zero tone.

A basic influence on blade flutter, as also in the case of flexural-torsional wing flutter, is rendered by the torsional oscillations of a blade. Minimum values of n_f correspond to the 1st tone of torsional blade oscillations. Practical interest is, therefore, presented to the consideration of forms of flutter with the participation of torsional blade oscillations in the 1st tone. Forms of flutter with the participation of torsional blade oscillations of other tones usually have critical turns n_r which considerably exceed the maximum operational rotor turns.

Flutter of rotor blades can have two, three, and more degrees of freedom. Calculation of flutter with degrees of freedom of more than three presents considerable difficulties.

In all cases the combination of different flexural tones is usually considered with the form of the 1st tone of torsional blade oscillations. For example, during flutter with two degrees of freedom, torsional blade oscillations of the 1st tone and blade oscillations in the flapping plane in the zero or 1st tone are considered. During flutter with three degrees of freedom, torsional blade oscillations of the 1st tone and flexural blade oscillations in the flapping plane are considered in two tones (for instance, in the zero and 1st tone, or the 1st and 2nd tones of natural flexural blade oscillations).

Torsional blade oscillations appear due to elastic deformations of the blade itself, elastic deformations of the blade-control system, and due to the action of the blade-flapping control. Therefore, in calculation the blade is considered to be fixed to the shank on a flexible base with equivalent rigidity of the control system. Calculation is simplified if the blade can be considered to be absolutely torsionally rigid, while torsional blade oscillations basically occur due to elastic deformations of the control system. Such simplification of calculation can be made when the control system possesses small rigidity as compared to the torsional rigidity of a blade. In a very rigid control system one may assume that torsional blade oscillations occur basically due to elastic deformations of the blade itself. In this case the calculation may also be simplified.

Rigidity of the system of longitudinal and lateral control in the first approach may be considered as identical. Such an assumption in most cases does not lead to large errors. With the consideration of the distinction in rigidity of longitudinal and transverse control the calculation is complicated.

In flexural-torsional rotor flutter the blade oscillations in the plane of rotation do not render a large influence on n_f and in calculations they will be frequently disregarded.

The permissibility of those or other simplifications in the analysis of flutter of rotor blades is estimated in every specific case.

Selection of a calculation form of flutter in many respects depends on the experience of the researcher. Therefore, a study of the cases of flutter, encountered in the use of different helicopters, helps in the correct determination of a calculation form of flutter for the rotor of a new helicopter.

In a number of cases the calculation case of flutter with two degrees of freedom may be considered as the simplest; for instance joint torsional oscillations and blade flapping as a whole with respect to the flapping hinge. Under certain assumptions, with respect to the form of torsional blade oscillations, flutter equations in this case can be reduced to a system of two differential equations with two variables: angle of rotation with respect to the feathering hinge φ and angle of rotation with respect to the flapping hinge β.

In those cases when such a simplification can lead to large errors, flutter of a more complicated form is considered, but the analysis of flutter is strongly complicated because of this.

A large influence on rotor flutter is rendered by centering of blades, the magnitude of the blade-flapping control factor k_{bfc}, and the rigidity of rotor control. With rear centering of blades n_f decreases and with forward displacement of the center of gravity n_f is increased. There then exists such a value of centering $x^*_{c.g.}$ that if $x_{c.g.} \leq x^*_{c.g.}$, flutter is possible neither at any rotor speeds nor at any speeds of flight. Due to this, in the creation of the necessary centering of blades, flutter of rotor blades is removed. On finished rotors the magnitude n_f can be increased by installing balancing weights on the blade nose, especially on its tips.

With the decrease of the blade-flapping control factor k_{bfc}, the purpose of which is to change the blade-setting angle during its flapping about the flapping hinge, n_f is increased. By changing the magnitude of this factor, it is possible to affect flutter in the needed direction.

A large influence on critical flutter speed is rendered by the torsional rigidity of a blade. The frequencies of natural oscillations of blade torsion in a strong degree depend on the rigidity of control of its setting angle. Due to this, the rigidity of rotor control strongly affects flutter of blades. With the increase of torsional rigidity of blades and rigidity of control, n_f is increased.

Blade flutter is largely influenced also by friction in the hinges. With the increase of friction (especially in the feathering hinge) n_f is increased.

In calculations of flutter only friction in the feathering hinge, which is loaded by the centrifugal force of the blade, usually is considered. Friction in the other hinges is disregarded. In this instance the possible change of the coefficient of friction is considered with the change of temperature of the lubricant of the feathering hinge.

Flutter of rotor blades can arise in conditions of hovering and in flight at defined critical rotor speed n_f. In this case, in forward flight n_f is lowered. Due to this, the rotor, which safe from flutter on the ground, can be unsafe upon the appearance of flutter in flight.

The influence of forward velocity of flight on flutter of rotor blades has not yet been studied sufficiently. It is known that the same factors can differently affect the characteristics of flutter in conditions of flight with forward velocity and in conditions of hovering.

In flight, a strong influence on flutter is rendered by the compressibility of air, which in the first place appears in the blade tips. Due to the influence of compressibility of air the position of the aerodynamic focus and the aerodynamic coefficients c_y^α and c_m^α become dependent on Mach number. In forward flight the aerodynamic coefficients and the position of the focus of blade sections periodically change in azimuth. With the increase of the speed of flight the range of these changes increases, which can essentially lower the flutter characteristics of blades.

Inasmuch as flutter is influenced by a number of parameters (centering of blades, friction in hinges and others), which can change in operation due to various causes in defined limits, the rotors must possess a defined flutter margin.

For guarantee of helicopter safety from rotor blade flutter it is necessary that two conditions simultaneously be executed:

$$n_{\phi} > (1{,}20-1{,}35)\, n_{max.}$$
$$V_{\phi} > (1{,}20-1{,}35)\, V_{max\ max.}$$

where n_{max} is the maximum permissible rotor speed;

$V_{max\ max}$ is the maximum permissible flight speed of the helicopter.

Sometimes there two conditions can be replaced by the equivalent requirement of guarantee of a definite centering margin of blades. Fulfillment of this requirement can be monitored in the manufacture of blades and in operation.

The magnitude of the margin depends on the rotor speed, the centering of blades, the degree of reliability in determining n_f and V_f, and the degree of facility in exceeding n_{max} and $V_{max\ max}$ in piloting errors.

The safety of rotors from flutter is checked in ground conditions directly on helicopters at rotor speeds which are determined taking into account the margin, and in the centering of blades which are artificially shifted back taking into account the required centering margin. Inasmuch as in forward flight n_f is somewhat lowered, in the ground check of rotor safety from the appearance of flutter, this lowering of dynamic stability of blades is simulated by corresponding backward displacement of the center of gravity of the blades.

Investigation of flutter directly on helicopters in flight is extremely dangerous. Therefore, large propagation has been obtained by laborat y methods of investigating rotor flutter in an oblique flow on dynamically similar models in wind tunnels and by an experimental safety check of rotors for flutter in ground conditions directly on the helicopter.

9.5. Ground Resonance

Ground resonance denotes the self-exciting oscillations of a helicopter, which appear in ground conditions due to the interaction of oscillations of the helicopter on flexible landing gear with oscillations of blades near the drag hinges. The name "ground" is connected with the fact that this phenomenon usually occurs in ground conditions, e.g., during takeoff, landing, and during operation of a helicopter on the ground (secured and unsecured).

An analogous phenomenon under certain conditions is also possible in flight due to the influence of elasticity of the structure which the rotor is mounted on. In particular, if the frequency of natural oscillations of the fuselage is close to the rotor speed, the danger of appearance of the indicated oscillations in flight becomes quite realistic. In this case, the tandem-rotor helicopters in which the antinode of fuselage oscillations in the first tone is near the rotor are more predisposed to such oscillations than single-rotor helicopters in which near the rotor we usually find the node of natural fuselage, oscillations. The most possible oscillations on helicopters are transverse ones, in which large masses (rotors and engines) are located on the ends of the transverse boom or wing.

The appearance of self-exciting oscillations of the ground resonance type is connected with the presence of drag hinges in the blade mounting, which allows displacement of blades in the plane of rotation. In the absence of drag hinges ground resonance is practically impossible.

The mechanism of the appearance of self-exciting oscillations in ground resonance is the following. With an asymmetric impact of the landing gear of a helicopter on the ground, during a landing or upon takeoff, the blades are displaced at an angle with respect to the drag hinge (Fig. 9.14). There then appears a large magnitude unbalanced centrifugal rotor force $P_{cen.\ rot}$ (perturbing force), which rocks the helicopter. If the frequency of natural oscillations of the helicopter on the landing gear coincides with or is close to the frequency of the perturbing force $P_{cen.\ rot}$, there appears the phenomenon of ground resonance. Swaying of the helicopter (amplitude of oscillations) then increases, the unbalanced centrifugal force on the rotor increase, and the prerequisite for increase of oscillations is created, which leads to helicopter failure.

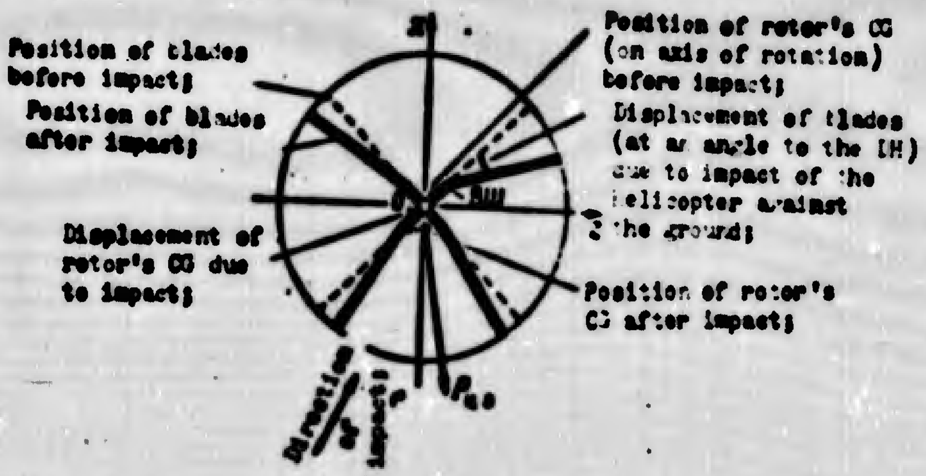

Fig. 9.14. Diagram of the appearance of an unbalanced centrifugal force on a rotor upon impact of the landing gear of a helicopter against the ground.

Ground resonance can also appear without an initial "impact" of the helicopter against the ground, if the rotor is unbalance in the weight aspect and there is a sufficiently large unbalanced centrifugal force $P_{cen.\ rot}$. However, in this case the ground resonance is usually less intense.

The pendular frequency of oscillations of an absolutely rigid blade with respect to the DH, in accordance with formula (3.126), is equal to

$$p_0=\sqrt{p_0^2+\nu_0^2\omega^2};\quad \nu_0=\sqrt{a_0-1}=\sqrt{\frac{l_{hm}S_{hm}}{J_{hm}}}. \qquad (9.36)$$

where $S_{d.h.}$ and $J_{d.h.}$ are the static moment and moment of inertia of the blade with respect to the DH, correspondingly.

The angular velocity of motion of the centers of gravity of the blades in the plane of rotation, considering $\bar{P}_{\cup} = 0$, is

$$\omega_{c.g.} = (1 - \nu_0)\omega. \tag{9.37}$$

The magnitude of $\omega_{c.g.}$ is 25-30% less than the angular velocity of rotor rotation.

Centrifugal force is

$$P_c = m_b \omega^2_{c.g.} r_{c.g.}. \tag{9.38}$$

Ground resonance appears upon coincidence of the frequency of natural oscillations of the helicopter on the landing gear P_{rot} with frequency of perturbing force P_{cen} (9.38):

$$p_0 = (1 - \nu_0)\omega. \tag{9.39}$$

Hence, critical rotor speed in terrestrial resonance can be determined from the relationship

$$\omega_{cr} = \frac{p_0}{1 - \nu_0}. \tag{9.40}$$

The problem of ground resonance is complicated by the fact that upon change of rotor thrust the natural frequencies of oscillations of the helicopter on its landing gear change in very large limits. This is connected with the fact that the landing gear is affected by the difference in the weight of the helicopter G and the rotor thrust T. If we schematize a helicopter on its landing gear as an oscillatory system with one degree of freedom, then in accordance with formula (3.2) the frequency of natural oscillations strongly depends on the difference of G - T and the rigidity of damping, which changes with the change of the difference of G - T:

$$p=\sqrt{\frac{Kg}{G-T}}. \qquad (9.41)$$

Due to what has been pointed out, it is difficult to avoid the coincidence of frequenices of natural helicopter oscillations on the landing gear with the frequency of the perturbing force. Therefore, the conflict against ground resonance is conducted mainly by means of damping the oscillations. For this, the drag hinges are equipped with special shock-absorbers (frictional or hydraulic). In the absence of such shock-absorbers the self-exciting oscillations of a helicopter on the ground having a rotor with drag hinges, are practically inevitable.

However, shock-absorbers lead to the appearance of a considerable bending moment in the blade shanks. The latter is very undesirable, since the blades of helicopter rotors experience large loads. Therefore, the characteristics of shock-absorbers are selected so that they do not lead to considerable loading of blades. In this case the application of shock-absorbers for the drap hinges would be insufficient preventing ground resonance. Additional shock-absorption is attained by the selection of landing gear shock-absorbers or by the introduction of special shock-absorbing devices in the landing gear system.

For the determination of the necessary shock-absorption the helicopter is calculated for ground resonance.

In the calculation of a helicopter for ground resonance a number of simplifying assumptions are made, since it is too complicated to conduct such a calculation in full volume.

The assumptions made in the calculation of helicopters for ground resonance include the following. A helicopter fuselage is considered to be absolutely rigid, since the elasticity of a fuselage hardly affects ground resonance. However, this assumption is unacceptable if we are considering natural oscillations of the ground resonance type, which can appear in flight when elastic oscillations of the fuselage (or rotor shaft) are necessary conditions of excitation of such oscillations. Rotor blades are considered to be absolutely flexurally rigid in the plane of rotation. In the presence of drag hinges the elasticity of blades practically does not show up in the characteristics of ground resonance. However, in certain special cases it is theoretically possible to have ground resonance (in the absence of drag hinges in the blade mounting) due to the influence of elasticity of the blades.

The nonlinear characteristics of elasticity and shock-absorption of landing gear are replaced by certain equivalent linear characteristics. This makes it possible to compose differential equations, which are necessary for the analysis of ground resonance, in linear form.

Further simplification of the problem consists of in that individual longitudinal (in the plane of symmetry) and transverse oscillations of the helicopter are considered on elastic landing gear. Since a helicopter fuselage always has a plane of symmetry, the consideration of individual longitudinal and transverse oscillations of the helicopter is fully permissible. This makes it possible to considerably simplify the problem of analysis of ground resonance.

Instead of a system from six differential equations, describing the motion of an absolutely rigid fuselage with six degrees of freedom, we consider two systems with three differential equations each, which determine the longitudinal and transverse oscillations of a helicopter.

If the difference between individual natural frequencies of oscillations of the helicopter on its landing gear are sufficiently large, then in rough calculations it is possible to consider the fuselage on landing gear with one degree of freedom (for each tone of natural oscillations separately).

Ground resonance in the form of transverse oscillations of a helicopter is more intense and consequently it presents a larger danger than ground resonance in the form of longitudinal oscillations. Therefore, in the analysis of ground resonance, in the first place transverse oscillations of the helicopter are considered.

The calculation diagram of a helicopter in each specific case can be different. For the investigation of transverse oscillations a diagram with three degrees of freedom is usually used: vertical shift of helicopter on landing gear, lateral shift, and angular shift of helicopter (Fig. 9.15).

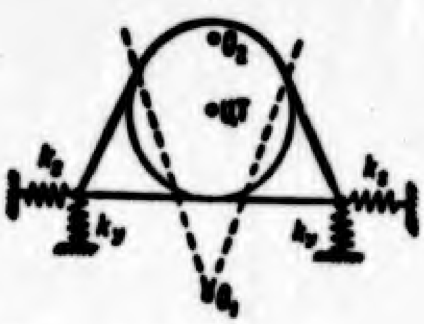

Fig. 9.15. Diagram of a helicopter for the calculation of ground resonance.

The frequency of vertical oscillations $P_y = \sqrt{2k_y/m}$ practically does not influence ground resonance. Ground resonance is determined by two other degrees of freedom. A system with two degrees of freedom has two frequencies of natural oscillations: the frequency of lateral oscillations of the helicopter P_z and the frequency of torsional oscillations P_φ. In actual helicopters the oscillations with these frequencies are always collective. They can only be separate when the line connecting the spring with rigidity k_z passes through the center of gravity of the helicopter.

In helicopters, which are schematized in accordance with Fig. 9.5, there exist two tones of collective helicopter oscillations on the landing gear. In the first tone the helicopter oscillates near a certain point O_1, which is located below the center of gravity of the helicopter. During the oscillations the helicopter deviates and turns to one side. The node of oscillations of the second tone is located above the center of gravity of the helicopter (point O_2). With these oscillations the helicopter deviates and turns in different directions.

Inasmuch as the natural frequencies of oscillations of a helicopter on landing gear can change in a wide range depending upon rotor thrust, a check for ground resonance is necessary for all combinations of thrust and rotor speeds. In the determination of the necessary damping the calculation selects minimum damping according to the considered tones of oscillations. The selected minimum damping of blades and the shock-absorption should be taken with a definite margin, inasmuch as the characteristics of damping for various reasons can change in operation in defined limits.

Ground resonance is very intense. Based on its consequences it is like flutter on aircraft. If oscillations do not stop development in good time during ground resonance, a helicopter accident is practically inevitable. The structure will be destroyed in several seconds.

A basic means of stopping ground resonance is turning off the motor. Sometimes it is sufficient to decrease the collective rotor pitch. The source of energy which supports the oscillations is the motor, the power of which is expended in rotating the rotor and thus will almost completely be converted into the energy of the perturbing forces which support the oscillatory motion. If we stop the entry of energy into the self-oscillation system (which is a helicopter in the presence of freedom of rotation of blades about drag hinges and freedom of movement of the entire helicopter on its landing gear) or we decrease the entry of energy to a level which is less than is necessary for overcoming the work of the resisting forces (analogous to how this is shown in Fig. 6.4), the oscillations will be damped and the ground resonance will cease. If a helicopter during ground resonance still does not "rock" severely, and there is a possibility of leaving the ground by means of increasing the rotor pitch, then such a measure leads to the cessation of oscillations, since the closed cycle of energy exchange between degrees of freedom of the oscillatory system is disturbed. If, however, the helicopter still cannot get off the ground, a similar measure can only add to the situation. Such cases have been encountered in practice and have led to helicopter failures.

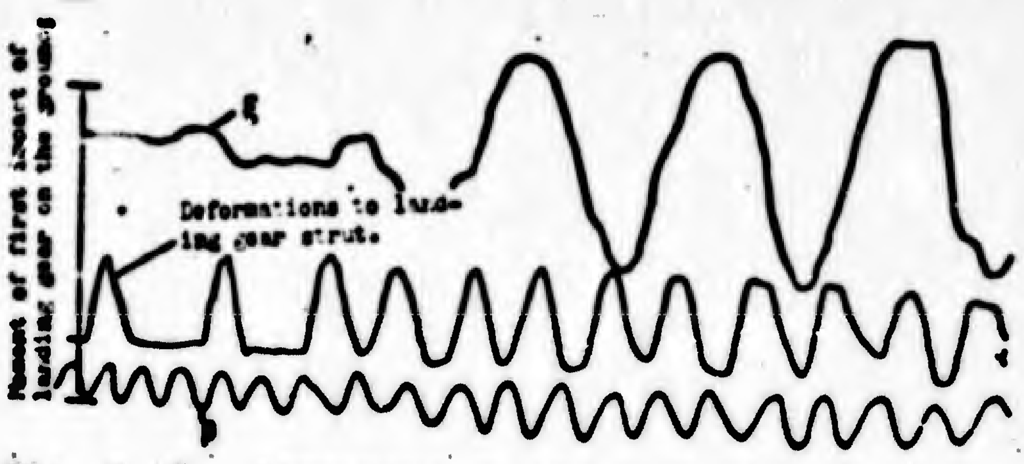

Fig. 9.16. Recording of the beginning of ground resonance on a helicopter. ξ – lag angle of blade (with respect to DH); β – blade-flapping angle (with respect to FH).

Figure 9.16 shows the moment of the beginning of ground resonance on a helicopter which was the subject on an investigation of this phenomenon. Before landing the helicopter was rocked by the control stick and ground resonance was brought about by a sharp impact of the helicopter against the ground during landing on one strut. At the time when the increasing oscillations began, they were stopped by decreasing the collective rotor pitch or by turning off the motor. As can be seen, even in several cycles the oscillations of rotor blades around the drag hinge reach a great magnitude. Oscillation of the entire helicopter on the landing gear are also increased in this proportion. The oscillations of blades around the flapping hinge in the initial moment of development of ground resonance remain practically constant. The suddenness of the appearance of ground resonance and its emergency character create a large danger for the operation of helicopters.

Ground resonance is a complicated phenomenon. Recently all helicopters in some measure were subject to the danger of the appearance of ground resonance. Due to this, it was considered that constructive measures cannot, completely exclude ground resonance and therefore ground resonance is an inevitable hazard. The pilot in good time had to cease oscillations in case of their appearance, not giving to them the chance to develope to dangerous values.

At present, ground resonance has been studied to a definite extent; methods of calculation and graphic constructions have been developed, in which it is possible to quickly and simply conduct checking calculations for specific types of helicopters; there is a number of successful constructive solutions which completely remove this phenomenon in certain helicopters. Theoretical research on ground resonance shows that the selection of parameters of the landing gear can prevent ground resonance for a helicopter. Since the removal of ground resonance on a completed vehicle is very complicated, in the designing of landing gear of a new helicopter it is necessary to consider the safety requirements against ground resonance. At present there has been developed a number of recommendations for certain types of helicopters, the fulfillment of which ensures the prevention of ground resonance. Safety of a new helicopter from ground resonance is checked by flying tests.

9.6. Dynamic Strength of Helicopter Structures

Increased vibrations on helicopters are a basic factor of dynamic loading, which determine their service life and operational reliability.

The determination of forced oscillations and variable stresses in structural elements of helicopters by means of calculation is difficult. Therefore, of large value are the experimental methods of study of dynamic loading of helicopter assemblies. The data presented below is based mainly on the results of experiments.

Dynamic Strength of Rotors

The conducted measurements of stresses in rotor blades of a number of helicopters indicate that elastic oscillations of blades have a complicated character (see Figures 9.6 and 9.7). In conditions of hovering and horizontal flight the predominant oscillations are those with frequencies which are equal to the rotor speed; however, the high-frequency impositions are also substantial. In other conditions the character of the oscillations of blades, and consequently the stresses in them, changes. In particular, during deceleration before landing, the predominant oscillations are the high-frequency ones.

The greatest variable normal stresses in rotor blades appear in the flapping plane (Fig. 9.17). Variable normal stresses in the plane of rotation are usually considerably smaller. Tangential stresses from torsional blade strain also are small and they sometimes will be disregarded in the determination of the service life of a blade in laboratory conditions due to the technical difficulties of their reproduction.

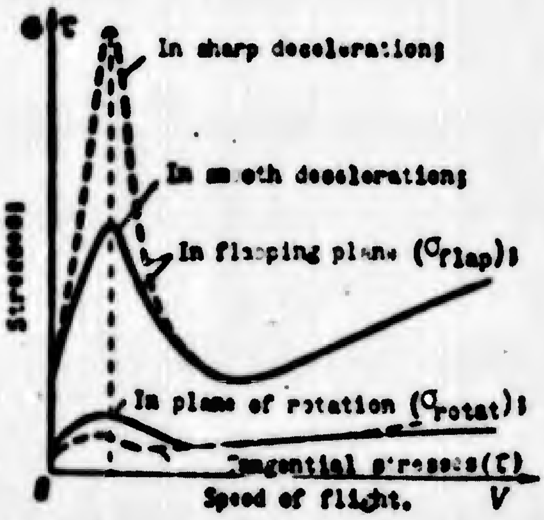

Fig. 9.17. Dependence of variable stresses in the spar of a rotor blade on the speed of flight.

Stresses in rotor blades attain maximum magnitudes at speeds of flight 20-40 km/hr. With the increase of speed of flight the stresses decrease, and then again increase (see Fig. 9.17). The smallest stresses in rotor blades are observed in conditions of hovering (without wind) and the largest are witnessed in conditions of deceleration before landing. In deceleration before landings, executed with a landing run, the stresses in blades are considerably less than in deceleration before landings without a run. In transitional regimes of flight the magnitudes of stresses can change in wide limits. In steady regimes of flight the oscillations of blades and the variable stresses caused by them also become steady.

The dynamic strength of rotor blades is characterized, first of all, by the fatigue limit σ_r of the supporting blade members (for spar blades it is characterized by the fatigue limit of the spar as the basic supporting member of a blade) and secondly, by the level of dynamic loading of blades in operation.

In the variable stresses in a blade spar under any conditions of flight, including brief flights, do not exceed the fatigue limit σ_r, and under conditions of sustained flight, are not more than 0.5 σ_r to 0.6 σ_r, the service life of such blades will be increased (on the order of several thousand flying hours) and will depend not so much on the dynamic strength of the supporting member, as on the wear and state of covering and the internal set of blades. If, however, under certain conditions of flight, although brief, the stresses in a spar exceed the fatigue limit ($\sigma > \sigma_r$), the service life of such blades will be sharply lowered. This lowering will then be even greater, the larger the inequality $\sigma > \sigma_r$. Thus, if $\sigma = 1.5\ \sigma_r$, the lowering of the service life with respect to number of cycles to destruction can attain several multiples, and when $\sigma = 2.0\ \sigma_r$, several hundred multiples. Therefore, the service life of blades is strongly lowered even after a brief period in conditions where there appear stresses which considerably exceed the fatigue limit.

The most important factor, which affects loads of rotor blades and hubs, is the proximity of natural frequencies (especially the lowest tones) of revolving blades to the frequencies of perturbing forces and the phenomenon of resonance connected with this.

The possible growth of stresses in blades due to resonance cannot be compensated by a corresponding increase of the fatigue limit. Therefore, the absence of blade resonance is the most important condition for increasing the service life of blades in operation. For preventing resonance in designing parameters are selected for blades so as to ensure the needed dynamic response characteristics of blades in the range of operational rotor speeds.

Another important index of dynamic strength of a blade is the magnitude of the fatigue limit σ_r. The magnitude of σ_r in many respects is determined by the design of the main supporting member of the blade, in particular the spar. Depending upon the presence of stress concentrators, the magnitude of σ_r can change a few times. From past experience it is known that in blades which have spars made from several steel pipes, united by means of rivet joints, the fatigue limit was small. Therefore, the fatigue strength and service life of such blades were also small. Replacement of these blades by blades with homogenous steel spars considerably increased their fatigue strength and service life.

For the creation of reliable rotor blades with long service life it is necessary that the stresses under no conditions exceed the fatigue limit. This requirement in a defined measure is satisfied by all-metal blades with spars pressed from a light alloy and which have a honeycomb filler. The use of adhesive connections in these blades reduces the concentration of stresses to a minimum.

At present, to a sufficient extent we have studied the factors which determine the dynamic strength of rotors. Thus, for instance, for the Soviet helicopters Mi-1 and Mi-4, rotors have been made that ensure sustained and reliable helicopter operation.

It is necessary to consider that the selection of an incorrect technique in the manufacture of rotors and a deviation from a fixed technique can lead to considerable lowering of the fatigue characteristics of a rotor.

Steel and especially aluminum alloys are extraordinarily sensitive to stress concentrators. Therefore, the variance of fatigue characteristics of blades, made from these materials, remains considerable even with the observance of all rules of the technological process of their manufacture. Due to this the service lives of such blades are established with a large margin.

Sufficiently good results (with respect to reliability of blades) were exhibited by the perennial use of wooden blades made from special kinds of wood with the application of plastics. Such blades are used for tail and main rotors with respect to small diameter. They are less sensitive to the concentration of stresses and have a smaller variance of fatigue characteristics. But wooden blades, especially for rotors with large diameter, are inconvenient for operation, since due to weather effects (moisture in blades) they change their mass characteristics, which leads to the necessity of frequent balancing of blades (especially of the main rotors).

The physico-mechanical properties of certain new plastics indicate that from them it is possible to manufacture blades for rotors. It is possible to consider that the application of plactics will considerably increase the safe period of service of blades as compared to the service lives of metal and wooden blades.

Dynamic Loads of Tail Rotors

The oscillations of tail rotor blades in flight are basically analogous to the oscillations of main rotors. The blade shanks and the hub of a tail rotor experience considerable dynamic loads in the plane of their rotation from the Coriolis forces due to the absence of hinges which are similar to the drag hinge of the main rotor blades. The frequency of change of dynamic loads is equal to the doubled angular velocity of rotation of the rotor (see Fig. 9.10, curve 2). The other components of dynamic loads differ considerably from the bending moment in the plane of rotation and contain large high-frequency impositions. However, the total quantities of these loads are small and do not have a decisive value in the loading of tail rotors.

Dynamic loads on blades of the tail rotor, just as in the main rotor, increase with the growth of the speed of flight, attaining their maximum at speeds from 20 to 50 km/hr, then decrease, and again increase with the increase of the speed of flight (Fig. 9.18). Large dynamic loads are experienced by tail rotors during hovering turns, during sharp deflections (depressions) of a pedal in flight, and during side-slips (especially during recovery from skidding).

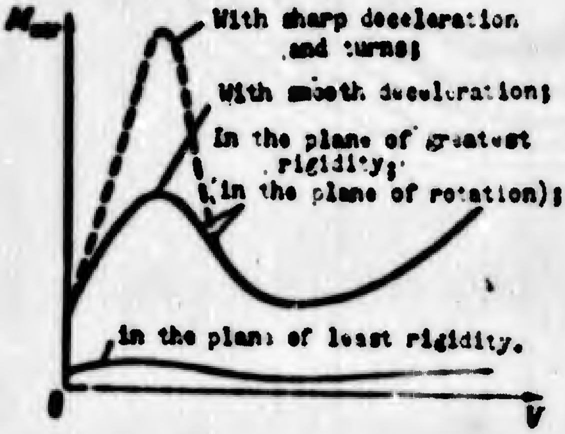

Fig. 9.18. Dependence of variable bending moments in a tail rotor blade on the speed of flight.

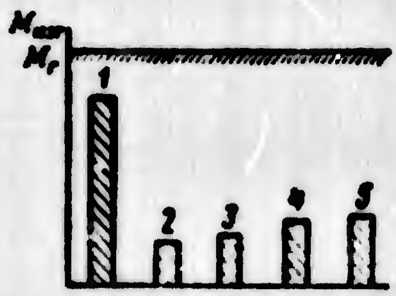

Fig. 9.19. Loading diagram of tail rotor blades. 1) during a turn; 2) in all conditions of horizontal flight; 3) on curves; 4) during side-slips; 5) in conditions of sharp deceleration before landing.

The service life of tail rotors, just as of main rotors, is determined by the relationship between the fatigue limit and the effective dynamic loads. Figure 9.19 shows the loads effective in the plane of rotation on a tail rotor blade of a helicopter.

Loads (variable bending moment M_{bend}) on a blade of this rotor almost in all conditions are lower than the fatigue limit (with respect to bending moment M_r). This ensures the blades and the rotor on the whole with high dynamic strength.

Figure 3.26 shows the characteristics of a rotor which has resonance of blades in operating conditions of flight (1st variant of blades in Fig. 3.26). Due to the proximity of the frequency of natural bending oscillations in the plane of rotation to the frequency of basic dynamic loads on the blade, i.e., the Coriolis forces (second harmonic to turns of rotor), the loads on the blade, and consequently also on the hub, increase a few times. Especially large loads are experienced by the tail rotor in turns on the ground, in curves, side-slips, at low speeds of flight near the ground, and in certain other conditions of flight with large tail-rotor pitch (Fig. 9.20).

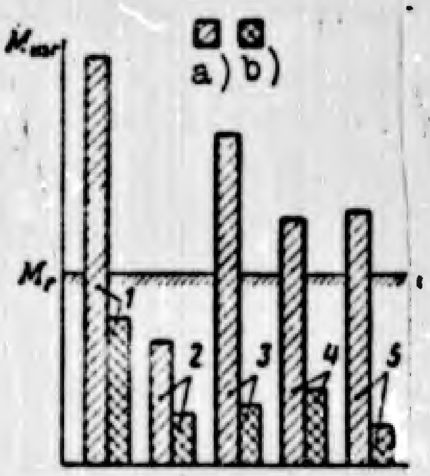

Fig. 9.20. Loading diagram of blades of two tail rotors. a) with unsatisfactory dynamic response characteristic (see Fig. 3.26, 1st variant); b) with improved dynamic response characteristic (see Fig. 3.26, 2nd variant).

Upon replacement of this rotor by another with more rigid blades, which also correspondingly possessed higher natural frequencies of oscillations, the resonance of blades shifted to the region of non-operating turns and blade-setting angles (Fig. 3.26, 2nd variant). Therefore, the dynamic loads on the tail rotor under the same conditions of flight were considerably lowered.

Dynamic Strength of Helicopter Fuselage Assemblies

As shown above, the basic dynamic loads on a fuselage and its assemblies arrive from the main rotor. The tail rotor renders an influence basically only on the end and tail booms and on the place of its mounting.

The change (in amplitude) of dynamic loads of the majority of fuselage assemblies with respect to speed of flight is analogous to the change of loads on the main rotor. Lowering of variable loads on the main rotor as a rule leads to lowering of vibrations and dynamic loading of the entire helicopter.

The biggest dynamic loads (with the exception of the control and transmission of a helicopter) are experienced by the rotor mountints, in particular the reductor frames. Figure 9.21 shows the change in amplitudes of variable normal stresses in frame rods according to speed of flight. It is clear that in a number of conditions of flight the frame experiences considerable variable stresses.

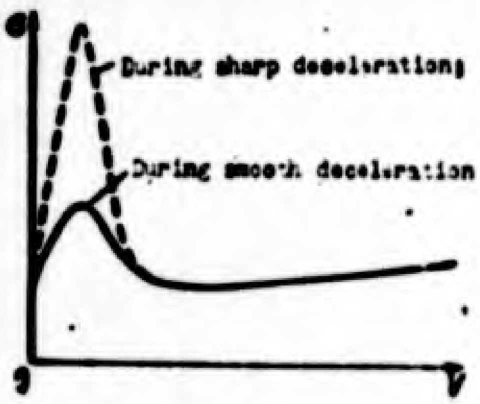

Fig. 9.21. Dependence of variable normal stresses in the reductor frame of a helicopter on the speed of flight.

In the tail and end booms of helicopters the stresses under all conditions of flight have such magnitude that within the limits of ordinary flying service lives of helicopters the dynamic strength of the fuselage, tail, and end booms is basically sufficient. However, upon further increase of the service life of helicopters, it will apparently be necessary to consider the influence on dynamic strength exerted by large loads which appear during landings.

The variable forces on the main and tail rotors create considerable variable loads on the helicopter controls. The strength of the control system during the action of these loads within the limits of comparatively short service lives of contemporary helicopters is not noticeably lowered. However, dynamic loads on controls require thorough study for determining a safe service life.

The most sensitive to variable loads are the various welded components. Operational experience of helicopters testifies to the small reliability of assemblies with welded joints. Such joints have small fatigue limits due to the great concentration of stresses in the places of welding. Furthermore, the reliability of welded joints in a considerable measure depends on the quality of the welding, the monitoring of which is complicated.

Welded joints are applied in the reductor and engine mounts and in other assemblies of the helicopter which possess comparatively low fatigue limits. However, the design of these assemblies is continuously improving, and at present they have sufficiently long service lives.

9.7. Estimation of the Service Life of Helicopters

Of prime importance in the problem of strength and reliability of helicopters is the correct determination and guarantee of safe service life. The main methods of estimating dynamic strength and establishing a safe service life of a structure at the present are fatigue tests of full-scale samples.

As shown in Chapter VII, the fatigue strength of a structure is influenced by many factors, including the magnitude and frequency of change of loads, the static load, the order of alternation of loads of different magnitude, the imposition of components with another frequency on the base load, and others. Therefore, the basis of estimating dynamic strength is the programmed fatigue test.

Programming, i.e., establishing a law of change of magnitudes, frequencies, and quantities of load cycles, which are encountered in operation, is carried out on the basis of data obtained experimentally or by means of calculation. More reliable data is obtained experimentally. The development of a program of fatigue tests originates from the necessity of calculating the loads which are encountered in all, including brief, conditions of flight.

Programmed tests undoubtedly are the best approach to real operating conditions, a safe service life, established in this way, is more reliable than an estimate of dynamic strength only with respect to one equivalent load. The basis for compiling the program of such tests could be the results of investigation of recurrence of loads in flight. These loads are measured in several flights during the entire time of their fulfillment, whereby flights are conducted according to a definite program which includes all conditions of flight. The program of every flight is composed by taking into account the probable flying time of the helicopter in the given conditions of flight.

Flying time for different types of helicopters is determined on the basis of collecting and studying statistics on the conditions of flight in accordance with the assignment of the helicopter approximately according to the following chart:

Number of rating (see Fig. 9.23)	Rating	Flying time, % of service life.
1	Ground conditions	
2	Hovering	
3	Ground acceleration	
4	Climb	
5	Horizontal flight	
	at low ground speeds	
	at cruising speeds	
	at maximum speeds	
	flight in bumpy air	
6	Curves, turns, side-slips	
7	Transitional flight rating	
8	Turns while hovering	
9	Power gliding	
10	Deceleration before landing	
11	Gliding and landing during autorotation of main rotor	

For an example, Figures 9.22 and 9.23 show the load capacity of the main structural assemblies of a helicopter in different flight conditions.

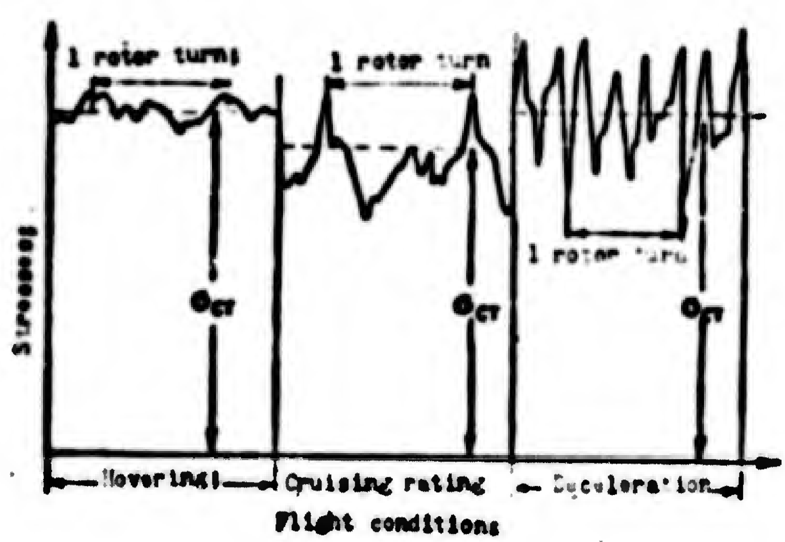

Fig. 9.22. Stresses appearing in the main rotor blade of a helicopter in different flight conditions (σ_{st} – stresses from static load).

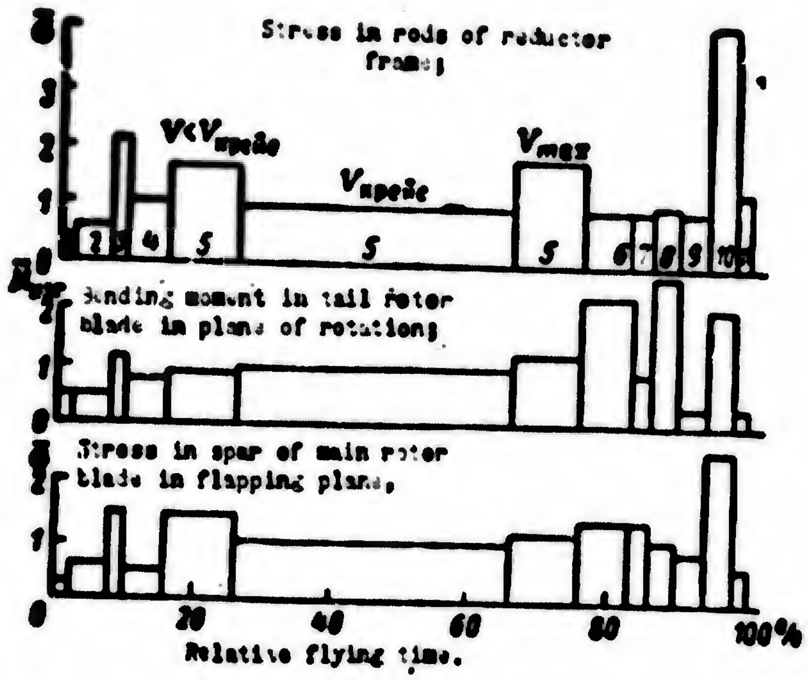

Fig. 9.23. Relative load capacity of assemblies of a single-rotor helicopter in different flight conditions (variable bending moment $\overline{M}_{bend}$ and stresses $\overline{\sigma}$ in every structural assembly refer to the moment and stress which appear in horizontal flight at cruising speed).

In establishing the service life of a structure on the basis of results of laboratory tests it is very important to determine the safety factors. During flying tests the safety factors cannot be detected in view of the extreme danger of such experiments. In laboratory tests the dynamic (fatigue) safety factor is taken simultaneously both for stresses (loads), and also for the number of loading cycles.

Laboratory tests, even if they are conducted taking into account the required safety factors, do not give a direct answer about the safe service life of a helicopter and its assemblies in actual operating conditions, since these tests are conducted under certain ideal conditions. In operation, besides loads, the dynamic strength is influenced by a number of factors, the main ones of which are the atmospheric conditions, corrosion, wear of parts, and several others.

Therefore, the service life, which is determined with the help of laboratory fatigue tests, is checked by endurance (operational) flight tests.

Such tests are conducted on several helicopter models of the leader group to full performance of a fixed service life. The program of these tests is developed by taking into account the necessary flying time in all basic operational conditions of flight. Although these tests cannot establish dynamic safety factors, they can determine the reliability probability of a helicopter within the limits of a fixed service life. Furthermore, the results of laboratory tests on assemblies, which have undergone the full flying service life, can be the basis for increasing the service life of structural assemblies above that which was initially established. According to such tests it is also possible to determine actual the fatigue safety factors of assemblies of a helicopter.

Only a group of strength tests (laboratory, flight with the measurement of stresses, and flight endurance) can allow an estimate of the dynamic strength, the service life, and the reliability of a helicopter.

In conclusion one should note that the basic criterion of a good helicopter is its operational reliability, which is understood as the ability of the structure to operate without accident in actual operating conditions within the limits of a defined service life. Bringing the reliability of helicopters, with respect to dynamic strength, up to such a level so that the probability of destruction of the helicopter from the dynamic loads would be not greater than the probability of destruction from static loads, is the most important problem.

9.8. External Loads and Strength of Helicopters

External loads of a helicopter are determined by the conditions of its normal operation. The design should ensure safe operation of the helicopter in accordance with its assignment. For a strength analysis, and also for static and dynamic tests, there have been determined a number of cases of loading, which have been encountered in practice and determine the strength of a helicopter and the assemblies of its structure. The basic conditions of loading of a helicopter are regulated by strength norms.

Cases of loading in strength norms are divided into three groups: flying cases of loading, landing cases of loading, and cases of loading in ground conditions.

The flight conditions of a helicopter are determined by its gross weight, the altitude and speed of flight, the overload in the center of gravity of the helicopter, the power supplied to the rotor, and the action of the controls. The gross weight of a helicopter during calculations in all cases of loading in flight and during landing is taken to be equal to normal takeoff weight. In ground conditions of loading (during tie-down tests) the calculation uses the minimum weight of the helicopter. Altitude and speed of flight are determined by the purpose of the helicopter and are assigned by the technical requirements for the helicopter.

The basic index of static loading of a helicopter is the magnitude of overload which appears during operation. The magnitude of overload determines the maneuvering possibilities of the helicopter in flight. If aircraft can theoretically have an overload in flight with a magnitude of $n^r = 15$ to 20 and maximum operational overload n^{op}_{max} is limited by the selection of corresponding characteristics of control, then for helicopters the maximum overloads, determined by the aerodynamic possibilities, are comparatively small and usually do not exceed n^r = 4 to 6. During overloads greater than this magnitude there appears rotor stall. Therefore, usually for helicopters the magnitude of n^{op}_{max} is taken from 2.5 to 4.0, depending on the assignment of the helicopter.

Maximum permissible overload is complicated to obtain in flight. During zooming and in emergence from gliding the maximum overloads on nonmaneuvering helicopters usually do not exceed n_{max} = 1.5 to 2.5 (depending upon the type of helicopter). During landing, helicopter overloads also usually do not exceed n = 2.0 to 2.5. Due to this, the guarantee of static strength of helicopters does not present any serious difficulties.

The strength norms of helicopters use the principles of standardization which were founded in the creation of aircraft strength norms. The development of strength norms of helicopters also uses the experience of autogyroconstruction. But their basis contained the results of generalization of operational experience of helicopters and operational experience of designing bureaus for the creation of helicopters. The basic cases of loading in strength norms of helicopters are determined by the results of numerous theoretical and experimental works.

The most important peculiarity of helicopters is the high level of dynamic (vibration) loading of their assemblies. This determines the large value of fatigue strength for guarantee of safe operation of helicopters. Inasmuch as the methods of studying the strength of structures up to now have almost been completely experimental, the possibilities of calculating fatigue characteristics, during the designing of a new helicopter with the help of calculation methods, are very limited. Calculation basically determines only the frequency of natural oscillations of a structure (in particular, the rotor blades), in order to exclude resonance with frequencies of perturbing forces, which always are multiple to the rotor speed.

Calculations of dynamic stresses and fatigue strength are insufficiently reliable for estimating the fatigue strength of structures, especially those whose failure presents a danger for flight. Therefore, at the basis of estimating the fatigue strength of helicopters and their assemblies we find experimental methods. They consist of laboratory methods, with the help of which the carrier ability of a structure is determined with respect to strength, and of the methods of measurement of loads acting upon a structure in actual operating conditions. The combination of these methods makes it possible to determine the fatigue strength of a helicopter or its separate equipment during the action of variable loads which appear in operation.

Conditions for determinating the safety of helicopters with respect to fatigue strength are regulated by the strength norms.

In the process of creating a new helicopter, the most important individual structural elements undergo preliminary fatigue tests for the purpose of estimating the dynamic strength. These tests are conducted on loads which are determined by calculation and are taken with a sufficiently large safety factor with respect to stresses. The magnitude of the selected safety factors depends on the degree of reliability of the calculation determination of loads. These preliminary tests terminate the construction of the vehicle or its assemblies and determine measures for increasing fatigue strength.

The order and volume of work, which is performed for checking the dynamic strength of new helicopters, depend on the type of structure and usually are based on the experience of industry. However, both the Soviet designing bureaus, and also foreign helicopter construction firms are trying to check the dynamic strength (fatigue strength, flutter) of a helicopter as fully as possible before beginning flights. The possibilities of lowering the level of variable stresses in the supporting members of the structure and methods of increasing their fatigue strength are carefully studied. The most responsible ready articles (usually full-scale equipment in assembled form) are checked on corresponding rigs or directly on the helicopter in ground conditions.

At present, variable external loads on structural assemblies cannot be determined accurately enough by means of calculation. Therefore, the state of strain of the structure is usually investigated directly on the helicopter.

During flying tests of a new helicopter, from the very first flights the stresses and dynamic loads are measured in the supporting members of all basic structural assemblies of the helicopter, the failure of which in the air leads directly to an accident. Such assemblies in the first place include the blades of the main and tail rotors, their hubs, the automatic pitch-control mechanism, the helicopter controls, the reductor and motor mounts, etc. The parameters of oscillations of the helicopter structure are simultaneously measured.

These measurements are conducted in all basic operating conditions of flight, including limiting conditions. The program of tests should anticipate especially thorough measurements in conditions which are characteristic for loading of the inspected part of the structure. Thus, for the main rotor, its blades, hub, and reductor frame, a thorough investigation is conducted on loading in all conditions of horizontal flight with normal and maximum gross weight at different rotor speeds and helicopter centering, during acceleration and deceleration before landing, during zooming and emergence from gliding with maximum overloads, during climbing, and other conditions. For tail rotors, furthermore, the loads which appear during entry and exit from side-slips, in the execution of curves, during ground turns with critical angular speeds of the helicopter, and in other conditions are thoroughly measured. For the tail boom it is important to study dynamic loading during landings.

On the basis of the results of measurements a program of laboratory fatigue tests is composed for the basic structural assemblies of the helicopter. The results of such tests serve as a basis for establishing the service life of the helicopter and its assemblies. The service life is calculated in accordance with the principles which are presented in Chapter VII.

During flying tests a check is also made on the safety of the helicopter from the appearance of ground resonance. The technique of these tests consists in that at different rotor speeds and thrusts ground resonance is attempted by means of asymmetric impacts of the landing gear of the helicopter against the ground during simulation of landings (vertical and with a run) and running takeoffs. The helicopter, before ground contact, is rocked by the control stick (transverse, longitudinal, or circular motions).

For determing the influence of individual operational parameters on the characteristics of ground resonance (friction in DH dampers, pressure in struts and tires of landing gear, etc.), these parameters are varied in defined limits, corresponding to their possible change in actual operating conditions. Control of the appearance of ground resonance, in addition to visual observation, is carried out by recordings of appropriate parameters, e.g., compression of shock-absorping struts of landing gear, blade flapping with respect to mounting hinges, and others. Preliminary simulation of ground resonance is produced, in which the influence of different parameters on ground resonance is studied. The results of this simulation serve as the basis for the defined change of separate parameters during flying tests of a helicopter in ground resonance.

Thus the estimate of strength of a new helicopter is produced by a group of tests, including both laboratory, and also flying tests. Before a helicopter becomes operational, it undergoes an extensive check on the strength of the vehicle and all its most important assemblies.

It is necessary to note that the results of checking the strength of a helicopter are impossible to automatically transfer to all its possible variants. Thus, for instance, it is known that conditions of low speeds of flight (conditions of low uniform speeds of horizontal flight near the ground, acceleration, and deceleration) are accompanied by increased vibrations and dynamic loads. These conditions, with respect to flying time, compose a relatively small percent of the service life of the helicopter. If, however, a helicopter is used as a rescue vehicle or helicopter-crane, the indicated conditions become basic, and most of the time it experiences increased loads. Consequently, the estimate of strength and especially the estimate of service life of a helicopter must be definitized in accordance with the change of loading conditions.

CHAPTER X

EXPERIMENTAL INVESTIGATION OF THE STRENGTH OF FLIGHT VEHICLES

List of Designations Appearing in Cyrillic

пр = w = wire

к = com = compensating

б = bal = balancing

д = d = diagnonal

тар = cal = calibration

рез = res = resonance

т = cal = calibration

доп = add = additional

г = g = galvanometer

э = e = electrical

сбр = dr = drop

сек = sec

э = op = operational

цт = cg = center of gravity

кон = t = tip

корн = r = root

н = act = actual

фм = fm = model flutter

фн = f. act = actual flutter

ст = st = static

в = up = upper

н = low = lower

кр = tor = torque

ом = ohm

ш = l.g. = landing gear

т = sg = strain gauge

аэр = aer = aerodynamic

з = m = measurement

д = en = engine

з = rec = recording

изг = bend = bending

кр = w = wing

ф = f = fuselage

л = lft = left

пр = rt = right

изм = meas = measurement

For the investigation of strength of a structure, along with theoretical calculations, experimental methods are widely used. These methods are divided into two basic forms: investigation of the loading conditions of a flight vehicle and investigation of the carrying capacity of a structure and the peculiarities of its performance.

Investigation of external loads is carried out in wind tunnels and during flying tests.

Investigations of the carrying capacity and the peculiarities of performance of a structure include static tests of full-scale structures (exact models), fatigue tests, dynamic tests of the landing gear and sometimes the aircraft on the whole, frequency (resonance) tests for determining the characteristics of natural oscillations, thermal tests (for flights vehicles whose structures are essentially heated in flight), simulated tests, and flying tests in limiting flight conditions.

An experimental estimate of the actual strength of a structure, i.e., determination of the degree of conformity of the carrying capacity of the structure to external loads, requires the harmonious development of both forms of investigation. However, in practice the investigations of carrying capacity of a structure are conducted in a larger volume than investigations of external loads. This is explained by the fact that, first of all, investigations of the carrying capacity of a structure basically have a laboratory character and can be carried out more simply than a flight experiment; secondly, a flight experiment is frequently connected with a definite risk and therefore can not always be conducted in sufficient volume.

Experimental methods of investigating the strength of aircraft structures are very extensive and frequently are very complicated. Below we shall consider some of the basic experimental methods that are applied at the present. Each of these methods has its own developed theory and a corresponding method of carrying out experiments. More detailed information on experimental methods of investigating the strength characteristics of aircraft structures are presented in special literature concerning this question, and in handbooks and techniques for carrying out the experiments.

10.1. Equipment for Structural Performance Tests

Testing equipment which is used in structural performance tests of aircraft and helicopters can be divided into three basic groups:

1. Airborne recording equipment. This group contains the

mechanical and optical-mechanical recorders, oscillographs, and magnetic recorders with transducers and commutating devices.

2. Telemetric equipment. In the use of equipment of this type, on board the flight vehicle there are installed transducers with converters and commutating devices. Signals from transducers, through an airborne radio station, are transmitted to a ground point, where the investigated parameters are recorded and the appropriate automatic processing of measurements is conducted.

3. Motion picture equipment and photorecorders. This group contains motion picture photorecorders for measuring deformations and motion picture equipment for aerial photographs and for filming the takeoff and landing.

At present, testing equipment has obtained a large development and it can ensure measurement of almost all parameters which characterize the loading conditions of structural parts of an aircraft and helicopter. Equipment for monitoring flight conditions (recorders of speed, altitude, angles of deflection of controls, etc.) is described in sufficient detail in a number of works and is not considered here (see, for example, V. S. Vedrov and M. A. Tayts "Aircraft flight tests," Oborongiz, 1951).

A special group is composed by statistical instruments which permit the recording of the necessary parameters which characterize loading of a structure in conditions of mass operation (see Chapter I).

A flight experiment for the investigation of strength is connected with the registration of a large quantity of parameters. Of important value for fast processing of recordings and analysis of recorded processes is the application of automatic and semiautomatic systems. In particular, in the investigation of random dynamic processes spectral analyzers and autocorrelators are used.

In conditions of mass measurements it is expedient to apply analog computers. Although they have somewhat smaller accuracy as compared to digital computers, they possess large productivity and permit the introduction of different converters which are necessary in the analysis of recordings. They are simpler in design and less expensive than digital computers, and they permit the obtainment of sufficiently full data on dynamic processes (spectral density, autocorrelation function, average magnitude of amplitude, standard deviation, and integral distribution function).

At present such equipment is being continuously improved.

Equipment for Measurement of Stresses and Loads (Tensometeric Equipment)

At present, stresses and loads in aircraft structures are measured in many points. Such wide measurements, especially under conditions of flight tests, can be carried out only on the basis of electrical methods.

The electrical measurement of stresses in a structure requires transducers which convert the change of physical parameters into proportional electrical signals. These signals are recorded by appropriate instruments (airborne or ground).

For measurement of stresses, capacitance and inductance methods and methods of resistance measurement are applicable in principle. Wound (not glued) resistance transducers, capacitance and inductance pickups are applied in measurements of large shifts and in such instruments as pressure transducers, accelerometers, etc.

For measurement of loads and stresses on flight vehicles the most frequently used are wire strain gauges. These strain gauges have small dimensions, small weight, and are easily glued to any part of the structure. Wire strain gauges are simple, inexpensive, reliable in operation, can be applied in remote recording, and permit the construction of systems which make it possible to determine loads with a minimum quantity of recording channels. Strain gauges can work at elongations of up to 1-2% without damages. Specially designed transducers ensure measurements at elongations of to 10%. The frequency measured by them is practically unlimited.

Strain gauges can utilize power supplies by both alternating and direct current. Temperature compensation is easily carried out by application of an additional compensational transducer. The advantage of this transducer is its simplicity of assembly of measuring circuits. All this permits the wide application of tensometeric methods of measurement in structural performance tests.

The strain gauge is a converter of a mechanical magnitude — elongation — into an electrical magnitude — increase of ohmic resistance — which can be measured by electrical methods.

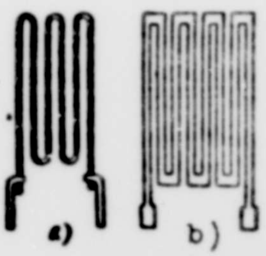

Fig. 10.1. Diagrams of strain gauges. a) wire strain gauge; b) strain gauge made from foil.

Strain gauges applied on flight vehicles consist of a sensitive grid made from special wire in the form of several loops or in the form of a flat grid made from foil (Fig. 10.1), which is attached by special glue to the base. Such a transducer, glued to the surface of the investigated component, is deformed (is stretched or compressed) together with it. Due to the deformation of the transducer grid, its ohmic resistance changes in proportion to the deformation of the component. The property of wire, made from certain materials, to change its resistance during deformation — strain sensitivity — may be characterized by the relation

$$\gamma = \frac{\Delta R}{R} / \varepsilon \quad \text{or} \quad \gamma\varepsilon = \frac{\Delta R}{R}. \qquad (10.1)$$

where $\frac{\Delta R}{R}$ is the relative change of ohmic resistance;

ε is the relative deformation.

The strain sensitivity of the transducer grid is less than the strain sensitivity of separate wire, since the wire does not completly enter work on curvatures. The formula for computing the strain sensitivity of a loop transducer has the form

$$\gamma = \gamma_w \frac{nl + \frac{\pi r}{2}(1+\mu)(n-1)}{nl + \pi r(n-1)}. \qquad (10.2)$$

where γ_w is the strain sensitivity of the wire;

n is the number of rectilinear sections of wire;

l is the length of rectilinear sections of wire;

r is half the distance between rectilinear sections of wire;

μ is Poisson's ratio.

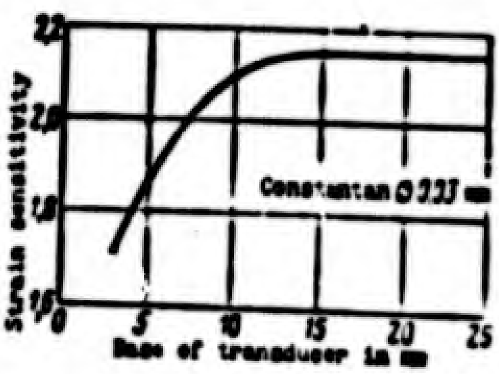

Fig. 10.2. Graph of the dependence of strain sensitivity of a wire gauge on its base.

From formula (10.2) it is clear that the strain sensitivity of the transducer depends not only on the strain sensitivity of the wire, but also on the dimensions of the transducer.

The most wide-spread material for the manufacture of strain gauges is constantan wire with a diameter from 0.025 to 0.050 mm, which possesses relatively high strain sensitivity (γ_w = 2.1).

The dependence of strain sensitivity of the transducer on its dimensions (base) is represented in Fig. 10.2, from which it is clear that for transducers with a base less than 10 mm the strain sensitivity sharply drops. The largest distribution has been obtained by strain gauges with base 25 mm. With limited dimensions of a component strain gauges with a small base (to 3 mm) are used. However, in these cases one should consider the influence of transverse sensitivity of the transducer.

There exist many types of strain gauges. For structural performance tests on aircraft equipment the biggest propagation has been obtained by strain gauges with a flat wire loop grid or with a flat grid made from constantan foil. For preservation of form the transducer grid is glued to a paper base or to a polymer base. The ends of the strain-sensitive grid have welded discharge conductors made from copper tinned wire with a diameter from 0.15 to 0.25 mm.

Wire transducers are widely applied with nominal resistance of 120, 200, and 400 ohm and maximum working current 25-30 ma, which ensure measurement of deformations at temperatures from +40 to 80°C. Certain special types of transducers work stably at temperatures from +[illegible] to 750°C. Transducers, made in the form of a thin foil grid, have nominal resistance from 45 to 200 ohm and maximum working current from 50 to 500 ma.

Strain gauges are most often glued to the surface of a component with polymerized glues. The gluing technique is determined by the type of glue.

Registration of the change in resistance of strain gauges in most cases employs bridge measuring circuits.

The circuit of a bridge consists of four resistors (arms of bridge) which are series-connected in the form of a ring. The opposite points of the connection of the bridge arms have a supply source

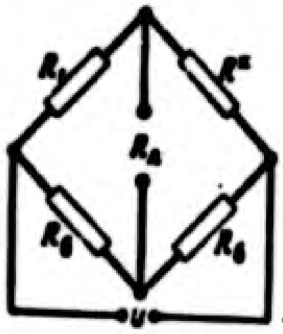

Fig. 10.3. Diagram of a measuring bridge.

and a measuring device (Fig. 10.3). The circuit shown in Fig. 10.3 contains the following designations.

R_1 is the working strain gauge;

R_{com} is the compensating strain gauge, which is equal in resistance to the working strain gauge and usually serves for temperature compensation during measurements;

R_{bal} are balancing resistors for balancing the measuring bridge;

R_d is the resistance of the bridge diagonal (recording galvanometer or amplifier input);

u is the voltage of the power source of the measuring bridge.

The sensitivity of bridge circuits may be raised both by increasing the feeding current, and also by applying highly sensitive loops (galvanometers) for the measurements. Furthermore, foil strain gauges are used, the working current in which may be increased up to 200-250 ma (in special transducers up to 500 ma). The magnitude of maximum permissible working current is determined in every case separately depending upon the design of the transducer and the mass of the component on which the transducer is glued. Sensitivity can be increased also by including two and more transducers in each arm.

With the use of electronic amplifiers AC bridges are employed. Usually two arms of the bridge are formed by transducers which are glued to the investigated component, while the two other arms are structurally connected with the amplifier. Sometimes for the registration of dynamic stresses DC feeding of the bridge is employed.

The measurements can determine the stresses in the elements of a structure and the forces acting on one of its assemblies. A separate strain gauge reacts to the total relative deformations which appear on the surface of the component in the place where it is glued. For isolating the components of stresses and loads in a combined state of strain of a structure the inclusion of strain gauges in the measuring circuits is employed. The principles of such combined connection of strain gauges are presented below.

For strain measurement of revolving components, in particular propeller blades, special slip-rings are used. The basic requirement for slip-rings is to guarantee the constancy of contact resistances. As contact pairs we find the use of mercury – copper, silver – silver-graphite, and others. In the application of slip-rings the measuring bridge is made up from transducers which are glued to the revolving components. In another diagram of transducer connection it is difficult to avoid the influence of the change of contact resistances.

Tensometric measurements in flight employ amplifying electronic equipment and oscillographs with highly sensitive loops. At present there exists a large variety of tensometeric equipment. The equipment with amplifiers consists of a measuring bridge, electronic amplifier, power unit, and recording device, e.g., an oscillograph or magnetic recorder.

A block diagram of a tensometric amplifier is shown in Fig. 10.4. The input on this diagram serves for connecting the external half-bridge from the transducers, which together with the internal resistances from the measuring bridge. The inputs usually have balancing attachments for balancing the stress components of the measuring bridge. From the input a modulated signal proceeds to the control grid of the voltage amplifier stage. Usually every measuring channel has several amplifier stages. Output stages are power amplifiers (during recording on an oscillograph loop). A phase-sensitive detector serves for demodulation of the amplified modulated signal. Signals are recorded with the help of a loop, the deviations of which are recorded on the photographic film of the oscillograph or another recorder.

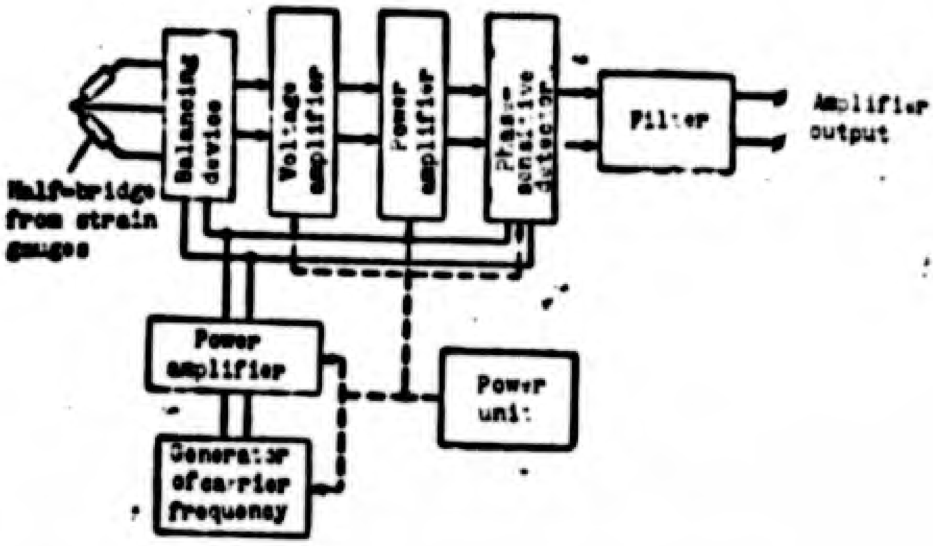

Fig. 10.4. Block diagram of tensometric equipment with amplifier.

Highly sensitive loops permit the use of equipment with limiting small dimensions. But such loops have a small working frequency range. Usually the working frequency range of an entire tensometric channel is determined by the frequency-response curve of the oscillograph loop.

Different types of tensometric equipment for the most part have from 4 to 8 channels for simultaneous measurement. With a large quantity of channels the dimensions of the equipment are increased and it frequently is difficult to install on a flight vehicle.

The equipment has several stages of sensitivity and ranges of measured aspect ratios. Such ranges are from 2 to 8. During the measurements, depending upon the magnitude of measured stresses (forces), this permits the sensitivity of the equipment to be changed and the necessary scale of recording of signals to be obtained.

The advantages of tensometric amplifiers include:

a) measurement with sufficient accuracy of small aspect ratios (0.1–$0.2 \cdot 10^{-4}$) and variable stresses with great frequency of change;

b) decrease of quantity of glued transducers in connection with the application of half-bridges;

c) simplification of calibration, since it can be done with small loads with large amplification of the equipment.

Along with this, tensometric amplifiers have deficiencies, including their relatively large dimensions, great sensitivity to external interferences (which requires more thorough shielding of wires and insulation of strain gauges), and the continuous heating of the equipment for stabilization of electrical zero.

Oscillographs with highly sensitive loops possess a number of advantages as compared to electronic amplifiers. Their application reduces the overall dimensions of equipment and lowers the sensitivity to external interferences. However, highly sensitive loops have a limited working frequency range near 0 to 40 oscillations per second, a relatively small sensitivity of the measuring circuit, and insufficient stability of loops during the action of high accelerations in flight.

Selection of equipment for measurements is determined by the possibility of its installation (with respect to dimensions) on the investigated object and the frequency range of the investigated processes. For high-frequency processes (more than 50-80 oscillations per second) equipment with highly sensitive loops should be employed only after an appropriate check.

Calibration of strain measurement equipment is executed in the laboratory with the help of a special calibration beam of equal resistance or with the help of an aspect ratio equivalent to the full range of aspect ratios expected during measurement. Calibration is usually conducted before installation of equipment on the object and after termination of measurements and removal from the object. In necessary cases control calibrations are conducted directly on the object with the help of portable calibration devices.

The problem of calibration of tensometric equipment with respect to stresses consists in obtaining a graph of the dependence of the ordinate of the recording on photographic film of an oscillograph or on another recorder on the aspect ratio of the structural material. For this, strain gauges, which are glued to the calibration beam, are connected to the equipment, then the beam is loaded and signals are recorded. Thus a number of measurements are obtained with defined loads on the beam. The dependence of the aspect ratio of the beam on the load is known beforehand.

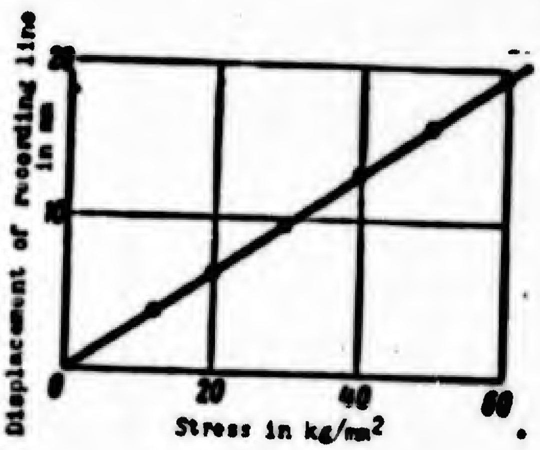

Fig. 10.5. Typical calibration graph of tensometric equipment.

Calibration is accomplished with various sensitivities of the equipment (for equipment with amplifiers); the strain gauges during calibration and tests have to be of the same type. As a result of calibration, calibration graphs are obtained for tensometric equipment depending upon the aspect ratio ε or stress σ (Fig. 10.5). The calibration coefficient of the equipment with respect to aspect ratio is determined by the formula

$$k_{\varepsilon}=\frac{\varepsilon}{\Delta h}. \qquad (10.3)$$

where Δh is the deviation of the recording line in mm.

Strain gauges can be glued to components that are made from different materials. The calibration coefficient for stresses is determined from the following relationships:

$$k_\sigma = \frac{\sigma}{\Delta h} = \frac{\varepsilon E}{\Delta h} = k_\varepsilon E \ \frac{\mathrm{kg/mm^2}}{\mathrm{mm}} \qquad (10.4)$$

where E is the elastic modulus of the material.

Inasmuch as th characteristics of the equipment within the limits of the ranges of measurements are usually linear, coefficients k_ε and k_σ are constants.

In calibration, along with obtaining calibration coefficients there is a final check of the equipment and measuring circuit before carrying out the measurements.

It is necessary to consider that in flight while carrying out measurements the amplification factor of the tensometric equipment can change in defined limits. The causes of instability of the amplification factor o the equipment are connected with the defined instability of the supply voltage of the equipment, with the influence of ambient temperature, which can essentially change in flight, and also with the influence of a number of other factors, which are difficult to consider precisely. For calculation of the possible change of amplification of the equipment during measurements the calibration signal is recorded, the magnitude of which corresponds to a definite magnitude of unbalance of the measuring bridge, i.e., definite magnitude ε_{cal}. The equipment anticipates devices for supply of the calibration signal from the generator of carrier frequency. According to the changes of the recording scale of the calibration signal, which is accomplished in flight during measurements and in the laboratory during calibration, the change of the amplification factor of the equipment is considered. In the absence of a device for supplying the calibrated signal, for instance, with the use of DC measuring circuits without an amplifier, on an oscillograph (recorder) recordings are made of the supply source stresses. Such recording also makes it possible to consider the changes in sensitivity of the equipment, which increases the accuracy of measurements.

Equipment for Measurements of Oscillations and Overloads

In connection with the study of dangerous oscillations (buffeting, flutter) and motor vibrations, the 1930's saw the development of aircraft vibration-measuring equipment, which began to be widely used in flying tests.

At present there exists a large quantity of types and designs of vibration-measuring equipment. Let us consider the basic characteristics of certain types of this equipment.

Principles of action of instruments for measurement of oscillations (overloads). The basic elements of any instrument for measurement of oscillations or overloads is the transducer which "measures" oscillations (overload). The sensing element of such a transducer is a seismic mass which is suspended on an elastic spring (see Fig. 3.3b).

For a transducer the motion of the point of the structure where it is attached is assigned. The body of the transducer moves together with the flight vehicle, and the motion of the mass of the sensing device, with respect to the body of the transducer, measured in the appropriate way, gives information about the parameters of oscillatory motion of the structure in the place of installation of the transducer.

For the solution of practical problems in most cases it is sufficient to know the frequencies, amplitudes of displacements of oscillatory motion of the structure, and amplitudes of accelerations (overloads), which appear in flight. The problem of measurement consists in ensuring that the readings of the transducer (relative motion of the mass of the sensing device) are in proportion to the measured parameter. If the readings of the transducer are

$$y(t) \sim \xi(t), \tag{10.5}$$

where ξ is the motion of the transducer body, the transducer measures displacements during oscillations. Such a transducer is called a vibrometer, and a transducer with an attachment for recording is known as a vibrograph. If the transducer readings are

$$y(t) \sim \dot{\xi}(t), \tag{10.6}$$

the transducer measures speeds during oscillations. Such a transducer is called a velocimeter. And finally, if proportionality is observed

$$y(t) \sim \ddot{\xi}(t). \tag{10.7}$$

the transducer measures accelerations (overloads) during oscillations. Transducers which are founded on the principle of measurement of acceleration are called accelerometers, and special self-recording instruments for measurement of overloads are designated as overload recorders.

It is necessary to note that this classification is conditional, since contemporary measuring equipment employs the conversion of mechanical oscillations of transducers into electrical or other magnitudes, which then can be integrated or differentiated, and the final recording on the recording instrument can be other than that indicated above.

The principles of work of seismic instruments can be completely explained on the basis of the theory of oscillations of linear systems with one degree of freedom. Detaching ourselves from the methods of recording the readings of transducers of seismic instruments, we shall consider their work.

Let us assume that on a transducer (see Fig. 33b) there acts a harmonic perturbation, whereupon the body of the transducer moves according to the law

$$\xi(t) = \xi_0 \sin \omega t. \qquad (10.8)$$

In this case the equation of relative motion of the seismic mass of the transducer coincides in form with equation (3.51), and its solution coincides with solution (3.56). If in formula (3.56) both parts are divided by ξ_0, we will obtain the expression

$$k = \frac{z_0}{\xi_0} = \frac{q^2}{\sqrt{(1-q^2)^2 + \gamma^2 q^2}}, \qquad (10.9)$$

which is analogous to expression (3.39) for the dynamic coefficient. The magnitude k is called the <u>sensitivity factor of the transducer</u> and constitutes an increase in the amplitude of oscillations of its seismic mass as compared to the amplitude of oscillations of the transducer body.

The coefficient of sensitivity k (10.9) differs from the dynamic coefficient λ (3.39) by the factor q^2:

$$k = \lambda q^2. \qquad (10.10)$$

The dependence of the coefficient of sensitivity on frequency is called a <u>frequency-response curve</u> (Fig. 10.6). It differs from the analogous curve in Fig. 3.5 when a perturbing force is applied to the mass of the system.

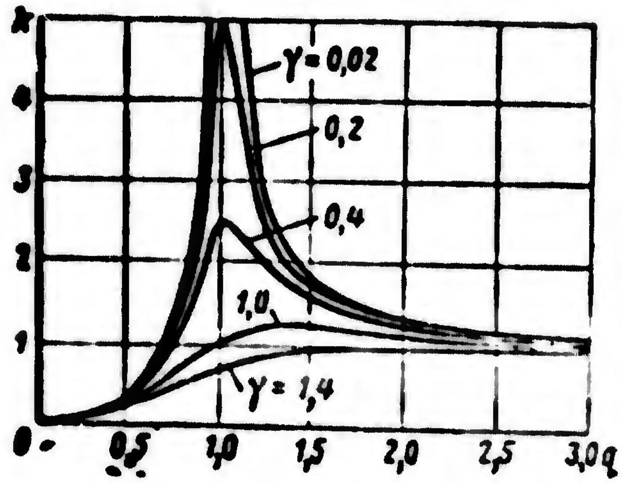

Fig. 10.6. Frequency-response curves of a vibrometric transducer.

From the graph on Fig. 10.6 it is clear that when q >> 1 the response curves converge to the value of k = 1. Consequently, at frequencies of oscillations, which are considerably larger than the natural frequency of the seismic element, the transducer measures displacements of oscillations. When q << 1 the transducer readings change approximately in proportion to the frequency squared, and consequently, it measures accelerations of oscillations, since the amplitude of acceleration

$$\ddot{y}_0 = \omega^2 y_0 \qquad (10.11)$$

changes according to the same law with respect to q (Fig. 10.7).

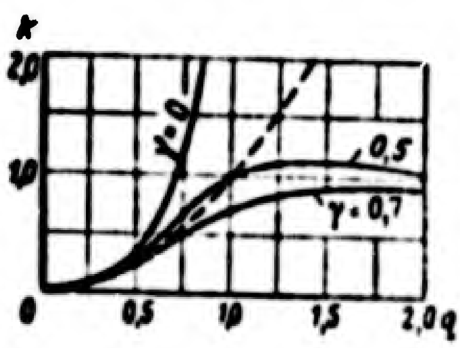

Fig. 10.7. Frequency-response curves of an accelerometer with various damping (dotted curve is a parabola).

Thus, seismic transducers for measurement of oscillations may be classified in the following way.

A vibrometer is an instrument for the measurement of oscillations, whose natural frequency of the seismic element is considerably lower than the lowest frequency of measured oscillatory motion.

An accelerometer is an instrument for the measurement of accelerations, in which the natural frequency of the seismic element is considerably higher than the highest frequency of measured oscillations.

The resonance region of the amplitude-response curve of a transducer is not commonly used for measurements due to the great dependence of its readings on the degree of damping. In accordance with formula (3.40)

$$\mu_{рез} = \frac{1}{\gamma}.$$

Taking into account that in many cases γ strongly changes with the change of temperature, and it depends on other factors, which usually in measurements on flight vehicles do not yield to exact calculation, the errors of measurements can be very large. The degree of approximation the "working" frequency-response curves of transducers to the natural frequency depends on the permissible measuring error.

In principle the same seismic instrument can measure both displacements (in the right part of the frequency-response curve), and also accelerations (in the extreme left part of the curve). In practice, however, different instruments are used. Vibrometers are designed for measurement of high-frequency oscillations, and accelerometers for measurement of low-frequency oscillations.

The necessity of different transducers for measurement of high-frequency and low-frequency oscillations is caused by the fact that one transducer cannot combine both functions without damage to the quality of measurements.

Vibrometers, due to the low rigidity of their springs, can work only under conditions when the linear overload, which is acting on the transducer, insignificantly differs from unity (by not more than ± 0.5). During large overloads the seismic mass descends to the base of the transducer and it ceases to function. Thus, vibrometers on flight vehicles can be applied basically only in rectilinear flight and under conditions where the overloads, acting in the place of installation of the transducer, insignificantly differ from the overloads in horizontal flight.

Permissible operating frequency ranges of transducers. Beginning from $q > 2$ (see Fig.10.6) the frequency-response curves straighten out and the relative oscillations of the seismic mass of a vibrometer become practically equal to the oscillations of its base. This coincidence is more exact, the larger q. Deviation of the curve from $k = 1$ is greater, the nearer the resonance period is to the natural frequency of the transducer. For practical problems a measuring error of amplitudes of oscillations from 5 to 10% is considered fully permissible. This condition corresponds to the value of $q = 2$ to 3. This error can be decreased and even completely excluded if for every frequency of measured oscillations one considers the change of the coefficient of sensitivity k. Thus the vibrometer measures oscillations with frequencies that are 2-3 times larger its natural frequency.

It is necessary to note that damping hardly affects the vibrometer readings. Therefore, vibrometers are frequently constructed without damping. However, during the work of a vibrometer there always are possible random perturbations (shocks), which cause natural oscillations of the seismic mass, building up on the forced oscillations. For decreasing the influence of such perturbations and faster damping of natural oscillations damping is introduced into the transducer.

The readings of an accelerometric transducer within the limits of $0 \leq q \leq 0.5$ practically do not depend on the degree of damping (see Fig. 10.7) and sufficiently accurately follow parabolic law, i.e., its readings are proportional to the effective acceleration. When $q > 0.5$ the readings of the accelerometric transducer to a strong degree depend on damping. With damping $\gamma = 0.6$ to 0.7 the transducer readings sufficiently well approximate parabolic law up to the value of $q = 0.7$ to 0.8. Consequently, if the accelerometer has no damping, it can be applied for measurement of accelerations with frequencies from zero to half the natural frequency of the transducer. If the accelerometer receives damping, constituting 0.6-0.7 critical, the working frequency range of the transducer is expanded to 0.7-0.8 of its natural frequency.

Depending upon the applied equipment with seismic transducers or the conditions of its work, the recording of oscillations will be represented in a certain scale by a graph of the time change of displacement, speed, or acceleration of the investigated oscillatory process. In all these cases the recording should satisfy conditions (10.5)-(10.7). This means that the frequency spectra of the recording and the investigated oscillations should be identical, the relationships of amplitudes of harmonic components of the recording and the investigated oscillations should also be identical, and there should be no phase distortions. The first two requirements are usually fulfilled if the vibration-measuring equipment works within the limits of the linearity of its frequency and amplitude response curves. The last condition can be exactly carried out only in the full absence of resisting forces. However, in real measuring instruments with damping $\gamma \approx 1.4$, the phase shift of different harmonic components for values of q from 0 to 1 approximately follows the law (see Fig. 3.6)

$$\varepsilon_i = \omega_i, \qquad (10.12)$$

where τ is the proportionality factor.

Putting formula (10.12) for the i-th harmonic component in the solution of the motion equation of the transducer's seismic mass, in a form coinciding with expression (3.56), we obtain

$$y_1 = y_{0i} \sin \omega_i (t - \tau). \tag{10.13}$$

It follows from this that there is a constant time shift of the recording with respect to the real process, which is immaterial. The magnitude of phase distortions is determined by the deviation of the phase response from a straight line, which in damping γ = 0.6 to 1.0 is small. For the values of $q > 2$ there is a constant phase shift $\alpha_1 \approx \pi$ (see Fig. 3.6), and phase distortions of the recording are insignificant. In the majority of practical problems only the frequencies and amplitudes of oscillations are determined and the phases of different oscillation components do not have value.

<u>Measurement of displacements of oscillations.</u> Frequencies and amplitudes of displacements are the basic parameters of an oscillatory process.

The equation of motion of the seismic mass of a transducer under the action of oscillations of its base (point of attachment of spring) has the form

$$\ddot{y} + 2h\dot{y} + p^2 y = -\ddot{\xi}(t), \tag{10.14}$$

where $\xi(t)$ (10.8) represents oscillations in the place of installation of the transducer.

Subsequently we will not make a distinction between the motion of the seismic mass of a transducer and the recording of this motion, since in virtue of the linearity of the frequency and amplitude response curves of the equipment they differ only in scale.

Considering, for convenience of use, the coefficient of sensitivity to be equal to $k = 1/k_a$ and constant, and considering (10.12), formula (3.56) may be reduced to the form

$$y = \frac{1}{k_a} \xi_0 \sin(\omega t - \alpha). \qquad (10.15)$$

From a comparison of formulas (10.15) and (10.8) it is clear that the recording of oscillations $y(t)$ differs from the real process $\xi(t)$ by constant factor $1/k_a$ and by phase lag (the latter is immaterial). Thus, the recording in a certain scale constitutes a graph of measured oscillatory motion. The scale of the recording (sensitivity of the equipment) can be a fully defined constant, as, for example, in mechanical recorders, or it can change in defined limits on the desire of the experimenter, as, for example, in electronic vibration-measuring equipment.

The scale of the recording – the coefficient of sensitivity k_a – can be calculated. However, in practice it is determined by the results of calibration of equipment. Knowing the coefficient of sensitivity k_a, on the basis of recording (10.15) it is easy to determine the amplitude of displacements of the investigated oscillations ξ_0.

During the action of a combined perturbation on the transducer

$$\xi(t) = \sum_{i=1}^{n} \xi_{0i} \sin(\omega_i t + \varphi_i). \qquad (10.16)$$

Formula (10.15) is reduced to the form

$$y = \sum_{i=1}^{n} y_i = \frac{1}{k_a} \sum_{i=1}^{n} \xi_{0i} \sin(\omega_i t + \varphi_i - \alpha), \qquad (10.17)$$

where ξ_{0i} and φ_i correspondingly are the amplitude and phase angle of the i-th component of the investigated oscillatory process.

From a comparison of formulas (10.17) and (10.16) it is clear that recording y(t) differs from the investigated process $\xi(t)$ by the common constant factor $1/k_a$ and by the phase shift of the harmonic components when $q > 2$ by magnitude $\alpha_1 \approx \pi$ (for estimating the amplitudes and frequencies of oscillations the latter is immaterial). Thus, in this case the recording also differs from the measured oscillations only by scale. Knowing the coefficient of sensitivity k_a, it is easy to determine both the amplitudes of displacements of components of measured oscillations, and also total displacement.

<u>Measurement of accelerations (overloads)</u>. In this case the acceleration of oscillatory motion of the point of spring suspension of the transducer $\ddot{\xi}(t)$ is given. Let us assume that $\xi(t)$ as before is determined by formula (10.8). The amplitude of acceleration is equal to

$$\ddot{\xi}_0 = \omega^2 \xi_0. \tag{10.18}$$

Then equation (10.14) can be written in the form

$$\ddot{y} + 2h\dot{y} + p^2 y = \ddot{\xi}_0 \sin \omega t. \tag{10.19}$$

Expression (3.56) is the solution of this equation. The amplitude of forced oscillations is

$$y_0 = \frac{1}{\sqrt{(1-q^2)^2 + q^2\gamma^2}} \cdot \frac{\ddot{\xi}_0}{p^2}. \tag{10.20}$$

The coefficient of acceleration sensitivity

$$k_1 = \frac{1}{k_j} = \frac{y_0}{\ddot{\xi}_0} p^2 = \frac{1}{\sqrt{(1-q^2)^2 + q^2\gamma^2}} \tag{10.21}$$

does not differ from the dynamic coefficient (3.39) and it determines the frequency-response acceleration curve (see Fig.3.5). The phase response of acceleration coincides with the phase response of displacement (see Fig. 3.6). In the measurement of accelerations, just as in the measurement of displacements, the phase distortions in recordings are immaterial.

Assuming, as before, that the value of y(t) corresponds to the recording of the instrument, the conclusion can be made that the recording in a certain scale represents a graph of the measured accelerations

$$y(t) = \frac{1}{k_j}\ddot{\xi}(t). \tag{10.22}$$

where coefficient k_j has the value of (10.21). It can be calculated or determined by the results of calibration. Knowing coefficient k_j, it is easy to determine acceleration on the basis of the recording of the instrument.

In case of complex measured oscillation the motion of the seismic mass of the transducer is determined by the formula

$$y = \sum_{i=1}^{n} y_i = \frac{1}{k_j}\sum_{i=1}^{n} \ddot{\xi}_i(t). \tag{10.23}$$

The recording of accelerations of complex oscillations has the same frequency spectrum as the measured oscillations themselves. Amplitudes of sinusoidal components of the recording, as may be seen from the structure of coefficient (10.21), are directly proportional to the square of the frequency of corresponding components of measured oscillations at identical amplitudes. Knowing coefficient $k_1 = 1/k_j$, on the basis of the recording one can determine the amplitudes of accelerations of the oscillation components or total acceleration in any moment of time by simple multiplication of the ordinate of the recording by coefficient k_j.

Measurement of overloads in principle does not differ at all from measurement of accelerations.

<u>Measurement of speed of oscillations.</u> By itself the speed of oscillations usually is of no interest and is rarely determined in practice. However, the recording of speed of oscillations as a method for extensive manifestation of the peculiarities of oscillations during flying tests is applied frequently.

The advantages of a recording of the speed of oscillations are evident from the following example. Let us assume that a transducer is influenced by complex oscillations with the frequencies and amplitudes shown in Table 10.1. The oscillations approximately with such parameters correspond to real ones (for instance, on passenger turboprop aircraft). Let us assume that displacements, speeds, and accelerations of oscillations are consecutively recorded. We shall then consider that the equipment does not have phase distortions, and its amplitude and frequency-response curves are linear. Then the investigated oscillations will be completely reproduced on the recording in certain scale.

Table 10.1

Order of components of complex oscillation (i)	Frequency, osc/sec	Amplitude of displacement		Amplitude of speed		Amplitude of acceleration	
		[illegible] mm	[illegible]	[illegible] mm/sec	[illegible]	[illegible] mm/sec²	[illegible]
1	2	2.50	250	31.4	2	395	1
5	10	0.50	50	31.4	2	1 975	5
25	50	0.10	10	31.4	2	9 875	25
125	250	0.01	1	15.7	1	24 700	62.5

Such a recording, for the example given in Table 10.1, is shown in Fig. 10.8.

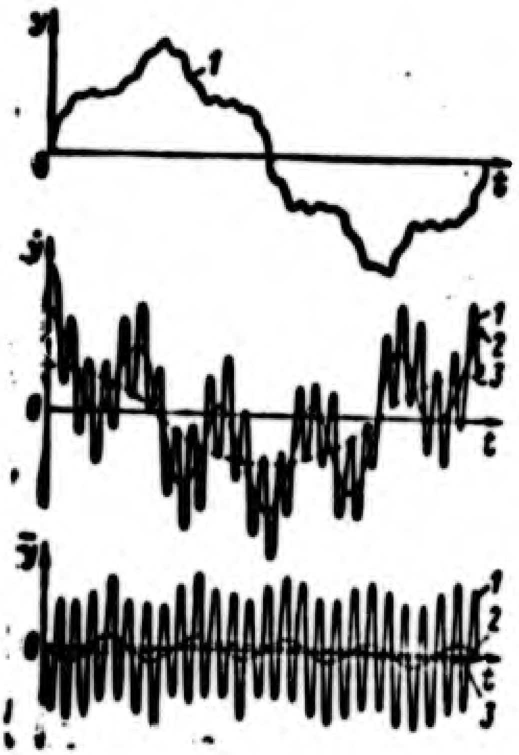

Fig. 10.8. Graphs of displacements y, speeds ẏ, and accelerations ÿ of the same oscillatory motion (illustration to Table 10.1). 1) composite graph of oscillations with frequencies of 2, 10, and 50 oscillations per second; 2) composite graph of oscillations with frequencies of 2 and 10 oscillations per second; 3) graph of oscillations with frequency of 2 oscillations per second.

For the considered example the amplitudes of displacements of high-frequency and low-frequency oscillations differ by 250 times, and the amplitudes accelerations by 62.5 times. Such recordings present difficulties during processing if it is necessary to determine the frequencies and amplitudes of all oscillation components. At the same time, in the recording of speeds, oscillations with different frequencies are obtained equally as well. Therefore, in the study of complex oscillations it is frequently useful to record the speeds, inasmuch as it is possible, without extra effort, to determine all components of complex oscillations on the basis of the recording.

Transducers for Measurement of Oscillations and Overloads

The basic types of transducers for measurement of oscillations are accelerometric and vibrometric transducers. Instruments for measurement of overloads have as their basic sensing device an accelerometric unit whose readings are appropriately recorded by a device which is incorporated in the instrument's design. Instruments for measurement of oscillations and overloads can be mechanical and electrical. In the last case for measurement of overloads vibration-measuring equipment with accelerometric transducers is used.

Electrical systems for measurement of oscillations and overloads possess a number of advantages over mechanical instruments. Electrical systems permit simultaneous measurement and recording on one photographic film of parameters of oscillations in large quantity of points of a structure, and they allow remote-control measurement. Furthermore, along with recording of oscillations and overloads, the same film can be used to record other parameters which are necessary for subsequent analysis of the investigated phenomenon.

The measurement of oscillations and overloads by electrical methods requires appropriate transducers which convert the mechanical oscillatory motions of the seismic mass of the transducer into an electrical signal that is convenient for measurement. The broadest application has been found by magnetoelectric, electromagnetic, piezoelectric, and ohmic systems of conversion.

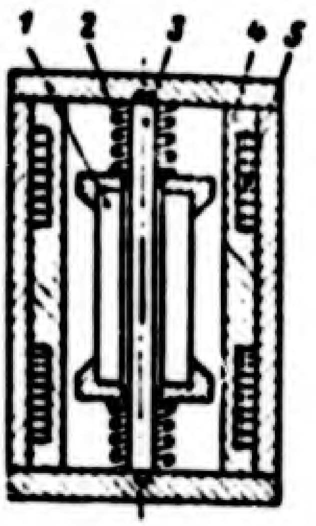

Fig. 10.9. Diagram of a magnetoelectric (inductive) vibrometric transducer.

The magnetoelectric system of conversion uses the phenomenon of electromagnetic induction. In transducers which are built according to this principle (Fig. 10.9) the mass of the seismic element consists of a magnet 1 which is attached to springs 2 and moves in the direction of axis 3. The body of the transducer 4 has a built-in wire coil 5. During oscillations the magnet moves with respect to the coil and induces e.m.f. into it, which is proportional to the rate of motion:

$$E = BlV \sin\varphi. \qquad (10.24)$$

where B is the magnetic induction of the field;

φ is the angle between the axis of the transducer and the vector of the magnetic field;

l is the overall length of the conductor;

V is the relative speed of the conductor in the magnetic field (in this case it is equal to the speed of the seismic mass of the transducer $V = \dot{y}$).

The magnetoelectric system of conversion is widely applied in vibrometric transducers. These transducers have a rather low frequency of natural oscillations near 4-7 oscillations per second and they ensure measurement of oscillations with frequencies from 10-12 to 300-500 oscillations per second. Transducers of this type can work with corresponding amplifiers, integrators, and differentiators. In this case it is possible (at the desire of the operator) to record displacements, speeds, or accelerations of the oscillatory process. In the presence of loops in the oscillograph with sensitivity 15-20 mm/ma such transducers can be employed without an amplifier by connecting them directly to the oscillograph. In this case the speed of the oscillatory process will be recorded. In the use of integrating loops the recording of readings of the transducer on an oscillograph is a recording of displacements in a defined scale.

The application of transducers without an amplifier has an important advantage, since the dimensions of the equipment are sharply decreased.

The electromagnetic system of conversion of mechanical oscillations into an electrical signal uses an interconnection between the change in the magnitude of the magnetic flux in the magnetic circuit and the magnitude of inductance of coil 5, inside which there passes a magnetic flux (Fig. 10.10). The magnetic circuit is carried out in the form of an iron core 6 which has an air clearance. The permeability of iron is 500-600 times more than that of air. Therefore, the main part of the resistance of the magnetic circuit is obtained at the expense of the air clearance. Inductance of the coil with iron core varies in inverse proportion to the magnitude of the air clearance.

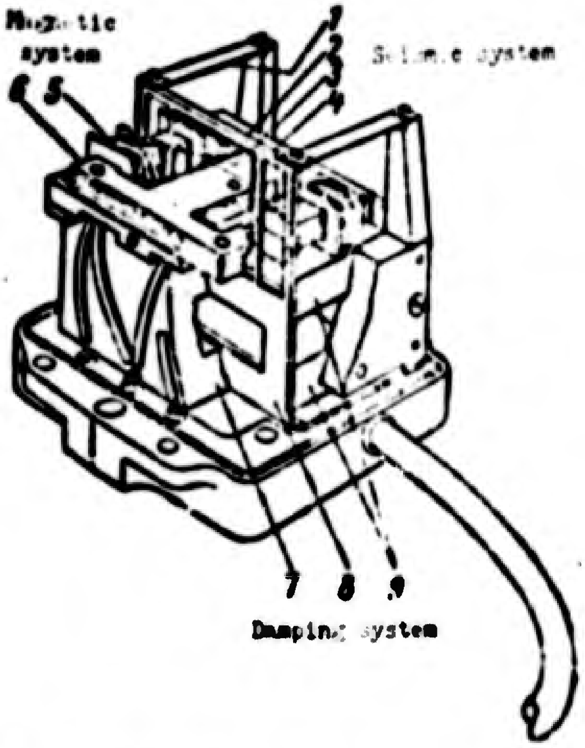

Fig. 10.10. Electromagnetic accelerometric transducer.

The change in conductivity of the magnetic circuit is attained by the introduction of iron plates 3 and 4 into the air clearance. These plates and spring 1, on which they are suspended, constitute the sensing device of the transducer. The seismic mass in this case consists of the iron plates. During oscillatory motion of the transducer, frame 2 moves with the plates, and in coil 5 the modulated voltage varies in proportion to movements of the frame. Separate inductive coils are connected in the circuit of the AC measuring bridge. One or two arms are in the transducer and the others are inside the electronic amplifier. The signals, taken from the measuring diagonal of the bridge, are fed to the inlet of the electronic amplifier.

The electromagnetic systems of conversion is widely used for accelerometric transducers with natural frequency of sensing device 40-1000 oscillations per second. Electromagnetic transducers in defined limits are insensitive to the change of ambient temperature.

Damping in transducers with natural frequency to 100 oscillations per second is carried out by vortex currents which are induced into the lower part of frame 8 during its oscillations around constant magnets 9 with pole pieces 7. The electromagnetic field, appearing from this current and interacting with the constant magnetic field of the transducer, creates a resisting force to the free oscillations of the frame.

Electromagnetic accelerometric transducers permit the measurement of oscillations and overloads with frequency to 0.7-0.8 of the natural frequency of the transducer.

The piezoelectric system of conversion uses the properties of certain substances to create electrical charges during deformations. For this, plates are usually employed that are made from quartz crystals or artificially prepared sensing devices made from barium titanate. The magnitude of the charge, taken from the sensing device, is very small, and therefore for decreasing the influence of leakage of charges near the transducer a cathode follower is usually installed.

Transducers with piezoelectric sensing devices are usually of the accelerometric type with sufficiently great natural frequency (in certain cases over 10,000 oscillations per second). Due to this, the sensitivity of such transducers to oscillations with low frequency is lowered. Piezoelectric transducers have small dimensions and weight. Their shortcoming is the increased sensitivity to changes of external conditions (humidity, temperature).

The ohmic system of conversion uses an ordinary strain gauge which is glued to a laminar spring. A seismic mass is attached to the spring. The deformations of such a sensing device are in proportion to the amplitudes of oscillations of the seismic mass. A signal, taken from the strain gauge, is fed to the conventional tensometric equipment.

Vibration-Measuring Equipment

The power of signals from electrical transducers is frequently insufficient for measurement with the help of loops of magnetoelctric oscillographs. Futheremore, in the measurements it is frequently necessary to integrate or differentiate signals from transducers. Therefore vibration-measuring equipment includes electronic amplifiers, integrators, and differentiators. Electronic amplifiers of vibration equipment in principle do not at all differ from amplifiers of strain measurement equipment, but include blocks of integration and differentiation.

The block diagram of an amplifier of vibration-measuring equipment with electromagnetic transducers of the accelerometric type is shown in Fig. 10.11. Amplification is produced on the carrier frequency. The input serves for balancing of the measuring circuit of the AC bridge. Two arms of the measuring bridge are in the transducer and the two others are in the amplifier. Amplifiers have a regulating device for changing the amplification factor. After several voltage amplifier stages the signal enters the power amplifier and phase sensitive detector. Further, this signal can be fed to the oscillograph loop. In this case the recording in a certain scale represents a graphic of the change of acceleration (overload) in time. Upon necessity the signal

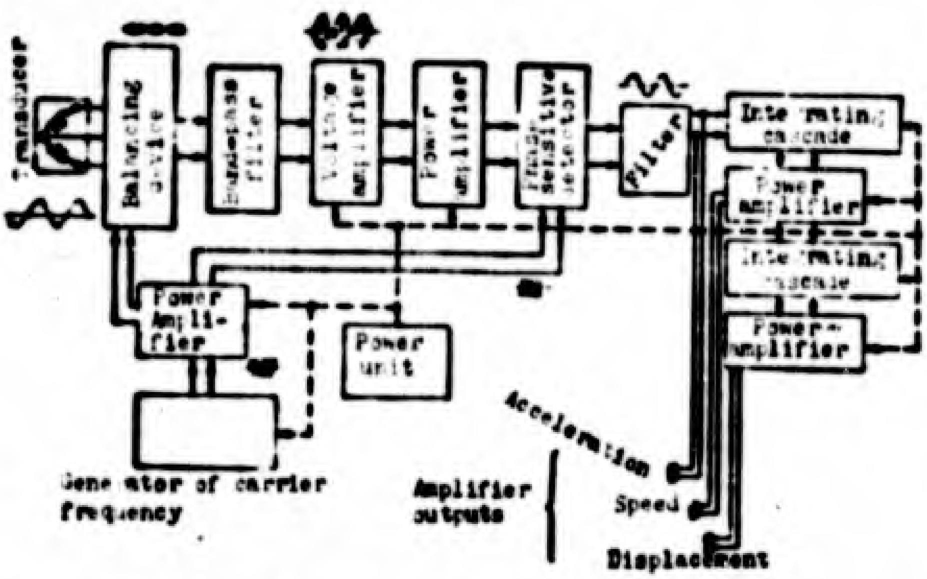

Fig. 10.11. Block diagram of vibration-measuring equipment with electromagnetic transducers.

can be fed to the integrating cascades. After integration and additional power amplification the signal is fed to the oscillograph loop. In this case, in a single integration the recording constitutes a graph of the change of the speed of oscillations, while in double integration it represents a graph of displacements. In certain cases for integration there can be applied special integrating oscillograph loops.

Mechanical Recorders of Oscillations and Overloads

These instruments use kinematic methods of increasing displacement of the needle which records the oscillations, as compared to the motion of the mass of the sensing device. The simplest method of such an increase is the use of a lever. The relation of the needle lever arm to the seismic mass lever arm characterized the increase of amplitude of the recording as compared to the amplitude of oscillations of the sensing device. Usually the transmission ratio in such instruments composes a magnitude from 3 to 10.

In mechanical recorders the transducer, amplifier, and recording device are combined in one instrument. Because of the pen-recording on paper (stencil, blueprint) the usual development and processing for electrical systems of measurement is not required.

The sensor of recorders of oscillations is a transducer of the vibrometric type with a natural frequency of 6-8 oscillations per second. The range of frequencies of measured oscillations composes from 10-15 to 200-250 oscillations per second.

The sensing device of recorders of overloads is a transducer of the accelerometric type with a natural frequency from 8-10 to 15 to 20 oscillations per second. Recorders of overloads are distinguished by the range of measured overloads and by the system of recording.

Furthermore, they can be one-, two-, and three-component, and can measure overloads correspondingly in the direction of one, two, or three coordinate axes of the instrument.

Mechanical recorders of oscillations and overloads have been applied for a very long time. There is large quantity of types and designs of such instruments. They are durable, reliable, and simple to operate, and therefore are presently in use. Recorders of oscillations are used basically for control measurements in separate structural points os aircraft and helicopters.

For measurements on transport aircraft we frequently find the use of mechanical instruments, i.e., vibroprobes. The sensing device of this instrument is pressed to the vibrating surface. An estimate of the magnitude of amplitudes of oscillations is produced on the scale of the instrument or on a tape recording.

Calibration of Equipment for Measurement of Oscillations and Overloads

The basic problem of calibration is the obtainment of coefficients for transition from recording to the parameters of the investigated process. Within the limits of the linearity of work of the equipment these coefficients determine the recording scale of the investigated motion.

Calibration of vibration-measuring equipment utilizes a special calibration stand, on which it is possible to create sinusoidal oscillatory motion with different frequency and amplitude. Calibration is produced in the following way. Transducers are rigidly mounted on the platform of the calibration stand and connected to the channels of equipment and oscillograph to which they will be connected during the measurements. The range of revolutions (frequencies of oscillations) of the stand and the amplitudes of oscillations of its platform should correspond to the expected frequencies and amplitudes of the investigated oscillations of the flight vehicle structure. Then a series of recordings of transducer signals are made at fixed revolutions of the calibration stand.

Calibration coefficients are determined according to the following formulas:

1. In the recording of displacements

$$k_s = \frac{S}{2A_{т}}. \qquad (10.25)$$

2. In the recording of speed

$$k_v = k_s\omega = \frac{2\pi f S}{2A_{т}}. \qquad (10.26)$$

3. In the recording of acceleration (overload)

$$k_j = k_a = k_s\frac{\omega^2}{g} = \frac{4\pi^2 f^2 S}{2A_{т} g}. \qquad (10.27)$$

Formulas (10.25) - (10.27) contain the following designations:

S – amplitude of oscillation of the platform of the calibration stand in mm;

f – frequency of oscillations of the platform of the calibration stand in oscillations per second;

ω – angular frequency of oscillations of the platform of the stand in 1/sec.

$2A_{cal}$ – sweep of calibration recording of oscillations in mm.

Calibration of overload recorders is carried out on centrifuges. For these instruments, which frequently do not have optimum damping, it is very important to determine the dynamic coefficient and thereby establish the limit of applicability of every instrument with respect to frequency. Such a check can be produced on the calibration stands, which are used for calibration of vibration-measuring equipment, and on special stands for dynamic calibration of overload recorders, which make it possible to simulate single forces of small duration with different change of their magnitude in time. The range of magnitudes of measured overloads, the natural frequency, and the dynamic response of an instrument usually are indicated in the log book of every overload recorder.

Thermomeasuring Equipment

The registration of temperatures of a structure in different points employs thermomeasuring equipment. Such equipment consists of transducers, which are intended for measurement of temperatures, an amplifier and a converter, plus switching and recording equipment. The transducers in the thermomeasuring equipment are thermocouples and film resistance transducers.

Measurement of temperatures with the help of thermocouples is based on thermoelectric effect. This consists in the fact that in a closed electrical circuit, which is composes of various materials, there appears electromotive force under the condition that in the places of contacts different temperature is maintained. In this case the simplest electrical circuit from two various conductors carries the name of thermocouple.

Thermoelectromotive force (TEMF) depends not only on the temperatures of hot and cold joints (places of conductor contacts), but also on the nature of the materials making up the thermocouple. The TEMF of a thermocouple does not change if the electrical circuit consecutively includes any quantity of other materials. However, it is then necessary to the observe condition that in the additional places of contacts a constant temperature is maintained.

The best pairs of metals, giving the biggest TEMF, are Chromel-Copel and Chromel-Alumel. The measuring circuit of temperature with the help of a thermocouple and galvanometer is shown in Fig. 10.12. Stabilization of thermocouple readings is attained by welding a hot joint to a 10 x 10 mm copper plate. In turn the copper plate is attached to the surface, the temperature which is measured. In the installation of thermocouples the conductors are thoroughly isolated from each other and from the structure. For lowering heat withdrawal a wire 15 to 20 mm in length is inserted along an isotherm, beginning from the hot joint.

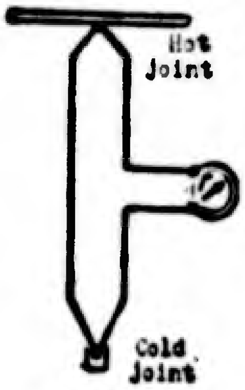

Fig. 10.12. Measuring circuit of temperatures with the help of a thermocouple and galvanometer.

In view of the complexity of installation of a thermocouple, the necessity of a sufficiently reliable cold joint, and other inconveniences of work with thermocouples, resistance transducers began to be used (Fig. 10.13) for the measurement of temperatures of a structure in flight. The sensing device of the film resistance transducer is a grid made from copper wire in an enamel insulation approximately 0.02 mm in diameter. Besides the copper wire, the sensing device uses nickel wire, and in certain cases platinum. The wire grid of the transducer is glued to a base, for instance to thermoresistant film with a thickness of about 0.05 mm. As a rule, such transducers work in a range of temperatures from -60 to 250°C. The error of the transducer is about 2%.

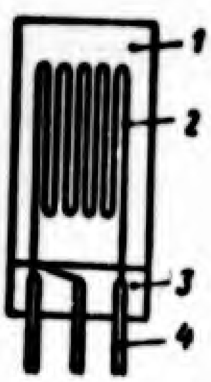

Fig. 10.13. Diagram of a film resistance transducer for measurement of temperatures. 1) base of transducer; 2) copper wire; 3) base for attaching connecting wires; 4) connecting wire.

Transducers placed in a special body are also used. Resistance transducers in the form of a plate, tube , or plug can be attached to different places of the structure. Receivers of temperatures in the form of resistance transducers, placed in the body, can be used at higher temperatures.

With an insufficiency of the thermotransducer signal amplifying equipment is used. The recording equipment employed for measurements of temperatures are ordinary loop oscillographs. Increase of the quantity of points of the structure, in which temperature is recorded, during work with oscillographs is attained by the use of switching devices.

A schematic diagram of thermomeasuring equipment is shown in Fig. 10.14. Transducers are included in the arms of the measuring bridges, one of which consists of a receiver resistance and the other, a line wire and corresponding meter multiplier, while the third and fourth arms are formed by resistances R_1 and R_2, which are common for each group (channel) of receivers. The bridge diagonal with the help of a third line wire is removed directly from the receiver. The latter excludes the error due to heating of the other two line wires which enter the bridge arms which are adjacent to the diagonal. Signals from diagonals of bridges are fed to the commutator, which in turn connects them at the amplifier input. Voltages of already direct current are taken from the amplifier output; they are proportionate to the temperatures of the

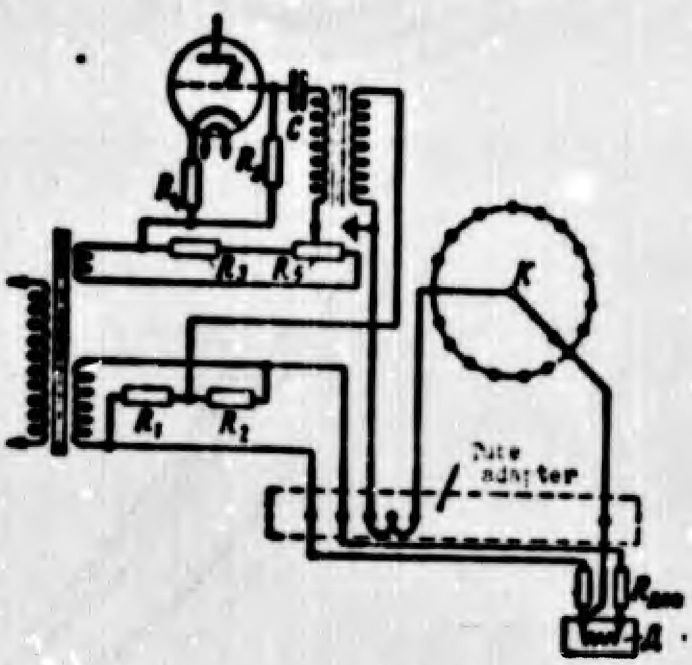

Fig. 10.14. Schematic diagram of equipment for measurement of temperatures. Д - transducer, $R_{доп}$ - additional resistance, R_1, ..., R_c - resistance, Л - tube, K - commutator.

receivers. All receivers are united in groups which form channels of measurements.

Calibration of thermocouples is usually produced on aligned control thermometers or on the basis of known physical constants: the melting point of snow (0°C), the boiling point of water at normal pressure (100°C), the fusing point of sulfur (236°C).

During calibration of thermomeasuring equipment with film resistance transducers the dependence between resistance of a transducer and ambient temperature is determined in the beginning. This dependence, with sufficient accuracy, is described by the equation

$$R_T = R_0(1 + \alpha_e T), \tag{10.28}$$

where R_T is transducer resistance at temperature T;

R_0 is transducer resistance at 0°C;

α_e is the thermal coefficient of electrical resistance of transducer wire;

During calibration the resistance transducers are glued to material which is analogous to the material of the object of measurements. Knowing the resistance of the transducer, which is glued to the object, at constant temperature and mean coefficient of electrical resistance for the given group of transducers, it is possible to construct a calibration curve. This curve is used subsequently in deciphering the results of tests. After calibration of transducers calibration of the equipment itself is conducted by assigning corresponding changes of resistance in the bridge circuit.

In measurements of non-stationary temperatures it is obligatory to consider the thermal inertia of the transducers. The distinction of the transducer readings from the actual values of temperatures depends on the structural layout of the transducer mounting. The true values of temperature are obtained by introducing a corresponding correction into the results of measurements. This correction is determined from the relationship

$$\Delta T = k\frac{dT}{dt},$$

where k is the time delay constant of the transducer; it depends on the design of the transducer, the material of the sensing device, and the coefficient of heat radiation of flow.

Magnitude k is determined by means of processing the recording of the change of temperature of standard and test transducers in time.

10.2. Laboratory Tests of Aircraft Structures

Static Tests of Aircraft Structures

Static tests are a basic means for controlling the strength of airplane designs, for checking the methods of calculation, for selecting a rational type of design, and for giving it the necessary strength.

Static tests of elements and models of structures. In the process of designing a flight vehicle, static tests are conducted on a large number of separate supporting structural members. Such tests definitize the constructive solution of a given supporting member which is brought to the necessary strength, and the tests definitize the method of its strength analysis. Separate tests are usually conducted on rods, samples of panels, spars and stringers, attachment joints, and so forth.

For a more precise definition of the method of calculation and selection of an optimum constructive solution structural models are sometimes tested.

The models are made with full similarity to the original with respect to geometric shape and applied materials. Sometimes models are prepared with fulfillment of only the basic supporting members.

Static tests of full-scale assemblies of airplane designs. This form of testing was introduced for the first time in the practice of aircraft building in 1910-1912. At present, static tests of full-scale assemblies are the most wide-spread experimental method of checking the strength of a structure.

In principle, static tests are a check of strength analysis. The structure is loaded with approximately the same loads which were accepted during calculation.

In serial production of flight vehicles static tests are a check of the conformity of their strength to a standard sample (experimental model).

The basic deficiency of static tests is the incomplete conformity of load distribution of the design to the actual conditions of loading in flight. In particular, large difficulties are presented by the calculation of the influence of deformations on the distribution of the aerodynamic load. For the majority of calculation cases the dynamic load is replaced by a static load, which distorts the character of application of the loads. Furthermore, it is impossible to correctly calculate the influence of local skin damages on the change of aerodynamic forces and the character of destruction of the structure.

For a long time loading of a structure during static tests was produced with sacks of sand or shot. Subsequently loading began to be done with the help of hydraulic or electrical power-exciters with the application of a lever system which permits carrying out distribution of total load on the structure (10.15). Aerodynamic load is applied to the surface of an assembly through canvas straps or rubber washers which are glued to the surface of the aircraft. In static tests on the whole the aircraft is in a suspended state under the action of mutually balanced loads (see Fig. 10.15). Separate parts of the aircraft can be attached to stands or support columns during tests (Fig. 10.16).

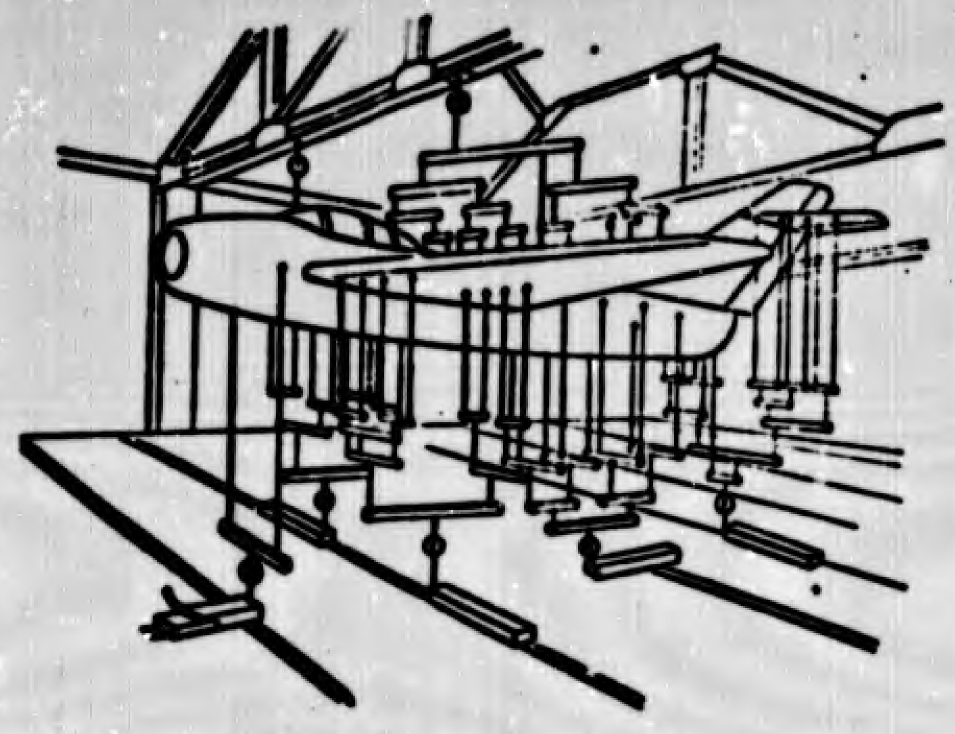

Fig. 10.15. Diagram of static tests of an aircraft.

Simultaneously with the manifestation of carrying capacity of structures while carrying out static tests, the stresses in different points of the structure and its rigidity are determined. Deformations of the structure are measured by rods which are suspended from it, and by a level. Stresses are measured basically with the help wire strain gauges (up to several thousand wire strain gauges are installed). The registration of signals from strain gauges employs

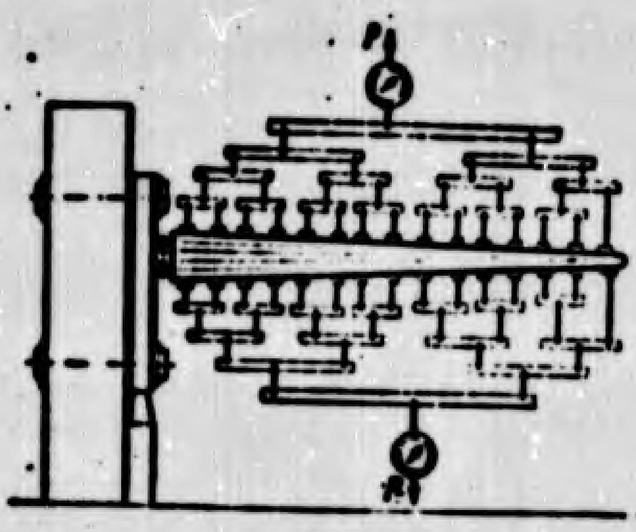

Fig. 10.16. Diagram of column tests.

tensometric equipment with automatic switching to 100 and more strain gauges and with automatic recording on paper in the form of graphs of the dependence of deformations on load or in the form of tables.

Before the proof (examination) test the structure is "stretched," i.e., the entire system is checked up to a load that is equal to 40-50% of the rated load. After the "stretching" stage-by-stage (through 10% of the rated load) loading is accomplished to a load equal to 67% of the rated load. For uniform loading of a large quantity of structural points automatic programming devices can be applied for controlling the power-exciters.

On every stage stress and strain is measured. For manifestation of stresses, which considerably exceed the stresses corresponding to those rated for a given stage of loading, the tests are continued and the cause of their appearance is clarified. Upon necessity, local reinforcement of the structure is accomplished.

During the tests they thoroughly check for permanent deformations, local loss of stability of skin and structural elements, and so forth. When there are considerable deformations the tests stop, the cause of the appearance of these deformations is cleared up, and the structure is reinforced.

After achievement of a load, equal to 67% of rated, the structure is unloaded to the primary state. A thorough check is then made on the state of the structure and permanent deformations are examined in detail. If local and general permanent deformations do not exceed permissible values, the static tests are continued until achievement of the rated load.

Testing to destruction for the purpose of finding the actual safety factors is conducted for a rated case which corresponds to the biggest load of the structure.

During static tests of experimental structures a considerable part of the structures is destroyed under a load less than 100% of rated. According to British investigations, in which 67 tests of full-scale assemblies and 100 tests of components (elements) of airplane designs were generalized, 20% of the full-scale assemblies are destroyed under a load less than the maximum operational and 55% under a load less than 95% of rated. Combined data on these tests are shown in Fig. 10.17. These data show that in spite of the great experience of aircraft construction plants and the development of methods of strength analysis, static tests are necessary for control and finishing the strength of aircraft structures.

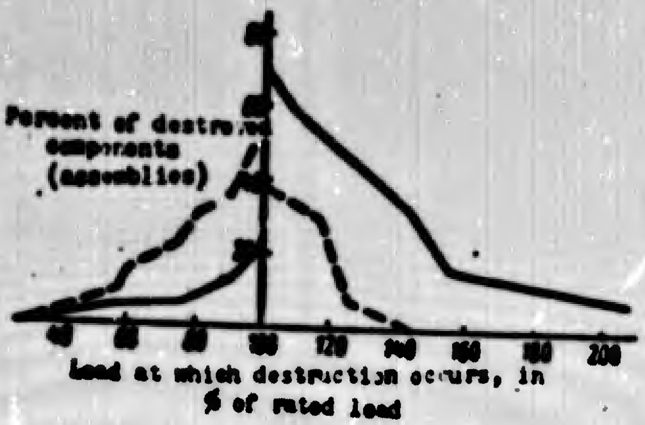

Fig. 10.17. Results of static tests. —— components, --- full-scale assemblies.

Pile-Driver Tests of Aircraft Structures

During landing, the structure of a flight vehicle should perceive a definite magnitude of kinetic energy without damages. For checking the shock-absorption, a landing gear strut, which is loaded by part of the weight of the aircraft, is dropped on a pile-driver (Fig. 10.18). Drop height is determined proceeding from the magnitude of absorbed energy:

$$A = \frac{mv^2}{2} + (h + \delta) G k_p, \tag{10.29}$$

where m and G correspondingly are the mass and weight of the load;

k_p is the coefficient of load decrease of an aircraft wing during the drop (it characterized the decrease of wing lift during landing);

h is the movement of the shock-absorber;

δ is the magnitude of pressure in the pneumatic tire.

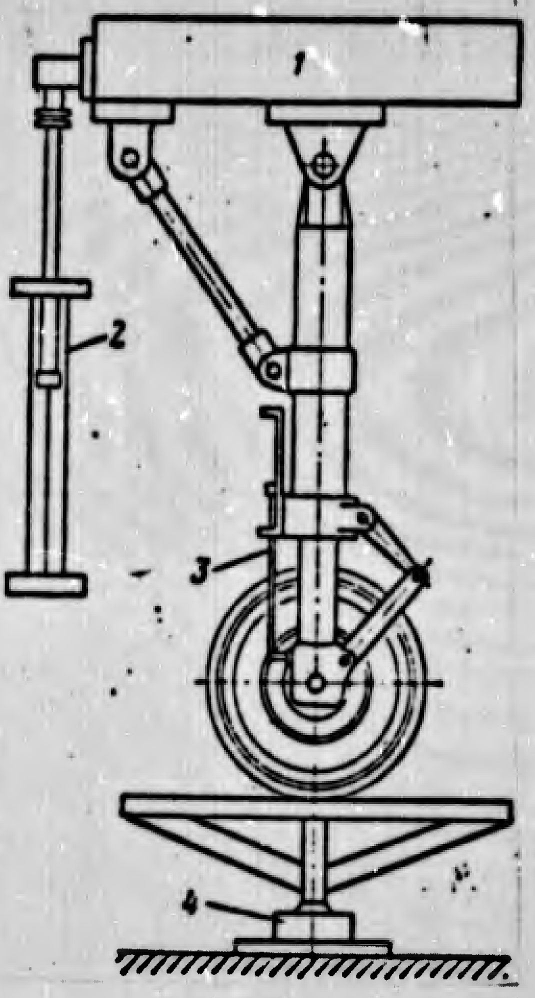

Fig. 10.18. Diagram of pile-driver installation. 1) load; 2) slide wire for recording the movements of the center of gravity of dropped load; 3) slide wire for recording the process of shock-absorption. 4) hydraulic dynamometer.

During free fall the drop height is

$$H_{\text{сбр}}=\frac{V_y^2}{2g}. \qquad (10.30)$$

From expression (10.29) we obtain

$$V_y=\sqrt{2\frac{A-k_p(h+\delta)G}{m}}. \qquad (10.31)$$

Placing this expression in formula (10.30), we determine

$$H_{\text{сбр}}=\frac{A}{G}-(h+\delta)k_p. \qquad (10.32)$$

For reproduction of frontal loads on a strut they sometimes employ a drop to a slanted surface. In this case the frontal load is

$$P_x=P_y\,\mathrm{tg}\,\alpha,$$

where α is the angle of inclination of the support surface.

A more exact simulation of frontal loads can be attained by dropping a strut on a movable support (drum) which has a speed that is equal to the landing speed of an aircraft. The preliminary acceleration of the wheels before the drop can also be used for this purpose.

In the drop of landing gear on a pile-driver the movement of the shock-absorber, the pneumatic tire pressure, the reaction of the strut to the support, the forces and stresses in the basic elements of the landing gear, and other parameters are measured and recorded by oscillograph. These measurements can subsequently be used for calibration of transducers of forces and movements for a flight experiment.

Figure 10.19 shows the approximate form of an oscillogram of the recording of support reaction and movement of a shock-absorber during tests of a strut on a pile-driver.

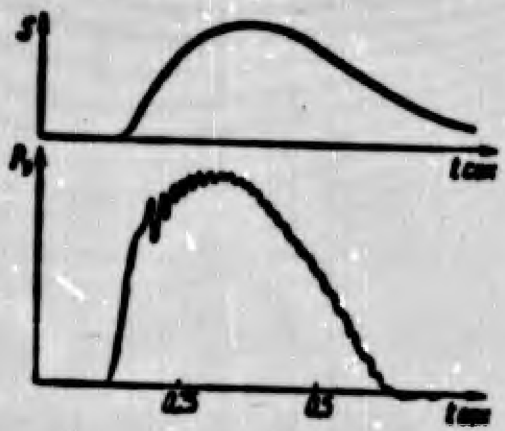

Fig. 10.19. Diagram of the change of the support reaction P_y and the movement of shock-absorption S during the drop of landing gear on a pile-driver.

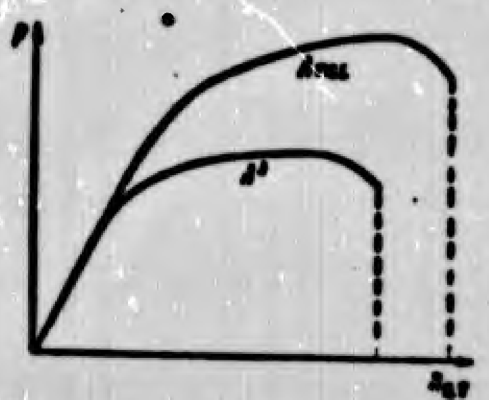

Fig. 10.20. Diagram of work of landing gear. A_{max} – maximum work, A^{op} – operational work.

The results of measurements during pile-driver tests are presented in the form of a diagram (Fig. 10.20) and are compared with calculation data. By means of introducing corresponding structural changes and repeated tests the characteristics of shock-absorption are brought to those required for normal operation.

On an actual aircraft kinetic energy is perceived not only by shock-absorbers and pneumatic tires, but also by the aircraft structure. For a more exact appraisal of the work of the landing of the landing gear and structure of an aircraft during landing, the whole aircraft is sometimes dropped from a given height. These tests additionally measure forces and stresses in the basic elements of the airframe structure, and also overloads in different parts of the aircraft (on the wing tips and empennage, in the nose and afterbodies, in the center of gravity of the aircraft, and so forth). In the drop of the whole aircraft it is possible to estimate the dynamic coefficients for its basic assemblies during landing.

For an appraisal of the performance characteristics of landing gear and a check of the strength of its structure, multiple drop tests are employed. Periodically, in a certain number of drops, a diagram of work is made for checking the functioning of the shock-absorption system. On the basis of the number of drops, which the structure sustains, it is possible to judge the number of permissible takeoffs and landings in operation.

Experimental Determination of Natural Frequencies and Forms of Oscillations

Every flight vehicle undergoes frequency (resonance) tests for determining its natural frequencies and forms of oscillations. Such tests are conducted so that by means of comparison of experimentally determined frequencies and forms of natural oscillations with rated ones the calculations of flutter and dynamic loading of a structure are refined.

The method of frequency testing consists in the fact that to the flight vehicle or a separate part of it there is applied an external perturbation, the frequency of which can be changed at the desire of the operator. Upon coincidence of one of the frequencies of natural oscillations of the structure with the frequency of the perturbing force, there appears resonance which is determined by the sharp increase of amplitudes of oscillations. Frequency and form of oscillations during resonance are taken as the natural frequency and form of oscillations of the structure.

In general, the reaction of a structure to an arbitrary perturbing force is a summation of a series of normal (natural) forms of oscillations of the structure. For isolation of separate forms and frequencies it is necessary to select the form and place of application of the perturbing force. Usually a sinusoidal disturbance is applied with a variable frequency. Analysis of the influence of a sinusoidal perturbing force on an elastic structure shows that for the excitation of oscillations of corresponding form it is necessary that with the equality of frequencies the amplitude of perturbing force in every point of the structure would be proportionate to the product of the amplitude of standardized initial form and the reduced mass in this point.

The excitation of oscillations on full-scale objects employs vibrators of several types:

1) vibrator with revolving unbalanced load, which constitutes an unbalanced flywheel fastened to the structure and set into rotation by an elastic shaft;

2) electromagnetic vibrator with generator of audio-frequencies. A sinusoidally changing current in the vibrator windings excites a corresponding force in the structure. These vibrators are convenient to use in the electrical registration of structural movements;

3) spring-eccentric vibrator, in which one end of the spring is attached to the structure, and the other moves according to sinusoidal law. In this case the amplitude and phase of the perturbation depend on the relative displacement of the structure and the end of the spring, which is connected with the drive of motion.

For excitation of oscillations of models air-jet vibrators can be applied in which the structure reflects pulsating air flows directed towards its opposite surfaces.

During installation of a vibrator on a structure it is necessary that its mass not be too great as compared to the mass of the structure. If the additional mass composes several percent of the local mass of the structure, its influence may be disregarded.

For determination of oscillation forms of a structure during frequency tests it is necessary to measure the amplitude of oscillations in a large quantity of sections during sustained excitation at resonance frequency. The measurement of amplitudes employs optical or electrical transducers. An optical transducer (vibroscope) is made in the form of a mirror whose angle of rotation is proportional to displacement of the structure. A beam of light, reflected from the fluctuating mirror on a screen, given an image of the amplitude of oscillations with a large increase. This method gives a graphic image of the distribution of amplitudes in the structure.

During the use of electrical transducers observation is conducted on an oscillograph screen and recorded on photographic film. Application of electrical transducers permits the complete automation of registration of the results of frequency tests up to construction of forms.

Sometimes stroboscopic illuminating devices are applied for detailed study of oscillation form.

With the appropriate vibrator parameters one can determine any quantity of frequencies and forms of natural oscillations of a structure. In practice we usually are limited to the determination of several first tones of natural oscillations of the structure or its separate parts.

During frequency tests it is necessary to simulate the conditions of free flight. This requires suspension of the aircraft or another flight vehicle on soft springs (rubber shock absorbers), which are mounted on the vehicle in sites of large loads. The natural frequency of the craft on the suspension should be considerably lower than the lowest natural frequency of elastic oscillations of the structure. During the analysis of results of frequency tests the influence of the suspension and vibrators on the natural modes of vibration of the structure are thoroughly analyzed.

Tests of Elastic Models

For checking theoretical calculations and developing new calculation methods in the area of aeroelasticity we find the wide application of tests of flight vehicle models. Models are prepared in different forms depending upon the type of tests. At present, models are used for investigations of flutter, reversal, the influence of gusts of bumpy air, loading during landing, and so forth.

Models for investigations of flutter started to be applied in the 1930's. Models began to be used later for other problems of aeroelasticity.

The main object of simulation is to obtain a similarity of the investigated phenomenon in flight to one reproduced in the laboratory. In this instance the selection of appropriate simulation scales and constructive fulfillment of the model is very important.

The basis of selection of simulation scales is the reduction of equations, which determine the given phenomenon, to dimensionless form. Typical dimensionless parameters in aerodynamics are elongation, Mach number, Reynolds number, given frequency, and so forth.

In the reduction of an equation, which describes a physical phenomenon, to dimensionless form, it is always possible to decrease the number of independent dimensionless variables as compared to the number of measured parameters.

Introduction of dimensionless parameters into simulation has a number of advantages. First, the problem is conveniently formulated with a minimum amount of variables (parameters) and, secondly, the dimensionless equation does not depend on the scale effect. The magnitudes of dimensionless parameters have to be identical for a full-scale design and its model. This is formulated in the Π-theorem, which establishes that if a physical phenomenon can be described by means of the equation

$$\phi(S_1, S_2, \ldots, S_n) = 0 \tag{10.33}$$

(where n arguments include all basic magnitudes, derivatives, and measured constants, which must be considered in the problem), then equation (10.33) can be written in the form

$$\phi(\Pi_1, \Pi_2, \Pi_3, \ldots, \Pi_{n-m}) = 0, \tag{10.34}$$

where $\Pi_1, \Pi_2, \Pi_3, \ldots, \Pi_{n-m}$ represents (n-m) independent combinations of arguments $S_1, S_2, \ldots, S_n$. These combinations are dimensionless values with respect to m basic magnitudes. The form of these dimensionless values with respect to m basic magnitudes. The form of these dimensionless values of Π can be determined, by expressing S through measures $P_1, P_2, \ldots, P_m$ of a corresponding series of basic magnitudes:

$$S = CP_1^{k_1}P_2^{k_2}\ldots P_m^{k_m}, \tag{10.35}$$

where C is a dimensionless number.

Indices k_i are called the dimension of the derivative with respect to basic P_i. For instance, through the basic magnitudes - mass M, length L, and time T - force F will be expressed in the form

$$P = CMLT^{-2}.$$

The form of Π can also be determined with the help of direct investigations and general considerations.

As an example we shall consider the problem of investigations with the help of a model of natural forms and frequencies of a wing.

Oscillations of the wing structure are described by the equation

$$[EJ(z)f''(z)]'' - p^2 m(z) f(z) = 0. \qquad (10.36)$$

Part of the parameters may be expressed in standardized forms

$$f(z) = f_{\text{конц}}\varphi(z);$$
$$J(z) = J_{\text{корн}} J_N(z);$$
$$m(z) = m_{\text{корн}} m_N(z),$$

where m_r and J_r are correspondingly the measured magnitude of current mass and moment of inertia in the root section;

$m_N(z)$ and $J_N(z)$ are standardized magnitudes which have values in the root section that are equal to unity;

f_t is the sag on the wingtip;

$\varphi(z)$ is the standardized form of oscillations.

Then equation (10.36) will take on the form

$$[EJ_{\text{корн}} J_N(z)\varphi''(z)]'' - p^2 m_{\text{корн}} m_N(z)\varphi(z) = 0. \qquad (10.37)$$

The dimensions of parameters z, E, J_r, p, and m are combinations of three basic magnitudes, i.e., mass M, length L, and time T:

$$z \sim L;$$
$$E \sim ML^{-1}T^{-2};\quad J_{\text{корн}} \sim L^4;$$
$$p \sim T^{-1};\quad m_{\text{корн}} \sim ML^{-1}.$$

Parameters $J_N(z)$, $m_N(z)$, and $\varphi(z)$ are dimensionless.

The measured parameters can be combined in order to obtain a series of dimensionless values of the form

$$\frac{z}{l},\ \frac{J_{\text{сопр}}}{l^4},\ \frac{p^2 m_{\text{сопр}}}{E}\quad (l - \text{semi-span of wing})$$

In virtue of the Π-theorem the number of dimensionless parameters are three units less than those measured, since in our case the dimensionless parameters are combinations of the three basic magnitudes.

Then the dimensionless form of the motion equation (10.37) takes on the form

$$\left[J_N\left(\frac{z}{l}\right)\varphi'\left(\frac{z}{l}\right)\right]'' - \left[\frac{l^4 p^2 m_{\text{сопр}}}{EJ_{\text{сопр}}}\right] m_N\left(\frac{z}{l}\right)\varphi\left(\frac{z}{l}\right) = 0, \tag{10.38}$$

where the primes signify the derivative with respect to $\frac{z}{l}$.

In this case the independent parameters are referred to the linear dimension L, time T, and elastic modulus E. During the construction of a model the linear scale k_L is determined by the dimensions of the wind tunnel and by structural considerations:

$$k_L = \frac{L_M}{L_a}.$$

where L_M is the size of the model;
where L_{act} is the actual size.

Usually k_L = 1/5 to 1/20.

The time scale $k_T = T_M/T_{act}$ is determined by the capabilities of the measuring equipment.

The scale of elasticity of the material is determined from the relationship

$$k_E = \frac{E_м}{E_н} = \frac{(ML^{-1}T^{-2})_м}{(ML^{-1}T^{-2})_н}. \quad (10.39)$$

These three scale factors determine all necessary parameters of the model. For instance, after solving relationship (10.39) with respect to masses, we obtain the coefficient of the scale of masses

$$k_m = \frac{m_м}{m_н} = \frac{E_м L_м T_м^2}{E_н L_н T_н} = k_E k_L k_T^2.$$

One can analogously determine the scales for the other parameters of the model.

The location of the axis of rigidity, the line of centers of gravity of sections, and centers of gravity of all concentrated loads of the model should be similar to their location in an actual wing.

The manufacture of a flutter model should ensure actual similarity with respect to distribution of rigidity of the structure, distribution of mass, and with respect to external form in the air flow. If one prepares a model, which is an exact copy of an actual design with all similar supporting members (spars, stringers, ribs, skin, etc.), there will be obtained very small skin thicknesses (less than 0.2 mm). In this case there appears a number of difficulties of a structural character in making the connections of the skin, wing ribs, stringers, and so forth. Therefore, wide propagation has been obtained by models (in the form of beams of rectangular cross section) which satisfy the necessary rigidity requirements.

Since the outer skin can considerably increase rigidity of the model, the external skin is made in the form of sections (Fig. 10.21). The main part of the model is sufficiently light, in order to obtain a corresponding mass reserve for all sections of the model. For changing (more precise definition) the mass of the model additional loads are applied in separate sections.

Fig. 10.21. Form of a flutter model with sections.

The flutter model is tested in a wind tunnel. During the wind test of the model the flow rate is increased gradually until the appearance of signs of flutter. During strong oscillations of the model the flow rate is immediately lowered, in order to prevent breakage of the model. When oscillations of the model terminate, the flow rate is again brought up to critical, in order to definitize its magnitude. The speed of flutter of the model V_{fm}, obtained in an experiment, is recomputed for a full-scale (actual) design in accordance with the scale of speeds:

$$V_{ф.н} = \frac{1}{k_v} V_{ф.м}$$

In case of necessity, additional corrections for compressibility are introduced.

Wind tests of dynamically similar models make it possible to definitize flutter calculations and to develop measures for increasing critical flutter speed.

Besides the method of simulation according to the beam system, the investigation of flutter employs structural simulation with the application of plastics which have a small elastic modulus.

During investigations of flutter there usually are applied the following types of models:

1) structurally-similar models;

2) conditionally-structural (dynamically similar) models;

3) control systems with amplifiers and automatic pilot controls;

4) flying models with accelerators;

5) electronic and electronic-mechanical models.

Different methods of simulating flutter have advantages and disadvantages and not one of them can be given explicit preference. It all depends on the complexity of the phenomenon, the urgency of its solution, and the required accuracy of results.

In recent years methods of electronic and electronic-mechanical simulation began to be widely applied not only for the investigation of flutter, but also for the investigation of certain dynamic processes during loading of flight vehicles. The methods of electronic simulation, when mechanical oscillations of a structure are simulated by an appropriate electrical circuit, make it possible to investigate a large variety of forms of dynamic processes. However, this method is limited with respect to the number of investigated oscillation modes, since the majority of electronic models usually do not permit more than 10-20 first order equations to be investigated.

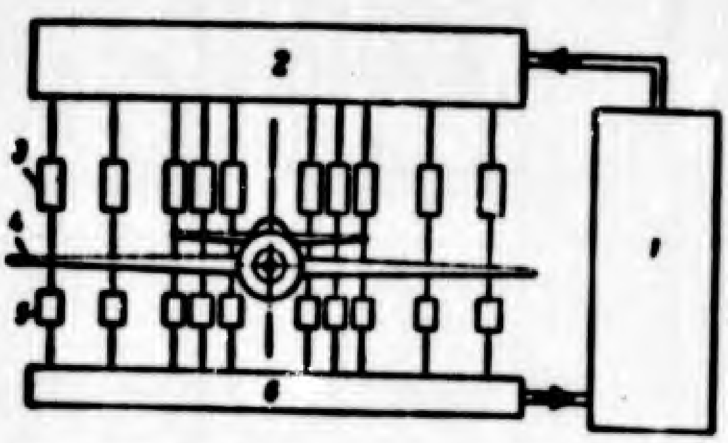

Fig. 10.22. Diagram of electronic-mechanical simulation.

Electronic-mechanical models combine a dynamically similar structural model with an electronic model (Fig. 10.22). All external forces are simulated on the electronic model, which consists of a computer block 1, that sends out pulses which are proportional to the aerodynamic forces corresponding to deformations of the model, and an excitation pulse generator 2. These forces are transmitted with the help of special power-exciters 3 to a dynamically similar model of a flight vehicle 4. Feedback is carried out with the help of bias pickups 5 which are located along the length of the structure, and a corresponding switching device 6 which transmits signals from the pickups to the computer block 1. This form of simulation makes it possible to investigate dynamic phenomena, taking into account more than 50 oscillation modes of an aircraft.

Models for investigating static aeroelasticity phenomena (divergence, reversal, and others). These investigations study the elastic deformations caused by air loads, and their influence on the redistribution of air loads. The model for such investigations should reproduce the aerodynamic shape of the aircraft, the rigidity distribution, and the relationship between aerodynamic forces and elastic characteristics of the structure. Mass distribution usually is not reproduced, but flutter should be excluded within the limits of the investigated speeds.

Let us consider the criteria of similarity in an example of a model for investigating aileron reversal. As was shown above, the torsion angle of an elastic wing on a spring in an air flow, having speed V, is determined from equation (2.27), which upon transition from a unit section to wing area S has the form

$$\theta=\frac{\frac{1}{k_\theta}\left[c_y^\alpha e\alpha+c_m^\delta\right]qbS}{1-\frac{1}{k_\theta}c_y^\alpha eqbS}. \qquad (10.40)$$

Inasmuch as the considered problem is a static one, it is possible to take force F and length L as the basic parameters. The measured magnitudes, entering expression (10.40), will be $k_\theta \sim FL$, $b \sim L$, $q \sim FL^{-2}$, $S \sim L^2$, α, c_y^α, θ, e, c_m^δ, i.e., dimensionless coefficients.

From the parameters in equation (10.40) it is possible to form the following independent dimensionless values:

$$\frac{qSb}{k_\theta},\ \frac{\nu}{b},\ \theta,\ \alpha,\ c_y^{\alpha},\ c_m^{0},\ c_y^{0},\ e.$$

In this case, according to the Π-theorem, the number of dimensionless relations is two units less than the number of measured parameters.

In dimensionless parameters relationship (10.40) will be

$$\theta=\frac{\left(c_y^{\alpha}\alpha+c_m^{0}\right)\frac{qSb}{k_\theta}}{1-c_y^{\alpha}e\left(\frac{qSb}{k_\theta}\right)}. \qquad (10.41)$$

From this relationship it is clear that a model and an actual object must have the same wing profile, identical dimensionless distance e of the elastic line from the line of the center of gravity of wing sections, identical initial angle of attack α, and equal relation of aerodynamic forces to elastic forces qSb/k_θ.

Two independent scale parameters b and q are determined by the parameters of the wind tunnel and the type of model.

The scale of forces is determined by linear scale and by the relation of dynamic pressure in real conditions to dynamic pressure, which can be obtained during model tests.

Relationships can be obtained analogously for similarity of modeling during the investigation of static problems for an elastic wing with variable torsional and flexural rigidity. During wind tests of a model the Re number should be as high as possible, and Mach number should be equal to the actual Mach number.

During the investigation of aeroelasticity special requirements are presented for bracing of the models as compared to the usual wind tests of rigid models in a wind tunnel, since it should not introduce additional errors due to the influence of deformation.

Models for the investigation of landing can be similar only in their rigidity and mass characteristics. During tests such a model is placed in the position of free flight with lowered landing gear, on which there act perturbing forces which are similar to real forces during landing. Sometimes it is expedient to investigate the influence of vertical and frontal loads separately.

Forces in structural elements of the model are measured with the help of wire strain gauges with recording on an oscillograph. They simultaneously record overloads in different points of the structure with the help of seismic transducers.

For investigations of dynamic loads during landing it is possible to use the models that were applied for the investigation of flutter and additionally equipped with landing gear struts. The influence of a gust of bumpy air on the structure can also be investigated on flutter models. Tests are conducted in a wind tunnel, where turbulent perturbations are simulated. These tests determine the field of overloads and the forces in the control sections of the model.

On the basis the results of model tests it is possible to definitize the magnitude of the correction factor that is utilized during conversion of the measured overload to the speed of the gust of bumpy air. In a wide variation range of frequencies of perturbations it is possible to determine the function of mechanical conductivity $H(i\omega)$.

Test of Structures at Raised Temperatures

In carrying out actual tests of airplane designs in conditions of high temperatures testing-units are necessary, in which the processes of heating and loading are mutually connected. These installations must ensure the fulfillment of a number of conditions in carrying out the tests:

1) heating of the structure, which is applied for simulating aerodynamic heating, should be used in combination with loading by air and inertial forces;

2) the heating element should be deformed together with the structure;

3) the systems of loading and heating should ensure the simulation of boundary conditions;

4) the heating system should allow for the change of density of thermal energy both as a function of space, and also as a function of time;

5) heating elements should not render an influence on the strength of the structure and should not cause a considerable change of inertial forces during dynamic tests.

The reproduction of aerodynamic heating during tests of aircraft structures employs different methods, as for instance:

a) heating by electrical heaters;

b) heating at the expense of heat radiation from a heated body;

c) heating of the structure during testing in a wind tunnel;

d) heating by hot gases;

e) the induction method of heating, and so forth.

Heating of a structure by electrical heaters (contact methods). Contact methods of heating propose a tight contact between the heated surface and the heating element. Heating elements are made in the form of blankets, tape elements, and various coatings which conduct an electrical current well.

A heating blanket consists of an electric lead which is placed in a flexible matrix made from insulating material.

The structure is usually loaded with the help of cables which pass through the heating elements and are fastened directly to the skin of the flight vehicle or to the internal elements of its structure. A thorough check is made of the electric insulation of the heated structure and the load-carrying parts of the loading system.

Density of energy that is obtained with the use of heating blankets, which are glued to the structure usually with silicon glue, makes it possible to create a heat flow of about 10,000 kcal/$\underline{m}^2$·hr with an efficienty of η = 0.9 that corresponds to a heating temperature of ~ 250°C.

Heating blankets are applied in tests of structures under conditions of steady-state and transient temperatures with limited capacities of heat flow.

The deficiencies of heating blankets include the drop of thermal conduction during heating, the possibility of electrical interlocking in places of application of loads, the complexity of replacement or repair of structural elements, and also the complexity of monitoring the state of the surface.

The tape heating element is analogous in its principle of operation to the heating blanket; however, it will not form a monolithic structure. Such a heating element consists of tape with aluminum foil on it. The foil has one surface insulated with an anode film made from aluminum oxide. The insulated surface of the aluminum foil comes into contact with the heating tape when its second, uninsulated surface, touches the heated surface. The external surface of tape heating elements is insulated by several layers of fabric made from fiberglass. With the help of such heating elements it is possible to create a heat flow with a density of approximately 300,000 kcal/m^2·hr, and the temperature of the structure can be raised to 300-350°C with an efficienty of $\eta = 0.9$.

Besides contact heating devices, so-called film heating elements are employed. Such elements are usually glued to the structure. The surface on which they are placed is preliminarily covered by a layer of electric insulating material.

Heating at the expense of heat radiation from a heated body (methods of radiant heating). The sources of radiant energy employed are Nichrome heating elements, infrared lamps, graphite rods, and so forth.

Nichrome spirals are usually placed in the focus of parabolic reflectors. With the close location of spiral coils there can be obtained a density of heat flow up to 200,000 - 300,000 kcal/m^2·hr with $\eta = 0.5$.

The deficiencies of Nichrome heating elements include their large thermal inertia and the limitation of maximum temperature.

Nichrome heating elements are expediently used when it is required to obtain low rates of heating and when stationary heating is being investigated.

The investigation of strength of structures in conditions of non-stationary heating at high temperatures utilizes infrared lamps. Reflectors for infrared lamps are prepared from plated aluminum alloy. The necessary distribution of heat flow through the structure is attained by separation of all lamps into sections, each of which creates a specific heat flow.

For simulation of transient heating conditions it is possible to apply graphite rods as heating elements. This type of heating element makes it possible to create extraordinarily large densities of thermal energy of order of 1,000,000 kcal m^2·hr.

In the radiant method of heating a structure it is usually difficult to create an external load, since the elements, through which loads are transmitted to the test structure, must occupy a minimum surface area in order to lower the effect of shielding the structure from infrared lamps. In this case loading is also most conveniently carried out with the help of a system of cables which are fastened directly to the investigated structure. A lever system and hydraulic power-exciters are placed outside the heated area.

Heating by hot gases. Heating of a structure by hot gases is usually carried out in special furnaces, or thermochambers. Although in a thermochamber it is impossible to obtain a high rate of heating, owing to the dimensions and the hot gaseous environment such a chamber is convenient for testing different actual constructions during stationary heat flow.

Besides the enumerated methods, in the investigation of strength in conditions of raised temperatures, the induction method can be applied for heating a structure. In this method, with the help of a magnetic field, vortex currents are induced in the material. By the selection of the frequency of alternating current there can be obtained different heating of the surface of the structure, which ensures simulation of the effect of aerodynamic heating. This method of heating can obtain a temperature of the structure of about 600°C.

Heating elements in the form of flat induction coils are braced to the heated surface with the help of vacuum cover plates made from silicon rubber. Loading of the structure is accomplished by methods that are analogous to the above-indicated ones.

During thermal tests automatic heating control is carried out. This makes it possible to preserve the boundary conditions, depending on time, to regulate the thermal load, and to synchronize it with loading of the structure by external power loads. In automatic control the coefficient of heat radiation from the boundary layer and the determining temperature (temperature of adiabatic wall) are programmed.

10.3. Structural-Performance Tests

Above we considered the main forms of laboratory tests. However, the fulfillment of a complex of laboratory tests for checking the strength of contemporary flight vehicle structures is only the first preliminary stage of evaluating strength, since the standardized loads, which are adopted during strength analysis, can essentially differ from the actual loads during the operation of an aircraft. Furthermore, laboratory tests do not completely consider the redistribution of aerodynamic loads due to structural deformations. Upon replacement of dynamic loads by static ones the conditions of work of the supporting members of the structure are changed. In conditions of static tests it is impossible to create full similarity of distribution of loads.

It is considered that laboratory tests are the basic preliminary stage of checking strength before the beginning of flying tests. However, only on the basis of a special complex of flying tests and comparative analysis of the results of laboratory and flying tests can there be given a final evaluation of the strength of a contemporary flight vehicle. Based on the actual state of strength of a flight vehicle, flying and operational limitations are definitized, in particular the terminal velocity of flight, maximum permis· ble overloads, flight and landing weight, the variant of loading, the type of airport, (degree of permissible roughness) and so forth. The complex of operations for checking the strength of a flight vehicle in flight is commonly called structural-performance testing.

It is necessary to consider that a crew cannot, on the basis of their sensations, judge the sufficienty of structural strength. A crew can note only intense oscillations of the structure or the beginning of failure of structural elements. In connection with this, the strength evaluation of a flight vehicle during flying tests requires the complex measurement of a large quantity of parameters. In most cases, on the basis of the materials of measurements, it is required to estimate the highest possible loads under the most unfavorable conditions of operation i.e., to extrapolate the results of the measurements carried out. Furthermore, during structural-performance tests it is necessary to execute flights in limiting conditions, which presents special requirements for ensuring the safety of these flights. Due to this, the strength check of a flight vehicle is very time-consuming and more complicated as compared to the evaluation of other characteristics during flying tests.

The volume of structural performance tests was very limited for a long time due to the absence of the necessary equipment. After the development of remote-control vibration-measuring equipment, wire strain gauges, oscillographs, and corresponding electronic equipment, structural-performance tests began to develope quickly. At present they are widely used for investigating the strength of aircraft structures, for improving their quality, for increasing reliability, for lowering the weight of the structure, and for improving the performance data of a flight vehicle.

During structural-performance tests, as was noted, flights are conducted in limiting-permissible conditions. In these flights, and also in flights that are not connected with the achievement of limiting conditions, measurements are conducted. The main ones are:

a) determination of loads acting upon structural assemblies under the main conditions of operation;

b) determination of parameters of structural oscillations (vibrations);

c) determination of general structural deformations in flight;

d) measurement of stresses in separate supporting members of the structure;

e) measurement of temperatures of structural elements (for flight vehicles in which heating of the structure to more than 100-150°C is possible).

Furthermore, during mass operation of flight vehicles, statistical measurements of overloads are conducted. The order of carrying out and the content of structural-performance tests depends on the problem on hand.

Tests in Limiting Flight Conditions

The character and magnitude of a load are determined by the conditions of flight and deformations of the flight vehicle structure. Recalculation of measured loads in other flight conditions is connected with difficulties and in certain cases does not give reliable data. Therefore the strength evaluation of a flight vehicle structure requires that all conditions, which are decided upon for operation, be checked during flying tests with corresponding reserves. During structural-performance tests all conditions are attained that are accompanied by the appearance of the biggest loads on the flight vehicle on the whole or its separate assemblies. These conditions are commonly called limiting.

Usually limiting conditions are considered to be such conditions in which there is attained the biggest value of overload, dynamic head, Mach number, speed of flight with lowered landing gear and wing mechanization, speed of flight with various open hatch doors, angles of side-slip, angular velocities around axes x and y, and deviations of controls (vanes and ailerons). Limiting conditions also include takeoff, flight, and landing with corresponding maximum weight of the flight vehicle.

In the process of flying tests conditions are also attained which correspond to the possible combinations of limiting values of the enumerated parameters. Upon the achievement of limiting conditions the appropriate flight parameters and performance conditions (loads, stresses, oscillations, temperature, general deformation, and so forth) are measured.

Before the beginning of structural-performance tests an analysis is conducted on the strength calculations and results of laboratory tests. A thorough study is made of structural units which have new materials; new design forms, and also those places of the structure, where permanent deformations were observed during laboratory tests. There is an analysis of the behavior of the main supporting members of the structure before destruction (based on the results of static tests). On the basis of this information one can determine which structure elements should be given special attention during the pre-flight and postflight inspections of the flight vehicle.

Before beginning the tests in limiting conditions, an external inspection is made of the state of the wing, empennage, landing gear, motor mounts, etc.

In the composition of a test program main attention is given to the safety of achieving limiting conditions. In the assignment of conditions for structural-performance tests we originate from the fact that in flight there are reproduced limiting conditions which are possible during operation, and also all cases that are accompanied by the biggest load (by calculation) of the flight vehicle on the whole or its separate assemblies. A gradual approach to limiting conditions of flight should be ensured.

The pilot should be ensured with the possibility of objective control of the conditions to be executed by visual instruments. It is expedient to use light or sound signalling in the approach to limiting conditions, which are difficult to control by the crew. Visual instruments for control of limiting conditions must be thoroughly checked in preliminary flight. After every flight there is an obligatory thorough inspection of the structure.

Determination of General Structural Deformations in Flight

Measurement of general structural deformations makes it possible to judge the magnitude of general external load on a given assembly under the accepted law of load distribution on its surface. However, it is difficult to have an opinion on the correctness of the selected law of load distribution on the surface of an assembly. The determination of general deformations has large value for estimating their influence on the stability and controllability of a flight vehicle, and the work of different equipment.

The measurement of general deformations utilized optical methods with the use of special cameras having continuous film feed (optographs) or movie cameras. In the first method the assemblies in the control points are equipped with special mirrors. Registration of deformations is conducted with the help of an optograph with several objectives. Each objective fixes the motion of an investigated point of the structure where there is a mirror (Fig. 10.23). From the light source 1 a beam proceeds to the mirror 2, from which it is reflected, and with the help of prism 3 it proceeds to lens 4. On photographic film 5 there is obtained an image A of a luminescent point which is called the standard point. During deformation of a structure the image of the point moves along the width of the film. During continuous motion of the film there is obtained a recording 6 of deformation of the structure in time.

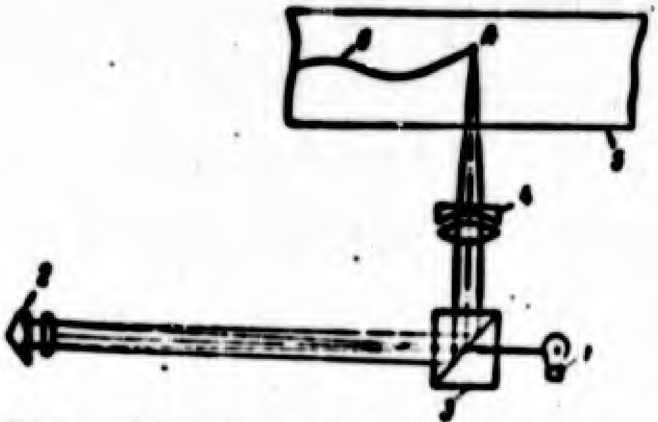

Fig. 10.23. Diagram of measurement of general deformations by the optical method.

With the use of a movie camera it is possible to place any markings (little pins, noticeable bands, and so forth) on the structure. By photographing the structure in flight, we obtain data on its deformations. The deficiency of this method is the complicated and time-consuming deciphering of photographs. Photographs can be taken by a modified movie camera with continuous film motion.

The registration of deformations can also employ the cinetheodolite method. With this method it is convenient to record local deformations.

Determination of Load Magnitudes by the Method of Load Measurement

Measurement of overloads gives an important loading characteristic of a flight vehicle, since the product of overload and weight characterizes the inertial load of an aircraft. For flight vehicles, when elastic deformations are small, the overload in the center of gravity characterizes the total magnitude of the external aerodynamic load. In this case for overload-registration they use ordinary overload recorders which are placed in the center of gravity.

In evaluating dynamic loads, when oscillations of the structure play an essential role, it is necessary to measure the distribution of overloads around the structure, i.e., determine the field of overloads. For this purpose transducers of oscillations of the accelerometeric type are usually applied.

The magnitudes of overloads, measured in different points, are referred to the overload in the center of gravity:

$$\Delta\bar{n}_i = \frac{\Delta n_i}{\Delta n_{c.g}}, \qquad (10.42)$$

where $\Delta\bar{n}_i$ is the relative increase of overload in the i-th point;

Δn^i is the measured increase of overload in the i-th point;

Δn_{cg} is the corresponding increase of overload in the center of gravity.

According to measurements, graphs of the distribution of overloads along the fuselage, wing, and so forth are constructed (see Fig. 4.28).

To determine loads the structure is divided into sections. The product of the weight of a section G_i and the magnitude of overload n_i gives the magnitude of inertial load p_i on the given section:

$$P_i = n_i G_i. \qquad (10.43)$$

The magnitude of overload and the position of the center of gravity of a section have to be definitized taking into account the irregularity of distribution of the magnitude of overload along the length of the section. Transducers for measuring overloads on aircraft are usually placed in the center of gravity, on the end and in the center parts of the wing, in the fuselage (in the center of gravity, in two points of the nose section and the two points of the tail section), on the end sections of the stabilizer and fin, and on the motor.

Figure 10.24 gives an approximate diagram of the distribution of accelerometers. Depending upon the peculiarities of arrangement of the flight vehicle, the diagram of distribution of transducers is changed. In a more precise definition of the diagram, it should anticipate the installation of transducers in places of distribution of large loads on the wing and fuselage.

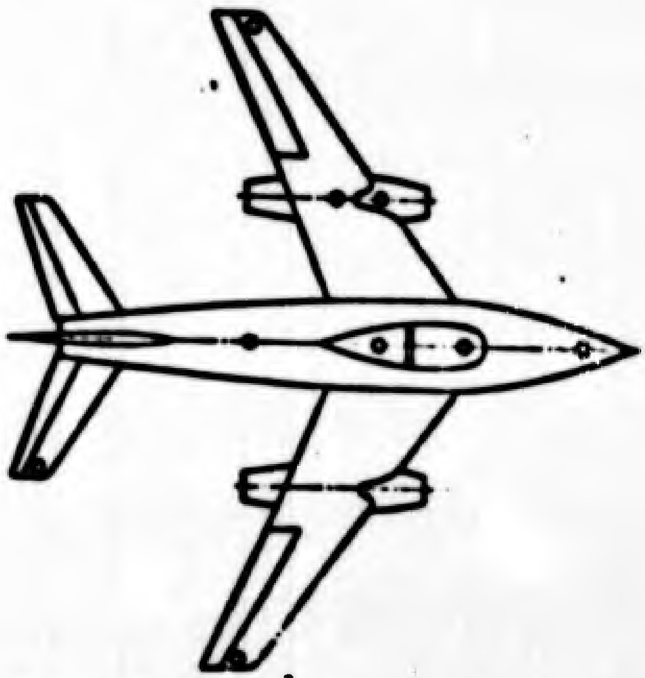

Fig. 10.24. Diagram of arrangement of overload transducers. 0 – overload transducers.

During the analysis of measurements one should consider that the recording of overloads, measured on the structure in the region of the center of gravity, can have impositions from elastic oscillations of the structure. In this case we introduce corresponding corrections for the magnitude of measured overload.

Investigation of Pressure Distribution Along the Surface of a Flight Vehicle

The study of distribution of air loads along the surface of an assembly utilizes the method of pressure measurement in different points. This method began to be applied in the 1930's with the carrying out of detailed investigations of loads acting on an aircraft. The surface of the investigated assembly is drained, i.e., to every point there is attached an individual pipe of small diameter (1.0 – – 2.5 mm). On the surface of the assembly the pipe terminates in a receiving hole. The other end of the pipe is joined to a multiple pressure recorder. Such a recorder makes it possible to record pressure in 10-20 points of the surface. Usually the recorder also receives static pressure p_{st} and then excess pressure $p_i - p_{st}$ is recorded (p_i is the pressure in the i-th point of the structure's surface). During the analysis of the results of measurements the magnitudes themselves of excess pressure are not used, but the so-called pressure coefficient

$$\bar{p} = \frac{p_i - p_{st}}{q}. \tag{10.44}$$

Distribution of pressure along the surface is usually depicted in the form of diagrams (Fig. 10.25). By summarizing the forces of aerodynamic pressure along the surface of an assembly, one can determine the necessary aerodynamic loads (lift, moment, and so forth).

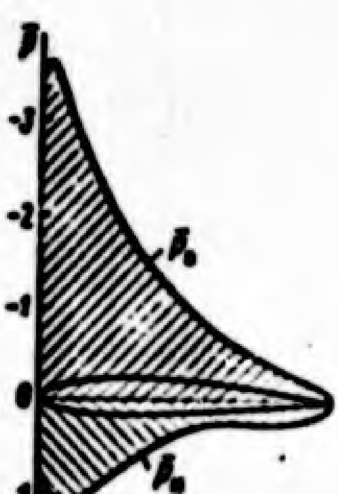

Fig. 10.25. Diagram of pressure distribution along a wing profile. $\bar{p}$ is the pressure coefficient, $\bar{p}_{up}$ and $\bar{p}_{low}$ correspondingly are the pressure coefficients on the upper and lower surfaces of the wing.

A long length of pipes from the surface of an assembly to the recording instrument leads to considerable delays during investigations of transient conditions. Therefore such investigations began to employ electrical transducers, i.e., pressure converters (tensometric or capacitance), which are practically inertialess and make it possible to investigate pressure in transient conditions (during oscillations, stalls, and so forth). These transducers may be used for the time of investigations, for instance instead of rivets. In this case the measurements are usually recorded with the help of tensometric equipment. Methods of investigation of pressure distribution are more specifically described in experimental aerodynamics courses.

Determination of Loads by the Electrotensometric Method

On any assembly of a flight vehicle there act simultaneously several components of loads. Thus, on a landing gear strut during landing there is a frontal load p_x, a vertical load p_y, a lateral load p_z, and torque M_{tor}. During test flights it is necessary to determine the magnitude of the basic components of loads and their dependence on operating conditions. Considering that frequently a flight vehicle can only hold a limited quantity of equipment, it is expedient to perform the measurements in such a way that for determining one load component one channel of the measuring equipment is used.

In general a structural assembly experiences six basic components: P_x, P_y, P_z, M_x, M_y, and M_z (three components of force and three components of moment correspondingly along axes x, y, and z). Let us designate these components Q_1, Q_2, ..., Q_6, respectively.

In order to analyze the state of strain of the structure, it is necessary to make certain assumptions.

Hypothesis of stationarity. During repeated structural loads the dependence of deformations on loads is kept constant and linear and it does not depend on the sign and character of change of the load in time. In the case of a dynamic load, the effective load (with respect to force in a given section) and the dynamic coefficient are determined.

Principle of independence of deformation. Deformation of any structural element during the combined action of all loads is equal to the sum of deformations which appear during the separate action of these loads.

Within the limits of operational loads (during elastic deformations of the structure) these hypotheses are valid and are confirmed by measurements of stresses during static tests.

In virtue of the first hypothesis, for a strain gauge which is glued to the surface of an assembly, we have the dependence

$$\varepsilon_{ik} = a_{ik} Q_k \quad (k = 1, 2, \ldots, 6), \tag{10.45}$$

where ε_{ik} is deformation of the i-th strain gauge during the action of load Q_k;

a_{ik} is a constant coefficient which is determined by calibration of the strain gauge that is glued to the given structures.

During the simultaneous action of all load components, in virtue of the second dypothesis it is possible to write

$$\varepsilon_i = a_{i1} Q_1 + a_{i2} Q_2 + \ldots + a_{i6} Q_6. \tag{10.46}$$

We then consider that the assembly experiences all six load components which to not depend on each other. In case of their interconnection the number of investigated components correspondingly decreases.

In view of the independence of the action of load components in a given section of an assembly it is possible to glue correspondingly six strain gauges in such a way that their deformations will be linearly independent. In this case, for deformations of strain gauges we obtain the system of equations

$$\left.\begin{aligned} \varepsilon_1 &= a_{11} Q_1 + a_{12} Q_2 + \ldots + a_{16} Q_6; \\ \varepsilon_2 &= a_{21} Q_1 + a_{22} Q_2 + \ldots + a_{26} Q_6; \\ &\ldots\ldots\ldots\ldots\ldots\ldots \\ \varepsilon_6 &= a_{61} Q_1 + a_{62} Q_2 + \ldots + a_{66} Q_6. \end{aligned}\right| \tag{10.47}$$

In virtue of the linear independence of the equations the determinant of system (10.47) $\Delta \neq 0$, and the system will have only one solution. Consequently, any load component may be expressed through deformations of strain gauges:

$$Q_k = \frac{1}{\Delta}(A_{1k}\varepsilon_1 + A_{2k}\varepsilon_2 + \dots + A_{nk}\varepsilon_n). \tag{10.48}$$

where A_{1k} is the cofactor of a_{1k}($\alpha_{1k} = A_{1k}/A_{1k}$);

Let us assume that A_{1k} is the lowest of coefficients A_{1k} (if another coefficient is the highest, then it is possible to change the order of designation in the appropriate way). Then dependence (10.48) can be presented in the form of

$$Q_k = \frac{A_{1k}}{\Delta}(\varepsilon_1 + \alpha_{2k}\varepsilon_2 + \dots + \alpha_{nk}\varepsilon_n). \tag{10.49}$$

Introducing the designation $A_{1k}/\Delta = B_k$, we obtain

$$Q_k = B_k \sum_{i=1}^{n} \alpha_{ik}\varepsilon_i. \tag{10.50}$$

Condition $|\alpha_{1k}| < 1$ is then fulfilled. Here magnitude B_k is constant for the given diagram of attachment of strain gauges to the structure and is determined by calibration.

From expression (10.50) it is clear that the determination of one load component requires the measurement of deformation of several strain gauges and then the corresponding calculations for every moment of time. Therefore the method of load measurement by means of separate registration of deformations of strain gauges is very time-consuming and can be used only for the measurement of static loads. By using the summation of electrical signals, it is possible to connect the strain gauges in such a way that on the recorder there will be signal which is directly proportional to the load, i.e., the sum

$$S=\sum_{i=1}^{6} a_{ik}\varepsilon_i \qquad (10.51)$$

For this we change the sensitivity of the strain gauges by means of series or parallel connection of additional ohmic resistances to them in such a way that, by connecting the strain gauges in a group, we obtain, at the output, a signal which is proportional to the sum of (10.51).

For a number of cases it is possible to simplify the working formula (10.50) and to reduce it to the form of

$$Q_k=B_k\sum_{i=1}^{6}\varepsilon_{i_k} \qquad (10.52)$$

if coefficients α_{ik} are equal to one or zero. In the last case it is possible to apply series or parallel connection of strain gauges without additional resistances. During measurement of loads on aircraft, the reduction of worker formula (10.50) to the form of (10.52) in most cases is possible owing to the fact that in an aircraft structure there exists a distribution of different forms of loads on separate structural elements. For instance, in the wing the bending moment is basically perceived by the spars, torque is experienced by the skin, and so forth.

For measurement of loads the strain gauges should be placed on those structural elements which perceive the main part of the given form of load. The accuracy of measurements may be increased by placing strain gauges in places of the biggest stresses, since with the increase of the level of stresses the relative error introduced by the measuring equipment is lowered.

Figure 10.26 gives the approximate distribution of strain gauges

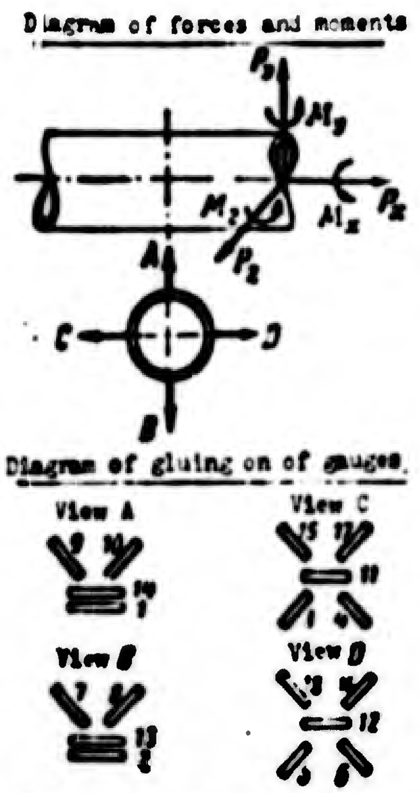

Fig. 10.26. Distribution of strain gauges on a thin-walled shell for measuring the main load components.

in case of the action of six load components on a thin-walled shell. To simultaneously measure all components, it is necessary to use 13 strain gauges, since in the connection to the measuring circuit each strain gauge can be included in only one bridge.

Figure 10.27 shows the diagram of connection of strain gauges and corresponding working formulas. In the measurement of a smaller number of components the measuring circuits can be correspondingly simplified.

In measurements with the help of wire strain gauges, as a rule, the bridge measuring circuit is used (see Fig. 10.3). The following basic dependences take place in this instance:

a) for equipment with amplifier (diagram I)

$$u_d = \frac{u}{4}\frac{\Delta R_1}{R_1}, \tag{10.53}$$

where u_d is the voltage in the measuring bridge diagonal;

u is the supply voltage (usually alternating current), brought in to the bridge;

ΔR_1 is the change in the resistance of the working strain gauge during deformation.

Considering dependence (10.1), we obtain

$$u_d = \frac{uS\varepsilon}{4}; \tag{10.54}$$

Diagram	Component	Working formula	Diagram of connection of strain gauges to bridge
I	P_x	$P_x = \dfrac{e_1 + e_2}{\dfrac{1}{a_1} + \dfrac{1}{a_2}}$	
II	P_y	$P_y = \dfrac{e_3 - e_4 + e_5 - e_6}{\dfrac{1}{a_3} + \dfrac{1}{a_4} + \dfrac{1}{a_5} + \dfrac{1}{a_6}}$	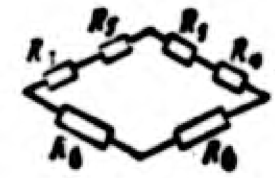
III	P_z	$P_z = \dfrac{e_7 - e_8 + e_9 - e_{10}}{\dfrac{1}{a_7} + \dfrac{1}{a_8} + \dfrac{1}{a_9} + \dfrac{1}{a_{10}}}$	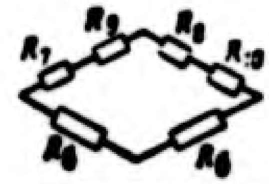
IV	M_y	$M_y = \dfrac{e_{11} - e_{12}}{\dfrac{1}{a_{11}} + \dfrac{1}{a_{12}}}$	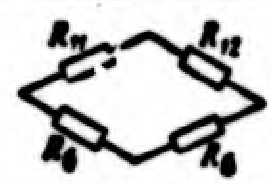
V	M_z	$M_z = \dfrac{e_{13} - e_{14}}{\dfrac{1}{a_{13}} + \dfrac{1}{a_{14}}}$	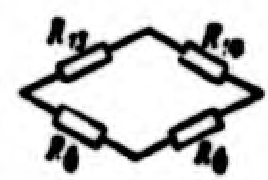
VI	M_x	$M_x = \dfrac{e_{15} + e_{16} - e_{17} + e_{18}}{\dfrac{1}{a_{15}} + \dfrac{1}{a_{16}} + \dfrac{1}{a_{17}} + \dfrac{1}{a_{18}}}$	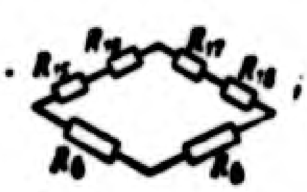

Fig. 10.27. Diagram of connection of strain gauges for measurement of basic load components. R_1, R_2, ... R_{18} - resistance of 1, 2, ..., 18 strain gauges, glued according to the diagram shown in Fig. 10.26, R_{bal} - balancing resistances, R_1^{com} and R_2^{com} - compensating strain gauges.

b) for equipment without amplifier (diagram II):

$$J_d = \frac{e}{2} \frac{\Delta R_1}{R} \frac{1}{R_1 + R_{bal} + 2R_d}. \tag{10.55}$$

where J_d is the current intensity in the measuring bridge diagonal.

If resistances of opposite arms of the bridge are equal ($R_1 = R_{bal} = R$), then

$$J_d = \frac{e}{4} \frac{\gamma\varepsilon}{R + R_d}. \tag{10.56}$$

Sensitivity of the bridge (relation of output signal to relative deformation), during work of equipment of the first type will be

$$S_0 = \frac{dU_d}{d\varepsilon} = \frac{e\gamma}{4}. \tag{10.57}$$

Figure 10.28 gives the approximate dependence of sensitivity on the resistances of the strain gauges. In a wide range of change of R the sensitivity of the bridge according to diagram I is kept constant.

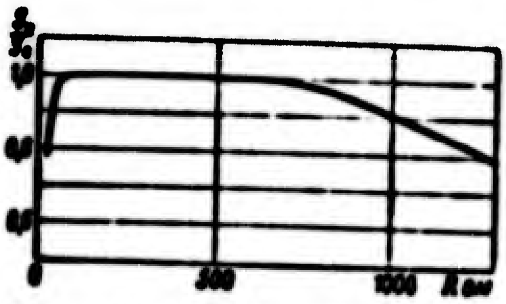

Fig. 10.28. Change of sensitivity of equipment with amplifier (diagram I) depending upon resistance of transducer R. S_0 is sensitivity at nominal resistance of transducers (120 ohms).

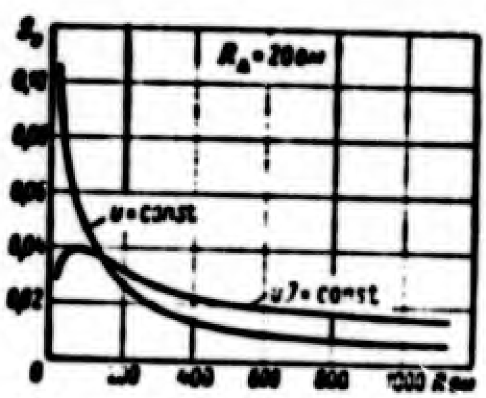

Fig. 10.29. Change of sensitivity of equipment according to diagram II, depending upon resistance of strain gauge.

Sensitivity of bridge in diagram II

$$S_I = \frac{\varepsilon}{4}\frac{\gamma}{R+R_d} \tag{10.58}$$

to a considerable extent is determined by the magnitudes of resistances R (Fig. 10.29) and R_d. For increasing the sensitivity of this circuit, low-resistance strain gauges are employed with high permissible current intensity. The most expedient in this case is the use of flat strain gauges made from foil.

Connection of Several Strain Gauges to One Bridge Arm

By combining the series and parallel methods of connecting strain gauges, it is possible during the measurements to separate specific components of total load and to affect the sensitivity of the measuring bridge.

Parallel connection (Fig. 10.30). The working arm has transducers with resistances R_1, R_2, ..., R_n. During deformation the resistance of every transducer is changed correspondingly by magnitude ΔR_1, ΔR_2, ..., ΔR_n.

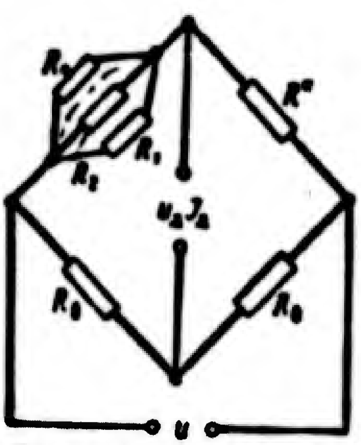

Fig. 10.30. Parallel connection of strain gauges.

Total resistance of arm is

$$R_\Sigma = \frac{1}{\sum\limits_{i=1}^{n}\frac{1}{R_i}}. \tag{10.59}$$

Let us introduce the designation $\rho_1 = R/R_1$, where R is the magnitude of resistance, taken as nominal.

Then

$$R_\Sigma = \frac{R}{\sum\limits_{i=1}^{n} \beta_i}.$$

Full change of resistance of bridge arm during deformation of strain gauges will be

$$\Delta R_\Sigma = \frac{\sum\limits_{i=1}^{n} \beta_i^2 \Delta R_i}{\left(\sum\limits_{i=1}^{n} \beta_i\right)^2}. \tag{10.60}$$

For diagram I the signal magnitude is

$$U_\Delta = \frac{U}{4} \frac{\sum\limits_{i=1}^{n} \beta_i^2 \Delta R_i}{R \sum\limits_{i=1}^{n} \beta_i}; \tag{10.61}$$

correspondingly for diagram II,

$$J_\Delta = \frac{U}{2} \frac{\sum\limits_{i=1}^{n} \beta_i^2 \Delta R_i}{\left[(R_G + 2R_{bal}) \sum\limits_{i=1}^{n} \beta_i + R\right] R}. \tag{10.62}$$

Usually $R_{bal} = R_\Sigma$. Then

$$J_\Delta = \frac{U}{4R} \frac{\sum\limits_{i=1}^{n} \beta_i^2 \Delta R_i}{R + R_G \sum\limits_{i=1}^{n} \beta_i}. \tag{10.63}$$

Series connection (Fig. 10.31). Total resistance of arm in series connection of n transducers will be

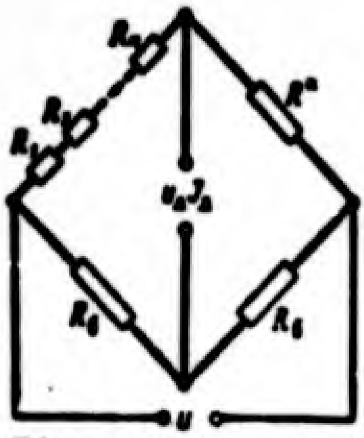

Fig. 10.31. Series connection of strain gauges.

$$R_\Sigma = \sum_{i=1}^{n} R_i \tag{10.64}$$

Full change of arm resistance during deformations of transducers is

$$\Delta R_\Sigma = \sum_{i=1}^{n} \Delta R_i \tag{10.65}$$

Let us introduce the designation $\lambda_1 = R_1/R$. Then

$$R_\Sigma = R\sum_{i=1}^{n} \lambda_i. \tag{10.66}$$

For diagram I the signal magnitude is

$$u_a = \frac{u}{4}\,\frac{\sum_{i=1}^{n} \Delta R_i}{R\sum_{i=1}^{n} \lambda_i}; \tag{10.67}$$

correspondingly for diagram II,

$$J_a = \frac{u}{2}\,\frac{\sum_{i=1}^{n} \Delta R_i}{R_g + R\sum_{i=1}^{n} \lambda_i + 2R_6}\cdot\frac{1}{R\sum_{i=1}^{n} \lambda_i}. \tag{10.68}$$

When $R_{bal} = R_\Sigma$,

$$J_a = \frac{u}{4}\,\frac{\sum_{i=1}^{n}\Delta R_i}{R\sum_{i=1}^{n}\lambda_i + R_a}\cdot\frac{1}{R\sum_{i=1}^{n}\lambda_i}. \qquad (10.69)$$

Having these basic dependences for the bridge circuit, it is possible to rationally apply connection circuits of strain gauges.

<u>Combined connection of strain gauges</u>. Let us consider the main ways of connecting transducers in groups for producing a recording signal which is directly proportional to force, i.e., sum (10.51), and let us give the relationship for the sensitivity of these circuits.

In the series connection of strain gauges (Fig. 10.32) for changing the sensitivity of the measuring circuit we connect shunting resistors r_i parallel to the strain gauges so that the change in resistance of the bridge arm would be equal to $\alpha_{ik}\gamma\varepsilon_i$. Then, considering that

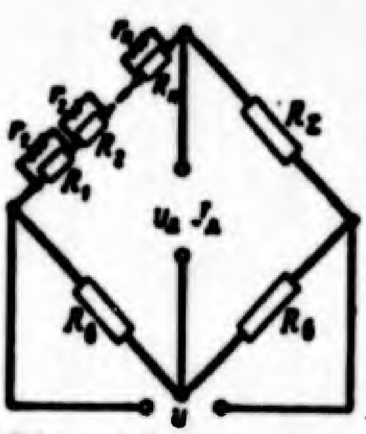

Fig. 10.32. Series connection of strain gauges with shunting resistors r_i.

$$R_\Sigma = \frac{Rr_i}{R+r_i} \quad \text{and} \quad \Delta R_\Sigma = \frac{r_i^2}{(R+r_i)^2}\,\Delta R_i,$$

we obtain

$$R_\Sigma = R\sqrt{\alpha_{ik}}.$$

With such connection of transducers the magnitude of voltage on the measuring instrument will be

$$u_a = \frac{u\gamma}{4R}\,\frac{\sum_{i=1}^{n}\alpha_{ik}\varepsilon_i}{\sum_{i=1}^{n}\sqrt{\alpha_{ik}}}. \qquad (10.70)$$

Shunting resistance is

$$r_i = \frac{\sqrt{|a_{i\Delta}|}}{1 - \sqrt{|a_{i\Delta}|}} R. \tag{10.71}$$

The recording line of the instrument with voltage on the measuring bridge diagonal u_d [formula (10.70)] deviates by the magnitude

$$h_1 = C_1 u_{\Delta}, \text{ or } h_1 = \frac{C_1 \varepsilon \gamma}{4R \sum_{i=1}^{6} \sqrt{|a_{i\Delta}|}} \sum_{i=1}^{6} a_{i\Delta} \varepsilon_i.$$

Considering expression (10.51), we have a signal which is proportionate to force:

$$h_1 = \frac{1}{k_Q} Q_{\Delta}, \tag{10.72}$$

where

$$\frac{1}{k_Q} = \frac{C_1 \varepsilon \gamma}{4RB_{\Delta} \sum_{i=1}^{6} \sqrt{|a_{i\Delta}|}}.$$

For diagram II

$$J_{\Delta} = \frac{\varepsilon \gamma}{4} \frac{\sum_{i=1}^{6} a_{i\Delta} \varepsilon_i}{R \sum_{i=1}^{6} \sqrt{|a_{i\Delta}|} + R_{\Delta}} \cdot \frac{1}{\sum_{i=1}^{6} \sqrt{|a_{i\Delta}|}}; \tag{10.73}$$

$$h_2 = C_2 J_{\Delta} \text{ or } h_2 = \frac{1}{k_Q},$$

where

$$\frac{1}{k_Q} = \frac{\varepsilon \gamma k}{4B_{\Delta}} \cdot \frac{1}{R \sum_{i=1}^{6} \sqrt{|a_{i\Delta}|} + R_{\Delta}} \cdot \frac{1}{\sum_{i=1}^{6} \sqrt{|a_{i\Delta}|}}. \tag{10.74}$$

In this case the measured force Q is obtained by simple multiplication of readings n of the recording instrument by the coefficient of sensitivity k_Q. This coefficient is a constant and is determined by taking into account the data of the equipment, the sensitivity of the measuring bridge, and the structural parameters.

Analogous dependences can be obtained for parallel connection of strain gauges.

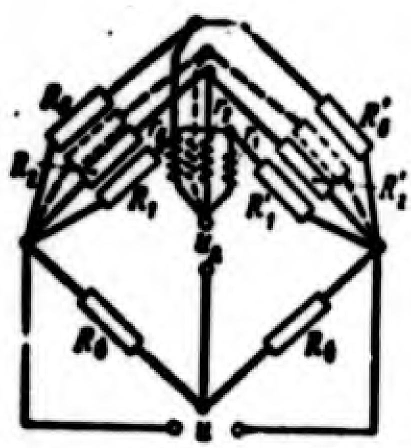

Fig. 10.33. Simplified diagram of parallel connection of strain gauges.

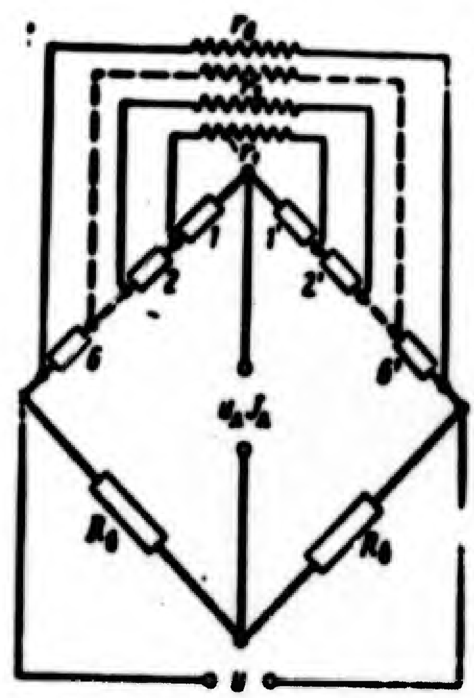

Fig. 10.34. Simplified diagram of series connection of strain gauges.

In practice it is expedient to simplify the bridge circuit by replacing the two additional resistances by one resistance. Figures 10.33 and 10.34 give working diagrams for simplified connection of strain gauges. The working formulas for parallel connection of transducers and additional resistances r_1 (see Fig. 10.33) have the following form:

with the use of an amplifier (diagram I)

$$u_a = \frac{\alpha\gamma}{4}\frac{1}{\Sigma|\mu_{ai}|}\sum_{i=1}^{6} a_{ai}\varepsilon_i; \tag{10.75}$$

with registration without an amplifier (diagram II)

$$J_a = \frac{\alpha\gamma}{4} \frac{1}{R + R_a \sum_{i=1}^{6} |\mu_{ik}|} \sum_{i=1}^{6} a_{ik} e_i, \tag{10.76}$$

$$r_i = \frac{R}{r}\left(\frac{1}{a_{ik}} - 1\right).$$

With total shuntin resistors (see Fig. 10.34) the working formulas have the form:

for diagram I

$$u_a = \frac{\alpha\gamma}{4} \cdot \frac{1}{\sum_{i=1}^{6} |\mu_{ik}|} \sum_{i=1}^{6} a_{ik} e_i; \tag{10.77}$$

for diagram II

$$J_a = \frac{\alpha\gamma}{4} \frac{1}{\sum_{i=1}^{6} |\mu_{ik}|} \frac{1}{R_a + nR} \sum_{i=1}^{6} a_{ik} e_i, \tag{10.78}$$

where

$$r_a = R \frac{|\mu_{ak}|}{1 - |\mu_{ak}|};$$

$$r_i = (2R + r_{i+1}) \frac{|\mu_{ik}|}{1 - |\mu_{ik}|}.$$

Thus, the combined circuits of connection of strain gauges ensure an output signal which is proportional to $\sum_{i=1}^{6} a_{ik} e_i$ (10.51). During work with equipment without an amplifier it is more expedient to use parallel connection of strain gauges with additional resistances. In the use of equipment with an amplifier it is more profitable to use series connection of strain gauges with total shunting resistors.

In many cases it is possible to apply special amplifying tensometric equipment which has several inputs on each channel with sealing resistors that ensure the change of sensitivity in accordance with magnitude a_{ik}.

The use of electronic mathematical machines makes it possible to perform the necessary calculations rather quickly after measurements. In this case the results of measurements should be recorded on magnetic tape by applying code recording or frequency modulation of the signal.

In certain cases during flying tests it is necessary to clarify the state of strain of separate elements of the structure. If the direction of the main stresses is known, then two transducers are glued along the axes of main stresses. If the direction of the main stresses is not known, then a rosette of three or four strain gauges is glued. The form of the rosettes and corresponding formulas for calculation of main stresses are shown in Fig. 10.35.

In selecting the place of installation of strain gauges on the structure while carrying out measurements we consider the following:

a) stresses in the place of installation of a strain gauge must be sufficiently large during the action of the investigated load component;

b) the structural element in the region of installation of a strain gauge should not lose stability within the limits of the measured loads;

c) based on the results of measurements during static tests, the dependence of deformations of a strain gauge on the load should be linear;

d) the place of installation of a strain gauge should be convenient for measurements.

Required solution	Type of rosette: two transducers	angular	delta	T-delta
				
Maximum normal stress σ_{max}	$\frac{E}{1-\mu^2}(\varepsilon_1+\mu\varepsilon_2)$	$\frac{E}{2}\left\{\frac{\varepsilon_1+\varepsilon_3}{1-\mu}+\frac{1}{1+\mu}\times \times\sqrt{(\varepsilon_1-\varepsilon_3)^2+[2\varepsilon_2-(\varepsilon_1+\varepsilon_3)]^2}\right\}$	$E\left[\frac{\varepsilon_1+\varepsilon_2+\varepsilon_3}{3(1-\mu)}+\frac{1}{1+\mu}\times \times\sqrt{\left(\varepsilon_1-\frac{\varepsilon_1+\varepsilon_2+\varepsilon_3}{3}\right)^2+\left(\frac{\varepsilon_2-\varepsilon_3}{\sqrt{3}}\right)^2}\right]$	$\frac{E}{2}\left[\frac{\varepsilon_1+\varepsilon_4}{1-\mu}+\frac{1}{1+\mu}\times \times\sqrt{(\varepsilon_1-\varepsilon_4)^2+\frac{4}{3}(\varepsilon_2-\varepsilon_3)^2}\right]$
Minimum normal stress σ_{min}	$\frac{1}{1-\mu^2}(\varepsilon_2+\mu\varepsilon_1)$	$\frac{E}{2}\left\{\frac{\varepsilon_1+\varepsilon_3}{1-\mu}-\frac{1}{1+\mu}\times \times\sqrt{(\varepsilon_1-\varepsilon_3)^2-[2\varepsilon_2-(\varepsilon_1-\varepsilon_3)]^2}\right\}$	$E\left[\frac{\varepsilon_1+\varepsilon_2+\varepsilon_3}{3(1-\mu)}-\frac{1}{1+\mu}\times \times\sqrt{\left(\varepsilon_1-\frac{\varepsilon_1+\varepsilon_2+\varepsilon_3}{3}\right)^2+\left(\frac{\varepsilon_2-\varepsilon_3}{\sqrt{3}}\right)^2}\right]$	$\frac{E}{2}\left[\frac{\varepsilon_1+\varepsilon_4}{1-\mu}-\frac{1}{1+\mu}\times \times\sqrt{(\varepsilon_1-\varepsilon_4)^2+\frac{4}{3}(\varepsilon_2-\varepsilon_3)^2}\right]$
Maximum tangential stress τ_{max}	$\frac{E}{2(1+\mu)}(\varepsilon_1-\varepsilon_2)$	$\frac{E}{2(1+\mu)}\times \times\sqrt{(\varepsilon_1-\varepsilon_3)^2+[2\varepsilon_2-(\varepsilon_1+\varepsilon_3)]^2}$	$\frac{E}{1+\mu}\times \times\sqrt{\left(\varepsilon_1-\frac{\varepsilon_1+\varepsilon_2+\varepsilon_3}{3}\right)^2+\left(\frac{\varepsilon_2-\varepsilon_3}{\sqrt{3}}\right)^2}$	$\frac{E}{2(1+\mu)}\times \times\sqrt{(\varepsilon_1-\varepsilon_4)^2+\frac{4}{3}(\varepsilon_2-\varepsilon_3)^2}$
Angle between axis of transducer and axis of maximum stress φ	0	$\frac{1}{2}\,\mathrm{arc\,tg}\,\frac{2\varepsilon_2-(\varepsilon_1+\varepsilon_3)}{\varepsilon_1-\varepsilon_3}$	$\frac{1}{2}\,\mathrm{arc\,tg}\,\frac{\frac{1}{\sqrt{3}}(\varepsilon_2-\varepsilon_3)}{\varepsilon_1-\frac{\varepsilon_1+\varepsilon_2+\varepsilon_3}{3}}$	$\frac{1}{2}\,\mathrm{arc\,tg}\,\frac{2(\varepsilon_2-\varepsilon_3)}{\sqrt{3}(\varepsilon_1-\varepsilon_4)}$

Fig. 10.35. Diagram of rosettes for investigating the combined state of strain of a structure.

An approximate diagram of installation of strain gauges is shown in Fig. 10.36.

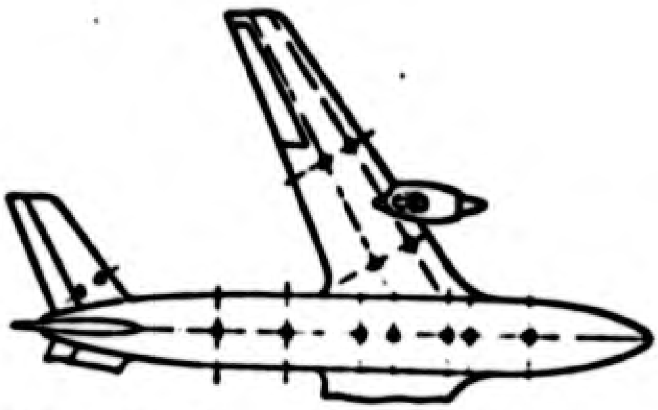

Fig. 10.36. Diagram of installation of strain gauges for the investigation of loads. ▲ - place of installation of strain gauges.

Strain gauges are glued and are protected by a special coating according to the technology fixed for the given type of transducers and glue. During assembly a thorough check is made of the waterproofing of the strain gauges.

Before the measurements, calibration of strain gauges and measuring equipment is made. During calibration, simultaneously with the determination of calibration coefficients, a final check is made of the measuring circuit and the work of the strain gauges. The calibration coefficient (with respect to load) is the magnitude of the load, which causes displacement of the line of recording by 1 mm, i.e.,

$$k_Q = Q/h, \qquad (10.79)$$

where h is the displacement of the recording line under load Q.

Calibration coefficients may be determined by means of calibration of an aircraft prototype by specified loads in a static testing laboratory, either under airport conditions, or by calculation based on the materials of measurements that were obtained during static tests of another of flight vehicle prototype.

Calculation methods do not give the possibility of checking the efficiency of equipment and strain gauges; therefore, they should be considered as preliminary methods.

Calibration of a flight vehicle prototype is conducted by loading it with specified loads which are applied in one or two sections (Fig. 10.37). During loading, special collars are used with soft linings, in order not to damage the structure. The magnitude of the load during calibration should not exceed 60% of the rated value for the most loaded section. During calibration the measuring circuit is assembled into a final variant in accordance with the working formulas. In the process of calibration the influence of other load components on the sensitivity of the measuring circuit should be estimated.

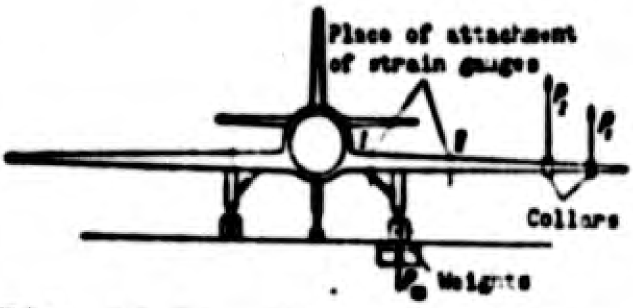

Fig. 10.37. Diagram of calibration of equipment for measurement of wing bending moment. P_1, P_2 are the forces applied to the wing, $P_{l.g.}$ is the force acting on the wing from a landing gear strut.

Calibration coefficients can be preliminarily determined by means of calculation. Based on the results of strength calculations, the magnitude of stress Q_{sg} is estimated in the place of installation of the strain gauge under a specified load Q. The calibration coefficient is

$$k_Q = \frac{Q}{h} = \frac{QE}{h\sigma_T}, \tag{10.80}$$

where k is the amplification factor of the equipment, determined on the basis of the calibration signal: $k = h/\varepsilon$.

For instance, for structural elements which are working under extension or compression, the calibration coefficient during registration on an oscillograph without an amplifier can be determined in the following way:

$$k_Q = \frac{4EF(R+R_g)}{\sigma\eta h}. \tag{10.81}$$

where F is the size of a component;

E is the elastic modulus.

For structural elements which are working under flexure,

$$k_q = \frac{4WE(R+R_0)}{\alpha\gamma h}. \qquad (10.82)$$

where W is the moment of flexural resistance.

Measurement of Loads Acting Upon a Flight Vehicle Under Conditions of Aerodynamic Heating

For flight vehicles of high supersonic speeds, during flying tests it is necessary to investigate not only loads, but also heating of the structure. The heat flow, which influence the structure of a flight vehicle, can be determined by means of analysis of the basic Fourier relationship:

$$q = -\lambda\left(\frac{\partial T}{\partial n}\right)_{n=0}. \qquad (10.83)$$

where $\frac{\partial T}{\partial n}$ is the gradient of temperatures in a structural element which is normal to its external surface;

n is a coordinate which is normal to the external surface (with respect to the source of heat) of the considered structural element.

The indicated gradient of temperatures, with respect to a body which is normal to the surface, is easy to determine with the known field of temperatures. Inasmuch as in the very general case an aircraft structure is a body of volume measurement, for the manifestation of a temperature field the temperature is measured along three axes.

As shown in Chapter VIII, the question is solved most simply in the case of a one-dimensional thermal space. Examples of structural elements, in which it is possible to consider the field of temperatures to be one-dimensional, could be structural elements in the form of plates and rods: skin, spar wall, and so forth.

For determination of any heat flow, which acts upon a structure, it is necessary to measure the change of temperatures along the thickness of the structural element. The temperature profile along the thickness is determined by the values of temperatures in no less than three points. This requires the installation of additional testing equipment.

For thin metallic elements of structures the temperature gradient along the thickness can be considered as insignificant and it may be disregarded. If we do not place the receivers of temperatures on these structural elements near the places of thermal drains (requirement of uniformity of heat flow), we can determine the thermal load of structural surfaces of the flight vehicle and compare it with the rated load.

Heat flow is calculated according to the equation

$$q_{exp}=c\gamma\delta\frac{\partial T}{\partial\tau}+\varepsilon\sigma T^{4}-q_{c}\cos\beta, \tag{10.84}$$

which is valid for every point of the structure. For manifestation of general regularities we compare the rated and actual coefficients of heat radiation:

$$\alpha=\frac{q_{exp}}{T_{0}-T}. \tag{10.85}$$

<u>Determination of external load</u>. Heating of a flight vehicle at a supersonic speed of flight leads to a drop in rigidity. Due to this, the calibrations of assemblies of a flight vehicle, obtained in ground conditions at normal temperature, for the determination of external loads in conditions of aerodynamic heating are impossible to use. At the same time, calibrations on full-scale (actual) objects

under the condition of observance of simulation of aerodynamic heating are also extraordinarily complicated to conducted. However, in the selection of places of distribution of strain gauges on the structure, one can determine the external loads of assemblies of the flight vehicle by the usual method strain measurement with the application of calibrations under normal temperature conditions. Corrections are then introduced for the influence of temperature:

$$P(T) = P_0 k_T, \tag{10.86}$$

where k_T is the coefficient which considers the influence of temperatures;

P_0 is the load which is determined for a "cold" structure.

Measurement of Oscillations (Vibrations) of Aircraft Structures

The basic purposes of oscillation measurements are:

a) quantitative determination of characteristics of oscillations (amplitudes and frequencies) under different operating conditions of a flight vehicle;

b) manifestation of the character and type of oscillations with the determination of the causes of their appearance;

c) development of recommendations for decreasing of increased oscillations;

d) estimating the permissibility of oscillations from the condition of strength of the main assemblies of a flight vehicle taking into account the assumed service life.

Proceeding from the problem of investigation, we determine the diagram of installation of oscillation transducers (vibration pickups) on the structure. Usually vibration pickups are mounted on the main structural assemblies for measuring the flexural and torsional oscillations. In the determination of flexural oscillation modes the vibration pickups should be placed near the axis of rigidity. In the selection of places of installation of vibration pickups one should also consider the data of frequency tests of the full-scale structure. Vibration pickups should not be placed near the nodes of the investigated oscillations.

For the measurement of torsional oscillations, vibration pickups are placed at approximately identical distances (symmetrically) from the axis of rigidity. Figure 10.38 gives the approximate distribution of vibration pickups in the investigation of wing oscillations. The places of installation of vibration pickups should be as accessible as possible for checking and mounting the pickups during measurements. During the mounting of vibration pickups the rigidity of their attachment to the structure is checked. A mounted pickup should have a frequency of natural oscillations higher than the top investigated one by 5-10 times. The frequency of natural oscillations of the pickup mounting is usually checked by tapping along the bracket with simultaneous recording of oscillations.

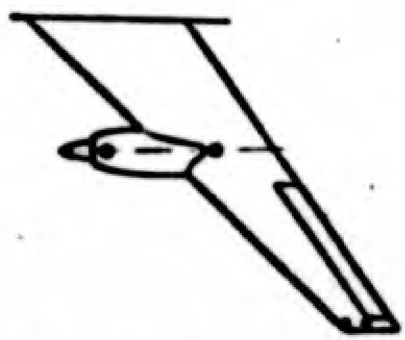

Fig. 10.38. Diagram of distribution of vibration pickups on a wing.

The type of applied vibration pickups and recording equipment is determined by the mode of the investigated oscillations. Here we consider the frequency and amplitude range of measurements, the sensitivity (amplification factor), the form of recording, the number of channels of registration, and the dimensions of the equipment.

In a number of cases, for estimating the permissibility of oscillations it is expedient to apply tensometric equipment, since it is possible to estimate the magnitude of stresses in the structure during oscillations with it. Measurement of oscillations is conducted under basic operating conditions of flight with a gradual approach to limiting conditions.

In an intensive increase of oscillations with the increase of speed of flight, overload, or other parameters which characterize the approach to critical conditions of flight, the materials of measurements are thoroughly analyzed for determinating the safety of further increasing these parameters. In this case for expanding the conditions of flight in the first place we are guided by the data of instrument recordings, inasmuch as the crew can give only a subjective estimate of oscillations in places of its distribution. The crew's estimate of oscillations of other parts of the structure usually has a too approximate character.

All conditions of flight during measurements of oscillations are usually repeated several times. It is expedient to use long recordings of oscillations for manifestation of conditions with a high level of oscillations and for an estimate of the relative time of the flight vehicle stays in different conditions of flight.

In the investigation of oscillations in the crew and passenger compartments it is expedient to use manual vibrographs (vibration probes) which permit fast inspection of a large number of points.

An estimate of the permissibility of structural oscillations is produced with respect to the level of variable stresses. For a rough estimate of the level of variable stresses in certain cases it is possible to convert the amplitudes of oscillations into the stresses of the structure, considering the oscillation mode. For a more precise definition of the level of stresses in separate points measurements of stresses are made with the help of wire strain gauges. In certain cases the magnitude of permissible oscillations of a flight vehicle is limited by the physiologic sensations of the crew or the passengers. Figure 10.39 gives curves which make it possible to estimate oscillations in a cabin*.

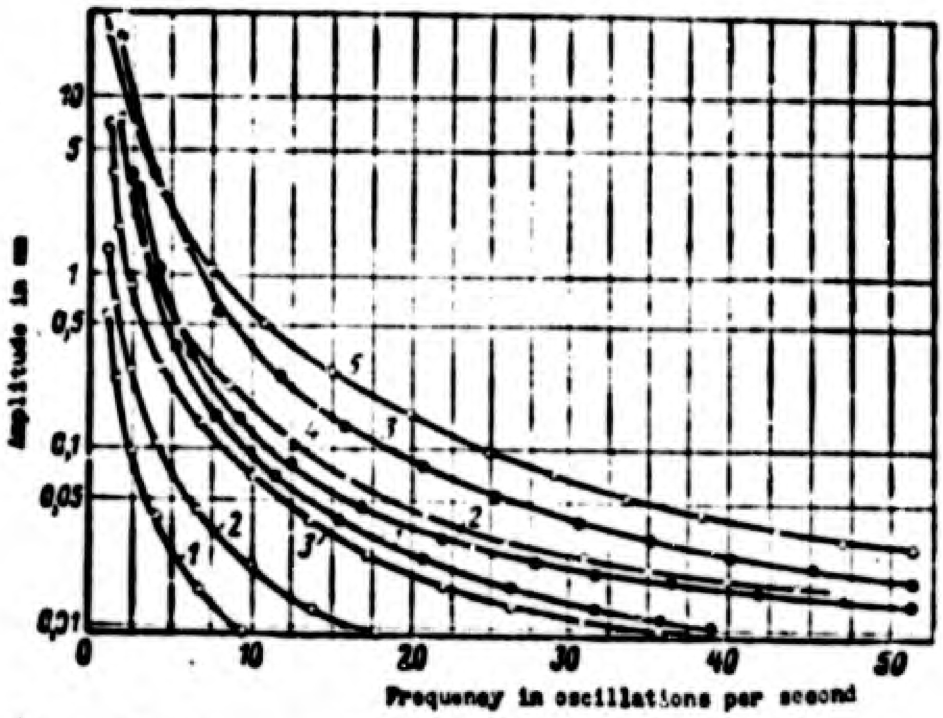

Fig. 10.39. Graphs for estimating oscillations from conditions of physiologic sensations. 0 — 0 – based on the results of generalization of test data of helicopters and aircraft: 0-1 – not noticeable, 1-2 – hardly noticeable, 2-3 – noticeable, 3-4 – slightly unpleasent, 4-5 – unpleasent to a limit, 5 – very unpleasent, ●-● – based on the results of laboratory and flying tests: 1) recommended limit; 2) uncomfortable; 3) very uncomfortable.

Estimation of Flight Safety from Flutter Conditions

The contemporary technique of making measurements of structural oscillations with the help of vibration-measuring and tensometric equipment makes it possible to investigate the reserves for critical speed of flutter during flying tests.

---

*R. Ya. Yang, Theory and design of a helicopter, English translation, Oborongiz, 1951. Gillmore, Helicopter Flight Vibration Problems, Aeronaut, Eng. Rev., 1955.

At present, on aircraft with subsonic speeds, owing to laboratory tests, the probability of the onset of flutter, with the exception of the trim tab of control form, is small. For supersonic speeds, especially during aerodynamic heating, the estimation of critical speed of flutter by calculation methods or simulation methods is considerably complicated and becomes less reliable. In connection with this the value of flying tests for flutter increases.

During flying tests for flutter we originate from the following:

1) the approach to critical conditions of flutter should be determined by observation of the structure's reaction to perturbations;

2) the approach to these conditions should be conducted quickly with the observance of safety conditions;

3) during the installation of experimental equipment the probability of the appearance of flutter should not be increased.

The diagram of aircraft equipment and the method of excitation depend on the form of flutter, on the part of the aircraft which is enveloped by flutter, and on the required range of frequencies and the expected danger of development of flutter. During the investigation of flutter we study the character of change of the damping decrement of oscillations with the increase of flight speed in case of pulse disturbance or change of amplitudes of forced oscillations during sinusoidal excitations.

For safety of flying tests the assumed perturbation calculation and character of change of damping decrement should be estimated during laboratory model testing. During the flying experiment we compare the obtained data with the data of laboratory investigations. On the basis of this comparison we estimate the reliability of preliminary data on the critical speed of flutter.

Let us consider the main methods of investigating flutter in flight.

Excitation by means of pulses of the control system. During manual control the pilot can transmit different forms of pulses by a lever (control stick) or by pedals. Such sharp pulses can excite oscillation modes with a frequency of up to 5-7 oscillations per second. If the aircraft has an automatic pilot, then it is possible to connect a signal transducer to it in order to create a shock or a sinusoidal disturbance to the controls. During control with amplifiers the system can also be equipped with exciters of oscillations of the controls.

Pulse excitation can be created by installing charges on different parts of the aircraft. By the corresponding selection of the grade of powder and the form of its grains there can be obtained pulses of different form and duration. Adjustment of pulse length makes it possible to bring about the appropriate frequency of oscillations. With a smooth change of force during the time of action of the pulse, equal to approximately half the period of oscillations with respect to a given mode, the energy which is absorbed by this mode tends to maximum. The advantage of this method is that the pulse disturbance makes it possible to reduce the time of flight at speeds which are close to limiting and, consequently, dangerous for flutter tests. Equipment for such tests can be made sufficiently light and small-size.

Some difficulty in the use of this method consists in transient response analysis.

Resonance method. With such a method sinusoidal oscillations of different modes are excited. The amplitude of forced oscillations with the approach to critical speed of flight sharply increases. The excitation of sinusoidal oscillations employs a vibrator with an unbalanced flywheel which transmits a force to the structure that is variable in direction and is in the form of a vector of force. Such a vibrator should have a light powerful motor with good speed regulation. With this method of excitation of oscillations there appears much difficulty in frequency control of the exciting force near the resonance peaks. Since vibrators require a large amount of room, they are difficult to place on the end sections of the wing and empennage. Therefore, they are mounted in the fuselage, the motor nacelles, and in special cowls on the wing.

Flying tests with a vibrator are more dangerous than during shock excitation, since they require a comparatively long flight near critical speed. Upon the appearance of resonance it is expedient to suddenly terminate excitation and record the process of oscillation damping. This process is repeated at all resonance peaks. Based on the analysis of damping, it is possible to estimate if the speed of flight is close to the critical speed of flutter.

At present, owing to the development of the theory of random influences of gusts of bumpy air on a structure, it is possible to estimate the approach of speed of flight to critical speed of flutter on the basis of an analysis of the influence of gusts on different speeds of flight.

During flutter tests, after every flight the measurement materials must be thoroughly analyzed. The safety of transition to the following conditions should be determined at a high speed of flight. The analysis of measurements utilized the construction of polar diagrams of excitation amplitude per unit of reaction amplitude at a constant speed of flight. The approach of curves for high speeds of flight to the origin of coordinates indicates a decrease of dynamic stability.

10.4. Treatment and Analysis of Results of Measurements

The main part of the parameters during structural-performance tests is usually recorded with the help of optical, magnetic, mechanical, and other recorders. With the use of a magnetoelectric oscillograph which records on Photographic film, the initial material for treatment is the oscillogram. The recording lines of the oscillogram must be easy to distinguish. This is carried out by automatic marking of the recording lines in the form of breaks which are alternated on the oscillogram in a definite sequence. Sometimes a color recording is used. The recording lines should not exceed the bounds of the film or go beyond the limits of the recording sweep, which is determined by the linear section of the amplification characteristic of the electronic measuring equipment. The duration of the recordings should be sufficient for estimating the main characteristics of the recorded process.

During measurements of static loads and overloads, the oscillogram should have a recording of the "zero" lines which correspond to their values in the initial position.

Depending upon the required accuracy and speed, the treatment of results of measurements can be executed with the help of drafting meters, scale and slide rules, special patterns and nomographs, key-actuated computers, mechanical and electonic harmonic analyzers. Furthermore, electronic computers can be applied. They may be digital, continuous action, and special computers, for instance, for determinating correlation functions, spectral density, recurrence characteristics, etc.

Depending upon the investigated parameter and the measurement problem, we distinguish the following forms of recording processing:

1) measuring the maximum values of the registered parameter under

specific conditions;

2) carrying out frequency-amplitude analysis of measured parameters;

3) determinating the dependence of magnitudes of measured parameters on time, speed, overload, and other arguments;

4) obtaining the spectral density and other dependences by methods of mathematical statistics.

The calculations terminate with a graphic formation in the required system of coordinates, i.e., right-angle, logarithmic, and similogarithmic. Sometimes for this purpose a probability scale is applied (see Fig. 4.8).

One of the peculiarities of carrying out flight tests, and in particular, structural-performance tests, consists in that the results of measurements must be processed as quickly as possible. During tests of aircraft and helicopters, frequently every subsequent flight is executed by taking into account the results of the preceding flight. In such conditions the application of time-consuming, although exact, methods of treatment of flight material is hampered. Due to this, development has been obtained by methods of approximation processing which, with sufficient accuracy of results, give the possibility in a short time to process a large quantity of recordings of different parameters and to obtain basic information on the investigated question.

The most time spent in the processing of results is connected with harmonic analysis and determination of statistical dependences for the measured parameters. Therefore, such processing is applied only when carrying out special investigations.

As shown above, wide development was obtained by the system of measurements with automatic and semiautomatic processing. In such measuring systems the required statistical dependences are obtained directly in the form of tables and graphs.

Methods of Processing the Recordings of Dynamic Processes

Harmonic analysis of periodic curves is based on the known Fourier theorem which establishes that any periodic function, satisfying certain conditions of continuity (Dirichlet conditions), can be presented in a specific trigonometric series. Curves of recordings of oscillations and variable stresses (forces) practically always satisfy the required conditions of continuity.

If under these conditions the function f(x) is determined in any point of the interval $0 \leq x \leq 2\pi$, and for points outside this interval the relationship $f(x + 2\pi) = f(x)$ is executed, then

$$f(x)=\frac{a_0}{2}+\sum_{k=1}^{\infty}(a_k\cos kx+b_k\sin kx), \tag{10.87}$$

where

$$a_k=\frac{1}{\pi}\int_0^{2\pi}f(x)\cos kx\,dx;\quad b_k=\frac{1}{\pi}\int_0^{2\pi}f(x)\sin kx\,dx\ (k=0,1,2,\ldots). \tag{10.88}$$

Expression (10.87) constitutes a Fourier series, while a_k and b_k are Fourier coefficients. Expressions (10.88), for the determination of these coefficients, are called Cauchy integrals.

There exists a proposition (known under the name of the Riemann theorem), which consists in that a periodic function can be expanded in a Fourier series by a single method. The application of methods of numerical harmonic analysis for processing recordings during flying tests is limited due to the cumbersomeness of calculating work. During tests of even one aircraft hundreds of recordings are obtained for different parameters of a dynamic process. Therefore, special equipment is used for harmonic analysis.

The envelope method has been quite fully developed and has been widely applied during the processing of recordings of dynamic processes. The envelope method is approximation method for processing the recordings of oscillations. However, in most cases this method gives sufficient accuracy of processing and makes it possible to conduct a fast analysis of recordings. During the practical carrying out of measurements the envelope method is almost the only method of amplitude-frequency analysis of recordings.

The comparison of the data of preliminary processing by the envelope method and subsequent harmonic analysis of recordings shows that with sufficient qualification of the processor in most cases the difference is insignificant. However, use of the envelope method requires considerable skills in processing and assumes that the analyst has a complete understanding of the investigated phenomenon. Formal application of this method, without proper analysis of obtained results, can lead to incorrect conclusions. With a sufficient amount of experience the calculator can visually determine the main harmonic (sinusoidal) components of the analyzed recordings.

Processing of oscillation recordings or recordings of other dynamic process consists in determining the sinusoids, whose sum reproduces the form of the initial curve. The envelope method is based on the properties of total curves which are obtained as a result of addition of sinusoids. Therefore, the essence of the envelope method is most easily comprehended in examples.

Curves with two components having a large frequency ratio are characterized by the following (Fig. 10.40):

a) the envelopes are similar to one another and are sinusoids;

b) the high-frequency components of the recording have the form of the sinusoid lying between the envelopes;

c) the distance between envelopes is constant and is equal to the sweep of the high-frequency component.

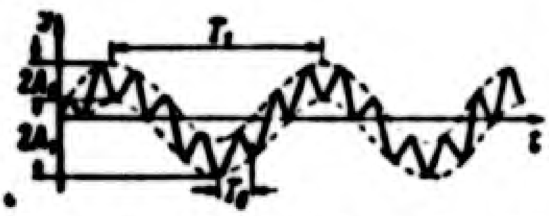

Fig. 10.40. Breakdown of a curve which consists of two sinusoids with frequency ratio 6 : 1.

Curves with three components have a more complicated form (Fig. 10.41).

In the use of the envelope method one should determine the period of the initial curve. If the recording has insignificant interferences (for instance, in the form of the high-frequency component from the amplifier), they can be disregarded. By further construction of a center line we separate the high-frequency component from the others. This is done by drawing envelopes; the center line is located in the middle between the envelopes.

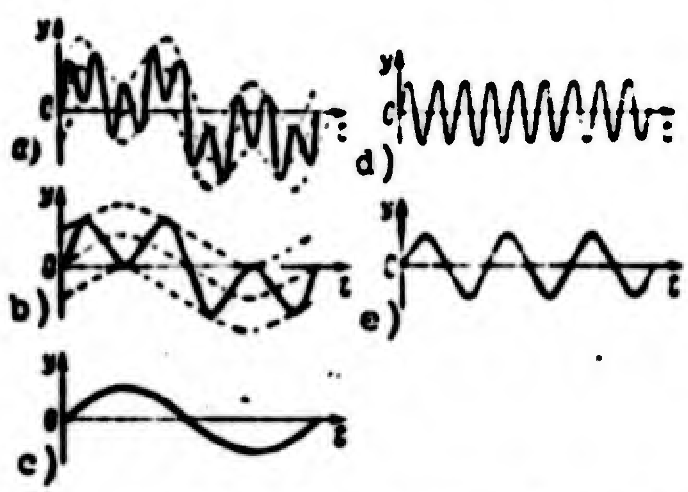

Fig. 10.41. Breakdown of a complicated curve into simple sinusoidal components.

The center line of the envelopes always constitutes the low-frequency component (or the sum of low-frequency components if the initial curve is complicated). Thus, on Fig. 10.41b, the curve is the center line of the initial curve which is shown in Fig. 10.41a; curve b differs from curve a by the absence of a high-frequency component (see Fig. 10.41d).

The same method is applied to the obtained center line of the initial curve: envelopes are drawn and the center line of the envelopes is constructed; a curve is then obtained with more low-frequency components (see Fig. 10.41b, and c; curve c differs from curve b by the absence of a second component). This process continues until the center line of the curve of the lowest order becomes a straight line in the final result (see Fig. 10.41c).

If both envelopes are identical, the center line is not constructed, since it will be similar to the envelopes. In this case there is only one high-frequency component (see Fig. 10.40).

The frequencies of separate components are determined by the timing on the oscillogram. In an extreme case the frequency can be determined by the speed of the tape on which the oscillations were recorded. The order of harmonics is calculated with respect to the base period which was taken for analysis of the oscillation recording. Upon necessity the harmonics can be referred to engine revolutions or to another characteristic frequency.

The frequencies of sinusoidal components of the recording are determined in the following way. Take a segment of the recording in two or three of the lowest periods and on it count the amount of waves with an identical period. First count the frequencies of sinusoidal components of the lowest period, then the frequencies of components of a higher order. The frequencies of oscillations are determined by the formula

$$f = \frac{N}{t} \tag{10.89}$$

where N is the quantity of waves of the investigated sinusoidal component on a selected segment of recording;

t is the time (usually in seconds) which is counted off on the recording with respect to the time notation.

The amplitudes of sinusoidal components of the recording are determined by the envelopes (or center lines). The bandwidth between envelopes constitutes the double amplitude (sweep) of a single high-frequency component (see Fig. 10.40). Amplitude is determined by the distance between the center line and the envelope.

The accuracy of determination of amplitudes of sinusoidal components by the envelope method can be increased, by increasing the initial curve with the photographic method. The frequencies of sinusoidal components are obtained with great accuracy and without magnification. For this, the section of the recording should be sufficiently large.

Imposition method. In certain cases the envelope method does not give an accuracy in processing the recordings of dynamic processes. This pertains to curves with frequency ratios 2 : 1, 3 : 1, 3 : 2 : 1, and others.

The imposition method is a certain average between the envelope method and harmonic analysis. It reduces basically to the division of the recording period into a series of smaller periods and to the determination of the mean value of the ordinate in these periods.

The theory of the method is simple and consists in the division of even and odd functions, and also in the separation of components with an order that is multiple to three.

If we divide the period in half and make a reading of the abscissa from the middle of the period, according to Fourier's theorem,

$$f(x)=\frac{a_0}{2}+\sum_{k=1}^{\infty}a_k\cos kx+\sum_{k=1}^{\infty}b_k\sin kx,$$

$$f(-x)=\frac{a_0}{2}+\sum_{k=1}^{\infty}a_k\cos kx-\sum_{k=1}^{\infty}b_k\sin kx.$$

Hence

$$f(x)+f(-x)=a_0+2\sum_{k=1}^{\infty}a_k\cos kx,$$

$$f(x)-f(-x)=2\sum_{k=1}^{\infty}a_k\sin kx.$$

Thus, if on the initial curve (Fig. 10.42a) one half-period AB is put on the other BD, then the half-sum of ordinates determines the c.-sinusoidal component, while the half-difference determines the sinusoidal one. Figure 10.41b gives a curve which is an even harmonic (cosine curve), and Fig. 10.42c shows an odd harmonic (sinusoid).

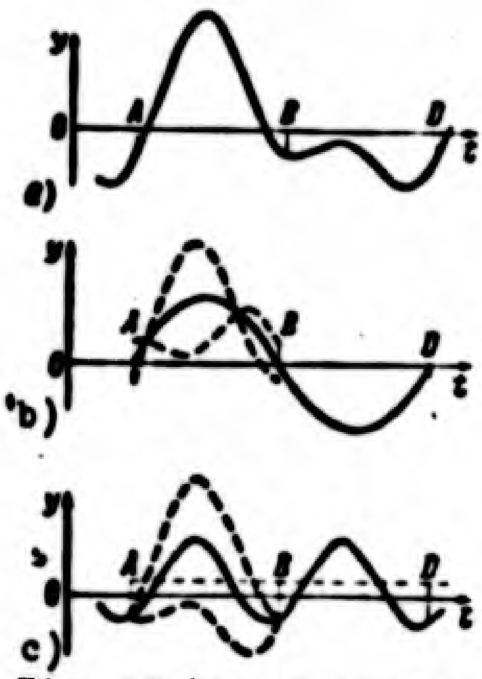

Fig. 10.42. Determination of sinusoidal components by the imposition method.

In general, the period on the investigated recording i. divided into equal parts and their "imposition" is produced in tables. For this it is also possible to transfer the curve on tracing paper, and by bending it in the central part of the period, put one part on the other and add or subtract the ordinates. Harmonics which are multiple to three cannot be subtracted if the period on the recording is divided into three parts and their imposition has been carried out.

The imposition method is rarely applied in practice due to its comparative time-consumption. The necessary amplitude-frequency analysis of complex recordings can be obtained more simply with the help of mechanical harmonic analyzers. However, in individual cases the imposition method turns out to be useful.

Treatment and Analysis of Oscillation Recordings

Recordings of oscillations, depending upon the measurement method, can be graphs of displacements, speeds, or accelerations. As a result of processing, the frequency and amplitude of displacements, and in certain cases the amplitude of accelerations of the recorded oscillatory process should be determined. Coefficients for transition from amplitudes of the recording to real magnitudes are obtained, as noted above, from the results of calibration of vibration-measuring equipment.

The processing of oscillation recordings includes an amplitude-frequency analysis. The main method of such analysis is the envelope method. As the result of primary processing of oscillograms the frequency and amplitude of sinusoidal components of recordings are determined. In certain cases, for instance in the determination of the magnitude of total acceleration on an acceleration recording or the magnitude of total deviation of a structure during oscillations from its average position on a displacement recording, it is sufficient to determine maximum deviations of a recording from its average ("zero") value, not conducting a breakdown of the recording into sinusoidal components and not determining their frequencies in this instance.

Frequencies of sinusoidal components of a recording are determined by formula (10.89). It is necessary to note that during processing of a recording by the envelope method, the physical values of frequencies are obtained. For the most part they are not multiple to each other or to some other magnitude. This especially pertains to recordings of aerodynamic oscillations (see Chapter V). During the processing of oscillation recordings by methods of harmonic analysis the frequencies of sinusoidal components are always multiple to one magnitude which frequently is conditionally taken on an oscillogram. The latter must be considered in the determination of oscillation sources.

If the amplitudes of displacements are determined on the recording of displacements, then in this case the values of the measured ordinates of the recording are multiplied by the corresponding calibration coefficient k_a (10.25). Analogously, the amplitudes of speed can be determined on the recording of speed and the amplitudes of acceleration on the recording of acceleration. Characteristics of speeds of oscillatory motion during structural-performance tests usually are not determined.

In many cases it is necessary, on the recording of displacements (speeds or accelerations), to determine both displacements, and also accelerations of real oscillatory motion. Besides the amplitudes of components of resultant motion, sometimes the total amplitudes of displacement and acceleration of oscillatory motion are determined according to the following formulas.

1. If the recording constitutes a graph of displacements, then the total quantity of displacement is determined by the formula

$$A_{\Sigma} = 2A_m k_a, \tag{10.90}$$

where A_m is the measurement deviation of the recording line from its average position;

k_a is the calibration coefficient, which is determined by formula (10.25).

Amplitudes of displacements A_{Σ} for sinusoidal components are also determined by formula (10.90), taking that $2A_m$ is the total amplitude (double amplitude) of the corresponding sinusoidal component on the recording.

Amplitudes of accelerations j (in percent of g) for sinusoidal components are determined by the formula

$$j = 2A_m f^2 k_{j(a)}, \tag{10.91}$$

where the calibration coefficient for acceleration is

$$k_{j(a)} = \frac{4\pi^2}{g} k_a = \frac{4\pi^2 S}{2A_{cal} g}; \tag{10.92}$$

f is the frequency of the corresponding sinusoidal component;

A_{cal} is the amplitude on the calibration recording;

S is the amplitude of the platform of the calibration stand.

Amplitudes of accelerations or vibration overload may be also calculated by formulas (3.8) and (3.9) according to the known values of f and A. Total acceleration usually is not determined on the recording of displacements due to the complexity of calculation of the shift of phases of different components of the complex recording.

2. If the recording constitutes a graph of speeds, then the amplitudes of displacements are determined by the formula*

$$A = \frac{2A_v}{f} k_{a(v)}, \tag{10.93}$$

where the calibration coefficient for displacement is

$$k_{a(v)} = \frac{k_v}{2\pi} = \frac{Sf}{2A_{cal}}; \tag{10.94}$$

Amplitudes of accelerations (in percent of g) we found by the formula

$$j = 2A_v f k_{j(v)}. \tag{10.95}$$

---

*Calibration coefficient subscripts signify: first subscript (a or j) – assignment of coefficient (for calculation of displacements or accelerations); second subscript (in parentheses a, v, j) – form of recording (recording of displacements, speeds, or accelerations). For instance, coefficient $k_{a(v)}$ intended for the determination of amplitudes of displacements on the recording of speed.

where the calibration coefficient for acceleration is

$$k_{j(v)} = \frac{2\pi}{g}\cdot k_v = \frac{4\pi^2 Sf}{2A_1 g}. \qquad (10.96)$$

Coefficient k_v in formulas (10.94) and (10.96) has the value of (10.26). Total amplitudes of displacements and accelerations on the recording of speed usually are not determined.

3. If recording constitutes a graph of acceleration, then the amplitude of displacements of sinusoidal components is determined by the formula

$$A = \frac{2A_j}{p}k_{s(j)}, \qquad (10.97)$$

where the calibration coefficient for displacement is

$$k_{s(j)} = \frac{g}{4\pi^2}\cdot k_j = \frac{Sp^2}{2A_j}. \qquad (10.98)$$

Amplitudes of accelerations of sinusoidal components are

$$j = 2A_j k_j, \qquad (10.99)$$

where k_j is determined by formula (10.27).

Total acceleration is

$$J = 2A_j k_j. \qquad (10.100)$$

On the basis of recordings of accelerations one can determine overload by the formula

$$n = A_j k_n, \qquad (10.101)$$

where k_n is the calibration coefficient for overload:

$$k_a = \frac{a}{A_m}; \qquad (10.102)$$

A_m is the total deviation of the recording line from its average ("zero") position.

In accordance with formula (10.102) the recordings of overload recorders are also processed. During determination of overloads on acceleration recordings the high-frequency impositions must be averaged, since they do not reflect the total load of the structure, but are a consequence of the high-frequency oscillations of the structure in the place of installation of the transducer.

The values of all shown calibration coefficients in formulas (10.25) – (10.27) and (10.90) – (10.102) are constants (within the limits of the linear characteristics of work of the measuring equipment), which is very convenient when carrying out the calculations.

Data on the frequencies and amplitudes obtained as a result of processing the oscillation recordings, for convenience of subsequent analysis are usually presented in the form of graphs.

Frequency analysis of measured oscillations does not depend on the method of oscillation measurement and can be conducted before obtaining the final processing data. In certain cases it is sufficient to conduct only a frequency analysis.

In the frequency analysis the source of structural oscillations is established. This is accomplished by constructing graphs of $f = f(n_{en})$ (n_{en} is the number of engine revolutions) on the basis of processing data, where for uniform location of frequency-response curves on the graph the logarithmic scale of frequencies is usually taken. This graph makes it possible to distinguish motor vibration and oscillations which appear during propeller rotation and from aerodynamic oscillations of the structure. The dependence of the frequency of motor (propeller) vibration on engine revolutions is always linear. Depending upon the order of harmonics, we determine the source of the onset of oscillations (motor or propeller), and then we find the cause of the vibrations. The frequencies of oscillations of aerodynamic origin are not changed or have little change upon change of engine revolutions.

It has also been recommended to construct graphs of the change of frequencies from speed of flight $f = f(V)$ or from the characteristic of rotor operating conditions $f = f(\mu)$ (for helicopters). These graphs make it possible to trace the change of the frequency spectrum of oscillations with the change of the conditions of flight. Furthermore, during processing of recordings of oscillations, frequency graphs make it possible to control the processing: if during processing there is an accidental ommission of some compoment of a combined recording, then on the frequency graph this error can be revealed. Frequency graphs are also necessary for constructing the amplitude characteristics of oscillations.

After the determination of amplitudes of sinusoidal components of oscillations, graphs are usually constructed, which reflect the dependence of amplitude on the parameters that characterize the conditions of measurements (rpm rate of engine shaft, speed, etc.), for instance, $A = A(n)$, $A = A(V)$, $A = A(M)$, and $A = A(f)$.

These graphs are constructed for every sinusoidal component.

The graph of $A = A(n)$ makes it possible to trace the change of amplitudes with respect to engine or propeller revolutions and to reveal the possible cases of resonance. Graphs of $A = A(V)$ or $A = A(M)$ give an understanding of the character of change of oscillations depending upon speed (Mach number) of flight. The graph of

A = A(f) makes it possible to judge the distribution of amplitudes of oscillations with respect to frequencies and to determine the most dangerous frequencies of oscillations.

The results of processing, and also frequency and amplitude analysis, should provide material for a subsequent estimate of the permissibility of oscillations.

In certain cases a statistical analysis of oscillations is performed. The fundamentals of the statistical method are presented in Chapter IV. Based on the results of oscillation processing, graphs are constructed for the distribution of probability density (see Fig. 4.4) and integral recurrence in the probability scale (see Fir. 4.8). These data make is possible to determine more fully the characteristics of non-stationary oscillations and to proceed to the estimate of fatigue damage of the structure, from the action of oscillations on it.

Processing and Analysis of Recordings of Stresses and Forces

Depending upon the investigated process, the recording of stresses and forces, according to character, can be of two types:

- recording of the oscillatory process of loading;
- recording of a single process of loading with respect to type of forces of small duration, shown in Fig. 3.8.

A recording of the first type is obtained as a result of measurement of stresses in a structure during vibrations, the investigation of stresses in rotor blades, reductor frames, and in other helicopter assemblies, the measurement of variable bending moments of helicopter tail-rotor blades, the measurement of loads on an aircraft during the takeoff run, landing run, during flight in a bumpy atmosphere, etc. In this case the problem of processing is:

– determination of the amplitude-frequency spectrum of stresses and forces;

– determination of maximum total stresses (forces) and time of action of different magnitudes of stresses.

In this case, amplitude-frequency analysis is analogous to analysis of an oscillation recording that is obtained with the help of vibration-equipment. The recording curves are usually processed by the envelope method. Frequencies of change of stresses (forces) are determined by formula (10.39). Amplitudes of sinusoidal components of recorded stresses are determined by the formula

$$\sigma = A_{rec} k_{\sigma}. \qquad (10.103)$$

where A_{rec} is the amplitude of the recording of stresses on an oscillogram;

k_{σ} is the calibration coefficient, which is determined by formula (10.4).

Amplitudes of forces are determined by the same formula (10.103), but in this case the calibration coefficient is obtained in accordance with formulas (10.79) or (10.80). Total stresses (forces) are determined also by formula (10.103). In this case A_{rec} is the maximum deviation of the recording from its average position (in the determination of oscillatory loads) or from the level from which the load increase is calculated (in the determination of total static and dynamic load components).

Recordings of the second type are obtained in measurements of loads (stresses) during the first landing impacts, in the execution of different maneuvers in flight, when firing an airborne weapon, etc. (Fig. 10.43). In these cases the form of the recording is like a graph of a force of small duration (Fig. 3.3). Frequency-amplitude analysis of such recordings is usually not conducted.

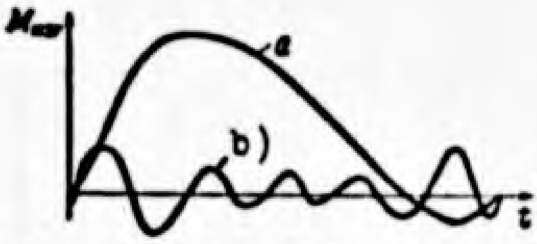

Fig. 10.43. Example of a recording of wing bending moment of an aircraft. a) when executing a zoom; b) during landing run.

During the processing of oscillograms (Fig. 10.44), with recordings of stresses and forces, the reading of recorded parameter variation is conducted from a base line. Instead of a base line it is possible to use the recording line of a timer or free loop, whose position is stable.

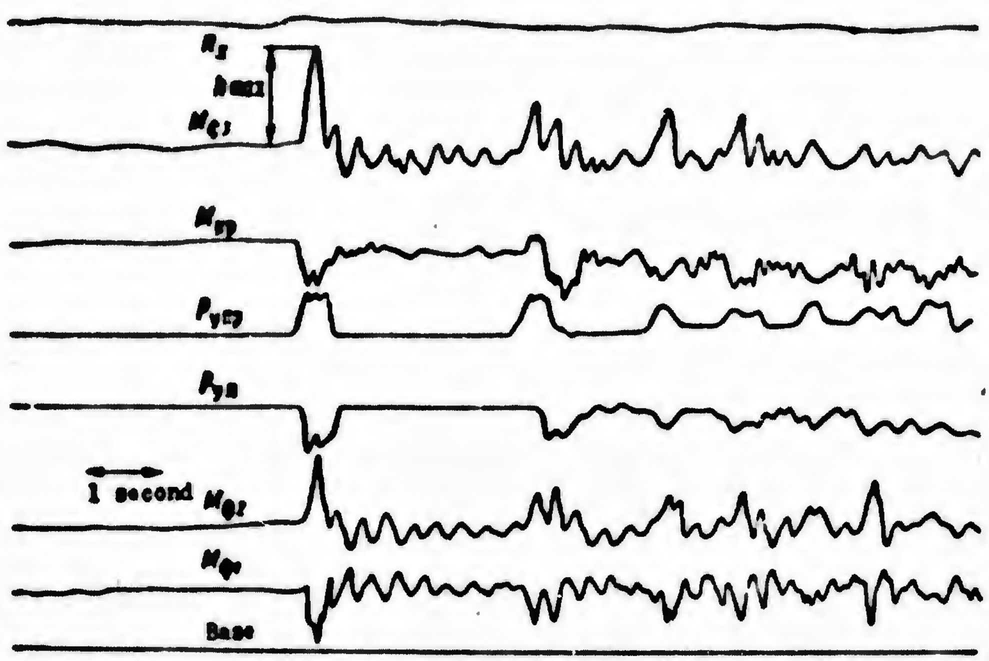

Fig. 10.44. Example of deciphering recorded parameters: n_x – overload, M_W – bending moment of wing, M_{f1}, M_{f2}, and M_{f3} – bending moments of fuselage in 1, 2, and 3 sections, $P_{y\ lft}$ and $P_{y\ rt}$ – vertical compoments of forces on left and right landing gear strut, h_{max} – magnitude of ordinate in mm, corresponding to maximum deviation of measured magnitude from reading level.

On the oscillogram it is necessary to have a recording of the parameter at zero or another initial value, with respect to which the increase in the magnitude of the measured parameter is calculated. Thus, during measurements of bending moment in a wing under the action of an overload, a recording is made before executing a maneuver in conditions of horizontal flight (n = 1.0). Furthermore, a recording of "zeroes" is made before landing and after landing. The process of recording other parameters proceeds in a similar manner.

During measurements a recording of calibration signals is made from the electronic amplifier equipment before takeoff, after landing, and control recordings of these signals in flight. For equipment without amplifiers, the same oscillograph is used to record the voltage of the power source for the measuring bridges of the tensometric equipment. For calculation of the change in the calibration signal during measurements, as compared to its value during calibration, the obtained values of the magnitudes of stresses (forces) are multiplied by a coefficient which equal to the relation

$$k = h_{\text{изм}}/h_{\text{тар}},$$

where h_{cal} is the loop deviation on the oscillogram during the recording of a calibration signal during calibration;

h_{meas} is the same value during measurements in flight.

We analogously consider the change of voltage of the power source for measuring circuits without amplifiers.

For facilitating the processing of recordings that are performed at different equipment sensitivity, calibration and recording of calibration signals is conducted at all positions of the equipment-sensitivity switch. Furthermore, the frequency-response curves of every measurement channel (amplifier - oscillograph) are determined.

For subsequent analysis, the results of processing tensometric recordings are plotted on corresponding graphs. During the analysis of oscillatory processes one should construct graphs which are analogous to those utilized during the analysis of frequencies and amplitudes of oscillations: frequency graphs $f = f(n_{en})$, $f = f(V)$,

$f = f(M)$, $f = f(n)$ and amplitude graphs $\sigma = \sigma(n_{en})$, $\sigma = \sigma(f)$, $\sigma = \sigma(n)$, $\sigma = \sigma(V)$, $\sigma = \sigma(M)$, $\sigma = \sigma(u)$ (in this case n_{en} equals the engine or rotor revolutions, and n is the overload in the center of gravity of the aircraft or helicopter).

For an analysis of loads we construct graphs $P = P(n)$, $P = P(V)$, $P = P(M)$, and other graphs of the dependences of load on the investigated parameters.

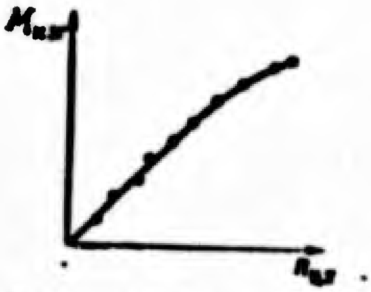

Fig. 10.45. Change of bending moment in the root section of a wing with respect to the overload in the center of gravity of an aircraft.

For an example, Fig. 10.45 shows a graph of the bending moment of a wing with respect to the overload in the center of gravity of an aircraft.

Statistical analysis of measured loading parameters of a structure is conducted in accordance with the methods presented in Chapter IV.

Literature

G. G. Abdrashitov. Concerning the question of tail buffeting, Transactions of TsAGI, No. 399, 1939.

V. S. Avduyevskiy et al, Fundamentals of heat transfer in aircraft and rocket technology, Oborongiz, 1960.

I. V. Anan'yev. Investigations in the region of strength during variable loads beyond the limit. Collection: "Strength and wear of mining equipment," Gosgortekhizdat, 1959.

I. V. Anan'yev. Reference book for the calculation of natrual oscillations of elastic systems, State Technical Press, 1946.

I. V. Anan'yev and M. M. Belyayev. Technology of measurement of oscillations, BNT, Central Aero-Hydrodynamic Institute, 194(.

Atmospheric turbulence, provoking aircraft bumping, edited by N. Z. Pinus, Gidrometeoizdat, 1962.

Aerodynamics of aircraft parts at high speeds, English translated, Collection edited by A. F. Donovan and G. R. Lawrence, IL, 1959.

P. L. Bisplinghoff, H. Ashly, and R. L. Halfman. Aeroelasticity. English translation, IL, 1958.

V. V. Bolotin. Statistical methods in structural mechanics, Gosstroyizdat, 1961.

V. S. Vedrov and M. A. Tayts. Flying tests of aircraft, Oborongiz, 1951.

T. A. Gevondyan and L. T. Kiselev. Instruments for measurement and registration of oscillations, Mashgiz, 1962.

B. E. Gatewood. Thermal stresses, English translation, IL, 1959.

A. Gessow and G. Meyers. Aerodynamics of a helicopter, English translation, Oborongiz, 1954.

Ye. P. Grossman. Course on vibrations of aircraft parts, Oborongiz, 1940.

Ye. P. Grossman and Ya. G. Panovko. Elastic oscillations of aircraft parts, LK VVIA Publishing House, 1947.

A. A. Goryainov and N. G. Kuz'min. Strength norms of aircraft and static tests. Transactions of the Central Aero-Hydrodynamic Institute, No. 25, 1926.

J. P. Den-Hartog. Mechanical oscillations, Fizmatgiz, 1961.

I. I. Drakin. Aerodynamic and radiant heating in flight, Oborongiz, 1961.

A. M. Zagordan. Elementary helicopter theory, Military Publishing House, 1960.

Yu. I. Iorish. Measurement of vibration, Mashgiz, 1956.

Yu. I. Iorish. Protection of aircraft equipment from vibrations, Oborongiz, 1949.

S. N. Kan and I. A. Sverdlov. Aircraft strength analysis, Oborongiz, 1958.

T. Karman and M. Biot. Mathematical methods in engineering, English translation, State Technical Press, 1948.

A. N. Krylov. Certain differential equations of mathematical physics, State Press for Technical and Theoretical Literature. 1950.

A. N. Krylov. Ship vibrations. Collected works, vol. 10, Academy of Sciences USSR, 1948.

A. V. Lykov. Theory of Heat Conductivity, GITTL, 1952.

A. I. Makarevskiy. Influence of longitudinal static stability on possible overload of an aircraft in curvilinear flight, Technical Reports of the Central Aero-Hydrodynamic Institute, 1940.

A. I. Makarevskiy. Strength of an aircraft at high speeds, Central Aero-Hydrodynamic Institute, 1944.

A. I. Makarevskiy and T. A. Frantsuz. Forces acting upon an aircraft in flight and during landing, BNT NKAP, 1943.

N. I. Marin. Influence of repeated loads on the strength of machine structures, Collection: "Strength and wear of mining equipment", Gosgortekhizdat, 1959.

M. A. Mikheyev. Fundamentals of heat transfer, State Power Engineering Publishing House, 1957.

R. Manly. Analysis and processing of oscillation recordings, English translation, Mashgiz, 1948.

Ya. G. Panovko. Fundamentals of the applied theory of elastic oscillations, Mashgiz, 1957.

Ya. M. Parkhomovskiy. Features of forced oscillations of distributed systems with damping, Reports of the Academy of Sciences of the USSR, Vol. 72, No. 9, 1950.

S. D. Ponomarev, and V. L. Biderman, et al. Strength analysis in machine building, Mashgiz, 1959.

A. P. Rayevskiy. Methods of experimental investigation of mechanical parameters of machines, Academy of Sciences of the USSR, 1952.

P. M. Riz and A. I. Pozhalostin. Vibrations and dynamic strength of propellers, Transactions of the Central Aero-Hydrodynamic Institute, No. 609, 1947.

Z. Ruzga. Electrical resistance strain gauges, State Power Engineering Publishing House, 1961.

M. G. Serebrennikov. Harmonic analysis, State Technical Press, 1948.

S. V. Serensen, I. M. Tetel'baum, and N. I. Prigorovskiy. Dynamic strength in machine building, Mashgiz, 1945.

N. V. Smirnov and I. V. Dunin-Barkovskiy. Short course on mathematical statistics for technical applications, Fizmatgiz, 1959.

V. V. Solodovnikov. Statistical dynamics of linear systems of automatic control, Fizmatgiz, 1960.

J. Stoker. Nonlinear oscillations in mechanical and electrical systems, IL, 1952.

S. P. Strelkov and Yu. M. Romanovskiy. The influence of atmospheric turbulence on an aircraft with flexible wings at different speeds of flight, News of the Academy of Sciences of the USSR, Mechanics and machine building, No. 4, 1959.

S. P. Strelkov and A. Ye. Ordanovich. Electronic model of flexural-torsional oscillations of an aircraft wing. Scientific Reports of the Higher School, physics and mathematics series, No.2, 1958.

Fatigue of aircraft structures, trans. from Eng., edited by I. I. Eskin, Oborongiz, 1961.

S. P. Timoshenko. Theory of oscillations in engineering, Fizmatgiz, 1959.

T. A. Frantsuz and V. L. Raykher. Methods of determination of service life of an aircraft from the action of loads repeated in operation, Transactions of the Central Aero-Hydrodynamic Institute, No. 727, 1958.

Ya. Ts. Fyn. Introduction to the theory of aeroelasticity, trans. from Eng., Fizmatgiz, 1959.

O. Khorna. Tensometric bridges, Energoizdat, 1962.

S. N. Shishkin. Concerning the question of new classification of aircraft in norms of strength, "Technology of the Air Fleet", 1933, No. 8.

S. N. Shishkin. Active loads on landing gear, Transactions of the Central Aero-Hydrodynamic Institute, No. 296, 1936.

G. N. Shur. Instruments for investigation of the spectrum of atmospheric turbulence by the method of harmonic analysis with the use of magnetic recording, Transactions of TsAO, No. 31, 1959.

B. N. Yur'yev. Aerodynamic design of helicopters, Oborongiz, 1958.

B. N. Yur'yev and V. Ye. Kastorskiy. Helicopters, Zhukovskiy VVIA Publishing House, 1951.

R. A. Yang. Theory and design of a helicopter, Oborongiz, 1951.

Alfred M. Freudenthal and Robert A. Heller. On stress interaction in fatigue and cumulative damage rule. Aero-Space Science, 1959, V. 26. No. 7.

Internal Stress and Fatigue Metals, Proc. of the Symposium on Internal Stress an Fatigue Metals, Detroit, 1960.

Mangurian, Brooks, Effects of Operational Factors on Structural Fatigue in Fighter Type Aircraft, SAE Preprint, 1954, X, N 387.

Metal Fatigue, New York-Toronto-London, 1959.

P. R. Payne. Helicopter Dynamics and Aerodynamics, London, 1959.

H. Press and B. Maselsky. A study of the Application of Power Spectral Methods, Washington, 1954.

H. Press, M. T. Meadors, and J. A. Hadlock. Re-evaluation of Data on Atmospheric Turbulence and Airplane Gust Loads for Application in Spectral Calculations, NACA, Report, N 1272, 1956.